Politecnico di Torino

ScuDo
Scuola di Dottorato ~ Doctoral School
WHAT YOU ARE, TAKES YOU FAR

Doctoral Dissertation
Doctoral Program in Pure and Applied Mathematics (38^{th}cycle)

Methods of Analytical Mechanics in Continuum Mechanics:

A unifying approach to growth, remodeling, and evolution of defects in simple and grade-one materials

By

Andrea Pastore

******

Supervisor(s):
Prof. Alfio Grillo, Supervisor
Prof. Luca Lussardi, Co-Supervisor

Doctoral Examination Committee:
Prof. Olga Barrera, Referee, Oxford Brookes University
Dr. Marco Coco, Referee, Polytechnic University of Marche
Prof. Marina Pirulli, Polytechnic of Turin

Politecnico di Torino
2026

Declaration

I hereby declare that, the contents and organization of this dissertation constitute my own original work and does not compromise in any way the rights of third parties, including those relating to the security of personal data.

Andrea Pastore
2026

* This dissertation is presented in partial fulfillment of the requirements for **Ph.D. degree** in the Graduate School of Politecnico di Torino (ScuDo).

I would like to dedicate this thesis to my loving parents

Acknowledgements

This PhD thesis is the result of three years of intense and deeply rewarding scientific work, which would not have been possible without the support of many people who accompanied me throughout this journey.

First and foremost, I wish to express my deepest gratitude to my PhD supervisor, Prof. Alfio Grillo, for the invaluable mentorship he has provided—and continues to provide—in my life. I first met Prof. Grillo during my Master's studies at the Politecnico di Torino. He was among the very first to believe in me, offering me the incredible opportunity to work alongside him, to learn from him, and to grow both scientifically and personally. He gave me the chance to explore different scientific environments, to participate in numerous conferences and workshops, and to take an active role in the Mathematical Physics community.

I am also very grateful to my co-supervisor, Prof. Luca Lussardi, for his support and in particular for the opportunity to serve as his teaching assistant for the Analisi Matematica I courses. Teaching has been an immensely rewarding experience, and I wish to thank my students for their patience, enthusiasm, and collaboration.

I would also like to thank all those with whom I have had the pleasure and honor of collaborating during these three years. In particular, I wish to thank the members of Prof. Grillo's group—Dr. Alessandro Giammarini, Dr. Salvatore Di Stefano, and Dr. Ariel Ramírez-Torres—for their constant support and availability. My sincere gratitude goes to Prof. Pierluigi Cesana for hosting me twice (in 2024 and 2025) at the Institute of Mathematics for Industry (IMI), Kyushu University, within the Q-PELS program. I also warmly thank Prof. Marco Morandotti for his guidance, and my dear friend Dr. Edoardo Fabbrini, who made me fall in love with Fukuoka. I am profoundly grateful to Prof. Eliot Fried for welcoming me both for an internship (in 2024) and a research visit (in 2025) at the Research Unit of Mechanics and Materials, Okinawa Institute of Science and Technology (OIST). I wish to sincerely thank all

the members of the Unit for their kind support, with special mention to my dear friend Mr. Geoffrey Garcia. Finally, I would like to express my heartfelt thanks to Dr. Ariel Ramírez-Torres for hosting me at the Department of Mathematics and Statistics, University of Glasgow, in 2025. My deepest appreciation also goes to Mr. Alejandro Roque Piedra, Ms. Zita "Bori" Fülöp, and Ms. Mariam M. Almudarra for their friendship and support.

I am profoundly grateful to all the wonderful people I have met at the Department of Mathematical Sciences "G.L. Lagrange" (DISMA)—professors, technicians, and staff alike. In particular, I would like to express my heartfelt thanks to my fellow PhD students, who have been the best friends one could ever wish for. They are far too many to list individually, but I am deeply thankful to each of them. They stood by me through both the highest and the most difficult moments, and even if life may one day take us far from each other, we will always remain a family.

Finally, I would like to thank my friends from Torino, Pinerolo and Pinasca —Alberto, Kevin, Giulio, Alessandro, Davide, Rosario, "Brusse", Valeria and all the *Paco Dynamite*'s band members— for always being by my side and for being the kind of friends one could only dream of. My deepest gratitude goes to my family, who has supported me and believed in me unconditionally since the very beginning. And above all, I want to thank my girlfriend Letizia, for believing in me even when I doubted myself, and for being my constant source of love, strength, and support.

Fig. 1 A selection of pictures I took while traveling abroad during my PhD. From left to right, top to bottom: Himeji Castle, Kansai (Japan, 2025); sand dunes near Jeddah (Saudi Arabia, 2025); Itsukushima Island, Hiroshima (Japan, 2025); Manzamo Cape, Onna (Okinawa, 2024); Gion Shrine, Fukuoka (Japan, 2024); Exeter Cathedral (England, 2025); the port of Castro Urdiales (Spain, 2025); the streets of Glasgow (Scotland, 2025); and the fields around Heraklion (Crete, 2025).

Abstract

The core of this PhD thesis is the extension and adaptation of concepts, originally envisioned in the context of Analytical Mechanics, to the study of mechanical problems—discrete, semi-discrete, and continuous—in which constraints, either internal or external, are considered. Rather than trying to address each class of problems separately, in this work we employ the enlightening language of Analytical Mechanics with the purpose of unifying such problems and contributing to a paradigmatic approach to mechanics. The main target of this PhD Thesis is to extend some fundamental concepts of the mechanics of constrained systems, such as Chetaev's conditions, quasi-velocities, quasi-coordinates, and transpositional relations, from their classical "discrete" definition to the semi-discrete continuous contexts. This adaptation demonstrates the versatility of Analytical Mechanics across biological and industrial problems, beyond enriching this discipline itself.

This PhD thesis is structured in three main parts.

Part I focuses on constrained discrete systems subjected to nonholonomic constraints, which are restrictions on system's generalized velocities that cannot be equivalently reformulated as conditions on the admissible configurations of the system itself. Constraints of this kind are rather typical in robotics, control theory, and other fields of the like but, to our knowledge, have received less attention in Continuum Mechanics. We analyze the dynamics of nonholonomic constrained systems by providing a modified version of a variational method originally suggested by Kozlov in the 1980s and subsequently expanded by other authors. Our work sets itself the scope of healing inconsistencies that arise in some problems of Classical Mechanics when some logical steps of the traditional formulations of d'Alembert and Lagrange are modified. In this respect, two problems that fall into this "gray zone", and that are analyzed in the present work, are the rolling coin problem and the *Gedankenexperiment* of a charged nonholonomic skate subjected to a magnetic field.

In Part II, we develop continuous models, inspired by the mechanics of constrained discrete systems, for mechanical problems stemming from biology, with emphasis on the biomechanics of growth and remodeling of tissues. In the case volumetric growth, we look at the mass balance law as a nonholonomic constraint on the growth tensor and, thus, we formulate a variational framework based on the Hamilton–Suslov principle, from which governing equations can be derived variationally. This perspective may provide new insights into the mechanics of growth and may pave the way to future investigations on the symmetries and conservation laws in growth mechanics. In the case remodeling, we extend Gurtin and Anand's strain-gradient theory of plasticity to the biphasic case in order to address multicellular aggregates, thereby coupling the deformation of the solid constituents with a Darcy–Brinkman model for the hydraulic part of the problem. Using the principles of Virtual Power and Maximum Dissipation, we derive a constitutive framework able to capture *boundary effects* related to the fluid flow and to remodeling.

Part III addresses semi-discrete mechanical systems in the industrial context, focusing on the dynamics of concentrated defects in elastic media, as is the case of *disclinations*. These defects, even though less studied than dislocations, are known to play a crucial role in some strengthening processes occurring in technologically relevant materials. By starting our discussion with a variational principle for the mechanical description of a plane-strain linear elastic medium in small deformations, we analyze the dynamics of a finite number of disclinations by showing how the defects interact reciprocally in a manner resembling *charged particles*. In doing so, we establish existence results of solutions, and we explore both the isotropic and the crystalline settings (with constrained, predefined "glide" directions), also through the use of numerical experiments.

Contents

Preface

These are the works that have been either published, accepted or put under revision by research journals during my PhD.

[1] Pastore A., Giammarini A. & Grillo A.: "Reconciling Kozlov's vakonomic method with the traditional non-holonomic method: solution of two benchmark problems". *Acta Mech* **235**, 2341– 2379 (2024).
https://doi.org/10.1007/s00707-023-03811-z

[2] Grillo A., Pastore A. & Di Stefano S.: "An Approach to Growth Mechanics Based on the Analytical Mechanics of Nonholonomic Systems". *J Elast* **157**, 3 (2025).
https://doi.org/10.1007/s10659-024-10092-7

[3] Cesana P., Grillo A., Morandotti M. & Pastore A.: "Dissipative Dynamics of Volterra Disclinations". *SIAM J. Appl. Math.* **85**(4), 1361–1386 (2025).
https://doi.org/10.1137/24M1688096

[4] Giammarini A., Pastore A. & Grillo A.: "A model of fiber reorientation in fiber-reinforced biological materials combining statistical and configurational mechanics". *Math. Mech. Solids* **30**(11), 2619–2656 (2025).
https://doi.org/10.1177/10812865251327765

[5] Giammarini A., Pastore A., Ramírez-Torres A. & Grillo A.: "A first-gradient approach to the remodeling and fluid flow in saturated porous media". *Math. Mech. Solids* **30**(9), 2185–2223 (2025).
https://doi.org/10.1177/10812865251364540

[6] Pastore A., Grillo A. & Fried E.: "Internal constraints and gauge relations in the theory of uniaxial nematic elastomers". *J Elast* **158**, 10 (2026).
https://doi.org/10.1007/s10659-025-10185-x.

Among these, in this PhD Thesis we focus on presenting the content and the main results of the sub-list [1–3, 5], even though some references to the remaining works [4, 6] are made throughout the Thesis.

Chapter 1

Introduction

The focus of this PhD Thesis is to employ concepts and tools native of Analytical Mechanics in the mathematical description of discrete, semi-discrete, and continuous mechanical systems characterized by the presence of *constraints* and pertaining to the biological and industrial contexts. On the one hand, this has required generalizing and adapting these concepts and tools to make them appropriate for a broader class of problems and to find the correct mechanical equivalent, while maintaining the mathematical structures of Variational Calculus and Differential Geometry. On the other hand, the *underlying philosophy* of Analytical Mechanics has made it possible to contextualize many mechanical problems of very different nature within a unified, paradigmatic framework. While some branches of mathematics, such as Operations Research, Financial Mathematics and Numerical Analysis, already do so, we have oriented our work towards specific problems in biomechanics, such as the growth and remodeling of soft tissues, and in materials science, such as the evolution of defects in crystalline solids.

Part I: Analytical Mechanics. The first part is devoted to the Analytical Mechanics of *discrete* mechanical systems featuring nonholonomic constraints, i.e., constraints that restrict the generalized velocities of a system of this type in a way that cannot be equivalently recast in the form of conditions on the system's configurations. These mechanical systems often appear in many branches of mechanics, among which robotics and control problems. Yet, to our knowledge, the study of this kind of problems has grown quite parallel with respect to Continuum Mechanics, and even when nonholonomicity has been investigated in the context of field theories [7–9],

there seems to be, at least in our opinion, a major highlight on Differential Geometry than on the modeling side of Mathematical Physics. Whereas we comprehend that it is necessary to develop rigorous languages to correctly formalize nonholonomic systems, we felt it was necessary to us to find a common ground in which a sufficiently rigorous formalism could meet the more physical aspects characterizing the specific problems of growth, remodeling and the evolution of defects. In this respect, our purpose was to propose models and approaches capable of framing, in a physical context, some abstract results of the differential geometric formalism, with the common ground being provided by Configurational Mechanics [10]. For this purpose, we begin our path starting from the treatise by Lanczos [11], Pars [12], Neimark&Fufaev [13], Gantmacher [14], and Bloch [15].

In Chapters 2 and 3, *(the following text is taken from the abstract of [1])* we study the dynamics of a class of mechanical systems subjected to nonholonomic constraints by employing a method termed "modified vakonomic method" (MVM), and developed by Llibre, Ramírez and Sadovskaia in 2014 [16]. In particular, we test the MVM for the "rolling coin" problem and a variant of the "non-holonomic skate" problem. For our purposes, we divide our work in two parts. For the first one, our point of departure is a paper published in the journal "Acta Mechanica" by Lemos in 2022 [17], in which, for the "rolling coin" problem, Kozlov's vakonomic method is shown to lead to inconsistencies with the so-called d'Alembert–Lagrange traditional nonholonomic method (TNHM). In this case, we prove that, if the MVM is used, the equivalence with the TNHM can be restored, and the two methods can be reconciled. In the second part, we formulate a thought experiment consisting of an electrically charged "nonholonomic skate" interacting with a magnetic field, and we examine its dynamics by means of the MVM. In this case, we point out the differences with the predictions of the TNHM, and we propose a reformulation of the MVM capable of retrieving the results obtained with the TNHM. Moreover, we give some insight into the main computational aspects related to the MVM for nonholonomic constraints linear in the generalized velocities.

Part II: Biomechanical Problems. The second part is instead devoted to systematically develop dynamic models, based on the Analytical Mechanics concepts native of constrained discrete systems, for two continuous mechanical systems representative of materials stemming from *biological contexts*. In particular, we study some problems

regarding the biomechanics of *growth and remodeling*, two very prominent subjects in the current scientific scenario.

In Chapter 5, *(the following text is taken from the abstract of [2])* motivated by the convenience, in some biomechanical problems, of interpreting the mass balance law of a growing medium as a nonholonomic constraint on the time rate of a structural descriptor known as growth tensor, we employ some results of analytical mechanics to show that such constraint can be studied variationally. Our purpose is to move a step forward in the formulation of a field theory of the mechanics of volumetric growth by defining a Lagrangian function that incorporates the nonholonomic constraint of the mass balance. The knowledge of such Lagrangian function permits, on the one hand, to deduce the dynamic equations of a growing medium as the result of a variational procedure known as Hamilton–Suslov Principle (clearly, up to non-potential generalized forces that are accounted for by extending this procedure), and, on the other hand, to study the symmetries and conservation laws that pertain to a given growth problem. While this second issue is not investigated in this work, we focus on the first one, and we show that the Euler–Lagrange equations of the considered growing medium, which describe both its motion and the evolution of the growth tensor, can be obtained by reformulating a variational method developed by other authors. We discuss the main features of this method in the context of growth mechanics, and we show how our procedure is able to improve them.

In Chapter 6, *(the following text is taken from the abstract of [5])* we rephrase Gurtin and Anand's formulation of strain-gradient plasticity [18] to describe the isochoric structural transformations (remodeling) of multicellular aggregates in *in silico* compression tests. We consider solid-fluid biphasic media, thereby accounting for interactions that cannot arise in classical elasto-plastic materials. To gain insight into the behavior of the fluid, especially in the proximity of the aggregate's boundary, we introduce a Darcy–Brinkman model, coupled with the deformation of the solid. This results in a constitutive framework of grade one in the fluid velocity (Darcy's law is of grade zero), wherein the stress tensor of the fluid acquires a dissipative contribution. To obtain the equations determining the system's evolution, we adopt the Principle of Virtual Power, which allows us to handle explicitly the internal constraints of incompressibility of the solid-fluid mixture, and of isochoricity and null-spin of the remodeling rate tensor. Furthermore, we enforce the Principle of Maximum Dissipation to justify the generalized dissipative forces of our model. Lastly, we discuss some relevant results of a numerical experiment and we provide a brief

computational background for the initial- and boundary-value problem representing our model.

Part III: Materials science problems. The third part is devoted to the description and the analysis, via techniques proper of constraints, of the dynamics of semi-continuous mechanical systems stemming from *materials science* and related to defects (disclinations) in elastic media. Together with dislocations, disclinations are commonly found in many materials of technological relevance, e.g. graphene, and their presence significantly alters the thermo-electro-mechanical properties of such materials. Whereas dislocation dynamics gathered more interest during the years, disclination dynamics received less attention. However, disclinations have recently been recognized as playing a crucial role in the *"strengthening by kink formation"* [19] process, discovered in Japan, and already widely employed in the Japanese heavy industry to produce steel and metal alloys. The initial modeling work by Inamura [20] clarified the influence of disclinations on the kinematics of kink formation. Yet, a comprehensive modeling of the energetics and dynamics of disclination systems, aimed at understanding the kink strengthening process, is still lacking for the design of improved, tougher materials.

In Chapter 7, *(the following text is taken from the abstract of [3])* the dissipative dynamics of a system of particles subject to a fourth order potential field modeling the evolution of wedge disclinations is studied, focusing on finite systems of disclinations within a circular domain. Existence theorems for the trajectories of these disclinations are presented, considering both the dynamics without predefined preferred directions of motion in an isotropic medium and the dynamics in which the disclinations move parallel to predefined directions, modeling a crystalline material. The analysis is illustrated with a number of numerical solutions to demonstrate various relevant configurations.

1.1 Basic concepts of constrained mechanics

In this section, we recall some concepts of constrained mechanics that are vastly employed throughout the Thesis: *constraints, Chetaev's conditions, quasi-velocities, quasi-coordinates and transpositional relations*. To provide the reader with a *primer*

on these concepts, the content of the following subsections is self-contained, and can be consulted independently of the notation employed in the following chapters.

1.1.1 Chetaev's conditions

The content of this section is taken from [5].

In Analytical Mechanics (see, e.g., the work by Flannery [21]), Chetaev's conditions[1] are relations that indicate how to select generalized virtual fields and variations in compliance with the imposed constraints. They generalize the selection criteria for the virtual displacements or velocities of holonomic systems to the case of nonholonomic constraints. In other words, Chetaev's conditions identify the virtual variations that are physically admissible for the system at hand, and make it possible to extend the Principle of Virtual Power or the d'Alembert–Lagrange Principle to systems featuring nonholonomic constraints (see, e.g., the treatises by Pars [12], Neimark and Fufaev [13], and Gantmacher [14]). To briefly contextualize Chetaev's conditions, let us consider a (discrete) mechanical system characterized by $n \geq 1$, $n \in \mathbb{N}$, generalized coordinates, collected in the array $q = (q^1, \dots, q^n)$, and by n generalized velocities, represented by $\dot{q}$ (we recall that, at each time t, $\dot{q}(t)$ is a tangent vector at the point $q(t)$ of the system's configuration manifold). In addition, let us assume that the system is subjected to $m \leq n$, $m \in \mathbb{N}$, constraints of the type $\mathcal{C}^k = \hat{\mathcal{C}}^k \circ (q, \dot{q}, \tau) = 0$, which, for $k = 1, \dots, m$, may be nonholonomic or holonomic, but all expressed in differential form. Here, q and $\dot{q}$ are functions of time t, and τ is an auxiliary map such that $\tau(t) = t$ for each t. Note that, among these m constraints, the holonomic ones are either linear or, at the most, affine in the generalized velocities (indeed, if $\mathcal{C}^k$, for some $k \in \{1, \dots, m\}$, is holonomic, it is obtained by taking the total time derivative of a condition of the type $f^k = \hat{f}^k \circ (q, \tau) = 0$; hence, the corresponding $\hat{\mathcal{C}}^k$ is linear in $\dot{q}$ if $\partial_\tau \hat{f} = 0$, and affine in $\dot{q}$ otherwise). However, the nonholonomic constraints can be linear or nonlinear in the generalized velocities, depending on the problem at hand. Then, given the tangent vector field of the generalized virtual velocities, here denoted by $\boldsymbol{u}$, Chetaev's conditions are defined as the Gâteaux derivatives of the given constraints, evaluated at $(q, \dot{q}, \tau)$ and along $\boldsymbol{u}$,

[1] Sometimes they are also referred to as Lagrange–Chetaev conditions.

i.e.,

$$\mathcal{A}^k := \hat{\mathcal{A}}^k \circ (q, \dot{q}, \tau; \boldsymbol{u}) = \left(\frac{\partial \hat{\mathfrak{C}}^k}{\partial \dot{q}} \circ (q, \dot{q}, \tau) \right) [\boldsymbol{u}]$$
$$= \sum_{i=1}^{n} \left(\frac{\partial \hat{\mathfrak{C}}^k}{\partial \dot{q}^i} \circ (q, \dot{q}, \tau) \right) [u^i] = 0, \tag{1.1}$$

for $k = 1, \ldots, m$. Hence, Chetaev's conditions are by construction linear in the generalized virtual velocities, even when the corresponding constraints are nonlinear in $\dot{q}$ (e.g., when they are affine in $\dot{q}$). Clearly, when the constraints $\hat{\mathfrak{C}}^1, \ldots, \hat{\mathfrak{C}}^m$ are all linear in the generalized velocities (as is the case for the constraints considered in this work), Chetaev's conditions are obtained by replacing the generalized velocities with the virtual ones. Yet, it should be remarked that there also exist constraints for which Chetaev's conditions are not applicable (see, e.g., the work by Borisov and Tsiganov [22] and the references therein). However, this is not the case for the constraints studied in our work.

1.1.2 Quasi-velocities and transpositional relations

The content of this section is taken from the Supplementary Material of [2].

Let $\mathfrak{M}$ be a discrete mechanical system with $n \in \mathbb{N}$, $n \geq 1$, Lagrangian parameters collected in $q \equiv (q^1, \ldots, q^n)$, and let $\mathscr{C}$ and $T\mathscr{C}$ be the system's configuration manifold and tangent bundle, respectively. Moreover, let us suppose that the system presents $m \in \mathbb{N}$, $1 \leq m \leq n$, linearly independent nonholonomic constraints that are *affine* in the generalized velocities $\dot{q}^1, \ldots, \dot{q}^n$, i.e., [23, Appendix I]

$$\mathcal{V}^\alpha \equiv \hat{\mathcal{V}}^\alpha \circ (q, \dot{q}, \tau) := \sum_{k=1}^{n} [\hat{a}^\alpha{}_k \circ (q, \tau)] \dot{q}^k + \hat{b}^\alpha \circ (q, \tau)$$
$$\equiv \sum_{k=1}^{n} a^\alpha{}_k \dot{q}^k + b^\alpha = 0, \qquad \alpha = 1, \ldots, m, \tag{1.2}$$

where $\tau : \mathscr{I} \to \mathscr{I}$ is the *time-identity* map [24], such that $\tau(t) = t$ for all t in the timeline $\mathscr{I}$, and the matrix $[a^\alpha{}_k]_{k=1,\ldots,n}^{\alpha=1,\ldots,m}$ has rank m almost everywhere in the time window in which the system is observed. Starting from some considerations done in [1, Remark 1], we consider only constraints *affine* in the generalized velocities

because such constraints are of the same type as the one representing the growth law in Equation (5.4).

A set of *quasi-velocities* for $\mathfrak{M}$ is *any* collection of functions $\omega \equiv (\omega^1, ..., \omega^n)$, such that each ω^b, for $b = 1, \ldots, n$, is defined as $\omega^b := \hat{\omega}^b \circ (q, \dot{q}, \tau)$, and the Jacobian matrix $J^b{}_k := \partial_{\dot{q}^k} \hat{\omega}^b \circ (q, \dot{q}, \tau)$ is non-singular almost everywhere [13, 16]. Although being arbitrary, quasi-velocities ought to improve, or simplify, the kinematics of the problem at hand and the physics related to it. For this reason, a rather consolidated praxis consists in identifying the first m quasi-velocities with the constraints themselves (possibly rescaled appropriately, so that they take on the correct physical dimensions), and the remaining $n - m$ quasi-velocities with arbitrary functions $\hat{\Phi}^\beta \circ (q, \dot{q}, \tau)$, such that the transformation is non-singular. This choice renders the quasi-velocities *"consistent"* [25] with the constraints. Hence, we set

$$\omega^\alpha \equiv \hat{\omega}^\alpha \circ (q, \dot{q}, \tau) := \hat{\mathcal{V}}^\alpha \circ (q, \dot{q}, \tau) = 0, \qquad \alpha = 1, \ldots, m, \tag{1.3a}$$

$$\omega^\beta \equiv \hat{\omega}^\beta \circ (q, \dot{q}, \tau) := \hat{\Phi}^\beta \circ (q, \dot{q}, \tau), \qquad \beta = m + 1, \ldots, n. \tag{1.3b}$$

A typical example of a discrete mechanical system for which quasi-velocities are useful is provided by the motion of *Chaplygin's nonholonomic skate* on a fixed inclined plane [13, 26, 27, 15, 16, 1]: the velocity of the skate's center of mass, $\boldsymbol{v}$, is constrained to be parallel, at all times, to the axis $\boldsymbol{n}$ of the skate itself. Then, if the *true* velocities of such a system are employed, the constraint reads $\boldsymbol{v} \times \boldsymbol{n} = \boldsymbol{0}$, where $\times$ denotes the cross product and, in a fixed reference frame, $\boldsymbol{v}$ has components equal to the time derivatives of the two coordinate functions of the skate's center of mass. Although this description is correct, a more direct characterization of the kinematics of the skate is achieved if one defines the functions $\omega_1 := n_2 v_1 - n_1 v_2 = 0$ and $\omega_2 := n_1 v_1 + n_2 v_2$ (Cartesian coordinates are used here for simplicity). These are *quasi-velocities* because they are a (linear) transformation of v_1 and v_2, but none of them is a total time derivative of a function of time *and* of the system's Lagrangian parameters.

Besides purely kinematic issues, quasi-velocities are powerful tools to highlight differential geometry aspects of nonholonomic systems, i.e., those related to the possible non-trivial curvature or torsion of the affine connections induced by the constraints [25]. In particular, these geometrical features are associated with the *transpositional relations* [13, 28, 29], which express the generally nonzero difference

between the derivative of a variation of a given Lagrangian parameter and the variation of its associated generalized velocity.

Along with the quasi-velocities, it is also possible to introduce a collection of functions termed *quasi-coordinates*. In the case of m *affine* nonholonomic constraints, and when the first m quasi-velocities are taken coincident with these constraints, Neimark&Fufaev [13, Page 126, Equation (5.18)] define the quasi-coordinates through linear differential forms of the type $\mathrm{d}\theta^\alpha = a^\alpha{}_k \mathrm{d}q^k + b^\alpha \mathrm{d}\tau$, with $\alpha = 1, \dots, m$, and $k = 1, \dots, n$. However, one can also write $\dot\theta^\alpha := a^\alpha{}_k \dot q^k + b^\alpha = \omega^\alpha$, for $\alpha = 1, \dots, m$, and $\dot\theta^\beta = \omega^\beta$, for $\beta = m+1, \dots, n$. Consequently, granted that all the quasi-velocities are continuous functions of time in a given interval $[t_{\mathrm{in}}, t_{\mathrm{fin}}]$, where t_{fin} could also be infinite, the Fundamental Theorem of Calculus permits to express the quasi-coordinates, for $t \in [t_{\mathrm{in}}, t_{\mathrm{fin}}]$, as

$$\theta^\alpha(t) = \theta^\alpha(t_{\mathrm{in}}) + \int_{t_{\mathrm{in}}}^{t} \hat\omega^\alpha(q(s), \dot q(s), s)\mathrm{d}s \equiv \theta^\alpha(t_{\mathrm{in}}), \quad \alpha = 1, \dots, m, \tag{1.4a}$$

$$\theta^\beta(t) = \theta^\beta(t_{\mathrm{in}}) + \int_{t_{\mathrm{in}}}^{t} \hat\omega^\beta(q(s), \dot q(s), s)\mathrm{d}s, \qquad \beta = m+1, \dots, n. \tag{1.4b}$$

Therefore, the quasi-coordinates $\theta^1(t), \dots, \theta^m(t)$ are constant in time because $\omega^1, \dots, \omega^m$ are all zero (since they are equal to the constraints), while $\theta^{m+1}(t), \dots, \theta^n(t)$ vary according to the corresponding quasi-velocities.

Note that the possibility of finding the functions θ^α, with $\alpha = 1, \dots, m$, does not mean that these can be represented as $\hat\theta^\alpha \circ (q, \tau)$. Indeed, if this were the case, then the quasi-velocities $\omega^\alpha = \hat{\mathcal{V}}^\alpha \circ (q, \dot q, \tau)$ would be integrable in the sense of differential forms; but that would lead to the absurd conclusion that the associated constraints are holonomic.

It is possible to determine a very important relation between the incremental function associated with the generic quasi-velocity ω^b and the time derivative of the incremental function related to the corresponding quasi-coordinate, hereafter denoted by η^b_θ. To this end, we introduce the homotopies associated to q and $\dot q$ as

$$q(t) \mapsto \tilde q(t, \varepsilon) = q(t) + \boldsymbol{\eta}_q(t)\varepsilon + o(\varepsilon), \qquad \varepsilon \to 0, \tag{1.5a}$$

$$\dot q(t) \mapsto \tilde{\boldsymbol{v}}(t, \varepsilon) = \dot q(t) + \boldsymbol{\eta}_{\dot q}(t)\varepsilon + o(\varepsilon), \qquad \varepsilon \to 0. \tag{1.5b}$$

These homotopies differ from the "classical" ones, introduced in Equation (5.14a), and employed in the standard formulation of Hamilton's Principle [11], in that the incremental functions $\boldsymbol{\eta}_q$ and $\boldsymbol{\eta}_{\dot{q}}$ are not assumed to fulfill automatically the equality $\dot{\boldsymbol{\eta}}_q = \boldsymbol{\eta}_{\dot{q}}$.

We introduce now the *increments of the quasi-coordinates* $\eta_\theta \equiv (\eta_\theta^1, \ldots, \eta_\theta^n)$. For each $b = 1, \ldots, n$, η_θ^b is expressed as $\eta_\theta^b \equiv \hat{\eta}_\theta^b \circ (q, \dot{q}, \tau)$, and, for a given t, $\eta_\theta^b(t) \equiv \hat{\eta}_\theta^b(q(t), \dot{q}(t), t)$ is defined by

$$\eta_\theta^b(t) \equiv \hat{\eta}_\theta^b(q(t), \dot{q}(t), t) := \sum_{k=1}^{n} \frac{\partial \hat{\omega}^b}{\partial \dot{q}^k}(q(t), \dot{q}(t), t)\eta_q^k(t), \quad b = 1, \ldots, n, \tag{1.6}$$

with $(q(t), \dot{q}(t), t) \in T\mathscr{C} \times \mathscr{I}$. Hence, it is identifiable with the result of the application of the linear map

$$\hat{\mathfrak{h}}_\theta^b(q(t), \dot{q}(t), t)[\,\cdot\,] := \sum_{k=1}^{n} \frac{\partial \hat{\omega}^b}{\partial \dot{q}^k}(q(t), \dot{q}(t), t)\boldsymbol{e}^k[\,\cdot\,] : T_{q(t)}\mathscr{C} \to \mathbb{R} \tag{1.7}$$

to the vector $\boldsymbol{\eta}_q(t) \in T_{q(t)}\mathscr{C}$, i.e.,

$$\begin{aligned} \hat{\mathfrak{h}}_\theta^b(q(t), \dot{q}(t), t)[\boldsymbol{\eta}_q(t)] &= \sum_{k=1}^{n} \frac{\partial \hat{\omega}^b}{\partial \dot{q}^k}(q(t), \dot{q}(t), t)\boldsymbol{e}^k[\boldsymbol{\eta}_q(t)] \\ &= \sum_{k=1}^{n} \frac{\partial \hat{\omega}^b}{\partial \dot{q}^k}(q(t), \dot{q}(t), t)\eta_q^k(t), \end{aligned} \tag{1.8}$$

where $\boldsymbol{e}^k \in T^*_{q(t)}\mathscr{C}$ is the kth element of the basis of linear maps of the cotangent space $T^*_{q(t)}\mathscr{C}$ of $\mathscr{C}$ at $q(t) \in \mathscr{C}$. By definition, it holds true that $\boldsymbol{e}^k[\boldsymbol{u}] = u^k$, for all $\boldsymbol{u} \in T_{q(t)}\mathscr{C}$.

By means of $\tilde{q}$ and $\tilde{\boldsymbol{v}}$ in Equations (1.5a) and (1.5b), we write the induced homotopy of the generic quasi-velocity ω^b as $\tilde{\omega}^b(t, \varepsilon) = \hat{\omega}^b(\tilde{q}(t, \varepsilon), \tilde{\boldsymbol{v}}(t, \varepsilon), t)$, with $b = 1, \ldots, n$. Then, by computing the increment $\eta_\omega^b(t) := \partial_\varepsilon \tilde{\omega}^b(t, 0)$ and the time derivative $\dot{\eta}_\theta^b(t)$, we obtain

$$\eta_\omega^b = \sum_{k=1}^{n} \left[\frac{\partial \hat{\omega}^b}{\partial q^k} \circ (q, \dot{q}, \tau)\right]\eta_q^k + \sum_{k=1}^{n} \left[\frac{\partial \hat{\omega}^b}{\partial \dot{q}^k} \circ (q, \dot{q}, \tau)\right]\eta_{\dot{q}}^k, \tag{1.9a}$$

$$\dot{\eta}_\theta^b = \sum_{k=1}^{n} \left[\frac{\mathrm{d}}{\mathrm{d}t}\left(\frac{\partial \hat{\omega}^b}{\partial \dot{q}^k} \circ (q, \dot{q}, \tau)\right)\right]\eta_q^k + \sum_{k=1}^{n} \left[\frac{\partial \hat{\omega}^b}{\partial \dot{q}^k} \circ (q, \dot{q}, \tau)\right]\dot{\eta}_q^k. \tag{1.9b}$$

Subtracting Equation (1.9b) from (1.9a) yields, for $b = 1, \ldots, n$,

$$\eta^b_\omega - \dot{\eta}^b_\theta = \sum_{k=1}^{n} [\mathcal{E}_k \hat{\omega}^b \circ (q, \dot{q}, \ddot{q}, \tau)] \eta^k_q + \sum_{k=1}^{n} \left[\frac{\partial \hat{\omega}^b}{\partial \dot{q}^k} \circ (q, \dot{q}, \tau) \right] (\eta^k_{\dot{q}} - \dot{\eta}^k_q), \quad (1.10)$$

where $\mathcal{E}_k \hat{\omega}^b \circ (q, \dot{q}, \ddot{q}, \tau)$ is the kth Euler–Lagrange operator applied to ω^b, i.e.,

$$\begin{aligned} &\mathcal{E}_k \hat{\omega}^b \circ (q, \dot{q}, \ddot{q}, \tau) \\ &:= \frac{\partial \hat{\omega}^b}{\partial q^k} \circ (q, \dot{q}, \tau) - \frac{\mathrm{d}}{\mathrm{d}t} \left(\frac{\partial \hat{\omega}^b}{\partial \dot{q}^k} \circ (q, \dot{q}, \tau) \right), \quad b, k = 1, \ldots, n. \end{aligned} \quad (1.11)$$

Equation (1.10) shows that, for systems featuring nonholonomic constraints (for which the characterizing condition $\mathcal{E}_k \hat{\omega}^b \neq 0$ applies, at least, for those values of b corresponding to such constraints, i.e., $b = \alpha = 1, \ldots, m$), the differences $\eta^b_\omega - \dot{\eta}^b_\theta$ and $\eta^k_{\dot{q}} - \dot{\eta}^k_q$ are not both *a priori* identically zero. In fact, there exists an infinite number of pairs $(\{\eta^b_\omega - \dot{\eta}^b_\theta\}^n_{b=1}, \{\eta^k_{\dot{q}} - \dot{\eta}^k_q\}^n_{k=1})$ satisfying (1.10). However, in the system of the quasi-velocities and quasi-coordinates, the nonholonomic constraints may be regarded to be *formally* "holonomic". Indeed, the quasi-coordinates associated with them are constant in time, and, thus, their only admissible incremental functions η^b_θ can be taken to be the null ones (this returns Chetaev's conditions), and, on the same footing, since the quasi-velocities expressing the constraints are identically null, η^b_ω can be taken null, too. In fact, according to [13, 28–30], Equation (1.10) can be fulfilled in two main ways: depending on the "school of thought" which is followed for defining the transpositional relations, one may require the vanishing either of $\eta^b_\omega - \dot{\eta}^b_\theta$, for $b = 1, \ldots, n$, or of $\eta^k_{\dot{q}} - \dot{\eta}^k_q$, for $k = 1, \ldots, n$. To compare the approach proposed in the present work with the *"Modified Vakonomic Method"* developed by Llibre et al. [16], we assume $\eta^b_\omega - \dot{\eta}^b_\theta = 0$, for all $b = 1, \ldots, n$. With this choice, Equation (1.10) leads to [16, 1]

$$\eta^h_{\dot{q}} - \dot{\eta}^h_q = \sum_{k=1}^{n} W^h{}_k \eta^k_q, \qquad W^h{}_k := -\sum_{b=1}^{n} [\mathrm{J}^{-1}]^h{}_b [\mathcal{E}_k \hat{\omega}^b \circ (q, \dot{q}, \ddot{q}, \tau)], \quad (1.12)$$

where $[\mathrm{J}^{-1}]$ is the inverse of the Jacobian $[J^b{}_k]^{b=1,\ldots,n}_{k=1,\ldots,n} = [\partial_{\dot{q}^k} \hat{\omega}^b \circ (q, \dot{q}, \tau)]^{b=1,\ldots,n}_{k=1,\ldots,n}$.

Since the first m quasi-velocities are taken equal to the functions expressing the m nonholonomic constraints, it holds that $\mathcal{E}_k \hat{\omega}^\alpha \neq 0$, for $\alpha = 1, \ldots, m$, thereby implying that the matrix of coefficients $W^h{}_k$ is different from the null matrix. Hence,

the incremental functions $\boldsymbol{\eta}_{\dot{q}}$ and $\dot{\boldsymbol{\eta}}_{q}$ are different from each other, and reciprocally related by the conditions in (1.12), which are referred to as *transpositional relations* [13, 30, 16].

Note that Equation (1.12) gives an operative way for computing the coefficients ${W^h}_k$, and, thus, the transpositional relations, by solving the $n \times n$ system of equations

$$\mathcal{E}_k \hat{\omega}^b \circ (q, \dot{q}, \ddot{q}, \tau) + \sum_{h=1}^{n} {J^b}_h {W^h}_k = 0, \qquad b, k = 1, \ldots, n. \tag{1.13}$$

For further insight on transpositional relations, see e.g. [16, 1].

Part I

Analytical Mechanics

Chapter 2

Nonholonomic constraints: a review of the Modified Vakonomic Method

The content of this chapter is taken from [1].

2.1 An overview on nonholonomic mechanics

The motivation for studying mechanical systems subjected to nonholonomic constraints is determined not only by their mathematical beauty, but also by their relevance in physics [31, 7], e.g. for modeling relativistic fluids; in biomechanics, for describing, e.g., tissue growth and remodeling [23, 32, 33], and animal or cellular motion [34]; and in engineering, especially in robotics [35–38]. The ever-green interest for these systems is the search for a *paradigmatic framework* formalizing nonholonomic mechanics, whose applicability should be as universal as possible. This applies, in particular, to problems exhibiting nonholonomic constraints that are either nonlinear in the generalized velocities of a given system [12, 14, 23, 32] or involving the accelerations [39, 21].

A peculiar feature of nonholonomic systems is their intrinsic tendency to involve several aspects of mathematics, such as analysis, differential geometry and numerics, with the aim of providing physically consistent formulations of their evolution. This has led to descriptions of nonholonomic systems different from those of standard analytical mechanics, which are based on the Lagrange–d'Alembert principle,

typically "augmented" by the technique of Lagrange multipliers, i.e., the so-called "traditional nonholonomic method" (TNHM) [11, 39, 21, 40]. For example, in the early 80's, Kozlov proposed a method for modeling nonholonomic mechanics, known as "vakonomic method" (VM) [41–44], and standing for mechanics of the *"variational axiomatic kind"* [17], which applies Hamilton's principle of stationary action [11] also to systems subjected to nonholonomic constraints. One of the main features of this method is the capability of describing nonholonomic systems through a fully variational procedure, based on the definition of an appropriate *constrained* Lagrangian function [41–44]. We remark that also other types of variational approaches have been introduced to study systems subjected to nonholonomic constraints (see, e.g., [45–49, 25]).

The vakonomic method [41–44], used *as is*, can lead, in same cases, to motions that differ from the ones obtained with the TNHM, which is known to supply solutions observable experimentally for the majority of mechanical problems [26, 50–52, 27, 17]. In particular, as recently shown by Lemos [17], one of such cases is the problem of the "rolling coin", which describes a rigid coin rolling without slipping on an inclined plane [17, 40], for which the VM is said to lead to unphysical results. Similar problems have also been investigated in [27, 16]. On the other hand, there are problems, e.g. in geometric control theory [15, 53, 34] and in field theory [31, 7], in which it is claimed that the TNHM does not provide physically consistent dynamics, while the VM provides *"interesting results"* [7].

Many authors have compared the VM and the TNHM on the basis of the *variations* introduced to define the associated variational principle [51, 26, 54–56, 52, 50, 57, 7, 31, 53], and in terms of the *geometrical meaning* of such variations [15, 55, 56, 58, 57, 49, 53]. Often, one of the purposes of these investigations is to provide conditions that allow to conclude that a solution to a mechanical problem obtained within the TNHM is also a solution of the VM, whereas the converse is, in general, not true (see [26] for a critique on Kozlov's approach). In fact, Lemos' work [17] places itself in this research line, thereby highlighting the discrepancies between the VM and the TNHM for a certain class of problems. Still, in our opinion, Kozlov's idea is worth of being investigated because of its conceptual potential, and, to the best of our understanding, it could be "saved" by performing suitable *modifications* to it (Llibre et al. [16] speak of *"modified vakonomic method"*). Indeed, if our interpretation is correct, it is with this attitude in mind that the works of Ramírez et al. [59] and Llibre et al. [16] have been conceived. From an operative point

of view, the modifications to the VM should be able to provide conditions on the variations of the Lagrangian parameters of a given system, and on the associated generalized velocities, in such a way that, under certain working hypotheses, the TNHM solutions can be recovered (see Section 2.3.3). To this end, the variations should satisfy Lagrange-Chetaev's conditions in addition to other conditions specified by the method employed.

To our knowledge, in fact, a possible reconciliation between the vakonomic method and the traditional methodologies is given in a paper by Llibre et al. [16], whose germinal idea was already present in [59], and in which the authors elaborate a modification to the original vakonomic method based on the Hamilton-Suslov variational principle [60, 61, 16] that accounts for the presence of non-vanishing *transpositional relations* [62, 13, 59, 25, 16]. Such relations express that, in the presence of a nonholonomic constraint, the variation of a generalized velocity involved in the constraint is generally not equal to the time derivative of the variation of the associated Lagrangian parameter. With this premise, Llibre et al. [16] prove that the equations of motion obtained with their so-called modified vakonomic method (MVM) [16] are equivalent to the ones obtained with the traditional nonholonomic method, up to a *"zero Lebesgue-measure set"* [16]. For their purposes, Llibre et al. [16] propose two *paths*: one is based on the introduction of auxiliary functions that augment the Lagrangian function of the considered problem in a suitable way (see Theorem 2 of [16] and Section 2.3 below), while the other one imposes *a priori* conditions that compel the equivalence of their approach with the TNHM (see Theorem 3 of [16] and our Corollary 2.1).

Within the context explained above, the scope of this chapter is to present a reformulation of the MVM that, on the one hand, retrieves the equivalence with the TNHM, and, on the other hand, merges the two *paths* of [16] in a physics-driven way. More in detail, we propose a way to indicate, on physical grounds (e.g. compliance with evident conservation laws), which *path* should be followed.

It should be noticed that, in the following, our efforts are concentrated on the reconciliation of the VM with the TNHM for a class of mechanical problems known to be reliably described by the TNHM, i.e., for which the TNHM is known to produce solutions consistent with the experiments. In fact, our interest for such reconciliation does not require that the TNHM should always be used as a reference, but it resides in the possibility of describing the dynamics of a given mechanical system through

a variational approach that supplies the same solutions as the TNHM, and, thus, the experimentally observable motions. In this respect, our work can be seen as a "gym" for testing the MVM [59, 16], and for understanding whether fundamental results of Analytical Mechanics holding in the nonholonomic setting [13] can be extended to study the symmetries of mechanical systems (see Noether's theorem and its extension to nonholonomic problems [63]), and whether, and with which modifications, the MVM can be imported to field theories (e.g. inelastic processes in continuum systems [23, 32]). Hence, in this work we are not interested in comparing the VM and the TNHM, neither on theoretical nor on experimental bases. Rather, we would just like to present our reformulation of the MVM of Llibre et al. [16], which enjoys the efficacy and elegance of the Lagrangian formalism, while providing solutions that are in harmony with the TNHM.

Outline of the content of Chapter 2. As for the structure of this chapter, Section 2.2 is dedicated to give the reader an *overview* on the mathematical foundations of the MVM [16]. In particular, in Section 2.2.1 we establish the geometrical setting used for describing the kinematics of a nonholonomically constrained system and the need for introducing non-vanishing *"transpositional relations"* [62, 13, 25, 16]; in Section 2.3, we have explicit recourse to the Hamilton–Suslov variational principle [60, 61, 16] that leads us to the dynamic equations for the system under investigation, which are then closed under the assumption of suitable *solvability conditions* discussed in Section 2.3.1; in Section 2.3.2, we further elaborate on some computational aspects regarding the MVM, which help us draw the differences and similarities between the MVM and the TNHM, as expanded in Sections 2.3.3 and 2.3.4. Some geometric remarks related to the analyzed constraints are summarized in Appendix A.

2.2 Modified Vakonomic Method: kinematic aspects

In this section, we summarize the fundamental aspects of the modified vakonomic method developed by Llibre et al. [16] that are relevant for our work. Hereafter, for the sake of brevity, we shall refer to the "modified vakonomic method" [16] as MVM, in order to distinguish it from the original "vakonomic method", referred to as VM, introduced by Kozlov [41–44].

2.2.1 Constraints, variations and Chetaev's conditions

Let $\mathfrak{M}$ be a mechanical system whose evolution is characterized by $n \geq 1$, $n \in \mathbb{N}$, Lagrangian parameters, i.e., n functions of time, collected in the array $q := (q^1, \ldots, q^n) : [t_{\text{in}}, t_{\text{fin}}] \subseteq \mathscr{I} \to \mathscr{C}$, where $[t_{\text{in}}, t_{\text{fin}}]$ is a closed interval of the *time line* $\mathscr{I}$ [24], and $\mathscr{C}$ is referred to as the *configuration space* of $\mathfrak{M}$ [11]. The latter is regarded here as an n-dimensional manifold representing the set of all possible configurations for $\mathfrak{M}$ and, as required in [16], it is assumed to be smooth in the sequel. In this sense, $q : [t_{\text{in}}, t_{\text{fin}}] \to \mathscr{C}$ is a one-parameter family of configurations of $\mathscr{C}$, thereby parameterizing a curve on this manifold, such that, for each $t \in [t_{\text{in}}, t_{\text{fin}}]$, ϑ is the unique element of $\mathscr{C}$ satisfying $\vartheta = q(t) \in \mathscr{C}$.

For each configuration $\vartheta \in \mathscr{C}$, $T_\vartheta\mathscr{C}$ denotes the tangent space of $\mathscr{C}$ at ϑ, and $T\mathscr{C} = \cup_{\vartheta\in\mathscr{C}}\big(\{\vartheta\}\times T_\vartheta\mathscr{C}\big)$ is the tangent bundle of $\mathscr{C}$, so that, for each pair $(\vartheta, \boldsymbol{\nu}) \in T\mathscr{C}$, $\boldsymbol{\nu} \in T_\vartheta\mathscr{C}$ is a realization of the generalized velocity vector attached at ϑ. Moreover, under the hypothesis that q is differentiable, we denote by $(q, \dot{q}) :]t_{\text{in}}, t_{\text{fin}}[\to T\mathscr{C}$ the map such that, for each time $t \in]t_{\text{in}}, t_{\text{fin}}[$, $\dot{q}(t) \in T_{q(t)}\mathscr{C}$ is the tangent vector to the curve parameterized by q at $q(t)$, and is equal to the vector of generalized velocities attached at $q(t) \in \mathscr{C}$, i.e., there exists $\boldsymbol{\nu} \in T_{q(t)}\mathscr{C}$ such that $\dot{q}(t) = \boldsymbol{\nu}$.

We assume that the system $\mathfrak{M}$ is subjected to $m \in \mathbb{N}$, with $m \leq n$, linearly independent *nonholonomic constraints*, represented by the functions $\hat{\mathcal{V}}^\alpha : T\mathscr{C}\times\mathscr{I} \to \mathbb{R}$, for $\alpha = 1, \ldots, m$. The presence of such constraints restricts the admissible generalized velocities to the following sub-manifold of the tangent bundle $T\mathscr{C}$ (see e.g. [51, 64])

$$T\mathscr{C}_{\text{c}} := \big\{(\vartheta, \boldsymbol{\nu}) \in T\mathscr{C} \,:\, \hat{\mathcal{V}}^\alpha(\vartheta, \boldsymbol{\nu}, t) = 0, \quad \alpha = 1, \ldots, m, \quad \forall\, t \in [t_{\text{in}}, t_{\text{fin}}]\big\}. \tag{2.1}$$

Moreover, as done in [59, 16], in this chapter and in Chapter 3, we focus on nonholonomic constraints *linear* in the generalized velocities. To this end, for each $\alpha = 1, \ldots, m$, and for all $\vartheta \in \mathscr{C}$ and $t \in \mathscr{I}$, we introduce a linear map $\mathcal{G}^\alpha(\vartheta, t)[\,\cdot\,] : T_\vartheta\mathscr{C} \to \mathbb{R}$, i.e., an element of the cotangent space $T^*_\vartheta\mathscr{C}$, represented by

$$\mathcal{G}^\alpha(\vartheta, t)[\,\cdot\,] := \sum_{k=1}^{n} \hat{a}^\alpha{}_k(\vartheta, t)\boldsymbol{e}^k(\vartheta)[\,\cdot\,], \tag{2.2}$$

with $\boldsymbol{e}^k(\vartheta)[\,\cdot\,]$ denoting the kth basis co-vector of $T^*_\vartheta\mathscr{C}$, and defined such that

$$\mathcal{G}^\alpha(\vartheta,t)[\boldsymbol{\nu}] \coloneqq \sum_{k=1}^{n} \hat{a}^\alpha{}_k(\vartheta,t)\nu^k \equiv \hat{\mathcal{V}}^\alpha(\vartheta,\boldsymbol{\nu},t), \tag{2.3}$$

where the identity $\boldsymbol{e}^k(\vartheta)[\boldsymbol{\nu}] \equiv \nu^k$ is exploited for each $k = 1,\dots,n$, and, for varying $\alpha = 1,\dots,m$ and $k = 1,\dots,n$, $\hat{a}^\alpha{}_k : \mathscr{C}\times\mathscr{I}\to\mathbb{R}$ determines a collection of given scalar-valued functions.

When $\hat{\mathcal{V}}^\alpha$ is evaluated for $\vartheta = q(t)$ and $\boldsymbol{\nu} = \dot{q}(t)$, we use the notation

$$\hat{\mathcal{V}}^\alpha(q(t),\dot{q}(t),t) = [\hat{\mathcal{V}}^\alpha \circ (q,\dot{q},\tau)](t) =: \mathcal{V}^\alpha(t), \tag{2.4}$$

where we have employed the composition of maps to define the scalar-valued function $\mathcal{V}^\alpha : \mathscr{I}\to\mathbb{R}$, with $\tau : \mathscr{T}\to\mathscr{T}$ being the *time-identity* function [24] defined as $\tau(t) \coloneqq t$. Finally, for all the pairs $(q,\dot{q})$ that are admissible in the sense specified by Equation (2.1), i.e., $(q,\dot{q}) :]t_{\text{in}}, t_{\text{fin}}[\to T\mathscr{C}_{\text{c}}$,

$$\hat{\mathcal{V}}^\alpha \circ (q,\dot{q},\tau) = [\hat{a}^\alpha{}_k \circ (q,\tau)]\dot{q}^k = 0, \qquad \alpha = 1,\dots,m. \tag{2.5}$$

In Equation (2.5), we have used Einstein's notation to imply a summation over the repeated index k, and, in the following, we will make large use of such notation, unless otherwise specified. Note that the *linear independence* of the constraints is fulfilled by requiring the functions $[\hat{a}^\alpha{}_k]^{\alpha=1,\dots,m}_{k=1,\dots,n}$ to defined a (rectangular) matrix of rank m.

Now that the kinematics of the system $\mathfrak{M}$ is described, we can introduce the variations of q and $\dot{q}$ as

$$\tilde{q} : [t_{\text{in}}, t_{\text{fin}}]\times\,]-\varepsilon_0,+\varepsilon_0[\to \mathscr{C}, \tag{2.6a}$$
$$\tilde{\boldsymbol{\nu}} : [t_{\text{in}}, t_{\text{fin}}]\times\,]-\varepsilon_0,+\varepsilon_0[\to T_{\tilde{q}}\mathscr{C}, \tag{2.6b}$$

with $\varepsilon_0 > 0$ being a smallness parameter, and we require them to be such that

$$\tilde{q}(t,\varepsilon) \in \mathscr{C}, \qquad \tilde{q}(t,0) = q(t), \qquad \forall\, t\in[t_{\text{in}},t_{\text{fin}}], \tag{2.7a}$$
$$\tilde{\boldsymbol{\nu}}(t,\varepsilon) \in T_{\tilde{q}(t,\varepsilon)}\mathscr{C}, \qquad \tilde{\boldsymbol{\nu}}(t,0) = \dot{q}(t), \qquad \forall\, t\in[t_{\text{in}},t_{\text{fin}}], \tag{2.7b}$$

where, in Equation (2.7b), $\dot{q}$ is prolonged by continuity to t_{in} and t_{fin}.

By varying $t \in [t_{\text{in}}, t_{\text{fin}}]$ and $\varepsilon \in]-\varepsilon_0, +\varepsilon_0[$, one can determine the two-parameter family of tangent spaces $T_{\tilde{q}}\mathscr{C}$, such that $T_{\tilde{q}(t,\varepsilon)}\mathscr{C}$ is the element of this family obtained for fixed $(t, \varepsilon) \in [t_{\text{in}}, t_{\text{fin}}]\times\,]-\varepsilon_0, +\varepsilon_0[$, and $T_q\mathscr{C} \equiv T_{\tilde{q}(\,\cdot\,,0)}\mathscr{C}$ is the one-parameter family of tangent spaces identified by $\varepsilon = 0$ and t varying in $[t_{\text{in}}, t_{\text{fin}}]$.

To avoid technicalities, we assume that both $\tilde{q}$ and $\tilde{\boldsymbol{v}}$ are C^2 maps over their domain, i.e., $[t_{\text{in}}, t_{\text{fin}}] \times\,]-\varepsilon_0, +\varepsilon_0[$, and we set

$$\boldsymbol{\eta}_q(t) \coloneqq \frac{\partial \tilde{q}}{\partial \varepsilon}(t, 0), \qquad \forall t \in [t_{\text{in}}, t_{\text{fin}}], \tag{2.8a}$$

$$\boldsymbol{\eta}_{\dot{q}}(t) \coloneqq \frac{\partial \tilde{\boldsymbol{v}}}{\partial \varepsilon}(t, 0), \qquad \forall t \in [t_{\text{in}}, t_{\text{fin}}], \tag{2.8b}$$

where $\boldsymbol{\eta}_q : [t_{\text{in}}, t_{\text{fin}}] \to T_q\mathscr{C}$ and $\boldsymbol{\eta}_{\dot{q}} : [t_{\text{in}}, t_{\text{fin}}] \to T_q\mathscr{C}$ are the *first-order variations* of q and $\dot{q}$, respectively, and $\boldsymbol{\eta}_q$ is such that $\boldsymbol{\eta}_q(t_{\text{in}}) = \boldsymbol{\eta}_q(t_{\text{fin}}) = \mathbf{0}$ [24, 11, 16]. Before proceeding, to simplify the notation, in analogy with the maps $\tilde{q}$ and $\tilde{\boldsymbol{v}}$, we introduce the auxiliary map $\tilde{\tau} : [t_{\text{in}}, t_{\text{fin}}] \times\,]-\varepsilon_0, +\varepsilon_0[\to [t_{\text{in}}, t_{\text{fin}}]$ defined as $\tilde{\tau}(t, \varepsilon) = t$ so that $\partial_\varepsilon \tilde{\tau}(t, \varepsilon) = 0$ applies everywhere in its domain.

We evaluate now the constraints for the varied configuration and varied velocity, defined in Equations (2.6a) and (2.6b), and we set [16]

$$\tilde{\mathcal{V}}^\alpha \coloneqq \hat{\mathcal{V}}^\alpha \circ (\tilde{q}, \tilde{\boldsymbol{v}}, \tilde{\tau}\,) = [\hat{a}^\alpha{}_k \circ (\tilde{q}, \tilde{\tau}\,)]\tilde{v}^k. \tag{2.9}$$

Clearly, evaluating $\tilde{\mathcal{V}}^\alpha$ at $\varepsilon = 0$ for each $\alpha = 1, \ldots, m$ yields the original set of constraints, i.e.,

$$\tilde{\mathcal{V}}^\alpha(\,\cdot\,, 0) = \hat{\mathcal{V}}^\alpha \circ (q, \dot{q}, \tau) = [\hat{a}^\alpha{}_k \circ (q, \tau)]\dot{q}^k = 0. \tag{2.10}$$

However, following [16], we also require that each $\tilde{\mathcal{V}}^\alpha$, for $\alpha = 1, \ldots, m$, satisfies the corresponding constraint at the first order in ε, i.e., up to orders $o(\varepsilon)$ in the limit $\varepsilon \to 0$. This requirement, in turn, is expressed by enforcing the set of conditions:

$$\frac{\partial \tilde{\mathcal{V}}^\alpha}{\partial \varepsilon}(\,\cdot\,, 0) = \left[\frac{\partial \hat{a}^\alpha{}_i}{\partial q^k} \circ (q, \tau)\right]\eta_q^k\,\dot{q}^i + [\hat{a}^\alpha{}_k \circ (q, \tau)]\eta_{\dot{q}}^k = 0, \quad \alpha = 1, \ldots, m. \tag{2.11}$$

Furthermore, by adhering to the framework developed in [59, 16], we *hypothesize* that, in the jargon of [16], all the constraints considered in this work are *ideal*, in the sense that they satisfy the so-called *Lagrange–Chetaev conditions* [16, 7, 52], which

are expressed in the form

$$\sum_{k=1}^{n}\Big[\frac{\partial\hat{\mathcal{V}}^{\alpha}}{\partial\dot{q}^{k}}\circ(q,\dot{q},\tau)\Big]\eta_{q}^{k}=\sum_{k=1}^{n}[\hat{a}^{\alpha}{}_{k}\circ(q,\tau)]\eta_{q}^{k}=0,\qquad\alpha=1,\dots,m.\tag{2.12}$$

Note that, since, for each $\alpha=1,\dots,m$, $\hat{\mathcal{V}}^{\alpha}$ is linear in the velocities, Equation (2.12) returns the constraints in the form $\hat{\mathcal{V}}^{\alpha}\circ(q,\boldsymbol{\eta}_{q},\tau)=0$, i.e., with $\boldsymbol{\eta}_{q}$ replacing $\dot{q}$, thereby prescribing the conditions that must be fulfilled by the first-order variations $\eta_{q}^{1},\dots,\eta_{q}^{n}$ (see [12, 14]). Thus, by computing the derivative of Equation (2.12) with respect to time, we obtain

$$\begin{aligned}&\frac{\mathrm{d}}{\mathrm{d}t}\Big\{\sum_{k=1}^{n}\Big[\frac{\partial\hat{\mathcal{V}}^{\alpha}}{\partial\dot{q}^{k}}\circ(q,\dot{q},\tau)\Big]\eta_{q}^{k}\Big\}=\frac{\mathrm{d}}{\mathrm{d}t}\Big\{\sum_{k=1}^{n}[\hat{a}^{\alpha}{}_{k}\circ(q,\tau)]\eta_{q}^{k}\Big\}\\&=\Big[\frac{\partial\hat{a}^{\alpha}{}_{k}}{\partial q^{i}}\circ(q,\tau)\Big]\eta_{q}^{k}\dot{q}^{i}+\Big[\frac{\partial\hat{a}^{\alpha}{}_{k}}{\partial\tau}\circ(q,\tau)\Big]\eta_{q}^{k}+[\hat{a}^{\alpha}{}_{k}\circ(q,\tau)]\dot{\eta}_{q}^{k}=0.\end{aligned}\tag{2.13}$$

Moreover, by computing the difference between Equations (2.11) and (2.13), and by changing the indexes appropriately, we obtain, for each $\alpha=1,\dots,m$, the relation [16, 39, 21]

$$\begin{aligned}0=&\frac{\partial\tilde{\mathcal{V}}^{\alpha}}{\partial\varepsilon}(\,\cdot\,,0)-\frac{\mathrm{d}}{\mathrm{d}t}\Big\{\sum_{k=1}^{n}\Big[\frac{\partial\hat{\mathcal{V}}^{\alpha}}{\partial\dot{q}^{k}}\circ(q,\dot{q},\tau)\Big]\eta_{q}^{k}\Big\}\\=&\Big[\Big(\frac{\partial\hat{a}^{\alpha}{}_{i}}{\partial q^{k}}-\frac{\partial\hat{a}^{\alpha}{}_{k}}{\partial q^{i}}\Big)\circ(q,\tau)\Big]\eta_{q}^{k}\dot{q}^{i}+\Big[-\frac{\partial\hat{a}^{\alpha}{}_{k}}{\partial\tau}\circ(q,\tau)\Big]\eta_{q}^{k}\\&+[\hat{a}^{\alpha}{}_{h}\circ(q,\tau)](\eta_{\dot{q}}^{h}-\dot{\eta}_{q}^{h}).\end{aligned}\tag{2.14}$$

Equation (2.14) produces a set of m linear relations between the components of $\boldsymbol{\eta}_{\dot{q}}-\dot{\boldsymbol{\eta}}_{q}$ and the components of $\boldsymbol{\eta}_{q}$. Thus, by following the framework established in [59, 16], we *hypothesize* (see Section 2.2.2) the existence of a linear transformation between $\boldsymbol{\eta}_{\dot{q}}-\dot{\boldsymbol{\eta}}_{q}$ and $\boldsymbol{\eta}_{q}$ represented by a matrix $\mathsf{W}:=[W^{h}{}_{k}]_{k=1,\dots,n}^{h=1,\dots,n}$ such that

$$\eta_{\dot{q}}^{h}-\dot{\eta}_{q}^{h}=\sum_{k=1}^{n}W^{h}{}_{k}\eta_{q}^{k},\qquad\qquad h=1,\dots,n.\tag{2.15}$$

In the terminology of [62, 13, 25, 16, 59, 64], the relations reported in Equation (2.15) are referred to as *"transpositional relations"*, since they express, at the first order in ε, the fact that, for each $h=1,\dots,n$, the variation of the time derivative of

the Lagrangian parameter q^h, i.e., η_q^h, is not equal, in general, to the time derivative of the variation of q^h, i.e., $\dot{\eta}_q^h$. The statement just given here contains a deep geometric meaning, and can be formalized quite rigorously by employing the language of Differential Geometry developed, e.g., in [57]. In this respect, one should introduce the concept of *second tangent bundle* of $\mathscr{C}$, denoted by $T T\mathscr{C}$, and declare $\boldsymbol{\eta}_{\dot{q}}$ and $\dot{\boldsymbol{\eta}}_q$ as elements of $T T\mathscr{C}$, but belonging to different fibers of $T T\mathscr{C}$. A study of constrained mechanical systems conducted by having recourse to such concepts of Differential Geometry can be found in [57], which, in turn, employs the framework established in [65].

To the best of our understanding, the variations taken in the MVM proposed by Llibre et al. [16] live in the intersection between two sets of variations introduced in a work by Jóźwikowski&Respondek [52] (based on the paper by Gràcia et al. [53]), i.e., the set of *"nonholonomic admissible variations"* [52], defined according to *"Chetaev's principle"* [52], and the set of *"vakonomic admissible variations"* [52]. The latter variations are also in agreement with those presented in the vakonomic approach provided by Lemos [17]. The reason for requiring that the variations of the MVM belong to the intersection mentioned above is that we need the consistency with Lagrange–Chetaev's conditions in order to look for coherence between the TNHM (based on the fulfillment of such conditions) and the MVM. More details are reported in Appendix A.

2.2.2 Quasi-velocities and transpositional relations

Granted the approach specified above [59, 16], which, as remarked in [16], places itself in the school of thought of *"Suslov, Voronets, Levi-Civita, Amaldi,. . . "* [16], the presence of nonholonomic constraints renders the operations of "variation" and "time differentiation" non-commutative in general [39, 21]. More in detail, as discussed in [13, 30, 59, 16, 64], if a generalized velocity featuring in a given constraint is taken as *dependent*, i.e., as a function of the other *independent* velocities, then its corresponding transpositional relation does not vanish. On the contrary, *indipendent* velocities produce null transpositional relations [13, 30, 59, 16, 64].

To contextualize the introduction of the *square* matrix $\mathsf{W} = [W^h{}_k]_{k=1,\dots,n}^{h=1,\dots,n}$ in Equation (2.15), we briefly review the point of view of Jarzębowska [30], who summarized the discussion of Neimark and Fufaev [13] on the transpositional

relations and the analysis of motion in terms of *quasi-velocities* and *quasi-coordinates*. Hence, by slightly modifying Jarzębowska's notation [30], we denote here by $\omega^1, \ldots, \omega^n$ the n quasi-velocities of a given mechanical system (they must be as many as the "true" velocities). Each quasi-velocity ω^h, with $h = 1, \ldots, n$, is, in general, a function defined as $\omega^h := \hat{\omega}^h \circ (q, \dot{q}, \tau)$, which supplies a convenient reformulation of the system's kinematics. For systems featuring $m \leq n$ nonholonomic constraints ($m \geq 1$), it is useful to identify the first m quasi-velocities with the functions expressing the constraints themselves, i.e., $\omega^\alpha := \hat{\omega}^\alpha \circ (q, \dot{q}, \tau) \equiv \hat{\mathcal{V}}^\alpha \circ (q, \dot{q}, \tau) = 0$, with $\alpha = 1, \ldots, m$ [13, 30] (indeed, this way, the constraints are satisfied as $\omega^1 = 0, \ldots, \omega^m = 0$), while, as remarked in [13], the remaining $n - m$ quasi-velocities can be assigned *arbitrarily* through generic functions $\mathcal{F}^\beta$, i.e., $\omega^\beta := \hat{\omega}^\beta \circ (q, \dot{q}, \tau) \equiv \hat{\mathcal{F}}^\beta \circ (q, \dot{q}, \tau)$, with $\beta = m + 1, \ldots, n$, provided that they represent a change of variables in the "space" of the velocities. Thus, by denoting by ${J^h}_k := \partial_{\dot{q}^k} \hat{\omega}^h \circ (q, \dot{q}, \tau)$ the coefficients of the non-singular Jacobian matrix $\mathsf{J} = [{J^h}_k]_{k=1,\ldots,n}^{h=1,\ldots,n}$ associated with the quasi-velocities, and adapting Jarzębowska's procedure [30] to ours, we rewrite Equation (16) of [30] as

$$\eta^h_{\dot{q}} - \dot{\eta}^h_q = -[\mathsf{J}^{-1}]^h{}_i \left\{ \frac{\partial \hat{\omega}^i}{\partial q^k} \circ (q, \dot{q}, \tau) - \frac{\mathrm{d}}{\mathrm{d}t} \left[\frac{\partial \hat{\omega}^i}{\partial \dot{q}^k} \circ (q, \dot{q}, \tau) \right] \right\} \eta^k_q, \tag{2.16}$$

which is obtained by identifying our $\eta^h_{\dot{q}}$, $\dot{\eta}^h_q$, and η^k_q in Equation (2.15) with $\delta \dot{q}_\lambda$, $(\delta q_\lambda)^{\cdot}$, and δq_λ of [30], respectively, and assuming that the difference $\delta \omega_r - (\delta \pi_r)^{\cdot}$ is null for each $r = 1, \ldots, n$ (here $\delta \pi_r$ is the rth form defined by "$\delta \pi_r := [\partial_{\dot{q}_\sigma} \omega_r] \delta q_\sigma$" in [30]). We emphasize that the latter assumption is not made in [30], although Neimark and Fufaev [13] explain that it can be done always. At this stage, if in Equation (2.16) we set

$${W^h}_k := -[\mathsf{J}^{-1}]^h{}_i \left\{ \frac{\partial \hat{\omega}^i}{\partial q^k} \circ (q, \dot{q}, \tau) - \frac{\mathrm{d}}{\mathrm{d}t} \left[\frac{\partial \hat{\omega}^i}{\partial \dot{q}^k} \circ (q, \dot{q}, \tau) \right] \right\}, \tag{2.17}$$

we retrieve Equation (2.15). Note that the matrix W obtained this way is related to the one defined in [30] through $\mathsf{W}_{\mathrm{Jar}} = \mathsf{J}\,\mathsf{W}\,\mathsf{J}^{-1}$, where "Jar" stands for "Jarzębowska".

If m is the number of nonholonomic constraints *linear* in the velocities, i.e., if $\omega^\alpha = \hat{\omega}^\alpha \circ (q, \dot{q}, \tau) = [\hat{a}^\alpha{}_k \circ (q, \tau)] \dot{q}^k$, as is the case addressed in this work, the

terms between braces in Equation (2.17), evaluated for $i = \alpha = 1, \ldots, m$, become

$$\begin{aligned}&\frac{\partial \hat{\omega}^{\alpha}}{\partial q^{k}} \circ (q, \dot{q}, \tau) - \frac{\mathrm{d}}{\mathrm{d}t}\left[\frac{\partial \hat{\omega}^{\alpha}}{\partial \dot{q}^{k}} \circ (q, \dot{q}, \tau)\right] \\ &= \left[\left(\frac{\partial \hat{a}^{\alpha}{}_{i}}{\partial q^{k}} - \frac{\partial \hat{a}^{\alpha}{}_{k}}{\partial q^{i}}\right) \circ (q, \tau)\right] \dot{q}^{i} - \frac{\partial \hat{a}^{\alpha}{}_{k}}{\partial \tau} \circ (q, \tau),\end{aligned} \tag{2.18}$$

which, after multiplication by η_{q}^{k}, is the sum of the first two terms on the right-hand side of Equation (2.14). In conclusion, in deriving Equation (2.15), we have hypothesized the existence of the linear transformation relating $\boldsymbol{\eta}_{\dot{q}} - \dot{\boldsymbol{\eta}}_{q}$ with $\boldsymbol{\eta}_{q}$ because in Equation (2.14) the matrix corresponding to $[\hat{a}^{\alpha}{}_{h} \circ (q, \tau)]$ is rectangular, and, thus, cannot be inverted to obtain Equation (2.16) at once.

2.2.3 Transpositional relations and the "Canonical flip"

A relevant result of the work by Grabowska&Grabowski [57] is their Equation (2.5), which reproposes the tranpositional relations discussed by Neimark&Fufaev [13], and establishes a peculiar relationship between the quantities that, in our context, are denoted by $\boldsymbol{\eta}_{\dot{q}}$ and $\dot{\boldsymbol{\eta}}_{q}$. In our notation, which follows the one adopted in [13], the transpositional relations could be written as [13, 57, 52]

$$\eta_{\dot{q}}^{h} = \dot{\eta}_{q}^{h} + \sum_{\ell,k=1}^{n} \mathcal{C}^{h}{}_{\ell k} \dot{q}^{\ell} \eta_{q}^{k}, \tag{2.19}$$

where $\mathcal{C}^{h}{}_{\ell k} = -\mathcal{C}^{h}{}_{k\ell}$ is a collection of functions that is skew-symmetric in the lower indices, and represents, in local coordinates, the fourth slot of the *"Canonical flip"* between $TT\mathscr{C}$ and itself [57, 52] (see Appendix A). However, adapted to our framework, in which the constraints are linear in the velocities as in (2.5), and are allowed to depend explicitly on time, Equation (2.19) is reformulated as

$$\eta_{\dot{q}}^{h} = \dot{\eta}_{q}^{h} + \sum_{k=1}^{n} \mathcal{C}^{h}{}_{0k} \eta_{q}^{k} + \sum_{\ell,k=1}^{n} \mathcal{C}^{h}{}_{\ell k} \dot{q}^{\ell} \eta_{q}^{k}. \tag{2.20}$$

This result, in fact, is consistent with the skew-symmetry of the first two terms on the far right-hand side of Equation (2.14)[1].

[1]Whereas the skew-symmetry of the first term is obvious, that of the second one becomes evident if, for each $\alpha = 1, \ldots, m$, we introduce an identically null function $\hat{a}^{\alpha}{}_{0} \circ (q, \tau)$, whose only role is to

Although obtained in a different context, Equation (2.15) (see [59, 16]) can be understood as an equivalent form of the relationship (2.20) adapted from [57], provided the following identification is made:

$$\begin{aligned}\eta^h_{\dot{q}} - \dot{\eta}^h_q &= \sum_{k=1}^{n} W^h{}_k \eta^k_q \equiv \sum_{k=1}^{n} \mathcal{C}^h{}_{0k} \eta^k_q + \sum_{\ell,k=1}^{n} \mathcal{C}^h{}_{\ell k}\, \dot{q}^\ell \eta^k_q \\ &= \sum_{k=1}^{n} \{\mathcal{C}^h{}_{0k} + \sum_{\ell=1}^{n} \mathcal{C}^h{}_{\ell k}\, \dot{q}^\ell\} \eta^k_q. \end{aligned} \tag{2.21}$$

In the remainder of our work, and, in particular, in the presentation of the benchmark problems analyzed in Chapter 3, we will show how relationships similar to Equation (2.21) are obtained. Moreover, we will emphasize that the skew-symmetry of the functions $\mathcal{C}^h{}_{\ell k}$ in the lower indices is respected as a consequence of the structure of the coefficients $W^h{}_k$. More specifically, we will present two situations in which Equation (2.21) is studied with special care: One case (see Section 3.2.4) requires redefining the coefficients $\mathcal{C}^h{}_{\ell k}$ as functions of q, $\dot{q}$, and τ (this will involve, in fact, the dependence of these coefficients on the generalized momenta of the problem); the second case (see Section 3.2.5), instead, requires redefining the generalized velocities $\dot{q}$ by suitably normalizing the generalized momenta mentioned above.

2.3 Hamilton–Suslov Variational Principle

Given the mechanical system $\mathfrak{M}$ introduced above, and assuming $\mathfrak{M}$ to be subjected to m nonholonomic constraints of the type specified in Equation (2.5), we denote by $\hat{\mathcal{L}} : T\mathscr{C} \times [t_{\text{in}}, t_{\text{fin}}] \to \mathbb{R}$ the Lagrangian function that would characterize $\mathfrak{M}$ if none of the m imposed constraints were present. Moreover, we adopt the composition $\mathcal{L} := \hat{\mathcal{L}} \circ (q, \dot{q}, \tau) : [t_{\text{in}}, t_{\text{fin}}] \to \mathbb{R}$ to rephrase $\hat{\mathcal{L}}$ as a function of time. Then, by following [41–44], we introduce also the *constrained Lagrangian function* of $\mathfrak{M}$ as

$$\mathcal{L}_{\text{c}} \equiv \hat{\mathcal{L}}_{\text{c}} \circ (q, \dot{q}, \tau; \lambda) := \hat{\mathcal{L}} \circ (q, \dot{q}, \tau) - \sum_{\alpha=1}^{m} \lambda_\alpha [\hat{\mathcal{V}}^\alpha \circ (q, \dot{q}, \tau)], \tag{2.22}$$

yield the expression $\left[\partial_k \hat{a}^\alpha{}_0 - \partial_\tau \hat{a}^\alpha{}_k\right] \circ (q, \tau)$. Note, however, that this is true because, throughout the remainder of Chapter 2 and in Chapter 3, we *are not* considering constraints *affine* in the velocities. Indeed, should these constraints be considered, as in Chapter 5 within the context of *growth mechanics* [2], the function $\hat{a}^\alpha{}_0 \circ (q, \tau)$ would not be identically zero, and Equations (2.19) and (2.20) would change accordingly (see also [46] for a discussion on constraints affine in the velocities).

where $\lambda_1, \ldots, \lambda_m$ are m Lagrange multipliers associated with the m nonholonomic constraints. For the sake of a compact notation, such Lagrange multipliers can be collected in the array $\lambda := (\lambda_1, \ldots, \lambda_m)$. Next, we define the action functional associated with $\mathcal{L}_\mathrm{c}$ over the time interval $[t_\mathrm{in}, t_\mathrm{fin}]$ as [41–44]

$$\begin{aligned}\mathscr{A}_\mathrm{c}(q;\lambda) &:= \int_{t_\mathrm{in}}^{t_\mathrm{fin}} \hat{\mathcal{L}}_\mathrm{c}(q(t), \dot{q}(t), \tau(t); \lambda(t))\,\mathrm{d}t = \int_{t_\mathrm{in}}^{t_\mathrm{fin}} \mathcal{L}_\mathrm{c}(t)\,\mathrm{d}t \\ &= \int_{t_\mathrm{in}}^{t_\mathrm{fin}} \Big\{\mathcal{L}(t) - \sum_{\alpha=1}^{m} \lambda_\alpha(t)\mathcal{V}^\alpha(t)\Big\}\mathrm{d}t. \end{aligned} \tag{2.23}$$

To perform the variation of the action functional $\mathscr{A}_\mathrm{c}$, and in analogy with the notation given in Equations (2.6a), (2.6b), and (2.9), we write $\tilde{\lambda}(t,\varepsilon)$ to indicate the collection of varied Lagrange multipliers, and [41–44, 16]

$$\tilde{\mathcal{L}}(t,\varepsilon) := \hat{\mathcal{L}}(\tilde{q}(t,\varepsilon), \tilde{\boldsymbol{\nu}}(t,\varepsilon), \tilde{\tau}(t,\varepsilon)) \tag{2.24}$$

to indicate the varied Lagrangian function. Note that, for each $\alpha = 1, \ldots, n$, we set $\tilde{\lambda}_\alpha(t,0) = \lambda_\alpha(t)$, and we call $\eta_{\lambda_\alpha}(t) := \partial_\varepsilon \tilde{\lambda}_\alpha(t,0)$ the first-order variation [16]. Accordingly, the varied action functional can be written as a function of ε, and reads [41–44]

$$\begin{aligned}\tilde{\mathscr{A}}_\mathrm{c}(\varepsilon) &:= \int_{t_\mathrm{in}}^{t_\mathrm{fin}} \hat{\mathcal{L}}_\mathrm{c}(\tilde{q}(t,\varepsilon), \tilde{\boldsymbol{\nu}}(t,\varepsilon), \tilde{\tau}(t,\varepsilon); \tilde{\lambda}(t,\varepsilon))\,\mathrm{d}t \\ &= \int_{t_\mathrm{in}}^{t_\mathrm{fin}} \Big\{\tilde{\mathcal{L}}(t,\varepsilon) - \sum_{\alpha} \tilde{\lambda}_\alpha(t,\varepsilon)\tilde{\mathcal{V}}^\alpha(t,\varepsilon)\Big\}\mathrm{d}t, \end{aligned} \tag{2.25}$$

where we have simplified the notation by using the convention according to which, in the summations, the index α runs from 1 to m. A similar notation will be employed in the sequel also for summations over indices running from 1 to n. We remark that, in Equations (2.23) and (2.25), the structure of the Lagrangian function $\mathcal{L}_\mathrm{c}$ is taken from [41–44], while the way in which the varied velocity $\tilde{\boldsymbol{\nu}}(t,\varepsilon)$ is defined rephrases the definition given in [16]. Finally, for the sake of brevity and for future use, from here on we denote by

$$\natural := (q, \dot{q}, \tau), \qquad\qquad \natural_\mathrm{a} := (q, \dot{q}, \tau; \lambda) \tag{2.26}$$

the lists of arguments of $\mathcal{L}$ and $\mathcal{L}_\mathrm{c}$, respectively, and by

$$\sharp \coloneqq (q, \dot{q}, \ddot{q}, \tau), \qquad \sharp_\mathrm{a} \coloneqq (q, \dot{q}, \ddot{q}, \tau; \lambda, \dot{\lambda}) \tag{2.27}$$

the lists of arguments of the corresponding Euler–Lagrange operators, i.e.,

$$\mathcal{E}_k \hat{\mathcal{L}} \circ \sharp \coloneqq \frac{\partial \hat{\mathcal{L}}}{\partial q^k} \circ \natural - \frac{\mathrm{d}}{\mathrm{d}t}\left[\frac{\partial \hat{\mathcal{L}}}{\partial \dot{q}^k} \circ \natural\right], \qquad k = 1, \dots, n, \tag{2.28a}$$

$$\mathcal{E}_k \hat{\mathcal{L}}_\mathrm{c} \circ \sharp_\mathrm{a} \coloneqq \frac{\partial \hat{\mathcal{L}}_\mathrm{c}}{\partial q^k} \circ \natural_\mathrm{a} - \frac{\mathrm{d}}{\mathrm{d}t}\left[\frac{\partial \hat{\mathcal{L}}_\mathrm{c}}{\partial \dot{q}^k} \circ \natural_\mathrm{a}\right], \qquad k = 1, \dots, n. \tag{2.28b}$$

With all the premises given above, the condition of stationary action at $\varepsilon = 0$ yields [11, 16]

$$\begin{aligned}\frac{\mathrm{d}\tilde{\mathscr{A}}_\mathrm{c}}{\mathrm{d}\varepsilon}(0) = &\int_{t_\mathrm{in}}^{t_\mathrm{fin}} \left\{\sum_k [\mathcal{E}_k \hat{\mathcal{L}}_\mathrm{c} \circ \sharp_\mathrm{a}] \eta_q^k + \sum_\alpha \left[\frac{\partial \hat{\mathcal{L}}_\mathrm{c}}{\partial \lambda_\alpha} \circ \natural_\mathrm{a}\right] \eta_{\lambda_\alpha}\right\}(t)\, \mathrm{d}t \\ &+ \int_{t_\mathrm{in}}^{t_\mathrm{fin}} \left\{\sum_h \left[\frac{\partial \hat{\mathcal{L}}_\mathrm{c}}{\partial \dot{q}^h} \circ \natural_\mathrm{a}\right] (\eta_{\dot{q}}^h - \dot{\eta}_q^h)\right\}(t)\, \mathrm{d}t = 0.\end{aligned} \tag{2.29}$$

Equation (2.29) can be further worked out by employing Equation (2.15) to rewrite the differences $\eta_{\dot{q}}^h - \dot{\eta}_q^h$ in terms of $\boldsymbol{\eta}_q$, by introducing the operators [59, 16]

$$\mathcal{D}_k \hat{\mathcal{L}}_\mathrm{c} \circ \sharp_\mathrm{a} \coloneqq \mathcal{E}_k \hat{\mathcal{L}}_\mathrm{c} \circ \sharp_\mathrm{a} + \sum_h \left[\frac{\partial \hat{\mathcal{L}}_\mathrm{c}}{\partial \dot{q}^h} \circ \natural_\mathrm{a}\right] W^h{}_k, \qquad k = 1, \dots, n, \tag{2.30}$$

and by noticing that the derivative of $\hat{\mathcal{L}}_\mathrm{c}$ with respect to λ_α returns, up to the sign, the αth constraint. These considerations lead to the following compact expression of the condition of stationary action:

$$\frac{\mathrm{d}\tilde{\mathscr{A}}_\mathrm{c}}{\mathrm{d}\varepsilon}(0) = \int_{t_\mathrm{in}}^{t_\mathrm{fin}} \left\{\sum_k [\mathcal{D}_k \hat{\mathcal{L}}_\mathrm{c} \circ \sharp_\mathrm{a}] \eta_q^k + \sum_\alpha [-\hat{\mathcal{V}}^\alpha \circ \natural] \eta_{\lambda_\alpha}\right\}(t)\, \mathrm{d}t = 0. \tag{2.31}$$

Since Equation (2.31) must hold for any possible choice of t_in and $t_\mathrm{fin} > t_\mathrm{in}$, we require the integrand to be zero, and, since the latter condition must be fulfilled for arbitrary variations $\eta_q^1, \dots, \eta_q^n$ and $\eta_{\lambda_1}, \dots, \eta_{\lambda_m}$, we obtain [16]

$$\mathcal{D}_k \hat{\mathcal{L}}_\mathrm{c} \circ \sharp_\mathrm{a} = 0, \qquad k = 1, \dots, n, \tag{2.32a}$$

$$-\hat{\mathcal{V}}^{\alpha} \circ \natural = 0, \qquad \alpha = 1, \ldots, m. \tag{2.32b}$$

This is a set of $n + m$ equations in the $n + m$ unknowns given by the n Lagrangian parameters $q^1, \ldots, q^n$ and by the m Lagrange multipliers $\lambda_1, \ldots, \lambda_m$. We notice that Equation (2.32a) are the dynamic equations of the problem, while Equation (2.32b) return the constraints.

It must be emphasized, however, that the system of equations just obtained differs from the one of standard Analytical Mechanics for the following facts:

(i) The dynamic equations (2.32a) search for functions $q^1, \ldots, q^n$ that yield, for each $k = 1, \ldots, n$, the vanishing of the quantity $\mathcal{D}_k \hat{\mathcal{L}}_{\mathrm{c}}$ introduced by Llibre et al. [16], instead of the *standard* Euler-Lagrange operator applied to $\hat{\mathcal{L}}_{\mathrm{c}}$, i.e., $\mathcal{E}_k \hat{\mathcal{L}}_{\mathrm{c}}$. In this respect, it should be noticed that, if one followed Kozlov's vakonomic method [41–44], the dynamic equations would still be formulated in terms of the standard Euler–Lagrange operators applied to $\hat{\mathcal{L}}_{\mathrm{c}}$, since the transpositional relations (2.15) would not be explicitly considered. Exactly at this point the "modification" to the vakonomic dynamics proposed in [59, 16] comes into play. Indeed, Llibre et al. [16] resolve explicitly the transpositional relations in Equation (2.15) through the introduction of the matrix W, which, in turn, leads to the definition of the quantity $\mathcal{D}_k \hat{\mathcal{L}}_{\mathrm{c}}$. From here on, with a slight abuse of notation, we shall refer to this quantity and to other similar ones as "operator". To conclude, we mention that, in the case of holonomic constraints, Equation (2.14) complies with the equalities $\eta^h_{\dot{q}} = \dot{\eta}^h_q$ for each $h = 1, \ldots, n$, thereby requiring W to be the null matrix.

(ii) Even though the number of equations (given by the sum of the number of the dynamic equations and of the constraints) equals the number of unknowns, Equations (2.32a) and (2.32b) are *not* closed, because, for each $k = 1, \ldots, n$, the operator $\mathcal{D}_k \hat{\mathcal{L}}_{\mathrm{c}}$ features the n^2 unknown coefficients of W. To overcome this problem, n^2 auxiliary conditions need to be imposed (see the difference with the approach sketched in Section 2.2.2).

(iii) In this theory, the equations for the Lagrange multipliers are first order differential equations, whereas they are algebraic in the TNHM.

2.3.1 Solvability conditions

Equations (2.32a) and (2.32b) can be rewritten as

$$\mathcal{D}_k\hat{\mathcal{L}} \circ \sharp + \sum_\alpha \dot{\lambda}_\alpha \left[\frac{\partial \hat{\mathcal{V}}^\alpha}{\partial \dot{q}^k} \circ \natural\right] - \sum_\alpha \lambda_\alpha [\mathcal{D}_k \hat{\mathcal{V}}^\alpha \circ \sharp] = 0, \quad k = 1, \dots, n, \tag{2.33a}$$

$$-\hat{\mathcal{V}}^\alpha \circ \natural = 0, \quad \alpha = 1, \dots, m. \tag{2.33b}$$

As anticipated in Section 2.3, we need to assign n^2 additional conditions, denoted hereafter as the *solvability conditions* of the MVM, in order to close the system (2.33a) and (2.33b). In particular, due to the properties of the constraints highlighted in Equations (2.14) and (2.15), mn conditions can be found by substituting Equation (2.15) into Equation (2.14), which amounts to setting

$$\mathcal{D}_k \hat{\mathcal{V}}^\alpha \circ \sharp = 0, \qquad k = 1, \dots, n, \qquad \alpha = 1, \dots, m. \tag{2.34}$$

The last $n(n-m)$ conditions are assigned via the prescription of *Ansätze*, in which either $n-m$ auxiliary functions satisfying certain conditions [16] are introduced or the fulfillment of some physics-based conditions is assumed.

Ansatz 1: approach based on the auxiliary functions

To solve Equations (2.33a) and (2.33b), Llibre et al. [16] determine univocally the coefficients of W by introducing $n-m$ auxiliary functions $\mathcal{F}^\beta \equiv \hat{\mathcal{F}}^\beta \circ (q, \dot{q}, \tau)$, with $\beta = m+1, \dots, n$, which yield the following $n(n-m)$ conditions

$$\mathcal{D}_k \hat{\mathcal{F}}^\beta \circ \sharp = 0, \qquad k = 1, \dots, n, \qquad \beta = m+1, \dots, n. \tag{2.35}$$

As anticipated in Section 2.2.2, the rationale behind the introduction of the set of functions $\{\mathcal{F}^\beta\}_{\beta=m+1}^n$ relies on the concept of quasi-velocities (see e.g. [13, 30, 25]), i.e., a set of functions $\{\omega^h\}_{h=1}^n$ constituting a reparameterization of the velocities $\{\dot{q}^k\}_{k=1}^n$ such that $\omega^h(t) = \hat{\omega}^h(q(t), \dot{q}(t), t)$, for all $h = 1, \dots, n$, and the Jacobian $J^h{}_k(t) \coloneqq \partial_{\dot{q}^k}\hat{\omega}^h(q(t), \dot{q}(t), t)$ is non-singular. In fact, for a mechanical system subjected to m constraints on the velocities, it is possible to choose the first m quasi-velocities coincident with the constraints themselves (see Section 2.2.2), and to identify the remaining $n-m$ quasi-velocities with the "arbitrary" functions

$\omega^{m+1} \equiv \mathcal{F}^{m+1}, \ldots, \omega^n \equiv \mathcal{F}^n$. However, in spite of this arbitrariness, some selection rules are necessary (see [59, 16]). To this end, the identification of the functions $\{\mathcal{F}^\beta\}_{\beta=m+1}^n$ with the corresponding quasi-velocities $\{\omega^\beta\}_{\beta=m+1}^n$ notwithstanding, it is instructive to critically review the method outlined in [16] because it involves conditions on the auxiliary functions that are called for by the variational procedure.

As a starting point, the functions $\mathcal{F}^{m+1}, \ldots, \mathcal{F}^n$ must be such that the matrix $\mathsf{J} = [J^i{}_k]_{k=1,\ldots,n}^{i=1,\ldots,n}$, with components

$$J^i{}_k = \begin{cases} [\partial_{\dot{q}^k} \hat{\mathcal{V}}^\alpha] \circ (q, \dot{q}, \tau), & i = \alpha = 1, \ldots, m, \qquad k = 1, \ldots, n, \\ [\partial_{\dot{q}^k} \hat{\mathcal{F}}^\beta] \circ (q, \dot{q}, \tau), & i = \beta = m+1, \ldots, n, \quad k = 1, \ldots, n, \end{cases} \tag{2.36}$$

is *non-singular*, i.e., $\det \mathsf{J} \neq 0$, almost everywhere in $T\mathscr{C} \times [t_{\text{in}}, t_{\text{fin}}]$. However, on this point, we would like to emphasize that:

(i) The conditions in Equation (2.35) may be regarded as *gauge conditions* [66] for the problem under study. In fact, through the introduction of $\mathcal{F}^{m+1}, \ldots, \mathcal{F}^n$, we can transform *a posteriori* the Lagrangian $\mathcal{L}_{\text{c}}$ in Equation (2.22) as [16]

$$\hat{\mathcal{L}}_{\text{c}} \circ \natural_{\text{a}} \mapsto \hat{\mathcal{L}}_{\text{c}} \circ \natural_{\text{a}} - \sum_\beta c_\beta [\hat{\mathcal{F}}^\beta \circ \natural] =: \hat{\mathcal{L}}_{\text{L}} \circ (\natural_{\text{a}}; \kappa), \tag{2.37}$$

where the summation over β is done from $m+1$ to n; $c_{m+1}, \ldots, c_n$ are constant-valued parameters, i.e., $c_\beta(t) = c_{\beta 0} \in \mathbb{R}$, for $\beta = m+1, \ldots, n$, and for all $t \in [t_{\text{in}}, t_{\text{fin}}]$; and $c := (c_{m+1}, \ldots, c_n)$ collects all such parameters. Therefore, by applying the variational procedure described in Section 2.3 to the case in which the Lagrangian is transformed as in Equation (2.37), it is necessary to impose Equation (2.35) in order for the dynamic equations associated with $\hat{\mathcal{L}}_{\text{L}}$ to be *invariant* with respect to those associated with $\hat{\mathcal{L}}_{\text{c}}$, reported in Equation (2.33a). However, this invariance of the dynamic equations is only sufficient for the equivalence of the descriptions provided by $\hat{\mathcal{L}}_{\text{L}}$ and $\hat{\mathcal{L}}_{\text{c}}$. Indeed, also the next remark has to be considered.

(ii) The transformation in Equation (2.37) has to be consistent with the Principle of Stationary Action [11], in the sense that the Action associated with the transformed Lagrangian needs to have the same stationary points as the

non-transformed Action. In other words, upon setting

$$\mathscr{A}_{\mathrm{L}}(q,\lambda;c) \coloneqq \int_{t_{\mathrm{in}}}^{t_{\mathrm{fin}}} \hat{\mathcal{L}}_{\mathrm{L}}(q(t),\dot{q}(t),t;\lambda(t);c(t))\mathrm{d}t, \tag{2.38}$$

it must hold true that $\mathscr{A}_{\mathrm{L}}(q;\lambda;c) = \mathscr{A}_{\mathrm{c}}(q;\lambda) + C$, where C is a real constant, i.e., the Actions $\mathscr{A}_{\mathrm{L}}(q;\lambda;c)$ and $\mathscr{A}_{\mathrm{c}}(q;\lambda)$ only differ additively by a constant term [11]. To this end, the generic function $\mathcal{F}^{\beta}$ will be chosen either as a total derivative, e.g. a generalized velocity, or as a function of the generalized velocities (quasi-velocity) that carries some physical interpretation for the problem at hand. Note that, in the second case, the associated coefficient c_{β} must be zero in order to satisfy the previous hypothesis on $\mathscr{A}_{\mathrm{L}}$ [16]. To see this, assume that there exists $\bar{\beta} \in \{m+1,\dots,n\}$ such that $\mathcal{F}^{\bar{\beta}}$ *is not* the total derivative of a function of the type $\hat{f} \circ (q,\tau)$, while all other functions $\mathcal{F}^{\beta}$ are so, with $\beta \in \{m+1,\dots,n\}\backslash\{\bar{\beta}\}$. Then, the Action $\mathscr{A}_{\mathrm{L}}(q;\lambda;c)$ becomes

$$\begin{aligned}
\mathscr{A}_{\mathrm{L}}(q;\lambda;c) &\coloneqq \mathscr{A}_{\mathrm{c}}(q;\lambda) - \sum_{\beta\neq\bar{\beta}} \int_{t_{\mathrm{in}}}^{t_{\mathrm{fin}}} c_{\beta}(t)\hat{\mathcal{F}}^{\beta}(\natural(t))\mathrm{d}t - \int_{t_{\mathrm{in}}}^{t_{\mathrm{fin}}} c_{\bar{\beta}}(t)\hat{\mathcal{F}}^{\bar{\beta}}(\natural(t))\mathrm{d}t \\
&= \mathscr{A}_{\mathrm{c}}(q;\lambda) \underbrace{- \sum_{\beta\neq\bar{\beta}} c_{\beta 0} \int_{t_{\mathrm{in}}}^{t_{\mathrm{fin}}} \hat{\mathcal{F}}^{\beta}(\natural(t))\mathrm{d}t}_{=:C} - c_{\bar{\beta}0} \int_{t_{\mathrm{in}}}^{t_{\mathrm{fin}}} \hat{\mathcal{F}}^{\bar{\beta}}(\natural(t))\mathrm{d}t \\
&= \mathscr{A}_{\mathrm{c}}(q;\lambda) + C - c_{\bar{\beta}0} \int_{t_{\mathrm{in}}}^{t_{\mathrm{fin}}} \hat{\mathcal{F}}^{\bar{\beta}}(\natural(t))\mathrm{d}t,
\end{aligned} \tag{2.39}$$

which means that $c_{\bar{\beta}0}$ must be zero.

(iii) Last but not least, the auxiliary functions must be chosen in such a way that the coefficients of W computed through Equation (2.35) must yield *zero transpositional relations* for those velocities that do not feature in the constraints or that, if featuring in them, can be varied independently of the other ones (see Section 2.2.2, and [46]). Operatively, if β^* corresponds to a velocity that can be chosen as independent or absent in the constraints, one can choose $\hat{\mathcal{F}}^{\beta^*} \circ \natural = \dot{q}^{\beta^*}$. A function of this type complies trivially with the requirements (i), (ii), and with the present one, and implies that the β^*th row of W is identically null.

Given these considerations on the choice of the auxiliary functions, Equations (2.34) and (2.35) can be rewritten in explicit form as [16]

$$\sum_h \left[\frac{\partial \hat{\mathcal{V}}^\alpha}{\partial \dot{q}^h} \circ \natural \right] W^h{}_k = -\mathcal{E}_k \hat{\mathcal{V}}^\alpha \circ \sharp, \quad k = 1, \dots, n, \quad \alpha = 1, \dots, m, \tag{2.40a}$$

$$\sum_h \left[\frac{\partial \hat{\mathcal{F}}^\beta}{\partial \dot{q}^h} \circ \natural \right] W^h{}_k = -\mathcal{E}_k \hat{\mathcal{F}}^\beta \circ \sharp, \quad k = 1, \dots, n, \quad \beta = m+1, \dots, n, \tag{2.40b}$$

so that the coefficients $W^h{}_k$ are obtained by solving (2.40a) and (2.40b). Note that, Equations (2.40a) and (2.40b) together are equivalent to Equation (2.17).

In spite of the selection rules mentioned above, we remark that, in the "charged skate" benchmark studied in Section 3.2, we found that an auxiliary function that works well in the uncharged case, yields to results that, in our opinion, are unphysical when the skate is charged and subjected to an interaction with a magnetic field. According to our calculations, indeed, there occur inconsistencies with the fulfillment of certain conservation laws, that can be related to the way in which the chosen auxiliary function depends on the velocities that *are* involved in the constraint. To amend these shortcomings, we suggest to switch to a different formulation, that we report in the following *Ansatz 2*.

Ansatz 2: physics-based conditions

In order to close Equation (2.33a) and (2.33b), we can require the system to respect the symmetries that may be naturally present in the Lagrangian function $\hat{\mathcal{L}}$ and in the constraints. For instance, if we assume the existence of a Lagrangian parameter $q^{\bar{k}}$ *"ignorable"* [11] in $\hat{\mathcal{L}}$, i.e., not explicitly featuring among its arguments, and such that $\partial_{\dot{q}^{\bar{k}}} \hat{\mathcal{V}}^\alpha \circ \natural = 0$ for all $\alpha = 1, \dots, m$, then, by consistency with classical Analytical Mechanics, expressed by the Lagrange–d'Alembert method, we may impose the condition

$$\sum_h p_h W^h{}_{\bar{k}} = 0, \qquad p_h \coloneqq \frac{\partial \hat{\mathcal{L}}}{\partial \dot{q}^h} \circ \natural, \tag{2.41}$$

to restore the conservation of the generalized momentum $p_{\bar{k}}$ [11].

Another scenario could be the one in which all the m constraints, say $\hat{f}^1 \circ (q, \tau) = 0, \dots, \hat{f}^m \circ (q, \tau) = 0$, are holonomic. In this case, it is known that the equations of

motion are $\mathcal{E}_k \mathcal{L} \circ \sharp + \sum_\alpha \mu_\alpha [\partial_{q^k} \hat{f}^\alpha \circ (q, \tau)] = 0$, for $k = 1, \ldots, n$ (see, e.g., [11]), and one can put the constraints in "nonholonomic"[2] form by setting $\hat{\mathcal{V}}^\alpha \circ \natural \equiv \mathrm{d}_t [\hat{f}^\alpha \circ (q, \tau)]$, with $\alpha = 1, \ldots, m$ and d_t indicating the total time derivative. In this case, however, it automatically applies $\mathcal{E}_k \hat{\mathcal{V}}^\alpha \circ \sharp = 0$, for all $k = 1, \ldots, n$, and for all $\alpha = 1, \ldots, m$. Thus, if we take $\hat{\mathcal{F}}^\beta \circ \natural = \mathrm{d}_t [\hat{g}^\beta \circ (q, \tau)]$, with $\beta = m+1, \ldots, n$, and $\hat{g}^\beta \circ (q, \tau)$ being arbitrary scalar functions such that the matrix J in Equation (2.36) is non-singular, then W turns out to be the null matrix, as prescribed by Equations (2.40a) and (2.40b).

Note that, the conditions in *Ansatz 2* are, in general, not enough to close the problem, so that a combination of the conditions featuring in *Ansatz 1* and *Ansatz 2* is required. From an operative point of view, our *Ansatz 2* suggests to introduce, as shown in *Ansatz 1*, a number ℓ^* of auxiliary functions $\{\mathcal{F}^\beta\}_{\beta=m+1}^{m+\ell^*}$, if this is the number of velocities that either do not feature in the constraints or can be chosen as independent. Then, to determine the remaining $n - (m + \ell^*)$ conditions, *Ansatz 2* indicates to apply a criterion that will be formalized in Theorem 2.1. Indeed, this criterion provides automatically the "physics-based conditions" mentioned at the beginning of this section, also for those cases in which it can be hard to impose them from the outset.

In conclusion, when matrix W is found, either by *Ansatz 1* or *Ansatz 2*, then the dynamic equations of the "modified vakonomic method" read [59, 16]

$$\mathcal{E}_k \hat{\mathcal{L}} \circ \sharp + \sum_h p_h W^h{}_k + \sum_\alpha \dot{\lambda}_\alpha \Big[\frac{\partial \hat{\mathcal{V}}^\alpha}{\partial \dot{q}^k} \circ \natural \Big] = 0, \qquad k = 1, \ldots, n, \tag{2.42a}$$

$$-\hat{\mathcal{V}}^\alpha \circ \natural = 0, \qquad \alpha = 1, \ldots, m. \tag{2.42b}$$

In the presence of generalized forces $\mathcal{Q}_1, \ldots, \mathcal{Q}_k$ that cannot be obtained from a scalar potential (Lanczos [11] refers to such forces as *"polygenic"*), Equation (2.42a) acquires, up to the sign, the right-hand side $\mathcal{Q}_k$, so that the set of Equations (2.42a) and (2.42b) becomes

$$\mathcal{E}_k \hat{\mathcal{L}} \circ \sharp + \sum_h p_h W^h{}_k + \sum_\alpha \dot{\lambda}_\alpha \Big[\frac{\partial \hat{\mathcal{V}}^\alpha}{\partial \dot{q}^k} \circ \natural \Big] = -\mathcal{Q}_k, \qquad k = 1, \ldots, n, \tag{2.43a}$$

$$-\hat{\mathcal{V}}^\alpha \circ \natural = 0, \qquad \alpha = 1, \ldots, m. \tag{2.43b}$$

[2] In other parts of this Thesis, the word "differential" is used in place of "nonholonomic" to refer to this reformulation of the constraint.

2.3.2 Some computational aspects regarding the MVM

In this section, we discuss some computational aspects regarding the solution of the set of Equations (2.42a) and (2.42b) (or (2.43a) and (2.43b)). We remark that having a general methodology for solving numerically the MVM dynamic equations is a key aspect of the theory, since not all problems allow for an analytical solution.

To include problems that involve electromagnetic interactions [66] as well as time-dependent holonomic constraints [11], we assume $\mathcal{L}$ to be of the type

$$\hat{\mathcal{L}} \circ \natural = \frac{1}{2} \sum_{h,k=1}^{n} [\hat{G}_{hk} \circ (q, \tau)] \dot{q}^h \dot{q}^k + \sum_{h=1}^{n} [\hat{Z}_h \circ (q, \tau)] \dot{q}^h + \hat{\mathcal{U}} \circ (q, \tau), \tag{2.44}$$

where $\hat{G}_{hk}$ is the generic component of the "metric tensor" associated with the kinetic energy [11]; $\hat{Z}_h$ is the hth component of a co-vector field accounting for Maxwell's (co-)vector potential [66], and for the possible explicit time-dependence of holonomic constraints; $\hat{\mathcal{U}}$ is a potential function that collects both electric and mechanical interactions as well as the contribution to the kinetic energy stemming from the possible presence of explicitly time-dependent holonomic constraints. Moreover, for such type of Lagrangian functions, their associated kth Euler–Lagrange operator reads

$$\begin{aligned} \mathcal{E}_k \hat{\mathcal{L}} \circ \sharp = &- [\hat{G}_{kh} \circ (q, \tau)] \left\{ \ddot{q}^h + [\hat{\Gamma}^h{}_{pl} \circ (q, \tau)] \dot{q}^p \dot{q}^l \right\} - \left[\frac{\partial \hat{G}_{kh}}{\partial \tau} \circ (q, \tau) \right] \dot{q}^h \\ &+ \left[\left(\frac{\partial \hat{Z}_h}{\partial q^k} - \frac{\partial \hat{Z}_k}{\partial q^h} \right) \circ (q, \tau) \right] \dot{q}^h + \left(\frac{\partial \hat{\mathcal{U}}}{\partial q^k} - \frac{\partial \hat{Z}_k}{\partial \tau} \right) \circ (q, \tau), \end{aligned} \tag{2.45}$$

where $\hat{\Gamma}^h{}_{pl} \circ (q, \tau)$ is the generic Christoffel symbol induced by the metric tensor, i.e. (see, e.g., [27, 67]),

$$\hat{\Gamma}^h{}_{pl} \coloneqq \frac{1}{2} \sum_{r=1}^{n} \hat{G}^{hr} \left(\frac{\partial \hat{G}_{rp}}{\partial q^l} + \frac{\partial \hat{G}_{rl}}{\partial q^p} - \frac{\partial \hat{G}_{pl}}{\partial q^r} \right), \tag{2.46}$$

and $\hat{G}^{hr}$ are the components of the inverse of the metric tensor.

Before going further, we notice that the substitution of Equation (2.45) into (2.42a) renders the latter one of second order in the Lagrangian parameters $q^1, \ldots, q^n$, whereas Equation (2.42b) is, by definition, of the first order in these variables.

Following [27], it is convenient to "promote" the constraints to second-order ordinary differential equations, as to store the constraints in the first non-singular matrix associated with the highest derivatives of q, i.e., the mass matrix. This can be accomplished by differentiating Equation (2.42b) with respect to time, thereby obtaining

$$\begin{aligned}&\frac{\mathrm{d}}{\mathrm{d}t}[\hat{\mathcal{V}}^{\alpha} \circ \natural] \\ &= [\hat{a}^{\alpha}{}_{k} \circ (q,\tau)]\ddot{q}^{k} + \left[\frac{\partial \hat{a}^{\alpha}{}_{k}}{\partial q^{h}} \circ (q,\tau)\right]\dot{q}^{k}\dot{q}^{h} + \left[\frac{\partial \hat{a}^{\alpha}{}_{k}}{\partial \tau} \circ (q,\tau)\right]\dot{q}^{k} = 0, \end{aligned} \tag{2.47}$$

and by solving the resulting equations together with Equation (2.45). For this purpose, it is convenient to introduce the following notation:

$$M_{kh} \coloneqq \hat{G}_{kh} \circ (q,\tau), \tag{2.48a}$$

$$C^{h}{}_{pl} \coloneqq \hat{\Gamma}^{h}{}_{pl} \circ (q,\tau), \tag{2.48b}$$

$$\Omega_{kh} \coloneqq \left[\frac{\partial \hat{Z}_{h}}{\partial q^{k}} - \frac{\partial \hat{Z}_{k}}{\partial q^{h}}\right] \circ (q,\tau) - \frac{\partial \hat{G}_{kh}}{\partial \tau} \circ (q,\tau), \tag{2.48c}$$

$$F_{k} \coloneqq \left[\frac{\partial \hat{\mathcal{U}}}{\partial q^{k}} - \frac{\partial \hat{Z}_{k}}{\partial \tau}\right] \circ (q,\tau), \tag{2.48d}$$

$$A^{\alpha}{}_{k} \coloneqq \hat{a}^{\alpha}{}_{k} \circ (q,\tau), \tag{2.48e}$$

$$\Lambda^{\alpha}{}_{kh} \coloneqq \frac{\partial \hat{a}^{\alpha}{}_{k}}{\partial q^{h}} \circ (q,\tau), \tag{2.48f}$$

$$\Theta^{\alpha}{}_{k} \coloneqq \frac{\partial \hat{a}^{\alpha}{}_{k}}{\partial \tau} \circ (q,\tau). \tag{2.48g}$$

Hence, by substituting Equation (2.45) in (2.42a), and changing sign to the resulting expression, Equations (2.42a) and (2.42b) take on the form

$$M_{kh}\ddot{q}^{h} + M_{kh}C^{h}{}_{pl}\dot{q}^{p}\dot{q}^{l} - \Omega_{kh}\dot{q}^{h} - F_{k} - p_{h}W^{h}{}_{k} - \dot{\lambda}_{\alpha}A^{\alpha}{}_{k} = 0, \tag{2.49a}$$

$$-A^{\alpha}{}_{h}\ddot{q}^{h} - \Lambda^{\alpha}{}_{pl}\dot{q}^{p}\dot{q}^{l} - \Theta^{\alpha}{}_{h}\dot{q}^{h} = 0. \tag{2.49b}$$

Moreover, Equations (2.49a) and (2.49b) can be recast in matrix form as

$$\begin{bmatrix} \mathsf{M} & -\mathsf{A}^{\mathrm{T}} \\ -\mathsf{A} & 0 \end{bmatrix} \begin{Bmatrix} \ddot{\mathsf{q}} \\ \dot{\lambda} \end{Bmatrix} = \begin{Bmatrix} -\mathsf{M}[\mathsf{C} : \dot{\mathsf{q}} \otimes \dot{\mathsf{q}}] + \Omega\dot{\mathsf{q}} + \mathsf{F} + \mathsf{W}^{\mathrm{T}}\mathsf{p} \\ \Lambda : \dot{\mathsf{q}} \otimes \dot{\mathsf{q}} + \Theta\dot{\mathsf{q}} \end{Bmatrix} \equiv \begin{Bmatrix} \mathsf{b}_{\mathsf{q}} \\ \mathsf{b}_{\mathsf{c}} \end{Bmatrix} + \begin{Bmatrix} \mathsf{W}^{\mathrm{T}}\mathsf{p} \\ 0 \end{Bmatrix}, \tag{2.50}$$

where the symbols in Sans Serif font represent the matrices and vectors (in the sense of arrays) associated with the quantities in Equations (2.49a) and (2.49b).

Moreover, we can exploit the saddle-point nature of the system (2.50) by employing the Schur complement technique [27], and, by doing so, we can recast the system (2.50) as

$$\ddot{\mathsf{q}} = \left[\mathsf{M}^{-1} - (\mathsf{M}^{-1}\mathsf{A}^{\mathrm{T}})\mathsf{S}^{-1}(\mathsf{A}\mathsf{M}^{-1})\right](\mathsf{b}_{\mathsf{q}} + \mathsf{W}^{\mathrm{T}}\mathsf{p}) - (\mathsf{M}^{-1}\mathsf{A}^{\mathrm{T}})\mathsf{S}^{-1}\mathsf{b}_{\mathrm{c}}, \tag{2.51a}$$

$$\dot{\lambda} = -\mathsf{S}^{-1}\left[(\mathsf{A}\mathsf{M}^{-1})(\mathsf{b}_{\mathsf{q}} + \mathsf{W}^{\mathrm{T}}\mathsf{p}) + \mathsf{b}_{\mathrm{c}}\right], \tag{2.51b}$$

with $\mathsf{S} \coloneqq \mathsf{A}\mathsf{M}^{-1}\mathsf{A}^{\mathrm{T}}$ being the Schur complement of the block-wise system. Note that the formalism used in Equation (2.51a) is similar to the one adopted in [63].

2.3.3 Differences and similarities with the TNHM

In this section, we will acknowledge the differences and the similarities between the MVM and the "traditional nonholonomic method", in short TNHM, which is based on a generalization of the Lagrange–d'Alembert Principle (see, e.g., [39, 21]). In particular, let us briefly recall the main results related to dynamic equations characterizing the TNHM [39, 21, 17, 7].

If we consider a mechanical system described by n Lagrangian parameters and constrained by m nonholonomic constraints $\hat{\mathcal{V}}^{\alpha} \circ \natural = 0$, with $\alpha = 1, \ldots, m$, then the TNHM is characterized by the $n + m$ equations [17, 27, 26]

$$\mathcal{E}_k\hat{\mathcal{L}} \circ \sharp + \sum_{\alpha=1}^{m} \mu_\alpha \left[\frac{\partial \hat{\mathcal{V}}^{\alpha}}{\partial \dot{q}^k} \circ \natural\right] = 0, \qquad k = 1, \ldots, n, \tag{2.52a}$$

$$-\hat{\mathcal{V}}^{\alpha} \circ \natural = 0, \qquad \alpha = 1, \ldots, m, \tag{2.52b}$$

in which μ_α is the αth Lagrange multiplier associated with the αth constraint.

By comparing Equation (2.42a) with Equation (2.52a) for the case of nonholonomic constraints linear in the generalized velocities, we notice that the quantities $\mathcal{E}_k\hat{\mathcal{L}} \circ \sharp$ are the same for both equations, and that the derivatives $\partial_{\dot{q}^k}\hat{\mathcal{V}}^{\alpha} \circ \natural$ return the coefficients $\hat{a}^{\alpha}{}_{k} \circ (q, \tau)$ of Equation (2.5), for all $\alpha = 1, \ldots, m$ and for all $k = 1, \ldots, n$. Therefore, the only visual differences between these equations are due to the presence of the quantities $\sum_{h=1}^{n} p_h W^h{}_k$ and of $\dot{\lambda}_\alpha$ in lieu of μ_α in Equation (2.42a). Moreover,

for each $\alpha = 1, \ldots, m$, the physical dimensions of the Lagrange multiplier λ_α in Equation (2.42a) are equal to the physical dimensions of the corresponding multiplier μ_α multiplied by a characteristic time [23, 32].

As previously done for the dynamic equations of the MVM in Equation (2.50), we can specialize Equations (2.52a) and (2.52b) for the case of the Lagrangian function in Equation (2.44). In particular, by referring to the same notation introduced in Equations (2.48a)–(2.48g), and by defining the array of Lagrange multipliers of the TNHM, i.e., $\mu := \{\mu_1, \ldots, \mu_m\}^{\mathrm{T}}$, Equations (2.52a) and (2.52b) can be written in matrix form as [27]

$$\begin{bmatrix} \mathsf{M} & -\mathsf{A}^{\mathrm{T}} \\ -\mathsf{A} & 0 \end{bmatrix} \begin{Bmatrix} \ddot{\mathsf{q}} \\ \mu \end{Bmatrix} = \begin{Bmatrix} -\mathsf{M}[\mathsf{C} : \dot{\mathsf{q}} \otimes \dot{\mathsf{q}}] + \Omega\dot{\mathsf{q}} + \mathsf{F} \\ \Lambda : \dot{\mathsf{q}} \otimes \dot{\mathsf{q}} + \Theta\dot{\mathsf{q}} \end{Bmatrix} \equiv \begin{Bmatrix} \mathsf{b}_{\mathsf{q}} \\ \mathsf{b}_{\mathsf{c}} \end{Bmatrix}. \tag{2.53}$$

Moreover, by defining $\mathsf{S} := \mathsf{A}\mathsf{M}^{-1}\mathsf{A}^{\mathrm{T}}$, the Schur complement technique allows us to invert Equation (2.53), which reads as follows:

$$\ddot{\mathsf{q}} = [\mathsf{M}^{-1} - (\mathsf{M}^{-1}\mathsf{A}^{\mathrm{T}})\mathsf{S}^{-1}(\mathsf{A}\mathsf{M}^{-1})]\mathsf{b}_{\mathsf{q}} - (\mathsf{M}^{-1}\mathsf{A}^{\mathrm{T}})\mathsf{S}^{-1}\mathsf{b}_{\mathsf{c}}, \tag{2.54a}$$

$$\mu = -\mathsf{S}^{-1}[(\mathsf{A}\mathsf{M}^{-1})\mathsf{b}_{\mathsf{q}} + \mathsf{b}_{\mathsf{c}}]. \tag{2.54b}$$

Note that, both for the MVM and for the TNHM, we obtain the same block-wise matrix on the left-hand side of Equations (2.50) and (2.53). However, the right-hand side of these equations is different since $\mathsf{W}^{\mathrm{T}}\mathsf{p}$ features in Equation (2.50), only, as a result of the followed procedure.

At this stage, we find it convenient to formalize the results obtained so far by providing a definition of *equivalence* between the "modified vakonomic method" (MVM) and the "traditional nonholonomic method" (TNHM).

Definition 2.1 (Equivalence between MVM and TNHM)**.** Given the same set of initial conditions on the generalized coordinates and velocities, we say that the MVM, i.e., Equations (2.42a) and (2.42b), and the TNHM, i.e., Equations (2.52a) and (2.52b), are *equivalent*, if they return the same solution q.

Theorem 2.1 (Characterization of the equivalence between MVM and TNHM)**.** *Let us consider a mechanical system described by a Lagrangian function of the type given in Equation* (2.44) *and by the set of nonholonomic constraints featuring in Equation* (2.5)*, which are linear in the generalized velocities. Then, the MVM, i.e.,*

Equations (2.51a) *and* (2.51b)*, and the TNHM, i.e., Equations* (2.54a) *and* (2.54b)*, are equivalent if, and only if, the following conditions are met*

$$\left[\mathsf{M}^{-1} - (\mathsf{M}^{-1}\mathsf{A}^{\mathrm{T}})\mathsf{S}^{-1}(\mathsf{A}\mathsf{M}^{-1})\right]\mathsf{W}^{\mathrm{T}}\mathsf{p} = 0, \tag{2.55a}$$

$$\dot{\lambda} = \mu - (\mathsf{S}^{-1}\mathsf{A}\mathsf{M}^{-1})\mathsf{W}^{\mathrm{T}}\mathsf{p}. \tag{2.55b}$$

Proof. If the MVM and the TNHM predict the same motion, which implies that the collection $q = (q^1, \ldots, q^n)$, represented by the array q, satisfies Equations (2.51a) and (2.51b) as well as Equations (2.54a) and (2.54b) at the same time, then subtracting Equation (2.54a) from Equation (2.51a), and (2.54b) from Equation (2.51b) yields Equations (2.55a) and (2.55b).

Conversely, if Equations (2.55a) and (2.55b) hold true, then Equation (2.51a) becomes identical to Equation (2.54a), and it is possible to establish a univocally determined relationship between the multipliers of the two methods, i.e., $\dot{\lambda}$ and μ, thereby predicting the same solution. □

As stated in Theorem 2.1, the fulfillment of Equations (2.55a) and (2.55b) provides the equivalence between the MVM and the TNHM. Moreover, it contributes to the understanding of whether a problem formulated with the vakonomic method yields, in a general context, the same solutions as the TNHM. In this sense, Theorem 2.1 seems to give an affirmative answer, since it prescribes the conditions under which the vakonomic method, modified as indicated by the MVM of [59, 16], returns the same results obtained within the TNHM.

We emphasize that, granted the equivalence between the MVM and the TNHM, the identification between the Lagrange multipliers in Equation (2.55b) is similar to the ones originally presented in [16]. Note also that, even though it is possible to *formally* find relations as in Equation (2.55b), they alone are not sufficient, in general, to guarantee the equivalence between the TNHM and the MVM.

Corollary 2.1 (Sufficient condition for the equivalence between MVM and TNHM)**.** *Given a mechanical system of the type addressed in Theorem 2.1, the MVM is* equivalent *to the TNHM, if it holds true that*

$$\mathsf{W}^{\mathrm{T}}\mathsf{p} = 0, \tag{2.56a}$$

$$\dot{\lambda} = \mu. \tag{2.56b}$$

Proof. If the condition $\mathsf{W}^{\mathrm{T}}\mathsf{p} = \mathsf{0}$ applies, then Equation (2.55a) is trivially satisfied, and, thus, the MVM is equivalent to the TNHM. In addition, Equation (2.56b) follows directly from Equation (2.55b). □

We emphasize that our Theorem 2.1 is a reinterpretation of Theorem 2 in [16], while our Corollary 2.1, and, by extension, also our *Ansatz 2*, aim to reinterpret Theorem 3 of Llibre et al. [16] and Section 3.2 of Ramírez et al. [59], as a sufficient condition for Theorem 2.1.

Remark 2.1 (On the role of the Lagrangian, its generalized momenta p, and W). The condition (2.56a) requires that the array of the generalized momenta p belongs to the kernel of the matrix W^{T}, and it amounts to requiring that the second term on the left-hand side of Equation (2.42a) vanishes identically, i.e., $\sum_{h=1}^{n} p_h W^h{}_k = 0$, for $k = 1, \ldots, n$. For a given Lagrangian function $\mathcal{L}$, which identifies the components $p_h = \partial_{\dot{q}^h}\hat{\mathcal{L}} \circ \natural$ of p, whether or not p belongs to the kernel of W^{T} depends both on W itself, and, thus, in general, on the conditions imposed to determine the coefficients of W, and on the form of p. The conditions on W, in fact, can be obtained by following the *Ansatz 1* and/or the *Ansatz 2*. On the other hand, for a given matrix W, determined e.g. through the assignment of suitable functions $\mathcal{F}^{m+1}, \ldots, \mathcal{F}^{n}$ (we recall that the constraints provide indications on the adequacy of such functions, which are none other than additional quasi-velocities), the array of momenta stemming from a given $\mathcal{L}$ does not necessarily belong to the kernel of W^{T}, depending on the interactions accounted for by $\mathcal{L}$. Indeed, the Lagrangian function addressed in our work, specified in Equation (2.44), is more general than the ones typically considered in the context of vakonomic mechanics, since it accounts for interactions that do not allow to write it as the sum of a kinetic energy plus a potential depending solely on the Lagrangian parameters and possibly on time. This will become clearer below, when we shall analyze a modification of the classical benchmark of the nonholonomic skate, by including magnetic interactions that yield the presence in the Lagrangian function of a term linear in the generalized velocities. In fact, this generalization leads to momenta that are affine in the velocities and that, because of their nature, cannot belong to the kernel of W^{T}, and do not trivially satisfy Theorem 2.1. This issue, however, will be discussed in Section 2.3.4, and specialized to the case of the "charged skate" in Section 3.2.3.

Before closing this section, we deem it worthwhile to emphasize that, to the best of our understanding, the MVM proposed by Llibre et al. [16] could be viewed as a

variational version of the method based on the quasi-velocities (see e.g. [13, 30]), in which the variational form of Newton's second law of dynamics is obtained by employing d'Alembert principle, but admitting that the time derivative of the variations are different from the variations of the velocities. In this respect, the sufficient conditions for the equivalence between the MVM and the TNHM, i.e., Equations (2.55a) and (2.55b), are a consequence of the method of the quasi-velocities.

2.3.4 The case of momenta linear in the velocities

In Equations (2.43a) and (2.43b) of Section 2.3.2, we have shown the equations of the MVM in the presence of *"polygenic forces"* [11]. In fact, it is possible to obtain the same form also in the case in which the interaction that leads to the term $\sum_{h=1}^{n}[\hat{Z}_h \circ (q,\tau)]\dot{q}^h$ in the Lagrangian function of Equation (2.44) is formally treated as a force of this type (although this force is not polygenic *per se*). Indeed, by making the identification

$$-\,\mathcal{Q}_k \equiv -\left[\left(\frac{\partial \hat{Z}_h}{\partial q^k} - \frac{\partial \hat{Z}_k}{\partial q^h}\right) \circ (q,\tau)\right]\dot{q}^h + \frac{\partial \hat{Z}_k}{\partial \tau} \circ (q,\tau), \tag{2.57}$$

and, thus, consistently omitting the term $\sum_{h=1}^{n}[\hat{Z}_h \circ (q,\tau)]\dot{q}^h$ in the Lagrangian function of Equation (2.44), i.e., redefining $\hat{\mathcal{L}} \circ \natural$ as

$$\hat{\mathcal{L}}_0 \circ \natural = \frac{1}{2}\sum_{h,k=1}^{n}[\hat{G}_{hk} \circ (q,\tau)]\dot{q}^h\dot{q}^k + \hat{\mathcal{U}} \circ (q,\tau), \tag{2.58}$$

Equations (2.42a) and (2.42b) are recast in the form

$$\mathcal{E}_k\hat{\mathcal{L}}_0 \circ \sharp + \sum_h p_{0h}W^h{}_k + \sum_\alpha \dot{\lambda}_\alpha\left[\frac{\partial \hat{\mathcal{V}}^\alpha}{\partial \dot{q}^k} \circ \natural\right] = -\mathcal{Q}_k, \qquad k = 1,\dots,n, \tag{2.59a}$$

$$-\hat{\mathcal{V}}^\alpha \circ \natural = 0, \qquad \alpha = 1,\dots,m, \tag{2.59b}$$

with $p_{0h} \coloneqq \partial_{\dot{q}^h}\hat{\mathcal{L}}_0 \circ \natural = \sum_{\ell=1}^{n}[\hat{G}_{h\ell} \circ (q,\tau)]\dot{q}^\ell$. This last result, which stipulates that the momenta are linear functions of the velocities, has deep repercussions on the fulfillment of conditions (2.55a) and (2.55b), with p_0 substituting p. More details on this issue will be discussed in Remark 3.5 of Section 3.2.3 for the specific case of the "charged skate".

Appendix A

Some geometric insight on the variations taken in the MVM

The content of this appendix is taken from the appendix of [1].

The scope of this appendix is to put the variations characterizing the MVM within the context of Differential Geometry. We start combining Jóźwikowski&Respondek's formalism [52], which implements the framework established by Gràcia et al. [53], with ours. In doing this, however, for the sake of simplicity, we consider here only constraints of the type $\hat{\mathcal{V}}^\alpha \circ (q, \dot{q}) = [\hat{a}^\alpha{}_k \circ q]\dot{q}^k = 0$, i.e., that do not depend explicitly on time. We denote by $\gamma := (q, \dot{q}) : [t_{\text{in}}, t_{\text{fin}}] \to T\mathscr{C}$ a *"path"* [52], identified with the *"tangent lift"* [52] of q at t, i.e., $\gamma(t) \equiv \mathrm{T}_t q(t) = (q(t), \dot{q}(t))$. In terms of $\tilde{q} : [t_{\text{in}}, t_{\text{fin}}] \times]-\varepsilon_0, +\varepsilon_0[\to \mathscr{C}$ (see Equation (2.6a)), we also define $\tilde{\gamma} := (\tilde{q}, \partial_t \tilde{q}) \equiv \mathrm{T}_t \tilde{q} : [t_{\text{in}}, t_{\text{fin}}] \times]-\varepsilon_0, +\varepsilon_0[\to T\mathscr{C}$, so that the chain of equalities

$$\gamma(t) = (q(t), \dot{q}(t)) = (\tilde{q}(t, 0), \partial_t \tilde{q}(t, 0)) = \mathrm{T}_t \tilde{q}(t, 0) = \tilde{\gamma}(t, 0) \tag{A.1}$$

applies. Moreover, by differentiating $\tilde{q}$ with respect to ε, and evaluating the result at $\varepsilon = 0$, we obtain, for each $t \in [t_{\text{in}}, t_{\text{fin}}]$, the quantity (see [52])

$$\xi(t) := \mathrm{T}_\varepsilon \tilde{q}(t, 0) = (\tilde{q}(t, 0), \partial_\varepsilon \tilde{q}(t, 0)) \equiv (q(t), \boldsymbol{\eta}_q(t)), \tag{A.2}$$

in which the identification $\boldsymbol{\eta}_q(t) \equiv \partial_\varepsilon \tilde{q}(t, 0) \in T_{q(t)}\mathscr{C}$ has been made by virtue of Equation (2.8a). Looking at the structure of $\xi(t)$, we notice that the second tangent bundle formalism arises naturally by iterating the operation of tangent lift, i.e., by

computing the tangent lift of ξ, which yields

$$\mathrm{T}_t\xi(t) = (q(t), \boldsymbol{\eta}_q(t), \dot{q}(t), \dot{\boldsymbol{\eta}}_q(t)) \in TT\mathscr{C}. \tag{A.3}$$

Finally, following [52], we compute the quantity

$$\begin{aligned}\mathrm{T}_\varepsilon\tilde{\gamma}(t,0) = \mathrm{T}_\varepsilon\mathrm{T}_t\tilde{q}(t,0) &= (q(t), \dot{q}(t), \partial_\varepsilon\tilde{q}(t,0), \partial_\varepsilon\partial_t\tilde{q}(t,0)) \\ &= (q(t), \dot{q}(t), \boldsymbol{\eta}_q(t), \dot{\boldsymbol{\eta}}_q(t)) \in TT\mathscr{C},\end{aligned} \tag{A.4}$$

thereby recovering the identity $\mathrm{T}_\varepsilon\tilde{\gamma}(t,0) = \kappa_{\mathscr{C}}(\mathrm{T}_t\xi(t))$, where the map $\kappa_{\mathscr{C}} : TT\mathscr{C} \to TT\mathscr{C}$ is referred to as *"canonical flip"* in [57, 52], since it changes the position of the entries of the second and third slots of the elements of $TT\mathscr{C}$. In the jargon adopted in [57, 52], the quantity $\mathrm{T}_\varepsilon\tilde{\gamma}(t,0)$ is referred to as *"natural variation"* and is also denoted by $\delta_\xi\gamma(t) \equiv \mathrm{T}_\varepsilon\tilde{\gamma}(t,0)$ to highlight that the natural variation is *generated* by $\xi(t)$ through the canonical flip.

In analogy with the reasoning leading to Equation (A.1), and with the purpose of putting the approach of Llibre et al. [16] in the language used in [52], we also define the pair $\tilde{\sigma} \coloneqq (\tilde{q}, \tilde{\boldsymbol{\nu}}) : [t_{\mathrm{in}}, t_{\mathrm{fin}}]\times\,]-\varepsilon_0, +\varepsilon_0[\to T\mathscr{C}$, where we require $\tilde{\boldsymbol{\nu}}$ to satisfy the condition $\tilde{\boldsymbol{\nu}}(t,0) = \dot{q}(t)$, for $t \in [t_{\mathrm{in}}, t_{\mathrm{fin}}]$ (see Equation (2.6b)). Hence, we compute $\mathrm{T}_\varepsilon\tilde{\sigma}(t,0)$, thereby obtaining

$$\begin{aligned}\mathrm{T}_\varepsilon\tilde{\sigma}(t,0) &= (\tilde{q}(t,0), \tilde{\boldsymbol{\nu}}(t,0), \partial_\varepsilon\tilde{q}(t,0), \partial_\varepsilon\tilde{\boldsymbol{\nu}}(t,0)) \\ &= (q(t), \dot{q}(t), \boldsymbol{\eta}_q(t), \boldsymbol{\eta}_{\dot{q}}(t)) \in TT\mathscr{C}, \quad \text{with } \boldsymbol{\eta}_{\dot{q}}(t) \coloneqq \partial_\varepsilon\tilde{\boldsymbol{\nu}}(t,0).\end{aligned} \tag{A.5}$$

The quantity $\mathrm{T}_\varepsilon\tilde{\sigma}(t,0)$ in Equation (A.5) defines a generic variation. To specify such variation for the MVM, we need to impose the following conditions:

(a) The path $(q, \dot{q})$ must satisfy the m given constraints $\hat{\mathcal{V}}^\alpha(q(t), \dot{q}(t)) = 0$, with $\alpha = 1, \ldots, m$, at all times, so that the pair $(q(t), \dot{q}(t))$ belongs to $T\mathscr{C}_{\mathrm{c}}$, defined in Equation (2.1).

(b) The pair $(q, \boldsymbol{\eta}_q) \in T\mathscr{C}$ is compelled to fulfill Lagrange–Chetaev's conditions (2.12), which, for $\alpha = 1, \ldots, m$, here become

$$[\partial_{\dot{q}}\hat{\mathcal{V}}^\alpha(q(t), \dot{q}(t))]\boldsymbol{\eta}_q(t) \equiv [\partial_{\dot{q}^k}\hat{\mathcal{V}}^\alpha(q(t), \dot{q}(t))]\eta_q^k(t) = 0. \tag{A.6}$$

(c) As specified in [16], for every $t \in [t_{\text{in}}, t_{\text{fin}}]$, the vector $\boldsymbol{\eta}_{\dot{q}}(t)$ is required to satisfy the constraints *at the first order in* ε. Thus, upon defining the functions $\tilde{\mathcal{V}}^{\alpha} : [t_{\text{in}}, t_{\text{fin}}] \times]-\varepsilon_0, +\varepsilon_0[\to \mathbb{R}$, such that $\tilde{\mathcal{V}}^{\alpha}(t, \varepsilon) := \hat{\mathcal{V}}^{\alpha}(\tilde{q}(t, \varepsilon), \tilde{\boldsymbol{v}}(t, \varepsilon))$, and $\tilde{\mathcal{V}}^{\alpha}(t, 0) \equiv \hat{\mathcal{V}}^{\alpha}(q(t), \dot{q}(t)) = 0$, for all $\alpha = 1, \ldots, m$ and for all $t \in [t_{\text{in}}, t_{\text{fin}}]$ (see Equations (2.9) and (2.10)), we write

$$\tilde{\mathcal{V}}^{\alpha}(t, \varepsilon) = \underbrace{\tilde{\mathcal{V}}^{\alpha}(t, 0)}_{=0} + \partial_{\varepsilon}\tilde{\mathcal{V}}^{\alpha}(t, 0)\varepsilon + o(\varepsilon), \qquad \varepsilon \to 0, \tag{A.7}$$

and we set $\partial_{\varepsilon}\tilde{\mathcal{V}}^{\alpha}(t, 0) = 0$, thereby obtaining Equation (2.11), i.e.,

$$0 = \partial_{\varepsilon}\tilde{\mathcal{V}}^{\alpha}(t, 0) = \frac{\partial \hat{\mathcal{V}}^{\alpha}}{\partial q^{k}}(q(t), \dot{q}(t))\eta_{q}^{k}(t) + \frac{\partial \hat{\mathcal{V}}^{\alpha}}{\partial \dot{q}^{k}}(q(t), \dot{q}(t))\eta_{\dot{q}}^{k}(t). \tag{A.8}$$

Equation (A.8), which characterizes the vakonomic variations, can be also worked out further as

$$\begin{aligned}
0 &= \left[\frac{\partial \hat{\mathcal{V}}^{\alpha}}{\partial q^{k}} \circ (q, \dot{q})\right]\eta_{q}^{k} + \left[\frac{\partial \hat{\mathcal{V}}^{\alpha}}{\partial \dot{q}^{k}} \circ (q, \dot{q})\right][\eta_{\dot{q}}^{k} - \dot{\eta}_{q}^{k}] + \left[\frac{\partial \hat{\mathcal{V}}^{\alpha}}{\partial \dot{q}^{k}} \circ (q, \dot{q})\right]\dot{\eta}_{q}^{k} \\
&= \left[\mathcal{E}_{k}\hat{\mathcal{V}}^{\alpha} \circ (q, \dot{q}, \ddot{q})\right]\eta_{q}^{k} + \left[\frac{\partial \hat{\mathcal{V}}^{\alpha}}{\partial \dot{q}^{k}} \circ (q, \dot{q})\right][\eta_{\dot{q}}^{k} - \dot{\eta}_{q}^{k}] + \frac{\mathrm{d}}{\mathrm{d}t}\left\{\left[\frac{\partial \hat{\mathcal{V}}^{\alpha}}{\partial \dot{q}^{k}} \circ (q, \dot{q})\right]\eta_{q}^{k}\right\} \\
&= \left[\mathcal{E}_{k}\hat{\mathcal{V}}^{\alpha} \circ (q, \dot{q}, \ddot{q})\right]\eta_{q}^{k} + \left[\frac{\partial \hat{\mathcal{V}}^{\alpha}}{\partial \dot{q}^{k}} \circ (q, \dot{q})\right][\eta_{\dot{q}}^{k} - \dot{\eta}_{q}^{k}],
\end{aligned} \tag{A.9}$$

with

$$\mathcal{E}_{k}\hat{\mathcal{V}}^{\alpha} \circ (q, \dot{q}, \ddot{q}) := \frac{\partial \hat{\mathcal{V}}^{\alpha}}{\partial q^{k}} \circ (q, \dot{q}) - \frac{\mathrm{d}}{\mathrm{d}t}\left[\frac{\partial \hat{\mathcal{V}}^{\alpha}}{\partial \dot{q}^{k}} \circ (q, \dot{q})\right], \tag{A.10}$$

and the last summand of Equation (A.9) being null by virtue of Lagrange–Chetaev's conditions (cf. Equation (A.9) with Equation (2.14): They are the same for nonholonomic constraints linear in the velocities and not depending explicitly on time).

With all the premises specified above, the set of the variations characterizing the MVM can be defined as:

$$\begin{aligned}
\mathscr{W}_{\text{c}}^{\text{MVM}} := \{&\mathrm{T}_{\varepsilon}\tilde{\sigma}(t, 0) \in TT\mathscr{C} |\ (q(t), \dot{q}(t)) \in T\mathscr{C}_{\text{c}},\ \ (q(t), \boldsymbol{\eta}_{q}(t)) \in T\mathscr{C}_{\text{c}}, \\
&\boldsymbol{\eta}_{\dot{q}}(t) |\ \partial_{\varepsilon}\tilde{\mathcal{V}}^{\alpha}(t, 0) = 0\}.
\end{aligned} \tag{A.11}$$

Note that, as written in Section 2.2.1, in Equation (A.9) we *guess* (this is, in fact, an educated guess, since we are aware of the existence of the transpositional relations) that $\eta^k_{\dot{q}} - \dot{\eta}^k_q$ can be expressed in terms of the linear transformation $\eta^k_{\dot{q}} - \dot{\eta}^k_q = W^k{}_\ell \eta^\ell_q$, in which $[W^k{}_\ell]^{k=1,\dots,n}_{\ell=1,\dots,n}$ are the coefficients of a *partially* unknown matrix W. Indeed, if the matrix made by the derivatives $\partial_{\dot{q}^k} \hat{\mathcal{V}}^\alpha \circ (q, \dot{q})$ were square (it is rectangular, here), the coefficients of W could be determined from Equation (A.9) by solving for $\eta^k_{\dot{q}} - \dot{\eta}^k_q$. However, this matrix can be made square by introducing suitable quasi-velocities, as is done in the standard procedure leading to the transpositional relations (see e.g. [13, 30] and cf. Equation (2.17)). This is, to our understanding, the philosophy underlying the approach proposed by Llibre et al. [16], whose main objective is to put the nonholonomic constraints in the variational framework, but with variations that *are not* only vakonomic, but both vakonomic and complying with Lagrange-Chetaev's conditions.

Finally, if the further identification $W^k{}_\ell \equiv \mathcal{C}^k{}_{h\ell} \dot{q}^h$ is made, where $\mathcal{C}^k{}_{h\ell}$ are the coefficients of the third-order tensor field defined in [57, 52], or in [13] (see Remark 2.2.3), and that characterizes the transpositional relations, then, in the formalism of [52], $\mathrm{T}_\varepsilon \tilde{\sigma}(t, 0)$ can be rewritten as

$$\mathrm{T}_\varepsilon \tilde{\sigma}(t, 0) = (q^a(t), \dot{q}^b(t), \eta^c_q(t), \underbrace{\dot{\eta}^d_q(t) + \mathcal{C}^d{}_{k\ell}(q(t)) \dot{q}^k(t) \eta^\ell_q(t))}_{\equiv \eta^d_{\dot{q}}(t)}. \tag{A.12}$$

Before closing this appendix, we remark that one crucial difference between the MVM and the VM is that, while the MVM is formulated by accounting explicitly for the *transpositional relations*, the VM is developed without even introducing such relations [41–44, 59, 16].

Chapter 3

Comparing the MVM with the TNHM over two benchmark problems

The content of this chapter is taken from [1].

The introduction of new methods that are, in a sense, ground-breaking, since they question the pillars of the standard variational procedures, requires them to be tested against the more traditional ones. This, indeed, has been done quite intensively by having recourse to widely studied and easy-to-reproduce "benchmark" problems, all encoded in the classical literature of Analytical Mechanics (see e.g. [13, 26, 51, 15, 50, 27, 52, 54–56, 58, 68]). Typical examples are a ball rolling over a moving or fixed surface [51, 26, 50], a skate moving on an inclined or horizontal plane [16, 27, 26], a disk rolling on an inclined plane [54–56, 40, 17, 52], and a two-wheeled carriage moving on a plane [51, 54, 56, 68, 52]. In spite of the fact that these case studies were formulated many years ago, and can be found in textbooks, they remain up-to-date (see e.g. [39, 21, 27, 31, 7, 59, 52], and, more recently, [16, 17]), since they are archetypal and, thus, serve as a reference even for much more complex physical situations in which the constraints can be reconducted to those characterizing the original case studies.

Granted all this, the scope of this chapter is twofold:

(i) To add a methodological note to the paper recently published by Lemos [17] by proving that the MVM and the TNHM are in agreement with each other for the "Rolling coin" problem [40, 17].

(ii) To apply the procedure developed in [59, 16] to a variant of the “Non-holonomic skate” presented in [16]. Specifically, we consider a nonholonomic and *electrically charged* skate interacting with an imposed magnetic field, and we show that, for this problem, if the MVM is formulated according to the first *path*, it is not equivalent to the TNHM. The second *path* is equivalent to the TNHM, but, *for our problem*, it is inconsistent with the first *path*. For our purposes, we generalize a benchmark taken from [25].

Outline of the content of Chapter 3. The “rolling coin” [15, 40, 17] and the “charged skate” [25, 16] benchmark problems are examined by means of both the MVM and the TNHM, as seen in Section 3.1 and Section 3.2, respectively. More specifically, a fully analytical resolution of the “rolling coin” problem is presented in Section 3.1.3, while in Section 3.2.2, and in the three subsequent sections, three possible choices of the collection of auxiliary functions are tested and discussed for the “charged skate” problem.

3.1 The “rolling coin” benchmark

In this section, we compute analytically the MVM equations of motion for the benchmark problem of the “rolling coin”, recently presented in [40, 17], and adopted as a *benchmark* for comparing the VM and the TNHM in [54–56, 52].

The mechanical system that we are considering is composed by a coin, hereafter denoted by $\mathfrak{C}$, idealized as a bi-dimensional rigid disk of radius R and mass m, that can roll without slipping over a plane inclined of an angle $\alpha \in]0, \pi/2[$ with respect to a horizontal plane. A graphical representation of $\mathfrak{C}$ is reported in Figure 3.1.

As done in [40, 17], we specify a coordinate system $\{O, (x, y, z)\}$ in which the y-axis is parallel to the inclined plane and is aligned along the direction of steepest descent; the z-axis “enters” the inclined plane and is orthogonal to it; the x-axis is such that the x-, y-, and z-axis form a right-handed triad, whose origin O is a point having the same z coordinate as the center of mass of $\mathfrak{C}$, hereafter denoted by G. Moreover, similarly to [40], we introduce the coordinates of G, i.e., $(x_G, y_G, 0)$; the angle of rolling, ϕ, taken clockwise from the z-axis; and the angle θ between the y-axis and the axis along which rolling occurs. Note that x_G, y_G, ϕ, and θ are the

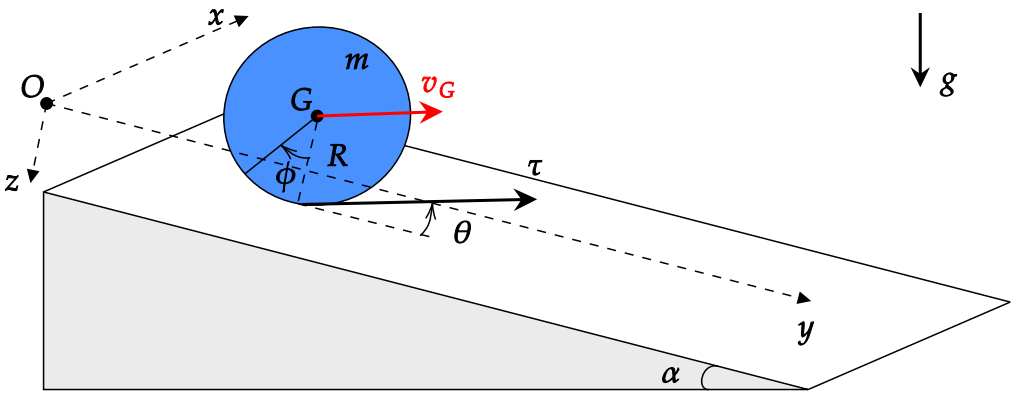

Fig. 3.1 Graphical representation of the "rolling coin" benchmark problem. This image was first showed during the conference "3rd International Conference on Nonlinear Solid Mechanics (ICoNSoM 2024)" held in Cagliari, Italy, on June 11-14, 2024, within the presentation of the abstract "A review on some "analytical" aspects of nonholonomic mechanics", authored by A. Pastore, A. Giammarini, A. Grillo.

Lagrangian parameters of the mechanical system under study, and are thus intended as functions of time, defined over the interval of observation $[t_{\text{in}}, t_{\text{fin}}]$.

From here on, the identification $q \equiv (q^1, q^2, q^3, q^4) = (x_G, y_G, \phi, \theta)$ is made, which implies that the system satisfies automatically two holonomic constraints: one requires G to experience only motions parallel to the inclined plane; the other one prescribes that the coin $\mathfrak{C}$ remains orthogonal to the inclined plane during its entire motion.

If gravity is the only interaction accounted for, the Lagrangian function of the mechanical system under study reads [17, 40, 13]

$$\hat{\mathcal{L}} \circ (q, \dot{q}) = \underbrace{\tfrac{1}{2}m\left[(\dot{q}^1)^2 + (\dot{q}^2)^2 + \tfrac{1}{2}R^2(\dot{q}^3)^2 + \tfrac{1}{4}R^2(\dot{q}^4)^2\right]}_{\hat{\mathcal{K}} \circ \dot{q}} + \underbrace{(mg\,\sin\alpha)q^2}_{\hat{\mathcal{U}} \circ q}, \tag{3.1}$$

where $\mathcal{K} \equiv \hat{\mathcal{K}} \circ \dot{q}$ is the kinetic energy; $\mathcal{U} \equiv \hat{\mathcal{U}} \circ q$ is the gravitational potential; and g denotes the magnitude of the gravitational acceleration.

The assumption that the coin *"rolls without slipping"* [40, 17] determines $m = 2$ nonholonomic constraints given by [13, 54–56, 68, 52]

$$\mathcal{V}^1 \equiv \hat{\mathcal{V}}^1 \circ (q, \dot{q}) := \dot{q}^1 - R\dot{q}^3\,\sin q^4 = 0, \tag{3.2a}$$

$$\mathcal{V}^2 \equiv \hat{\mathcal{V}}^2 \circ (q, \dot{q}) \coloneqq \dot{q}^2 - R\dot{q}^3 \cos q^4 = 0. \tag{3.2b}$$

Note that, by indicating with $\boldsymbol{\tau} = \sin\theta\, \boldsymbol{e}_x + \cos\theta\, \boldsymbol{e}_y$ the unit vector defining the direction of rolling, Equations (3.2a) and (3.2b) express, in terms of the Lagrangian parameters of the model and their derivatives, the fact that the velocity of the coin's center of mass, $\boldsymbol{v}_G$, satisfies the condition $\boldsymbol{v}_G = R\dot{\phi}\boldsymbol{\tau}$, given in the physical space.

3.1.1 The traditional nonholonomic approach

In the benchmark that we are analyzing, the dynamic equations of the TNHM, namely Equations (2.52a) and (2.52b), admit the expressions [40, 17, 54–56, 68, 52]

$$-m\ddot{q}^1 + \mu_1 = 0, \tag{3.3a}$$

$$mg\sin\alpha - m\ddot{q}^2 + \mu_2 = 0, \tag{3.3b}$$

$$-\tfrac{1}{2}mR^2\ddot{q}^3 - \mu_1 R\sin q^4 - \mu_2 R\cos q^4 = 0, \tag{3.3c}$$

$$-\tfrac{1}{4}mR^2\ddot{q}^4 = 0. \tag{3.3d}$$

As shown in [17], Equations (3.3a)–(3.3d) can be solved analytically by exploiting the direct integrability of Equation (3.3d), so we will not further investigate this solution.

3.1.2 The Modified Vakonomic approach

In this section, we study the benchmark problem introduced above by means of the MVM [16], thereby determining the motion from the dynamic equations (2.42a) and (2.42b) in compliance with the *solvability conditions* (2.40a) and (2.40b).

By applying the Euler–Lagrange operators defined in Equation (2.28a) to the Lagrangian function in Equation (3.1), we obtain

$$\mathcal{E}_1\hat{\mathcal{L}} \circ \sharp = -m\ddot{q}^1, \tag{3.4a}$$

$$\mathcal{E}_2\hat{\mathcal{L}} \circ \sharp = -m\ddot{q}^2 + mg\sin\alpha, \tag{3.4b}$$

$$\mathcal{E}_3\hat{\mathcal{L}} \circ \sharp = -\tfrac{1}{2}mR^2\ddot{q}^3, \tag{3.4c}$$

$$\mathcal{E}_4\hat{\mathcal{L}} \circ \sharp = -\tfrac{1}{4}mR^2\ddot{q}^4. \tag{3.4d}$$

Furthermore, we write explicitly the differential operators in Equation (2.34) for the expressions of the two constraints in (3.2a) and (3.2b), respectively. Hence, for $\alpha = 1$, we have

$$\mathcal{D}_1\hat{\mathcal{V}}^1 \circ \sharp = W^1{}_1 - (R\sin q^4)W^3{}_1 = 0, \tag{3.5a}$$
$$\mathcal{D}_2\hat{\mathcal{V}}^1 \circ \sharp = W^1{}_2 - (R\sin q^4)W^3{}_2 = 0, \tag{3.5b}$$
$$\mathcal{D}_3\hat{\mathcal{V}}^1 \circ \sharp = W^1{}_3 - (R\sin q^4)W^3{}_3 + (R\cos q^4)\dot{q}^4 = 0, \tag{3.5c}$$
$$\mathcal{D}_4\hat{\mathcal{V}}^1 \circ \sharp = W^1{}_4 - (R\sin q^4)W^3{}_4 - (R\cos q^4)\dot{q}^3 = 0, \tag{3.5d}$$

while, for $\alpha = 2$, we obtain

$$\mathcal{D}_1\hat{\mathcal{V}}^2 \circ \sharp = W^2{}_1 - (R\cos q^4)W^3{}_1 = 0, \tag{3.6a}$$
$$\mathcal{D}_2\hat{\mathcal{V}}^2 \circ \sharp = W^2{}_2 - (R\cos q^4)W^3{}_2 = 0, \tag{3.6b}$$
$$\mathcal{D}_3\hat{\mathcal{V}}^2 \circ \sharp = W^2{}_3 - (R\cos q^4)W^3{}_3 - (R\sin q^4)\dot{q}^4 = 0, \tag{3.6c}$$
$$\mathcal{D}_4\hat{\mathcal{V}}^2 \circ \sharp = W^2{}_4 - (R\cos q^4)W^3{}_4 + (R\sin q^4)\dot{q}^3 = 0. \tag{3.6d}$$

By choosing the arbitrary *auxiliary functions* as [59, 16]

$$\mathcal{F}^3 \equiv \hat{\mathcal{F}}^3 \circ \natural := \dot{q}^3, \tag{3.7a}$$
$$\mathcal{F}^4 \equiv \hat{\mathcal{F}}^4 \circ \natural := \dot{q}^4, \tag{3.7b}$$

Equation (2.35), for $\beta = 3$ and $\beta = 4$, implies that

$$\mathcal{D}_k\hat{\mathcal{F}}^3 \circ \sharp = W^3{}_k = 0, \qquad k = 1, \ldots, 4, \tag{3.8a}$$
$$\mathcal{D}_k\hat{\mathcal{F}}^4 \circ \sharp = W^4{}_k = 0, \qquad k = 1, \ldots, 4. \tag{3.8b}$$

We can represent the coefficients $W^h{}_k$ in a more compact way by assembling the 4×4 matrix W that, by having recourse to Equations (3.5a)–(3.5d), (3.6a)–(3.6d), and (3.8a) and (3.8b), is given by

$$\mathsf{W} = \begin{bmatrix} 0 & 0 & -(R\cos q^4)\dot{q}^4 & (R\cos q^4)\dot{q}^3 \\ 0 & 0 & (R\sin q^4)\dot{q}^4 & -(R\sin q^4)\dot{q}^3 \\ 0 & 0 & 0 & 0 \\ 0 & 0 & 0 & 0 \end{bmatrix}. \tag{3.9}$$

Our choice of the auxiliary functions in Equations (3.7a) and (3.7b) is done in compliance with Remark 2.2.2, since, by inspection of the constraints (3.2a) and (3.2b), the generalized velocities $\dot{q}^3$ and $\dot{q}^4$ are *independent*, thereby leading to the vanishing of the corresponding transpositional relations $\eta^3_{\dot{q}} - \dot{\eta}^3_q$ and $\eta^4_{\dot{q}} - \dot{\eta}^4_q$. In fact, this choice is a *strong* way of guaranteeing this result because the conditions (3.8a) and (3.8b), implied by the selected auxiliary functions, ensure that the third and fourth row of W are null.

Finally, if we substitute Equations (3.4a)–(3.4d) and the coefficients collected in Equation (3.9) into the Euler–Lagrange equations of the MVM written in (2.42a), we can recast Equations (2.42a) and (2.42b) in the form

$$m\ddot{q}^1 - \dot{\lambda}_1 = 0, \tag{3.10a}$$

$$m\ddot{q}^2 - \dot{\lambda}_2 = mg\sin\alpha, \tag{3.10b}$$

$$\tfrac{1}{2}mR^2\ddot{q}^3 + \dot{\lambda}_1 R\sin q^4 + \dot{\lambda}_2 R\cos q^4 = -mR(\dot{q}^1\cos q^4 - \dot{q}^2\sin q^4)\dot{q}^4, \tag{3.10c}$$

$$\tfrac{1}{4}mR^2\ddot{q}^4 = mR(\dot{q}^1\cos q^4 - \dot{q}^2\sin q^4)\dot{q}^3, \tag{3.10d}$$

$$\dot{q}^1 = R\dot{q}^3\sin q^4, \tag{3.10e}$$

$$\dot{q}^2 = R\dot{q}^3\cos q^4. \tag{3.10f}$$

Before going further, we notice that the quantity $\dot{q}^1\cos q^4 - \dot{q}^2\sin q^4$, which features both in Equations (3.10c) and (3.10d), is none other than the component along the axis $\boldsymbol{e}_z$ of the cross product $\boldsymbol{v}_G \times \boldsymbol{\tau}$, which is null because the velocity of the center of mass of the coin has to be parallel to the unit vector $\boldsymbol{\tau}$. In particular, it should be noticed that this condition is naturally satisfied by the constraint of rolling without slipping, but it is, in fact, more general than the latter, since it expresses a merely geometric fact. In conclusion, it applies that [13]

$$(\boldsymbol{v}_G \times \boldsymbol{\tau}) \cdot \boldsymbol{e}_z = \dot{q}^1\cos q^4 - \dot{q}^2\sin q^4 = 0. \tag{3.11}$$

By virtue of this result, Equations (3.10a)–(3.10f) become

$$m\ddot{q}^1 - \dot{\lambda}_1 = 0, \tag{3.12a}$$

$$m\ddot{q}^2 - \dot{\lambda}_2 = mg\sin\alpha, \tag{3.12b}$$

$$\tfrac{1}{2}mR^2\ddot{q}^3 + \dot{\lambda}_1 R\sin q^4 + \dot{\lambda}_2 R\cos q^4 = 0, \tag{3.12c}$$

$$\tfrac{1}{4}mR^2\ddot{q}^4 = 0. \tag{3.12d}$$

$$\dot{q}^1 = R\dot{q}^3 \sin q^4, \tag{3.12e}$$
$$\dot{q}^2 = R\dot{q}^3 \cos q^4. \tag{3.12f}$$

By making the identifications $\mu_\alpha \equiv \dot{\lambda}_\alpha$, for $\alpha = 1, \ldots, m$, the set of equations (3.12a)–(3.12d) is equal to the set of dynamic equations obtained within the TNHM, i.e. Equations (3.3a)–(3.3d). This shows that, in agreement with [16], the MVM is indeed *equivalent* with the TNHM for the "rolling coin" problem.

Remark 3.1 (The MVM and the TNHM for the "rolling coin" problem). It should be noticed that the equivalence between the MVM and the TNHM, and the identification between their respective Lagrange multipliers, could have been proven in advance since, in the case considered above, the matrix W in Equation (3.9) and the array of momenta p satisfy the hypothesis of Corollary 2.1, namely $\mathsf{W}^{\mathrm{T}}\mathsf{p} = \mathsf{0}$.

Remark 3.2 (*"Canonical flip"* [57, 52] for the "rolling coin" problem). Looking at the structure of the matrix W featuring in Equation (3.9), and computing the quantities $\eta^h_{\dot{q}} - \dot{\eta}^h_q$, with $h = 1, \ldots, n$, once as $\eta^h_{\dot{q}} - \dot{\eta}^h_q = \sum_{k=1}^n W^h{}_k \eta^k_q$ and once as $\eta^h_{\dot{q}} - \dot{\eta}^h_q = \sum_{\ell,k=1}^n \mathcal{C}^h{}_{\ell k} \dot{q}^\ell \eta^k_q$ (cf. Equation (2.21)), we can choose

$$\mathcal{C}^1{}_{43}\dot{q}^4 = W^1{}_3 = -(R\cos q^4)\dot{q}^4 \quad \Rightarrow \quad \mathcal{C}^1{}_{43} \equiv \hat{\mathcal{C}}^1{}_{43} \circ q = -R\cos q^4, \tag{3.13a}$$
$$\mathcal{C}^1{}_{34}\dot{q}^3 = W^1{}_4 = +(R\cos q^4)\dot{q}^3 \quad \Rightarrow \quad \mathcal{C}^1{}_{34} \equiv \hat{\mathcal{C}}^1{}_{34} \circ q = +R\cos q^4, \tag{3.13b}$$
$$\mathcal{C}^2{}_{43}\dot{q}^4 = W^2{}_3 = +(R\sin q^4)\dot{q}^4 \quad \Rightarrow \quad \mathcal{C}^2{}_{43} \equiv \hat{\mathcal{C}}^2{}_{43} \circ q = +R\sin q^4, \tag{3.13c}$$
$$\mathcal{C}^2{}_{34}\dot{q}^3 = W^2{}_4 = -(R\sin q^4)\dot{q}^3 \quad \Rightarrow \quad \mathcal{C}^2{}_{34} \equiv \hat{\mathcal{C}}^2{}_{34} \circ q = -R\sin q^4, \tag{3.13d}$$

while all the other entries of $\mathcal{C}^h{}_{\ell k}$ can be set equal to zero. We notice that, in the case studied in this remark, the nonzero entries of $\mathcal{C}^h{}_{\ell k}$, reported in Equations (3.13a)–(3.13d), depend on q, and, in particular, on q^4, only.

3.1.3 Analytical solution of the Modified Vakonomic Method

In this section, we are interested in finding an analytical solution to the dynamical equations previously obtained within the MVM, i.e., Equations (3.12a)–(3.12d). To this end, we introduce the following set of initial conditions, i.e., at $t = t_{\mathrm{in}}$, for the generalized coordinates and velocities:

$$q^1(t_{\mathrm{in}}) = q^1_{\mathrm{in}}, \qquad q^2(t_{\mathrm{in}}) = q^2_{\mathrm{in}}, \qquad q^3(t_{\mathrm{in}}) = q^3_{\mathrm{in}}, \qquad q^4(t_{\mathrm{in}}) = q^4_{\mathrm{in}}, \tag{3.14a}$$

$$\dot{q}^1(t_{\text{in}}) = v^1_{\text{in}}, \qquad \dot{q}^2(t_{\text{in}}) = v^2_{\text{in}}, \qquad \dot{q}^3(t_{\text{in}}) = v^3_{\text{in}}, \qquad \dot{q}^4(t_{\text{in}}) = v^4_{\text{in}}, \tag{3.14b}$$

where their specified values q^k_{in} and v^k_{in}, for $k = 1, \dots, 4$, should satisfy the constraints in Equations (3.10e) and (3.10f), both for physical and for numerical consistency [27]. Furthermore, we introduce the initial values for the multipliers

$$\lambda_1(t_{\text{in}}) = \lambda_{1\,\text{in}}, \qquad \lambda_2(t_{\text{in}}) = \lambda_{2\,\text{in}}. \tag{3.15}$$

By taking inspiration from the solution strategy employed by Lemos [17], from the direct integration of Equation (3.12d) we obtain that q^4 is *affine* in time, that is

$$q^4(t) = \Omega[t - t_{\text{in}}] + q^4_{\text{in}} = \Omega t + \theta_0, \qquad \forall\, t \in [t_{\text{in}}, t_{\text{fin}}], \tag{3.16}$$

where $\Omega \coloneqq \dot{q}^4(t) \equiv \dot{q}^4(t_{\text{in}}) = v^4_{\text{in}}$ for all $t \in [t_{\text{in}}, t_{\text{fin}}]$, and, for a better readability, we write $\theta_0 \coloneqq q^4_{\text{in}} - \Omega t_{\text{in}}$. Note that the angular velocity $\dot{q}^4(t) = \Omega$ is constant in time.

We can exploit the *saddle-point nature* of the system of equations under study by decoupling the dynamic equations (3.12a)–(3.12d) from the constraints, i.e., (3.12e) and (3.12f), so that the latter ones can be computed *a posteriori*. Hence, by substituting the constraints in (3.12e) and (3.12f) into Equations (3.12a) and (3.12b), we obtain

$$\dot{\lambda}_1 = m\ddot{q}^3 R \sin q^4 + m\dot{q}^3\dot{q}^4 R \cos q^4, \tag{3.17a}$$

$$\dot{\lambda}_2 = m\ddot{q}^3 R \cos q^4 - m\dot{q}^3\dot{q}^4 R \sin q^4 - mg \sin\alpha. \tag{3.17b}$$

With the expressions obtained in Equations (3.17a) and (3.17b) for the two time derivatives of the Lagrange multipliers, and with the expression of q^4 in Equation (3.16), we can re-frame Equation (3.12c) as follows

$$\ddot{q}^3(t) = \frac{2g \sin\alpha}{3R} \cos(\Omega t + \theta_0). \tag{3.18}$$

In the following, we introduce, for each $k = 1, \dots, 4$ and for each $\alpha = 1, 2$, the notations $q^k(t) \equiv \hat{q}^k(t; \Omega)$ and $\lambda_\alpha(t) \equiv \hat{\lambda}_\alpha(t; \Omega)$ in order to emphasize the dependence of the solution of the system under study on the parameter Ω. In particular, depending on the value of Ω, we can distinguish two cases.

Case 1. By assuming $\Omega \neq 0$, the right-hand side of Equation (3.18) represents an oscillatory forcing term with angular frequency Ω and initial phase θ_0. By integrating Equation (3.18), we obtain

$$q^3(t) \equiv \hat{q}^3(t;\Omega) = \hat{q}^3_{\text{osc}}(t;\Omega) + \nu^3_{\text{in}}[t - t_{\text{in}}] + q^3_{\text{in}}, \tag{3.19}$$

where we have introduced the auxiliary notation

$$\begin{aligned}\hat{q}^3_{\text{osc}}(t;\Omega) \coloneqq{}& \Phi_{\text{s}}(\Omega)\big\{\sin(\Omega t) - \sin(\Omega t_{\text{in}})\big\} - \Phi_{\text{c}}(\Omega)\big\{\cos(\Omega t) - \cos(\Omega t_{\text{in}})\big\} \\ &- \Omega[t - t_{\text{in}}]\big\{\Phi_{\text{c}}(\Omega)\sin(\Omega t_{\text{in}}) + \Phi_{\text{s}}(\Omega)\cos(\Omega t_{\text{in}})\big\}, \qquad (3.20\text{a})\\ \Phi(\Omega) \coloneqq{}& \frac{2g\sin\alpha}{3R\Omega^2}, \quad \Phi_{\text{c}}(\Omega) \coloneqq \Phi(\Omega)\cos\theta_0, \quad \Phi_{\text{s}}(\Omega) \coloneqq \Phi(\Omega)\sin\theta_0. \qquad (3.20\text{b})\end{aligned}$$

Note that, by virtue of Equation (3.19), the Lagrangian parameter $q^3(t)$ features an oscillatory contribution, given by Equation (3.20a), which is characterized by the amplitude $\Phi(\Omega)$ in Equation (3.20b), and a contribution that is affine in time, i.e., $\nu^3_{\text{in}}[t - t_{\text{in}}] + q^3_{\text{in}}$. Moreover, by differentiating in time Equation (3.20a), one obtains

$$\begin{aligned}\frac{\partial \hat{q}^3_{\text{osc}}}{\partial t}(t;\Omega) &= \Omega\big\{\Phi_{\text{s}}(\Omega)\big[\cos(\Omega t) - \cos(\Omega t_{\text{in}})\big] + \Phi_{\text{c}}(\Omega)\big[\sin(\Omega t) - \sin(\Omega t_{\text{in}})\big]\big\} \\ &= \Omega\Phi(\Omega)\big[\sin(\Omega t + \theta_0) - \sin(\Omega t_{\text{in}} + \theta_0)\big]. \qquad (3.21)\end{aligned}$$

Thus, by integrating Equations (3.12e) and (3.12f), $q^1(t)$ and $q^2(t)$ read as

$$\begin{aligned}q^1(t) \equiv \hat{q}^1(t;\Omega) = {}& -\tfrac{1}{4}R\Phi(\Omega)\big[\sin(2\Omega t + 2\theta_0) - \sin(2\Omega t_{\text{in}} + 2\theta_0)\big] \\ &- R\big[\tfrac{\nu^3_{\text{in}}}{\Omega} - \Phi(\Omega)\sin(\Omega t_{\text{in}} + \theta_0)\big]\big\{\cos(\Omega t + \theta_0) - \cos(\Omega t_{\text{in}} + \theta_0)\big\} \\ &+ \tfrac{1}{2}R\Omega\Phi(\Omega)[t - t_{\text{in}}] + q^1_{\text{in}}, \qquad (3.22\text{a})\\ q^2(t) \equiv \hat{q}^2(t;\Omega) = {}& -\tfrac{1}{4}R\Phi(\Omega)\big[\cos(2\Omega t + 2\theta_0) - \cos(2\Omega t_{\text{in}} + 2\theta_0)\big] \\ &+ R\big[\tfrac{\nu^3_{\text{in}}}{\Omega} - \Phi(\Omega)\sin(\Omega t_{\text{in}} + \theta_0)\big]\big\{\sin(\Omega t + \theta_0) - \sin(\Omega t_{\text{in}} + \theta_0)\big\} \\ &+ q^2_{\text{in}}. \qquad (3.22\text{b})\end{aligned}$$

In light of the calculations above, we conclude that, for $\Omega \neq 0$, $q^1(t)$ and $q^2(t)$ exhibit two oscillatory contributions: one with angular frequency Ω and the other one with angular frequency 2Ω. In particular, $q^1(t)$ is unbounded in the limit $t \to +\infty$, whereas $q^2(t)$ is bounded. Therefore, the center of mass of the coin moves indefinitely

along the x-axis and, in addition, will never reach the end of the inclined plane along the y-axis.

Finally, we compute the Lagrange multipliers *a posteriori* by integrating Equations (3.17a) and (3.17b) in light of the relations obtained for $q^3(t)$ and $q^4(t)$, i.e., Equations (3.16) and (3.21). By doing this, we obtain

$$\begin{aligned}\lambda_1(t) \equiv \hat{\lambda}_1(t;\Omega) = &-\tfrac{1}{2}mR\Omega\Phi(\Omega)\big[\cos(2\Omega t + 2\theta_0) - \cos(2\Omega t_{\text{in}} + 2\theta_0)\big] \\ &+ mR\big[v_{\text{in}}^3 - \Omega\Phi(\Omega)\sin(\Omega t_{\text{in}} + \theta_0)\big]\{\sin(\Omega t + \theta_0) - \sin(\Omega t_{\text{in}} + \theta_0)\} \\ &+ \lambda_{1\,\text{in}}, \end{aligned} \tag{3.23a}$$

$$\begin{aligned}\lambda_2(t) \equiv \hat{\lambda}_2(t;\Omega) = &\ \tfrac{1}{2}mR\Omega\Phi(\Omega)\big[\sin(2\Omega t + 2\theta_0) - \sin(2\Omega t_{\text{in}} + 2\theta_0)\big] \\ &+ mR\big[v_{\text{in}}^3 - \Omega\Phi(\Omega)\sin(\Omega t_{\text{in}} + \theta_0)\big]\{\cos(\Omega t + \theta_0) - \cos(\Omega t_{\text{in}} + \theta_0)\} \\ &- (mg\sin\alpha)[t - t_{\text{in}}] + \lambda_{2\,\text{in}}. \end{aligned} \tag{3.23b}$$

Case 2. In the case $\Omega = 0$, we find that $q^4(t) = \theta_0 \equiv q_{\text{in}}^4$ for all $t \in [t_{\text{in}}, t_{\text{fin}}]$, and that the right-hand side of Equation (3.18) is constant in time, thereby returning a uniformly accelerated angular motion for q^3. Thus, by integrating Equation (3.18) two times, we obtain

$$q^3(t) \equiv \hat{q}^3(t;0) = \tfrac{1}{2}\xi\,[t - t_{\text{in}}]^2 + v_{\text{in}}^3[t - t_{\text{in}}] + q_{\text{in}}^3, \quad \xi := \frac{2g\sin\alpha\cos\theta_0}{3R}, \tag{3.24}$$

where ξ represent the angular acceleration associated with q^3.

Since the evolution in time of q^3 is known, we can deduce the evolution of q^1 and q^2 by substituting Equation (3.24) in the constraints, i.e., Equations (3.12e) and (3.12f). By integrating the resulting expressions, we get

$$q^1(t) = \tfrac{1}{2}\xi(R\sin\theta_0)[t - t_{\text{in}}]^2 + \underbrace{v_{\text{in}}^3(R\sin\theta_0)}_{\equiv v_{\text{in}}^1}[t - t_{\text{in}}] + q_{\text{in}}^1, \tag{3.25a}$$

$$q^2(t) = \tfrac{1}{2}\xi(R\cos\theta_0)[t - t_{\text{in}}]^2 + \underbrace{v_{\text{in}}^3(R\cos\theta_0)}_{\equiv v_{\text{in}}^2}[t - t_{\text{in}}] + q_{\text{in}}^2. \tag{3.25b}$$

Finally, we can compute λ_1 and λ_2 *a posteriori* by integrating Equations (3.17a) and (3.17b) as follows:

$$\lambda_1(t) = m\xi(R\sin\theta_0)[t - t_{\text{in}}] + \lambda_{1\,\text{in}}, \tag{3.26a}$$

$$\lambda_2(t) = \{m\xi(R\cos\theta_0) - mg\sin\alpha\}[t - t_{\text{in}}] + \lambda_{2\,\text{in}}. \tag{3.26b}$$

We conclude noting that, for $\Omega = 0$, the Lagrange multipliers $\lambda_1(t)$ and $\lambda_2(t)$ are *affine* in time, whereas their time derivatives are constants. This means that, since $\dot{\lambda}_1(t)$ and $\dot{\lambda}_2(t)$ are equal to the Lagrange multipliers $\mu_1(t)$ and $\mu_2(t)$, respectively, of the TNHM (see Corollary 2.1 and Remark 3.1), and since the latter ones measure the magnitude of the reaction forces associated with the imposed constraints, we can say that the reaction forces are constants.

Remark 3.3 (Continuity of the third Lagrangian parameter with respect to Ω).
From Case 1 and Case 2, it follows that the solution of Equation (3.18) is defined as

$$q^3(t) \equiv \hat{q}^3(t;\Omega) = \begin{cases} \hat{q}^3_{\text{osc}}(t;\Omega) \quad + v^3_{\text{in}}[t - t_{\text{in}}] + q^3_{\text{in}}, & \text{if } \Omega \neq 0, \\ \frac{1}{2}\xi\,[t - t_{\text{in}}]^2 + v^3_{\text{in}}[t - t_{\text{in}}] + q^3_{\text{in}}, & \text{if } \Omega = 0, \end{cases} \tag{3.27}$$

where $\hat{q}^3_{\text{osc}}(t;\Omega)$ is reported in Equation (3.20a). In particular, we emphasize that $\hat{q}^3(t,\,\cdot\,)$ is continuous with respect to Ω uniformly in $[t_{\text{in}}, t_{\text{fin}}]$, since it holds that

$$\lim_{\Omega\to 0} \hat{q}^3(t;\Omega) = \hat{q}^3(t;0), \qquad t \in [t_{\text{in}}, t_{\text{fin}}]. \tag{3.28}$$

3.1.4 Numerical simulations

In this section, we present the graphical results of the "rolling coin" problem with the purpose of visualizing that the MVM is equivalent, for the considered problem, to the TNHM.

Hence, we numerically solve the system of Equations (3.12a)–(3.12f), put in a more general form as in Equation (2.50), over the interval $[t_{\text{in}}, t_{\text{fin}}] \equiv [0, T]$. To this end, we introduce the set of *normalized* Lagrangian parameters

$$\mathfrak{q}^1 := q^1/R, \qquad \mathfrak{q}^2 := q^2/R, \qquad \mathfrak{q}^3 := q^3, \qquad \mathfrak{q}^4 := q^4, \tag{3.29}$$

and the set of *normalized* Lagrange multipliers as

$$\lambda_1 \coloneqq \lambda_1/(mR), \qquad \lambda_2 \coloneqq \lambda_2/(mR). \tag{3.30}$$

Note that the normalization of a given Lagrangian parameter is necessary only when it represents a translational kinematic descriptor, and not an angular one, while both the normalized Lagrange multipliers "absorb" the coin's mass m and radius R. As a consequence of (3.29) and (3.30), Equations (3.12a)–(3.12f) are thus normalized as follows:

$$\ddot{\mathfrak{q}}^1 - \dot{\lambda}_1 = 0, \tag{3.31a}$$
$$\ddot{\mathfrak{q}}^2 - \dot{\lambda}_2 = \tfrac{g\sin\alpha}{R}, \tag{3.31b}$$
$$\tfrac{1}{2}\ddot{\mathfrak{q}}^3 + \dot{\lambda}_1 \sin\mathfrak{q}^4 + \dot{\lambda}_2 \cos\mathfrak{q}^4 = 0, \tag{3.31c}$$
$$\tfrac{1}{4}\ddot{\mathfrak{q}}^4 = 0, \tag{3.31d}$$
$$\dot{\mathfrak{q}}^1 = \dot{\mathfrak{q}}^3 \sin\mathfrak{q}^4, \tag{3.31e}$$
$$\dot{\mathfrak{q}}^2 = \dot{\mathfrak{q}}^3 \cos\mathfrak{q}^4. \tag{3.31f}$$

Finally, Equations (3.31a)–(3.31f) are solved numerically using the "trapezium rule" in the case in which the physical and numerical parameters are the ones reported in Table 3.1.

Parameter	Value	Units	Description
R	11.625	mm	Radius of the coin
m	7.5	g	Mass of the coin
g	9.81	$\mathrm{m/s^2}$	Gravitational acceleration
α	$\pi/6$	rad	Angle of the inclined plane
T	2	s	Total time of simulation
Δt	10^{-4}	s	Time-step

Table 3.1 Physical and numerical parameters chosen for the simulation of a standard "1 Euro" coin rolling down an infinitely long inclined plane.

Parametric sweep of Ω. The first scenario we examine is the case of a coin, initially tilted towards the direction of steepest descent of the plane, i.e., $q^4_{\mathrm{in}} = 0$, that rolls without slipping from the top of the inclined plane. Moreover, we consider the initial angular velocity $v^4_{\mathrm{in}} \equiv \Omega$, and we study its effect on the evolution of the system. Then,

we initialize the remaining generalized coordinates as $q^1_{\text{in}} = 0$, $q^2_{\text{in}} = 0$ and $q^3_{\text{in}} = 0$, and the Lagrange multipliers as $\lambda_{1\,\text{in}} = 0$ and $\lambda_{2\,\text{in}} = 0$. Further, we assume that $\nu^3_{\text{in}} = 0$, which implies that the initial velocities ν^1_{in} and ν^2_{in} are zero too, since they have to satisfy the constraints in Equations (3.2a) and (3.2b) at time $t = t_{\text{in}} = 0$.

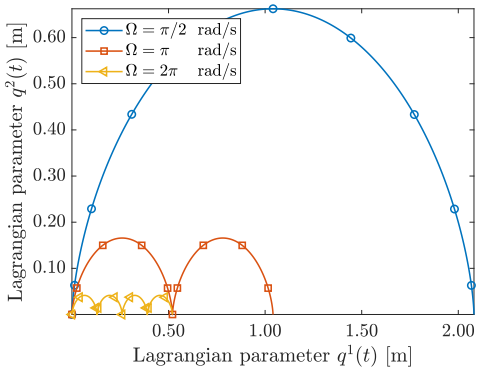

Fig. 3.2 Trajectories of the center of mass of the coin for different values of $\Omega \in \{\pi/2, \pi, 2\pi\}$ rad/s simulated from $t_{\text{in}} = 0\,\text{s}$ to $t_{\text{fin}} = 2\,\text{s}$.

In Figure 3.2, we show the trajectories of the center of mass of the coin for different values of Ω, e.g. $\Omega \in \{\pi/2, \pi, 2\pi\}$ rad/s. We observe that gyroscopic effects arise when non-vanishing values of Ω are considered, as predicted by the analytical solution of the problem (see e.g. Section 3.1.3) [40, 17]. These effects, which are produced by the action of the constraints, are due to an oscillatory contribution characterized by angular frequency 2Ω, since, if we specialize the analytical solution to the case under examination, the coordinates of the center of mass of the coin read

$$q^1(t) \equiv \hat{q}^1(t;\Omega) = -\tfrac{1}{4}R\Phi(\Omega)\sin(2\Omega t) + \tfrac{1}{2}R\Omega\Phi(\Omega)t, \tag{3.32a}$$
$$q^2(t) \equiv \hat{q}^2(t;\Omega) = -\tfrac{1}{4}R\Phi(\Omega)\big[\cos(2\Omega t) - 1\big]. \tag{3.32b}$$

Note that, by expanding Equations (3.32a) and (3.32b) in a neighborhood of $\Omega = 0$, and for a fixed time $t \in [t_{\text{in}}, t_{\text{fin}}]$, we obtain, in the limit $\Omega \to 0$, that

$$q^1(t) \equiv \hat{q}^1(t;\Omega) = \tfrac{1}{3}R\Phi(\Omega)\Omega^3 t^3 + o(\Omega) = \tfrac{2}{9}g\sin\alpha\,\Omega t^3 + o(\Omega), \tag{3.33a}$$
$$q^2(t) \equiv \hat{q}^2(t;\Omega) = \tfrac{1}{2}R\Phi(\Omega)\Omega^2 t^2 + o(1) = \tfrac{1}{3}g\sin\alpha\, t^2 + o(1). \tag{3.33b}$$

Therefore, we find that $\hat{q}^1(t;0) = \lim_{\Omega\to 0}\hat{q}^1(t;\Omega)$, and that the leading term of $\hat{q}^2(t;\Omega)$ does not depend on Ω and grows quadratically in time in the considered neighborhood.

In conclusion, if $\Omega = 0$, the coin rolls downwards indefinitely and reaches the end of the inclined plane, when the latter one is finite. On the other hand, when $\Omega \neq 0$, the center of mass of the coin exhibits a behavior similar to the one of a "yo-yo", since it oscillates back and forth in the direction of the y-axis, while moving indefinitely along the x-axis, and the amplitude of the oscillations depends on Ω. Moreover, even for inclined planes whose slope is finite, yet sufficiently longer than the amplitude of the y-oscillations, there exist values of Ω such that the coin does not reach the end of the slope.

In Figure 3.3, we have reported four plots describing the qualitative and quantitative behavior of the Lagrange multipliers λ_1 and λ_2 in the case in which Ω is either π rad/s or 2π rad/s. In particular, in Figure 3.3a–3.3c, we introduce ρ_1 and ρ_2 as the "reactive forces" associated to q^1 and q^2, respectively, and ρ_3 the "reactive moment" associated to q^3, so that the corresponding pairs of "Lagrangian parameter – reactive force" could be compared. Note that, the expressions of ρ_1, ρ_2 and ρ_3 follow from Equations (3.12a)–(3.12c) and read

$$\rho_1 \coloneqq \dot{\lambda}_1, \qquad \rho_2 \coloneqq \dot{\lambda}_2, \qquad \rho_3 \coloneqq -\dot{\lambda}_1 R \sin q^4 - \dot{\lambda}_2 R \cos q^4, \tag{3.34}$$

while, by virtue of Equation (3.12d), the "reactive moment" associated to q^4, i.e., ρ_4, is identically zero.

In Figure 3.3a we observe that in the instants of time in which the reactive force ρ_1 vanishes, the Lagrangian parameter q^1 exhibits, in the same instants, inflection points. This phenomenon is a direct consequence of Equation (3.12e). Moreover, as one can see in Figure 3.3b,c, for the instants of time in which q^2 or q^3 admit a local maximum, their corresponding reactive force and moment, i.e., ρ_2 and ρ_3, feature a local minimum, and vice versa. Indeed, this is in compliance with the analytical expressions of the Lagrange multipliers $\lambda_1(t)$ and $\lambda_2(t)$ featuring in Equations (3.23a) and (3.23b), and reported in Figure 3.3d, since, in the case we are considering, they read

$$\lambda_1(t) \equiv \hat{\lambda}_1(t;\Omega) = -\tfrac{1}{2} mR\Omega\Phi(\Omega)[\cos(2\Omega t) - 1], \tag{3.35a}$$

$$\lambda_2(t) \equiv \hat{\lambda}_2(t;\Omega) = \tfrac{1}{2} mR\Omega\Phi(\Omega)\sin(2\Omega t) - (mg\sin\alpha)t, \tag{3.35b}$$

which, in turn, produce the following reactions

$$\rho_1(t) = \tfrac{2}{3} mg \sin\alpha \, \sin(2\Omega t), \tag{3.36a}$$

$$\rho_2(t) = \tfrac{2}{3} mg \sin\alpha \, \cos(2\Omega t) - mg \sin\alpha, \tag{3.36b}$$

$$\rho_3(t) = \tfrac{1}{3} mgR \sin\alpha \, \cos(\Omega t). \tag{3.36c}$$

Therefore, by comparing the expression in Equations (3.36a)–(3.36c) with Equations (3.32a), (3.32b) and (3.19), we conclude that:

(i) The constraint $\mathcal{V}^1$ has the effect to change the curvature of the trajectory of the center of mass of the coin, i.e., the second time derivative of $q^1(t)$.

(ii) The constraint $\mathcal{V}^2$ produces a reaction force on q^2 opposing to the motion that, in turn, determines the oscillatory behavior of the center of mass of the coin along the y-axis.

Effect of a non-zero θ_0. The second scenario we examine for the "rolling coin" problem concerns how considering non-zero values of $\theta_0 \equiv q^4_{\text{in}}$, for the fixed value of $\Omega = 2\pi\,\text{rad/s}$, affects the overall motion of the system. In particular, we will compare the solutions when the chosen value of θ_0 belongs to the set $\{0, \pi/2\}$ (see Figure 3.4). Note that, the two cases above describe the situations in which the initial direction of rolling, indicated by the unit vector $\boldsymbol{\tau}$, is either aligned with the direction of steepest descent ($\theta_0 = 0$) or is orthogonal to it ($\theta_0 = \pi/2$). As in the study above, we initialize the remaining generalized coordinates as $q^1_{\text{in}} = 0$, $q^2_{\text{in}} = 0$ and $q^3_{\text{in}} = 0$, and the Lagrange multipliers as $\lambda_{1\,\text{in}} = 0$ and $\lambda_{2\,\text{in}} = 0$.

In Figure 3.4, we observe that in the case in which $\theta_0 = 0\,\text{rad}$, the trajectory of the center of mass of the coin features an oscillatory motion that makes the center of mass move in the positive direction of the x-axis without ever going backward in the same direction. Instead, for $\theta_0 = \pi/2\,\text{rad}$, the center of mass of the coin experiences an oscillatory motion that moves the coin initially in the negative direction of the x-axis. Since this behavior is periodic in the motion, a knot is produced in the trajectory of the center of mass when $t \simeq 1\,\text{s}$.

Finally, from Figure 3.5, we have compared, as done previously in Figure 3.3, the pairs of "Lagrangian parameters – Reactive forces" that are obtained when Ω is fixed at $2\pi\,\text{rad/s}$ and $\theta_0 \in \{0, \pi/2\}\,\text{rad}$. In this case, by looking at Figure 3.5a–3.5c,

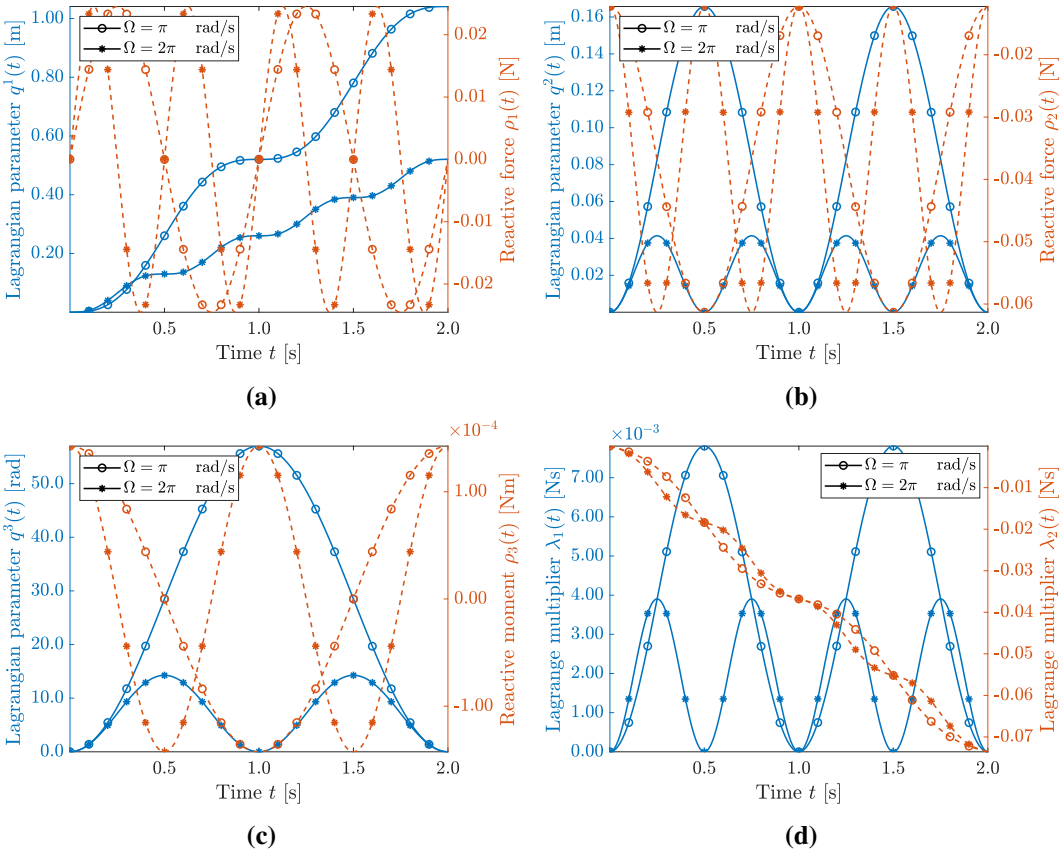

Fig. 3.3 In 3.3a–3.3c the pairs “Lagrangian parameter – Reactive force” are represented by continuous and dotted lines, respectively. In Figure 3.3d, $\lambda_1(t)$ and $\lambda_2(t)$ are represented with a continuous and a dotted line, respectively.

we can draw similar conclusions to what we draw for the parametric study on Ω. Nevertheless, we acknowledge the fact that, when $\theta_0 \neq 0$, then the reactive forces ρ_1 and ρ_2 are determined by an apposition of oscillatory motion with different angular frequencies (see Figure 3.5a–3.5b). On the other hand, as shown in Figure 3.5c, ρ_3 is defined by only one cosinusoidal contribution that is shifted by the presence of a non-zero θ_0. Indeed, these phenomena are explained by the analytical expressions for the three generalized reactive forces, which, in the case of $t_{\text{in}} = 0$ and $\theta_0 \neq 0$, read as follows:

$$\rho_1(t) = \tfrac{2}{3} mg \sin\alpha \big[\sin(2\Omega t + 2\theta_0) - \sin\theta_0 \cos(\Omega t + \theta_0) \big], \tag{3.37a}$$

$$\rho_2(t) = \tfrac{2}{3} mg \sin\alpha \big[\cos(2\Omega t + 2\theta_0) + \sin\theta_0 \sin(\Omega t + \theta_0) \big] - mg \sin\alpha, \tag{3.37b}$$

$$\rho_3(t) = \tfrac{1}{3} mg \sin\alpha R \cos(\Omega t). \tag{3.37c}$$

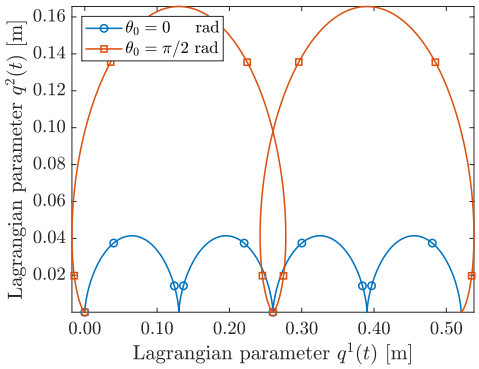

Fig. 3.4 Trajectories of the center of mass of the coin for $\theta_0 \in \{0, \pi/2\}$ rad which are simulated from $t_{\text{in}} = 0$ s to $t_{\text{fin}} = 2$ s.

Note that the presence of non-zero θ_0 provides the same "reactive moment" $\rho_3(t)$, i.e., Equation (3.37c), that we had in the case with $\theta_0 = 0$, i.e., Equation (3.36c), thereby manifesting the independence of $\rho_3(t)$ with respect to θ_0.

3.2 The "charged skate" benchmark

In this section, we study the dynamic equations for the benchmark problem of the "nonholonomic skate" (see e.g. [13, 15, 55, 51, 50, 27, 54, 16, 68]), which we have modified by introducing an electromagnetic interaction (see also [25]). Also in this case, we employ the "modified vakonomic method" (MVM) with the objective of showing how an interaction of this type can "break" the equivalence between the MVM and the TNHM, thereby violating the hypothesis of Theorem 2.1. In particular, the role of the *Ansätze*, needed for the closure of Equations (2.42a) and (2.42b), is investigated in the sequel.

We consider a three-dimensional rigid skate $\mathfrak{S}$, shaped as a rectangular parallelepiped having mass m, length ℓ, and cross section of area σ^2, that slides over an inclined plane of an angle α with respect to a horizontal plane. We assume that the skate is electrically charged, with volumetric charge density e distributed uniformly in $\mathfrak{S}$, so that the total electric charge of the skate is $Q := e\ell\sigma^2$. Moreover, we let the skate interact with a field of magnetic induction associated with the (co-)vector potential $\boldsymbol{A}$ [66]. A graphical representation of $\mathfrak{S}$ is reported in Figure 3.6.

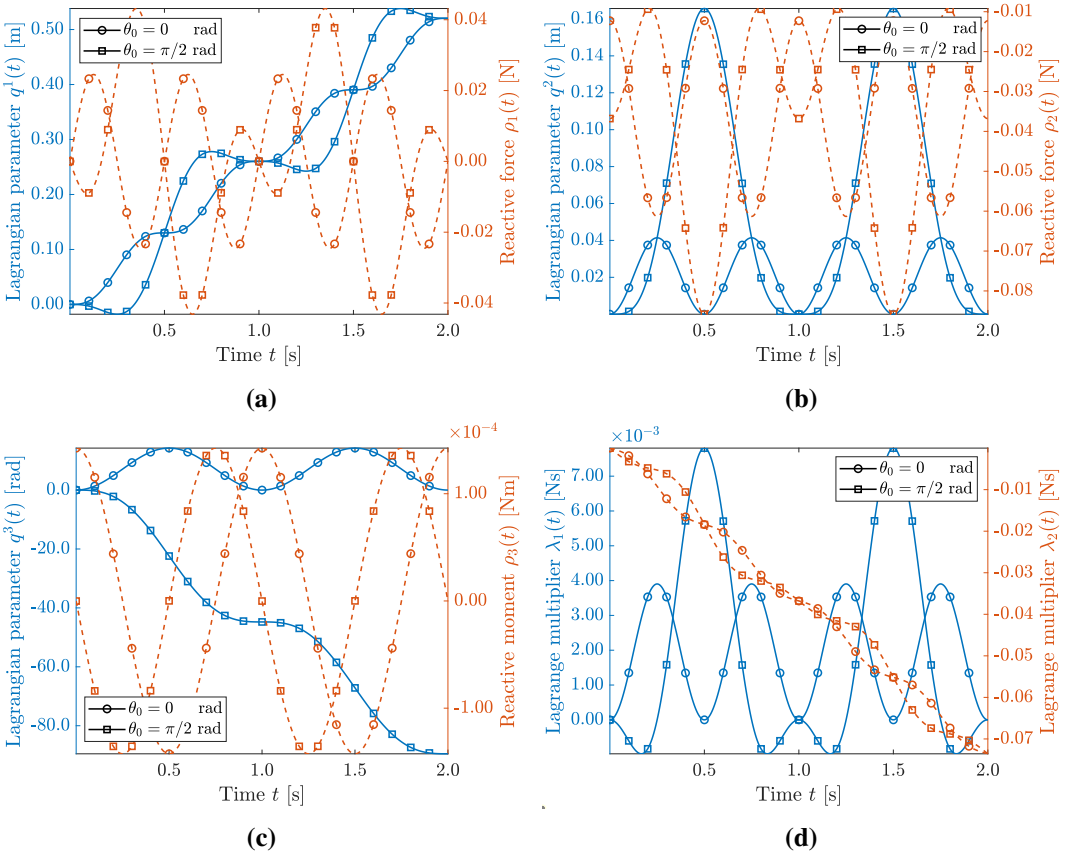

Fig. 3.5 In 3.5a, 3.5b and 3.5c the pairs “Lagrangian parameter – Reactive force” are represented by continuous and dotted lines, respectively. In Figure 3.5d, $\lambda_1(t)$ and $\lambda_2(t)$ are represented with a continuous and a dotted line, respectively.

A coordinate system $\{O, (x, y, z)\}$ is prescribed such that the x-axis is parallel to the inclined plane and is aligned with the direction of steepest descent; the z-axis “exits” the inclined plane and is orthogonal to it; the y-axis is such that the x-, y- and z-axis form a right-handed triad; the origin O is fixed at the same z-coordinate as the center of mass of the skate, hereafter denoted by G. Furthermore, we denote by $\{\boldsymbol{e}_x, \boldsymbol{e}_y, \boldsymbol{e}_z\}$ and $\{\boldsymbol{e}^x, \boldsymbol{e}^y, \boldsymbol{e}^z\}$ the basis unit vectors and co-vectors, respectively, associated with the coordinate system $\{O, (x, y, z)\}$.

By introducing $(x_G, y_G, 0)$ as the coordinates of G, and θ as the angle between the x-axis and the axis of the skate, we choose x_G, y_G and θ as the $n = 3$ Lagrangian parameters of the mechanical system under study, thereby leading to the identification $q \equiv (q^1, q^2, q^3) \equiv (x_G, y_G, \theta)$ [16].

In the following, we will only consider the case in which the magnetic induction field $\boldsymbol{B} = \text{curl}\boldsymbol{A}$ is homogeneous in space and orthogonal to the inclined plane, i.e., $\boldsymbol{B}(x, y, z, t) = B_0(t)\boldsymbol{e}_z$, so that the resulting Lorentz force, acting on the skate, is parallel to the inclined plane itself. To this end, we design the (co-)vector potential to be $\boldsymbol{A}(x, y, z, t) = [-\frac{1}{2}B_0(t)y]\boldsymbol{e}^x + [\frac{1}{2}B_0(t)x]\boldsymbol{e}^y$.

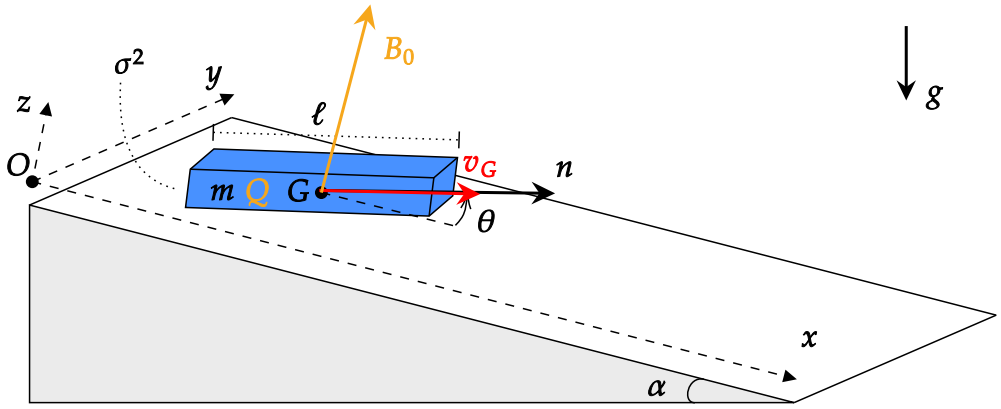

Fig. 3.6 Graphical representation of the "charged skate" benchmark problem. This image was first showed during the conference "The coupled nonlinear continuum theory horizon" held in Castro Urdiales, Spain, on July 1-5, 2024, within the presentation of the abstract "Towards a variational theory of nonholonomic continuum media: the discrete mechanics scenario", authored by A. Pastore, A. Giammarini, A. Grillo.

Given the premises above, and if, in addiction to the considered magnetic interactions, we also account for the gravitational interaction, then the Lagrangian of the skate reads [16, 27, 54, 50]

$$\begin{aligned}\hat{\mathcal{L}} \circ (q, \dot{q}, \tau) = &\underbrace{\tfrac{1}{2}m\left[(\dot{q}^1)^2 + (\dot{q}^2)^2 + \tfrac{\ell^2+\sigma^2}{12}(\dot{q}^3)^2\right]}_{\hat{\mathcal{K}} \circ \dot{q}} + \underbrace{(mg\,\sin\alpha)q^1}_{\hat{\mathcal{U}}_{\mathrm{g}} \circ q} \\ &\underbrace{+\left[-\tfrac{QB_0}{2}q^2\right]\dot{q}^1 + \left[\tfrac{QB_0}{2}q^1\right]\dot{q}^2 + \left[\tfrac{QB_0(\ell^2+\sigma^2)}{24}\right]\dot{q}^3}_{\hat{\mathcal{U}}_{\mathrm{m}} \circ (q,\dot{q},\tau)},\end{aligned} \tag{3.38}$$

where $\mathcal{K} \equiv \hat{\mathcal{K}} \circ \dot{q}$ is the kinetic energy; $\mathcal{U}_{\mathrm{g}} \equiv \hat{\mathcal{U}}_{\mathrm{g}} \circ q$ and $\mathcal{U}_{\mathrm{m}} \equiv \hat{\mathcal{U}}_{\mathrm{m}} \circ (q, \dot{q}, \tau)$ are the gravitational and magnetic potential functions, respectively; g is the magnitude of the gravity acceleration vector, and $B_0 \equiv B_0 \circ \tau$ is the magnitude of the magnetic induction field.

By denoting by $\boldsymbol{n} = \cos\theta \boldsymbol{e}_x + \sin\theta \boldsymbol{e}_y$ the unit vector aligned with the skate's axis, we assume the velocity of the center of mass of the skate, $\boldsymbol{v}_G$, to remain always parallel to $\boldsymbol{n}$. This condition, written in the physical space as $\boldsymbol{v}_G \times \boldsymbol{n} = \boldsymbol{0}$, prescribes the nonholonomic constraint to be [16, 27, 54–56, 50]

$$\mathcal{V}^1 \equiv \hat{\mathcal{V}}^1 \circ (q, \dot{q}) \coloneqq (\sin q^3)\dot{q}^1 - (\cos q^3)\dot{q}^2 = 0. \tag{3.39}$$

Note that the absence of $\dot{q}^3$ in the constraint (3.39) is sufficient to conclude that the transpositional relation $\eta^3_{\dot{q}} - \dot{\eta}^3_q$ must be zero, i.e., $\eta^3_{\dot{q}} - \dot{\eta}^3_q = \sum_{h=1}^{3} W^3{}_h \eta^h_q = 0$. In turn, this means that the coefficients $W^3{}_1$, $W^3{}_2$, and $W^3{}_3$ must be either identically zero or such that their combination with η^1_q, η^2_q, and η^3_q is zero because of Lagrange–Chetaev's conditions (2.12).

3.2.1 The traditional nonholonomic approach

In this section, we compute the dynamic equations produced by the TNHM for the “charged skate” problem. Hence, we specify the Euler–Lagrange operators in Equation (2.28a) for the Lagrangian in Equation (3.38), i.e.,

$$\mathcal{E}_1 \hat{\mathcal{L}} \circ \sharp = -m\ddot{q}^1 + QB_0\dot{q}^2 + \tfrac{1}{2}Q\dot{B}_0 q^2 + mg\sin\alpha, \tag{3.40a}$$
$$\mathcal{E}_2 \hat{\mathcal{L}} \circ \sharp = -m\ddot{q}^2 - QB_0\dot{q}^1 - \tfrac{1}{2}Q\dot{B}_0 q^1, \tag{3.40b}$$
$$\mathcal{E}_3 \hat{\mathcal{L}} \circ \sharp = -\tfrac{1}{12}m(\ell^2 + \sigma^2)\ddot{q}^3 - \tfrac{1}{24}Q\dot{B}_0(\ell^2 + \sigma^2), \tag{3.40c}$$

and, by substituting Equations (3.40a)–(3.40c) as well as the constraint (3.39) into Equations (2.52a) and (2.52b), we find the TNHM dynamic equations for the “charged skate” problem to be as follows:

$$m\ddot{q}^1 - \mu_1 \sin q^3 = mg\sin\alpha + QB_0\dot{q}^2 + \tfrac{1}{2}Q\dot{B}_0 q^2, \tag{3.41a}$$
$$m\ddot{q}^2 + \mu_1 \cos q^3 = -QB_0\dot{q}^1 - \tfrac{1}{2}Q\dot{B}_0 q^1, \tag{3.41b}$$
$$\tfrac{1}{12}m(\ell^2 + \sigma^2)\ddot{q}^3 = -\tfrac{1}{24}Q(\ell^2 + \sigma^2)\dot{B}_0, \tag{3.41c}$$
$$(\sin q^3)\dot{q}^1 - (\cos q^3)\dot{q}^2 = 0. \tag{3.41d}$$

We notice that Equations (3.41a)–(3.41c) can be recast in a more suggestive form by rewriting them in terms of the canonical momenta:

$$\frac{\mathrm{d}}{\mathrm{d}t}\underbrace{\left[m\dot{q}^1 - \tfrac{1}{2}QB_0q^2\right]}_{=:p_1} = \mu_1 \sin q^3 + mg\sin\alpha + \tfrac{1}{2}QB_0\dot{q}^2, \tag{3.42a}$$

$$\frac{\mathrm{d}}{\mathrm{d}t}\underbrace{\left[m\dot{q}^2 + \tfrac{1}{2}QB_0q^1\right]}_{=:p_2} = -\mu_1 \cos q^3 - \tfrac{1}{2}QB_0\dot{q}^1, \tag{3.42b}$$

$$\frac{\mathrm{d}}{\mathrm{d}t}\underbrace{\left[\tfrac{1}{12}m[\ell^2+\sigma^2]\dot{q}^3 + \tfrac{1}{24}Q[\ell^2+\sigma^2]B_0\right]}_{=:p_3} = 0. \tag{3.42c}$$

Note also that, since the Lagrangian parameter q^3 is *"ignorable"* [11], Equation (3.42c) is equivalent to state the conservation of the generalized momentum conjugated with q^3, which, thus, turns out to be an integral of the motion, i.e.,

$$p_3(t) = \frac{\partial\hat{\mathcal{L}}}{\partial\dot{q}^3}(\natural(t)) = \tfrac{1}{12}m[\ell^2+\sigma^2]\dot{q}^3(t) + \tfrac{1}{24}[\ell^2+\sigma^2]QB_0(t) = C, \tag{3.43}$$

with C being an integration constant.

3.2.2 The Modified Vakonomic approach

Now, we apply the procedure reported in Section 2.2 to the problem under study. Hence, we solve Equations (2.42a) and (2.42b) in compliance with the *solvability conditions* (2.40a) and (2.40b), for the case in which the Lagrangian function and the constraint are of the type specified in Equations (3.38) and (3.39), respectively.

To this end, we express the conditions in Equation (2.34), for $k \in \{1,2,3\}$ and with $\alpha = 1$, in the case in which the considered constraint is the one reported in Equation (3.39):

$$\mathcal{D}_1\hat{\mathcal{V}}^1 \circ \sharp = (\sin q^3)W^1{}_1 - (\cos q^3)W^2{}_1 - (\cos q^3)\dot{q}^3 = 0, \tag{3.44a}$$

$$\mathcal{D}_2\hat{\mathcal{V}}^1 \circ \sharp = (\sin q^3)W^1{}_2 - (\cos q^3)W^2{}_2 - (\sin q^3)\dot{q}^3 = 0, \tag{3.44b}$$

$$\mathcal{D}_3\hat{\mathcal{V}}^1 \circ \sharp = (\sin q^3)W^1{}_3 - (\cos q^3)W^2{}_3 + (\cos q^3)\dot{q}^1 + (\sin q^3)\dot{q}^2 = 0. \tag{3.44c}$$

To find all the coefficients $W^h{}_k$, we proceed as follows:

3.2.3 Case A: Llibre et al.’s auxiliary functions

In the sequel, we take the same auxiliary functions as those suggested by Llibre et al. [16] for the case of the “nonholonomic skate” without magnetic field (see also [25] for comparison). However, we flip their order from the one reported in [16], thereby writing

$$\mathcal{F}^2 \equiv \hat{\mathcal{F}}^2 \circ \natural := \dot{q}^3, \tag{3.45a}$$

$$\mathcal{F}^3 \equiv \hat{\mathcal{F}}^3 \circ \natural := (\cos q^3)\dot{q}^1 + (\sin q^3)\dot{q}^2, \tag{3.45b}$$

to emphasize that the choice of these functions must respect the criterion given in *Ansatz 1*. In particular, this means that they must respect the transpositional relation $\eta^3_{\dot{q}} - \dot{\eta}^3_q = \sum_{h=1}^3 W^3{}_h \eta^h_q = 0$, and, indeed, $\hat{\mathcal{F}}^2 \circ \natural = \dot{q}^3$ ensures the fulfillment of this condition in *strong* way, as can be seen by the equations

$$\mathcal{D}_1\hat{\mathcal{F}}^2 \circ \sharp = W^3{}_1 = 0, \tag{3.46a}$$

$$\mathcal{D}_2\hat{\mathcal{F}}^2 \circ \sharp = W^3{}_2 = 0, \tag{3.46b}$$

$$\mathcal{D}_3\hat{\mathcal{F}}^2 \circ \sharp = W^3{}_3 = 0. \tag{3.46c}$$

Conversely, the auxiliary function in Equation (3.45b) leads to the conditions

$$\mathcal{D}_1\hat{\mathcal{F}}^3 \circ \sharp = (\cos q^3)W^1{}_1 + (\sin q^3)W^2{}_1 + (\sin q^3)\dot{q}^3 = 0, \tag{3.47a}$$

$$\mathcal{D}_2\hat{\mathcal{F}}^3 \circ \sharp = (\cos q^3)W^1{}_2 + (\sin q^3)W^2{}_2 - (\cos q^3)\dot{q}^3 = 0, \tag{3.47b}$$

$$\mathcal{D}_3\hat{\mathcal{F}}^3 \circ \sharp = (\cos q^3)W^1{}_3 + (\sin q^3)W^2{}_3 - \underbrace{[(\sin q^3)\dot{q}^1 - (\cos q^3)\dot{q}^2]}_{=0} = 0. \tag{3.47c}$$

We remark that, as anticipated in the *Ansatz 1* of Section 2.3.1, Equation (3.45b) identifies $\mathcal{F}^3$ with the component of the projection of $\boldsymbol{v}_G$ onto the unit vector $\boldsymbol{n}$, namely $\mathcal{F}^3 \equiv \boldsymbol{v}_G \cdot \boldsymbol{n}$, which is the geometric interpretation of a quasi-velocity.

By solving the linear algebraic system in Equations (3.44a)–(3.44c), (3.46a)–(3.46c), and (3.47a)–(3.47c) for the unknown coefficients ${W^h}_k$, we have [16]

$$\mathsf{W} = \begin{bmatrix} 0 & \dot{q}^3 & -\dot{q}^2 \\ -\dot{q}^3 & 0 & \dot{q}^1 \\ 0 & 0 & 0 \end{bmatrix}. \tag{3.48}$$

Hence, by substituting Equations (3.40a)–(3.40c) and (3.48) into Equations (2.42a) and (2.42b), we obtain that the dynamic equations returned by the MVM for the "charged skate" problem read

$$m\ddot{q}^1 - \dot{\lambda}_1 \sin q^3 = mg\sin\alpha - m\dot{q}^2\dot{q}^3 + QB_0\dot{q}^2 + \tfrac{1}{2}Q\dot{B}_0 q^2 - \tfrac{1}{2}QB_0 q^1\dot{q}^3, \tag{3.49a}$$

$$m\ddot{q}^2 + \dot{\lambda}_1 \cos q^3 = m\dot{q}^1\dot{q}^3 - QB_0\dot{q}^1 - \tfrac{1}{2}Q\dot{B}_0 q^1 - \tfrac{1}{2}QB_0 q^2\dot{q}^3, \tag{3.49b}$$

$$\tfrac{1}{12}m(\ell^2+\sigma^2)\ddot{q}^3 = -\tfrac{1}{24}Q(\ell^2+\sigma^2)\dot{B}_0 + \tfrac{1}{2}QB_0(q^1\dot{q}^1 + q^2\dot{q}^2), \tag{3.49c}$$

$$(\sin q^3)\dot{q}^1 - (\cos q^3)\dot{q}^2 = 0. \tag{3.49d}$$

For ease of comparison with the TNHM, we rewrite Equations (3.49a)–(3.49c) by highlighting the canonical momenta, i.e.,

$$\frac{\mathrm{d}}{\mathrm{d}t}\underbrace{\left[m\dot{q}^1 - \tfrac{1}{2}QB_0q^2\right]}_{=:p_1} = \dot{\lambda}_1\sin q^3 + mg\sin\alpha + \tfrac{1}{2}QB_0\dot{q}^2 - p_2\dot{q}^3, \tag{3.50a}$$

$$\frac{\mathrm{d}}{\mathrm{d}t}\underbrace{\left[m\dot{q}^2 + \tfrac{1}{2}QB_0q^1\right]}_{=:p_2} = -\dot{\lambda}_1\cos q^3 - \tfrac{1}{2}QB_0\dot{q}^1 + p_1\dot{q}^3, \tag{3.50b}$$

$$\frac{\mathrm{d}}{\mathrm{d}t}\underbrace{\left[\tfrac{1}{12}m[\ell^2+\sigma^2]\dot{q}^3 + \tfrac{1}{24}Q[\ell^2+\sigma^2]B_0\right]}_{=:p_3} = \underbrace{\tfrac{1}{2}QB_0[q^1\dot{q}^1 + q^2\dot{q}^2]}_{=-p_1\dot{q}^2+p_2\dot{q}^1}. \tag{3.50c}$$

From Equation (3.50c), we notice that the generalized momentum p_3 is not conserved with the functions $\mathcal{F}^2$ and $\mathcal{F}^3$ of Equations (3.45a) and (3.45b) characterizing *Ansatz 1* for this problem. The criticality with this choice of functions is that they do not guarantee the equivalence between the MVM and the TNHM, i.e., the characterizing condition of Theorem 2.1 in Equation (2.55a) is not satisfied. Indeed, such condition

would require the vanishing of the quantities

$$(\cos q^3)(\mathsf{W}^{\mathrm{T}}\mathsf{p})_1 + (\sin q^3)(\mathsf{W}^{\mathrm{T}}\mathsf{p})_2 \qquad \text{and} \qquad (\mathsf{W}^{\mathrm{T}}\mathsf{p})_3, \tag{3.51}$$

which, in the case considered, i.e., with W as in Equation (3.48), are instead

$$(\cos q^3)(\mathsf{W}^{\mathrm{T}}\mathsf{p})_1 + (\sin q^3)(\mathsf{W}^{\mathrm{T}}\mathsf{p})_2 = -\tfrac{1}{2}QB_0[q^1\cos q^3 + q^2\sin q^3]\dot{q}^3 \neq 0, \tag{3.52a}$$

$$(\mathsf{W}^{\mathrm{T}}\mathsf{p})_3 = \tfrac{1}{2}QB_0[q^1\dot{q}^1 + q^2\dot{q}^2] \neq 0, \tag{3.52b}$$

where the right-hand sides of Equations (3.52a) and (3.52b) stem from the terms making the momenta *affine* in the velocities.

Hence, if we take the same auxiliary functions as in [16] for the problem at hand, then, although the transpositional relations are maintained, the MVM is *not equivalent* to the TNHM, since Equation (2.55a) of Theorem 2.1 is not satisfied, and a conservation law, which should exist, is lost.

Remark 3.4 (*"Canonical flip"* [57, 52] for the Case A of the "charged skate"). Similarly to what has been done in Remark 3.2, the matrix W in Equation (3.48) allows to choose the coefficients $\mathcal{C}^h{}_{\ell k}$ of the associated "Canonical flip" as follows

$$\mathcal{C}^1{}_{32}\dot{q}^3 = W^1{}_2 = +\dot{q}^3 \qquad \Rightarrow \qquad \mathcal{C}^1{}_{32} \equiv \hat{\mathcal{C}}^1{}_{32} \circ q = +1, \tag{3.53a}$$

$$\mathcal{C}^1{}_{23}\dot{q}^2 = W^1{}_3 = -\dot{q}^2 \qquad \Rightarrow \qquad \mathcal{C}^1{}_{23} \equiv \hat{\mathcal{C}}^1{}_{23} \circ q = -1, \tag{3.53b}$$

$$\mathcal{C}^2{}_{31}\dot{q}^3 = W^2{}_1 = -\dot{q}^3 \qquad \Rightarrow \qquad \mathcal{C}^2{}_{31} \equiv \hat{\mathcal{C}}^2{}_{31} \circ q = -1, \tag{3.53c}$$

$$\mathcal{C}^2{}_{13}\dot{q}^1 = W^2{}_3 = +\dot{q}^1 \qquad \Rightarrow \qquad \mathcal{C}^2{}_{13} \equiv \hat{\mathcal{C}}^2{}_{13} \circ q = +1. \tag{3.53d}$$

As for the "rolling coin", all the other entries of $\mathcal{C}^h{}_{\ell k}$ can be set equal to zero.

Remark 3.5 (The "charged skate" in the case of momenta linear in the velocities). The fact that, with the matrix W of Equation (3.48), the results (3.52a) and (3.52b) spoil the fulfillment of Theorem 2.1, and make, thus, the MVM not equivalent to the TNHM, is a direct consequence of the last three summands of the Lagrangian function (3.38), which correspond to $\sum_{h=1}^{3}[\hat{Z}_h \circ (q,\tau)]\dot{q}^h$, and render the momenta affine (rather than linear) in the generalized velocities. However, if we follow the approach presented in Section 2.3.4, so that we deal with Equations (2.59a) and (2.59b), the dynamic equations (3.49a)–(3.49d) for the charged nonholonomic skate

with the magnetic interactions regarded as (pseudo-)polygenic [11] become

$$m\ddot{q}^1 - \dot{\lambda}_1 \sin q^3 = \underbrace{-m\dot{q}^2\dot{q}^3}_{=(\mathsf{W}^{\mathrm{T}}\mathsf{p}_0)_1} + \underbrace{[QB_0\dot{q}^2 + \tfrac{1}{2}Q\dot{B}_0 q^2]}_{=\mathcal{Q}_1} + mg\sin\alpha, \tag{3.54a}$$

$$m\ddot{q}^2 + \dot{\lambda}_1 \cos q^3 = \underbrace{+m\dot{q}^1\dot{q}^3}_{=(\mathsf{W}^{\mathrm{T}}\mathsf{p}_0)_2} + \underbrace{[-QB_0\dot{q}^1 - \tfrac{1}{2}Q\dot{B}_0 q^1]}_{=\mathcal{Q}_2}, \tag{3.54b}$$

$$\tfrac{1}{12}m(\ell^2+\sigma^2)\ddot{q}^3 = \underbrace{0}_{=(\mathsf{W}^{\mathrm{T}}\mathsf{p}_0)_3} + \underbrace{[-\tfrac{1}{24}Q(\ell^2+\sigma^2)\dot{B}_0]}_{=\mathcal{Q}_3}, \tag{3.54c}$$

$$(\sin q^3)\dot{q}^1 - (\cos q^3)\dot{q}^2 = 0. \tag{3.54d}$$

Accordingly, the condition (2.55a) of Theorem 2.1, *instead of* Equations (3.52a) and (3.52b), produces

$$\begin{aligned}(\cos q^3)(\mathsf{W}^{\mathrm{T}}\mathsf{p}_0)_1 + (\sin q^3)(\mathsf{W}^{\mathrm{T}}\mathsf{p}_0)_2 &= -(\cos q^3)m\dot{q}^2\dot{q}^3 + (\sin q^3)m\dot{q}^3\dot{q}^1 \\ &= m\dot{q}^3[(\sin q^3)\dot{q}^1 - (\cos q^3)\dot{q}^2] = 0, \end{aligned} \tag{3.55a}$$

$$(\mathsf{W}^{\mathrm{T}}\mathsf{p}_0)_3 = -\dot{q}^2 m\dot{q}^1 + \dot{q}^1 m\dot{q}^2 = 0, \tag{3.55b}$$

with the right-hand side of Equation (3.55a) being null by virtue of the constraint. Therefore, within the present formulation, Equation (2.55a) of Theorem 2.1 is automatically satisfied, and Equation (2.55b) follows by working out the terms $\dot{\lambda}_1 \sin q^3 - m\dot{q}^2\dot{q}^3$ and $-\dot{\lambda}_1 \cos q^3 + m\dot{q}^1\dot{q}^3$.

3.2.4 Case B: Direct use of Theorem 2.1

In addition to what has been done in Remark 3.5, we may also reason in a different way, which constitutes the core of *Ansatz 2*. Specifically, to compute W, we adopt the conditions supplied in Equations (3.44a)–(3.44c) and (3.46a)–(3.46c), which stem from the constraint and from the use of $\hat{\mathcal{F}}^2 \circ \natural = \dot{q}^3$, respectively, and, in lieu of introducing $\mathcal{F}^3$, we invoke directly Theorem 2.1, thereby requiring the vanishing of the quantities in Equation (3.51):

$$\begin{aligned}&(\cos q^3)(\mathsf{W}^{\mathrm{T}}\mathsf{p})_1 + (\sin q^3)(\mathsf{W}^{\mathrm{T}}\mathsf{p})_2 \\ &= p_1 \cos q^3 W^1{}_1 + p_1 \sin q^3 W^1{}_2 + p_2 \cos q^3 W^2{}_1 + p_2 \sin q^3 W^2{}_2 = 0, \end{aligned} \tag{3.56a}$$

$$(\mathsf{W}^{\mathrm{T}}\mathsf{p})_3 = p_1 W^1{}_3 + p_2 W^2{}_3 = 0. \tag{3.56b}$$

This guarantees the equivalence between the MVM and the TNHM.

It is important to remark that the conditions (3.56a) and (3.56b) amount to requiring that the vector associated with $\mathsf{W}^{\mathrm{T}}\mathsf{p}$ lies on the plane on which the skate's motion takes place and *is orthogonal* to the skate's axis. Thus, the plane projection of this vector is orthogonal also to the velocity of the skate's center of mass $\boldsymbol{v}_G$, so that the force $\mathsf{W}^{\mathrm{T}}\mathsf{p}$ produces no power on $\boldsymbol{v}_G$. Moreover, by virtue of Equation (3.56b), $\mathsf{W}^{\mathrm{T}}\mathsf{p}$ produces no source/sink of momentum for p_3, so that it does not spoil its conservation.

The eight conditions (3.44a)–(3.44c), (3.46a)–(3.46c), (3.56a) and (3.56b) permit to determine the nine coefficients of the resulting matrix W up to an arbitrary function ϱ, i.e.,

$$W^1{}_1 = \varrho, \tag{3.57a}$$

$$W^1{}_2 = \frac{p_2\dot{q}^3}{\sin q^3[p_1\cos q^3 + p_2\sin q^3]} - \varrho\cot q^3, \tag{3.57b}$$

$$W^1{}_3 = -p_2\frac{\dot{q}^1\cos q^3 + \dot{q}^2\sin q^3}{p_1\cos q^3 + p_2\sin q^3}, \tag{3.57c}$$

$$W^2{}_1 = -\dot{q}^3 + \varrho\tan q^3, \tag{3.57d}$$

$$W^2{}_2 = -\dot{q}^3\frac{p_1\sin q^3 - p_2\cos q^3}{p_1\cos q^3 + p_2\sin q^3} - \varrho, \tag{3.57e}$$

$$W^2{}_3 = p_1\frac{\dot{q}^1\cos q^3 + \dot{q}^2\sin q^3}{p_1\cos q^3 + p_2\sin q^3}, \tag{3.57f}$$

$$W^3{}_1 = W^3{}_2 = W^3{}_3 = 0. \tag{3.57g}$$

Hence, the equations of motion (2.42a) and (2.42b) take on the form

$$\dot{p}_1 = \quad \dot{\lambda}_1\sin q^3 + mg\sin\alpha + \tfrac{1}{2}QB_0\dot{q}^2 - p_2\dot{q}^3 + \varrho\big[p_1 + p_2\tan q^3\big], \tag{3.58a}$$

$$\dot{p}_2 = -\dot{\lambda}_1\cos q^3 - \tfrac{1}{2}QB_0\dot{q}^1 + p_2\dot{q}^3\cot q^3 - \varrho\big[p_2 + p_1\cot q^3\big], \tag{3.58b}$$

$$\dot{p}_3 = 0. \tag{3.58c}$$

Thus, as predicted by Theorem 2.1, the MVM is equivalent to the TNHM, provided the following identification of the Lagrange multipliers is made:

$$\mu_1 \equiv \dot{\lambda}_1 - p_2\dot{q}^3\csc q^3 + \varrho\big[p_1\csc q^3 + p_2\sec q^3\big]. \tag{3.59}$$

Note that, because of the equivalence between the two methods, the present reformulation of the MVM conserves the momentum p_3, that is, Equation (3.58c) is identical to Equation (3.42c). In this respect, it should also be noticed that, even though Equations (3.58a)–(3.58c) apparently depend on ϱ, which is still unknown, this dependence is not effective. Indeed, if the MVM has to be equivalent to the TNHM, this dependence cancels out by virtue of Equation (2.55a) of Theorem 2.1 when the equations of motion are put in the form (2.51a). This means that, if the equivalence between the MVM and the TNHM is maintained, the determination of the motion does not require the complete knowledge of W and, thus, of ϱ. However, as predicted by Equation (2.51b), the Lagrange multiplier λ_1 does depend on ϱ, thereby yielding a one-parameter family of solutions that are *all* equivalent to those obtained by the TNHM and lead to one, and only one, μ_1. Clearly, as anticipated in *Ansatz 2*, ϱ can be determined through a physics-based condition, or by adopting Corollary 2.1, which requires $\mathsf{W}^{\mathrm{T}}\mathsf{p} = \mathsf{0}$. In particular, the latter case retrieves the condition pointed out by Ramírez and Sadovskaia [59], and, later, by Llibre et al. [16] (see, in particular, Theorem 3 of [16]).

Before closing this section, we find it convenient to summarize the results that we deem particularly noteworthy in the following Remarks.

Remark 3.6 (Consequences of the adopted methodology).
Transpositional relations. Given the matrix W, whose coefficients are reported in Equations (3.57a)–(3.57g), the transpositional relations characterizing the problem at hand are

$$\eta^1_{\dot{q}} - \dot{\eta}^1_q = \frac{p_2\dot{q}^3}{\sin q^3\left[p_1\cos q^3 + p_2\sin q^3\right]}\eta^2_q - \frac{p_2\dot{q}^2}{\sin q^3\left[p_1\cos q^3 + p_2\sin q^3\right]}\eta^3_q, \tag{3.60a}$$

$$\eta^2_{\dot{q}} - \dot{\eta}^2_q = -\dot{q}^3\eta^1_q + \frac{p_2\cos q^3 - p_1\sin q^3}{p_1\cos q^3 + p_2\sin q^3}\dot{q}^3\eta^2_q + \frac{\dot{q}^1\cos q^3 + \dot{q}^2\sin q^3}{p_1\cos q^3 + p_2\sin q^3}p_1\eta^3_q, \tag{3.60b}$$

$$\eta^3_{\dot{q}} - \dot{\eta}^3_q = 0. \tag{3.60c}$$

It is interesting to notice that the unknown parameter ϱ featuring in some coefficients of W, i.e., in Equations (3.57a), (3.57b), (3.57d) and (3.57e), does not enter the transpositional relations in Equations (3.60a)–(3.60c) because of the *Lagrange-Chetaev condition* in Equation (2.12).
Indetermination of the matrix W. Our formulation of the MVM according to *Ansatz 2*, which renounces to one of the auxiliary functions, and invokes directly Theorem

2.1, does not determine univocally all the 9 entries of W. This is testified by the independent unknown ϱ, and follows from the fact that the conditions delivered by Equation (2.55a) are only two (difference between the total number of Lagrangian parameters, i.e., 3, and number of constraints, i.e., 1). Even though this could seem to be a deficiency of our approach with respect to the one developed in [16], one can assign or determine ϱ through other conditions, e.g. physically inspired, as suggested by *Ansatz 2*.

Remark 3.7 (*“Canonical flip”* [57, 52] for the Case B of the “charged skate”). Although the case analyzed here shares some similarities with Remark 3.4, some changes arise, which are worth of being investigated. This time, we start looking at Equations (3.60a)–(3.60c), and we compare them with the relationships (2.21). To this end, we notice that Equations (3.60a) and (3.60b) can be rewritten as

$$\eta^1_{\dot{q}} - \dot{\eta}^1_q = \frac{p_2 \csc q^3}{p_1 \cos q^3 + p_2 \sin q^3}\dot{q}^3\eta^2_q - \frac{p_2 \csc q^3}{p_1 \cos q^3 + p_2 \sin q^3}\dot{q}^2\eta^3_q, \tag{3.61a}$$

$$\begin{aligned}\eta^2_{\dot{q}} - \dot{\eta}^2_q = &- \frac{p_1 \cos q^3}{p_1 \cos q^3 + p_2 \sin q^3}\dot{q}^3\eta^1_q + \frac{p_1 \cos q^3}{p_1 \cos q^3 + p_2 \sin q^3}\dot{q}^1\eta^3_q \\ &- \frac{p_1 \sin q^3}{p_1 \cos q^3 + p_2 \sin q^3}\dot{q}^3\eta^2_q + \frac{p_1 \sin q^3}{p_1 \cos q^3 + p_2 \sin q^3}\dot{q}^2\eta^3_q,\end{aligned} \tag{3.61b}$$

where, to obtain Equation (3.61b), we have made use of the Lagrange–Chetaev condition $(\sin q^3)\eta^1_q - (\cos q^3)\eta^2_q = 0$. Hence, a direct inspection yields

$$\mathcal{C}^1{}_{32} \equiv \hat{\mathcal{C}}^1{}_{32} \circ (q,p) = \frac{p_2 \csc q^3}{p_1 \cos q^3 + p_2 \sin q^3} = -\mathcal{C}^1{}_{23} \equiv -\hat{\mathcal{C}}^1{}_{23} \circ (q,p), \tag{3.62a}$$

$$\mathcal{C}^2{}_{31} \equiv \hat{\mathcal{C}}^2{}_{31} \circ (q,p) = -\frac{p_1 \cos q^3}{p_1 \cos q^3 + p_2 \sin q^3} = -\mathcal{C}^2{}_{13} \equiv -\hat{\mathcal{C}}^2{}_{13} \circ (q,p), \tag{3.62b}$$

$$\mathcal{C}^2{}_{32} \equiv \hat{\mathcal{C}}^2{}_{32} \circ (q,p) = -\frac{p_1 \sin q^3}{p_1 \cos q^3 + p_2 \sin q^3} = -\mathcal{C}^2{}_{23} \equiv -\hat{\mathcal{C}}^2{}_{23} \circ (q,p), \tag{3.62c}$$

whereas all the other coefficients of $\mathcal{C}^h{}_{\ell k}$ can be set equal to zero. It should be noticed that, in the present situation, the nonzero coefficients reported in Equations (3.62a)–(3.62c) are functions of *both* the Lagrangian parameters q *and* of the generalized momenta p. This result is, in fact, a consequence of the Lagrangian function featuring a term linear in the velocities, which, in turn, renders the momenta affine functions of the velocities themselves, and is in harmony with the functional dependence prescribed in [59, 16] for the entries of the matrix W. We emphasize that, in

Equations (3.62a)–(3.62c), the identifications of the functions ${}^{h}\mathcal{C}_{\ell k}$ is *purely* formal, since we have not determined them through the assignment of a set of quasi-velocities.

Remark 3.8 (Absence of electromagnetic interactions [16]). If the interaction with the magnetic field is switched off (i.e., if $B_0(t) = 0$ is zero at all times), Equations (3.50a)–(3.50c), as well as Equations (3.58a)–(3.58c) upon setting $\varrho = 0$, simplify to the case already addressed in [16]. In particular, we obtain the same dynamic equations found by Llibre et al. [16] by employing W as in Equation (3.48) for the "nonholonomic skate" problem, i.e., [16]

$$\dot{p}_1 \equiv m\ddot{q}^1 = -m\dot{q}^2\dot{q}^3 + mg\,\sin\alpha + \dot{\lambda}_1\,\sin q^3, \tag{3.63a}$$

$$\dot{p}_2 \equiv m\ddot{q}^2 = \quad m\dot{q}^1\dot{q}^3 - \dot{\lambda}_1\,\cos q^3, \tag{3.63b}$$

$$\dot{p}_3 = 0. \tag{3.63c}$$

Moreover, the matrix W with coefficients in Equations (3.57a)–(3.57g) trivially reduces to the one in Equation (3.48). Hence, by removing the magnetic interaction, the equivalence between the MVM and the TNHM is restored again for Case A, while, in Case B, the equivalence was already present even with the magnetic interaction. In both cases, the assumptions $B_0 \equiv 0$ and $\varrho = 0$ induce the same relation between the Lagrange multipliers of the two methods, which reads

$$\mu_1 \equiv \dot{\lambda}_1 - m\dot{q}^2\dot{q}^3\,\csc q^3 = \dot{\lambda}_1 - m\left[\dot{q}^1\,\cos q^3 + \dot{q}^2\,\sin q^3\right]\dot{q}^3, \tag{3.64}$$

where the last equality is obtained by working out $\csc q^3$ and employing the constraint. Finally, the absence of the magnetic interaction allows the transpositional relations to simplify to the ones found in [16], i.e.,

$$\eta^1_{\dot{q}} - \dot{\eta}^1_q = \dot{q}^3\eta^2_q - \dot{q}^2\eta^3_q, \qquad \eta^2_{\dot{q}} - \dot{\eta}^2_q = \dot{q}^1\eta^3_q - \dot{q}^3\eta^1_q, \qquad \eta^3_{\dot{q}} - \dot{\eta}^3_q = 0. \tag{3.65}$$

3.2.5 Case C: New formulation of the constraint

Looking at the relationship connecting the generalized velocities and the momenta, the constraint (3.39), the expression of the functions $\mathcal{F}^2$ and $\mathcal{F}^3$ supplied by Llibre et al. [16], and the matrix W of Equation (3.48), we notice that there exists a sort of "natural pattern" among all these characteristic features of the considered problem. Indeed, by referring to Case A, both in Equation (3.39) and in $\mathcal{F}^3$ there appear the

same *constrained velocities*, whereas $\mathcal{F}^2$ involves the "unconstrained velocity" $\dot{q}^3$. Moreover, the structure of W is such that: its first 2×2 block is skew-symmetric in $\dot{q}^3$; its last column features the components of the vector $\boldsymbol{e}_3 \times \boldsymbol{v}_G$, which has zero projection onto the skate's unit vector $\boldsymbol{n}$, so that the mixed product $(\boldsymbol{e}_3 \times \boldsymbol{v}_G) \cdot \boldsymbol{n}$ vanishes, thereby returning the constraint; and its last row is null. These results render the MVM equivalent to the TNHM in the absence of the magnetic field, as highlighted in Remark 3.8, although they lead to a loss of equivalence in the presence of the magnetic field, as made evident in Equations (3.50a)–(3.50c) and in the subsequent discussion. It was indeed this broken equivalence, and the need for restoring it, that made us "re-design" W to obtain the matrix in Equations (3.57a)–(3.57g) under the guidance of Theorem 2.1. However, this required to renounce to the "natural pattern" mentioned above. Yet, this pattern can be recovered by redefining the constraint in such a way that the *effective velocities* of the skate, i.e., p_1/m and p_2/m (or $(\mathsf{M}^{-1}\mathsf{p})_1$ and $(\mathsf{M}^{-1}\mathsf{p})_2$, in matrix notation), rather than $\dot{q}^1$ and $\dot{q}^2$, are constrained. Clearly, this amounts to modifying the original problem, but in a still physically sound way, so as to account for the velocity shift induced by the magnetic field by passing from a constraint linear in the velocities $\dot{q}^1$ and $\dot{q}^2$ to one *affine* in these velocities (see Equation (3.66) below).

By virtue of the discussion above, and setting $\chi \coloneqq \frac{QB_0}{2m}$, we introduce

$$\begin{aligned}\mathcal{V}^1_{\text{new}} \equiv \hat{\mathcal{V}}^1_{\text{new}} \circ \natural &= (\sin q^3)\tfrac{p_1}{m} - (\cos q^3)\tfrac{p_2}{m} \\ &= \sin q^3\left[\dot{q}^1 - \chi q^2\right] - \cos q^3\left[\dot{q}^2 + \chi q^1\right] \\ &= (\sin q^3)\dot{q}^1 - (\cos q^3)\dot{q}^2 - \chi\left[(\sin q^3)q^2 + (\cos q^3)q^1\right] \\ &= 0. \end{aligned} \tag{3.66}$$

The new constraint expressed in Equation (3.66) suggests that the "natural pattern" discussed above can be recovered by defining also the auxiliary functions in terms of the effective velocities, i.e.,

$$\mathcal{F}^2_{\text{new}} \equiv \hat{\mathcal{F}}^2_{\text{new}} \circ \natural = \underbrace{\dot{q}^3 + \chi}_{=:\, 12p_3/m[\ell^2+\sigma^2]}, \tag{3.67a}$$

$$\mathcal{F}^3_{\text{new}} \equiv \hat{\mathcal{F}}^3_{\text{new}} \circ \natural = \cos q^3 \underbrace{\left[\dot{q}^1 - \chi q^2\right]}_{=:\, p_1/m} + \sin q^3 \underbrace{\left[\dot{q}^2 + \chi q^1\right]}_{=:\, p_2/m}. \tag{3.67b}$$

Accordingly, the new solvability conditions read

$$\mathcal{D}_1\hat{\mathcal{V}}^1_{\text{new}} \circ \sharp = (\sin q^3)W^1{}_1 - (\cos q^3)W^2{}_1 - (\cos q^3)\left[\dot{q}^3 + \chi\right] = 0, \tag{3.68a}$$
$$\mathcal{D}_2\hat{\mathcal{V}}^1_{\text{new}} \circ \sharp = (\sin q^3)W^1{}_2 - (\cos q^3)W^2{}_2 - (\sin q^3)\left[\dot{q}^3 + \chi\right] = 0, \tag{3.68b}$$
$$\mathcal{D}_3\hat{\mathcal{V}}^1_{\text{new}} \circ \sharp = (\sin q^3)W^1{}_3 - (\cos q^3)W^2{}_3 + (\cos q^3)\tfrac{p_1}{m} + (\sin q^3)\tfrac{p_2}{m} = 0, \tag{3.68c}$$
$$\mathcal{D}_1\hat{\mathcal{F}}^2_{\text{new}} \circ \sharp = W^3{}_1 = 0, \tag{3.68d}$$
$$\mathcal{D}_2\hat{\mathcal{F}}^2_{\text{new}} \circ \sharp = W^3{}_2 = 0, \tag{3.68e}$$
$$\mathcal{D}_3\hat{\mathcal{F}}^2_{\text{new}} \circ \sharp = W^3{}_3 = 0, \tag{3.68f}$$
$$\mathcal{D}_1\hat{\mathcal{F}}^3_{\text{new}} \circ \sharp = (\cos q^3)W^1{}_1 + (\sin q^3)W^2{}_1 + (\sin q^3)\left[\dot{q}^3 + \chi\right] = 0, \tag{3.68g}$$
$$\mathcal{D}_2\hat{\mathcal{F}}^3_{\text{new}} \circ \sharp = (\cos q^3)W^1{}_2 + (\sin q^3)W^2{}_2 - (\cos q^3)\left[\dot{q}^3 + \chi\right] = 0, \tag{3.68h}$$
$$\mathcal{D}_3\hat{\mathcal{F}}^3_{\text{new}} \circ \sharp = (\cos q^3)W^1{}_3 + (\sin q^3)W^2{}_3 \underbrace{-(\sin q^3)\tfrac{p_1}{m} + (\cos q^3)\tfrac{p_2}{m}}_{=0} = 0. \tag{3.68i}$$

Finally, by virtue of these results, the new matrix W_{new}, which solves Equations (3.68a)–(3.68i), takes on the form

$$\mathsf{W}_{\text{new}} = \begin{bmatrix} 0 & \left(\dot{q}^3 + \chi\right) & -\left(\dot{q}^2 + \chi q^1\right) \\ -\left(\dot{q}^3 + \chi\right) & 0 & \left(\dot{q}^1 - \chi q^2\right) \\ 0 & 0 & 0 \end{bmatrix}, \tag{3.69}$$

which corresponds to *shifting* the original matrix W_{old} in Equation (3.48) by a matrix

$$\mathsf{W}_{\text{mag}} = \chi \begin{bmatrix} 0 & 1 & -q^1 \\ -1 & 0 & -q^2 \\ 0 & 0 & 0 \end{bmatrix}, \tag{3.70}$$

which accounts for the interaction of the skate with the magnetic field, i.e., $\mathsf{W}_{\text{new}} = \mathsf{W}_{\text{old}} + \mathsf{W}_{\text{mag}}$.

We notice that, since the new constraint $\mathcal{V}^1_{\text{new}}$ in Equation (3.66) is the sum of the original constraint in Equation (3.39) and of an additional term not involving the generalized velocities, the condition in Equation (2.55a), which guarantees the equivalence between the MVM and the TNHM, requires the vanishing of the same terms displayed in Equation (3.51). Indeed, by computing the product $\mathsf{W}^{\mathrm{T}}_{\text{new}}\mathsf{p}$, we

observe that the equivalence is satisfied, since the following identities hold:

$$(\cos q^3)(\mathsf{W}_{\text{new}}^{\mathrm{T}}\mathsf{p})_1 + (\sin q^3)(\mathsf{W}_{\text{new}}^{\mathrm{T}}\mathsf{p})_2 = \frac{12 p_3}{\ell^2 + \sigma^2}\left[\sin q^3 \frac{p_1}{m} - \cos q^3 \frac{p_2}{m}\right] = 0, \tag{3.71a}$$

$$(\mathsf{W}_{\text{new}}^{\mathrm{T}}\mathsf{p})_3 = -\frac{p_2}{m} p_1 + \frac{p_1}{m} p_2 = 0. \tag{3.71b}$$

Moreover, the dynamic equations returned by the MVM with the new formulation of both the constraint in Equation (3.66) and the auxiliary functions in Equations (3.67a) and (3.67b) read

$$\dot{p}_1 = \dot{\lambda}_1 \sin q^3 + mg \sin\alpha + \tfrac{1}{2} Q B_0 \dot{q}^2 - p_2 \left(\dot{q}^3 + \chi\right), \tag{3.72a}$$

$$\dot{p}_2 = -\dot{\lambda}_1 \cos q^3 - \tfrac{1}{2} Q B_0 \dot{q}^1 + p_1 \left(\dot{q}^3 + \chi\right), \tag{3.72b}$$

$$\dot{p}_3 = 0. \tag{3.72c}$$

Finally, the relation between the Lagrange multipliers of the MVM and the TNHM is a direct consequence of Equations (3.72a) and (3.72b), and, following the same procedure as in Equation (3.59), it holds that

$$\mu_1 \equiv \dot{\lambda}_1 - (p_1 \cos q^3 + p_2 \sin q^3)\left(\dot{q}^3 + \chi\right). \tag{3.73}$$

Remark 3.9 (*“Canonical flip”* [57, 52] for the Case C of the “charged skate”). Looking at Equation (3.69), it is immediate to notice that, in spite of the presence of the factor χ, the structure of the “new” matrix W_{new} is the same as the one obtained for the Case A (see Equation (3.48)), with the sole difference that the entries of W_{new} coincide with the components of the momenta of the theory, p, normalized by the corresponding components of the mass matrix. A direct consequence of this fact is that the coefficients ${\mathcal{C}^h}_{\ell k}$ of the “Canonical flip” characterizing this version of the considered problem are exactly those determined in Remark 3.4, provided that the transpositional relations are written as

$$\eta_{\dot{q}}^1 - \dot{\eta}_q^1 = +(\dot{q}^3 + \chi)\eta_q^2 - (\dot{q}^2 + \chi q^1)\eta_q^3 = + \underbrace{\frac{12\, p_3}{m[\ell^2 + \sigma^2]}}_{=:\pi^3} \eta_q^2 - \underbrace{\frac{p_2}{m}}_{=:\pi^2} \eta_q^3, \tag{3.74a}$$

$$\eta^2_{\dot{q}} - \dot{\eta}^2_q = -(\dot{q}^3 + \chi)\eta^1_q + (\dot{q}^1 - \chi q^2)\eta^3_q = -\underbrace{\frac{12\,p_3}{m[\ell^2 + \sigma^2]}}_{=:\pi^3}\eta^1_q + \underbrace{\frac{p_1}{m}}_{=:\pi^1}\eta^3_q, \quad (3.74b)$$

$$\eta^3_{\dot{q}} - \dot{\eta}^3_q = 0, \quad (3.74c)$$

where π^1, π^2, and π^3 are the normalized momenta, and can be interpreted as the *effective velocities* of the problem at hand (in the sense that they are the physical quantities, having physical dimensions of velocities, that are effectively constrained).

Chapter 4

Concluding remarks of Part I

The content of this chapter is taken from [1].

In Part I, we have employed the "modified vakonomic method" (MVM), introduced by Llibre et al. [16], to achieve four main results that, in our opinion, may deepen the understanding of vakonomic mechanics:

(i) We have shown that, for the "rolling coin" problem, the TNHM and MVM are equivalent. By doing so, we have proven that the methodology outlined in [16], which, however, was not adopted therein for this problem, allows to reconcile the vakonomic approach with the traditional one, at least for the considered case. This result, in fact, confirms the statement given by Lemos [17], who spoke of *"complete inequivalence between the vakonomic and the non-holonomic method"*, but it contextually indicates how to overcome this inconsistency by using the procedure developed in [16].

(ii) After testing the methodological power of the MVM with the "rolling coin", we have considered another widely studied problem, namely, the "non-holonomic skate", and we have elaborated a variant of it obtained by assuming the skate to be electrically charged and exposed to an imposed, homogeneous magnetic field (we have, in fact, modified the framework outlined in [25]). We emphasize, in this respect, that, whereas Llibre et al. [16] studied the uncharged "non-holonomic skate" by using their MVM, we have studied the variant to this problem described above in two steps. First, we have employed the MVM *as is* (i.e., as formulated in [16]), and we have seen that, according to

our results, it *is not* equivalent to the TNHM as long as the auxiliary functions of the MVM are taken like in [16]. However, our second step was to show that, by following the rationale supplied by Theorem 2.1, the equivalence can be restored through a suitable set of conditions on W entering the transpositional relations.

(iii) Theorem 2.1, in fact, is the result that states the characterizing conditions by which the MVM can always be made consistently equivalent to the TNHM. This, however, requires to further modify the MVM according to the physical motivations given in *Ansatz 2*. Although the germinal idea of this modification is already present in [59] (cf. the condition $\mathsf{W}^{\mathrm{T}}\mathsf{p} = 0$, in our notation) and in [16] (cf. the unnumbered equation in the Remark 19 of [16] with our Equations (2.55a) and (2.55b)), we have reinterpreted and expanded it to formulate a new criterion, which we may call "M^{2}VM", where "M^2" stands for "Modified Modified". The reason for this, as remarked in Section 3.2, is that one can formulate problems for which it is not straightforward to find a full set of auxiliary functions guaranteeing the equivalence between the MVM and the TNHM. Therefore, in our opinion, the approach outlined in [16] should be augmented by invoking Theorem 2.1.

(iv) In Section 3.2.5, we have highlighted the existence of a "natural pattern", and we have discussed how this "pattern" is not respected when the charged nonholohomic skate is subjected to the classical constraint (3.39), and the auxiliary functions supplied in Equations (3.45a) and (3.45b) are used (cf. [16]). Thus, we have proposed a variant of the constraint in which the constrained velocities are the *effective ones*, i.e., those obtained by dividing the momenta p_1 and p_2 by the mass, and p_3 by the corresponding coefficient of the mass matrix, and we have re-defined the auxiliary functions in terms of such velocities. As reported in Section 3.2.5, this restores the pattern and allows to apply the MVM by Llibre et al. [16] *as is*. In addition, this way of looking at a given mechanical problem could lead to a more physical conception of the constraints which may result, for instance, in the passage from a constraint linear in the velocities to one that is affine in them.

We are aware of studies (see, e.g., [15, 31, 7]) suggesting that, for some problems of field theory or geometric control theory, the vakonomic method leads to results that are sometimes believed to be physically remarkable in comparison with those

obtained with the traditional non-holonomic method. This belief, in our opinion, promotes further investigations on the vakonomic method, with its generalizations, and on its relationship with the TNHM. In this respect, it is important to emphasize that the aim of our work is not to affirm that the TNHM should always be taken as reference for all types of problems, and that, thus, other methods (e.g. the MVM) should always be made equivalent to it. However, we are saying that, if there are physical reasons —even very subtle ones— hinting that the MVM can be made equivalent to the TNHM, then this equivalence must be accounted for. Indeed, following this philosophy, we highlighted, through Theorem 2.1, the possibility of applying the variational approach of Llibre et al. [16] to a class of problems that the scientific community regards as correctly described by the TNHM.

It should be noted that, by promoting the further study of the *vakonomic procedure*, we intend the study of *generalized variational procedures* that well-suit the nonholonomic setting and, when expected, should be consistent with the TNHM. In fact, to our knowledge, there is no experimental evidence implying that the VM is better than the TNHM in modeling classical mechanical systems subjected to nonholonomic constraints (see e.g. [26, 50]), but this discussion is out of the scope of our work. In light of the previous sentence, our interest for the MVM relies on the possibility of having a fully-variational procedure specialized to non-holonomic systems, which, while being consistent with the TNHM, allows to exploit the Lagrangian formalism.

As a last remark, we would like to emphasize that our work served, essentially, two main purposes. The first one was to satisfy our need to test the MVM in its original formulation by [16] against both standard (see Section 3.1) and non-standard (see Section 3.2) problems in order to see whether or not the consistency with the TNHM holds. Exactly in this spirit, we view our work as an instructive “exercise” on the MVM. The second purpose, instead, was to propose some *modifications* of the MVM that ensure both the consistency with the TNHM (see Theorem 2.1) and the fulfillment of the appropriate transpositional relations (see Remark 2.2.2). Given the results above, future investigations could make use of the insight gained in this work on the MVM to look for symmetries in complicated systems (see [63] for a review on Noether’s theorem in non-holonomic systems), and for extending the MVM to the continuum setting as a tool for approaching the rheonomy and non-holonomy of the inelastic processes [23, 32].

Part II

Biomechanical problems

Chapter 5

An approach to growth mechanics based on nonholonomic constraints

The content of this chapter is taken from [2], as well as from its Supplementary Material. Note that the labels employed in some of the figures reported in Section 5.6 differ from those reported in the Supplementary Material of [2] to adhere with the change in notation from "$\boldsymbol{K}$" to "$\boldsymbol{F}_\gamma$".

5.1 *Return ticket* from growth to Analytical Mechanics

The primary purpose of this chapter[1] is to construct a *quasi-variational theory* of the mechanics of volumetric growth. By "quasi-variational" we mean that, even though we formulate a field theory of growth, with its own Lagrangian density function and action functional, we also need to consider peculiar interactions that do not admit a potential, not even in generalized sense. These interactions can rather be described by force-like entities [69] (see also [70], and [10, 71] for the rationale behind this approach), which have to be deduced constitutively when they are regarded as internal, or assigned phenomenologically when they are rated as external. In both cases, however, they can be so complicated and problem specific, that they cannot be determined from a single scalar function. For this reason, such

[1]The wording *"return ticket"* in this context was first used during the conference "Giornata Signorini" held in Florence, Italy, on December 15, 2023, within the presentation of the abstract "A revisitation of Kozlov's Vakonomic Mechanics: modifications, reconciliation, and new perspectives", authored by A. Pastore, A. Giammarini, A. Grillo.

forces are referred to as non-potential, or *"polygenic"* in the terminology of [11], while those that can be obtained by differentiation of a generalized potential are said to be *"monogenic"*, or "*single-generated*" [11].

While non-potential forces must be allotted in a model of growth to study biologically relevant situations, the Lagrangian density function of a growing medium is *"apodeictic"*[2], i.e., it represents a model that is "true" by itself, since it is assigned on the basis of all the hypotheses done on the body (see also [72]). In other words, the Lagrangian density function is constructed so as to account for all the items of information that can be "condensed" in one (pseudo-)scalar quantity. Therefore, if the body is assumed to be hyperelastic, and if one can find, or design, interactions that admit generalized potentials, such as inertial forces (although they are often negligible), gravity, and forces acting on the body's internal structure, then the Lagrangian function will consist of the body's kinetic energy, strain energy, and all the other potential terms that participate in the body's dynamics.

Why a Lagrangian theory of growth: advantages and problems. Aside from mathematical elegance, a Lagrangian theory of growth has some advantages. To mention a few: it is self-contained; up to non-potential forces, it encloses both the *"direct"* and the *"configurational"* dynamics of a body [73, 10, 74], and it unfolds each of them depending on the variations that are performed on the arguments of the body's Lagrangian function (here, the adjectives *"direct"* and *"configurational"* are intended as in [73], and [10], respectively); through Noether's Theorem (see, e.g., [75, 76, 74, 63, 77]), it provides the natural device for investigating the symmetries of a body, the related conservation laws, and the symmetry breaking brought about by growth along with its consequences on the body's overall dynamics [77]. In addition, a field-theoretical approach to growth can be inherently geometrized [78–80], so as to account for the phenomenological aspects connected with the incompatibility of the distortions induced by growth [81], and it supplies the basis for including other theories, like that of micromorphic media [82].

Yet, to benefit from all these advantages, one has to answer the question as to whether the Lagrangian density function of a growing body is able to account also for the core feature of the mechanics of volumetric growth, which is the presence

[2]We are thankful to Prof. Gaetano Giaquinta (1945–2016) for teaching us the meaning of this word in relation to Lagrangian functions.

of mass sources that, acting in the body's interior, trigger its variation of mass [83]. These sources are positive when mass increases, as is the case for cell proliferation in tumors, and negative when mass is depleted due to removal processes such as necrosis or apoptosis [84, 85]. In both situations, they appear in the body's mass balance law, and must be characterized very accurately in order to capture the combination of the biochemical, biophysical, and mechanical stimuli from which they originate (see, e.g., [69, 86]).

Mass sources: a posteriori and a priori approaches. To our knowledge, two distinct paths can be followed for characterizing mass sources in accordance with experimental evidences. As reported in [87], the functional form expressing a mass source is called *"growth law"*, and it can be determined by employing *"a posteriori approaches"* or *"a priori approaches"*. Both rely on the Bilby–Kröner–Lee (BKL) decomposition of the deformation gradient tensor of the growing medium under study. The anelastic factor of such decomposition, termed *growth tensor*, is identified with the descriptor of the medium's structural transformations accompanying its growth. A crucial aspect is that the mass balance law of the medium can be recast in the form of a relationship between the mass source active in it and the trace of the time rate of the growth tensor (see, e.g., [83, 73, 88–90]).

In the a posteriori approaches, an initial and boundary value problem is formulated for determining both the motion and the growth tensor of the body, and, once the growth tensor is known, the source of mass is obtained *"a posteriori"* [87, 91] by setting it equal to the trace of the growth tensor time rate [73, 90, 77]. It should be noticed that, even describing the evolution of the growth tensor very accurately, the growth laws obtained with the a posteriori approaches, being calculated quantities, may exhibit discrepancies with the ones observed experimentally.

In the a priori approaches, the growth law is prescribed by the modeler to reproduce experiments [92–94], to comply with phenomenology [88, 89, 95, 84, 96–98], or to test the response of a medium to a mass source designed to match some target biomechanical behavior. This may occur, for instance, in control problems, or when a specific medicament is analyzed. In all these cases, using the knowledge of the given growth law in the mass balance of the medium under study amounts to imposing a condition on the time rate of its growth tensor. If the latter is viewed as a generalized kinematic variable [69, 86], this condition acquires the meaning of a

constraint [23, 32]. In particular, unless very specific growth laws are considered, this constraint can only be expressed as a differential relationship, and is thus classified as *nonholonomic* [11, 13, 12, 14], i.e., it cannot be obtained by time differentiation of a scalar function of the sole growth tensor, material points and time. We recall that, on the contrary, a constraint is said to be holonomic when the converse is true [11].

As discussed in [23, 32], interpreting the mass balance of a growing medium as a nonholonomic constraint on the growth tensor ensures that the evolution of this quantity complies with the growth law taken as target, while granting the freedom of modeling other interactions as necessary. Hence, no further restrictions are placed on the growth tensor, if unneeded (see, e.g., [92, 93], and [23] for some remarks on this issue), and its dynamics is dictated by the constraint and the balance of the configurational forces obtained through the quasi-variational procedure outlined in the forthcoming sections.

Nonholonomic constraints: Kozlov's Method and its modifications. The considerations reported so far lead to the fundamental question as to whether a nonholonomic constraint can be handled *variationally*. While the answer is affirmative for holonomic constraints, which can be appended to the Lagrangian function of a given mechanical system through the Lagrange multiplier technique (see, e.g., [11]), the extension of such procedure to nonholonomic constraints is not trivial, and has been the subject of a whole branch of literature. In particular, this was the main point of the works by Kozlov [41–44, 99], who developed a formulation of analytical mechanics in which it was claimed that Hamilton's Principle of stationary action can be employed also to Lagrangian functions augmented with the Lagrange multiplier method applied to nonholonomic constraints. In the literature, Kozlov's approach is termed "Vakonomic Method" (VM).

If, on the one hand, exploiting Kozlov's idea would allow to cast the nonholonomic constraint on the growth tensor in the variational picture which we are looking for —and that, as previously discussed, is the primary scope of our work—, on the other hand, a lot of caution is necessary to "import" Kozlov's method *as is*. Indeed, many critiques have been raised towards it (see, e.g., [26, 50, 17]), because, in several cases, it has been proven to be inconsistent with the well consolidated results of the analytical mechanics of nonholonomic systems, based on *Extended Hamilton's Method* or, equivalently, on the *d'Alembert–Lagrange Principle* [11, 39]. In the

sequel, we shall refer to both approaches as the *"Traditional Non-Holonomic Method"* (TNHM) [1].

In spite of the problems related to the VM, a work by Llibre et al. [16] proposes a *"Modified Vakonomic Method"* (MVM) [16], which, for the class of constraints analyzed by the authors, is able to save the idea of handling nonholonomic constraints variationally. This is achieved by raising a technical issue: namely, the variations performed on the generalized velocities restricted by the considered nonholonomic constraints should not be taken equal to the time derivatives of the variations of the associated Lagrangian parameters. This non-commutativity between time differentiation and variation of a given kinematic descriptor is known as *"transpositional relation"* [13, 30, 16], and constitutes a fundamental concept of the mechanics of nonholonomic systems.

Llibre et al. [16] employ transpositional relations in conjunction with a variational procedure referred to as *Hamilton–Suslov Variational Principle* [61, 60], which they apply to a Lagrangian function augmented with the considered nonholonomic constraints, just as Kozlov would do, but taking the variations on the system's generalized velocities consistently with the transpositional relations. Moreover, Llibre et al. [16] develop their MVM in two ways, which they formalize in two corresponding theorems (see Theorem 1 and Theorem 3 of [16]). In the present work, we are interested in comparing our approach with the formulation of the MVM provided in their Theorem 1, and in studying how it applies to our growth problem. Hence, from here on, Llibre et al.'s MVM [16] refers to their Theorem 1.

Outline of the content of Chapter 5. While the MVM has been recently reviewed in [1], in the present chapter we investigate whether the MVM can be used for handling variationally the nonholonomic constraint placed on the growth tensor. Although for this purpose we take much inspiration from [16], we find that we need to reformulate it remarkably in order to reach our goal. Indeed, rather than adhering to the theory presented in [16], we follow a different path, which, to a certain extent, could be regarded as the "inverse" of the one developed in [16]. However, also other noticeable differences arise, and the main novelties of our work are:

N1. Upon considering the mass balance law of the growing medium under study as a nonholonomic constraint on the growth tensor [23, 32], we determine the transpositional relations associated with it by having recourse to the concept

of *quasi-velocities* [13, 100], which we suitably adapt to the problem at hand. We remark that quasi-velocities constitute a pillar of the analytical mechanics of nonholonomic systems, but, to the best of our knowledge, they have not been employed to describe growth, yet. For our purposes, we use the algebra of fourth-order tensors, as shown in Sections 5.3.1 and 5.3.2.

N2. We show that, by means of our reformulation of the MVM by Llibre et al. [16], it is possible to obtain the full equivalence between our approach and the TNHM (see Section 5.4). This is the *core result* of our work because, starting from the dynamic equations of a growing body, written in the system of the quasi-velocities (Section 5.4.1), it allows us to conclude that one can determine a Lagrangian density function even in the presence of the nonholonomic constraint on the growth tensor (Section 5.4.2).

N3. We analyze in detail the quasi-static case, since it is the most relevant one in the biomechanical problems of interest, and we show that our method is able to recover other formulations [69, 90, 101, 102] (Section 5.4.3).

N4. We highlight the main differences between our results and those of Llibre et al. [16], and we provide a theorem and a corollary to state the conditions under which the latter ones can be used for modeling growth.

To present our results, we review some well-established formulations of growth mechanics based on the Principle of Virtual Work [69, 86, 90, 101, 103, 104, 32, 87, 91] (Section 5.2.1) and the Extended Hamilton Method [11, 105, 77] (Section 5.2.2). Although both of them are rather consolidated, it is important for us to recapitulate their most essential logical steps to compare the resulting dynamic equations with those obtained in the present work (Section 5.4).

5.1.1 Main notations employed

To express the ideas presented in the following, it is convenient to start with the presentation of the main notation used throughout this chapter.

Let us denote by $\mathscr{B}$ the reference placement of the medium under investigation (an open subset of the three-dimensional Euclidean space $\mathscr{S}$), by $\partial\mathscr{B}$ its boundary, and by $\mathscr{I}$ the *time line* [24].

In our setting, $\mathscr{B}$ is assumed to be a smooth differentiable manifold, endowed, for all $X \in \mathscr{B}$, with the metric tensor $\boldsymbol{G}(X) : T_X\mathscr{B} \to T_X^*\mathscr{B}$, where $T_X\mathscr{B}$ and $T_X^*\mathscr{B}$ are the tangent space and cotangent space of $\mathscr{B}$ at $X \in \mathscr{B}$, respectively. For future use, we also introduce the tangent bundle $T\mathscr{B} := \cup_{X\in\mathscr{B}}\big(\{X\} \times T_X\mathscr{B}\big)$ and the cotangent bundle $T^*\mathscr{B} := \cup_{X\in\mathscr{B}}\big(\{X\} \times T_X^*\mathscr{B}\big)$.

By letting $(Z^I)_{I=1}^3$ and $(X^A)_{A=1}^3$ be a system of Cartesian and curvilinear coordinates, and $(\Phi^I)_{I=1}^3$ the collection of real-valued C^∞-functions such that $Z^I = \Phi^I(X^1, X^2, X^3)$, for $I = 1, 2, 3$, with non-singular Jacobian $[\partial_K\Phi^I]_{I,K=1}^3$ [24], the components of $\boldsymbol{G}$ are given by $G_{AB} = \delta_{IK}\partial_A\Phi^I\partial_B\Phi^K$, where δ_{IK} is the Kronecker Delta [24]. Together with $\boldsymbol{G}$, $\mathscr{B}$ is endowed with an affine connection, which, for our purposes, can be taken equal to the one induced by the chosen curvilinear coordinates.

Let us consider the list of the kinematic and space-time variables that are necessary for our minimal description of the medium's volumetric growth:

$$\natural := (\chi, D\chi, \boldsymbol{F}, \boldsymbol{F}_\gamma; \dot{\chi}, \overset{\cdot}{\overline{D\chi}} \equiv \mathrm{Grad}\dot{\chi}, \dot{\boldsymbol{F}}, \dot{\boldsymbol{F}}_\gamma; \mathfrak{X}, \mathfrak{T}). \tag{5.1}$$

Each entry of $\natural$ is a function defined over the Cartesian product $\mathscr{B} \times \mathscr{I}$, and valued in an appropriate set of points, or in a vector or tensor space. To be specific, the following identifications apply:

1. $\chi : \mathscr{B} \times \mathscr{I} \to \mathscr{S}$ defines, for varying time $t \in \mathscr{I}$, the one-parameter family of embeddings $\chi(\,\cdot\,, t) : \mathscr{B} \to \mathscr{S}$ mapping the points $X \in \mathscr{B}$ in the three-dimensional Euclidean space $\mathscr{S}$ at time $t \in \mathscr{I}$.

2. For each pair $(X, t) \in \mathscr{B} \times \mathscr{I}$, $D\chi(X, t) : T_X\mathscr{B} \to T_{\chi(X,t)}\mathscr{S}$ is the two-point tensor defining the Jacobian tensor of $\chi(\,\cdot\,, t)$ at $X \in \mathscr{B}$. Here, $T_{\chi(X,t)}\mathscr{S}$ is the tangent space of $\mathscr{S}$ at $\chi(X, t) \in \mathscr{S}$. The tensor $D\chi(X, t)$ represents the deformation gradient tensor of the body, and with respect to two local coordinate systems, covering a neighborhood of $X \in \mathscr{B}$ and a neighborhood of $x = \chi(X, t) \in \mathscr{S}$, respectively, the components of $D\chi$ are given by the partial derivatives $[D\chi]^a{}_A \equiv \partial_A\chi^a \equiv \partial\chi^a/\partial X^A$, with $a, A = 1, 2, 3$.

3. $\boldsymbol{F}$ is an "auxiliary" deformation gradient tensor field, which, for our purposes, is regarded as a generalized kinematic variable on its own. Later, it will be identified with $D\chi$. This is done in order to unfold a variational procedure similar to the Hu–Washizu variational principle [106].

4. $\boldsymbol{F}_\gamma$ is referred to as *growth tensor* (see, e.g., [89]), and represents the time-dependent anelastic tensor field describing the structural distortions associated with growth [89, 80]. The tensor $\boldsymbol{F}_\gamma(X,t)$ maps the vectors of $T_X\mathscr{B}$ into the linear vector space, denoted by $\mathscr{N}_X(t)$ [107, 108], that defines the *natural state* of $T_X\mathscr{B}$ at time $t \in \mathscr{I}$ (see, e.g., [69, 80, 109, 103]). Hence, we can write $\boldsymbol{F}_\gamma(X,t) : T_X\mathscr{B} \to \mathscr{N}_X(t)$. We recall that $T_X\mathscr{B}$ is referred to as *"body element"* in [69]. For a given $t \in \mathscr{I}$, $\mathscr{N}(t) := \cup_{X\in\mathscr{B}}\big(\{X\} \times \mathscr{N}_X(t)\big)$ denotes the bundle of linear spaces representing the natural state of the body at time t. Once $\mathscr{N}(t)$ is introduced, we indicate with $\boldsymbol{F}_\gamma(\,\cdot\,,t)$ the tensor field $\boldsymbol{F}_\gamma(\,\cdot\,,t) : \mathscr{B} \to \mathscr{N}(t) \otimes T^*\mathscr{B}$. Moreover, we also define the collection of natural states $\mathscr{N} := \cup_{t\in\mathscr{I}}\big(\cup_{X\in\mathscr{B}}\big(\{X\} \times \mathscr{N}_X(t)\big)\big)$.

5. $\dot{\chi} : \mathscr{B} \times \mathscr{I} \to T\mathscr{S}$ is the (Lagrangian) velocity field associated with χ, so that $\dot{\chi}(X,t) \in T_{\chi(X,t)}\mathscr{S}$. The superimposed dot means $\dot{\chi}(X,t) \equiv \partial_t\chi(X,t)$. Analogously, $\dot{\boldsymbol{F}} \equiv \partial_t\boldsymbol{F}$ and $\dot{\boldsymbol{F}}_\gamma \equiv \partial_t\boldsymbol{F}_\gamma$.

6. $\mathfrak{X} : \mathscr{B} \times \mathscr{I} \to \mathscr{B}$ and $\mathfrak{T} : \mathscr{B} \times \mathscr{I} \to \mathscr{I}$ denote the projections $\mathfrak{X}(X,t) = X$ and $\mathfrak{T}(X,t) = t$. For any physical quantity f defined as a function $\hat{f}$ of $\boldsymbol{F}$ and $\boldsymbol{F}_\gamma$, and exhibiting explicit dependence on points and time, we write $f = \hat{f} \circ (\boldsymbol{F}, \boldsymbol{F}_\gamma, \mathfrak{X}, \mathfrak{T})$ and $f(X,t) = \hat{f}(\boldsymbol{F}(X,t), \boldsymbol{F}_\gamma(X,t), X, t)$ [110].

For any second-order tensor $\boldsymbol{T}$, we use the wordings "$\boldsymbol{A}$-deviatoric part" and "$\boldsymbol{A}$-spherical part" of $\boldsymbol{T}$, with $\boldsymbol{A}$ being an appropriate non-singular second-order tensor, to indicate $\boldsymbol{T} - \frac{1}{3}\mathrm{tr}(\boldsymbol{A}^{-1}\boldsymbol{T})\boldsymbol{A}$ and $\frac{1}{3}\mathrm{tr}(\boldsymbol{A}^{-1}\boldsymbol{T})\boldsymbol{A}$, respectively.

To perform operations involving vectors, tensors, and their dual entities, we employ the notation of duality pairs between a generic vectorial or tensorial quantity $\boldsymbol{V}$ and its dual entity $\boldsymbol{\Omega}$. Hence, we denote by $\langle\boldsymbol{\Omega}|\boldsymbol{V}\rangle$ the real-valued application of the linear map $\boldsymbol{\Omega}$ to $\boldsymbol{V}$. For example, if $\boldsymbol{V}$ is a vector and $\boldsymbol{\Omega}$ is a co-vector, we obtain $\langle\boldsymbol{\Omega}|\boldsymbol{V}\rangle = \Omega_A V^A$. Similarly, if $\boldsymbol{V}$ and $\boldsymbol{\Omega}$ are mixed second-order tensors with components $V^L{}_M$ and $\Omega_P{}^Q$ in some coordinate system, then we find $\langle\boldsymbol{\Omega}|\boldsymbol{V}\rangle = \Omega_A{}^B V^A{}_B = \mathrm{tr}(\boldsymbol{\Omega}^{\mathrm{T}}\boldsymbol{V})$.

Given two fourth-order tensors $\mathbb{L}$ and $\mathbb{K}$ having components, e.g., $\mathbb{L}^A{}_B{}^C{}_D$ and $\mathbb{K}_P{}^Q{}_{RS}$, we define the operation $\mathbb{L} \diamond \mathbb{K}$ as the contraction of the second pair of indices of the first tensor with the first pair of indices of the second tensor, i.e., in components, $[\mathbb{L} \diamond \mathbb{K}]^A{}_{BRS} := \mathbb{L}^A{}_B{}^M{}_N \mathbb{K}_M{}^N{}_{RS}$.

By viewing a fourth-order tensor $\mathbb{L}$ as a linear map $\mathbb{L} : \mathscr{U} \to \mathscr{V}$ between the spaces of second-order tensors $\mathscr{U}$ and $\mathscr{V}$, possibly of different kind, we write

$\mathbb{L}[\boldsymbol{U}] = \boldsymbol{V}$ to denote the application of $\mathbb{L}$ to $\boldsymbol{U} \in \mathscr{U}$ returning $\boldsymbol{V} \in \mathscr{V}$. For example, if $\mathbb{L}$ and $\boldsymbol{U}$ have components $\mathbb{L}^A{}_B{}^C{}_D$ and $U_P{}^Q$, then $\boldsymbol{V}$ has components given by $V^A{}_B = \mathbb{L}^A{}_B{}^M{}_N U_M{}^N$. The transpose of $\mathbb{L}$ is defined through $\langle \boldsymbol{\Omega} | \mathbb{L}[\boldsymbol{U}] \rangle = \langle \mathbb{L}^{\mathrm{T}}[\boldsymbol{\Omega}] | \boldsymbol{U} \rangle$, and $\mathbb{L}^{\mathrm{T}}$ has components $[\mathbb{L}^{\mathrm{T}}]^C{}_D{}^A{}_B$.

5.1.2 An overview from *geometric* to *configurational* mechanics

The process of volumetric growth manifests itself through a source of mass, hereafter denoted by R, and yields a variation in time of the mass density of the body under study. This is captured by the mass balance law, which, in the body's reference placement $\mathscr{B}$, is given by $\dot{\varrho}_{\mathrm{R}} = \varrho_{\mathrm{R}} R$, with ϱ_{R} being the body's mass density per unit volume of $\mathscr{B}$ (see, e.g., [73]).

In general, the variation of ϱ_{R} represents a reorganization of the internal structure of the body that is virtually independent of deformation. Moreover, it introduces inhomogeneities [111, 76, 112] that do not amount only to nonuniform redistributions of mass within the body, and that, similarly to dislocations [113–115], cannot be eliminated by deformation alone.

Growth can be accompanied also by other structural reorganizations, which, although possibly related to R, do not directly induce changes of ϱ_{R}. All these structural processes lead to *incompatible rearrangements* of the body elements, often termed *anelastic*. When such rearrangements occur, the body elements tend to find themselves in a state in which they do not *"fit together"* [80]. This produces *residual stresses* [81, 116], which are the mechanical manifestation of incompatibility [117, 116].

Incompatibility is a geometric concept expressing that, in general, the above mentioned rearrangements cannot be reduced to maps transforming $\mathscr{B}$ into other body material manifolds in the Euclidean space. For these reasons, a second-order tensor field —in fact, $\boldsymbol{F}_\gamma$— that is not defined as the tangent map [24] of a deformation is a suitable descriptor for growth and for the other structural reorganization processes related to it.

From the mechanical point of view, the residual stresses accumulated in the body elements in response to growth can be relaxed by virtually isolating each body element from the other ones, and letting it grow alone. By doing this, the body element undergoing growth will be in a stress-free state at each time $t \in \mathscr{I}$. This

state is, in fact, the linear space $\mathscr{N}_X(t)$ introduced in Section 5.1.1, and the ideal operation of relaxation is $\boldsymbol{F}_\gamma(X,t) : T_X\mathscr{B} \to \mathscr{N}_X(t)$.

The incompatibility of $\boldsymbol{F}_\gamma$, i.e., its intrinsic non-integrability, leads to frame the mechanics of growth within non-Euclidean geometry. Indeed, it allows to introduce a non-Euclidean metric and affine connections by means of which several geometric settings can be studied, such as the Riemannian, Riemann–Cartan, Weitzenböck, or Weyl manifolds (see, e.g., [78, 79, 118–120, 80, 121–125]).

By referring to *configuration* of a body as the manifold described by its deformation *and* growth tensor $\boldsymbol{F}_\gamma$, one can augment its kinematics. This way, it is possible to resolve, aside deformation, the structural changes due both to the mass variation and to the other reorganization processes associated with it. This fact suggests that *configurational mechanics* [10] is a natural framework to study growth.

In this chapter, we consider the minimal context of a theory of grade zero in $\boldsymbol{F}_\gamma$ [69] (see also [70] for plasticity). This choice is dictated by simplicity, but it allows to study the geometric aspects of growth as "byproducts" of our theory, and is sufficient to handle growth as a problem of configurational mechanics.

5.2 Growth mechanics as a constrained field theory

In this section, we review the peculiar points of some previous works [23, 32, 87, 91].

The continuum theories of volumetric growth in monophasic media often adopt the Bilby–Kröner–Lee (BKL) decomposition of $\boldsymbol{F}$ (see, e.g., [73, 88, 89, 95, 93, 126, 127, 80, 107, 77]), and recast the mass balance law in the form of a differential relationship between $\boldsymbol{F}_\gamma$ and the (rescaled) source of mass R, i.e.,

$$\langle \boldsymbol{F}_\gamma^{-\mathrm{T}} | \dot{\boldsymbol{F}}_\gamma \rangle \equiv \operatorname{tr}(\boldsymbol{F}_\gamma^{-1}\dot{\boldsymbol{F}}_\gamma) = R. \tag{5.2}$$

In the BKL decomposition $\boldsymbol{F} = \boldsymbol{F}_\mathrm{e}\boldsymbol{F}_\gamma$, $\boldsymbol{F}_\mathrm{e}$ denotes the tensor field of the elastic distortions that accommodate for the growth distortions, described by $\boldsymbol{F}_\gamma$. It follows that $J := \det \boldsymbol{F} > 0$ is given by $J = J_\mathrm{e}J_\gamma$, with $J_\mathrm{e} := \det \boldsymbol{F}_\mathrm{e} > 0$ and $J_\gamma := \det \boldsymbol{F}_\gamma > 0$. For details, see, e.g., [80] and the references therein.

Starting from the mass balance law $\dot{\varrho}_\mathrm{R} = \varrho_\mathrm{R} R$, and exploiting the BKL decomposition, Equation (5.2) is obtained under the assumption that, for each $X \in \mathscr{B}$ and

time $t \in \mathscr{I}$, $\dot{\varrho}_{\mathrm{R}}(X,t)$ is "absorbed" by the volumetric part of the ideal relaxation process $\boldsymbol{F}_\gamma(X,t) : T_X\mathscr{B} \to \mathscr{N}_X(t)$. To this end, we decompose $\boldsymbol{F}_\gamma$ as $\boldsymbol{F}_\gamma = J_\gamma^{1/3}\boldsymbol{F}_{\gamma,\mathrm{u}}$, where J_γ accounts for the volume change of the body elements from the reference placement to the body's natural state, and $\boldsymbol{F}_{\gamma,\mathrm{u}}$ describes the isochoric (volume-preserving) part of $\boldsymbol{F}_\gamma$. Then, if ϱ is the mass density in the current placement of the body, so that $\varrho_{\mathrm{R}} := J\varrho$, we write ϱ_{R} as $\varrho_{\mathrm{R}} = J_\gamma\varrho_\nu$, where $\varrho_\nu := J_{\mathrm{e}}\varrho$ is such that $\varrho_\nu(X,t)$ defines the mass density of the body element attached at X in its relaxed state at time t. However, due to the assumption that has been made, the function $\varrho_\nu(X,\,\cdot\,)$ can be taken constant in time, and, thus, upon dropping the dependence on X, it holds that $\dot{\varrho}_{\mathrm{R}} = \dot{J}_\gamma\varrho_\nu$. Finally, because of the chain of identities $\dot{J}_\gamma = J_\gamma\mathrm{tr}(\boldsymbol{F}_\gamma^{-1}\dot{\boldsymbol{F}}_\gamma) = J_\gamma\langle\boldsymbol{F}_\gamma^{-\mathrm{T}}|\dot{\boldsymbol{F}}_\gamma\rangle$, we obtain $\dot{\varrho}_{\mathrm{R}} = J_\gamma\langle\boldsymbol{F}_\gamma^{-\mathrm{T}}|\dot{\boldsymbol{F}}_\gamma\rangle\varrho_\nu = \varrho_{\mathrm{R}}\langle\boldsymbol{F}_\gamma^{-\mathrm{T}}|\dot{\boldsymbol{F}}_\gamma\rangle$, which yields Equation (5.2).

Equation (5.2) places a condition both for $\boldsymbol{F}_\gamma$ and for R, and it can be viewed either as a way for defining R, once $\boldsymbol{F}_\gamma$ is determined (see, e.g., [73, 112, 108, 77]), or as a *constraint* on $\boldsymbol{F}_\gamma$ [23, 32], if R is assumed to be given from the outset, for example, phenomenologically [89, 95, 84, 85, 102, 96].

In the present work, we concentrate on the second point of view, which we refer to as *"a priori approach"* [87]. Moreover, following the phenomenological framework developed for tumor growth in [85, 102], we hypothesize that R can be expressed as a function of $\boldsymbol{F}$ and $\boldsymbol{F}_\gamma$ through an appropriate function of mechanical stress. In addition, R must be related to chemical factors as well as to any other factor that enhances or hinders growth. Hence, we set

$$R := \hat{R} \circ \natural_\gamma, \qquad\qquad \natural_\gamma := (\boldsymbol{F}, \boldsymbol{F}_\gamma; \mathfrak{X}, \mathfrak{T}). \tag{5.3}$$

We view Equation (5.2) as a constraint. This way, one is sure of describing growth as necessary, with the possibility of developing a dynamic model for the full tensor field $\boldsymbol{F}_\gamma$ [23, 32]. This procedure permits to consider the remodeling that accompanies growth for any type of material, without the necessity of "guessing" the form of $\boldsymbol{F}_\gamma$ on the basis of material symmetries (see, e.g., [88, 128, 93]). Thus, we write:

$$\mathcal{C} \equiv \hat{\mathcal{C}} \circ \natural_{\mathrm{c}} := \langle\boldsymbol{F}_\gamma^{-\mathrm{T}}|\dot{\boldsymbol{F}}_\gamma\rangle - \hat{R} \circ \natural_\gamma = 0, \qquad \natural_{\mathrm{c}} := (\boldsymbol{F}, \boldsymbol{F}_\gamma; \dot{\boldsymbol{F}}_\gamma; \mathfrak{X}, \mathfrak{T}). \tag{5.4}$$

Remark 5.1 (Nonholonomic nature of the constraint). If R is zero, no variation of mass occurs, and the constraint (5.4) becomes $\langle \boldsymbol{F}_\gamma^{-\mathrm{T}} | \dot{\boldsymbol{F}}_\gamma \rangle = 0$, which is holonomic. Indeed, one can take $h := \log J_\gamma$, to retrieve $\dot{h} = \langle \boldsymbol{F}_\gamma^{-\mathrm{T}} | \dot{\boldsymbol{F}}_\gamma \rangle = 0$. In such a situation, $\boldsymbol{F}_\gamma$ is constrained to be isochoric, as is often assumed in the biomechanics of remodeling (see e.g. [84, 129, 130]). There can also be other functional forms of $\hat{R}$ that make the constraint (5.4) holonomic (see, e.g., [23]), but they are rather special. Hence, with the purpose of virtually including any biologically plausible form of $\hat{R}$, we regard the constraint (5.4) as *nonholonomic* with respect to $\boldsymbol{F}_\gamma$. This means that no scalar function $h := \hat{h} \circ \natural_\gamma$ exists, such that $\dot{h} = \hat{\mathcal{C}} \circ \natural_{\mathfrak{c}} = 0$. In particular, $\hat{\mathcal{C}} \circ \natural_{\mathfrak{c}}$ is affine in $\dot{\boldsymbol{F}}_\gamma$.

Remark 5.2 (Biological scenario and differentiability of R). In some studies on tumor growth (see, e.g., [85]), $\hat{R}$ depends on $\boldsymbol{F}$ and $\boldsymbol{F}_\gamma$ through mechanical stress. More specifically, one is interested in capturing the inhibitory effect that compressive stresses exert on the cell proliferation processes, like mitosis [131], which precedes vascularization. In this stage, the mass variation of the tumor is mainly due to the accessibility of the tumor cells to nourishment, which is supplied in the form of *nutrient* chemical substances, such as glucose and oxygen [89, 131, 84, 85, 102, 96]. The concentration of nutrients at each point $X \in \mathscr{B}$ and time $t \in \mathscr{I}$, hereafter denoted by $\mathfrak{c}(X, t)$, evolves by following a diffusion-reaction equation coupled with the other mechanical variables of the problem (see e.g. [89, 131, 102, 91]). To model the influence of stress on growth, $\hat{R}$ can be related to the positive part of the mechanical pressure $\wp := -\frac{1}{3}\mathrm{tr}\boldsymbol{\sigma}$, where $\boldsymbol{\sigma}$ is the Cauchy stress tensor of the medium, expressed as a function of $\boldsymbol{F}$ and $\boldsymbol{F}_\gamma$, as is the case when the mechanical response of the tumor is hypothesized to be elastic. Hence, upon setting $\langle \wp \rangle_+ = \frac{1}{2}(\wp + |\wp|)$ for the positive part of $\wp$, the effect of mechanical stress is switched off for $\wp \leq 0$, and switched on for $\wp > 0$ [85]. In particular, $\hat{R}$ decreases with increasing $\wp$. Finally, by expressing $\wp$ constitutively as $\wp = \hat{\wp} \circ \natural_\gamma$, $\hat{R}$ is made dependent on $\boldsymbol{F}$ and $\boldsymbol{F}_\gamma$. To account for these facts, and imitating an expression of $\hat{R}$ prescribed in [85, 102], Grillo&Di Stefano [87, 91] suggested the functional form

$$R \equiv \hat{R} \circ \natural_\gamma := \zeta_{\mathrm{a}} \left\langle \frac{\mathfrak{c} - \mathfrak{c}_{\mathrm{cr}}}{\mathfrak{c}_{\mathrm{env}} - \mathfrak{c}_{\mathrm{cr}}} \right\rangle_+ \left[1 - \frac{\alpha \langle \hat{\wp} \circ \natural_\gamma \rangle_+}{\sigma_{\mathrm{c}} + \langle \hat{\wp} \circ \natural_\gamma \rangle_+} \right] - \zeta_{\mathrm{r}} \left\langle 1 - \frac{\mathfrak{c}}{\mathfrak{c}_{\mathrm{cr}}} \right\rangle_+ . \tag{5.5}$$

Here, ζ_{a} and ζ_{r} are non-negative, constant material coefficients associated with mass "accretion" and "resorption", respectively, having units of the reciprocal of time [87]; $\mathfrak{c}_{\mathrm{cr}}$ is a constant threshold value of the nutrients' concentration; $\mathfrak{c}_{\mathrm{env}} > \mathfrak{c}_{\mathrm{cr}}$ is a constant

value of the nutrients' concentration in the tumor's environment [87]; $\alpha \geq 0$ is a non-dimensional material constant; σ_{c} is a constant characteristic reference value of stress. Growth laws of the kind given in Equation (5.5) render $\hat{R}$ continuous but not everywhere differentiable, because $\langle \wp \rangle_+$ is not differentiable in $\wp = 0$. Thus, when the differentiability of $\hat{R}$ is needed, $\langle \wp \rangle_+$ is mollified, and $\hat{R}$ is taken to be at least C^1.

5.2.1 Principle of Virtual Work and a nonholonomic constraint

Following the methodology outlined in [23, 32], which, in turn, is based on the approaches developed in [70, 69], the constraint (5.4) has to be appended to the Principle of Virtual Work (PVW), formulated for the growing body under study. To this end, it is necessary to introduce the virtual variations of the basic kinematic descriptors χ, $\boldsymbol{F}$, and $\boldsymbol{F}_\gamma$. Thus, since the present context is of grade one in χ, and of grade zero in $\boldsymbol{F}$ and $\boldsymbol{F}_\gamma$ [69, 86], we write

$$(\chi, D\chi, \boldsymbol{F}, \boldsymbol{F}_\gamma; \delta\chi, \delta D\chi \equiv \mathrm{Grad}\delta\chi, \delta\boldsymbol{F}, \delta\boldsymbol{F}_\gamma; \mathfrak{X}, \mathfrak{T}). \tag{5.6}$$

Within the *"canonical doctrine"* [32], the *varied form* of the constraint to be appended to the PVW is supplied by the so-called *Chetaev condition* [12, 14, 51, 39, 16], which holds true for *"ideal"* constraints [16], and reads [32]

$$\begin{aligned} &\mathcal{A}_{\natural_{\mathrm{c}}}(\delta\boldsymbol{F}_\gamma) := \langle \partial_{\dot{\boldsymbol{F}}_\gamma} \hat{\mathcal{C}} \circ \natural_{\mathrm{c}} | \delta\boldsymbol{F}_\gamma \rangle = 0 \\ &\Rightarrow \quad \mathcal{A}_{\natural_{\mathrm{c}}}(\delta\boldsymbol{F}_\gamma) = \langle \boldsymbol{F}_\gamma^{-\mathrm{T}} | \delta\boldsymbol{F}_\gamma \rangle \equiv \langle \boldsymbol{I}^{\mathrm{T}} | \boldsymbol{F}_\gamma^{-1} \delta\boldsymbol{F}_\gamma \rangle \equiv \mathrm{tr}(\boldsymbol{F}_\gamma^{-1}\delta\boldsymbol{F}_\gamma) = 0, \end{aligned} \tag{5.7}$$

where $\boldsymbol{I}^{\mathrm{T}} : T^*\mathscr{B} \to T^*\mathscr{B}$ is the transpose of the identity tensor [24].

In conjunction with Equation (5.4), and in order to postulate the PVW in a form *à la* Hu–Washizu [106], we enforce the condition that $\boldsymbol{F}$ must be equal to $D\chi$ at all times and at all points, thereby introducing the auxiliary constraint $\mathfrak{C}_{\mathrm{a}} := D\chi - \boldsymbol{F} = \boldsymbol{O}$, where $\boldsymbol{O}$ is the null second-order tensor field. By introducing the tensorial Lagrange multiplier $\boldsymbol{T}$, this condition can be associated with the weak forms

$$\langle \boldsymbol{T} \,|\, D\chi - \boldsymbol{F} \rangle = 0, \qquad \langle \delta\boldsymbol{T} \,|\, D\chi - \boldsymbol{F} \rangle + \langle \boldsymbol{T} \,|\, \mathrm{Grad}\delta\chi - \delta\boldsymbol{F} \rangle = 0. \tag{5.8}$$

By assuming that, in addition to the prescribed constraints, growth occurs under the action of the generalized forces $\boldsymbol{Y}_{\mathrm{u}}$ and $\boldsymbol{Z}$ [70, 69], introduced by duality with the

generalized virtual displacement $\boldsymbol{F}_\gamma^{-1}\delta\boldsymbol{F}_\gamma$, and interpreted as internal and external, respectively, the PVW can be cast in the form [23, 32]

$$\mathcal{W}_{\mathrm{v}}^{(\mathrm{i})} + \mathcal{W}_{\mathrm{v}}^{(\mathrm{c})} = \mathcal{W}_{\mathrm{v}}^{(\mathrm{e})}, \tag{5.9}$$

where $\mathcal{W}_{\mathrm{v}}^{(\mathrm{i})}$, $\mathcal{W}_{\mathrm{v}}^{(\mathrm{c})}$, and $\mathcal{W}_{\mathrm{v}}^{(\mathrm{e})}$ are the "internal", "constrained", and "external" virtual work, respectively, and are defined by

$$\mathcal{W}_{\mathrm{v}}^{(\mathrm{i})} := \int_{\mathscr{B}} \big\{\langle \boldsymbol{P}|\delta\boldsymbol{F}\rangle + \langle \boldsymbol{Y}_{\mathrm{u}}|\boldsymbol{F}_\gamma^{-1}\delta\boldsymbol{F}_\gamma\rangle\big\}, \tag{5.10a}$$

$$\mathcal{W}_{\mathrm{v}}^{(\mathrm{c})} := \int_{\mathscr{B}} \big\{\langle \mu\,\boldsymbol{I}^{\mathrm{T}}|\boldsymbol{F}_\gamma^{-1}\delta\boldsymbol{F}_\gamma\rangle + \langle \boldsymbol{T}|\mathrm{Grad}\delta\chi - \delta\boldsymbol{F}\rangle + \delta\mu\, t_{\mathrm{c}}\mathcal{C} + \langle \delta\boldsymbol{T}|\mathcal{C}_{\mathrm{a}}\rangle\big\}, \tag{5.10b}$$

$$\mathcal{W}_{\mathrm{v}}^{(\mathrm{e})} := \int_{\mathscr{B}} \big\{\langle \boldsymbol{f}|\delta\chi\rangle + \langle \boldsymbol{Z}|\boldsymbol{F}_\gamma^{-1}\delta\boldsymbol{F}_\gamma\rangle\big\} + \int_{\partial_{\mathrm{N}}^{\chi}\mathscr{B}} \langle \boldsymbol{\tau}|\delta\chi\rangle. \tag{5.10c}$$

Here, $\boldsymbol{P}$ is the first Piola–Kirchhoff stress tensor; μ is the real-valued Lagrange multiplier associated with the Chetaev condition (5.7); $\delta\mu$ and $\delta\boldsymbol{T}$ are the virtual variations of μ and $\boldsymbol{T}$; t_{c} is a strictly positive characteristic time introduced to make the term $\delta\mu\, t_{\mathrm{c}}\mathcal{C}$ dimensionally homogeneous with all the other addends of Equation (5.10b); $\boldsymbol{f}$ and $\boldsymbol{\tau}$ represent the external body forces and the external surface forces dual to $\delta\chi$. Note that $\boldsymbol{\tau}$ is defined over the Neumann portion of $\partial\mathscr{B}$, denoted by $\partial_{\mathrm{N}}^{\chi}\mathscr{B}$. In the sequel, $\partial\mathscr{B}$ is partitioned as $\partial\mathscr{B} = \partial_{\mathrm{D}}^{\chi}\mathscr{B} \sqcup \partial_{\mathrm{N}}^{\chi}\mathscr{B}$, where $\partial_{\mathrm{D}}^{\chi}\mathscr{B}$ is referred to as Dirichlet boundary.

The strong form of the dynamic problem associated with Equations (5.9) and (5.10a)–(5.10c) is given by the set of equations

$$\mathrm{Div}\boldsymbol{T} + \boldsymbol{f} = \boldsymbol{0}, \qquad \text{in } \mathscr{B}, \tag{5.11a}$$

$$\boldsymbol{\tau} - \boldsymbol{T}\boldsymbol{N} = \boldsymbol{0}, \qquad \text{on } \partial_{\mathrm{N}}^{\chi}\mathscr{B}, \tag{5.11b}$$

$$\boldsymbol{P} = \boldsymbol{T}, \qquad \text{in } \mathscr{B}, \tag{5.11c}$$

$$\boldsymbol{Y}_{\mathrm{u}} + \mu\boldsymbol{I}^{\mathrm{T}} - \boldsymbol{Z} = \boldsymbol{O}, \qquad \text{in } \mathscr{B}, \tag{5.11d}$$

$$\mathcal{C}_{\mathrm{a}} = D\chi - \boldsymbol{F} = \boldsymbol{O}, \qquad \text{in } \mathscr{B}, \tag{5.11e}$$

$$\mathcal{C} = \langle \boldsymbol{F}_\gamma^{-\mathrm{T}}|\dot{\boldsymbol{F}}_\gamma\rangle - R = 0, \qquad \text{in } \mathscr{B}, \tag{5.11f}$$

which has to be completed with Dirichlet boundary conditions on χ, and with all the necessary initial conditions. As for the Hu–Washizu method (see e.g. [106]), Equation (5.11c) identifies $\boldsymbol{T}$ with $\boldsymbol{P}$.

Because of the difference of formulation with respect to the one recently presented in [23, 32], the physical quantities featuring in Equations (5.11a)–(5.11f) can be grouped as follows: 21 kinematic variables χ, $\boldsymbol{F}$, and $\boldsymbol{F}_\gamma$; 10 Lagrange multipliers μ and $\boldsymbol{T}$; 18 constitutive functions $\boldsymbol{P}$ and $\boldsymbol{Y}_\mathrm{u}$; 15 external forces $\boldsymbol{f}$, $\boldsymbol{\tau}$, and $\boldsymbol{Z}$. The kinematic variables and the Lagrange multipliers yield a set of 31 scalar unknowns to be determined by solving the 31 scalar equations given by the balance laws (5.11a), (5.11c), (5.11d), and by the constraints (5.11e), (5.11f).

The presentation of the full boundary value problem (5.11a)–(5.11f) serves as comparison for the dynamic equations that will be determined in the sequel.

5.2.2 The hyperelastic case and the Extended Hamilton Method

Although some biological tissues show viscoelastic behavior in certain dynamic regimes [132, 133], a case of particular interest is when the growing medium under study can be assumed to be hyperelastic [73, 88, 89, 95, 90, 69, 102, 77, 134]. Then, the constitutive representation of $\boldsymbol{P}$ can be obtained as

$$\boldsymbol{P} = \frac{\partial \hat{\Psi}}{\partial \boldsymbol{F}} \circ (\boldsymbol{F}, \boldsymbol{F}_\gamma; \mathcal{X}, \mathcal{T}) = J_\gamma \left[\frac{\partial \hat{\Psi}_\nu}{\partial \boldsymbol{F}_\mathrm{e}} \circ (\boldsymbol{F}_\mathrm{e}; \mathcal{X}, \mathcal{T}) \right] \boldsymbol{F}_\gamma^{-\mathrm{T}}, \tag{5.12}$$

where $\Psi := \hat{\Psi} \circ (\boldsymbol{F}, \boldsymbol{F}_\gamma; \mathcal{X}, \mathcal{T}) = J_\gamma [\hat{\Psi}_\nu \circ (\boldsymbol{F}_\mathrm{e}; \mathcal{X}, \mathcal{T})]$ is the strain energy density of the medium per unit volume of its reference placement; $\Psi_\nu := \hat{\Psi}_\nu \circ (\boldsymbol{F}_\mathrm{e}; \mathcal{X}, \mathcal{T})$ is the same physical quantity, but expressed per unit volume of the medium's natural state. Note that the arguments of $\hat{\Psi}$ are the same as the collection $\natural_\gamma$, so that we can write $\Psi = \hat{\Psi} \circ \natural_\gamma$.

Typically, the growth of a biological medium, such as a tumor or a cellular aggregate, occurs over time scales that allow to neglect its kinetic energy. However, nothing forbids, in principle, to consider the "classical" kinetic energy density, $\mathcal{K} = \frac{1}{2} J_\gamma \varrho_\nu \|\dot{\chi}\|^2$, and define the *medium's Lagrangian density function* $\mathcal{L}_\mathrm{b} := \mathcal{K} - \Psi$ [73].

The function $\mathcal{L}_\mathrm{b}$ can be generalized by including other interactions that the medium can experience. These could be represented by the kinetic energy density associated with $\dot{\boldsymbol{F}}_\gamma$ [135], and potential densities that may depend both on χ and on $\boldsymbol{F}_\gamma$. Therefore, to include such contributions, we consider, in lieu of $\mathcal{L}_\mathrm{b}$, a more general Lagrangian density function, defined as $\mathcal{L} := \hat{\mathcal{L}} \circ \natural$. However, in the

hyperelastic case, $\dot{\boldsymbol{F}}$ is ignorable, since it holds that $\partial_{\dot{\boldsymbol{F}}}\hat{\mathcal{L}} \circ \natural = \boldsymbol{O}$. We also notice that $\hat{\mathcal{L}}$ can be assumed to be formally independent of $D\chi$, since the dependence on the deformation gradient tensor is already accounted for through $\boldsymbol{F}$, which is one of the arguments of $\hat{\Psi}$. Hence, we set $\partial_{D\chi}\hat{\mathcal{L}} \circ \natural = \boldsymbol{O}$.

To imitate the Hu–Washizu formulation of the PVW [106] of Section 5.2.1, it is convenient to augment $\mathcal{L}$ with $\langle \boldsymbol{T} \mid \boldsymbol{F} - D\chi \rangle$, so that one finds

$$\mathcal{L}_{\mathrm{a}} \equiv \hat{\mathcal{L}}_{\mathrm{a}} \circ (\natural; \boldsymbol{T}) = \hat{\mathcal{L}} \circ \natural + \langle \boldsymbol{T} \mid \boldsymbol{F} - D\chi \rangle, \tag{5.13a}$$

$$\mathscr{A}_{\mathrm{a}}(\chi, \boldsymbol{F}, \boldsymbol{F}_\gamma; \boldsymbol{T}) := \int_{t_{\mathrm{in}}}^{t_{\mathrm{fin}}} \left\{ \int_{\mathscr{B}} \hat{\mathcal{L}}_{\mathrm{a}}(\natural(X,t); \boldsymbol{T}(X,t)) \mathrm{dV}(X) \right\} \mathrm{d}t. \tag{5.13b}$$

The Lagrange multiplier $\boldsymbol{T}$ has to be included among the arguments both of the *augmented Lagrangian density function* $\hat{\mathcal{L}}_{\mathrm{a}}$ and of the *augmented action* $\mathscr{A}_{\mathrm{a}}$, obtained by integration over the time interval $[t_{\mathrm{in}}, t_{\mathrm{fin}}]$. Moreover, since $\boldsymbol{F}$ is regarded here as an independent kinematic variable, $\mathscr{A}_{\mathrm{a}}$ has to be defined as a functional of $\boldsymbol{F}$ as well as of χ and $\boldsymbol{F}_\gamma$. Note that, because of the hypothesis of hyperelastic material, $\hat{\mathcal{L}}_{\mathrm{a}}$ and $\hat{\mathcal{L}}$ are independent of $\dot{D\chi}$, that is, $\partial_{\dot{D\chi}}\hat{\mathcal{L}}_{\mathrm{a}} \circ (\natural; \boldsymbol{T}) = \partial_{\dot{D\chi}}\hat{\mathcal{L}} \circ \natural = \boldsymbol{O}$.

No matter how accurate $\mathcal{L}_{\mathrm{a}}$ can be, it is not sufficient, in general, to provide a comprehensive description of a growing medium. There are at least two reasons for this. First, one should expect the presence of generalized forces for which no potential density exists. Second, in the *classical formulation* of Variational Calculus, one cannot attach the nonholonomic constraint (5.4) to $\mathcal{L}$ or $\mathcal{L}_{\mathrm{a}}$, as one could instead do if the constraint were holonomic (see e.g. [11, 13, 28, 29, 40]). Still, to obtain the dynamic equations of the problem under study, one may have recourse to *Extended Hamilton's Principle* [11, 105]. To this end, we introduce a smallness parameter $\varepsilon \in \mathscr{Y}(\varepsilon_0)$, where $\mathscr{Y}(\varepsilon_0)$ is an open neighborhood of zero with radius $\varepsilon_0 > 0$, and we define the homotopies

$$(\natural(X,t); \boldsymbol{T}(X,t)) \;\mapsto\; (\tilde{\natural}(X,t,\varepsilon); \tilde{\boldsymbol{T}}(X,t,\varepsilon)), \tag{5.14a}$$

$$\tilde{\natural}(X,t,\varepsilon) = \tilde{\natural}(X,t,0) + \partial_\varepsilon \tilde{\natural}(X,t,0)\varepsilon + o(\varepsilon), \qquad \varepsilon \to 0, \tag{5.14b}$$

$$\tilde{\boldsymbol{T}}(X,t,\varepsilon) = \tilde{\boldsymbol{T}}(X,t,0) + \partial_\varepsilon \tilde{\boldsymbol{T}}(X,t,0)\varepsilon + o(\varepsilon), \qquad \varepsilon \to 0, \tag{5.14c}$$

with $\tilde{\natural}(X,t,0) = \natural(X,t)$, $\tilde{\boldsymbol{T}}(X,t,0) = \boldsymbol{T}(X,t)$.

Since the Extended Hamilton Principle relies on "classical variations" [11, 105], we proceed as follows. By indicating with φ a generic variable of $\natural$, $\varphi(X,t)$ is varied

into $\tilde{\varphi}(X,t,\varepsilon)$, and we denote by $\boldsymbol{\eta}_\varphi(X,t) := \partial_\varepsilon\tilde{\varphi}(X,t,0)$ the entity defining the direction (in a generalized sense) along which the infinitesimal first-order variation of $\varphi(X,t)$ is computed, that is, $\delta\varphi(X,t,\varepsilon) \equiv \varepsilon\boldsymbol{\eta}_\varphi(X,t)$. However, with a slight abuse of terminology, from here on we shall refer to $\boldsymbol{\eta}_\varphi(X,t)$ and $\boldsymbol{\eta}_\varphi$ as the first-order *increment* and *incremental field* associated with $\varphi(X,t)$ and φ, respectively (in fact, since in the sequel these quantities are attributed only to first-order variations, we shall omit the specification "first-order"). Analogously, we call $\boldsymbol{\eta}_{\boldsymbol{T}}(X,t) = \partial_\varepsilon\tilde{\boldsymbol{T}}(X,t,0)$ the increment associated with $\boldsymbol{T}(X,t)$. If φ is the time derivative of another variable ψ of $\natural$, i.e., if $\varphi = \dot{\psi}$, then the hypothesis of "classical variations" implies the commutative relationship $\boldsymbol{\eta}_{\dot{\psi}} = \dot{\boldsymbol{\eta}}_\psi$. Moreover, it holds that $\boldsymbol{\eta}_{D\chi} = \mathrm{Grad}\boldsymbol{\eta}_\chi$, and $\boldsymbol{\eta}_{\dot{D\chi}} = \dot{\boldsymbol{\eta}}_{D\chi} = \mathrm{Grad}\dot{\boldsymbol{\eta}}_\chi$. The incremental fields $\boldsymbol{\eta}_\chi$ and $\boldsymbol{\eta}_{\boldsymbol{F}_\gamma}$ are required to vanish at t_{in} and t_{fin}, while $\boldsymbol{\eta}_\chi$ must be null also on the Dirichlet boundary of $\mathscr{B}$. Finally, we clarify that the incremental fields associated with $\mathcal{X}$ and $\mathcal{T}$ are taken to be null.

Now, we let $\boldsymbol{f}_{\mathrm{np}}$ and $\mathfrak{S}_{\mathrm{np}}$ be the non-potential forces dual to $\boldsymbol{\eta}_\chi$ and $\boldsymbol{\eta}_{\boldsymbol{F}_\gamma}$, respectively. The former represents all the non-potential contributions to the balance of *"deformational forces"* [10], while the latter collects the non-potential contributions to the quantity $\boldsymbol{F}_\gamma^{-\mathrm{T}}[\boldsymbol{Z} - \boldsymbol{Y}_{\mathrm{u}}]$ that can be defined from Equation (5.11d). In addition, following Lanczos' approach [11] to nonholonomic systems, we consider also the constraint (5.4), which contributes to the overall virtual work through the term $\langle \mu\boldsymbol{F}_\gamma^{-\mathrm{T}} \,|\, \boldsymbol{\eta}_{\boldsymbol{F}_\gamma}\rangle$, with $\mu\boldsymbol{F}_\gamma^{-\mathrm{T}}$ acquiring the meaning of the associated reactive force, up to the sign. Therefore, by integrating the virtual work produced by $\boldsymbol{f}_{\mathrm{np}}$, $\mathfrak{S}_{\mathrm{np}}$, and $\mu\boldsymbol{F}_\gamma^{-\mathrm{T}}$ over $[t_{\mathrm{in}}, t_{\mathrm{fin}}]$, we write Extended Hamilton's Principle [11, 105, 136] as

$$\begin{aligned}\frac{\mathrm{d}\tilde{\mathscr{A}}_{\mathrm{a}}}{\mathrm{d}\varepsilon}(0) = &-\int_{t_{\mathrm{in}}}^{t_{\mathrm{fin}}}\left\{\int_{\mathscr{B}}\left[\langle \boldsymbol{f}_{\mathrm{np}}|\boldsymbol{\eta}_\chi\rangle + \langle \mathfrak{S}_{\mathrm{np}} - \mu\boldsymbol{F}_\gamma^{-\mathrm{T}} \,|\, \boldsymbol{\eta}_{\boldsymbol{F}_\gamma}\rangle\right]\mathrm{dV}\right\}\mathrm{d}t \\ &-\int_{t_{\mathrm{in}}}^{t_{\mathrm{fin}}}\left\{\int_{\partial_{\mathrm{N}}^{\chi}\mathscr{B}}\langle \boldsymbol{\tau}|\boldsymbol{\eta}_\chi\rangle\,\mathrm{dA}\right\}\mathrm{d}t,\end{aligned} \tag{5.15}$$

with $\tilde{\mathscr{A}}_{\mathrm{a}}(\varepsilon) := \int_{t_{\mathrm{in}}}^{t_{\mathrm{fin}}}\left\{\int_{\mathscr{B}}\hat{\mathcal{L}}_{\mathrm{a}}(\tilde{\natural}(X,t,\varepsilon);\tilde{\boldsymbol{T}}(X,t,\varepsilon))\mathrm{dV}(X)\right\}\mathrm{d}t$.

Computing the left-hand side of Equation (5.15), grouping together the terms dual to the same variation, and localizing the resulting expression yield

$$\mathcal{E}_\chi\hat{\mathcal{L}} + \mathrm{Div}\boldsymbol{T} = -\boldsymbol{f}_{\mathrm{np}}, \qquad \text{in } \mathscr{B}, \tag{5.16a}$$

$$\boldsymbol{T}\boldsymbol{N} = \boldsymbol{\tau}, \qquad \text{on } \partial_{\mathrm{N}}^{\chi}\mathscr{B}, \tag{5.16b}$$

$$\mathcal{E}_{\boldsymbol{F}}\hat{\mathcal{L}} + \boldsymbol{T} = \boldsymbol{O}, \qquad \text{in } \mathscr{B}, \tag{5.16c}$$

$$\boldsymbol{F} - D\chi = \boldsymbol{O}, \qquad \text{in } \mathscr{B}, \tag{5.16d}$$

$$\mathcal{E}_{\boldsymbol{F}_\gamma}\hat{\mathcal{L}} = -\mathfrak{S}_{\text{np}} + \mu \boldsymbol{F}_\gamma^{-\text{T}}, \qquad \text{in } \mathscr{B}, \tag{5.16e}$$

$$\langle \boldsymbol{F}_\gamma^{-\text{T}} | \dot{\boldsymbol{F}}_\gamma \rangle - R = 0, \qquad \text{in } \mathscr{B}, \tag{5.16f}$$

where, for a given variable φ of $\natural$, $\mathcal{E}_\varphi\hat{\mathcal{L}} := \partial_\varphi\hat{\mathcal{L}} \circ \natural - \partial_t(\partial_{\dot{\varphi}}\hat{\mathcal{L}} \circ \natural)$ denotes the associated Euler–Lagrange operator applied to $\mathcal{L} = \hat{\mathcal{L}} \circ \natural$. In particular, we obtain $\mathcal{E}_{\boldsymbol{F}}\hat{\mathcal{L}} = \partial_{\boldsymbol{F}}\hat{\mathcal{L}} \circ \natural$, since $\dot{\boldsymbol{F}}$ is ignorable for $\hat{\mathcal{L}}$, and, thus, $\partial_{\dot{\boldsymbol{F}}}\hat{\mathcal{L}} \circ \natural = \boldsymbol{O}$.[3]

The sets of Equations (5.16a)–(5.16f) and (5.11a)–(5.11f) are equivalent to each other, and the following identifications can be made:

$$\boldsymbol{f} = \mathcal{E}_\chi\hat{\mathcal{L}} + \boldsymbol{f}_{\text{np}}, \tag{5.17a}$$

$$\boldsymbol{Z} - \boldsymbol{Y}_{\text{u}} = \boldsymbol{F}_\gamma^{\text{T}}[\mathcal{E}_{\boldsymbol{F}_\gamma}\hat{\mathcal{L}} + \mathfrak{S}_{\text{np}}]. \tag{5.17b}$$

In the sequel, when we speak of *"Traditional NonHolonomic Method"* (TNHM) [1], we refer equivalently either to Equations (5.11a)–(5.11f) or to (5.16a)–(5.16f).

5.2.3 A note on the configurational generalized forces

In the paradigm of the Principle of Virtual Work [137, 138], the configurational forces $\boldsymbol{Y}_{\text{u}}$, $\mu\boldsymbol{I}^{\text{T}}$, and $\boldsymbol{Z}$ are the entities that represent the real-valued linear functional defining the growth part of the virtual work [69], i.e.,

$$\delta\boldsymbol{F}_\gamma \;\mapsto\; \mathscr{W}_{\text{g}}(\delta\boldsymbol{F}_\gamma) := \int_{\mathscr{B}} \langle \mathfrak{F} | \boldsymbol{F}_\gamma^{-1}\delta\boldsymbol{F}_\gamma \rangle = 0, \qquad \mathfrak{F} \equiv \boldsymbol{Z} - \boldsymbol{Y}_{\text{u}} - \mu\boldsymbol{I}^{\text{T}} = \boldsymbol{O}. \tag{5.18}$$

By its own definition, $\mathscr{W}_{\text{g}}(\,\cdot\,)$ is dual to $\delta\boldsymbol{F}_\gamma$ (viewed as a *test* tensor field), while $\mathfrak{F}$ is dual to the tensor field given by $\boldsymbol{F}_\gamma^{-1}\delta\boldsymbol{F}_\gamma$.

Since growth requires an irreversible expenditure of energy, $\boldsymbol{Y}_{\text{u}}$ must feature a dissipative contribution, which we denote by $\boldsymbol{Y}_{\text{ud}}$. If $\boldsymbol{Y}_{\text{ud}}$ can be expressed constitutively (see, e.g., [70, 69, 89, 86, 139, 23, 32]); if the chosen constitutive representation is continuous and differentiable in all the values of $\boldsymbol{F}_\gamma^{-1}\dot{\boldsymbol{F}}_\gamma$ in which it is defined, including $\boldsymbol{F}_\gamma^{-1}\dot{\boldsymbol{F}}_\gamma = \boldsymbol{O}$; if it vanishes for $\boldsymbol{F}_\gamma^{-1}\dot{\boldsymbol{F}}_\gamma = \boldsymbol{O}$; and if one is interested in the evolution of $\boldsymbol{F}_\gamma$ only in a small neighborhood of $\boldsymbol{F}_\gamma^{-1}\dot{\boldsymbol{F}}_\gamma = \boldsymbol{O}$, then $\boldsymbol{Y}_{\text{ud}}$ can be taken

[3] To reduce the notational burden, throughout this chapter we suppress the compositions in the definition of the Euler–Lagrange operators $\mathcal{E}_\varphi\hat{\mathcal{L}}$ with respect to their arguments, differently from what has been done in Section 1.1.2 and in Chapters 2 and 3 (see the definitions (1.11) and (2.28a)).

linear in $\boldsymbol{F}_\gamma^{-1}\dot{\boldsymbol{F}}_\gamma$. This yields a relation of the type $\boldsymbol{Y}_{\mathrm{ud}} = \mathbb{T}[\boldsymbol{F}_\gamma^{-1}\dot{\boldsymbol{F}}_\gamma]$, where $\mathbb{T}$ is a positive semi-definite fourth-order tensor field enjoying the major symmetry, i.e., such that $\langle \mathbb{T}[\boldsymbol{F}_\gamma^{-1}\dot{\boldsymbol{F}}_\gamma] | \boldsymbol{F}_\gamma^{-1}\dot{\boldsymbol{F}}_\gamma \rangle \geq 0$, for all $\boldsymbol{F}_\gamma^{-1}\dot{\boldsymbol{F}}_\gamma$, and $\mathbb{T} = \mathbb{T}^{\mathrm{T}}$. Clearly, $\mathbb{T}$ may depend on $\boldsymbol{F}$, $\boldsymbol{F}_\gamma$, and other variables, apart from $\dot{\boldsymbol{F}}_\gamma$. In fact, $\mathbb{T}$ represents a generalized tensorial viscosity independent of $\dot{\boldsymbol{F}}_\gamma$[101, 103, 104, 23, 87, 91].

The study of dissipation permits to conclude that $\boldsymbol{Y}_{\mathrm{u}}$ consists also of a non-dissipative term, given by the Eshelby stress tensor $\boldsymbol{H}$. This is found also in many other approaches to growth [73, 69, 126, 90, 127] and to configurational mechanics in general. It descends from $\boldsymbol{H}$ being naturally conjugate to the kinematic variables describing the structural transformations of a body, such as plastic distortions [140, 141, 70, 142] and remodeling of biological media [143, 144]. In all these situations, the pairing $\langle \boldsymbol{H} | \boldsymbol{F}_\gamma^{-1}\dot{\boldsymbol{F}}_\gamma \rangle$ occurs, and, in the examined case of growth, it holds that $\boldsymbol{Y}_{\mathrm{u}} = \boldsymbol{H} + \boldsymbol{Y}_{\mathrm{ud}}$. In more general frameworks, tensors similar to $\boldsymbol{H}$ arise, e.g., in the evolution of interfaces [145, 10] and of the chemical composition of mixtures [146, 139].

For hyperelastic bodies, and in the quasi-static case, $\boldsymbol{H}$ can be expressed by differentiation of the body's strain energy density with respect to $\boldsymbol{F}_\gamma$ (see Equation (5.86a) below). Thus, the physical meaning of $\boldsymbol{Y}_{\mathrm{ud}}$ and $\boldsymbol{H}$ is embedded in the constitutive relations by which they are determined. In particular, since $\boldsymbol{Y}_{\mathrm{ud}}$ is a non-potential force, it contributes to the overall non-potential force $\mathfrak{S}_{\mathrm{np}}$.

Quite differently, since $\boldsymbol{Z}$ is external, it may feature, in general, inertial-like terms as well as other contributions that can be assigned phenomenologically either through the differentiation of the Lagrangian density function with respect to $\boldsymbol{F}_\gamma$ or as generalized forces that generally do not admit a potential. The latter ones, in particular, should capture, at least, how the most relevant chemo-mechanical processes occurring at lower scales influence growth at the scale of the body as a whole [69, 23]. Following [87, 91] (see Remark 5.2), when the inertial-like terms are negligible, and the contributions that stem from the Lagrangian density function are disregarded, one can supply $\boldsymbol{Z}$ as (in the sequel $\boldsymbol{C}$ is the right Cauchy-Green deformation tensor induced by $\boldsymbol{F}$)

$$\boldsymbol{Z} = \tfrac{1}{3} J_\gamma \beta R \boldsymbol{I}^{\mathrm{T}} + J_\gamma Q_{\nu\mathfrak{t}} \|\mathrm{Grad}\mathfrak{c}\|_{\boldsymbol{C}^{-1}} \boldsymbol{I}^{\mathrm{T}} + J_\gamma [Q_{\nu\ell} - Q_{\nu\mathfrak{t}}] \frac{\mathrm{Grad}\mathfrak{c} \otimes \boldsymbol{C}^{-1}\mathrm{Grad}\mathfrak{c}}{\|\mathrm{Grad}\mathfrak{c}\|_{\boldsymbol{C}^{-1}}}. \quad (5.19)$$

The first term on the right-hand side of Equation (5.19) is a purely volumetric contribution that directly induces the mass variation within the body ($\beta > 0$ gives the correct physical dimensions); the second and third terms represent a configurational force driving the evolution of $\boldsymbol{F}_\gamma$ in response to the material gradient of the nutrients' concentration. In Equation (5.19), the parameters $Q_{\nu\ell}$ and $Q_{\nu\mathrm{t}}$ are strictly positive, and presumed, since we are aware of no experiment determining them. For any material co-vector field $\boldsymbol{\Phi}$, $\|\boldsymbol{\Phi}\|_{\boldsymbol{C}^{-1}} := \sqrt{\boldsymbol{\Phi}\boldsymbol{C}^{-1}\boldsymbol{\Phi}}$.

5.3 Quasi-velocities and transpositional relations

In Analytical Mechanics, the terminology *quasi-velocities* refers to the result of a "change of variables" in the collection of the generalized velocities of a given mechanical system [45, 13, 30, 16]. It is done to describe the system's kinematics in a way that best "fits" the system at hand [25]. This is because many important features of the constraints are made explicit by the most appropriate choice of quasi-velocities.

Before studying how quasi-velocities work in growth mechanics, we refer the reader to Section 1.1.2 for further details on their employment for discrete mechanical systems.

Within our context, the generalized velocities are the time derivatives that feature in the list of variables $\natural$ of Equation (5.1), i.e., $\dot{\chi}$, $\mathrm{Grad}\dot{\chi}$, $\dot{\boldsymbol{F}}$, and $\dot{\boldsymbol{F}}_\gamma$. However, only $\dot{\boldsymbol{F}}_\gamma$ is constrained through Equation (5.4), while all the other ones are unconstrained. In fact, the holonomic condition $D\chi = \boldsymbol{F}$ implies *a posteriori* that $\mathrm{Grad}\dot{\chi} = \dot{\boldsymbol{F}}$, but these velocities are not restricted *a priori*, and also $D\chi$ and $\boldsymbol{F}$, in spite of their being constrained to be equal to each other, are varied independently of one another at the price of introducing the tensorial Lagrange multiplier $\boldsymbol{T}$. For these reasons, and on the basis of the rationale outlined above, there is no physical advantage in transforming $\dot{\chi}$, $\mathrm{Grad}\dot{\chi}$, and $\dot{\boldsymbol{F}}$. On the contrary, it is meaningful to transform $\dot{\boldsymbol{F}}_\gamma$.

5.3.1 Quasi-velocities

Let us denote by $\Omega^\alpha{}_A$ the generic component of the tensor of quasi-velocities $\boldsymbol{\Omega}$, which represents a "change of variables" performed on $\dot{\boldsymbol{F}}_\gamma$, and let us define it through

the transformation (cf. Section 1.1.2)

$$\Omega^{\alpha}{}_{A} = \hat{\Omega}^{\alpha}{}_{A} \circ (\boldsymbol{F}, \boldsymbol{F}_{\gamma}; \dot{\boldsymbol{F}}_{\gamma}; \mathcal{X}, \mathcal{T}) \equiv \hat{\Omega}^{\alpha}{}_{A} \circ \natural_{\mathrm{c}}, \qquad \alpha, A = 1, 2, 3, \tag{5.20}$$

where the arguments of $\hat{\Omega}^{\alpha}{}_{A}$ are the same as those of $\hat{\mathcal{C}}$.

Together with the quasi-velocities, we introduce the *quasi-coordinates* and their virtual incremental fields (cf. Section 5.3) [13, 30]

$$\dot{\Theta}^{\alpha}{}_{A} := \hat{\Omega}^{\alpha}{}_{A} \circ \natural_{\mathrm{c}}, \tag{5.21a}$$

$$[\boldsymbol{\eta}_{\boldsymbol{\Theta}}]^{\alpha}{}_{A} := \left(\frac{\partial \hat{\Omega}^{\alpha}{}_{A}}{\partial (\dot{\boldsymbol{F}}_{\gamma})^{\beta}{}_{B}} \circ \natural_{\mathrm{c}} \right) [\boldsymbol{\eta}_{\boldsymbol{F}_{\gamma}}]^{\beta}{}_{B} \equiv (\hat{\mathbb{J}}^{\alpha}{}_{A\beta}{}^{B} \circ \natural_{\mathrm{c}}) [\boldsymbol{\eta}_{\boldsymbol{F}_{\gamma}}]^{\beta}{}_{B}. \tag{5.21b}$$

Equation (5.21b) is, for each pair of indices α and A, a linear differential form in the *virtual incremental field* $\boldsymbol{\eta}_{\boldsymbol{F}_{\gamma}}$ of $\boldsymbol{F}_{\gamma}$, which defines *explicitly* the new virtual incremental field $[\boldsymbol{\eta}_{\boldsymbol{\Theta}}]^{\alpha}{}_{A}$. Equation (5.21a), instead, defines quasi-coordinates *implicitly*, i.e., as the functions $\Theta^{\alpha}{}_{A}$ that solve the differential equations that it represents. Hence, for given α and A, there exists a function $\Theta^{\alpha}{}_{A}$ that satisfies Equation (5.21a), and is, thus, a primitive of $\Omega^{\alpha}{}_{A} \equiv \hat{\Omega}^{\alpha}{}_{A} \circ \natural_{\mathrm{c}}$ in the sense of the Fundamental Theorem of Calculus, i.e.,

$$\Theta^{\alpha}{}_{A}(X, t) = \Theta^{\alpha}{}_{A}(X, t_{\mathrm{in}}) + \int_{t_{\mathrm{in}}}^{t} \Omega^{\alpha}{}_{A}(X, s) \mathrm{d}s, \qquad \forall\, X \in \mathscr{B}, \tag{5.22}$$

provided $\Omega^{\alpha}{}_{A}$ is continuous in time. However, as expanded in Section 1.1.2, this does not imply a representation of $\Theta^{\alpha}{}_{A}$ of the form $\hat{\Theta}^{\alpha}{}_{A} \circ (\boldsymbol{F}, \boldsymbol{F}_{\gamma}; \mathcal{X}, \mathcal{T})$.

The functions $\dot{\Theta}^{\alpha}{}_{A}$ and $[\boldsymbol{\eta}_{\boldsymbol{\Theta}}]^{\alpha}{}_{A}$ can be identified with the components of the two two-point second-order tensor fields defined by the right-hand sides of Equations (5.21a) and (5.21b), respectively.

The non-singularity of the transformation (5.20) requires that the collection of functions

$$\mathbb{J}^{\alpha}{}_{A\beta}{}^{B} = \hat{\mathbb{J}}^{\alpha}{}_{A\beta}{}^{B} \circ \natural_{\mathrm{c}} := \frac{\partial \hat{\Omega}^{\alpha}{}_{A}}{\partial (\dot{\boldsymbol{F}}_{\gamma})^{\beta}{}_{B}} \circ \natural_{\mathrm{c}}, \qquad \alpha, A, \beta, B = 1, 2, 3, \tag{5.23}$$

gives the components of the non-singular fourth-order tensor $\mathbb{J}$ that represents the Jacobian of the transformation itself. Hence, in compact notation, we write $\boldsymbol{\eta}_{\boldsymbol{\Theta}} = \mathbb{J}[\boldsymbol{\eta}_{\boldsymbol{F}_{\gamma}}]$, with $\mathbb{J} = \hat{\mathbb{J}} \circ \natural_{\mathrm{c}} = \partial_{\dot{\boldsymbol{F}}_{\gamma}} \hat{\boldsymbol{\Omega}} \circ \natural_{\mathrm{c}}$.

5.3.2 Transpositional relations and choice of the quasi-velocities

As anticipated in the previous section, the choice of the most appropriate system of quasi-velocities permits to compute the associated "transpositional relations" (see, e.g., [13, 30, 16]), which express the fact that, in general, the operations of "virtual variation" and of "time differentiation" are not commutative when nonholonomic constraints are featured [13].

To compute the transpositional relations characterizing our problem of growth mechanics, we adapt a procedure reported in a work by Jarzębowska [30], and recently reviewed in [1], that is based on the quasi-velocities and on the variations of the quasi-coordinates introduced in Equations (5.20) and (5.21b). To recall the main steps of such procedure, we refer the reader to Section 1.1.2, in which we explain it for the case of a generic discrete mechanical problem. For our problem of growth mechanics, we introduce the homotopies

$$\boldsymbol{F}(X,t) \mapsto \tilde{\boldsymbol{F}}(X,t,\varepsilon) = \boldsymbol{F}(X,t) + \boldsymbol{\eta}_{\boldsymbol{F}}(X,t)\varepsilon + o(\varepsilon), \qquad \varepsilon \to 0, \tag{5.24a}$$

$$\boldsymbol{F}_\gamma(X,t) \mapsto \tilde{\boldsymbol{F}}_\gamma(X,t,\varepsilon) = \boldsymbol{F}_\gamma(X,t) + \boldsymbol{\eta}_{\boldsymbol{F}_\gamma}(X,t)\varepsilon + o(\varepsilon), \quad \varepsilon \to 0, \tag{5.24b}$$

$$\dot{\boldsymbol{F}}_\gamma(X,t) \mapsto \tilde{\boldsymbol{V}}(X,t,\varepsilon) = \dot{\boldsymbol{F}}_\gamma(X,t) + \boldsymbol{\eta}_{\dot{\boldsymbol{F}}_\gamma}(X,t)\varepsilon + o(\varepsilon), \quad \varepsilon \to 0, \tag{5.24c}$$

$$\mathcal{X}(X,t) \mapsto \tilde{\mathcal{X}}(X,t,\varepsilon) = \mathcal{X}(X,t) = X, \qquad \forall\, \varepsilon \in \mathscr{Y}(\varepsilon_0), \tag{5.24d}$$

$$\mathcal{T}(X,t) \mapsto \tilde{\mathcal{T}}(X,t,\varepsilon) = \mathcal{T}(X,t) = t, \qquad \forall\, \varepsilon \in \mathscr{Y}(\varepsilon_0), \tag{5.24e}$$

where, as before, $\mathscr{Y}(\varepsilon_0)$ is an open neighborhood of zero having radius $\varepsilon_0 > 0$, and $\boldsymbol{\eta}_\varphi$ is the field associated with the generic variable φ of $\mathfrak{h}_\mathrm{c}$.

Within the present framework, the increment $\boldsymbol{\eta}_{\dot{\boldsymbol{F}}_\gamma}(X,t)$ on the generalized velocity $\dot{\boldsymbol{F}}_\gamma(X,t)$ is allowed to be different from $\dot{\boldsymbol{\eta}}_{\boldsymbol{F}_\gamma}(X,t)$. Hence, in general, we set $\boldsymbol{\eta}_{\dot{\boldsymbol{F}}_\gamma} \neq \dot{\boldsymbol{\eta}}_{\boldsymbol{F}_\gamma}$. The homotopies $\tilde{\mathcal{X}}$ and $\tilde{\mathcal{T}}$ are formal, since material points and time are not transformed. They are introduced with the sole purpose of defining rigorously the variation of a generic function $f = \hat{f} \circ \mathfrak{h}_\mathrm{c}$ as $\tilde{f} := \hat{f} \circ \tilde{\mathfrak{h}}_\mathrm{c}$, with the understanding that $\tilde{\mathfrak{h}}_\mathrm{c} := (\tilde{\boldsymbol{F}}, \tilde{\boldsymbol{F}}_\gamma; \tilde{\boldsymbol{V}}; \tilde{\mathcal{X}}, \tilde{\mathcal{T}})$, and

$$\tilde{f}(X,t,\varepsilon) = \hat{f}(\tilde{\mathfrak{h}}_\mathrm{c}(X,t,\varepsilon)) = \hat{f}(\tilde{\boldsymbol{F}}(X,t,\varepsilon), \tilde{\boldsymbol{F}}_\gamma(X,t,\varepsilon); \tilde{\boldsymbol{V}}(X,t,\varepsilon); X, t). \tag{5.25}$$

Equation (5.25) permits to formalize the homotopy $\tilde{\boldsymbol{\Omega}} := \hat{\boldsymbol{\Omega}} \circ \tilde{\natural}_{\mathrm{c}}$, and to write the increment associated with it, i.e., $\boldsymbol{\eta}_{\boldsymbol{\Omega}}(X,t) := \partial_{\varepsilon}\tilde{\boldsymbol{\Omega}}(X,t,0)$, as

$$\boldsymbol{\eta}_{\boldsymbol{\Omega}} = \left(\frac{\partial\hat{\boldsymbol{\Omega}}}{\partial\boldsymbol{F}} \circ \natural_{\mathrm{c}}\right)[\boldsymbol{\eta}_{\boldsymbol{F}}] + \left(\frac{\partial\hat{\boldsymbol{\Omega}}}{\partial\boldsymbol{F}_{\gamma}} \circ \natural_{\mathrm{c}}\right)[\boldsymbol{\eta}_{\boldsymbol{F}_{\gamma}}] + \left(\frac{\partial\hat{\boldsymbol{\Omega}}}{\partial\dot{\boldsymbol{F}}_{\gamma}} \circ \natural_{\mathrm{c}}\right)[\boldsymbol{\eta}_{\dot{\boldsymbol{F}}_{\gamma}}]. \tag{5.26}$$

We also compute the time derivative of $\boldsymbol{\eta}_{\boldsymbol{\Theta}}$, i.e.,

$$\dot{\boldsymbol{\eta}}_{\boldsymbol{\Theta}} = \left[\frac{\partial}{\partial t}\left(\frac{\partial\hat{\boldsymbol{\Omega}}}{\partial\dot{\boldsymbol{F}}_{\gamma}} \circ \natural_{\mathrm{c}}\right)\right][\boldsymbol{\eta}_{\boldsymbol{F}_{\gamma}}] + \left(\frac{\partial\hat{\boldsymbol{\Omega}}}{\partial\dot{\boldsymbol{F}}_{\gamma}} \circ \natural_{\mathrm{c}}\right)[\dot{\boldsymbol{\eta}}_{\boldsymbol{F}_{\gamma}}], \tag{5.27}$$

so that the difference $\boldsymbol{\eta}_{\boldsymbol{\Omega}} - \dot{\boldsymbol{\eta}}_{\boldsymbol{\Theta}}$ yields (cf. Section 1.1.2)

$$\boldsymbol{\eta}_{\boldsymbol{\Omega}} - \dot{\boldsymbol{\eta}}_{\boldsymbol{\Theta}} = (\mathcal{E}_{\boldsymbol{F}}\hat{\boldsymbol{\Omega}})[\boldsymbol{\eta}_{\boldsymbol{F}}] + (\mathcal{E}_{\boldsymbol{F}_{\gamma}}\hat{\boldsymbol{\Omega}})[\boldsymbol{\eta}_{\boldsymbol{F}_{\gamma}}] + \left(\frac{\partial\hat{\boldsymbol{\Omega}}}{\partial\dot{\boldsymbol{F}}_{\gamma}} \circ \natural_{\mathrm{c}}\right)[\boldsymbol{\eta}_{\dot{\boldsymbol{F}}_{\gamma}} - \dot{\boldsymbol{\eta}}_{\boldsymbol{F}_{\gamma}}], \tag{5.28}$$

where the Euler–Lagrange operators $\mathcal{E}_{\boldsymbol{F}}$ and $\mathcal{E}_{\boldsymbol{F}_{\gamma}}$ applied to $\hat{\boldsymbol{\Omega}}$ are given by the following fourth-order tensor fields

$$\mathcal{E}_{\boldsymbol{F}}\hat{\boldsymbol{\Omega}} := \frac{\partial\hat{\boldsymbol{\Omega}}}{\partial\boldsymbol{F}} \circ \natural_{\mathrm{c}}, \tag{5.29a}$$

$$\mathcal{E}_{\boldsymbol{F}_{\gamma}}\hat{\boldsymbol{\Omega}} := \frac{\partial\hat{\boldsymbol{\Omega}}}{\partial\boldsymbol{F}_{\gamma}} \circ \natural_{\mathrm{c}} - \frac{\partial}{\partial t}\left(\frac{\partial\hat{\boldsymbol{\Omega}}}{\partial\dot{\boldsymbol{F}}_{\gamma}} \circ \natural_{\mathrm{c}}\right). \tag{5.29b}$$

We remark that $\mathcal{E}_{\boldsymbol{F}}\hat{\boldsymbol{\Omega}}$ reduces to $\partial_{\boldsymbol{F}}\hat{\boldsymbol{\Omega}} \circ \natural_{\mathrm{c}}$ because the variable $\dot{\boldsymbol{F}}$ is ignorable in the present framework and has thus been excluded from the list $\natural_{\mathrm{c}}$.

According to [13, 28–30], Equation (5.28) can be simplified by assuming the vanishing either of $\boldsymbol{\eta}_{\boldsymbol{\Omega}} - \dot{\boldsymbol{\eta}}_{\boldsymbol{\Theta}}$ or of $\boldsymbol{\eta}_{\dot{\boldsymbol{F}}_{\gamma}} - \dot{\boldsymbol{\eta}}_{\boldsymbol{F}_{\gamma}}$. For our purposes, we consider here the case $\boldsymbol{\eta}_{\boldsymbol{\Omega}} - \dot{\boldsymbol{\eta}}_{\boldsymbol{\Theta}} = \boldsymbol{O}$, and, upon setting $\mathbb{J} = \partial_{\dot{\boldsymbol{F}}_{\gamma}}\hat{\boldsymbol{\Omega}} \circ \natural_{\mathrm{c}}$, we achieve the important result (cf. Section 1.1.2)

$$\begin{aligned}\boldsymbol{\eta}_{\dot{\boldsymbol{F}}_{\gamma}} - \dot{\boldsymbol{\eta}}_{\boldsymbol{F}_{\gamma}} &= -(\mathbb{J}^{-1} \diamond \mathcal{E}_{\boldsymbol{F}}\hat{\boldsymbol{\Omega}})[\boldsymbol{\eta}_{\boldsymbol{F}}] - (\mathbb{J}^{-1} \diamond \mathcal{E}_{\boldsymbol{F}_{\gamma}}\hat{\boldsymbol{\Omega}})[\boldsymbol{\eta}_{\boldsymbol{F}_{\gamma}}] \\ &= \mathbb{W}_{\boldsymbol{F}_{\gamma}\boldsymbol{F}}[\boldsymbol{\eta}_{\boldsymbol{F}}] + \mathbb{W}_{\boldsymbol{F}_{\gamma}\boldsymbol{F}_{\gamma}}[\boldsymbol{\eta}_{\boldsymbol{F}_{\gamma}}],\end{aligned} \tag{5.30}$$

where the fourth-order tensor fields $\mathbb{W}_{\boldsymbol{F}_{\gamma}\boldsymbol{F}}$ and $\mathbb{W}_{\boldsymbol{F}_{\gamma}\boldsymbol{F}_{\gamma}}$ are given by

$$\mathbb{W}_{\boldsymbol{F}_{\gamma}\boldsymbol{F}} := -\mathbb{J}^{-1} \diamond \mathcal{E}_{\boldsymbol{F}}\hat{\boldsymbol{\Omega}}, \qquad \mathbb{W}_{\boldsymbol{F}_{\gamma}\boldsymbol{F}_{\gamma}} := -\mathbb{J}^{-1} \diamond \mathcal{E}_{\boldsymbol{F}_{\gamma}}\hat{\boldsymbol{\Omega}}. \tag{5.31}$$

Equation (5.30) is referred to as *transpositional relation*, since it shows that, if the quantities $\mathcal{E}_{\boldsymbol{F}}\hat{\boldsymbol{\Omega}}$ and $\mathcal{E}_{\boldsymbol{F}_\gamma}\hat{\boldsymbol{\Omega}}$ are not null, $\boldsymbol{\eta}_{\dot{\boldsymbol{F}}_\gamma}$ is different from $\dot{\boldsymbol{\eta}}_{\boldsymbol{F}_\gamma}$ [13, 30].

5.3.3 Conditions on the quasi-velocities

By plugging the last sum on the right-hand side of Equation (5.30) into Equation (5.28), grouping together the factors of $\boldsymbol{\eta}_{\boldsymbol{F}}$ and $\boldsymbol{\eta}_{\boldsymbol{F}_\gamma}$, and setting $\boldsymbol{\eta}_{\boldsymbol{\Omega}} - \dot{\boldsymbol{\eta}}_{\boldsymbol{\Theta}} = \boldsymbol{O}$, we obtain the equality

$$\boldsymbol{O} = \left\{\mathcal{E}_{\boldsymbol{F}}\hat{\boldsymbol{\Omega}} + \mathbb{J} \diamond \mathbb{W}_{\boldsymbol{F}_\gamma \boldsymbol{F}}\right\}[\boldsymbol{\eta}_{\boldsymbol{F}}] + \left\{\mathcal{E}_{\boldsymbol{F}_\gamma}\hat{\boldsymbol{\Omega}} + \mathbb{J} \diamond \mathbb{W}_{\boldsymbol{F}_\gamma \boldsymbol{F}_\gamma}\right\}[\boldsymbol{\eta}_{\boldsymbol{F}_\gamma}]. \tag{5.32}$$

Following the line of thought developed in [16], we can now use Equation (5.32) as a condition to compute $\mathbb{W}_{\boldsymbol{F}_\gamma \boldsymbol{F}}$ and $\mathbb{W}_{\boldsymbol{F}_\gamma \boldsymbol{F}_\gamma}$, as done in Section 1.1.2 for the discrete case, thereby requiring

$$\mathcal{E}_{\boldsymbol{F}}\hat{\boldsymbol{\Omega}} + \mathbb{J} \diamond \mathbb{W}_{\boldsymbol{F}_\gamma \boldsymbol{F}} = \mathbb{O}, \qquad \mathcal{E}_{\boldsymbol{F}_\gamma}\hat{\boldsymbol{\Omega}} + \mathbb{J} \diamond \mathbb{W}_{\boldsymbol{F}_\gamma \boldsymbol{F}_\gamma} = \mathbb{O}, \tag{5.33}$$

where $\mathbb{O}$ is the null fourth-order tensor. We remark that this can be done if $\boldsymbol{\eta}_{\boldsymbol{F}}$ and $\boldsymbol{\eta}_{\boldsymbol{F}_\gamma}$ are linearly independent. In the present framework, they are regarded to be such, because the Lagrange multiplier technique is employed.

The conditions (5.33) are thus equivalent to those in Equation (5.31), and are preferable since they allow to determine $\mathbb{W}_{\boldsymbol{F}_\gamma \boldsymbol{F}}$ and $\mathbb{W}_{\boldsymbol{F}_\gamma \boldsymbol{F}_\gamma}$ without directly inverting $\mathbb{J}$ (as will be seen later). It is also worth to remark that Equations $(5.33)_1$ and $(5.33)_2$ can be viewed as characterizing properties for $\hat{\boldsymbol{\Omega}}$ [16].

5.3.4 Best choice of the quasi-velocities

Let us decompose the growth tensor as $\boldsymbol{F}_\gamma = J_\gamma^{1/3}\boldsymbol{F}_{\gamma,\mathrm{u}}$, where $\det \boldsymbol{F}_{\gamma,\mathrm{u}} = 1$, and let us write the rate $\boldsymbol{F}_\gamma^{-1}\dot{\boldsymbol{F}}_\gamma$ in the form

$$\boldsymbol{F}_\gamma^{-1}\dot{\boldsymbol{F}}_\gamma = \boldsymbol{F}_{\gamma,\mathrm{u}}^{-1}\dot{\boldsymbol{F}}_{\gamma,\mathrm{u}} + \tfrac{1}{3}\mathrm{tr}(\boldsymbol{F}_\gamma^{-1}\dot{\boldsymbol{F}}_\gamma)\boldsymbol{I} = \boldsymbol{F}_{\gamma,\mathrm{u}}^{-1}\dot{\boldsymbol{F}}_{\gamma,\mathrm{u}} + \tfrac{1}{3}(\dot{J}_\gamma/J_\gamma)\boldsymbol{I}. \tag{5.34}$$

Since it holds that $\mathrm{tr}(\boldsymbol{F}_\gamma^{-1}\dot{\boldsymbol{F}}_\gamma) = \dot{J}_\gamma/J_\gamma$, only the spherical part of $\boldsymbol{F}_\gamma^{-1}\dot{\boldsymbol{F}}_\gamma$ is restricted by the constraint (5.4), which, indeed, becomes $\mathcal{C} = \dot{J}_\gamma/J_\gamma - R = 0$. On the other hand, the time derivative of the isochoric part of $\boldsymbol{F}_\gamma$, i.e., $\dot{\boldsymbol{F}}_{\gamma,\mathrm{u}}$, is not involved in the

constraint. In fact, $\dot{\boldsymbol{F}}_{\gamma,\mathrm{u}}$ is subjected to no restrictions, except that it has to satisfy the property $\mathrm{tr}(\boldsymbol{F}_{\gamma,\mathrm{u}}^{-1}\dot{\boldsymbol{F}}_{\gamma,\mathrm{u}}) = 0$, true by construction, as can be deduced from Equation (5.34), or, equivalently, from the expression

$$\dot{\boldsymbol{F}}_{\gamma,\mathrm{u}} = J_\gamma^{-1/3}\dot{\boldsymbol{F}}_\gamma - \tfrac{1}{3}\mathrm{tr}(\boldsymbol{F}_\gamma^{-1}\dot{\boldsymbol{F}}_\gamma)J_\gamma^{-1/3}\boldsymbol{F}_\gamma. \tag{5.35}$$

Hence, $\dot{\boldsymbol{F}}_{\gamma,\mathrm{u}}$ has only 8 independent tensor components. On the basis of these considerations, we choose as quasi-velocities the constraint (5.4) itself and eight independent components of $\dot{\boldsymbol{F}}_{\gamma,\mathrm{u}}$. Thus, we set (cf. Section 1.1.2)

$$\Omega^1{}_1 = \hat{\Omega}^1{}_1 \circ \natural_\mathrm{c} := \hat{\mathcal{C}} \circ \natural_\mathrm{c} = \mathrm{tr}(\boldsymbol{F}_\gamma^{-1}\dot{\boldsymbol{F}}_\gamma) - \hat{R} \circ \natural_\gamma, \tag{5.36a}$$

$$\Omega^1{}_B = \hat{\Omega}^1{}_B \circ \natural_\mathrm{c} := J_\gamma^{-1/3}\big[(\dot{\boldsymbol{F}}_\gamma)^1{}_B - \tfrac{1}{3}\mathrm{tr}(\boldsymbol{F}_\gamma^{-1}\dot{\boldsymbol{F}}_\gamma)(\boldsymbol{F}_\gamma)^1{}_B\big], \quad B = 2,3, \tag{5.36b}$$

$$\Omega^\beta{}_1 = \hat{\Omega}^\beta{}_1 \circ \natural_\mathrm{c} := J_\gamma^{-1/3}\big[(\dot{\boldsymbol{F}}_\gamma)^\beta{}_1 - \tfrac{1}{3}\mathrm{tr}(\boldsymbol{F}_\gamma^{-1}\dot{\boldsymbol{F}}_\gamma)(\boldsymbol{F}_\gamma)^\beta{}_1\big], \quad \beta = 2,3, \tag{5.36c}$$

$$\Omega^\beta{}_B = \hat{\Omega}^\beta{}_B \circ \natural_\mathrm{c} := J_\gamma^{-1/3}\big[(\dot{\boldsymbol{F}}_\gamma)^\beta{}_B - \tfrac{1}{3}\mathrm{tr}(\boldsymbol{F}_\gamma^{-1}\dot{\boldsymbol{F}}_\gamma)(\boldsymbol{F}_\gamma)^\beta{}_B\big], \quad \beta, B = 2,3. \tag{5.36d}$$

We now employ the definitions (5.36a)–(5.36d) in the conditions (5.33), which, thus, acquire a block-wise structure. Specifically, Equation $(5.33)_1$ gives

$$\left(\frac{\partial\hat{\Omega}^1{}_1}{\partial(\dot{\boldsymbol{F}}_\gamma)^\lambda{}_L} \circ \natural_\mathrm{c}\right)(\mathbb{W}_{\boldsymbol{F}_\gamma\boldsymbol{F}})^\lambda{}_{La}{}^A = -\frac{\partial\hat{\Omega}^1{}_1}{\partial F^a{}_A} \circ \natural_\mathrm{c}$$

$$\Rightarrow \quad (\mathbb{W}^{\mathrm{T}}_{\boldsymbol{F}_\gamma\boldsymbol{F}}[\boldsymbol{F}_\gamma^{-\mathrm{T}}])_a{}^A = \frac{\partial\hat{R}}{\partial F^a{}_A} \circ \natural_\gamma, \tag{5.37a}$$

$$\left(\frac{\partial\hat{\Omega}^1{}_B}{\partial(\dot{\boldsymbol{F}}_\gamma)^\lambda{}_L} \circ \natural_\mathrm{c}\right)(\mathbb{W}_{\boldsymbol{F}_\gamma\boldsymbol{F}})^\lambda{}_{La}{}^A = -\frac{\partial\hat{\Omega}^1{}_B}{\partial F^a{}_A} \circ \natural_\mathrm{c}$$

$$\Rightarrow \quad J_\gamma^{-1/3}\left\{(\mathbb{W}_{\boldsymbol{F}_\gamma\boldsymbol{F}})^1{}_{Ba}{}^A - \frac{1}{3}(\boldsymbol{F}_\gamma)^1{}_B(\mathbb{W}^{\mathrm{T}}_{\boldsymbol{F}_\gamma\boldsymbol{F}}[\boldsymbol{F}_\gamma^{-\mathrm{T}}])_a{}^A\right\} = 0, \tag{5.37b}$$

$$\left(\frac{\partial\hat{\Omega}^\beta{}_1}{\partial(\dot{\boldsymbol{F}}_\gamma)^\lambda{}_L} \circ \natural_\mathrm{c}\right)(\mathbb{W}_{\boldsymbol{F}_\gamma\boldsymbol{F}})^\lambda{}_{La}{}^A = -\frac{\partial\hat{\Omega}^\beta{}_1}{\partial F^a{}_A} \circ \natural_\mathrm{c}$$

$$\Rightarrow \quad J_\gamma^{-1/3}\left\{(\mathbb{W}_{\boldsymbol{F}_\gamma\boldsymbol{F}})^\beta{}_{1a}{}^A - \frac{1}{3}(\boldsymbol{F}_\gamma)^\beta{}_1(\mathbb{W}^{\mathrm{T}}_{\boldsymbol{F}_\gamma\boldsymbol{F}}[\boldsymbol{F}_\gamma^{-\mathrm{T}}])_a{}^A\right\} = 0, \tag{5.37c}$$

$$\left(\frac{\partial\hat{\Omega}^\beta{}_B}{\partial(\dot{\boldsymbol{F}}_\gamma)^\lambda{}_L} \circ \natural_\mathrm{c}\right)(\mathbb{W}_{\boldsymbol{F}_\gamma\boldsymbol{F}})^\lambda{}_{La}{}^A = -\frac{\partial\hat{\Omega}^\beta{}_B}{\partial F^a{}_A} \circ \natural_\mathrm{c}$$

$$\Rightarrow \quad J_\gamma^{-1/3}\left\{(\mathbb{W}_{\boldsymbol{F}_\gamma\boldsymbol{F}})^\beta{}_{Ba}{}^A - \frac{1}{3}(\boldsymbol{F}_\gamma)^\beta{}_B(\mathbb{W}^{\mathrm{T}}_{\boldsymbol{F}_\gamma\boldsymbol{F}}[\boldsymbol{F}_\gamma^{-\mathrm{T}}])_a{}^A\right\} = 0, \tag{5.37d}$$

with $\beta, B = 2, 3$, $\lambda, L = 1, 2, 3$, and $a, A = 1, 2, 3$. The system (5.37a)–(5.37d) can be solved by substituting the right-hand side of Equation (5.37a) in all other equations. This provides all the components of $\mathbb{W}_{\boldsymbol{KF}}$ except $(\mathbb{W}_{\boldsymbol{F}_\gamma \boldsymbol{F}})^1{}_{1a}{}^A$. Hence, by using these results in the first relation of Equation (5.33), $\mathbb{W}_{\boldsymbol{F}_\gamma \boldsymbol{F}}$ becomes

$$\mathbb{W}_{\boldsymbol{F}_\gamma \boldsymbol{F}} = \frac{1}{3}\boldsymbol{F}_\gamma \otimes \left(\frac{\partial \hat{R}}{\partial \boldsymbol{F}} \circ \natural_\gamma\right). \tag{5.38}$$

Next, we turn to Equation $(5.33)_2$ to compute $\mathbb{W}_{\boldsymbol{F}_\gamma \boldsymbol{F}_\gamma}$. Since $\mathrm{tr}(\boldsymbol{F}_\gamma^{-1}\dot{\boldsymbol{F}}_\gamma)$ in Equation (5.36a) is the time derivative of $\log(\det \boldsymbol{F}_\gamma)$, it belongs to the kernel of the Euler–Lagrange operator $\mathcal{E}_{\boldsymbol{F}_\gamma}$, and, thus, we find $\mathcal{E}_{\boldsymbol{F}_\gamma}\hat{\Omega}^1{}_1 = -\partial_{\boldsymbol{F}_\gamma}\hat{R} \circ \natural_\gamma$. Analogously, since all the components of $\dot{\boldsymbol{F}}_{\gamma,\mathrm{u}}$ written explicitly in Equations (5.36b)–(5.36d) are time derivatives of functions of $\boldsymbol{F}_\gamma$, we find $\mathcal{E}_{\boldsymbol{F}_\gamma}\hat{\Omega}^1{}_B = \boldsymbol{O}$, $\mathcal{E}_{\boldsymbol{F}_\gamma}\hat{\Omega}^\beta{}_1 = \boldsymbol{O}$, and $\mathcal{E}_{\boldsymbol{F}_\gamma}\hat{\Omega}^\beta{}_B = \boldsymbol{O}$. Therefore, Equation $(5.33)_2$ yields

$$\begin{aligned}
&\left(\frac{\partial \hat{\Omega}^1{}_1}{\partial (\dot{\boldsymbol{F}}_\gamma)^\lambda{}_L} \circ \natural_{\mathrm{c}}\right)(\mathbb{W}_{\boldsymbol{F}_\gamma \boldsymbol{F}_\gamma})^\lambda{}_{L\mu}{}^M = -\mathcal{E}_{(\boldsymbol{F}_\gamma)^\mu{}_M}\hat{\Omega}^1{}_1 \\
&\Rightarrow \quad (\mathbb{W}^{\mathrm{T}}_{\boldsymbol{F}_\gamma \boldsymbol{F}_\gamma}[\boldsymbol{F}_\gamma^{-\mathrm{T}}])_\mu{}^M = \frac{\partial \hat{R}}{\partial (\boldsymbol{F}_\gamma)^\mu{}_M} \circ \natural_\gamma, && (5.39a) \\
&\left(\frac{\partial \hat{\Omega}^1{}_B}{\partial (\dot{\boldsymbol{F}}_\gamma)^\lambda{}_L} \circ \natural_{\mathrm{c}}\right)(\mathbb{W}_{\boldsymbol{F}_\gamma \boldsymbol{F}_\gamma})^\lambda{}_{L\mu}{}^M = -\mathcal{E}_{(\boldsymbol{F}_\gamma)^\mu{}_M}\hat{\Omega}^1{}_B \\
&\Rightarrow \quad J_\gamma^{-1/3}\left\{(\mathbb{W}_{\boldsymbol{F}_\gamma \boldsymbol{F}_\gamma})^1{}_{B\mu}{}^M - \frac{1}{3}(\boldsymbol{F}_\gamma)^1{}_B(\mathbb{W}^{\mathrm{T}}_{\boldsymbol{F}_\gamma \boldsymbol{F}_\gamma}[\boldsymbol{F}_\gamma^{-\mathrm{T}}])_\mu{}^M\right\} = 0, && (5.39b) \\
&\left(\frac{\partial \hat{\Omega}^\beta{}_1}{\partial (\dot{\boldsymbol{F}}_\gamma)^\lambda{}_L} \circ \natural_{\mathrm{c}}\right)(\mathbb{W}_{\boldsymbol{F}_\gamma \boldsymbol{F}_\gamma})^\lambda{}_{L\mu}{}^M = -\mathcal{E}_{(\boldsymbol{F}_\gamma)^\mu{}_M}\hat{\Omega}^\beta{}_1 \\
&\Rightarrow \quad J_\gamma^{-1/3}\left\{(\mathbb{W}_{\boldsymbol{F}_\gamma \boldsymbol{F}_\gamma})^\beta{}_{1\mu}{}^M - \frac{1}{3}(\boldsymbol{F}_\gamma)^\beta{}_1(\mathbb{W}^{\mathrm{T}}_{\boldsymbol{F}_\gamma \boldsymbol{F}_\gamma}[\boldsymbol{F}_\gamma^{-\mathrm{T}}])_\mu{}^M\right\} = 0, && (5.39c) \\
&\left(\frac{\partial \hat{\Omega}^\beta{}_B}{\partial (\dot{\boldsymbol{F}}_\gamma)^\lambda{}_L} \circ \natural_{\mathrm{c}}\right)(\mathbb{W}_{\boldsymbol{F}_\gamma \boldsymbol{F}_\gamma})^\lambda{}_{L\mu}{}^M = -\mathcal{E}_{(\boldsymbol{F}_\gamma)^\mu{}_M}\hat{\Omega}^\beta{}_B \\
&\Rightarrow \quad J_\gamma^{-1/3}\left\{(\mathbb{W}_{\boldsymbol{F}_\gamma \boldsymbol{F}_\gamma})^\beta{}_{B\mu}{}^M - \frac{1}{3}(\boldsymbol{F}_\gamma)^\beta{}_B(\mathbb{W}^{\mathrm{T}}_{\boldsymbol{F}_\gamma \boldsymbol{F}_\gamma}[\boldsymbol{F}_\gamma^{-\mathrm{T}}])_\mu{}^M\right\} = 0, && (5.39d)
\end{aligned}$$

with $\beta, B = 2, 3$ and $\lambda, \mu, L, M = 1, 2, 3$. Also in this case, substitution of Equation (5.39a) into (5.39b)–(5.39d) and using the second of Equation (5.33) lead to

$$\mathbb{W}_{\boldsymbol{F}_\gamma \boldsymbol{F}_\gamma} = \frac{1}{3}\boldsymbol{F}_\gamma \otimes \left(\frac{\partial \hat{R}}{\partial \boldsymbol{F}_\gamma} \circ \natural_\gamma\right). \tag{5.40}$$

5.3.5 Quasi-coordinates and their variation for growth

Comparing Equations (5.36a)–(5.36d) with the general definitions (5.21a), we notice that, apart from $\hat{\Omega}^1{}_1 \circ \natural_c$, all the other quasi-velocities are total time derivatives of $\boldsymbol{F}_{\gamma,u}$, which is a function of $\boldsymbol{F}_\gamma$, only. Accordingly, by virtue of the relations

$$\dot{\Theta}^1{}_1 = \Omega^1{}_1 = \mathcal{C} \equiv \hat{\mathcal{C}} \circ \natural_c = \mathrm{tr}(\boldsymbol{F}_\gamma^{-1}\dot{\boldsymbol{F}}_\gamma) - \hat{R} \circ \natural_\gamma = 0, \tag{5.41a}$$

$$\Omega^1{}_B \equiv \hat{\Omega}^1{}_B \circ \natural_c = [\partial_t(J_\gamma^{-1/3}\boldsymbol{F}_\gamma)]^1{}_B = \dot{\Theta}^1{}_B, \qquad B = 2,3, \tag{5.41b}$$

$$\Omega^\beta{}_1 \equiv \hat{\Omega}^\beta{}_1 \circ \natural_c = [\partial_t(J_\gamma^{-1/3}\boldsymbol{F}_\gamma)]^\beta{}_1 = \dot{\Theta}^\beta{}_1 \qquad \beta = 2,3, \tag{5.41c}$$

$$\Omega^\beta{}_B \equiv \hat{\Omega}^\beta{}_B \circ \natural_c = [\partial_t(J_\gamma^{-1/3}\boldsymbol{F}_\gamma)]^\beta{}_B = \dot{\Theta}^\beta{}_B, \qquad \beta, B = 2,3, \tag{5.41d}$$

and with appropriate initial conditions, the quasi-coordinates are given by

$$\Theta^1{}_1(X,t) - \Theta^1{}_1(X,t_{in}) = \int_{t_{in}}^{t} \hat{\mathcal{C}}(\boldsymbol{F}(X,s), \boldsymbol{F}_\gamma(X,s); \dot{\boldsymbol{F}}_\gamma(X,s); X, s)\mathrm{d}s = 0, \tag{5.42a}$$

$$\Theta^1{}_B = [\boldsymbol{F}_{\gamma,u}]^1{}_B, \quad \Theta^\beta{}_1 = [\boldsymbol{F}_{\gamma,u}]^\beta{}_1, \quad \Theta^\beta{}_B = [\boldsymbol{F}_{\gamma,u}]^\beta{}_B, \tag{5.42b}$$

where, as above, β and B take on the values 2, 3, and $\Theta^1{}_1(X,t_{in})$ is to be provided by means of suitable initial conditions. The nonholonomic nature of the quasi-velocity $\Omega^1{}_1 = \hat{\mathcal{C}} \circ \natural_c$ implies that the quasi-coordinate $\Theta^1{}_1$ has to be a functional of $\boldsymbol{F}$ and $\boldsymbol{F}_\gamma$ and a function of material points and time. Indeed, by exploiting Equation (5.41a), it follows from (5.42a) that

$$\begin{aligned}&\Theta^1{}_1(X,t) - \Theta^1{}_1(X,t_{in})\\ &= \log\left(\frac{J_\gamma(X,t)}{J_\gamma(X,t_{in})}\right) - \int_{t_{in}}^{t} \hat{R}(\boldsymbol{F}(X,s), \boldsymbol{F}_\gamma(X,s); X, s)\mathrm{d}s = 0.\end{aligned} \tag{5.43}$$

In addition, the fulfillment of $\mathcal{C} = 0$ implies $\Theta^1{}_1(X,t) - \Theta^1{}_1(X,t_{in}) = 0$, and, thus, that $\Theta^1{}_1(X,t)$ equals its initial value $\Theta^1{}_1(X,t_{in})$ at all times $t \geq t_{in}$, which returns the formal solution to $\dot{J}_\gamma - J_\gamma R = 0$, i.e., the constraint itself.

From Equation (5.43), we notice that, *if* we take $\Theta^1{}_1(X,t_{in}) = \log J_\gamma(X,t_{in})$, and *if* we assume that the body finds itself in an initial state for which $J_\gamma(X,t_{in}) = 1$, then we obtain $\Theta^1{}_1(X,t) = 0$ at all times $t \geq t_{in}$, and for all $X \in \mathscr{B}$. Thus, if we further suppose $\boldsymbol{F}_\gamma = J_\gamma^{1/3}\boldsymbol{I}$ (some authors [84] refer to this situation as *"spherical*

growth"), then Equations (5.42a) and (5.42b) give

$$\Theta^1{}_1(X,t) = \Theta^1{}_1(X,t_{\text{in}}) = 0, \qquad \Theta^1{}_B(X,t) = 0, \qquad B = 2,3, \tag{5.44a}$$

$$\Theta^\beta{}_1(X,t) = 0, \quad \beta = 2,3, \qquad \Theta^\beta{}_B(X,t) = \delta^\beta{}_B, \qquad \beta, B = 2,3, \tag{5.44b}$$

which means that the matrix associated with the quasi-coordinates is *singular* in the just analyzed case (whereas $\boldsymbol{F}_\gamma$ is non-singular). This result is coherent with the fact that choosing the quasi-velocity $\Omega^1{}_1$ as coincident with the expression of the constraint implies that, if the constraint is fulfilled, the quasi-velocity $\Omega^1{}_1$ is zero. Consequently, the corresponding quasi-coordinate defines a state of rest, which becomes equal to the "origin" $\Theta^1{}_1(X,t_{\text{in}}) = 0$ of an appropriate reference frame, if $J_\gamma(X,t_{\text{in}}) = 1$. On the other hand, if one starts from a perturbed state $0 < J_\gamma(X,t_{\text{in}}) \neq 1$, then $\Theta^1{}_1(X,t_{\text{in}}) = \log J_\gamma(X,t_{\text{in}})$ is different from zero (it could be negative, if $J_\gamma(X,t_{\text{in}}) < 1$), and so is also $\Theta^1{}_1(X,t)$ at all times $t \geq t_{\text{in}}$. This property descends from the fact that $\Theta^1{}_1(X,t_{\text{in}})$ represents $J_\gamma(X,t_{\text{in}})$ in logarithmic scale.

In conclusion, the representation of quasi-velocities and quasi-coordinates amounts to selecting a frame that co-moves with growth, in which, thus, no growth is perceived. For this reason, the (virtual) incremental field associated with $\Theta^1{}_1$, i.e., $[\boldsymbol{\eta}_{\boldsymbol{\Theta}}]^1{}_1$, must return Equation (5.7) divided by ε, that is,

$$[\boldsymbol{\eta}_{\boldsymbol{\Theta}}]^1{}_1 = \left(\frac{\partial \hat{\Omega}^1{}_1}{\partial(\dot{\boldsymbol{F}}_\gamma)^\beta{}_B} \circ \natural_{\text{c}}\right)[\boldsymbol{\eta}_{\boldsymbol{F}_\gamma}]^\beta{}_B = \left(\frac{\partial \hat{\mathcal{C}}}{\partial(\dot{\boldsymbol{F}}_\gamma)^\beta{}_B} \circ \natural_{\text{c}}\right)[\boldsymbol{\eta}_{\boldsymbol{F}_\gamma}]^\beta{}_B = 0, \tag{5.45}$$

as can be deduced from Equation (5.21b).

5.4 Equivalence with the TNHM

In this section, we present the result that we deem most fundamental for our formulation of growth. Specifically, we show that, although being nonholonomic, *the constraint* (5.4) *can be included in a suitably defined Lagrangian density function of the growing body*. In other words, one is able to handle the constraint "as if" it were holonomic, thereby allowing for a variational study of growth, up to the irreducible non-potential forces $\boldsymbol{f}_{\text{np}}$ and $\mathfrak{S}_{\text{np}}$.

5.4.1 Dynamic equations in the system of the quasi-velocities

Written in the system of the quasi-velocities $\boldsymbol{\Omega} \equiv \hat{\boldsymbol{\Omega}} \circ \natural_{\mathrm{c}}$, the Lagrangian density function of the growing medium becomes

$$\check{\mathcal{L}} \circ \natural_{\boldsymbol{\Omega}} = \hat{\mathcal{L}} \circ \natural = \mathcal{L}, \tag{5.46}$$

where $\natural_{\boldsymbol{\Omega}}$ is the same collection of variables as $\natural$, with the exception of $\dot{\boldsymbol{F}}_\gamma$, which is replaced with $\boldsymbol{\Omega}$.

If φ is a variable of $\natural$ such that neither φ nor $\dot{\varphi}$ are included in $\natural_{\mathrm{c}}$, then $\mathcal{E}_\varphi \check{\mathcal{L}}$ is identical to $\mathcal{E}_\varphi \hat{\mathcal{L}}$. However, if ψ is a variable of $\natural$ such that ψ itself and/or $\dot{\psi}$ are included in $\natural_{\mathrm{c}}$ (in fact, here $\dot{\psi}$ can be only $\dot{\boldsymbol{F}}_\gamma$), then the chain rule implies the identities

$$\frac{\partial \hat{\mathcal{L}}}{\partial \psi} \circ \natural = \frac{\partial \check{\mathcal{L}}}{\partial \psi} \circ \natural_{\boldsymbol{\Omega}} + \left(\frac{\partial \check{\mathcal{L}}}{\partial \Omega^\alpha{}_A} \circ \natural_{\boldsymbol{\Omega}} \right) \left(\frac{\partial \hat{\Omega}^\alpha{}_A}{\partial \psi} \circ \natural_{\mathrm{c}} \right), \tag{5.47a}$$

$$\frac{\partial \hat{\mathcal{L}}}{\partial \dot{\psi}} \circ \natural = \left(\frac{\partial \check{\mathcal{L}}}{\partial \Omega^\alpha{}_A} \circ \natural_{\boldsymbol{\Omega}} \right) \left(\frac{\partial \hat{\Omega}^\alpha{}_A}{\partial \dot{\psi}} \circ \natural_{\mathrm{c}} \right), \tag{5.47b}$$

and the corresponding Euler–Lagrange operator $\mathcal{E}_\psi \hat{\mathcal{L}}$ transforms accordingly. Since Equations (5.47a) and (5.47b) apply to $\boldsymbol{F}$ and $\boldsymbol{F}_\gamma$ and $\dot{\boldsymbol{F}}_\gamma$, we obtain

$$\mathcal{E}_{\boldsymbol{F}} \hat{\mathcal{L}} \equiv \frac{\partial \hat{\mathcal{L}}}{\partial \boldsymbol{F}} \circ \natural = \check{\mathcal{E}}_{\boldsymbol{F}} \check{\mathcal{L}} + (\mathcal{E}_{\boldsymbol{F}} \hat{\boldsymbol{\Omega}})^{\mathrm{T}} \left[\frac{\partial \check{\mathcal{L}}}{\partial \boldsymbol{\Omega}} \circ \natural_{\boldsymbol{\Omega}} \right], \tag{5.48a}$$

$$\mathcal{E}_{\boldsymbol{F}_\gamma} \hat{\mathcal{L}} \equiv \frac{\partial \hat{\mathcal{L}}}{\partial \boldsymbol{F}_\gamma} \circ \natural - \frac{\partial}{\partial t} \left(\frac{\partial \hat{\mathcal{L}}}{\partial \dot{\boldsymbol{F}}_\gamma} \circ \natural \right) = \mathbb{J}^{\mathrm{T}} [\check{\mathcal{E}}_{\boldsymbol{F}_\gamma} \check{\mathcal{L}}] + (\mathcal{E}_{\boldsymbol{F}_\gamma} \hat{\boldsymbol{\Omega}})^{\mathrm{T}} \left[\frac{\partial \check{\mathcal{L}}}{\partial \boldsymbol{\Omega}} \circ \natural_{\boldsymbol{\Omega}} \right], \tag{5.48b}$$

where we have exploited the definitions of $\mathcal{E}_{\boldsymbol{F}} \hat{\boldsymbol{\Omega}} \equiv \partial_{\boldsymbol{F}} \hat{\boldsymbol{\Omega}} \circ \natural_{\mathrm{c}}$ and $\mathcal{E}_{\boldsymbol{F}_\gamma} \hat{\boldsymbol{\Omega}}$ given in Equations (5.29a) and (5.29b), and we have introduced the notation

$$\check{\mathcal{E}}_{\boldsymbol{F}} \check{\mathcal{L}} := \frac{\partial \check{\mathcal{L}}}{\partial \boldsymbol{F}} \circ \natural_{\boldsymbol{\Omega}}, \tag{5.49a}$$

$$\check{\mathcal{E}}_{\boldsymbol{F}_\gamma} \check{\mathcal{L}} := (\mathbb{J}^{-1})^{\mathrm{T}} \left[\frac{\partial \check{\mathcal{L}}}{\partial \boldsymbol{F}_\gamma} \circ \natural_{\boldsymbol{\Omega}} \right] - \frac{\partial}{\partial t} \left(\frac{\partial \check{\mathcal{L}}}{\partial \boldsymbol{\Omega}} \circ \natural_{\boldsymbol{\Omega}} \right) \tag{5.49b}$$

to denote the transformed Euler–Lagrange operators $\check{\mathcal{E}}_{\boldsymbol{F}}$ and $\check{\mathcal{E}}_{\boldsymbol{F}_\gamma}$ applied to the Lagrangian density function $\check{\mathcal{L}}$, expressed in the system of the quasi-velocities. On

the other hand, the quantity

$$\boldsymbol{\pi}_\gamma := \frac{\partial \check{\mathcal{L}}}{\partial \boldsymbol{\Omega}} \circ \natural_{\boldsymbol{\Omega}} \tag{5.50}$$

can be expressed in terms of the generalized momentum $\boldsymbol{p}_\gamma = \partial_{\dot{\boldsymbol{F}}_\gamma} \hat{\mathcal{L}} \circ \natural$, dual to $\dot{\boldsymbol{F}}_\gamma$ through $\hat{\mathcal{L}}$, by inverting the relationship

$$\boldsymbol{p}_\gamma = \left(\frac{\partial \hat{\boldsymbol{\Omega}}}{\partial \dot{\boldsymbol{F}}_\gamma} \circ \natural_{\mathrm{c}} \right)^{\mathrm{T}} [\boldsymbol{\pi}_\gamma] = \mathbb{J}^{\mathrm{T}} [\boldsymbol{\pi}_\gamma] \quad \Rightarrow \quad \boldsymbol{\pi}_\gamma = (\mathbb{J}^{-1})^{\mathrm{T}} [\boldsymbol{p}_\gamma]. \tag{5.51}$$

We could refer to $\boldsymbol{\pi}_\gamma$ as *quasi-momentum*, since it is dual to the quasi-velocity $\boldsymbol{\Omega}$ through the duality relationship introduced by $\check{\mathcal{L}}$.

Let us substitute Equation (5.51) into (5.48a) and (5.48b), and let us employ the definitions (5.31) to see how the Euler–Lagrange operators $\mathcal{E}_{\boldsymbol{F}}$ and $\mathcal{E}_{\boldsymbol{F}_\gamma}$ transform when switching from the collection $\natural$ to $\natural_{\boldsymbol{\Omega}}$, i.e., to the one of the quasi-velocities, for describing the medium's kinematics. By employing the notation $\diamond$ introduced in 5.1.1, we find (see also [13, 29])

$$\mathcal{E}_{\boldsymbol{F}} \hat{\mathcal{L}} = \check{\mathcal{E}}_{\boldsymbol{F}} \check{\mathcal{L}} + (\mathbb{J}^{-1} \diamond \mathcal{E}_{\boldsymbol{F}} \hat{\boldsymbol{\Omega}})^{\mathrm{T}} [\boldsymbol{p}_\gamma] = \check{\mathcal{E}}_{\boldsymbol{F}} \check{\mathcal{L}} - \mathbb{W}^{\mathrm{T}}_{\boldsymbol{F}_\gamma \boldsymbol{F}} [\boldsymbol{p}_\gamma], \tag{5.52a}$$

$$\mathcal{E}_{\boldsymbol{F}_\gamma} \hat{\mathcal{L}} = \mathbb{J}^{\mathrm{T}} [\check{\mathcal{E}}_{\boldsymbol{F}_\gamma} \check{\mathcal{L}}] + (\mathbb{J}^{-1} \diamond \mathcal{E}_{\boldsymbol{F}_\gamma} \hat{\boldsymbol{\Omega}})^{\mathrm{T}} [\boldsymbol{p}_\gamma] = \mathbb{J}^{\mathrm{T}} [\check{\mathcal{E}}_{\boldsymbol{F}_\gamma} \check{\mathcal{L}}] - \mathbb{W}^{\mathrm{T}}_{\boldsymbol{F}_\gamma \boldsymbol{F}_\gamma} [\boldsymbol{p}_\gamma], \tag{5.52b}$$

where $\mathbb{W}_{\boldsymbol{F}_\gamma \boldsymbol{F}}$ and $\mathbb{W}_{\boldsymbol{F}_\gamma \boldsymbol{F}_\gamma}$ are given in Equations (5.38) and (5.40), respectively.

By virtue of the results (5.52a) and (5.52b), we rephrase the dynamic equations (5.16c) and (5.16e) in the system of the quasi-velocities as (see [13, 28, 29] for the derivation of similar equations for noholonomic discrete mechanical systems)

$$\check{\mathcal{E}}_{\boldsymbol{F}} \check{\mathcal{L}} - \mathbb{W}^{\mathrm{T}}_{\boldsymbol{F}_\gamma \boldsymbol{F}} [\boldsymbol{p}_\gamma] + \boldsymbol{T} = \boldsymbol{O}, \tag{5.53a}$$

$$\mathbb{J}^{\mathrm{T}} [\check{\mathcal{E}}_{\boldsymbol{F}_\gamma} \check{\mathcal{L}}] = -\mathfrak{S}_{\mathrm{np}} + \mu (\partial_{\dot{\boldsymbol{F}}_\gamma} \hat{\mathcal{C}} \circ \natural_{\mathrm{c}}) + \mathbb{W}^{\mathrm{T}}_{\boldsymbol{F}_\gamma \boldsymbol{F}_\gamma} [\boldsymbol{p}_\gamma]. \tag{5.53b}$$

Before going further, the following remark is in order.

Remark 5.3 (The origin of the "extra terms"). Equations (5.53a) and (5.53b) are *Hamel equations* [13], up to the reactive forces $\boldsymbol{T}$ and $\mu(\partial_{\dot{\boldsymbol{F}}_\gamma} \hat{\mathcal{C}} \circ \natural_{\mathrm{c}})$. With respect to the "classical" Euler–Lagrange equations, they feature the "extra" generalized forces $\mathbb{W}^{\mathrm{T}}_{\boldsymbol{F}_\gamma \boldsymbol{F}} [\boldsymbol{p}_\gamma]$ and $\mathbb{W}^{\mathrm{T}}_{\boldsymbol{F}_\gamma \boldsymbol{F}_\gamma} [\boldsymbol{p}_\gamma]$, which both descend from the adoption of the quasi-velocities. In general, these terms are nonzero because the functions $\Omega^\alpha{}_A = \hat{\Omega}^\alpha{}_A \circ \natural_{\mathrm{c}}$

are not all the time derivatives of as many functions of $\boldsymbol{F}$, $\boldsymbol{F}_\gamma$, $\mathcal{X}$, and $\mathcal{T}$ (note that the just mentioned list of variables coincides with $\natural_\gamma$). Indeed, if for each pair of indices $\alpha, A = 1, 2, 3$ there existed a C^1 function $\mathcal{F}^\alpha{}_A := \hat{\mathcal{F}}^\alpha{}_A \circ \natural_\gamma$ such that $\Omega^\alpha{}_A = \partial_t \mathcal{F}^\alpha{}_A$, then the quantities $\mathcal{E}_{\boldsymbol{F}}\hat{\boldsymbol{\Omega}}$ and $\mathcal{E}_{\boldsymbol{F}_\gamma}\hat{\boldsymbol{\Omega}}$ would vanish identically (note that the first condition requires both $\hat{\mathcal{F}}^\alpha{}_A$ and $\hat{\Omega}^\alpha{}_A$ to be independent of $\boldsymbol{F}$). In fact, $\mathbb{W}^{\mathrm{T}}_{\boldsymbol{F}_\gamma \boldsymbol{F}}[\boldsymbol{p}_\gamma]$ and $\mathbb{W}^{\mathrm{T}}_{\boldsymbol{F}_\gamma \boldsymbol{F}_\gamma}[\boldsymbol{p}_\gamma]$ could be viewed as *fictitious "polygenic forces"* [11] generated by the choice of the quasi-velocities. In other words, whereas the Euler–Lagrange dynamic equations are form-invariant in every system of coordinates, they lose this property when one switches to a system of generic quasi-velocities, and, as a result of this loss of invariance, they acquire the extra forces $\mathbb{W}^{\mathrm{T}}_{\boldsymbol{F}_\gamma \boldsymbol{F}}[\boldsymbol{p}_\gamma]$ and $\mathbb{W}^{\mathrm{T}}_{\boldsymbol{F}_\gamma \boldsymbol{F}_\gamma}[\boldsymbol{p}_\gamma]$. However, these forces disappear when one goes back to the original system of generalized velocities.

Based on Remark 5.3, we add $\mathbb{W}^{\mathrm{T}}_{\boldsymbol{F}_\gamma \boldsymbol{F}}[\boldsymbol{p}_\gamma]$ and $\mathbb{W}^{\mathrm{T}}_{\boldsymbol{F}_\gamma \boldsymbol{F}_\gamma}[\boldsymbol{p}_\gamma]$ to both sides of Equations (5.16c) and (5.16e), respectively, thereby finding the *modified dynamic equations*

$$\mathcal{E}_{\boldsymbol{F}}\hat{\mathcal{L}} + \mathbb{W}^{\mathrm{T}}_{\boldsymbol{F}_\gamma \boldsymbol{F}}[\boldsymbol{p}_\gamma] + \boldsymbol{T} = \mathbb{W}^{\mathrm{T}}_{\boldsymbol{F}_\gamma \boldsymbol{F}}[\boldsymbol{p}_\gamma], \tag{5.54a}$$

$$\mathcal{E}_{\boldsymbol{F}_\gamma}\hat{\mathcal{L}} + \mathbb{W}^{\mathrm{T}}_{\boldsymbol{F}_\gamma \boldsymbol{F}_\gamma}[\boldsymbol{p}_\gamma] = -\mathfrak{S}_{\mathrm{np}} + \mu(\partial_{\dot{\boldsymbol{F}}_\gamma}\hat{\mathcal{C}} \circ \natural_{\mathrm{c}}) + \mathbb{W}^{\mathrm{T}}_{\boldsymbol{F}_\gamma \boldsymbol{F}_\gamma}[\boldsymbol{p}_\gamma]. \tag{5.54b}$$

Note that, in doing this, we are taking inspiration from the *"most general formulation of the principle of stationary action"* discussed in [13].

Although Equations (5.54a) and (5.54b) are a mere rewriting of (5.16c) and (5.16e), they unfold important properties:

P1. While the left-hand sides of Equations (5.16c) and (5.16e) are obtained by varying the action functional $\mathscr{A}_{\mathrm{a}}$ according to Hamilton's Principle, the left-hand sides of Equations (5.54a) and (5.54b) cannot be retrieved this way because of the extra forces $\mathbb{W}^{\mathrm{T}}_{\boldsymbol{F}_\gamma \boldsymbol{F}}[\boldsymbol{p}_\gamma]$ and $\mathbb{W}^{\mathrm{T}}_{\boldsymbol{F}_\gamma \boldsymbol{F}_\gamma}[\boldsymbol{p}_\gamma]$. However, they can be obtained by means of a variational procedure known as *Hamilton–Suslov Principle* (see, e.g., [16]). In brief, the Hamilton–Suslov method computes the variation of a given action functional by hypothesizing that, if φ is a Lagrangian parameter of the theory under consideration, and $\dot{\varphi}$ is its generalized velocity, then the incremental field $\boldsymbol{\eta}_{\dot{\varphi}}$ differs from the time derivative $\dot{\boldsymbol{\eta}}_{\varphi}$ of the variation by the so-called *transpositional relations* (see, e.g., Equation (5.30)). It can be proven that, if $\dot{\varphi}$ is not involved in any nonholonomic constraint, then the

associated transpositional relations are null, and one finds $\boldsymbol{\eta}_{\dot{\varphi}} = \dot{\boldsymbol{\eta}}_{\varphi}$. However, this is not true, in general, when $\dot{\varphi}$ has to comply with a nonholonomic constraint. This is indeed the case for $\dot{\boldsymbol{F}}_\gamma$ in the growth problem studied here, and the non-vanishing transpositional relations (5.30) are naturally accounted for by the Hamilton–Suslov method. In particular, they result into the extra forces $\mathbb{W}^{\mathrm{T}}_{\boldsymbol{F}_\gamma \boldsymbol{F}}[\boldsymbol{p}_\gamma]$ and $\mathbb{W}^{\mathrm{T}}_{\boldsymbol{F}_\gamma \boldsymbol{F}_\gamma}[\boldsymbol{p}_\gamma]$, which are, thus, an output of the procedure.

P2. Similarly to the right-hand side of Equation (5.16e), which collects the non-potential forces handled by means of the Extended Hamilton Principle [11][4], also the right-hand sides of Equations (5.54a) and (5.54b) can be framed by "extending" the Hamilton–Suslov method: the variation of $\mathscr{A}_{\mathrm{a}}$ performed with the Hamilton–Suslov variations is set equal to minus the integral in time of the work done on the variations associated with $\boldsymbol{\eta}_{\boldsymbol{F}}$ and $\boldsymbol{\eta}_{\boldsymbol{F}_\gamma}$ by all the non-potential forces dual to them, including the extra ones $\mathbb{W}^{\mathrm{T}}_{\boldsymbol{F}_\gamma \boldsymbol{F}}[\boldsymbol{p}_\gamma]$ and $\mathbb{W}^{\mathrm{T}}_{\boldsymbol{F}_\gamma \boldsymbol{F}_\gamma}[\boldsymbol{p}_\gamma]$ that feature on the right-hand sides. In doing this, one has to admit the existence of these fictitious extra forces *a priori*. Although, on the one hand, this may sound artificial, on the other hand, $\mathbb{W}^{\mathrm{T}}_{\boldsymbol{F}_\gamma \boldsymbol{F}}[\boldsymbol{p}_\gamma]$ and $\mathbb{W}^{\mathrm{T}}_{\boldsymbol{F}_\gamma \boldsymbol{F}_\gamma}[\boldsymbol{p}_\gamma]$ do have a physical meaning. Namely, they represent two rates of momentum introduced in the system by the constraint. In the specific case of growth, upon recognizing that $P_\gamma \coloneqq \frac{1}{3}\mathrm{tr}(\boldsymbol{F}_\gamma^{\mathrm{T}}\boldsymbol{p}_\gamma)$ is the spherical part of the fully material generalized momentum $\boldsymbol{F}_\gamma^{\mathrm{T}}\boldsymbol{p}_\gamma = \boldsymbol{F}_\gamma^{\mathrm{T}}(\partial_{\dot{\boldsymbol{F}}_\gamma}\hat{\mathcal{L}} \circ \natural)$, the results (5.38) and (5.40) are such that the extra forces

$$\mathbb{W}^{\mathrm{T}}_{\boldsymbol{F}_\gamma \boldsymbol{F}}[\boldsymbol{p}_\gamma] = \left\{\frac{1}{3}\boldsymbol{F}_\gamma \otimes \left(\frac{\partial \hat{R}}{\partial \boldsymbol{F}} \circ \natural_\gamma\right)\right\}^{\mathrm{T}}[\boldsymbol{p}_\gamma] = P_\gamma\left(\frac{\partial \hat{R}}{\partial \boldsymbol{F}} \circ \natural_\gamma\right), \tag{5.55a}$$

$$\mathbb{W}^{\mathrm{T}}_{\boldsymbol{F}_\gamma \boldsymbol{F}_\gamma}[\boldsymbol{p}_\gamma] = \left\{\frac{1}{3}\boldsymbol{F}_\gamma \otimes \left(\frac{\partial \hat{R}}{\partial \boldsymbol{F}_\gamma} \circ \natural_\gamma\right)\right\}^{\mathrm{T}}[\boldsymbol{p}_\gamma] = P_\gamma\left(\frac{\partial \hat{R}}{\partial \boldsymbol{F}_\gamma} \circ \natural_\gamma\right) \tag{5.55b}$$

can be interpreted as momentum rates due to the *coupling* of the mass source R with the system's degrees of freedom represented by $\boldsymbol{F}$ and $\boldsymbol{F}_\gamma$. Moreover, since the constraint (5.4) is made nonholonomic by R, the right-hand sides of Equations (5.55a) and (5.55b) "measure" how nonholonomic the constraint is.

[4]With reference to Equation (5.16e), this means that the variation of the action functional computed with Hamilton's variations, and through the derivative reported in Equation (5.15), is set equal to the time integral of the negative of the work done by the *"polygenic forces"* [11] dual to $\boldsymbol{\eta}_{\boldsymbol{F}_\gamma}$ on the variations associated with $\boldsymbol{\eta}_{\boldsymbol{F}_\gamma}$ itself.

In the remainder of this section, we show that Equations (5.54a) and (5.54b) can be obtained variationally by letting their left-hand sides originate from the Hamilton–Suslov Principle, and interpreting the terms $\mathbb{W}^{\mathrm{T}}_{\boldsymbol{F}_\gamma \boldsymbol{F}}[\boldsymbol{p}_\gamma]$ and $\mathbb{W}^{\mathrm{T}}_{\boldsymbol{F}_\gamma \boldsymbol{F}_\gamma}[\boldsymbol{p}_\gamma]$ on the right-hand sides as non-potential forces to be accounted for by means of an "Extended Hamilton–Suslov Principle". We accomplish this task by (i) taking the weak forms of Equations (5.54a) and (5.54b) through multiplication with $\boldsymbol{\eta}_{\boldsymbol{F}}$ and $\boldsymbol{\eta}_{\boldsymbol{F}_\gamma}$, respectively; (ii) combining the results with the weak forms of the dynamic equations (5.16a) and (5.16b); (iii) integrating over $\mathscr{B}$, $\partial^{\chi}_{\mathrm{N}}\mathscr{B}$, and $[t_{\mathrm{in}}, t_{\mathrm{fin}}]$; and (iv) showing that one achieves the variation of the action according to the Hamilton–Suslov Principle, set equal to minus the work done by the polygenic and the extra forces on their respective dual variations.

If, on the one hand, doing so amounts to going back along the procedure designated by Llibre et al. [16], on the other hand, our result seems to us more general and, to the best of our understanding, capable of explaining when and why the method proposed in [16] is equivalent to the TNHM. This seems to us a very important issue for the following reason.

According to *our* results, it seems that the constraint given in Equation (5.4) cannot be studied by means of the MVM formulated in [16], since this version of the MVM produces Equations (5.54a) and (5.54b) only *up to* the extra forces $\mathbb{W}^{\mathrm{T}}_{\boldsymbol{F}_\gamma \boldsymbol{F}}[\boldsymbol{p}_\gamma]$ and $\mathbb{W}^{\mathrm{T}}_{\boldsymbol{F}_\gamma \boldsymbol{F}_\gamma}[\boldsymbol{p}_\gamma]$ featuring on their right-hand sides. Hence, in our opinion, the MVM of [16] is not equivalent to the TNHM for growth mechanics viewed as a constrained field theory. On the other hand, $\mathbb{W}^{\mathrm{T}}_{\boldsymbol{F}_\gamma \boldsymbol{F}}[\boldsymbol{p}_\gamma]$ and $\mathbb{W}^{\mathrm{T}}_{\boldsymbol{F}_\gamma \boldsymbol{F}_\gamma}[\boldsymbol{p}_\gamma]$ on the right-hand sides of Equations (5.54a) and (5.54b) are necessary to grant the equivalence with the TNHM, and such equivalence is necessary to make the MVM applicable to the mechanics of growth. For this reason, the purpose of the forthcoming calculations is to show how to accommodate for this issue.

5.4.2 The Lagrangian density function of a growing medium

We set $\partial_{\dot{\boldsymbol{F}}_\gamma} \hat{\mathcal{C}} \circ \natural_{\mathrm{c}} = \boldsymbol{F}_\gamma^{-\mathrm{T}}$ in Equation (5.53b), as follows from Equation (5.4). However, the procedure outlined in the sequel applies to any non-singular second-order tensor field $\partial_{\dot{\boldsymbol{F}}_\gamma} \hat{\mathcal{C}} \circ \natural_{\mathrm{c}}$. Moreover, we write

$$\mathfrak{S}_{\boldsymbol{F}_\gamma \boldsymbol{F}} := \mathbb{W}^{\mathrm{T}}_{\boldsymbol{F}_\gamma \boldsymbol{F}}[\boldsymbol{p}_\gamma], \qquad \mathfrak{S}_{\boldsymbol{F}_\gamma \boldsymbol{F}_\gamma} := \mathbb{W}^{\mathrm{T}}_{\boldsymbol{F}_\gamma \boldsymbol{F}_\gamma}[\boldsymbol{p}_\gamma]. \tag{5.56}$$

Note that $\mathfrak{S}_{\boldsymbol{F}_\gamma \boldsymbol{F}}$ and $\mathfrak{S}_{\boldsymbol{F}_\gamma \boldsymbol{F}_\gamma}$ have components $[\mathfrak{S}_{\boldsymbol{F}_\gamma \boldsymbol{F}}]_a{}^A$ and $[\mathfrak{S}_{\boldsymbol{F}_\gamma \boldsymbol{F}_\gamma}]_\alpha{}^A$. It is also convenient to introduce the fully material quantities $\boldsymbol{F}^{\mathrm{T}}\mathfrak{S}_{\boldsymbol{F}_\gamma \boldsymbol{F}}$ and $\boldsymbol{F}_\gamma^{\mathrm{T}}\mathfrak{S}_{\boldsymbol{F}_\gamma \boldsymbol{F}_\gamma}$, and, accordingly, to transform Equations (5.54a) and (5.54b) as

$$\boldsymbol{F}^{\mathrm{T}}[\mathcal{E}_{\boldsymbol{F}}\hat{\mathcal{L}}] + \boldsymbol{F}^{\mathrm{T}}\mathfrak{S}_{\boldsymbol{F}_\gamma \boldsymbol{F}} + \boldsymbol{F}^{\mathrm{T}}\boldsymbol{T} = \boldsymbol{F}^{\mathrm{T}}\mathfrak{S}_{\boldsymbol{F}_\gamma \boldsymbol{F}}, \tag{5.57a}$$

$$\boldsymbol{F}_\gamma^{\mathrm{T}}[\mathcal{E}_{\boldsymbol{F}_\gamma}\hat{\mathcal{L}}] + \boldsymbol{F}_\gamma^{\mathrm{T}}\mathfrak{S}_{\boldsymbol{F}_\gamma \boldsymbol{F}_\gamma} = -\boldsymbol{F}_\gamma^{\mathrm{T}}\mathfrak{S}_{\mathrm{np}} + \mu\boldsymbol{I}^{\mathrm{T}} + \boldsymbol{F}_\gamma^{\mathrm{T}}\mathfrak{S}_{\boldsymbol{F}_\gamma \boldsymbol{F}_\gamma}. \tag{5.57b}$$

In Equation (5.57b), the term $\mu\boldsymbol{I}^{\mathrm{T}}$ suggests to project the equation itself onto the space of spherical tensors in order to compute μ. To this end, we consider the summand $\boldsymbol{F}_\gamma^{\mathrm{T}}\mathfrak{S}_{\boldsymbol{F}_\gamma \boldsymbol{F}_\gamma}$ on the right-hand side of Equation (5.57b), and we decompose it as

$$\boldsymbol{F}_\gamma^{\mathrm{T}}\mathfrak{S}_{\boldsymbol{F}_\gamma \boldsymbol{F}_\gamma} = \tfrac{1}{3}\mathrm{tr}(\boldsymbol{F}_\gamma^{\mathrm{T}}\mathfrak{S}_{\boldsymbol{F}_\gamma \boldsymbol{F}_\gamma})\,\boldsymbol{I}^{\mathrm{T}} + \mathrm{Dev}(\boldsymbol{F}_\gamma^{\mathrm{T}}\mathfrak{S}_{\boldsymbol{F}_\gamma \boldsymbol{F}_\gamma}). \tag{5.58}$$

Then, by introducing the *rescaled* Lagrange multiplier

$$\kappa := \mu + \tfrac{1}{3}\mathrm{tr}(\boldsymbol{F}_\gamma^{\mathrm{T}}\mathfrak{S}_{\boldsymbol{F}_\gamma \boldsymbol{F}_\gamma}), \tag{5.59}$$

and recalling that $\boldsymbol{p}_\gamma = \partial_{\dot{\boldsymbol{F}}_\gamma}\hat{\mathcal{L}} \circ \natural$, we rewrite Equation (5.57b) as

$$\mathcal{E}_{\boldsymbol{F}_\gamma}\hat{\mathcal{L}} + \mathbb{W}^{\mathrm{T}}_{\boldsymbol{F}_\gamma \boldsymbol{F}_\gamma}[\partial_{\dot{\boldsymbol{F}}_\gamma}\hat{\mathcal{L}} \circ \natural] = -\mathfrak{S}_{\mathrm{np}} + \kappa\,\boldsymbol{F}_\gamma^{-\mathrm{T}} + \mathrm{DEV}\mathfrak{S}_{\boldsymbol{F}_\gamma \boldsymbol{F}_\gamma}, \tag{5.60}$$

with $\mathrm{DEV}\mathfrak{S}_{\boldsymbol{F}_\gamma \boldsymbol{F}_\gamma} := \boldsymbol{F}_\gamma^{-\mathrm{T}}\mathrm{Dev}(\boldsymbol{F}_\gamma^{\mathrm{T}}\mathfrak{S}_{\boldsymbol{F}_\gamma \boldsymbol{F}_\gamma}) = \mathfrak{S}_{\boldsymbol{F}_\gamma \boldsymbol{F}_\gamma} - \frac{1}{3}\mathrm{tr}(\boldsymbol{F}_\gamma^{\mathrm{T}}\mathfrak{S}_{\boldsymbol{F}_\gamma \boldsymbol{F}_\gamma})\boldsymbol{F}_\gamma^{-\mathrm{T}}$ being the $\boldsymbol{F}_\gamma^{-\mathrm{T}}$-deviatoric part of $\mathfrak{S}_{\boldsymbol{F}_\gamma \boldsymbol{F}_\gamma}$.

By using Equations (5.54a) and (5.60) in lieu of (5.16c) and (5.16e), respectively, in the system (5.16a)–(5.16f), we can write

$$\mathcal{E}_\chi\hat{\mathcal{L}} + \mathrm{Div}\boldsymbol{T} = -\boldsymbol{f}_{\mathrm{np}}, \qquad \text{in } \mathscr{B}, \tag{5.61a}$$

$$\boldsymbol{\tau} - \boldsymbol{T}\boldsymbol{N} = \boldsymbol{0}, \qquad \text{on } \partial_{\mathrm{N}}^{\chi}\mathscr{B}, \tag{5.61b}$$

$$\mathcal{E}_{\boldsymbol{F}}\hat{\mathcal{L}} + \mathbb{W}^{\mathrm{T}}_{\boldsymbol{F}_\gamma \boldsymbol{F}}[\partial_{\dot{\boldsymbol{F}}_\gamma}\hat{\mathcal{L}} \circ \natural] + \boldsymbol{T} = \mathfrak{S}_{\boldsymbol{F}_\gamma \boldsymbol{F}}, \qquad \text{in } \mathscr{B}, \tag{5.61c}$$

$$\boldsymbol{F} - D\chi = \boldsymbol{O}, \qquad \text{in } \mathscr{B}, \tag{5.61d}$$

$$\mathcal{E}_{\boldsymbol{F}_\gamma}\hat{\mathcal{L}} + \mathbb{W}^{\mathrm{T}}_{\boldsymbol{F}_\gamma \boldsymbol{F}_\gamma}[\partial_{\dot{\boldsymbol{F}}_\gamma}\hat{\mathcal{L}} \circ \natural] = -\mathfrak{S}_{\mathrm{np}} + \kappa\,\boldsymbol{F}_\gamma^{-\mathrm{T}} + \mathrm{DEV}\mathfrak{S}_{\boldsymbol{F}_\gamma \boldsymbol{F}_\gamma}, \qquad \text{in } \mathscr{B}, \tag{5.61e}$$

$$\langle \boldsymbol{F}_\gamma^{-\mathrm{T}} | \dot{\boldsymbol{F}}_\gamma \rangle - R = 0, \qquad \text{in } \mathscr{B}. \tag{5.61f}$$

Recalling that $\boldsymbol{\eta}_\chi(X,t) = \mathbf{0}$ for $X \in \partial^\chi_{\mathrm{D}}\mathscr{B}$ and at all times, we consider the duality pairs between Equations (5.61a) and $\boldsymbol{\eta}_\chi$, and between (5.61b) and $\boldsymbol{\eta}_\chi$, we integrate the resulting expressions over $\mathscr{B}$ and $\partial^\chi_{\mathrm{N}}\mathscr{B}$, respectively, and we add them together. Then, after some algebraic passages, integrating over the time interval $[t_{\mathrm{in}}, t_{\mathrm{fin}}]$, and enforcing the conditions $\boldsymbol{\eta}_\chi(X,t_{\mathrm{in}}) = \boldsymbol{\eta}_\chi(X,t_{\mathrm{fin}}) = \mathbf{0}$, for all $X \in \mathscr{B}$, we obtain

$$\begin{aligned}&\int_{t_{\mathrm{in}}}^{t_{\mathrm{fin}}}\int_{\mathscr{B}}\left[\left\langle\frac{\partial\hat{\mathcal{L}}}{\partial\chi}\circ\natural\middle|\boldsymbol{\eta}_\chi\right\rangle+\left\langle\frac{\partial\hat{\mathcal{L}}}{\partial\dot{\chi}}\circ\natural\middle|\boldsymbol{\eta}_{\dot{\chi}}\right\rangle-\langle\boldsymbol{T}\mid\mathrm{Grad}\,\boldsymbol{\eta}_\chi\rangle\right]\\&=-\int_{t_{\mathrm{in}}}^{t_{\mathrm{fin}}}\int_{\mathscr{B}}\langle\boldsymbol{f}_{\mathrm{np}}|\boldsymbol{\eta}_\chi\rangle-\int_{t_{\mathrm{in}}}^{t_{\mathrm{fin}}}\int_{\partial^\chi_{\mathrm{N}}\mathscr{B}}\langle\boldsymbol{\tau}|\boldsymbol{\eta}_\chi\rangle,\end{aligned}\tag{5.62}$$

where we have used the abbreviated notations $\int_{t_{\mathrm{in}}}^{t_{\mathrm{fin}}}\int_{\mathscr{B}}[\ldots] \equiv \int_{t_{\mathrm{in}}}^{t_{\mathrm{fin}}}\{\int_{\mathscr{B}}[\ldots]\mathrm{dV}\}\mathrm{d}t$ and $\int_{t_{\mathrm{in}}}^{t_{\mathrm{fin}}}\int_{\partial^\chi_{\mathrm{N}}\mathscr{B}}[\ldots] \equiv \int_{t_{\mathrm{in}}}^{t_{\mathrm{fin}}}\{\int_{\partial^\chi_{\mathrm{N}}\mathscr{B}}[\ldots]\mathrm{dA}\}\mathrm{d}t$, and the identity $\dot{\boldsymbol{\eta}}_\chi = \boldsymbol{\eta}_{\dot{\chi}}$, which is true since the velocity $\dot{\chi}$ is not involved in the constraint.

Next, we take the duality pairs between Equation (5.61c) and $\boldsymbol{\eta}_{\boldsymbol{F}}$, and between Equation (5.61e) and $\boldsymbol{\eta}_{\boldsymbol{F}_\gamma}$, and we integrate over $\mathscr{B}$ and $[t_{\mathrm{in}}, t_{\mathrm{fin}}]$. Then, by recalling the identity $\mathcal{E}_{\boldsymbol{F}}\hat{\mathcal{L}} \equiv \partial_{\boldsymbol{F}}\hat{\mathcal{L}}\circ\natural$, the conditions $\boldsymbol{\eta}_{\boldsymbol{F}_\gamma}(X,t_{\mathrm{in}}) = \boldsymbol{\eta}_{\boldsymbol{F}_\gamma}(X,t_{\mathrm{fin}}) = \boldsymbol{O}$ for all $X \in \mathscr{B}$, and the transpositional relation in Equation (5.30), we find

$$\begin{aligned}&\int_{t_{\mathrm{in}}}^{t_{\mathrm{fin}}}\int_{\mathscr{B}}\left[\left\langle\frac{\partial\hat{\mathcal{L}}}{\partial\boldsymbol{F}}\circ\natural+\boldsymbol{T}\,\middle|\,\boldsymbol{\eta}_{\boldsymbol{F}}\right\rangle+\left\langle\frac{\partial\hat{\mathcal{L}}}{\partial\boldsymbol{F}_\gamma}\circ\natural\,\middle|\,\boldsymbol{\eta}_{\boldsymbol{F}_\gamma}\right\rangle+\left\langle\frac{\partial\hat{\mathcal{L}}}{\partial\dot{\boldsymbol{F}}_\gamma}\circ\natural\,\middle|\,\boldsymbol{\eta}_{\dot{\boldsymbol{F}}_\gamma}\right\rangle\right]\\&=\int_{t_{\mathrm{in}}}^{t_{\mathrm{fin}}}\int_{\mathscr{B}}\left[\langle\mathfrak{S}_{\boldsymbol{F}_\gamma\boldsymbol{F}}\,|\,\boldsymbol{\eta}_{\boldsymbol{F}}\rangle-\langle\mathfrak{S}_{\mathrm{np}}-\kappa\boldsymbol{F}_\gamma^{-\mathrm{T}}-\mathrm{DEV}\mathfrak{S}_{\boldsymbol{F}_\gamma\boldsymbol{F}_\gamma}\,|\,\boldsymbol{\eta}_{\boldsymbol{F}_\gamma}\rangle\right].\end{aligned}\tag{5.63}$$

An important step forward is done if it is possible to find a C^1-function of time, λ, such that $\dot{\lambda} = \kappa$. We assume that this is the case, and, after rewriting $\boldsymbol{F}_\gamma^{-\mathrm{T}}$ as $\partial_{\dot{\boldsymbol{F}}_\gamma}\hat{\mathcal{C}}\circ\natural_{\mathrm{c}}$, performing some algebraic calculations, and invoking the relationship (5.30), we work out the term $\langle\kappa\,\boldsymbol{F}_\gamma^{-\mathrm{T}}\,|\,\boldsymbol{\eta}_{\boldsymbol{F}_\gamma}\rangle$ in Equation (5.63) as

$$\begin{aligned}&\langle\kappa\,\boldsymbol{F}_\gamma^{-\mathrm{T}}\,|\,\boldsymbol{\eta}_{\boldsymbol{F}_\gamma}\rangle=\dot{\lambda}\left\langle\frac{\partial\hat{\mathcal{C}}}{\partial\dot{\boldsymbol{F}}_\gamma}\circ\natural_{\mathrm{c}}\middle|\boldsymbol{\eta}_{\boldsymbol{F}_\gamma}\right\rangle=\frac{\partial}{\partial t}\left[\lambda\left\langle\frac{\partial\hat{\mathcal{C}}}{\partial\dot{\boldsymbol{F}}_\gamma}\circ\natural_{\mathrm{c}}\middle|\boldsymbol{\eta}_{\boldsymbol{F}_\gamma}\right\rangle\right]\\&+\lambda\left\langle\mathcal{E}_{\boldsymbol{F}}\hat{\mathcal{C}}+\mathbb{W}^{\mathrm{T}}_{\boldsymbol{F}_\gamma\boldsymbol{F}}\left[\frac{\partial\hat{\mathcal{C}}}{\partial\dot{\boldsymbol{F}}_\gamma}\circ\natural_{\mathrm{c}}\right]\middle|\boldsymbol{\eta}_{\boldsymbol{F}}\right\rangle+\lambda\left\langle\mathcal{E}_{\boldsymbol{F}_\gamma}\hat{\mathcal{C}}+\mathbb{W}^{\mathrm{T}}_{\boldsymbol{F}_\gamma\boldsymbol{F}_\gamma}\left[\frac{\partial\hat{\mathcal{C}}}{\partial\dot{\boldsymbol{F}}_\gamma}\circ\natural_{\mathrm{c}}\right]\middle|\boldsymbol{\eta}_{\boldsymbol{F}_\gamma}\right\rangle\\&-\lambda\left\langle\frac{\partial\hat{\mathcal{C}}}{\partial\boldsymbol{F}}\circ\natural_{\mathrm{c}}\middle|\boldsymbol{\eta}_{\boldsymbol{F}}\right\rangle-\lambda\left\langle\frac{\partial\hat{\mathcal{C}}}{\partial\boldsymbol{F}_\gamma}\circ\natural_{\mathrm{c}}\middle|\boldsymbol{\eta}_{\boldsymbol{F}_\gamma}\right\rangle-\lambda\left\langle\frac{\partial\hat{\mathcal{C}}}{\partial\dot{\boldsymbol{F}}_\gamma}\circ\natural_{\mathrm{c}}\middle|\boldsymbol{\eta}_{\dot{\boldsymbol{F}}_\gamma}\right\rangle,\end{aligned}\tag{5.64}$$

where $\mathcal{E}_{\boldsymbol{F}}\hat{\mathcal{C}} = \partial_{\boldsymbol{F}}\hat{\mathcal{C}} \circ \natural_{\mathrm{c}}$.

Another important deduction stems from Equations (5.33), (5.37a) and (5.39a). Indeed, by virtue of the identification of $\mathcal{C}$ with the quasi-velocity $\Omega^1{}_1$, and since Equation (5.64) must hold at this stage for any λ, $\boldsymbol{\eta}_{\boldsymbol{F}}$, and $\boldsymbol{\eta}_{\boldsymbol{F}_\gamma}$, we obtain

$$\mathcal{E}_{\boldsymbol{F}}\hat{\mathcal{C}} + \mathbb{W}^{\mathrm{T}}_{\boldsymbol{F}_\gamma \boldsymbol{F}}[\partial_{\dot{\boldsymbol{F}}_\gamma}\hat{\mathcal{C}} \circ \natural_{\mathrm{c}}] = \boldsymbol{O}, \qquad \mathcal{E}_{\boldsymbol{F}_\gamma}\hat{\mathcal{C}} + \mathbb{W}^{\mathrm{T}}_{\boldsymbol{F}_\gamma \boldsymbol{F}_\gamma}[\partial_{\dot{\boldsymbol{F}}_\gamma}\hat{\mathcal{C}} \circ \natural_{\mathrm{c}}] = \boldsymbol{O}. \tag{5.65}$$

Moreover, by integrating Equation (5.64) over $\mathscr{B}$ and $[t_{\mathrm{in}}, t_{\mathrm{fin}}]$, we find

$$\begin{aligned}
&\int_{t_{\mathrm{in}}}^{t_{\mathrm{fin}}} \int_{\mathscr{B}} \langle \kappa \boldsymbol{F}_\gamma^{-\mathrm{T}} \mid \boldsymbol{\eta}_{\boldsymbol{F}_\gamma} \rangle \\
&= -\int_{t_{\mathrm{in}}}^{t_{\mathrm{fin}}} \int_{\mathscr{B}} \lambda \left[\left\langle \frac{\partial \hat{\mathcal{C}}}{\partial \boldsymbol{F}} \circ \natural_{\mathrm{c}} \middle| \boldsymbol{\eta}_{\boldsymbol{F}} \right\rangle + \left\langle \frac{\partial \hat{\mathcal{C}}}{\partial \boldsymbol{F}_\gamma} \circ \natural_{\mathrm{c}} \middle| \boldsymbol{\eta}_{\boldsymbol{F}_\gamma} \right\rangle + \left\langle \frac{\partial \hat{\mathcal{C}}}{\partial \dot{\boldsymbol{F}}_\gamma} \circ \natural_{\mathrm{c}} \middle| \boldsymbol{\eta}_{\dot{\boldsymbol{F}}_\gamma} \right\rangle \right].
\end{aligned} \tag{5.66}$$

Now, we introduce the *varied constraint* $\tilde{\mathcal{C}} = \hat{\mathcal{C}} \circ \tilde{\natural}_{\mathrm{c}}$, where $\tilde{\natural}_{\mathrm{c}}$ is the collection of the homotopies defined in Equations (5.24a)–(5.24e), and we consider also the homotopy $\lambda(X,t) \mapsto \tilde{\lambda}(X,t,\varepsilon) = \lambda(X,t) + \eta_\lambda(X,t)\varepsilon + o(\varepsilon)$, for $\varepsilon \to 0$, such that $\partial_\varepsilon \tilde{\lambda}(X,t,0) = \eta_\lambda(X,t)$ is the increment of $\lambda(X,t)$. Then, by exploiting the fact that the product $-\eta_\lambda[\hat{\mathcal{C}} \circ \natural_{\mathrm{c}}]$ returns the constraint up to the arbitrary factor η_λ, and is, thus, null, we can rephrase Equation (5.66) as

$$\int_{t_{\mathrm{in}}}^{t_{\mathrm{fin}}} \int_{\mathscr{B}} \langle \kappa \boldsymbol{F}_\gamma^{-\mathrm{T}} \mid \boldsymbol{\eta}_{\boldsymbol{F}_\gamma} \rangle = -\int_{t_{\mathrm{in}}}^{t_{\mathrm{fin}}} \int_{\mathscr{B}} \frac{\partial \{\tilde{\lambda}[\hat{\mathcal{C}} \circ \tilde{\natural}_{\mathrm{c}}]\}}{\partial \varepsilon}(X,t,0). \tag{5.67}$$

Granted (5.67), we introduce the *constrained Lagrangian density function* and the associated *constrained action functional*

$$\mathcal{L}_{\mathrm{c}} := \hat{\mathcal{L}}_{\mathrm{c}} \circ (\natural; \boldsymbol{T}, \lambda) = \hat{\mathcal{L}} \circ \natural + \langle \boldsymbol{T} \mid \boldsymbol{F} - D\chi \rangle + \lambda\, [\hat{\mathcal{C}} \circ \natural_{\mathrm{c}}], \tag{5.68a}$$

$$\mathscr{A}_{\mathrm{c}}(\chi, \boldsymbol{F}, \boldsymbol{F}_\gamma; \boldsymbol{T}, \lambda) := \int_{t_{\mathrm{in}}}^{t_{\mathrm{fin}}} \int_{\mathscr{B}} \hat{\mathcal{L}}_{\mathrm{c}} \circ (\natural; \boldsymbol{T}, \lambda), \tag{5.68b}$$

and we write the varied action $\tilde{\mathscr{A}_{\mathrm{c}}}$ and its first derivative with respect to ε, evaluated at $\varepsilon = 0$, as

$$\tilde{\mathscr{A}_{\mathrm{c}}}(\varepsilon) := \int_{t_{\mathrm{in}}}^{t_{\mathrm{fin}}} \int_{\mathscr{B}} \hat{\mathcal{L}}_{\mathrm{c}}(\tilde{\natural}(X,t,\varepsilon); \tilde{\boldsymbol{T}}(X,t,\varepsilon), \tilde{\lambda}(X,t,\varepsilon)), \tag{5.69a}$$

$$\frac{\mathrm{d}\tilde{\mathscr{A}}_{\mathrm{c}}}{\mathrm{d}\varepsilon}(0) = \int_{t_{\mathrm{in}}}^{t_{\mathrm{fin}}} \int_{\mathscr{B}} \frac{\partial[\hat{\mathcal{L}}_{\mathrm{c}} \circ (\tilde{\natural}; \tilde{\boldsymbol{T}}, \tilde{\lambda})]}{\partial \varepsilon}(X, t, 0). \tag{5.69b}$$

Then, a direct calculation shows that the sum of Equations (5.62) and (5.63) is identical to the compact expression

$$\begin{aligned}\frac{\mathrm{d}\tilde{\mathscr{A}}_{\mathrm{c}}}{\mathrm{d}\varepsilon}(0) = &- \int_{t_{\mathrm{in}}}^{t_{\mathrm{fin}}} \int_{\mathscr{B}} \langle \boldsymbol{f}_{\mathrm{np}} | \boldsymbol{\eta}_{\chi} \rangle - \int_{t_{\mathrm{in}}}^{t_{\mathrm{fin}}} \int_{\partial_{\mathrm{N}}^{\chi}\mathscr{B}} \langle \boldsymbol{\tau} | \boldsymbol{\eta}_{\chi} \rangle - \int_{t_{\mathrm{in}}}^{t_{\mathrm{fin}}} \int_{\mathscr{B}} \langle \mathfrak{S}_{\mathrm{np}} \mid \boldsymbol{\eta}_{\boldsymbol{F}_{\gamma}} \rangle \\ &+ \int_{t_{\mathrm{in}}}^{t_{\mathrm{fin}}} \int_{\mathscr{B}} \left\{ \langle \mathfrak{S}_{\boldsymbol{F}_{\gamma}\boldsymbol{F}} \mid \boldsymbol{\eta}_{\boldsymbol{F}} \rangle + \langle \mathrm{DEV}\mathfrak{S}_{\boldsymbol{F}_{\gamma}\boldsymbol{F}_{\gamma}} \mid \boldsymbol{\eta}_{\boldsymbol{F}_{\gamma}} \rangle \right\}. \end{aligned} \tag{5.70}$$

Equation (5.68a) defines the Lagrangian density function of the growing medium which we were looking for. Furthermore, the dynamics of the growing body is obtained variationally by "extending" the Hamilton–Suslov Principle at the price of considering the extra forces $\mathfrak{S}_{\boldsymbol{F}_{\gamma}\boldsymbol{F}}$ and $\mathrm{DEV}\mathfrak{S}_{\boldsymbol{F}_{\gamma}\boldsymbol{F}_{\gamma}}$, due to the nonholonomic nature of the constraint, in addition to the same non-potential forces $\boldsymbol{f}_{\mathrm{np}}$ and $\mathfrak{S}_{\mathrm{np}}$ appearing also in the TNHM. This confirms what has been said at the point P2 of Section 5.4.1. Thus, starting with Equation (5.70), taking the first-order increment of $\dot{\boldsymbol{F}}_{\gamma}$ as $\boldsymbol{\eta}_{\dot{\boldsymbol{F}}_{\gamma}}$ (which differs from $\dot{\boldsymbol{\eta}}_{\boldsymbol{F}_{\gamma}}$ as specified in the transpositional relation (5.30)), and going backward until (5.61a)–(5.61f) are recovered, the dynamic problem is entirely equivalent to the one stated in Equations (5.16a)–(5.16f), deduced from the TNHM. This is, in fact, our reformulation for growth mechanics of the MVM by Llibre et al. [16].

5.4.3 Implications of our formulation of the MVM for growth

The introduction of $\mathcal{L}_{\mathrm{c}}$ and the whole procedure shown in Sections 5.4.1 and 5.4.2 produce some results that we consider noteworthy.

The "true" dynamic equations

Since it holds that $\mathfrak{S}_{\boldsymbol{F}_{\gamma}\boldsymbol{F}} = \mathbb{W}^{\mathrm{T}}_{\boldsymbol{F}_{\gamma}\boldsymbol{F}}[\partial_{\dot{\boldsymbol{F}}_{\gamma}} \hat{\mathcal{L}} \circ \natural]$, Equation (5.61c) returns the well-established result $\boldsymbol{T} = -\mathcal{E}_{\boldsymbol{F}}\hat{\mathcal{L}} = -\partial_{\boldsymbol{F}}\hat{\mathcal{L}} \circ \natural$. Moreover, since Equation (5.61d) prescribes $\boldsymbol{F} = D\chi$, the replacement of $\boldsymbol{F}$ with $D\chi$ in the arguments of $\hat{\mathcal{L}}$ (redefining

$\hat{\mathcal{L}}$ accordingly) permits to write Equations (5.61a) and (5.61b) as [76]

$$\frac{\partial \hat{\mathcal{L}}}{\partial \chi} \circ \natural - \frac{\partial}{\partial t}\left(\frac{\partial \hat{\mathcal{L}}}{\partial \dot{\chi}} \circ \natural\right) - \mathrm{Div}\left(\frac{\partial \hat{\mathcal{L}}}{\partial D\chi} \circ \natural\right) = -\boldsymbol{f}_{\mathrm{np}}, \qquad \text{in } \mathscr{B}, \tag{5.71a}$$

$$\boldsymbol{\tau} = \left(-\frac{\partial \hat{\mathcal{L}}}{\partial D\chi} \circ \natural\right)\boldsymbol{N}, \qquad \text{on } \partial^{\chi}_{\mathrm{N}}\mathscr{B}. \tag{5.71b}$$

Thus, $\mathfrak{S}_{\boldsymbol{F}_\gamma \boldsymbol{F}}$ does not contribute to the "true" dynamics of the system, although it is necessary to formulate the variational procedure presented in Section 5.4.2.

We also notice that, if the Lagrangian density function $\hat{\mathcal{L}}$ is defined in such a way that its partial derivative with respect to $D\chi$ equals the negative of the partial derivative of the strain energy density $\hat{\Psi}$ with respect to the same quantity, then, from Equation (5.12), we obtain that $\boldsymbol{T}$ coincides with the first Piola–Kirchhoff stress tensor of the material, i.e.,

$$\boldsymbol{P} = \frac{\partial \hat{\Psi}}{\partial \boldsymbol{F}} \circ (\boldsymbol{F}, \boldsymbol{F}_\gamma; \mathfrak{X}, \mathfrak{T}) = \boldsymbol{T} = -\frac{\partial \hat{\mathcal{L}}}{\partial D\chi} \circ \natural, \qquad \boldsymbol{F} = D\chi. \tag{5.72}$$

Equations (5.71a) and (5.71b) must be solved together with those for $\boldsymbol{F}_\gamma$ and the new Lagrange multiplier λ. These, when deduced from Equation (5.70), are directly given by

$$\mathcal{E}_{\boldsymbol{F}_\gamma}\hat{\mathcal{L}} + \mathbb{W}^{\mathrm{T}}_{\boldsymbol{F}_\gamma \boldsymbol{F}_\gamma}[\partial_{\dot{\boldsymbol{F}}_\gamma}\hat{\mathcal{L}} \circ \natural] = -\mathfrak{S}_{\mathrm{np}} + \dot{\lambda}\,\boldsymbol{F}_\gamma^{-\mathrm{T}} + \mathrm{DEV}\mathfrak{S}_{\boldsymbol{F}_\gamma \boldsymbol{F}_\gamma}, \tag{5.73a}$$

$$\langle \boldsymbol{F}_\gamma^{-\mathrm{T}} | \dot{\boldsymbol{F}}_\gamma \rangle - R = 0, \tag{5.73b}$$

and replace (5.61e) and (5.61f) with $\kappa \equiv \dot{\lambda}$. Recall that $\mathfrak{S}_{\boldsymbol{F}_\gamma \boldsymbol{F}_\gamma} = \mathbb{W}^{\mathrm{T}}_{\boldsymbol{F}_\gamma \boldsymbol{F}_\gamma}[\partial_{\dot{\boldsymbol{F}}_\gamma}\hat{\mathcal{L}} \circ \natural]$.

Left-multiplying by $\boldsymbol{F}_\gamma^{\mathrm{T}}$, and extracting the hydrostatic and the volumetric parts of Equation (5.73a) yield [23, 32, 87, 91]

$$\mathrm{Dev}[\boldsymbol{F}_\gamma^{\mathrm{T}}(\mathcal{E}_{\boldsymbol{F}_\gamma}\hat{\mathcal{L}})] = -\mathrm{Dev}[\boldsymbol{F}_\gamma^{\mathrm{T}}\mathfrak{S}_{\mathrm{np}}], \tag{5.74a}$$

$$\dot{\lambda} = \tfrac{1}{3}\mathrm{tr}[\boldsymbol{F}_\gamma^{\mathrm{T}}(\mathcal{E}_{\boldsymbol{F}_\gamma}\hat{\mathcal{L}}) + \boldsymbol{F}_\gamma^{\mathrm{T}}\mathfrak{S}_{\mathrm{np}}] + \tfrac{1}{3}\mathrm{tr}[\boldsymbol{F}_\gamma^{\mathrm{T}}\mathfrak{S}_{\boldsymbol{F}_\gamma \boldsymbol{F}_\gamma}], \tag{5.74b}$$

$$\langle \boldsymbol{F}_\gamma^{-\mathrm{T}} | \dot{\boldsymbol{F}}_\gamma \rangle - R = 0. \tag{5.74c}$$

Therefore, the deviatoric term $\mathrm{DEV}\mathfrak{S}_{\boldsymbol{F}_\gamma \boldsymbol{F}_\gamma}$ does not contribute to the "true" dynamics of the problem, while only $\frac{1}{3}\mathrm{tr}[\boldsymbol{F}_\gamma^{\mathrm{T}}\mathfrak{S}_{\boldsymbol{F}_\gamma \boldsymbol{F}_\gamma}]$ plays a role in it. However, this generalized force does not influence directly the determination of $\boldsymbol{F}_\gamma$, and is indeed absorbed in $\dot{\lambda}$,

thereby quantifying the entity of the reactive force $\dot{\lambda}\boldsymbol{F}_\gamma^{-\mathrm{T}}$ predicted by the theory under consideration, and necessary to maintain the constraint. Also, the term $\frac{1}{3}\mathrm{tr}[\boldsymbol{F}_\gamma^{\mathrm{T}}\mathfrak{S}_{\boldsymbol{F}_\gamma\boldsymbol{F}_\gamma}]$ constitutes a fundamental aspect of the procedure, since it defines the Lagrange multiplier of the MVM, which is inherently different from the one characterizing the TNHM. Yet, Equation (5.74b) returns the identification (5.59), and makes the MVM equivalent to the TNHM, provided the equality $\mu = \frac{1}{3}\mathrm{tr}[\boldsymbol{F}_\gamma^{\mathrm{T}}(\mathcal{E}_{\boldsymbol{F}_\gamma}\hat{\mathcal{L}}) + \boldsymbol{F}_\gamma^{\mathrm{T}}\mathfrak{S}_{\mathrm{np}}]$ holds true, as can be deduced by extracting the hydrostatic part of Equation (5.16e) left-multiplied by $\boldsymbol{F}_\gamma^{\mathrm{T}}$. Hence, this yields $\dot{\lambda} = \mu + \frac{1}{3}\mathrm{tr}[\boldsymbol{F}_\gamma^{\mathrm{T}}\mathfrak{S}_{\boldsymbol{F}_\gamma\boldsymbol{F}_\gamma}]$. To our knowledge, this result represents a novelty in the context of growth mechanics, and generalizes a result reported in [16] for the case of discrete nonholonomic systems.

To gain further physical insight into the MVM, we deem it noteworthy to comment on the explicit expression of the term $\frac{1}{3}\mathrm{tr}[\boldsymbol{F}_\gamma^{\mathrm{T}}\mathfrak{S}_{\boldsymbol{F}_\gamma\boldsymbol{F}_\gamma}]$. Indeed, looking at the definition of $\mathfrak{S}_{\boldsymbol{F}_\gamma\boldsymbol{F}_\gamma}$ in Equation (5.56) and at the result reported in Equation (5.55b), we find

$$\tfrac{1}{3}\mathrm{tr}[\boldsymbol{F}_\gamma^{\mathrm{T}}\mathfrak{S}_{\boldsymbol{F}_\gamma\boldsymbol{F}_\gamma}] = \tfrac{1}{3}P_\gamma\mathrm{tr}\big[\boldsymbol{F}_\gamma^{\mathrm{T}}(\partial_{\boldsymbol{F}_\gamma}\hat{R}\circ\natural_\gamma)\big], \tag{5.75}$$

so that only the hydrostatic part of $\boldsymbol{F}_\gamma^{\mathrm{T}}(\partial_{\boldsymbol{F}_\gamma}\hat{R}\circ\natural_\gamma)$ contributes to $\dot{\lambda}$.

The nine tensor components of $\boldsymbol{F}_\gamma$ are determined by Equations (5.74a) and (5.74c), equivalent to eight and to one scalar equations, respectively (see also [23, 32, 87, 91]). In addition, λ is determined by integrating Equation (5.74b) in time. This requires an initial condition for λ, i.e., $\lambda(X, t_{\mathrm{in}}) = \lambda_{\mathrm{in}}(X)$, for all $X \in \mathscr{B}$, and to assign $\lambda_{\mathrm{in}}(X)$ consistently with the constraint at the initial time. Obtaining the Lagrange multiplier of the theory by solving a Cauchy problem constitutes a difference with respect to the TNHM, in which the Lagrange multiplier μ is computed algebraically, and is a characteristic of the MVM [16].

As noticed in [23, 32, 87, 91], Equation (5.74a) allows to evaluate the "remodeling part" of growth, and frees one from guessing particular forms of $\boldsymbol{F}_\gamma$, as is often done in tumor growth, growth in anisotropic media, or under the influence of interactions that define preferred growth directions. All these particular cases are physically sound for the problems that they are to model, but they also require to assume that some symmetries are maintained throughout the dynamics of the system. However, when this restriction cannot be guaranteed, and no *a priori* hypotheses are done on the generalized forces $\mathcal{E}_{\boldsymbol{F}_\gamma}\hat{\mathcal{L}}$ and $\mathfrak{S}_{\mathrm{np}}$, Equations (5.74a) and (5.74b) permit to compute $\boldsymbol{F}_\gamma$.

In conclusion, if the variational procedure defined by our formulation of the MVM is applied to growth mechanics, the dynamic equations to be solved are (5.71a), (5.71b), and (5.74a)–(5.74c), which have to be equipped with initial and Dirichlet boundary conditions for χ and with initial conditions for $\boldsymbol{F}_\gamma$ and λ.

Quasi-static case: the MVM seems to boil down to the TNHM

In almost all the biomechanical problems involving growth, the characteristic time scales of this phenomenon are such that a quasi-static approach is amply justified. Hence, if $\hat{\mathcal{L}}_\mathrm{c}$ depends on $\dot{\chi}$ only through the classical kinetic energy density $\mathcal{K} = \frac{1}{2} J_\gamma \varrho_\nu \|\dot{\chi}\|^2$, which contributes to $\hat{\mathcal{L}}$ in the general setting, one can neglect the inertial force density $-\partial_t[\partial_{\dot{\chi}} \hat{\mathcal{L}} \circ \natural]$ in Equation (5.71a). In fact, in the quasi-static case, $\hat{\mathcal{L}}$ is defined without $\mathcal{K}$, and, if we assume that Equation (5.72) applies, the dynamic equations (5.71a) and (5.71b) become

$$\frac{\partial \hat{\mathcal{L}}}{\partial \chi} \circ \natural + \mathrm{Div}\boldsymbol{P} = -\boldsymbol{f}_\mathrm{np}, \qquad \text{in } \mathscr{B}, \tag{5.76a}$$

$$\boldsymbol{\tau} = \boldsymbol{P}\boldsymbol{N}, \qquad \text{on } \partial_\mathrm{N}^\chi \mathscr{B}. \tag{5.76b}$$

Then, if we indicate with $\boldsymbol{f} := \boldsymbol{f}_\mathrm{p} + \boldsymbol{f}_\mathrm{np}$ the total body force, where $\boldsymbol{f}_\mathrm{p}$ is given here by $\boldsymbol{f}_\mathrm{p} = \partial_\chi \hat{\mathcal{L}} \circ \natural$, Equation (5.76a) returns the classical force balance $\boldsymbol{f} + \mathrm{Div}\boldsymbol{P} = \boldsymbol{0}$ of Continuum Mechanics. Note that $\boldsymbol{f}_\mathrm{np}$ includes non-potential forces due to growth and describes sources or sinks of linear momentum related to the variation of mass of the body under consideration (see, e.g., [73, 127]). In addition, to maintain the quasi-static hypothesis, $\boldsymbol{f}_\mathrm{np}$ and $\boldsymbol{\tau}$ must be taken accordingly. More details on $\boldsymbol{f}_\mathrm{np}$ are provided in the following remark.

Remark 5.4 (Some remarks on the non-potential force $\boldsymbol{f}_\mathrm{np}$). By exploiting Equation (5.72), and making the identifications $J_\gamma \varrho_\nu \boldsymbol{g}\dot{\chi} \equiv \partial_{\dot{\chi}} \hat{\mathcal{L}} \circ \natural$ and $\boldsymbol{f}_\mathrm{p} \equiv \partial_\chi \hat{\mathcal{L}} \circ \natural$, where $\boldsymbol{g}$ is the metric tensor associated with the current placement of the body, and $\boldsymbol{f}_\mathrm{p}$ designates a force density stemming from a potential density function, the balance of linear momentum (5.71a) can be recast in the more explicit form

$$\boldsymbol{f}_\mathrm{p} - \partial_t(J_\gamma \varrho_\nu \boldsymbol{g}\dot{\chi}) + \mathrm{Div}\boldsymbol{T} = -\boldsymbol{f}_\mathrm{np}, \qquad \text{in } \mathscr{B}. \tag{5.77}$$

Following, e.g., [73, 127], we prescribe $\boldsymbol{f}_{\mathrm{np}}$ to be expressed as

$$\boldsymbol{f}_{\mathrm{np}} = \varrho_{\mathrm{R}}^{(\mathrm{g})} R^{(\mathrm{g})} \boldsymbol{g}\boldsymbol{v}^{(\mathrm{g})} + \boldsymbol{f}_{\mathrm{np}}^{(\mathrm{oc})}, \tag{5.78}$$

where $\varrho_{\mathrm{R}}^{(\mathrm{g})}$ is the mass density, pulled back to the body's reference placement, of the material inserted into the body, or subtracted from it, because of growth; $R^{(\mathrm{g})}$ is the rate at which such insertion or remotion take place; $\boldsymbol{v}^{(\mathrm{g})}$ is the velocity of the incoming or outgoing material; $\boldsymbol{f}_{\mathrm{np}}^{(\mathrm{oc})}$ is a non-potential force density introduced to account, at the body scale, for any *other contributions* to growth, such as those of biophysical or biochemical nature, arising from the lower scales [73, 127] (for a more general framework, see [147]). As remarked in [127], $\varrho_{\mathrm{R}}^{(\mathrm{g})}$ and $\boldsymbol{v}^{(\mathrm{g})}$ are equal to ϱ_{R} and $\dot{\chi}$, respectively, when the material is subtracted from the body, while they can be different from the preexisting mass density and velocity when *"new material"* [73] is added. It is interesting to notice, however, that the mass balance law allows to write $\varrho_{\mathrm{R}}^{(\mathrm{g})} R^{(\mathrm{g})} = \varrho_{\mathrm{R}} R$, with $\varrho_{\mathrm{R}}^{(\mathrm{g})}$ and ϱ_{R} being strictly positive, and R being the rate introduced in Equation (5.2). This result can be used to work out the right-hand side of Equation (5.78) to obtain (see, e.g., [127])

$$\boldsymbol{f}_{\mathrm{np}} = \varrho_{\mathrm{R}} R \boldsymbol{g}\boldsymbol{v}^{(\mathrm{g})} + \boldsymbol{f}_{\mathrm{np}}^{(\mathrm{oc})} = \varrho_{\mathrm{R}} R \boldsymbol{g}\dot{\chi} + \varrho_{\mathrm{R}} R \boldsymbol{g}[\boldsymbol{v}^{(\mathrm{g})} - \dot{\chi}] + \boldsymbol{f}_{\mathrm{np}}^{(\mathrm{oc})}. \tag{5.79}$$

Then, by employing this explicit expression of $\boldsymbol{f}_{\mathrm{np}}$, expanding the time derivative on the left-hand side of Equation (5.77), and recalling the relationships $\varrho_{\mathrm{R}} = J_\gamma \varrho_\nu$ and $\dot{J}_\gamma = J_\gamma \mathrm{tr}(\boldsymbol{F}_\gamma^{-1}\dot{\boldsymbol{F}}_\gamma) = J_\gamma R$ (the last equality follows from the constraint (5.2)), the linear momentum balance law becomes

$$\boldsymbol{f}_{\mathrm{p}} - J_\gamma \varrho_\nu \boldsymbol{g}\ddot{\chi} + \mathrm{Div}\boldsymbol{T} = -J_\gamma \varrho_\nu \mathrm{tr}(\boldsymbol{F}_\gamma^{-1}\dot{\boldsymbol{F}}_\gamma)\boldsymbol{g}[\boldsymbol{v}^{(\mathrm{g})} - \dot{\chi}] - \boldsymbol{f}_{\mathrm{np}}^{(\mathrm{oc})}. \tag{5.80}$$

The right-hand side of Equation (5.80) defines, up to the sign, an *effective* non-potential force density.

Further simplifications are obtained for problems that allow to neglect all body forces, so that Equation (5.76a) reduces to $\mathrm{Div}\boldsymbol{P} = \boldsymbol{0}$.

Similarly to the conclusions drawn for $\mathcal{K}$, even though it is possible to define a generalized kinetic energy density $\mathcal{K}_\gamma := \frac{1}{2}\langle \mathbb{G}[\dot{\boldsymbol{F}}_\gamma] | \dot{\boldsymbol{F}}_\gamma \rangle$ associated with $\dot{\boldsymbol{F}}_\gamma$, where $\mathbb{G}$ is some suitable fourth-order inertial tensor field, the quantity $\mathcal{K}_\gamma$ does not contribute to $\hat{\mathcal{L}}$ in the quasi-static regime. Accordingly, if we further hypothesize that $\hat{\mathcal{L}}$ depends

on $\dot{\boldsymbol{F}}_\gamma$ only through $\mathcal{K}_\gamma$, then the generalized momentum $\boldsymbol{p}_\gamma = \partial_{\dot{\boldsymbol{F}}_\gamma}\hat{\mathcal{L}} \circ \natural$, which now reads $\boldsymbol{p}_\gamma = \mathbb{G}[\dot{\boldsymbol{F}}_\gamma]$, does not appear at all. Indeed, it disappears from $\mathcal{E}_{\boldsymbol{F}_\gamma}\hat{\mathcal{L}}$, which reduces to $\partial_{\boldsymbol{F}_\gamma}\hat{\mathcal{L}} \circ \natural$, and so do also the extra forces $\mathfrak{S}_{\boldsymbol{F}_\gamma \boldsymbol{F}}$ and $\mathfrak{S}_{\boldsymbol{F}_\gamma \boldsymbol{F}_\gamma}$, defined in Equation (5.56). Consequently, the dynamic equations deduced by means of our formulation of the MVM, i.e., Equations (5.74a)–(5.74c), become identical to those obtained with the TNHM in the quasi-static case, the only difference being that μ is replaced by $\dot{\lambda}$.

These results notwithstanding, there remains a methodological difference between the two methods, which is reflected in the way in which the Lagrange multipliers μ and λ are computed. Indeed, as remarked above, the multiplier μ is determined algebraically in the TNHM, while, in the MVM, one has to find λ by solving an ordinary differential equation in time also in the quasi-static case. One may say, in this case, that μ is the rate of λ.

On the basis of the considerations above, in the quasi-static approximation of growth, our formulation of the MVM seems to boil down to the TNHM. However, this is not the case because of an important conceptual and technical difference between the two approaches. Such difference becomes evident by comparing the Extended Hamilton Principle, presented in Equation (5.15), with Equation (5.70), which is the "heart" of our formulation of the MVM and, in the quasi-static regime, becomes

$$\frac{\mathrm{d}\tilde{\mathscr{A}}_{\mathrm{c}}}{\mathrm{d}\varepsilon}(0) = -\int_{t_{\mathrm{in}}}^{t_{\mathrm{fin}}}\int_{\mathscr{B}} \left\{\langle \boldsymbol{f}_{\mathrm{np}} | \boldsymbol{\eta}_\chi \rangle + \langle \mathfrak{S}_{\mathrm{np}} | \boldsymbol{\eta}_{\boldsymbol{F}_\gamma} \rangle\right\} - \int_{t_{\mathrm{in}}}^{t_{\mathrm{fin}}}\int_{\partial_{\mathrm{N}}^{\chi}\mathscr{B}} \langle \boldsymbol{\tau} | \boldsymbol{\eta}_\chi \rangle. \tag{5.81}$$

Indeed, whereas in the TNHM the nonholonomic constraint is handled by regarding the reactive force $\mu \boldsymbol{F}_\gamma^{-\mathrm{T}}$ as *"polygenic"* [11], thereby giving rise to $\langle \mu \boldsymbol{F}_\gamma^{-\mathrm{T}} | \boldsymbol{\eta}_{\boldsymbol{F}_\gamma} \rangle$ in Equation (5.15), no such term is present in Equation (5.81), since the constraint is handled variationally although it is nonholonomic.

Explicit form of the dynamic equations in the quasi-static case

Within the quasi-static regime, let us hypothesize that $\hat{\mathcal{L}}$ has expression

$$\hat{\mathcal{L}} \circ \natural = -\hat{\Psi} \circ (\boldsymbol{F}, \boldsymbol{F}_\gamma; \mathcal{X}, \mathcal{T}) - \hat{\Psi}_{\mathrm{g}} \circ (\boldsymbol{F}_\gamma; \mathcal{X}, \mathcal{T}) + \hat{\mathcal{U}} \circ (\chi, \boldsymbol{F}_\gamma; \mathcal{X}, \mathcal{T}), \tag{5.82}$$

where $-\hat{\Psi}$ defines the body Lagrangian density function $\mathcal{L}_{\mathrm{b}}$; $\hat{\Psi}_{\mathrm{g}}$ is an energy density depending solely on the growth tensor, material points, and time; while $\hat{\mathcal{U}}$ is the potential density that generates the body forces $\boldsymbol{f}_{\mathrm{p}}$.

The energy density $\hat{\Psi}_{\mathrm{g}}$ is introduced to highlight that a given configuration of the system, defined by the triad $(\chi, \boldsymbol{F} \equiv D\chi, \boldsymbol{F}_\gamma)$, may vary its energetic content in response to variations of $\boldsymbol{F}_\gamma$, for fixed χ and $\boldsymbol{F}$ (see, e.g., [77, 23], and a discussion on *"Cauchy's gauge"* [112]). We also notice that, in general, $\hat{\mathcal{U}}$ must depend on $\boldsymbol{F}_\gamma$. Indeed, if $\hat{\mathcal{U}}$ models, e.g., gravity, i.e.,

$$\hat{\mathcal{U}} \circ (\chi, \boldsymbol{F}_\gamma; \mathcal{X}, \mathcal{T}) = \langle (\det \boldsymbol{F}_\gamma) \varrho_\nu \boldsymbol{a}_{\mathrm{gr}} | \chi - \chi_0 \rangle =: \mathcal{U}, \tag{5.83}$$

where $\boldsymbol{a}_{\mathrm{gr}}$ is the gravity acceleration (co-)vector, and χ_0 defines a referential position, i.e., $\chi_0(X,t) = x_0$, for all $(X,t) \in \mathscr{B} \times \mathscr{I}$, then the dependence of $\hat{\mathcal{U}}$ on $\boldsymbol{F}_\gamma$ accounts for the redistribution of the mass density $\varrho_{\mathrm{R}} = (\det \boldsymbol{F}_\gamma)\varrho_\nu$ in the body's reference placement due to growth. Hence, we obtain

$$\partial_\chi \hat{\mathcal{U}} \circ (\chi, \boldsymbol{F}_\gamma; \mathcal{X}, \mathcal{T}) = \partial_\chi \hat{\mathcal{L}} \circ \natural = (\det \boldsymbol{F}_\gamma) \varrho_\nu \boldsymbol{a}_{\mathrm{gr}} =: \boldsymbol{f}_{\mathrm{p}}, \tag{5.84a}$$

$$\partial_{\boldsymbol{F}_\gamma} \hat{\mathcal{U}} \circ (\chi, \boldsymbol{F}_\gamma; \mathcal{X}, \mathcal{T}) = [\hat{\mathcal{U}} \circ (\chi, \boldsymbol{F}_\gamma; \mathcal{X}, \mathcal{T})] \boldsymbol{F}_\gamma^{-\mathrm{T}}, \tag{5.84b}$$

and Equations (5.76a) and (5.76b) take on the form

$$(\det \boldsymbol{F}_\gamma) \varrho_\nu \boldsymbol{a}_{\mathrm{gr}} + \mathrm{Div} \boldsymbol{P} = -\boldsymbol{f}_{\mathrm{np}}, \qquad \text{in } \mathscr{B}, \tag{5.85a}$$

$$\boldsymbol{\tau} = \boldsymbol{P}\boldsymbol{N}, \qquad \text{on } \partial^{\chi}_{\mathrm{N}}\mathscr{B}, \tag{5.85b}$$

with $\boldsymbol{P}$ given in Equation (5.12) or (5.72). The coupling with $\boldsymbol{F}_\gamma$ emerges both through the constitutive representation of $\boldsymbol{P}$ and through the body forces.

Switching to the dynamic sub-problem for the growth tensor, we notice that Equation (5.82) and the discussion reported in Section 5.2.3 lead to

$$\boldsymbol{H} \equiv \boldsymbol{F}_\gamma^{\mathrm{T}} \big(\partial_{\boldsymbol{F}_\gamma} \hat{\Psi} \circ (\boldsymbol{F}, \boldsymbol{F}_\gamma; \mathcal{X}, \mathcal{T}) \big) = \Psi \boldsymbol{I}^{\mathrm{T}} - \boldsymbol{F}^{\mathrm{T}} \boldsymbol{P}, \tag{5.86a}$$

$$\boldsymbol{Z}_{\mathrm{p}} \equiv -\boldsymbol{F}_\gamma^{\mathrm{T}} \big(\partial_{\boldsymbol{F}_\gamma} \hat{\Psi}_{\mathrm{g}} \circ (\boldsymbol{F}_\gamma; \mathcal{X}, \mathcal{T}) \big) + \boldsymbol{F}_\gamma^{\mathrm{T}} \big(\partial_{\boldsymbol{F}_\gamma} \hat{\mathcal{U}} \circ (\chi, \boldsymbol{F}_\gamma; \mathcal{X}, \mathcal{T}) \big), \tag{5.86b}$$

$$\boldsymbol{F}_\gamma^{\mathrm{T}} \mathfrak{S}_{\mathrm{np}} \equiv \boldsymbol{Z}_{\mathrm{np}} - \mathbb{T}[\boldsymbol{F}_\gamma^{-1} \dot{\boldsymbol{F}}_\gamma] \equiv \boldsymbol{Z}_{\mathrm{np}} - \boldsymbol{Y}_{\mathrm{ud}}, \tag{5.86c}$$

where $\boldsymbol{H}$ is the Eshelby stress tensor, $\boldsymbol{Z}_{\mathrm{p}}$ and $\boldsymbol{Z}_{\mathrm{np}}$ are the potential and non-potential contributions to $\boldsymbol{Z} = \boldsymbol{Z}_{\mathrm{p}} + \boldsymbol{Z}_{\mathrm{np}}$ introduced in Equation (5.10c), while $\mathbb{T}$ and $\boldsymbol{Y}_{\mathrm{ud}}$ are

defined in Section 5.2.3 (we recall that the inertial terms that, in general, would feature in $\boldsymbol{Z}$ are neglected here). Thus, Equations (5.74a)–(5.74c) become

$$\mathrm{Dev}\boldsymbol{Z} - \mathrm{Dev}\boldsymbol{H} = \mathrm{Dev}\big\{\mathbb{T}[\boldsymbol{F}_\gamma^{-1}\dot{\boldsymbol{F}}_\gamma]\big\}, \tag{5.87a}$$

$$\dot{\lambda} = -\tfrac{1}{3}\mathrm{tr}\boldsymbol{H} + \tfrac{1}{3}\mathrm{tr}\boldsymbol{Z} - \tfrac{1}{3}\mathrm{tr}\big\{\mathbb{T}[\boldsymbol{F}_\gamma^{-1}\dot{\boldsymbol{F}}_\gamma]\big\}, \tag{5.87b}$$

$$\langle \boldsymbol{F}_\gamma^{-\mathrm{T}} | \dot{\boldsymbol{F}}_\gamma \rangle - R = 0. \tag{5.87c}$$

The generalized force $\boldsymbol{Z}_{\mathrm{np}}$ can be prescribed as in Equation (5.19). Moreover, if $\mathcal{U}$ is given as in Equation (5.83), then the second term on the right-hand side of Equation (5.86b) reduces to $\mathcal{U}\boldsymbol{I}^{\mathrm{T}}$, and does not contribute to $\mathrm{Dev}\boldsymbol{Z}$, but to $\dot{\lambda}$.

Looking at Equation (5.87b), we notice that, since $\frac{1}{3}\mathrm{tr}\boldsymbol{Z}$ is conjugated to $\mathrm{tr}(\boldsymbol{F}_\gamma^{-1}\dot{\boldsymbol{F}}_\gamma)$, it does not contribute to trigger the variation of mass. Yet, it does contribute to determine the Lagrange multiplier associated with the constraint. On the other hand, $\mathrm{Dev}\boldsymbol{Z}$ guides, together with $\mathrm{Dev}\boldsymbol{H}$, the evolution of the volume-preserving part of $\boldsymbol{F}_\gamma^{-1}\dot{\boldsymbol{F}}_\gamma$, as indicated by Equation (5.87a).

5.5 Differences with the MVM of Llibre et al.

There are two differences between the MVM by Llibre et al. [16] and our reformulation of this method. To analyze them, we abandon the quasi-static case, and return to the full system of dynamic equations (5.61a)–(5.61f).

The first, and minor, difference is that, in its original conception [16], the MVM does not consider any non-potential force. This amounts to switching off $\boldsymbol{f}_{\mathrm{np}}$ and $\mathfrak{S}_{\mathrm{np}}$ in Equations (5.70) and (5.61a)–(5.61f). We maintain only $\boldsymbol{\tau}$ for including the case of non-vanishing tractions imposed on the body's boundary. Although eliminating $\boldsymbol{f}_{\mathrm{np}}$ and $\mathfrak{S}_{\mathrm{np}}$ could be unphysical for describing growth, especially for what concerns $\mathfrak{S}_{\mathrm{np}}$, we consider this situation to highlight how our version of the MVM differs from the one by Llibre et al. [16][5].

The second, and major, difference is that, to the best of our understanding, Llibre et al. [16] do not consider the extra forces $\mathfrak{S}_{\boldsymbol{F}_\gamma\boldsymbol{F}}$ and $\mathrm{DEV}\mathfrak{S}_{\boldsymbol{F}_\gamma\boldsymbol{F}_\gamma}$ on the right-hand side of Equation (5.70), although the variation of their action functional is performed

[5] In the quasi-static case, and in the absence of $\mathfrak{S}_{\mathrm{np}}$ (specifically, under the assumption that $\boldsymbol{Z}_{\mathrm{np}}$ and $\boldsymbol{Y}_{\mathrm{ud}}$ are both identically null), Equations (5.87a)–(5.87c) become $\mathrm{Dev}\boldsymbol{Z}_{\mathrm{p}} - \mathrm{Dev}\boldsymbol{H} = \boldsymbol{O}$; $\dot{\lambda} = -\frac{1}{3}\mathrm{tr}\boldsymbol{H} + \frac{1}{3}\mathrm{tr}\boldsymbol{Z}_{\mathrm{p}}$; and $\langle \boldsymbol{F}_\gamma^{-\mathrm{T}} | \dot{\boldsymbol{F}}_\gamma \rangle - R = 0$.

by employing the Hamilton–Suslov variational principle. Hence, with the procedure outlined in [16], our dynamic equations would become

$$\mathcal{E}_{\chi}\hat{\mathcal{L}} + \mathrm{Div}\boldsymbol{T} = \boldsymbol{0}, \qquad \text{in } \mathscr{B}, \tag{5.88a}$$

$$\boldsymbol{\tau} - \boldsymbol{T}\boldsymbol{N} = \boldsymbol{0}, \qquad \text{on } \partial_{\mathrm{N}}^{\chi}\mathscr{B}, \tag{5.88b}$$

$$\mathcal{E}_{\boldsymbol{F}}\hat{\mathcal{L}} + \mathbb{W}^{\mathrm{T}}_{\boldsymbol{F}_{\gamma}\boldsymbol{F}}[\partial_{\dot{\boldsymbol{F}}_{\gamma}}\hat{\mathcal{L}} \circ \natural] + \boldsymbol{T} = \boldsymbol{O}, \qquad \text{in } \mathscr{B}, \tag{5.88c}$$

$$\boldsymbol{F} - D\chi = \boldsymbol{O}, \qquad \text{in } \mathscr{B}, \tag{5.88d}$$

$$\mathcal{E}_{\boldsymbol{F}_{\gamma}}\hat{\mathcal{L}} + \mathbb{W}^{\mathrm{T}}_{\boldsymbol{F}_{\gamma}\boldsymbol{F}_{\gamma}}[\partial_{\dot{\boldsymbol{F}}_{\gamma}}\hat{\mathcal{L}} \circ \natural] = \dot{\lambda}\,\boldsymbol{F}_{\gamma}^{-\mathrm{T}}, \qquad \text{in } \mathscr{B}, \tag{5.88e}$$

$$\langle \boldsymbol{F}_{\gamma}^{-\mathrm{T}} | \dot{\boldsymbol{F}}_{\gamma} \rangle - R = 0, \qquad \text{in } \mathscr{B}. \tag{5.88f}$$

This formulation of dynamics produces important consequences, which require conditions for the MVM formulated in [16] to be equivalent to the TNHM and, thus, to our version of the MVM, as presented in Section 5.4. As we shall see in the two following sections, these conditions place restrictions on admissible functional forms of the mass source $\hat{R}$. In this respect, we remark that *no conditions of this type are required in our formulation of the MVM (see Section 5.4), since it is constructed to be always equivalent to the TNHM*.

5.5.1 First restriction on the mass source due to (5.88a)–(5.88f).

By recalling the identifications $\mathcal{E}_{\boldsymbol{F}}\hat{\mathcal{L}} = \partial_{\boldsymbol{F}}\hat{\mathcal{L}} \circ \natural$ and $\partial_{\dot{\boldsymbol{F}}_{\gamma}}\hat{\mathcal{L}} \circ \natural = \boldsymbol{p}_{\gamma}$, and using the results (5.38) and (5.55a), Equation (5.88c) implies that $\boldsymbol{T}$ now reads

$$\boldsymbol{T} = -\partial_{\boldsymbol{F}}\hat{\mathcal{L}} \circ \natural - \mathbb{W}^{\mathrm{T}}_{\boldsymbol{F}_{\gamma}\boldsymbol{F}}[\boldsymbol{p}_{\gamma}] = \boldsymbol{P} - P_{\gamma}(\partial_{\boldsymbol{F}}\hat{R} \circ \natural_{\gamma}), \tag{5.89}$$

where, in the last equality, we have assumed $-\partial_{\boldsymbol{F}}\hat{\mathcal{L}} \circ \natural = \partial_{\boldsymbol{F}}\hat{\Psi} \circ \natural_{\gamma} = \boldsymbol{P}$, thereby returning the body's first Piola–Kirchhoff stress tensor. Then, by plugging Equation (5.89) into (5.88a), one can write the result as

$$\mathcal{E}_{\chi}\hat{\mathcal{L}} + \mathrm{Div}\boldsymbol{T} \equiv \boldsymbol{f}_{\mathrm{p}} - \mathrm{Div}[P_{\gamma}(\partial_{\boldsymbol{F}}\hat{R} \circ \natural_{\gamma})] - \partial_{t}(\partial_{\dot{\chi}}\hat{\mathcal{L}} \circ \natural) + \mathrm{Div}\boldsymbol{P} = \boldsymbol{0}. \tag{5.90}$$

Since, in Equation (5.88c), nothing compensates for $\mathbb{W}^{\mathrm{T}}_{\boldsymbol{F}_{\gamma}\boldsymbol{F}}[\partial_{\dot{\boldsymbol{F}}_{\gamma}}\hat{\mathcal{L}} \circ \natural]$, it goes into Equation (5.88a), i.e., into the balance of linear momentum, where it generates the extra force $-\mathrm{Div}[P_{\gamma}(\partial_{\boldsymbol{F}}\hat{R} \circ \natural_{\gamma})]$. Consequently, for the considered growth problem, the original procedure by Llibre et al. [16] is equivalent to the well-consolidated

TNHM *only* if $\hat{R}$ is independent of $\boldsymbol{F}$, i.e., if $\partial_{\boldsymbol{F}}\hat{R} \circ \natural_\gamma = \boldsymbol{O}$, or in the quasi-static approximation, because $P_\gamma(\partial_{\boldsymbol{F}}\hat{R} \circ \natural_\gamma)$ is neglected, provided $\hat{\mathcal{L}}$ depends on $\dot{\boldsymbol{F}}_\gamma$ only through the generalized kinetic energy density $\mathcal{K}_\gamma$.

To us, the comments reported above place the question as to whether the procedure stemming from Theorem 1 of Llibre et al. [16] can be applied, *as is*, to the growth problem, at least for arbitrary $\hat{R}$. The "warning sign" for this applicability issue is the discrepancy of the momentum balance law (5.90) with Equation (5.16a), which originates from the TNHM and in which $\boldsymbol{T} = \boldsymbol{P}$.

5.5.2 Second restriction on the mass source due to (5.88a)–(5.88f).

Let us consider the case in which the generalized kinetic energy density induced by $\dot{\boldsymbol{F}}_\gamma$ is $\mathcal{K}_\gamma = \frac{1}{2}\langle \mathbb{G}[\dot{\boldsymbol{F}}_\gamma] \mid \dot{\boldsymbol{F}}_\gamma \rangle = \frac{1}{2} J_\gamma \mathfrak{m}_\nu \|\boldsymbol{\Lambda}_\gamma\|^2$, where $\mathfrak{m}_\nu > 0$ is a mass-like material parameter, and $\|\boldsymbol{\Lambda}_\gamma\|^2 := \mathrm{tr}(\boldsymbol{\Lambda}_\gamma^{\mathrm{T}} \boldsymbol{G} \boldsymbol{\Lambda}_\gamma \boldsymbol{G}^{-1})$ is the squared norm of the material rate of $\boldsymbol{F}_\gamma$, i.e., $\boldsymbol{\Lambda}_\gamma := \boldsymbol{F}_\gamma^{-1}\dot{\boldsymbol{F}}_\gamma$, while $\boldsymbol{G}$ is the metric tensor associated with the body's reference placement. In this formulation, $\mathbb{G}$ is given by $\mathbb{G} = J_\gamma \mathfrak{m}_\nu \, \boldsymbol{b}_\gamma^{-1} \underline{\otimes} \boldsymbol{G}^{-1}$, i.e., in components, $\mathbb{G}_\alpha{}^A{}_\beta{}^B = J_\gamma \mathfrak{m}_\nu \, [\boldsymbol{b}_\gamma^{-1}]_{\alpha\beta} G^{AB}$, with $\boldsymbol{b}_\gamma := \boldsymbol{F}_\gamma \boldsymbol{G}^{-1} \boldsymbol{F}_\gamma^{\mathrm{T}}$ being the left Cauchy-Green tensor generated by $\boldsymbol{F}_\gamma$.

If we further hypothesize that $\hat{\mathcal{L}}$ depends on $\dot{\boldsymbol{F}}_\gamma$ only through $\mathcal{K}_\gamma$, then, after differentiating Equation (5.88f) with respect to time, we can write

$$\mathbb{G}[\ddot{\boldsymbol{F}}_\gamma] + \boldsymbol{F}_\gamma^{-\mathrm{T}} \dot{\lambda} = \partial_{\boldsymbol{F}_\gamma}\hat{\mathcal{L}} \circ \natural - \dot{\mathbb{G}}[\dot{\boldsymbol{F}}_\gamma] + \mathfrak{S}_{\boldsymbol{F}_\gamma \boldsymbol{F}_\gamma}, \tag{5.91a}$$

$$\langle \boldsymbol{F}_\gamma^{-\mathrm{T}} | \ddot{\boldsymbol{F}}_\gamma \rangle = \mathrm{tr}\boldsymbol{\Lambda}_\gamma^2 + \dot{R}. \tag{5.91b}$$

To formally analyze Equations (5.91a) and (5.91b), it is convenient to recast them in the form of a block-wise system of second order ordinary differential equations. To this end, we multiply Equation (5.91a) by $\boldsymbol{b}_\gamma$ from the left, and by $\boldsymbol{G}$ from the right, thereby obtaining

$$J_\gamma \mathfrak{m}_\nu \ddot{\boldsymbol{F}}_\gamma + \boldsymbol{F}_\gamma \dot{\lambda} = \boldsymbol{b}_\gamma (\partial_{\boldsymbol{F}_\gamma}\hat{\mathcal{L}} \circ \natural)\boldsymbol{G} - \boldsymbol{b}_\gamma (\dot{\mathbb{G}}[\dot{\boldsymbol{F}}_\gamma])\boldsymbol{G} + \boldsymbol{b}_\gamma \mathfrak{S}_{\boldsymbol{F}_\gamma \boldsymbol{F}_\gamma} \boldsymbol{G}, \tag{5.92a}$$

$$\langle \boldsymbol{F}_\gamma^{-\mathrm{T}} | \ddot{\boldsymbol{F}}_\gamma \rangle = \mathrm{tr}\boldsymbol{\Lambda}_\gamma^2 + \dot{R}. \tag{5.92b}$$

Then, we rewrite the resulting expressions as [27, 1]

$$\begin{bmatrix} \mathsf{M} & \mathsf{N} \\ \mathsf{Q}^{\mathrm{t}} & \mathsf{O} \end{bmatrix} \begin{Bmatrix} \ddot{\mathsf{f}} \\ \dot{\lambda} \end{Bmatrix} = \begin{Bmatrix} \mathsf{b} + \sigma \\ \mathsf{c} \end{Bmatrix}, \tag{5.93}$$

where, by prescribing a convention for converting fourth-order tensors in 9×9 square matrices and second-order tensors either in 9×1 matrices or column vectors (or, depending on the situation, in 1×9 matrices or row vectors), we obtain that $\mathsf{M} = J_\gamma \mathfrak{m}_\nu \mathsf{I}$ is proportional to the 9×9 identity matrix I; N is the 9×1 matrix associated with $\boldsymbol{F}_\gamma$; Q^{t} is the 1×9 matrix representing $\boldsymbol{F}_\gamma^{-\mathrm{T}}$; $\ddot{\mathsf{f}}$ is the 9×1 column vector representing $\ddot{\boldsymbol{F}}_\gamma$; O is the 1×1 null matrix; b is the 9×1 column vector that represents the first two addends on the right-hand side of Equation (5.92a); σ is the 9×1 column vector associated with $\boldsymbol{b}_\gamma \mathfrak{S}_{\boldsymbol{F}_\gamma \boldsymbol{F}_\gamma} \boldsymbol{G}$; finally, c is the 1×1 column vector associated with $\mathrm{tr}\boldsymbol{\Lambda}_\gamma^2 + \dot{R}$. Note that, although $\dot{\lambda}$ is a scalar, in the system (5.93) we represent it with the 1×1 column vector $\dot{\lambda}$, and we use the same convention for $\mathrm{tr}\boldsymbol{\Lambda}_\gamma^2 + \dot{R}$ by renaming it c.

We remark that, although the system (5.93) is found by following a procedure similar to those outlined in [27, 1], its form is different in that the matrix Q^{t} *is not* the transpose of N.

By means of the Schur complement technique [27, 1], the system (5.93) becomes

$$\begin{cases} \ddot{\mathsf{f}} = \mathsf{M}^{-1}[\mathsf{I} - \mathsf{N}\mathsf{S}^{-1}\mathsf{Q}^{\mathrm{t}}\mathsf{M}^{-1}]\sigma + \mathsf{M}^{-1}[\mathsf{I} - \mathsf{N}\mathsf{S}^{-1}\mathsf{Q}^{\mathrm{t}}\mathsf{M}^{-1}]\mathsf{b} + \mathsf{M}^{-1}\mathsf{N}\mathsf{S}^{-1}\mathsf{c}, \\ \dot{\lambda} = \mathsf{S}^{-1}\mathsf{Q}^{\mathrm{t}}\mathsf{M}^{-1}\sigma + \mathsf{S}^{-1}\mathsf{Q}^{\mathrm{t}}\mathsf{M}^{-1}\mathsf{b} - \mathsf{S}^{-1}\mathsf{c}, \end{cases} \tag{5.94}$$

where $\mathsf{S} := \mathsf{Q}^{\mathrm{t}}\mathsf{M}^{-1}\mathsf{N}$ is the Schur matrix. For the problem at hand, S is a 1×1 matrix, and represents the scalar

$$\mathsf{S} = \mathsf{Q}^{\mathrm{t}}\mathsf{M}^{-1}\mathsf{N} = \mathsf{Q}^{\mathrm{t}}\frac{1}{J_\gamma \mathfrak{m}_\nu}\mathsf{I}\mathsf{N} = \frac{1}{J_\gamma \mathfrak{m}_\nu}\mathsf{Q}^{\mathrm{t}}\mathsf{N} = \frac{1}{J_\gamma \mathfrak{m}_\nu}\langle \boldsymbol{F}_\gamma^{-\mathrm{T}} | \boldsymbol{F}_\gamma \rangle = \frac{3}{J_\gamma \mathfrak{m}_\nu}. \tag{5.95}$$

Consequently, Equation (5.94) simplifies to

$$\begin{cases} \ddot{\mathsf{f}} = \frac{1}{J_\gamma \mathfrak{m}_\nu}\left[\mathsf{I} - \frac{1}{3}\mathsf{N}\mathsf{Q}^{\mathrm{t}}\right]\sigma + \frac{1}{J_\gamma \mathfrak{m}_\nu}\left[\mathsf{I} - \frac{1}{3}\mathsf{N}\mathsf{Q}^{\mathrm{t}}\right]\mathsf{b} + \frac{1}{3}\mathsf{N}\mathsf{c}, \\ \dot{\lambda} = \frac{1}{3}\mathsf{Q}^{\mathrm{t}}\sigma + \frac{1}{3}\mathsf{Q}^{\mathrm{t}}\mathsf{b} - \frac{J_\gamma \mathfrak{m}_\nu}{3}\mathsf{c}. \end{cases} \tag{5.96}$$

Before proceeding, the following remark is in order.

Remark 5.5 (Consistency with the direct calculation of $\dot{\lambda}$).
The products $\mathsf{Q}^{\mathrm{t}}\sigma$ and $\mathsf{Q}^{\mathrm{t}}\mathsf{b}$ are scalars, and admit the identifications

$$\mathsf{Q}^{\mathrm{t}}\sigma = \left\langle \boldsymbol{F}_\gamma^{-\mathrm{T}} | \boldsymbol{b}_\gamma \mathfrak{S}_{\boldsymbol{F}_\gamma \boldsymbol{F}_\gamma} \boldsymbol{G} \right\rangle = \mathrm{tr}(\boldsymbol{F}_\gamma^{\mathrm{T}} \mathfrak{S}_{\boldsymbol{F}_\gamma \boldsymbol{F}_\gamma}), \tag{5.97a}$$

$$\begin{aligned} \mathsf{Q}^{\mathrm{t}}\mathsf{b} &= \left\langle \boldsymbol{F}_\gamma^{-\mathrm{T}} | \boldsymbol{b}_\gamma (\partial_{\boldsymbol{F}_\gamma} \hat{\mathcal{L}} \circ \natural) \boldsymbol{G} \right\rangle - \left\langle \boldsymbol{F}_\gamma^{-\mathrm{T}} | \boldsymbol{b}_\gamma (\dot{\mathbb{G}}[\dot{\boldsymbol{F}}_\gamma]) \boldsymbol{G} \right\rangle \\ &= \mathrm{tr}\left[\boldsymbol{F}_\gamma^{\mathrm{T}} (\partial_{\boldsymbol{F}_\gamma} \hat{\mathcal{L}} \circ \natural)\right] - \mathrm{tr}\left[\boldsymbol{F}_\gamma^{\mathrm{T}} (\dot{\mathbb{G}}[\dot{\boldsymbol{F}}_\gamma])\right]. \end{aligned} \tag{5.97b}$$

Hence, $\dot{\lambda}$ is given by

$$\begin{aligned} \dot{\lambda} =& \tfrac{1}{3}\mathrm{tr}(\boldsymbol{F}_\gamma^{\mathrm{T}} \mathfrak{S}_{\boldsymbol{F}_\gamma \boldsymbol{F}_\gamma}) + \tfrac{1}{3}\mathrm{tr}\left[\boldsymbol{F}_\gamma^{\mathrm{T}} (\partial_{\boldsymbol{F}_\gamma} \hat{\mathcal{L}} \circ \natural)\right] - \tfrac{1}{3}\mathrm{tr}\left[\boldsymbol{F}_\gamma^{\mathrm{T}} (\dot{\mathbb{G}}[\dot{\boldsymbol{F}}_\gamma])\right] \\ & - \tfrac{1}{3} J_\gamma \mathfrak{m}_\nu [\mathrm{tr}\boldsymbol{\Lambda}_\gamma^2 + \dot{R}], \end{aligned} \tag{5.98}$$

and, by recalling Equation (5.92b), we obtain

$$\begin{aligned} \dot{\lambda} =& \tfrac{1}{3}\mathrm{tr}(\boldsymbol{F}_\gamma^{\mathrm{T}} \mathfrak{S}_{\boldsymbol{F}_\gamma \boldsymbol{F}_\gamma}) + \tfrac{1}{3}\mathrm{tr}\left[\boldsymbol{F}_\gamma^{\mathrm{T}} (\partial_{\boldsymbol{F}_\gamma} \hat{\mathcal{L}} \circ \natural)\right] - \tfrac{1}{3}\mathrm{tr}\left[\boldsymbol{F}_\gamma^{\mathrm{T}} (\dot{\mathbb{G}}[\dot{\boldsymbol{F}}_\gamma])\right] \\ & - \tfrac{1}{3} J_\gamma \mathfrak{m}_\nu \langle \boldsymbol{F}_\gamma^{-\mathrm{T}} | \ddot{\boldsymbol{F}}_\gamma \rangle. \end{aligned} \tag{5.99}$$

Finally, by considering the identity $J_\gamma \mathfrak{m}_\nu \langle \boldsymbol{F}_\gamma^{-\mathrm{T}} | \ddot{\boldsymbol{F}}_\gamma \rangle \equiv \mathrm{tr}[\boldsymbol{F}_\gamma^{\mathrm{T}} (\mathbb{G}[\ddot{\boldsymbol{F}}_\gamma])]$, obtained by assuming $\mathbb{G} = J_\gamma \mathfrak{m}_\nu \boldsymbol{b}_\gamma^{-1} \underline{\otimes} \boldsymbol{G}^{-1}$, we rewrite the sum of the last two terms of Equation (5.99) as $-\frac{1}{3}\mathrm{tr}[\boldsymbol{F}_\gamma^{\mathrm{T}} \partial_t (\mathbb{G}[\dot{\boldsymbol{F}}_\gamma])]$, and, thus, as $-\frac{1}{3}\mathrm{tr}[\boldsymbol{F}_\gamma^{\mathrm{T}} \partial_t (\partial_{\dot{\boldsymbol{F}}_\gamma} \hat{\mathcal{L}} \circ \natural)]$. Then, substituting this result into Equation (5.99), and using the definition of the Euler–Lagrange operator lead to

$$\dot{\lambda} = \tfrac{1}{3}\mathrm{tr}(\boldsymbol{F}_\gamma^{\mathrm{T}} \mathfrak{S}_{\boldsymbol{F}_\gamma \boldsymbol{F}_\gamma}) + \tfrac{1}{3}\mathrm{tr}[\boldsymbol{F}_\gamma^{\mathrm{T}} (\mathcal{E}_{\boldsymbol{F}_\gamma} \hat{\mathcal{L}})], \tag{5.100}$$

which is identical to Equation (5.74b), up to the presence of $\mathfrak{S}_{\mathrm{np}}$.

We notice that, since σ (representative of $\boldsymbol{b}_\gamma \mathfrak{S}_{\boldsymbol{F}_\gamma \boldsymbol{F}_\gamma} \boldsymbol{G}$) would not appear if the problem were formulated by means of the TNHM, Equations (5.16e) and (5.16f), rewritten in matrix formalism, become (if $\mathfrak{S}_{\mathrm{np}}$ is neglected)

$$\begin{cases} \ddot{\mathsf{f}}_{\mathrm{TNHM}} = \frac{1}{J_\gamma \mathfrak{m}_\nu} \left[\mathsf{I} - \frac{1}{3}\mathsf{N}\mathsf{Q}^{\mathrm{t}}\right] \mathsf{b} + \frac{1}{3}\mathsf{N}\mathsf{c}, \\ \mu = \frac{1}{3}\mathsf{Q}^{\mathrm{t}}\mathsf{b} - \frac{J_\gamma \mathfrak{m}_\nu}{3}\mathsf{c}. \end{cases} \tag{5.101}$$

Hence, as reported in a theorem of [1] (which rephrases a result given also in [16] and is reported in this Thesis as Theorem 2.1), the MVM formulated by Llibre et al. [16] is equivalent to the TNHM if, and only if, it holds that $\mathsf{f} = \mathsf{f}_{\mathrm{TNHM}}$ and $\dot{\lambda} = \mu + \frac{1}{3}\mathsf{Q}^{\mathrm{t}}\sigma$.

While the latter condition is a direct consequence of Equations (5.96) and (5.101), and is equivalent to Equation (5.59), provided the substitution $\kappa \equiv \dot{\lambda}$ is done, for the former one to be fulfilled it is necessary and sufficient that

$$\tfrac{1}{J_\gamma \mathfrak{m}_\nu}\left[\mathsf{I} - \tfrac{1}{3}\mathsf{N}\mathsf{Q}^{\mathsf{t}}\right]\sigma = \mathsf{0}. \tag{5.102}$$

This means that σ must belong to the kernel of the operator $\mathsf{I} - \frac{1}{3}\mathsf{N}\mathsf{Q}^{\mathsf{t}}$. This operator, in fact, is the matrix representation of the fourth-order tensor

$$\boldsymbol{\delta} \underline{\otimes} \boldsymbol{I}^{\mathrm{T}} - \tfrac{1}{3}\boldsymbol{F}_\gamma \otimes \boldsymbol{F}_\gamma^{-\mathrm{T}}, \tag{5.103}$$

which extracts the $\boldsymbol{F}_\gamma$-deviatoric part (see Equation (5.104a) below) of a generic second-order tensor $\boldsymbol{\Phi}$ with components $\Phi^{\alpha}{}_{A}$, and has kernel spanned by all tensors of the type $\boldsymbol{\Phi}_0 = \varphi \boldsymbol{F}_\gamma$, with $\varphi \in \mathbb{R}$ (in Equation (5.103), $\boldsymbol{\delta}$ is the identity tensor associated with the body's natural state). These two properties can be verified by a direct calculation, which yields

$$\left\{\boldsymbol{\delta} \underline{\otimes} \boldsymbol{I}^{\mathrm{T}} - \tfrac{1}{3}\boldsymbol{F}_\gamma \otimes \boldsymbol{F}_\gamma^{-\mathrm{T}}\right\}[\boldsymbol{\Phi}] = \boldsymbol{\Phi} - \tfrac{1}{3}\mathrm{tr}(\boldsymbol{F}_\gamma^{-1}\boldsymbol{\Phi})\boldsymbol{F}_\gamma, \qquad \forall\, \boldsymbol{\Phi}, \tag{5.104a}$$

$$\left\{\boldsymbol{\delta} \underline{\otimes} \boldsymbol{I}^{\mathrm{T}} - \tfrac{1}{3}\boldsymbol{F}_\gamma \otimes \boldsymbol{F}_\gamma^{-\mathrm{T}}\right\}[\varphi\, \boldsymbol{F}_\gamma] = \boldsymbol{O}, \qquad \forall\, \varphi. \tag{5.104b}$$

From these results, it follows that, since the column vector σ represents the second-order tensor $\boldsymbol{b}_\gamma \mathfrak{S}_{\boldsymbol{F}_\gamma \boldsymbol{F}_\gamma} \boldsymbol{G}$, Equation (5.102) requires the $\boldsymbol{F}_\gamma$-deviatoric part of $\boldsymbol{b}_\gamma \mathfrak{S}_{\boldsymbol{F}_\gamma \boldsymbol{F}_\gamma} \boldsymbol{G}$ to be null, i.e.,

$$\left\{\boldsymbol{\delta} \underline{\otimes} \boldsymbol{I}^{\mathrm{T}} - \tfrac{1}{3}\boldsymbol{F}_\gamma \otimes \boldsymbol{F}_\gamma^{-\mathrm{T}}\right\}[\boldsymbol{b}_\gamma \mathfrak{S}_{\boldsymbol{F}_\gamma \boldsymbol{F}_\gamma} \boldsymbol{G}] = \boldsymbol{O}, \tag{5.105}$$

which is equivalent to both of the following conditions

$$\mathrm{DEV}\mathfrak{S}_{\boldsymbol{F}_\gamma \boldsymbol{F}_\gamma} = \mathfrak{S}_{\boldsymbol{F}_\gamma \boldsymbol{F}_\gamma} - \tfrac{1}{3}\mathrm{tr}(\boldsymbol{F}_\gamma^{\mathrm{T}} \mathfrak{S}_{\boldsymbol{F}_\gamma \boldsymbol{F}_\gamma}) \boldsymbol{F}_\gamma^{-\mathrm{T}} = \boldsymbol{O}, \tag{5.106a}$$

$$\mathrm{Dev}(\boldsymbol{F}_\gamma^{\mathrm{T}} \mathfrak{S}_{\boldsymbol{F}_\gamma \boldsymbol{F}_\gamma}) = \boldsymbol{F}_\gamma^{\mathrm{T}} \mathfrak{S}_{\boldsymbol{F}_\gamma \boldsymbol{F}_\gamma} - \tfrac{1}{3}\mathrm{tr}(\boldsymbol{F}_\gamma^{\mathrm{T}} \mathfrak{S}_{\boldsymbol{F}_\gamma \boldsymbol{F}_\gamma}) \boldsymbol{I}^{\mathrm{T}} = \boldsymbol{O}. \tag{5.106b}$$

Equations (5.106a) and (5.106b) constitute the most important result of this section, and can be summarized in the following theorem, which particularizes a theorem reported in [1] (i.e., Theorem 2.1 of this Thesis).

Theorem 5.1 (The MVM by Llibre et al. [16] and the TNHM)**.** *Within the theory of growth under consideration, the MVM formulated in [16], which leads to Equations*

(5.88a)–(5.88f)*, is equivalent to the TNHM, and, thus, also to our formulation of the MVM, if, and only if,* $\mathfrak{S}_{\boldsymbol{F}_\gamma \boldsymbol{F}_\gamma}$ *has vanishing* $\boldsymbol{F}_\gamma^{-\mathrm{T}}$*-deviatoric part (and* $\mathfrak{S}_{\boldsymbol{F}_\gamma \boldsymbol{F}} = \boldsymbol{O}$*).*
Proof: To prove the necessary condition, we compare the systems (5.96) and (5.101), and we notice that, if they are equivalent to each other, then Equation (5.102) has to be fulfilled. Since this condition implies Equation (5.106a), or (5.106b), $\mathfrak{S}_{\boldsymbol{F}_\gamma \boldsymbol{F}_\gamma}$ must have null $\boldsymbol{F}_\gamma^{-\mathrm{T}}$-deviatoric part.

To prove the sufficient condition, we assume that Equation (5.106a), or (5.106b), holds true. Then, the system (5.96) returns (5.101), and, thus, the MVM formulated in [16] is equivalent to the TNHM. □

Hence, if the MVM by Llibre et al. [16] is to be used *as is*, then, in order for it to be equivalent to the TNHM, only tensors $\mathfrak{S}_{\boldsymbol{F}_\gamma \boldsymbol{F}_\gamma}$ proportional to $\boldsymbol{F}_\gamma^{-\mathrm{T}}$ are admissible. More specifically, on account of Equations (5.55b) and (5.106a), or (5.106b), to ensure the equivalence with the TNHM, $\mathfrak{S}_{\boldsymbol{F}_\gamma \boldsymbol{F}_\gamma}$ must be such that

$$\mathfrak{S}_{\boldsymbol{F}_\gamma \boldsymbol{F}_\gamma} = \tfrac{1}{3} P_\gamma \mathrm{tr}\big[\boldsymbol{F}_\gamma^{\mathrm{T}} (\partial_{\boldsymbol{F}_\gamma} \hat{R} \circ \natural_\gamma)\big] \boldsymbol{F}_\gamma^{-\mathrm{T}}. \tag{5.107}$$

By virtue of Equations (5.107), let us write $\mathfrak{S}_{\boldsymbol{F}_\gamma \boldsymbol{F}_\gamma} = \frac{1}{3}\mathrm{tr}(\boldsymbol{F}_\gamma^{\mathrm{T}} \mathfrak{S}_{\boldsymbol{F}_\gamma \boldsymbol{F}_\gamma}) \boldsymbol{F}_\gamma^{-\mathrm{T}}$ in Equation (5.88e). Then, by multiplying it by $\boldsymbol{F}_\gamma^{\mathrm{T}}$, and projecting it onto the subspaces of deviatoric and spherical tensors, we find

$$\mathrm{Dev}[\boldsymbol{F}_\gamma^{\mathrm{T}} (\mathcal{E}_{\boldsymbol{F}_\gamma} \hat{\mathcal{L}})] = \boldsymbol{O}, \tag{5.108a}$$

$$\tfrac{1}{3}\mathrm{tr}[\boldsymbol{F}_\gamma^{\mathrm{T}} (\mathcal{E}_{\boldsymbol{F}_\gamma} \hat{\mathcal{L}})] + \tfrac{1}{3}\mathrm{tr}[\boldsymbol{F}_\gamma^{\mathrm{T}} \mathfrak{S}_{\boldsymbol{F}_\gamma \boldsymbol{F}_\gamma}] = \dot{\lambda}, \tag{5.108b}$$

thereby providing another expression of the fact that the dynamic equations are now equivalent to those obtained via the TNHM or via our formulation of the MVM, up to the non-potential forces.

This result can be formalized in the following Corollary to Theorem 5.1. Before enunciating it, we emphasize that, also in this case, the restriction that it places on the mass source *is not* required in our formulation of the MVM.

Corollary 5.1 (Restriction on the constitutive form of the mass source)**.** *In order for* $\mathfrak{S}_{\boldsymbol{F}_\gamma \boldsymbol{F}_\gamma}$ *to be proportional to* $\boldsymbol{F}_\gamma^{-\mathrm{T}}$*, the functional form of the mass source, i.e.,* $\hat{R}$*, may depend on* $\boldsymbol{F}_\gamma$ *only through* $J_\gamma = \det \boldsymbol{F}_\gamma$*, i.e., on the volumetric part of the distortions induced by growth.*
Proof: To satisfy the first restriction on $\hat{R}$, discussed in Section 5.5.1, let us take

$\hat{R}$ independent of $\boldsymbol{F}$. Then, consistently with the hypothesis of this corollary, we write $R = \hat{R} \circ (\boldsymbol{F}_\gamma; \mathcal{X}, \mathcal{T}) = \check{R} \circ (J_\gamma; \mathcal{X}, \mathcal{T})$, and we calculate $\mathfrak{S}_{\boldsymbol{F}_\gamma \boldsymbol{F}_\gamma}$ as prescribed in Equation (5.55b), i.e.,

$$\mathfrak{S}_{\boldsymbol{F}_\gamma \boldsymbol{F}_\gamma} = P_\gamma \left(\frac{\partial \hat{R}}{\partial \boldsymbol{F}_\gamma} \circ (\boldsymbol{F}_\gamma; \mathcal{X}, \mathcal{T}) \right) = J_\gamma P_\gamma \left(\frac{\partial \check{R}}{\partial J_\gamma} \circ (J_\gamma; \mathcal{X}, \mathcal{T}) \right) \boldsymbol{F}_\gamma^{-\mathrm{T}}. \tag{5.109}$$

The tensor $\mathfrak{S}_{\boldsymbol{F}_\gamma \boldsymbol{F}_\gamma}$ computed this way is, by construction, proportional to $\boldsymbol{F}_\gamma^{-\mathrm{T}}$, and has, thus, null $\boldsymbol{F}_\gamma^{-\mathrm{T}}$-deviatoric part. This completes the proof and makes the growth law $R = \hat{R} \circ (\boldsymbol{F}_\gamma; \mathcal{X}, \mathcal{T}) = \check{R} \circ (J_\gamma; \mathcal{X}, \mathcal{T})$ admissible in the sense of Theorem 5.1, since the tensor $\mathfrak{S}_{\boldsymbol{F}_\gamma \boldsymbol{F}_\gamma}$ in Equation (5.109) makes the MVM by Llibre et al. [16] equivalent to the TNHM. □

A final remark concerns the fact that, if the dependence of $\hat{\mathcal{L}}$ on $\dot{\boldsymbol{F}}_\gamma$ is only through the kinetic energy density $\mathcal{K}_\gamma$, then, in the quasi-static case, the MVM by Llibre et al. [16] is equivalent to the TNHM because $\partial_{\dot{\boldsymbol{F}}_\gamma} \hat{\mathcal{L}} \circ \natural$ is neglected and, thus, the extra forces $\mathbb{W}^{\mathrm{T}}_{\boldsymbol{F}_\gamma \boldsymbol{F}} [\partial_{\dot{\boldsymbol{F}}_\gamma} \hat{\mathcal{L}} \circ \natural]$ and $\mathbb{W}^{\mathrm{T}}_{\boldsymbol{F}_\gamma \boldsymbol{F}_\gamma} [\partial_{\dot{\boldsymbol{F}}_\gamma} \hat{\mathcal{L}} \circ \natural]$ do not appear on the left-hand sides of Equations (5.88c) and (5.88e). However, we deem it important to reformulate this version of the MVM as shown in Section 5.4 because it allows to obtain the quasi-static limit in the correct way. In this regard, we refer the reader to the next section for the study of such quasi-static limit for a simple benchmark problem [89, 91].

5.6 A benchmark problem in the quasi-static limit

As indicated at the beginning of Section 5.1, our main purpose is to obtain the dynamic equations of a growing body within a *quasi-variational theory* of growth, although the evolution of $\boldsymbol{F}_\gamma$ is restricted by the *nonholonomic constraint* $\langle \boldsymbol{F}_\gamma^{-\mathrm{T}} | \dot{\boldsymbol{F}}_\gamma \rangle - R = 0$. In this respect, the dynamic equations for $\boldsymbol{F}_\gamma$ that we obtain with our procedure, i.e., Equations (5.73a) and (5.73b), are equivalent to those determined by the Principle of Virtual Work, as they should be. Apart from the reasons already explained in the paragraph *"Why a Lagrangian theory of growth: advantages and problems"* of Section 5.1, the advantage of this formulation is provided by the possibility of defining the Lagrangian density function $\hat{\mathcal{L}}_{\mathrm{c}}$ given in Equation (5.68a), which is comprehensive of the nonholonomic constraint and can be used as the starting point

for computational schemes based on finite element methods. While the detailed investigation of this issue is out of the scopes of the present work, the numerical simulation of a simple benchmark problem could be useful to see the role played by $\mathfrak{S}_{\boldsymbol{F}_\gamma \boldsymbol{F}}$ and $\mathfrak{S}_{\boldsymbol{F}_\gamma \boldsymbol{F}_\gamma}$, defined in Equation (5.56).

In line with previous studies of our research group, we concentrate on an academic problem of tumor growth in a *"breast duct"* [89], as recently described in [91, Section 3.1]. The mathematical model adopted therein neglects the inertial effects and all the body forces featuring in Equation (5.71a) and then specialized in Equation (5.80) below. Hence, the dynamic equation for χ (linear momentum balance law) becomes

$$\mathrm{Div}\boldsymbol{P} = \boldsymbol{0}, \qquad \text{in } \mathscr{B}, \tag{5.110}$$

and is, indeed, obtained from Equation (5.85a) by disregarding $(\det \boldsymbol{F}_\gamma)\varrho_\nu \boldsymbol{a}_{\mathrm{gr}}$ and $\boldsymbol{f}_{\mathrm{np}}$.

Within the considered approximation, the dynamic equations for $\boldsymbol{F}_\gamma$ are given by those of the quasi-static case, i.e., by Equations (5.87a)–(5.87c), which we rewrite here:

$$\mathrm{Dev}\boldsymbol{Z} - \mathrm{Dev}\boldsymbol{H} = \mathrm{Dev}\big\{\mathbb{T}[\boldsymbol{F}_\gamma^{-1}\dot{\boldsymbol{F}}_\gamma]\big\}, \tag{5.111a}$$

$$\dot{\lambda} = -\tfrac{1}{3}\mathrm{tr}\boldsymbol{H} + \tfrac{1}{3}\mathrm{tr}\boldsymbol{Z} - \tfrac{1}{3}\mathrm{tr}\big\{\mathbb{T}[\boldsymbol{F}_\gamma^{-1}\dot{\boldsymbol{F}}_\gamma]\big\}, \tag{5.111b}$$

$$\langle \boldsymbol{F}_\gamma^{-\mathrm{T}} | \dot{\boldsymbol{F}}_\gamma \rangle - R = 0. \tag{5.111c}$$

With $\dot{\lambda}$ playing the role of μ, these equations are identical to those solved in [91]. In fact, the condition $\dot{\lambda} = \mu$ follows from Equation (5.59), rewritten as $\dot{\lambda} = \mu + \frac{1}{3}\mathrm{tr}(\boldsymbol{F}_\gamma^{\mathrm{T}}\mathfrak{S}_{\boldsymbol{F}_\gamma \boldsymbol{F}_\gamma})$, when $\frac{1}{3}\mathrm{tr}(\boldsymbol{F}_\gamma^{\mathrm{T}}\mathfrak{S}_{\boldsymbol{F}_\gamma \boldsymbol{F}_\gamma})$ is zero or is neglected, as implied by Equation (5.82) of the Subsection *"Explicit form of the dynamic equations in the quasi-static case"* of Section 5.4.3.

To close the problem, we prescribe the same mechanical framework as in [91]. Therefore, we drop $\hat{\Psi}_{\mathrm{g}}$ and $\hat{\mathfrak{U}}$ from the Lagrangian density function $\hat{\mathcal{L}}$ in Equation (5.82), and, under the assumption of homogeneous and isotropic hyperelastic material, we set

$$\hat{\mathcal{L}} \circ \natural = -\hat{\Psi} \circ (\boldsymbol{F}, \boldsymbol{F}_\gamma) = -J_\gamma[\hat{\Psi}_\nu \circ \boldsymbol{F}_{\mathrm{e}}] = -J_\gamma[\hat{\mathcal{W}}_\nu \circ (I_{1\mathrm{e}}, I_{2\mathrm{e}}, I_{3\mathrm{e}})], \tag{5.112a}$$

$$\hat{\mathcal{W}}_\nu \circ (I_{1\mathrm{e}}, I_{2\mathrm{e}}, I_{3\mathrm{e}}) = \alpha_0\big\{\exp(\alpha_1[I_{1\mathrm{e}} - 3] + \alpha_2[I_{2\mathrm{e}} - 3] - \alpha_3 \log I_{3\mathrm{e}}) - 1\big\}, \tag{5.112b}$$

where $\hat{\mathcal{W}}_\nu$ is the strain energy density of the body per unit volume of the natural state, and expressed as a function of the principal invariants $I_{1\mathrm{e}}$, $I_{2\mathrm{e}}$, and $I_{3\mathrm{e}}$ of the right Cauchy-Green deformation tensor induced by $\boldsymbol{F}_\mathrm{e}$, i.e., $\boldsymbol{C}_\mathrm{e} = \boldsymbol{F}_\mathrm{e}^\mathrm{T}\boldsymbol{g}\boldsymbol{F}_\mathrm{e} = \boldsymbol{F}_\gamma^{-\mathrm{T}}\boldsymbol{C}\boldsymbol{F}_\gamma^{-1}$, with $\boldsymbol{C} = \boldsymbol{F}^\mathrm{T}\boldsymbol{g}\boldsymbol{F}$ and $\boldsymbol{g}$ being the metric associated with the three-dimensional Euclidean space hosting the body.

Given Equations (5.112a) and (5.112b), the first Piola–Kirchhoff stress tensor $\boldsymbol{P}$ and the Eshelby stress tensor $\boldsymbol{H}$ are determined by Equation (5.12), or (5.72), and (5.86a), respectively.

Since the Lagrangian density function in Equation (5.112a) implies that $\boldsymbol{Z}_\mathrm{p}$ is null, the external force $\boldsymbol{Z}$ is entirely non-potential in the present framework. Thus, we obtain $\boldsymbol{Z} = \boldsymbol{Z}_\mathrm{np}$, with the latter one being specified in Equation (5.19), Section 5.2.3. Moreover, the mass source R is supplied in Equation (5.5). Both $\boldsymbol{Z}$ and R are conceived starting from biological phenomenology, as explained in Remark 5.2. The nutrients' concentration $\mathfrak{c}$ evolves according to a diffusion-reaction equation, as the one reported in [91], where the diffusivity tensor is prescribed as a tensor-valued function of $\boldsymbol{F}$ and $\boldsymbol{F}_\gamma$, while the reaction rate is constant.

Finally, $\mathbb{T}$ is a fourth-order tensor field, defined in [23] in such a way that the dissipative generalized force $\boldsymbol{Y}_\mathrm{ud} = \mathbb{T}[\boldsymbol{F}_\gamma^{-1}\dot{\boldsymbol{F}}_\gamma]$ takes on the form

$$\begin{aligned}\mathbb{T}[\boldsymbol{F}_\gamma^{-1}\dot{\boldsymbol{F}}_\gamma] = {}& \tfrac{1}{3}J_\gamma a_\nu \mathrm{tr}(\boldsymbol{F}_\gamma^{-1}\dot{\boldsymbol{F}}_\gamma)\boldsymbol{I}^\mathrm{T} + 2J_\gamma b_\nu \boldsymbol{C}\,\mathrm{sym}[(\boldsymbol{F}_\gamma^{-1}\dot{\boldsymbol{F}}_\gamma)\boldsymbol{C}^{-1}] \\ & + 2J_\gamma c_\nu \boldsymbol{C}\,\mathrm{skew}[(\boldsymbol{F}_\gamma^{-1}\dot{\boldsymbol{F}}_\gamma)\boldsymbol{C}^{-1}],\end{aligned} \tag{5.113}$$

where a_ν, b_ν, and c_ν are constant material parameters assumed for the computed benchmark problem as in [91], but not taken from experiments. Also all the remaining values of the coefficients employed in the model are borrowed from [91].

Since the external force $\boldsymbol{Z}$ specified in Equation (5.19) is such that $\boldsymbol{C}^{-1}\mathrm{Dev}\boldsymbol{Z}$ is symmetric, and since $\boldsymbol{C}^{-1}\mathrm{Dev}\boldsymbol{H}$ is symmetric by construction, then Equation (5.111a) requires its right-hand side to be symmetric, too. This, according to Equation (5.113), implies that the skew-symmetric contribution to $\mathbb{T}[\boldsymbol{F}_\gamma^{-1}\dot{\boldsymbol{F}}_\gamma]$ must vanish, i.e., $\mathrm{skew}[(\boldsymbol{F}_\gamma^{-1}\dot{\boldsymbol{F}}_\gamma)\boldsymbol{C}^{-1}] = \boldsymbol{O}$. Details about this procedure are given in [23, 87, 91].

Equations (5.110), (5.111a)–(5.111c), and the diffusion-reaction equation for the nutrients are now solved for the case of a tumor that grows inside a breast duct of cylindrical shape and having fixed and non-deformable lateral boundary, and extremities free of contact forces. Moreover, it is assumed that the tumor does not

rotate about the geometric symmetry axis of the cylinder. By using cylindrical coordinates, the just provided description implies that Equation (5.110) is completed by homogeneous Dirichlet conditions for the radial and angular displacement of the tumor and by the homogeneous Neumann conditions $\boldsymbol{PN} = \boldsymbol{0}$ on the extremities of the duct. Furthermore, the benchmark assumes that, at the initial instant of time $t = t_{\text{in}} \in \mathscr{I}$, $\boldsymbol{F}_\gamma(X, t_{\text{in}})$ is given in components as $(\boldsymbol{F}_\gamma)^\alpha{}_A(X, t_{\text{in}}) = 1$, for $\alpha \equiv A = 1, 2, 3$, and $(\boldsymbol{F}_\gamma)^\alpha{}_A(X, t_{\text{in}}) = 0$ for $\alpha \neq A$.

In principle, given the form of Equation (5.111b), an initial condition for λ should be provided (see, e.g., [27, 1]). However, this is not necessary in the present framework, since the model has been formulated in such a way that only $\dot{\lambda}$ has to be computed.

The initial- and boundary-value subproblem for the nutrients' concentration is the same as the one studied in [91]. The diffusion-reaction equation for $\mathfrak{c}$ is equipped with homogeneous (zero-flux) Neumann boundary conditions on the lateral boundary of the cylinder and Dirichlet boundary conditions at the extremities, where $\mathfrak{c}$ is set equal to $\mathfrak{c}_{\text{env}}$ at all times. The initial value of $\mathfrak{c}$ is equal to $\mathfrak{c}_{\text{env}}$, too.

Finite elements have been used to solve Equations (5.110), (5.111a)–(5.111c) and the equation for $\mathfrak{c}$, together with the discussed boundary and initial conditions. The numerical simulations have been performed by using the commercial software COMSOL Multiphysics™ v. 5.3a. The axial-symmetric geometry of the duct has been exploited, so that the axis of the abscissae in Figures 5.1 and 5.2 represents the axial coordinate Ξ of the cylinder in the reference placement.

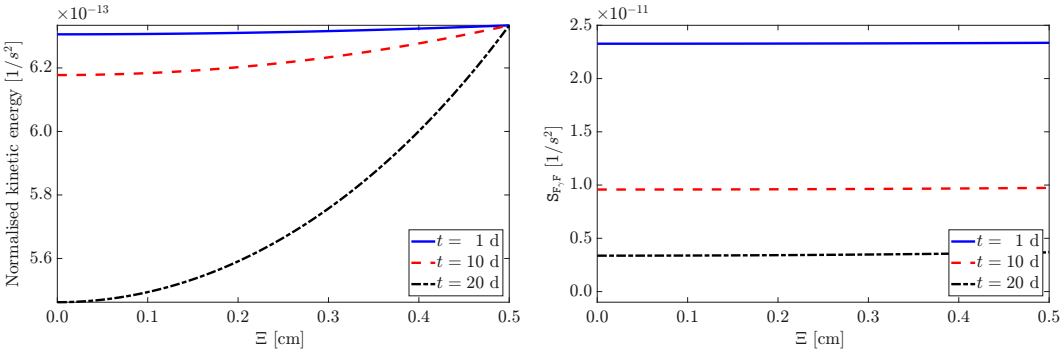

Fig. 5.1 (Left) Normalized kinetic energy $\mathcal{K}_\gamma / J_\gamma \mathfrak{m}_\nu$; (Right) Norm of the normalized extra force $\mathfrak{S}_{\boldsymbol{F}_\gamma \boldsymbol{F}}$.

The purpose of these simulations is to show that, since tumor growth is typically studied in the quasi-static regime, the limit of vanishing inertial contributions must be met in the correct way, if one wants to formulate a theory of growth as discussed in our work. Thus, one has to consider the extra forces $\mathfrak{S}_{\boldsymbol{F}_\gamma \boldsymbol{F}} = \mathbb{W}^{\mathrm{T}}_{\boldsymbol{F}_\gamma \boldsymbol{F}}[\partial_{\dot{\boldsymbol{F}}_\gamma}\hat{\mathcal{L}} \circ \natural]$ and $\mathfrak{S}_{\boldsymbol{F}_\gamma \boldsymbol{F}_\gamma} = \mathbb{W}^{\mathrm{T}}_{\boldsymbol{F}_\gamma \boldsymbol{F}_\gamma}[\partial_{\dot{\boldsymbol{F}}_\gamma}\hat{\mathcal{L}} \circ \natural]$ on both sides of the dynamic equations (5.54a) and (5.54b), and show that they are, in fact, negligible with respect to all the other terms. Since Equations (5.54a) and (5.54b) are obtained by adding $\mathfrak{S}_{\boldsymbol{F}_\gamma \boldsymbol{F}}$ and $\mathfrak{S}_{\boldsymbol{F}_\gamma \boldsymbol{F}_\gamma}$ on both sides of each equation, these forces are obviously always of the same order, and so will they be when they are sent to zero. However, this is not the case in the *"Modified Vakonomic Method"* (MVM) by Llibre et al. [16], according to which $\mathfrak{S}_{\boldsymbol{F}_\gamma \boldsymbol{F}}$ and $\mathfrak{S}_{\boldsymbol{F}_\gamma \boldsymbol{F}_\gamma}$ would appear *only* on the left-hand side of each equation. Therefore, as long as inertial effects are genuinely negligible, their formulation will yield the same results as ours. However, as soon as inertial terms are, for any reason, no longer negligible, their equations would still feature $\mathfrak{S}_{\boldsymbol{F}_\gamma \boldsymbol{F}}$ and $\mathfrak{S}_{\boldsymbol{F}_\gamma \boldsymbol{F}_\gamma}$ on the left-hand sides, but not on the right-hand sides. Therefore, $\mathfrak{S}_{\boldsymbol{F}_\gamma \boldsymbol{F}}$ and $\mathfrak{S}_{\boldsymbol{F}_\gamma \boldsymbol{F}_\gamma}$ would not be compensated for. This would lead to results discrepant not only with ours, but, more importantly, with those predicted by the Traditional Non-Holonomic Method (TNHM), on which the theories of growth usually rely.

For the reasons outlined above, we start showing that the kinetic energy density $\mathcal{K}_\gamma$ is negligible in the problem at hand. In the left panel of Figure 5.1, we report the normalized kinetic energy density $\mathcal{K}_\gamma / J_\gamma \mathfrak{m}_\nu$ at three different times (day 1, day 10 and day 20), corresponding to different values of the nutrients' concentration. We notice that it is essentially equal to the square of the source of mass (cfr. [91, Figure 2(a)]). This follows from the fact that, by virtue of the constraint (5.2), $\mathcal{K}_\gamma$ in Section 5.5.2 can be written as

$$\begin{aligned} \mathcal{K}_\gamma = \tfrac{1}{2} J_\gamma \mathfrak{m}_\nu \|\boldsymbol{\Lambda}_\gamma\|^2 &= \tfrac{1}{6} J_\gamma \mathfrak{m}_\nu (J_\gamma^{-1} \dot{J}_\gamma)^2 + \tfrac{1}{2} J_\gamma \mathfrak{m}_\nu \|\boldsymbol{\Lambda}_{\gamma,\mathrm{u}}\|^2 \\ &= \tfrac{1}{6} J_\gamma \mathfrak{m}_\nu (\hat{R} \circ \natural_\gamma)^2 + \tfrac{1}{2} J_\gamma \mathfrak{m}_\nu \|\boldsymbol{\Lambda}_{\gamma,\mathrm{u}}\|^2, \end{aligned} \tag{5.114}$$

where $\boldsymbol{\Lambda}_{\gamma,\mathrm{u}} := \boldsymbol{F}_{\gamma,\mathrm{u}}^{-1} \dot{\boldsymbol{F}}_{\gamma,\mathrm{u}}$ is the rate of the volume-preserving distortions due to growth, the square norm of which is negligible with respect to R^2. This result notwithstanding, $\mathcal{K}_\gamma$ is comprehensive of a contribution due to the growth law $R = \hat{R} \circ \natural_\gamma$, and a contribution associated with the rates of the isochoric distortions. Whereas the functional expression of the former one is assigned *a priori* by imposing R in Equation (5.2), the latter is computed from the dynamic equation (5.111a). Since the trend

of $\mathcal{K}_\gamma/J_\gamma \mathfrak{m}_\nu$ can be approximated with the trend of R^2, then the inertial effects on the evolution of $\boldsymbol{F}_\gamma$ are negligible whenever the values attained by $R \equiv \hat{R} \circ \natural_c$ are relatively small, as is indeed the case.

To represent the magnitudes of $\mathfrak{S}_{\boldsymbol{F}_\gamma \boldsymbol{F}}$ and $\mathfrak{S}_{\boldsymbol{F}_\gamma \boldsymbol{F}_\gamma}$, with the latter being decomposed in its $\boldsymbol{F}_\gamma^{-\mathrm{T}}$-spheric and $\boldsymbol{F}_\gamma^{-\mathrm{T}}$-deviatoric, we consider the norms

$$\mathsf{S}_{\mathsf{F}_\gamma \mathsf{F}} := \left\| \frac{\mathfrak{S}_{\boldsymbol{F}_\gamma \boldsymbol{F}}}{J_\gamma \mathfrak{m}_\nu} \right\|, \tag{5.115a}$$

$$\mathsf{S}^{\mathtt{sph}}_{\mathsf{F}_\gamma \mathsf{F}_\gamma} := \left\| \frac{\frac{1}{3}\mathrm{tr}(\boldsymbol{F}_\gamma^{\mathrm{T}} \mathfrak{S}_{\boldsymbol{F}_\gamma \boldsymbol{F}_\gamma}) \boldsymbol{F}_\gamma^{-\mathrm{T}}}{J_\gamma \mathfrak{m}_\nu} \right\|, \qquad \mathsf{S}^{\mathtt{dev}}_{\mathsf{F}_\gamma \mathsf{F}_\gamma} := \left\| \frac{\mathrm{DEV} \mathfrak{S}_{\boldsymbol{F}_\gamma \boldsymbol{F}_\gamma}}{J_\gamma \mathfrak{m}_\nu} \right\|. \tag{5.115b}$$

From the right panel of Figure 5.1, we can see that $\mathsf{S}_{\mathsf{F}_\gamma \mathsf{F}}$ is quite homogeneously distributed with respect to the axial coordinate Ξ, and, in particular, it decreases of one order of magnitude from day 1 to day 20. This may be attributed to the fact that $\mathfrak{S}_{\boldsymbol{F}_\gamma \boldsymbol{F}} \equiv \mathbb{W}^{\mathrm{T}}_{\boldsymbol{F}_\gamma \boldsymbol{F}}[\boldsymbol{p}_\gamma]$ depends on the source of mass through $\partial_{\boldsymbol{F}} \hat{R} \circ \natural_\gamma$ (see Equation (5.38)).

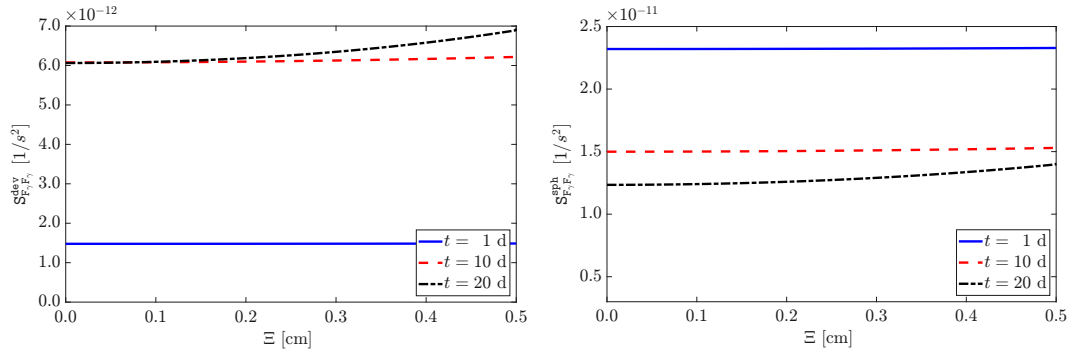

Fig. 5.2 (Left) Norm of the normalized extra force $\mathrm{DEV}\mathfrak{S}_{\boldsymbol{F}_\gamma \boldsymbol{F}_\gamma} = \mathfrak{S}_{\boldsymbol{F}_\gamma \boldsymbol{F}_\gamma} - \frac{1}{3}\mathrm{tr}(\boldsymbol{F}_\gamma^{\mathrm{T}} \mathfrak{S}_{\boldsymbol{F}_\gamma \boldsymbol{F}_\gamma}) \boldsymbol{F}_\gamma^{-\mathrm{T}}$. (Right) Norm of the normalized extra force $\frac{1}{3}\mathrm{tr}(\boldsymbol{F}_\gamma^{\mathrm{T}} \mathfrak{S}_{\boldsymbol{F}_\gamma \boldsymbol{F}_\gamma}) \boldsymbol{F}_\gamma^{-\mathrm{T}}$.

Concerning the extra force $\mathfrak{S}_{\boldsymbol{F}_\gamma \boldsymbol{F}_\gamma} \equiv \mathbb{W}^{\mathrm{T}}_{\boldsymbol{F}_\gamma \boldsymbol{F}_\gamma}[\boldsymbol{p}_\gamma]$, which depends on the source of mass through $\partial_{\boldsymbol{F}_\gamma} \hat{R} \circ \natural_\gamma$ (see Equation (5.40)), Figure 5.2 shows two different qualitative behaviors for the $\boldsymbol{F}_\gamma^{-\mathrm{T}}$-spheric and $\boldsymbol{F}_\gamma^{-\mathrm{T}}$-deviatoric parts of $\mathfrak{S}_{\boldsymbol{F}_\gamma \boldsymbol{F}_\gamma}$. By looking at the left panel of Figure 5.2, the quantity $\mathsf{S}^{\mathtt{dev}}_{\mathsf{F}_\gamma \mathsf{F}_\gamma}$ increases with time. It measures the influence of the chosen set of transpositional relations onto the volume-preserving part of $\boldsymbol{F}_\gamma$. In particular, $\mathsf{S}^{\mathtt{dev}}_{\mathsf{F}_\gamma \mathsf{F}_\gamma}$ evolves from a state of homogenous distribution to one that is non-homogeneous. On the contrary, by looking at the right panel of Figure 5.2, one can see that the quantity $\mathsf{S}^{\mathtt{sph}}_{\mathsf{F}_\gamma \mathsf{F}_\gamma}$, proportional to the mismatch

between the Lagrange multipliers $\dot{\lambda}$ and μ, decreases with time, and evolves towards a non-homogenous distribution, too. The normalized force $\mathtt{S}^{\mathtt{sph}}_{\mathtt{F}_\gamma\mathtt{F}_\gamma}$ diminishes with time because it scales with the availability of nutrients in the interior of the tumor, which decreases as time goes by, although the nutrients' concentration remains above the critical value $\mathfrak{c}_{\mathrm{cr}}$. The deviatoric force $\mathtt{S}^{\mathtt{dev}}_{\mathtt{F}_\gamma\mathtt{F}_\gamma}$, instead, increases with time because $\boldsymbol{F}_\gamma$ tends to deviate from its initial value, which is a spherical tensor, due to the spatial variability of the nutrients.

5.7 Concluding remarks

This work is the latest of a series of studies [23, 32, 87, 91] devoted to adapt concepts and methods of the analytical mechanics of nonholonomic systems [13, 16, 1] to the continuum mechanics of volumetric growth in biological media.

Our main conclusions can be summarized as follows:

C1. We have developed a *quasi-variational* theory of growth in which the growth law of a body is assigned *a priori*, for example, in compliance with experimental evidences or design choices. This compels to interpret the body's mass balance law as an affine and nonholonomic *constraint* on the time rate of the growth tensor, which is introduced by means of the BKL decomposition. We have *appended* this constraint to the Lagrangian density function of the body, and we have shown that the corresponding dynamic equations can be obtained variationally up to *"polygenic forces"* [11], which have to be considered for a general and physically sound model of growth. To us, this result is noteworthy, because it subsists even though the constraint is nonholonomic. To achieve it, we have started from the dynamic equations supplied by Hamilton's Extended Principle [11] (which are equivalent to those predicted by the Principle of Virtual Work), and we have modified them by introducing the extra forces $\mathfrak{S}_{\boldsymbol{F}_\gamma\boldsymbol{F}}$ and $\mathfrak{S}_{\boldsymbol{F}_\gamma\boldsymbol{F}_\gamma}$ that stem from the transformation rules of the Euler–Lagrange operators when passing from the true velocities to the quasi-velocities of the body. By virtue of these forces, the modified equations remain equivalent to the original ones. Then, we have found that the modified dynamic equations can be made descend from the variational procedure known as Hamilton–Suslov Principle, "corrected" in a fashion similar to Hamilton's Extended Principle,

as shown in Section 5.4.2, Equation (5.70). To do all this, we have taken the *"Modified Vakonomic Method"* MVM by Llibre et al. [16] as a point of departure, and we have reformulated it by considering the extra forces $\mathfrak{S}_{\boldsymbol{F}_\gamma \boldsymbol{F}}$ and $\mathfrak{S}_{\boldsymbol{F}_\gamma \boldsymbol{F}_\gamma}$. These forces must be accounted for to ensure that our formulation of the MVM is consistent with the TNHM [11, 39, 21]. In this regard, we have re-contextualized the work done by Llibre et al. [16] in light of the results provided in [1].

C2. We have compared our reformulation of the MVM with its original version [16] by specializing the latter to the mechanics of a growing medium. Our conclusion is that the original MVM *disagrees* with the TNHM for general growth laws employed in the nonholonomic constraint on the time rate of the growth tensor (see Section 5.5). The discrepancy is due to the fact that, if the procedure by Llibre et al. [16] is strictly followed, the extra forces $\mathbb{W}^{\mathrm{T}}_{\boldsymbol{F}_\gamma \boldsymbol{F}}[\partial_{\dot{\boldsymbol{F}}_\gamma} \hat{\mathcal{L}} \circ \natural] \equiv \mathfrak{S}_{\boldsymbol{F}_\gamma \boldsymbol{F}}$ and $\mathbb{W}^{\mathrm{T}}_{\boldsymbol{F}_\gamma \boldsymbol{F}_\gamma}[\partial_{\dot{\boldsymbol{F}}_\gamma} \hat{\mathcal{L}} \circ \natural] \equiv \mathfrak{S}_{\boldsymbol{F}_\gamma \boldsymbol{F}_\gamma}$, which are produced by the Hamilton–Suslov procedure [60, 61, 16, 1] (cf. with $\mathsf{W}^{\mathrm{T}}\mathsf{p}$ in [1], as well as Chapters 2 and 3), appear only on the left-hand sides of the dynamic equations (5.88c) and (5.88e). Therefore, since no other term balances them, they lead, for an arbitrary growth law, to dynamics that cannot be predicted by the TNHM (indeed, no extra force appears in the TNHM). In particular, $\mathfrak{S}_{\boldsymbol{F}_\gamma \boldsymbol{F}}$ is fully unbalanced, and, although the $\boldsymbol{F}_\gamma^{-\mathrm{T}}$-spherical part of $\mathfrak{S}_{\boldsymbol{F}_\gamma \boldsymbol{F}_\gamma}$ can be incorporated into $\dot{\lambda}$ [16], the $\boldsymbol{F}_\gamma^{-\mathrm{T}}$-deviatoric part of $\mathfrak{S}_{\boldsymbol{F}_\gamma \boldsymbol{F}_\gamma}$ remains unbalanced. Accordingly, to restore the equivalence of the original MVM [16] with the TNHM, $\mathfrak{S}_{\boldsymbol{F}_\gamma \boldsymbol{F}}$ and $\mathrm{DEV}\mathfrak{S}_{\boldsymbol{F}_\gamma \boldsymbol{F}_\gamma}$ must be null. This is the result of our Theorem 5.1. The requirement that $\mathrm{DEV}\mathfrak{S}_{\boldsymbol{F}_\gamma \boldsymbol{F}_\gamma}$ vanishes is coherent with the statement of a theorem [1] that supplies a necessary and sufficient condition for the original MVM [16] to be equivalent to the TNHM for discrete nonholonomic systems. In conclusion, when the Hamilton–Suslov procedure generates extra forces that are both null or that comply with the conditions stated previously, the equivalence between Llibre et al.'s MVM [16] and the TNHM is naturally fulfilled. In fact, the second case is true for the constraints studied in [16, 1], but, in general, not for the constraint considered in this present work.

C3. Since the constraint (5.4) is made nonholonomic by the mass source R, the equivalence conditions between Llibre et al.'s MVM [16] and the TNHM depend entirely on the functional form of $\hat{R}$. Our corollary 5.1 states that such

conditions require $\hat{R}$ to be independent of $\boldsymbol{F}$ and to depend on $\boldsymbol{F}_\gamma$ solely through J_γ. The first restriction can be used for some simple benchmark problems, but it is not realistic for many biological problems in which the growth law must depend on mechanical stress and, thus, on $\boldsymbol{F}$, as is the case for tumor growth models involving *"mechanosensing"* [148, 149] and *"mechanotransduction"* [85, 102]. The second restriction, instead, is often imposed when growth is assumed to be isotropic, as in tumors (see, e.g., [84, 102, 94]), but it should be relaxed when growth is not isotropic, as occurs in heart or skin mechanics (see, e.g., [93] for a review), or, more generally, in fiber-reinforced tissues (see, e.g., [88]). Therefore, these situations cannot be modeled by the original MVM. Nevertheless, our reformulation of the MVM, as presented in Section 5.4, can be adopted, since it is equivalent *by construction* with the TNHM, independently of the assigned growth law. Thus, in all the situations mentioned above, our work is able to provide a quasi-variational theory of growth.

C4. Since our theory is of grade zero in $\boldsymbol{F}_\gamma$, the geometric descriptors induced by $\boldsymbol{F}_\gamma$ are all determined as *outputs* of the dynamic problem. For example, if one solves Equations (5.61a)–(5.61f) in a sufficiently general setting, then, once $\boldsymbol{F}_\gamma$ is computed, one can determine a Riemannian manifold characterized by the metric tensor associated with $\boldsymbol{F}_\gamma$, and the corresponding Levi-Civita connection. This connection and the curvature that it produces are consequences of the forces accounted for in the model *and* of the mass source R given in the constraint, and are, thus, directly related to the bio-physics and bio-chemistry of the body [107]. Analogous considerations hold true, for instance, for the affine connection $\Gamma^A{}_{BC} = (\boldsymbol{F}_\gamma^{-1})^A{}_\alpha(\partial(\boldsymbol{F}_\gamma)^\alpha{}_B/\partial X^C)$.

It is worth noticing that, for the majority of the cases of biological interest, R is such that the constraint on the evolution of $\boldsymbol{F}_\gamma$ cannot be reduced to a holonomic condition. This nonholonomicity in time, in turn, induces the nonholonomicity of $\boldsymbol{F}_\gamma$ in space, and, thus, its incompatibility, especially with respect to its volumetric part, modeled by J_γ. In a previous work of some of us, we have called this type of models *"a priori approach"* [91], since R is prescribed by the phenomenology. Yet, this is not the only possible path. Indeed, one could put no constraints on $\boldsymbol{F}_\gamma$, and let it evolve according to a dynamic problem in which the force $\boldsymbol{Z}$ contains the biological information necessary to trigger and maintain growth [69, 90, 150, 103, 104]. This is what we called *"a posteriori approach"* [91]. In this case, the geometric descriptors

depend on $\boldsymbol{Z}$ and on the constitutive assumptions defining $\boldsymbol{Y}_{\text{ud}}$ and $\boldsymbol{H}$. A similar situation occurs for those models of growth that consider $\boldsymbol{F}_\gamma$ as an internal variable (see, e.g., [73, 88]), in which $\boldsymbol{F}_\gamma$ is introduced as the *"implant"* tensor within a theory of uniformity [140, 73, 112, 118, 79, 125].

However, a different situation is provided by theories of higher grade [79, 151, 124], in which the geometric descriptors, like affine connection and curvature, are part of the augmented kinematics and, thus, part of the solution of the dynamic problem. In this case, these descriptors can lead to even more complicated manifolds.

As a final remark, we would like to emphasize that our formulation of the MVM can be seen as based on an "Extended" Hamilton–Suslov Principle, since it augments the already existing theory by allowing for non-potential forces (cf. with Extend Hamilton's Principle in Section 5.2.2). In particular, the way in which the constraints are handled differs significantly from how Extended Hamilton's Principle operates. Indeed, whereas the latter binds the constraints to merely "polygenic" forces, and equates the first-order variation of the action to the time-integral of the virtual work done by the "reactive" forces, the Extended Hamilton–Suslov Principle directly varies a Lagrangian function that comprehends the constraint by operating variations that are of the Hamilton–Suslov kind [60, 61, 16, 1].

Moreover, it would be interesting to exploit the Extended Hamilton–Suslov Principle to study "broken" symmetries due to growth, and the related loss of conservation laws, by means of an appropriate formulation of Noether's Theorem for nonholonomic systems [63].

Appendix B

Revisiting the charged skate: the quasi-variational approach

In this appendix we revisit and further expand (in light of the results presented by Grillo et al. [2], see Chapter 5) the "charged skate" benchmark problem investigated by Pastore et al. [1] and reported in Section 3.2 of this Thesis. In particular, it is proven that the equivalence between the TNHM and the MVM can be guaranteed by the introduction of appropriate *polygenic forces*, which adapt the quasi-variational procedure put forward by Grillo et al. [2] for growth mechanics to the problem at hand. In fact, with respect to Sections 3.2.3–3.2.5, we might think of this appendix as the "Case D" of the benchmark analysis done in [1].

By referring to the notation employed in Part I, let us rewrite Equations (3.41a)–(3.41c), corresponding to the three dynamic equations for the "charged skate" benchmark provided by the TNHM, in the following form:

$$\underbrace{-\dot{p}_1 + mg\,\sin\alpha + \tfrac{1}{2}QB_0\dot{q}^2}_{=:\,\mathcal{E}_1\hat{\mathcal{L}}\circ\sharp} + \underbrace{\mu_1\,\sin q^3}_{=:\,(\mathsf{A}^{\mathrm{T}}\mu)_1} = 0, \tag{B.1a}$$

$$\underbrace{-\dot{p}_2 - \tfrac{1}{2}QB_0\dot{q}^1}_{=:\,\mathcal{E}_2\hat{\mathcal{L}}\circ\sharp} + \underbrace{(-\mu_1\,\cos q^3)}_{=:\,(\mathsf{A}^{\mathrm{T}}\mu)_2} = 0, \tag{B.1b}$$

$$\underbrace{-\dot{p}_3}_{=:\,\mathcal{E}_3\hat{\mathcal{L}}\circ\sharp} + \underbrace{0}_{=:\,(\mathsf{A}^{\mathrm{T}}\mu)_3} = 0. \tag{B.1c}$$

As put forward in Section 3.2, these dynamic equations are coupled with the nonholonomic constraint in Equation (3.39), reported here for convenience, as

$$\mathcal{V} \equiv \hat{\mathcal{V}} \circ (q, \dot{q}) \coloneqq (\sin q^3)\dot{q}^1 - (\cos q^3)\dot{q}^2 = 0. \tag{B.2}$$

Moreover, we further recall that

$$p_1 = \partial_{\dot{q}^1}\hat{\mathcal{L}} \circ \natural = m\dot{q}^1 - \tfrac{1}{2}QB_0q^2, \tag{B.3}$$
$$p_2 = \partial_{\dot{q}^2}\hat{\mathcal{L}} \circ \natural = m\dot{q}^2 + \tfrac{1}{2}QB_0q^1, \tag{B.4}$$
$$p_3 = \partial_{\dot{q}^3}\hat{\mathcal{L}} \circ \natural = \tfrac{1}{12}m(\ell^2 + \sigma^2)\dot{q}^3 + \tfrac{1}{24}Q(\ell^2 + \sigma^2)B_0 \tag{B.5}$$

are the conjugated momenta (affine in the velocities due to the presence of the magnetic interaction), and, for each $k \in \{1, 2, 3\}$, the quantity $\mathcal{E}_k\hat{\mathcal{L}} \circ \sharp$ represents the kth Euler–Lagrange operator applied to the Lagrangian function of the "charged skate" (see Equation (3.38)).

Following the procedure outlined in [2] and reported in Section 5.4, to show the equivalence between the TNHM and the MVM (granted the presence of non-potential forces) we need to: (i) select a system of quasi-velocities for the problem at hand; (ii) construct the associated collection of transpositional relations, as well as the matrix W; (iii) introduce the generalized forces $(\mathsf{W}^{\mathrm{T}}\mathsf{p})_1$, $(\mathsf{W}^{\mathrm{T}}\mathsf{p})_2$ and $(\mathsf{W}^{\mathrm{T}}\mathsf{p})_3$ characterizing the MVM in our case. In this respect, we select the same auxiliary functions employed in Case A of the "charged skate" benchmark (Section 3.2.3, Equations (3.39), (3.45a) and (3.45b)) since they are the most obvious choice of quasi-velocities for the nonholonomic skate when the interaction with the magnetic field is switched off (see Remark 3.8). This yields the matrix W reported in Equation (3.48) and the collection of generalized forces

$$(\mathsf{W}^{\mathrm{T}}\mathsf{p})_1 = -p_2\dot{q}^3 = -[m\dot{q}^2 + \tfrac{1}{2}QB_0q^1]\dot{q}^3, \tag{B.6a}$$
$$(\mathsf{W}^{\mathrm{T}}\mathsf{p})_2 = +p_1\dot{q}^3 = +[m\dot{q}^1 - \tfrac{1}{2}QB_0q^2]\dot{q}^3, \tag{B.6b}$$
$$(\mathsf{W}^{\mathrm{T}}\mathsf{p})_3 = -p_1\dot{q}^2 + p_2\dot{q}^1 = +\tfrac{1}{2}QB_0[q^1\dot{q}^1 + q^2\dot{q}^2]. \tag{B.6c}$$

Let us add on both sides of Equations (B.1a)–(B.1c) the appropriate terms featuring in (B.6a)–(B.6c), thereby obtaining

$$\mathcal{E}_1\hat{\mathcal{L}} \circ \sharp + (\mathsf{W}^{\mathrm{T}}\mathsf{p})_1 + (\mathsf{A}^{\mathrm{T}}\mu)_1 = (\mathsf{W}^{\mathrm{T}}\mathsf{p})_1, \tag{B.7a}$$

$$\mathcal{E}_2\hat{\mathcal{L}} \circ \sharp + (\mathsf{W}^{\mathrm{T}}\mathsf{p})_2 + (\mathsf{A}^{\mathrm{T}}\mu)_2 = (\mathsf{W}^{\mathrm{T}}\mathsf{p})_2, \tag{B.7b}$$

$$\mathcal{E}_3\hat{\mathcal{L}} \circ \sharp + (\mathsf{W}^{\mathrm{T}}\mathsf{p})_3 \qquad\quad = (\mathsf{W}^{\mathrm{T}}\mathsf{p})_3. \tag{B.7c}$$

Now, we rewrite the terms on the right-hand sides of Equations (B.7a)–(B.7c) in light of the decomposition suggested by Theorem 2.1. Indeed, upon introducing the mass matrix M and the constraint matrix A as

$$\mathsf{M} = \begin{bmatrix} m & 0 & 0 \\ 0 & m & 0 \\ 0 & 0 & \frac{1}{12}m\,(\ell^2+\sigma^2) \end{bmatrix}, \qquad \mathsf{A} = \begin{bmatrix} \sin q_3 & -\cos q_3 & 0 \end{bmatrix}, \tag{B.8}$$

and by having explicit recourse to the *effective velocities* $\mathsf{M}^{-1}\mathsf{p}$ (see Section 3.2.5), we can decompose the array $\mathsf{W}^{\mathrm{T}}\mathsf{p}$ as

$$\mathsf{W}^{\mathrm{T}}\mathsf{p} = \underbrace{[\mathsf{M} - \mathsf{A}^{\mathrm{T}}\mathsf{S}^{-1}\mathsf{A}](\mathsf{M}^{-1}\mathsf{W}^{\mathrm{T}}\mathsf{M})(\mathsf{M}^{-1}\mathsf{p})}_{=:\,\mathfrak{S}} + \underbrace{[\mathsf{A}^{\mathrm{T}}\mathsf{S}^{-1}\mathsf{A}](\mathsf{M}^{-1}\mathsf{W}^{\mathrm{T}}\mathsf{M})(\mathsf{M}^{-1}\mathsf{p})}_{=:\,\mathsf{A}^{\mathrm{T}}\rho}, \tag{B.9}$$

where $\mathsf{S} \coloneqq \mathsf{A}\mathsf{M}^{-1}\mathsf{A}^{\mathrm{T}}$ is the Schur matrix and $\rho \coloneqq \mathsf{S}^{-1}\mathsf{A}(\mathsf{M}^{-1}\mathsf{W}^{\mathrm{T}}\mathsf{M})(\mathsf{M}^{-1}\mathsf{p})$. Equation (B.9) is the counterpart of the force decomposition provided in Equation (5.106a) in the context of growth. In particular, by slightly simplifying the notation, we made the following identifications:

- The quantity "$\mathfrak{S}_{\boldsymbol{F}_\gamma \boldsymbol{F}}$" of Chapter 5 has no counterpart in this benchmark, while "$\mathfrak{S}_{\boldsymbol{F}_\gamma \boldsymbol{F}_\gamma}$" of Chapter 5 is identified with the array $\mathsf{W}^{\mathrm{T}}\mathsf{p}$.
- The quantity "$\mathrm{DEV}\mathfrak{S}_{\boldsymbol{F}_\gamma \boldsymbol{F}_\gamma}$" of Chapter 5 is identified here with $\mathfrak{S}$. In particular, the role played by the projection operator "DEV" is played here by the matrix $\mathsf{M} - \mathsf{A}^{\mathrm{T}}\mathsf{S}^{-1}\mathsf{A}$ and, as a consequence, the relation "$\mathrm{DEV}\mathfrak{S}_{\boldsymbol{F}_\gamma \boldsymbol{F}_\gamma} = \mathfrak{S}_{\boldsymbol{F}_\gamma \boldsymbol{F}_\gamma} - \frac{1}{3}\mathrm{tr}(\boldsymbol{F}_\gamma^{\mathrm{T}}\mathfrak{S}_{\boldsymbol{F}_\gamma \boldsymbol{F}_\gamma})\boldsymbol{F}_\gamma^{-\mathrm{T}}$" is the counterpart of $\mathfrak{S} = \mathsf{W}^{\mathrm{T}}\mathsf{p} - \mathsf{A}^{\mathrm{T}}\rho$ in the context of the problem at hand.
- Finally, the quantity "$\frac{1}{3}\mathrm{tr}(\boldsymbol{F}_\gamma^{\mathrm{T}}\mathfrak{S}_{\boldsymbol{F}_\gamma \boldsymbol{F}_\gamma})\boldsymbol{F}_\gamma^{-\mathrm{T}}$" of Equation (5.59) in Chapter 5 is identified here with the array $\mathsf{A}^{\mathrm{T}}\rho$.

By specializing Equation (B.9) to the case under study, we obtain that S reduces to the 1×1 matrix $\mathsf{S} = [1/m]$, the three components of $\mathfrak{S}$ read

$$\mathfrak{S}_1 = -\tfrac{1}{2}QB_0(\cos q^3)\big(q^1\cos q^3 + q^2\sin q^3\big)\,\dot{q}^3, \tag{B.10a}$$

$$\mathfrak{S}_2 = -\tfrac{1}{2}QB_0(\sin q^3)\big(q^1\cos q^3 + q^2\sin q^3\big)\dot{q}^3, \tag{B.10b}$$
$$\mathfrak{S}_3 = +\tfrac{1}{2}QB_0\left(q^1\dot{q}^1 + q^2\dot{q}^2\right), \tag{B.10c}$$

and the array ρ reduces to the 1×1 array

$$\rho = \left\{-m(\dot{q}^1\cos q^3 + \dot{q}^2\sin q^3)\dot{q}^3 - \tfrac{1}{2}B_0Q(q^1\sin q^3 - q^2\cos q^3)\dot{q}^3\right\}. \tag{B.11}$$

Hence, employing the decomposition $\mathsf{W}^{\mathrm{T}}\mathsf{p} = \mathfrak{S} + \mathsf{A}^{\mathrm{T}}\rho$ in the right-hand sides of (B.7a)–(B.7c), where $(\mathsf{A}^{\mathrm{T}}\rho)_3 \equiv 0$ and $(\mathsf{W}^{\mathrm{T}}\mathsf{p})_3 \equiv \mathfrak{S}_3$ by construction, yields

$$\mathcal{E}_1\hat{\mathcal{L}}\circ\sharp + (\mathsf{W}^{\mathrm{T}}\mathsf{p})_1 + (\mathsf{A}^{\mathrm{T}}\mu)_1 = \mathfrak{S}_1 + (\mathsf{A}^{\mathrm{T}}\rho)_1, \tag{B.12a}$$
$$\mathcal{E}_2\hat{\mathcal{L}}\circ\sharp + (\mathsf{W}^{\mathrm{T}}\mathsf{p})_2 + (\mathsf{A}^{\mathrm{T}}\mu)_2 = \mathfrak{S}_2 + (\mathsf{A}^{\mathrm{T}}\rho)_2, \tag{B.12b}$$
$$\mathcal{E}_3\hat{\mathcal{L}}\circ\sharp + (\mathsf{W}^{\mathrm{T}}\mathsf{p})_3 = \mathfrak{S}_3. \tag{B.12c}$$

We can now make the identifications [2]

$$\dot{\lambda} = \mu - \rho$$
$$\Longrightarrow \dot{\lambda} = \mu + m(\dot{q}^1\cos q^3 + \dot{q}^2\sin q^3)\dot{q}^3 + \tfrac{1}{2}B_0Q(q^1\sin q^3 - q^2\cos q^3)\dot{q}^3. \tag{B.13}$$

This permits us to relate the Lagrange multiplier λ of the MVM, collected in the 1×1 array λ, with the Lagrange multiplier μ of the TNHM, collected in the 1×1 array μ (cf. with Equations (2.55b) and (5.59)). Moreover, according to the provision (B.13), Equations (B.12a)–(B.12c) simplify to

$$\mathcal{E}_1\hat{\mathcal{L}}\circ\sharp + (\mathsf{W}^{\mathrm{T}}\mathsf{p})_1 + (\mathsf{A}^{\mathrm{T}}\dot{\lambda})_1 = \mathfrak{S}_1, \tag{B.14a}$$
$$\mathcal{E}_2\hat{\mathcal{L}}\circ\sharp + (\mathsf{W}^{\mathrm{T}}\mathsf{p})_2 + (\mathsf{A}^{\mathrm{T}}\dot{\lambda})_2 = \mathfrak{S}_2, \tag{B.14b}$$
$$\mathcal{E}_3\hat{\mathcal{L}}\circ\sharp + (\mathsf{W}^{\mathrm{T}}\mathsf{p})_3 = \mathfrak{S}_3. \tag{B.14c}$$

Following the procedure outlined in [2], we can make further progress by computing the weak form of Equations (B.14a)–(B.14c) and (B.2) by multiplying each equation by its dual virtual increment (here, for convenience, we denote the virtual increments by η_q^1, η_q^2, η_q^3 and η_λ), integrating the resulting products over the time interval $[t_{\mathrm{in}}, t_{\mathrm{fin}}]$ and summing the four integrals together. Thus, by noticing

that $(\mathsf{A}^{\mathrm{T}}\dot{\lambda})_3 \equiv 0$ and that $\mathsf{A} \equiv [\partial_{\dot{q}^k}\hat{\mathcal{V}} \circ \natural]_{k=1,2,3}$, the weak form of the system reads

$$\int_{t_{\mathrm{in}}}^{t_{\mathrm{fin}}} \sum_{k=1}^{3} \left\{ \mathcal{E}_k \hat{\mathcal{L}} \circ \sharp + \sum_{h=1}^{3} p_h W^h{}_k + \lambda \left[\frac{\partial \hat{\mathcal{V}}}{\partial \dot{q}^k} \circ \natural \right] \right\} \eta_q^k - \int_{t_{\mathrm{in}}}^{t_{\mathrm{fin}}} [\hat{\mathcal{V}} \circ \natural] \eta_\lambda$$
$$= \int_{t_{\mathrm{in}}}^{t_{\mathrm{fin}}} \sum_{k=1}^{3} \mathfrak{S}_k \eta_q^k. \tag{B.15}$$

By direct inspection of the left-hand side of the weak form (B.15), we can state the following theorem:

Theorem B.1 (Weak form and the Hamilton–Suslov Principle)**.** *By introducing the constrained Lagrangian function and the constrained action functional as [1]*

$$\mathcal{L}_{\mathrm{c}} \equiv \hat{\mathcal{L}}_{\mathrm{c}} \circ \natural_{\mathrm{a}} := \hat{\mathcal{L}} \circ \natural - \lambda[\hat{\mathcal{V}} \circ \natural], \qquad \mathscr{A}_{\mathrm{c}}(q;\lambda) := \int_{t_{\mathrm{in}}}^{t_{\mathrm{fin}}} \mathcal{L}_{\mathrm{c}}(t)\,\mathrm{d}t, \tag{B.16}$$

it holds that the left-hand side of Equation (B.15) *can be obtained by employing the* Hamilton–Suslov variations *[16] to $\mathscr{A}_{\mathrm{c}}(q;\lambda)$ according to the transpositional relations $\eta_{\dot{q}}^k - \dot{\eta}_q^k = \sum_{h=1}^{n} W^k{}_h \eta_q^h$ for $k = 1, \dots, n$. In other words, given the homotopies*

$$q(t) \mapsto \tilde{q}(t,\varepsilon) = q(t) + \boldsymbol{\eta}_q(t)\varepsilon + o(\varepsilon), \qquad \varepsilon \to 0, \tag{B.17a}$$
$$\dot{q}(t) \mapsto \tilde{\boldsymbol{v}}(t,\varepsilon) = \dot{q}(t) + \boldsymbol{\eta}_{\dot{q}}(t)\varepsilon + o(\varepsilon), \qquad \varepsilon \to 0, \tag{B.17b}$$
$$\tau(t) \mapsto \tilde{\tau}(t,\varepsilon) = \tau(t) = t, \qquad \forall \varepsilon > 0, \tag{B.17c}$$
$$\lambda(t) \mapsto \tilde{\lambda}(t,\varepsilon) = \lambda(t) + \eta_\lambda(t)\varepsilon + o(\varepsilon), \qquad \varepsilon \to 0, \tag{B.17d}$$

and the varied constrained action functional

$$\mathscr{A}_{\mathrm{c}}^{\tilde{}}(\varepsilon) := \int_{t_{\mathrm{in}}}^{t_{\mathrm{fin}}} \hat{\mathcal{L}}_{\mathrm{c}}(\tilde{q}(t,\varepsilon), \tilde{\boldsymbol{v}}(t,\varepsilon), \tilde{\tau}(t,\varepsilon); \tilde{\lambda}(t,\varepsilon)), \tag{B.18}$$

it holds true that

$$\frac{\mathrm{d}\mathscr{A}_{\mathrm{c}}^{\tilde{}}}{\mathrm{d}\varepsilon}(0)$$
$$= \int_{t_{\mathrm{in}}}^{t_{\mathrm{fin}}} \sum_{k=1}^{3} \left\{ \mathcal{E}_k \hat{\mathcal{L}} \circ \sharp + \sum_{h=1}^{3} p_h W^h{}_k + \lambda \left[\frac{\partial \hat{\mathcal{V}}}{\partial \dot{q}^k} \circ \natural \right] \right\} \eta_q^k - \int_{t_{\mathrm{in}}}^{t_{\mathrm{fin}}} [\hat{\mathcal{V}} \circ \natural] \eta_\lambda. \tag{B.19}$$

Proof. The procedure that we now use to prove Equation (B.19) is equivalent to that employed in [2] for growth (see Section 5.4.2), although we go through it in reverse order. Explicating $[\mathrm{d}\tilde{\mathscr{A}_{\mathrm{c}}}/\mathrm{d}\varepsilon](0)$ yields the relation (Einstein's notation is used in the following calculations)

$$\begin{aligned}\frac{\mathrm{d}\tilde{\mathscr{A}_{\mathrm{c}}}}{\mathrm{d}\varepsilon}(0) = &\int_{t_{\mathrm{in}}}^{t_{\mathrm{fin}}}\left[\frac{\partial\hat{\mathcal{L}}}{\partial q^k}\circ\natural\right]\eta_q^k + \int_{t_{\mathrm{in}}}^{t_{\mathrm{fin}}}\left[\frac{\partial\hat{\mathcal{L}}}{\partial\dot{q}^k}\circ\natural\right]\eta_{\dot{q}}^k \\ &- \int_{t_{\mathrm{in}}}^{t_{\mathrm{fin}}}\lambda\left[\frac{\partial\hat{\mathcal{V}}}{\partial q^k}\circ\natural\right]\eta_q^k - \int_{t_{\mathrm{in}}}^{t_{\mathrm{fin}}}\lambda\left[\frac{\partial\hat{\mathcal{V}}}{\partial\dot{q}^k}\circ\natural\right]\eta_{\dot{q}}^k - \int_{t_{\mathrm{in}}}^{t_{\mathrm{fin}}}[\hat{\mathcal{V}}\circ\natural]\eta_\lambda. \quad \text{(B.20)}\end{aligned}$$

Moreover, by having explicit recourse to the transpositional relations, it holds that

$$\begin{aligned}\frac{\mathrm{d}\tilde{\mathscr{A}_{\mathrm{c}}}}{\mathrm{d}\varepsilon}(0) = &\int_{t_{\mathrm{in}}}^{t_{\mathrm{fin}}}\left[\frac{\partial\hat{\mathcal{L}}}{\partial q^k}\circ\natural\right]\eta_q^k + \int_{t_{\mathrm{in}}}^{t_{\mathrm{fin}}}\left[\frac{\partial\hat{\mathcal{L}}}{\partial\dot{q}^k}\circ\natural\right](\dot{\eta}_q^k + W^k{}_h\eta_q^h) \\ &- \int_{t_{\mathrm{in}}}^{t_{\mathrm{fin}}}\lambda\left[\frac{\partial\hat{\mathcal{V}}}{\partial q^k}\circ\natural\right]\eta_q^k - \int_{t_{\mathrm{in}}}^{t_{\mathrm{fin}}}\lambda\left[\frac{\partial\hat{\mathcal{V}}}{\partial\dot{q}^k}\circ\natural\right](\dot{\eta}_q^k + W^k{}_h\eta_q^h) \\ &- \int_{t_{\mathrm{in}}}^{t_{\mathrm{fin}}}[\hat{\mathcal{V}}\circ\natural]\eta_\lambda. \quad \text{(B.21)}\end{aligned}$$

By using the integral relations

$$\int_{t_{\mathrm{in}}}^{t_{\mathrm{fin}}}\left[\frac{\partial\hat{\mathcal{L}}}{\partial\dot{q}^k}\circ\natural\right]\dot{\eta}_q^k = -\int_{t_{\mathrm{in}}}^{t_{\mathrm{fin}}}\left[\frac{\mathrm{d}}{\mathrm{d}t}\left(\frac{\partial\hat{\mathcal{L}}}{\partial\dot{q}^k}\circ\natural\right)\right]\eta_q^k, \quad \text{(B.22a)}$$

$$\int_{t_{\mathrm{in}}}^{t_{\mathrm{fin}}}\lambda\left[\frac{\partial\hat{\mathcal{V}}}{\partial\dot{q}^k}\circ\natural\right]\dot{\eta}_q^k = -\int_{t_{\mathrm{in}}}^{t_{\mathrm{fin}}}\lambda\left[\frac{\mathrm{d}}{\mathrm{d}t}\left(\frac{\partial\hat{\mathcal{V}}}{\partial\dot{q}^k}\circ\natural\right)\right]\eta_q^k - \int_{t_{\mathrm{in}}}^{t_{\mathrm{fin}}}\dot{\lambda}\left[\frac{\partial\hat{\mathcal{V}}}{\partial\dot{q}^k}\circ\natural\right]\eta_q^k, \quad \text{(B.22b)}$$

where the hypothesis $\boldsymbol{\eta}_q(t_{\mathrm{in}}) = \boldsymbol{\eta}_q(t_{\mathrm{fin}}) = \mathbf{0}$ is enforced, Equation (B.21) reduces to

$$\begin{aligned}\frac{\mathrm{d}\tilde{\mathscr{A}_{\mathrm{c}}}}{\mathrm{d}\varepsilon}(0) = &\int_{t_{\mathrm{in}}}^{t_{\mathrm{fin}}}[\mathcal{E}_k\hat{\mathcal{L}}\circ\sharp]\eta_q^k + \int_{t_{\mathrm{in}}}^{t_{\mathrm{fin}}}\left[\frac{\partial\hat{\mathcal{L}}}{\partial\dot{q}^k}\circ\natural\right](W^k{}_h\eta_q^h) \\ &- \int_{t_{\mathrm{in}}}^{t_{\mathrm{fin}}}\lambda[\mathcal{E}_k\hat{\mathcal{V}}\circ\sharp]\eta_q^k - \int_{t_{\mathrm{in}}}^{t_{\mathrm{fin}}}\lambda\left[\frac{\partial\hat{\mathcal{V}}}{\partial\dot{q}^k}\circ\natural\right](W^k{}_h\eta_q^h) + \int_{t_{\mathrm{in}}}^{t_{\mathrm{fin}}}\dot{\lambda}\left[\frac{\partial\hat{\mathcal{V}}}{\partial\dot{q}^k}\circ\natural\right]\eta_q^k \\ &- \int_{t_{\mathrm{in}}}^{t_{\mathrm{fin}}}[\hat{\mathcal{V}}\circ\natural]\eta_\lambda. \quad \text{(B.23)}\end{aligned}$$

Equation (B.23) can be further worked out by swapping the repeated indices h and k in the integrals featuring the entries $W^h{}_k$ and by recalling that $p_h = \partial_{\dot{q}^h}\hat{\mathcal{L}}\circ\natural$. This

yields

$$\begin{aligned}\frac{\mathrm{d}\tilde{\mathscr{A}}_{\mathrm{c}}}{\mathrm{d}\varepsilon}(0) = &\int_{t_{\mathrm{in}}}^{t_{\mathrm{fin}}} \left\{ \mathcal{E}_k \hat{\mathcal{L}} \circ \sharp + p_h W^h{}_k + \dot{\lambda} \left[\frac{\partial \hat{\mathcal{V}}}{\partial \dot{q}^k} \circ \natural \right] \right\} \eta_q^k \\ &- \int_{t_{\mathrm{in}}}^{t_{\mathrm{fin}}} \lambda \left\{ \mathcal{E}_k \hat{\mathcal{V}} \circ \sharp + \left[\frac{\partial \hat{\mathcal{V}}}{\partial \dot{q}^h} \circ \natural \right] W^h{}_k \right\} \eta_q^k \\ &- \int_{t_{\mathrm{in}}}^{t_{\mathrm{fin}}} [\hat{\mathcal{V}} \circ \natural] \eta_\lambda . \end{aligned} \tag{B.24}$$

Finally, by recalling that $\mathcal{D}_k \hat{\mathcal{V}} \circ \sharp \equiv \mathcal{E}_k \hat{\mathcal{V}} \circ \sharp + [\partial_{\dot{q}^h} \hat{\mathcal{V}} \circ \natural] W^h{}_k = 0$ (this is due to how W is constructed), Equation (B.19) is retrieved from (B.24). □

By virtue of Theorem B.1, Equation (B.15) can thus be rewritten as

$$\frac{\mathrm{d}\tilde{\mathscr{A}}_{\mathrm{c}}}{\mathrm{d}\varepsilon}(0) = \int_{t_{\mathrm{in}}}^{t_{\mathrm{fin}}} \sum_{k=1}^{3} \mathfrak{S}_k \eta_q^k . \tag{B.25}$$

Equation (B.25) shows that it is possible to *variationally* retrieve the TNHM dynamic equations (B.1a)–(B.1c), as well as the constraint (B.2), characterizing the "charged skate" benchmark by following the Hamilton–Suslov procedure augmented by the presence of the additional polygenic forces $\mathfrak{S}_1$, $\mathfrak{S}_2$ and $\mathfrak{S}_3$ reported in Equations (B.10a)–(B.10c). Note that this amounts to consider the general form of the dynamic equations (2.43a) where the identifications $-\mathcal{Q}_k \equiv \mathfrak{S}_k$ for $k = 1, 2, 3$ are made [2].

Remark B.1 (Equivalence with the TNHM according to Llibre et al. [16]).
According to the variational picture outlined by Llibre et al. [16], in which no polygenic forces are accounted for, the dynamic equations provided by their version of the MVM are

$$\mathcal{E}_1 \hat{\mathcal{L}} \circ \sharp + (\mathsf{W}^{\mathrm{T}}\mathsf{p})_1 + (\mathsf{A}^{\mathrm{T}}\dot{\lambda})_1 = 0, \tag{B.26a}$$

$$\mathcal{E}_2 \hat{\mathcal{L}} \circ \sharp + (\mathsf{W}^{\mathrm{T}}\mathsf{p})_2 + (\mathsf{A}^{\mathrm{T}}\dot{\lambda})_2 = 0, \tag{B.26b}$$

$$\mathcal{E}_3 \hat{\mathcal{L}} \circ \sharp + (\mathsf{W}^{\mathrm{T}}\mathsf{p})_3 = 0. \tag{B.26c}$$

Comparing these equations with the those reported in Equations (B.12a)–(B.12c), it is immediate to see that Llibre et al.'s methodology [16] is equivalent to the TNHM if and only if the forces $\mathfrak{S}_1$, $\mathfrak{S}_2$ and $\mathfrak{S}_3$ are all identically zero. This, in general, depends on the structure of the constraint (and of the choice of the quasi-velocities),

thereby notably limiting the applicability of a fully variational approach (i.e., one in which no polygenic contributions are allowed).

We conclude this remark by noticing that requiring the vanishing of $\mathfrak{S}_1$, $\mathfrak{S}_2$ and $\mathfrak{S}_3$ would amount to requiring the vanishing of the terms reported in Equation (3.51) of Case A (see Section 3.2.3). However, by direct computation, the relations (3.52a) and (3.52b) can be written solely in terms of the forces $\mathfrak{S}_1$, $\mathfrak{S}_2$ and $\mathfrak{S}_3$, i.e.,

$$\begin{aligned}(\cos q^3)(\mathsf{W}^{\mathrm{T}}\mathsf{p})_1 + (\sin q^3)(\mathsf{W}^{\mathrm{T}}\mathsf{p})_2 &= (\cos q^3)\mathfrak{S}_1 + (\sin q^3)\mathfrak{S}_2 \\ &= -\tfrac{1}{2}QB_0[q^1\cos q^3 + q^2\sin q^3]\dot{q}^3, \qquad \text{(B.27a)} \\ (\mathsf{W}^{\mathrm{T}}\mathsf{p})_3 &= \mathfrak{S}_3 \\ &= \tfrac{1}{2}QB_0[q^1\dot{q}^1 + q^2\dot{q}^2], \qquad \text{(B.27b)}\end{aligned}$$

which are in general non-zero.

Chapter 6

A first-gradient approach to the remodeling and the fluid flow in saturated porous media

The content of this chapter is taken from [5].

6.1 Introduction

The mechanical behavior of *soft* and *hydrated* biological tissues is often studied by having recourse to the theory of mixtures [152–154, 127, 155, 139]. Within a minimal modeling approach, a tissue of the aforementioned class may be described as a mixture comprehending a solid phase and a fluid phase [152, 156, 155, 157]. The solid phase idealizes the complex of cells, extracellular matrix, protein links and many other species. The fluid phase represents the tissue's interstitial fluid, mostly consisting of water, macromolecules, nutrients, ions, and various chemical substances or compounds.

In this work, with the terminology "biological tissues" we intend both true tissues (e.g., articular cartilage, muscles, blood vessels or skin) and cultures of cells. Such cultures are often referred to as *multicellular aggregates* and are important to study, through *in vitro* or *in silico* experiments, the mechanical behavior of tumor masses [158, 159] before vascularization begins.

As is common for living matter, biological tissues experience changes of their material properties [160, 83], which can be viewed as the result of the activation of some specific structural degrees of freedom. In general, such changes are dynamically coupled with transformations of morphology and shape, although being virtually independent of those. Given suitable time and length scales, the structural changes may be primarily related to genetics [83], physio-pathological events [161], aging [162], as well as to a variety of possibly concurring stimuli, which include mechanical, chemical, and electromagnetic interactions of the tissue with its surrounding environment.

The structural transformations experienced by a tissue are often conventionally classified on the basis of the phenomena by which they are predominantly characterized (see, e.g., [83]): the uptake or loss of mass, and the structural rearrangements associated with these processes, constitute *growth*; the (usually mass-preserving) reorganization of the internal structure of a tissue is referred to as *remodeling* and pertains, for example, to the transformations of the extracellular matrix or to the breaking and reconstruction of the intercellular bonds [159, 163]; the production of patterns, and the processes yielding the specific morphology and size of a tissue are the primary expressions of *morphogenesis* [164]. Other essential processes for the evolution of a tissue are cellular differentiation and migration.

Although the distinction among growth, remodeling and morphogenesis is not sharp [83], it is possible to determine time scales and experimental settings in which each of these phenomena is preponderant with respect to the others. In the remainder of this work, we concentrate exclusively on remodeling, and we consider the specific case in which it occurs in multicellular aggregates undergoing compression tests [158, 159].

The aforementioned tissutal transformations are often described by a second-order tensor field, termed *remodeling tensor* from here on, that is conceived with the property of being *incompatible*, i.e., not expressible as the Jacobian tensor field of a deformation (see, e.g., the seminal papers by Rodríguez et al. [81], Epstein and Maugin [73], and the works by Vandiver and Goriely [165], Yavari [78], Yavari and Goriely [118], and Goriely [166]). In fact, according to a somewhat standard praxis, the remodeling tensor is taken as one of the factors that decompose multiplicatively the *deformation gradient tensor* of a medium undergoing remodeling, which, instead, is by definition the Jacobian tensor field of the deformation. If such decomposition

features two factors only, the first factor is usually identified with an accommodating tensor field, which is incompatible, too, and compensates for the incompatibility of the remodeling tensor. Often, the accommodating tensor is assumed to describe elastic distortions, whereas the remodeling tensor is attributed intrinsically inelastic nature and is thus said to describe anelastic distortions.

The studies on remodeling available in the literature which we are aware of are mainly developed upon theories of *"grade zero"* [69] in the remodeling tensor. Accordingly, the dependence of the remodeling tensor on the points of a medium is not resolved explicitly by accounting for its gradient, or higher-order derivatives, in the list of the basic variables with which the mathematical models are constructed and, in particular, the constitutive framework is established (see, e.g., [81, 83, 69, 126, 155, 129, 92, 139, 167, 168, 93]). However, theories of remodeling and growth of grade one or higher can also be found, and were proposed, e.g., by Epstein and Maugin [73], Epstein [169, 170], Epstein and Elżanowski [112], Goriely [166], and, later, by Grillo et al. [108] and by Grillo and Di Stefano [23, 32, 91]. Still, to the best of our knowledge, they have not been given the attention that grade-0 theories have received.

Conversely, in plasticity, higher-order effects are well established and studied, since the inclusion of such effects is necessary for capturing size-related phenomena (see, e.g., the review of strain-gradient plasticity by Voyiadjis and collaborators [171]). Theories of plasticity that do not account for the gradients of their inelastic descriptors are unable to recover the stress-strain curves obtained, for example, in indentation, torsion and bending tests for metals at low scales. In biomechanics, however, low-scale mechanical tests on biological tissues are rather common, and assessing the effectiveness of the grade-0 theories of remodeling may become an interesting topic, especially to evaluate when it is convenient to switch to theories of higher grade. Aside from that, the theories of higher order are interesting, at least, for other two reasons: they may unravel boundary effects due to the contact interactions between the tested tissues and the experimental apparatus, and they make it possible to blend the mere phenomenological aspects of remodeling with those pertaining to phase transitions and to the generation of patterns typical of morphogenesis [73]. These are, in fact, our main motivations for undertaking a strain-gradient formulation of remodeling, which we obtain by re-proposing the work by Gurtin and Anand [142] on plasticity in the biomechanical context of the compression tests of multicellular aggregates.

In conjunction with remodeling, another major role on the evolution of the aforementioned systems is played by the interactions between the interstitial fluid and the solid phase. The models of fluid mostly encountered in the literature assume Darcy's law, which is often provided in the form of a linear relation between the velocity of the fluid relative to the solid and the pressure gradient of the fluid. The pressure gradient is multiplied from the left by the permeability tensor, which contains important pieces of information about the pore space and material symmetries of the porous medium under study, and is usually coupled with the deformation [152]. In our work, however, we abandon Darcy's law in favor of an enriched description of the fluid known as Darcy–Brinkman model. Our motivation is twofold. First, in addition to the interactions resolved within the Darcian approach, the Darcy–Brinkman model accounts also for self-interactions of the fluid, resulting in a dissipative contribution to the overall stress tensor, usually taken linear in the fluid velocity gradient. Indeed, due to the presence of macromolecules, nutrients and other substances dissolved in the fluid, the assumption of negligible viscosity may not hold, and the fluid flow may be non-Darcian. Second, at variance with Darcy's law, the Darcy–Brinkman model allows for describing *"boundary effects"* [172, 173]. We mention that, before us, other, pioneering, works employed an extension of Darcy's law, named *Brinkman equation* [174], to study the interstitial flow in biological media [175, 176].

Outline of the content of Chapter 6. This chapter is organized as follows: Section 6.2 presents the relevant modeling hypotheses for hydrated soft tissues, the kinematic framework (with all the considered constraints), and the mass balance laws; Section 3 summarizes all the force balances and the constraints, after formulating the Principle of Virtual Power [137, 138] (PVP) for constrained systems, and for a grade-1 theory both in the remodeling tensor [142] and in the velocity field of the fluid phase (at variance with previous works of our group —see, e.g., [23, 32, 4]— we provide some notions about the functional spaces involved in the formulation); Section 4 presents the constitutive framework; Section 5 shows the initial- and boundary-value problem to be solved and contains a discussion on some numerical results; Section 6 provides some concluding remarks.

6.2 Hydrated soft tissues as biphasic mixtures undergoing remodeling

We present the main hypotheses with which we describe the mechanics of fluid-saturated soft tissues undergoing remodeling of their internal structure. As "representative" for this kind of biological systems we refer to the so-called *"multicellular aggregates"* [159]. These are conglomerates of various types of cultured cells that are typically used in laboratory experiments on the mechanics of tumor spheroids [133]. The latter ones, in turn, inspire mechanical models of the evolution of *in situ* tumors in the stages of their growth that precede vascularization [177, 102].

In the mechanics of multicellular aggregates, it is often assumed that remodeling is a volume-preserving process, thereby requiring the isochoricity of the remodeling tensor. In fact, this requirement defines a constraint [178]. In the remainder of this section, we shall discuss the kinematics of the mechanical system describing our representation of a multicellular aggregate. Attention will be given to the isochoricity constraint imposed on the remodeling tensor and to the implications of such constraint in the mass balance law of each constituent of the aggregate. In particular, the aggregate will be described as a biphasic mixture comprising a porous "solid" constituent —or phase—, represented by cells and extracellular matrix, and an interstitial fluid, which saturates the pores of the solid constituent. Since the theory presented hereafter models a fluid-solid biphasic system as a biphasic mixture resulting from a suitable volume-averaging technique [179, 180], it is referred to as "Hybrid Mixture Theory" [153].

We remark that some parts of the model are unavoidably similar to previous works of our group on similar topics [23, 32, 4], some parts of which were reported in Chapter 5. In particular, the multiplicative decomposition of the deformation gradient tensor, the kinematics of biphasic mixtures and of the essential mass balance laws, as well as the handling of the constraints in Section 6.2.3 and of Chetaev's conditions in Section 6.2.4 expand the treatment of the same subjects outlined by Giammarini et al. [4]. However, in the present work we concentrate on quite a different type of remodeling (of grade 1) and consider a rather different dynamic regime for the fluid phase.

6.2.1 Basic kinematics and notation

Like in previous works of our group [181, 4], the description of the kinematics of the biphasic system under study is taken, with slight modifications, from the works by Quiligotti [146] and Quiligotti et al. [182]. Consistently with these approaches, we admit the existence of a reference placement for the system as a whole [159, 183, 184, 129, 102, 185]. The reference placement is indicated with $\mathscr{B}$ and is assumed to be a (smooth) differentiable manifold hosted in the three-dimensional Euclidean space $\mathscr{S}$. Hence, it holds that $\mathscr{B} \subset \mathscr{S}$. Moreover, we enforce the saturation condition, according to which the pore space of the solid phase is entirely filled with the interstitial fluid. This condition has to be respected at all points of $\mathscr{B}$ and at all times of the time window $\mathscr{I} :=]0, t_e[$, with t_e being the final time of observation of the system. The region of $\mathscr{S}$ occupied by the system at an instant of time $t \in \mathscr{I}$ is denoted by $\mathscr{B}(t) \subset \mathscr{S}$ and is referred to as current placement. In our description, the fluid and the solid coexist in each spatial point $x \in \mathscr{B}(t)$.

We denote by $\chi : \mathscr{B} \times \mathscr{I} \to \mathscr{S}$ the motion of the solid phase, so that $x = \chi(X, t) \in \mathscr{S}$ is the spatial point in which the point $X \in \mathscr{B}$ is mapped at time $t \in \mathscr{I}$. For $t \in \mathscr{I}$, the map $\chi_t \equiv \chi(\,\cdot\,, t) : \mathscr{B} \to \mathscr{S}$ defines a smooth embedding parameterized by time, and the current placement of the mixture is obtained as the image of $\mathscr{B}$ through χ_t, i.e., $\mathscr{B}(t) = \chi_t(\mathscr{B}) = \chi(\mathscr{B}, t)$. We remark that, even though $\mathscr{B}$ is originally associated with the solid constituent [146, 182], the fluid particle occupying a point $x \in \mathscr{B}(t)$ is mapped, at each time $t \in \mathscr{I}$, into the point $X = \hat{\chi}_t^{-1}(x) \in \mathscr{B}$ through the inverse map $\hat{\chi}_t^{-1} : \chi_t(\mathscr{B}) \to \mathscr{B}$, where $\hat{\chi}_t$ is defined as $\hat{\chi}_t : \mathscr{B} \to \chi_t(\mathscr{B})$.

For a given $x \in \mathscr{S}$, $T_x\mathscr{S}$ and $(T_x\mathscr{S})^*$ are the tangent space and the co-tangent space of $\mathscr{S}$ at x. Similarly, for a given point $X \in \mathscr{B}$, $T_X\mathscr{B}$ and $(T_X\mathscr{B})^*$ are the tangent space and the co-tangent space of $\mathscr{B}$ at X. For completeness, we recall that $T\mathscr{B} := \sqcup_{X\in\mathscr{B}} T_X\mathscr{B}$ and $(T\mathscr{B})^* := \sqcup_{X\in\mathscr{B}} (T_X\mathscr{B})^*$ are the tangent bundle and the co-tangent bundle associated with $\mathscr{B}$, respectively. For any given vector space $\mathscr{V}_X$ attached to $X \in \mathscr{B}$, "$\sqcup_{X\in\mathscr{B}} \mathscr{V}_X$" indicates the "disjoint union" of all $\mathscr{V}_X$, for X varying in $\mathscr{B}$ [24]. The same notation is used for vector spaces $\mathscr{V}_x$ attached to $x \in \mathscr{S}$, and we write $T\mathscr{S} = \sqcup_{x\in\mathscr{S}} T_x\mathscr{S}$ and $(T\mathscr{S})^* = \sqcup_{x\in\mathscr{S}} (T_x\mathscr{S})^*$ for the tangent and co-tangent bundles associated with $\mathscr{S}$.

As for the tangent and co-tangent spaces and bundles, here and in the following we adopt the $*$-notation to indicate the dual space $\mathscr{V}^*$ of a generic space $\mathscr{V}$, be it a vector, tensor or functional space. It is, indeed, to emphasize *duality* that, in this work, we denote the co-tangent spaces by $(T_x\mathscr{S})^*$ and $(T_X\mathscr{B})^*$ instead of using the more standard notation $T_x^*\mathscr{S}$ and $T_X^*\mathscr{B}$ (see, e.g., Marsden and Hughes [24]).

We endow $\mathscr{S}$ and $\mathscr{B}$ with the metric tensor fields $\boldsymbol{g}$ and $\boldsymbol{G}$. For each $x \in \mathscr{S}$ and $X \in \mathscr{B}$, $\boldsymbol{g}(x)$ and $\boldsymbol{G}(X)$ can be viewed as the linear maps $\boldsymbol{g}(x) \equiv \boldsymbol{g}_x : T_x\mathscr{S} \to (T_x\mathscr{S})^*$ and $\boldsymbol{G}(X) \equiv \boldsymbol{G}_X : T_X\mathscr{B} \to (T_X\mathscr{B})^*$, i.e., as the spatial and material *musical isomorphisms* that map univocally each vector $\boldsymbol{u} \in T_x\mathscr{S}$ and each vector $\boldsymbol{U} \in T_X\mathscr{B}$ into the co-vectors $\boldsymbol{g}_x\boldsymbol{u} \in (T_x\mathscr{S})^*$ and $\boldsymbol{G}_X\boldsymbol{U} \in (T_X\mathscr{B})^*$, respectively [24]. For instance, given the spatial musical isomorphism $\flat_x : T_x\mathscr{S} \mapsto (T_x\mathscr{S})^*$, it holds that $\boldsymbol{g}_x\boldsymbol{u} = \flat_x(\boldsymbol{u}) \in (T_x\mathscr{S})^*$, for each $\boldsymbol{u} \in T_x\mathscr{S}$. By definition, $\boldsymbol{g}(x)$ and $\boldsymbol{G}(X)$ are invertible, and their inverse maps are given by $\boldsymbol{g}^{-1}(x) \equiv \boldsymbol{g}_x^{-1} : (T_x\mathscr{S})^* \to T_x\mathscr{S}$ and $\boldsymbol{G}^{-1}(X) \equiv \boldsymbol{G}_X^{-1} : (T_X\mathscr{B})^* \to T_X\mathscr{B}$, thereby corresponding to the spatial and material musical isomorphisms that map univocally each co-vector $\boldsymbol{\omega} \in (T_x\mathscr{S})^*$ and each co-vector $\boldsymbol{\Omega} \in (T_X\mathscr{B})^*$ into $\boldsymbol{g}_x^{-1}\boldsymbol{\omega} \in T_x\mathscr{S}$ and $\boldsymbol{G}_X^{-1}\boldsymbol{\Omega} \in T_X\mathscr{B}$, respectively [24]. Also in this case, given the spatial musical isomorphism $\sharp_x : (T_x\mathscr{S})^* \mapsto T_x\mathscr{S}$, the identity $\boldsymbol{g}_x^{-1}\boldsymbol{\omega} = \sharp_x(\boldsymbol{\omega}) \in T_x\mathscr{S}$ applies, for each $\boldsymbol{\omega} \in (T_x\mathscr{S})^*$. It is commonly praxis to say that $\flat_x$ "lowers" indices and $\sharp_x$ "raises" indices.

Before going further, we recall that the metric tensors are often introduced as the tensor maps $\boldsymbol{g}(x) \equiv \boldsymbol{g}_x : T_x\mathscr{S} \times T_x\mathscr{S} \to \mathbb{R}$ and $\boldsymbol{G}(X) \equiv \boldsymbol{G}_X : T_X\mathscr{B} \times T_X\mathscr{B} \to \mathbb{R}$, such that, for any pair of spatial vectors $(\boldsymbol{u}, \boldsymbol{v}) \in T_x\mathscr{S} \times T_x\mathscr{S}$ and for any pair of material vectors $(\boldsymbol{U}, \boldsymbol{V}) \in T_X\mathscr{B} \times T_X\mathscr{B}$, the real numbers $\boldsymbol{g}_x(\boldsymbol{u}, \boldsymbol{v})$ and $\boldsymbol{G}_X(\boldsymbol{U}, \boldsymbol{V})$ are the scalar products between $\boldsymbol{u}$ and $\boldsymbol{v}$ and between $\boldsymbol{U}$ and $\boldsymbol{V}$ generated by the corresponding metrics. With this definition of the metric tensors, it makes no sense to speak of their inverse. When there is no room for confusion, in the remainder of this work we will use interchangeably both the latter definition and the one viewing metric tensors as linear maps between a tangent space and its associated co-tangent space.

Granted all the necessary regularity requirements for χ, we introduce the *deformation gradient tensor* $\boldsymbol{F}(X,t) \coloneqq T\chi_t(X) = D\chi_t(X)$, which is defined as the tangent map of χ_t at X [24], or as the Jacobian tensor of χ_t at X. By construction, $\boldsymbol{F}(X,t)$ is the two-point tensor map $\boldsymbol{F}(X,t) : T_X\mathscr{B} \to T_{\chi(X,t)}\mathscr{S}$. Accordingly, $\boldsymbol{F}(\,\cdot\,,t) : \mathscr{B} \to T\mathscr{S} \otimes (T\mathscr{B})^*$ is, for t varying in $\mathscr{I}$, the two-point tensor field

that associates the deformation gradient tensor $\boldsymbol{F}(X,t)$ with each $X \in \mathscr{B}$. At each pair $(X,t) \in \mathscr{B} \times \mathscr{I}$, the tensor $\boldsymbol{F}(X,t)$ is non-singular, and its determinant $J(X,t) \coloneqq \det \boldsymbol{F}(X,t)$ is strictly positive.

The remodeling tensor, hereafter denoted by $\boldsymbol{F}_\gamma(X,t)$, is introduced by having recourse to the Bilby–Kröner–Lee (BKL) decomposition of the deformation gradient tensor $\boldsymbol{F}(X,t)$ into an elastic (or accommodating) part and an anelastic (remodeling) part [109], i.e.,

$$\boldsymbol{F}(X,t) = \boldsymbol{F}_{\mathrm{e}}(X,t)\boldsymbol{F}_\gamma(X,t), \qquad (X,t) \in \mathscr{B} \times \mathscr{I}. \tag{6.1}$$

The tensor fields $\boldsymbol{F}_{\mathrm{e}}$ and $\boldsymbol{F}_\gamma$ have the property of being non-integrable, that is, none of them reduces, in general, to the Jacobian tensor field of a deformation map. Rather, $\boldsymbol{F}_\gamma$ represents the distortions induced by the process of remodeling, while $\boldsymbol{F}_{\mathrm{e}}$ is the accommodating tensor field that describes the elastic distortions necessary to restore the integrability of $\boldsymbol{F}$. Both $\boldsymbol{F}_{\mathrm{e}}$ and $\boldsymbol{F}_\gamma$ are non-singular for all pairs $(X,t) \in \mathscr{B} \times \mathscr{I}$ and their determinants $J_{\mathrm{e}} \coloneqq \det \boldsymbol{F}_{\mathrm{e}}$ and $J_\gamma \coloneqq \det \boldsymbol{F}_\gamma$ are strictly positive. Moreover, the Cauchy–Binet formula yields $J = J_{\mathrm{e}} J_\gamma$.

The remodeling tensor field $\boldsymbol{F}_\gamma$ can be viewed as the tissue-scale descriptor of the structural reorganizations that occur at different scales of a tissue, including those characterizing intercellular interactions. Moreover, $\boldsymbol{F}_\gamma$ relates the configurational changes of the microstructure of a medium that undergoes remodeling to the alterations in the medium's mechanical and hydraulic properties. In the terminology of DiCarlo and Quiligotti [69], $\boldsymbol{F}_\gamma(X,t)$ operates incompatible transformations on the *"body element"* $T_X\mathscr{B}$ in order to (virtually) mold it, at each instant of time $t \in \mathscr{I}$, into a relaxed and stress-free state. The result of these transformations is referred to as the *natural state* of $T_X\mathscr{B}$ at $t \in \mathscr{I}$, and can be identified with the image of $T_X\mathscr{B}$ through $\boldsymbol{F}_\gamma(X,t)$ [166], i.e., $\mathscr{N}_X(t) \coloneqq \boldsymbol{F}_\gamma(X,t)[T_X\mathscr{B}]$ (square brackets are used to emphasize that $\boldsymbol{F}_\gamma(X,t)$ operates linearly on the vectors of $T_X\mathscr{B}$). Hence, we may write $\boldsymbol{F}_\gamma(X,t) : T_X\mathscr{B} \to \mathscr{N}_X(t)$ and, consequently, $\boldsymbol{F}_{\mathrm{e}}(X,t) : \mathscr{N}_X(t) \to T_{\chi(X,t)}\mathscr{B}(t)$. Finally, the natural state at time $t \in \mathscr{I}$ of the body as a whole is obtained as the vector bundle collecting the natural states of all body elements, i.e., $\mathscr{N}(t) \coloneqq \sqcup_{X \in \mathscr{B}} \mathscr{N}_X(t)$.

To simplify the mathematical formulation, we make the hypothesis that $\mathscr{N}_X(t)$ is *"the relaxed version of* $T_X\mathscr{B}$*"* [4]. It is, thus, possible to identify $\boldsymbol{F}_\gamma$ with a mixed, but (formally) not two-point, tensor field. This way, the forthcoming calculations

gain the notational advantage of avoiding the introduction of an additional family of indices pertaining solely to the natural state, and uppercase Latin indices, proper of the reference placement, can be used to denote the components of $\boldsymbol{F}_\gamma$, as we now proceed to describe.

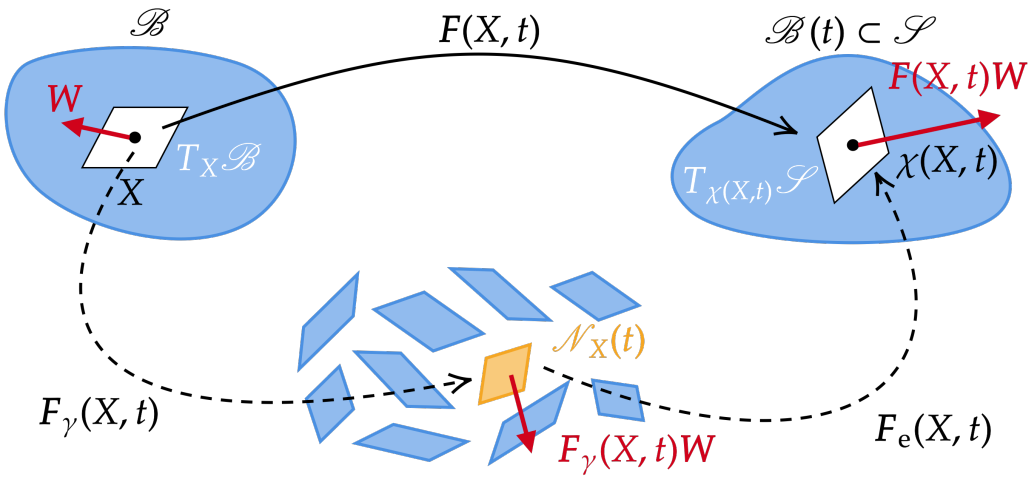

Fig. 6.1 Graphical representation of the Bilby–Kröner–Lee (BKL) decomposition of the deformation gradient tensor $\boldsymbol{F}(X,t)$. This image was first showed during the conference "XI International Conference on Computational Bioengineering (ICCB 2025)" held in Rome, Italy, on September 8-10, 2025, within the presentation of the abstract "Coupling inelastic distortions and Darcy–Brinkman fluid flow in the modeling of multicellular aggregates under compression", authored by A. Pastore, A. Giammarini, A. Ramírez-Torres, A. Grillo.

Given a point $X \in \mathscr{B}$, and by denoting by $\{\boldsymbol{E}_A(X)\}_{A=1}^3$ a basis of $T_X\mathscr{B}$ and by $\{\boldsymbol{E}^B(X)\}_{B=1}^3$ the dual basis of $(T_X\mathscr{B})^*$ (thus, $\boldsymbol{E}^B(X)[\boldsymbol{E}_A(X)] = \delta^B{}_A$, with $\delta^B{}_A$ being the Kronecker delta), $\boldsymbol{F}_\gamma(X,t)$ can be represented as $\boldsymbol{F}_\gamma(X,t) = [\boldsymbol{F}_\gamma(X,t)]^A{}_B\,\boldsymbol{E}_A(X)\otimes\boldsymbol{E}^B(X)$ and its time derivative $\dot{\boldsymbol{F}}_\gamma(X,t)$ is given by $\dot{\boldsymbol{F}}_\gamma(X,t) = [\dot{\boldsymbol{F}}_\gamma(X,t)]^A{}_B\,\boldsymbol{E}_A(X)\otimes\boldsymbol{E}^B(X)$. Furthermore, the components of the material gradient $\mathrm{Grad}\boldsymbol{F}_\gamma$ are identified with the components of the covariant derivative of $\boldsymbol{F}_\gamma$, i.e.,

$$\big[\mathrm{Grad}\boldsymbol{F}_\gamma\big]^A{}_{BC} = \frac{\partial[\boldsymbol{F}_\gamma]^A{}_B}{\partial X^C} + [\boldsymbol{F}_\gamma]^L{}_B\Gamma^A{}_{LC} - [\boldsymbol{F}_\gamma]^A{}_L\Gamma^L{}_{BC}. \tag{6.2}$$

Here, $\Gamma^R{}_{ST}$ are the Christoffel symbols associated with the material connection induced by $\boldsymbol{G}$ [186]. Throughout this work, Christoffel symbols are symmetric in the second and third (lower) indices, so that $\Gamma^R{}_{ST} = \Gamma^R{}_{TS}$, for all $R,S,T \in \{1,2,3\}$.

For the forthcoming discussions, also the material curl of $\boldsymbol{F}_\gamma$ will be relevant, i.e.,

$$\left[\mathrm{Curl}\boldsymbol{F}_\gamma\right]^{DA} \coloneqq \frac{1}{\sqrt{\det[\boldsymbol{G}]}}\epsilon^{DCB}\left[\mathrm{Grad}\boldsymbol{F}_\gamma\right]^{A}{}_{BC}, \tag{6.3}$$

where ϵ is the Levi–Civita symbol and $\det[\boldsymbol{G}]$ is the determinant of the matrix associated with the material metric tensor $\boldsymbol{G}$ (see, e.g., the work by Bîrsan and Neff [187]). Moreover, it is possible to introduce a kinematic quantity, constructed upon $\boldsymbol{F}_\gamma$ and $\mathrm{Curl}\boldsymbol{F}_\gamma$, which is invariant under smooth changes of the reference placement. This quantity is referred to as *Burgers tensor field* [188, 142] and reads

$$\mathfrak{B} \coloneqq J_\gamma^{-1}\boldsymbol{F}_\gamma\mathrm{Curl}\boldsymbol{F}_\gamma, \qquad [\mathfrak{B}]^{AB} = J_\gamma^{-1}[\boldsymbol{F}_\gamma]^{A}{}_{C}[\mathrm{Curl}\boldsymbol{F}_\gamma]^{CB}. \tag{6.4}$$

In accordance with the formulation of elasto-plasticity in finite deformations of Gurtin and Anand [142], we introduce the rate of the remodeling tensor field $\boldsymbol{L}_\gamma \coloneqq \dot{\boldsymbol{F}}_\gamma\boldsymbol{F}_\gamma^{-1}$, and we extract its symmetric and skew-symmetric parts with respect to the metric tensor field $\boldsymbol{G}$, i.e., $\boldsymbol{D}_\gamma = \mathrm{Sym}(\boldsymbol{G}\boldsymbol{L}_\gamma)$ and $\boldsymbol{W}_\gamma = \mathrm{Skew}(\boldsymbol{G}\boldsymbol{L}_\gamma)$. We refer to $\boldsymbol{D}_\gamma$ and $\boldsymbol{W}_\gamma$ as the *remodeling stretch rate* and the *remodeling spin tensor fields*. Finally, we introduce the anelastic Cauchy–Green deformation tensor field $\boldsymbol{C}_\gamma \coloneqq \boldsymbol{F}_\gamma^{\mathrm{T}}\boldsymbol{G}\boldsymbol{F}_\gamma$, its inverse $\boldsymbol{B}_\gamma \coloneqq \boldsymbol{C}_\gamma^{-1}$, and the elastic Cauchy–Green deformation tensor field $\boldsymbol{C}_\mathrm{e} \coloneqq \boldsymbol{F}_\mathrm{e}^{\mathrm{T}}\boldsymbol{g}\boldsymbol{F}_\mathrm{e}$.

In the remainder of this work, we will introduce spaces of tensor fields that, when expressed in components, may have contravariant, covariant or mixed indices. By assuming that the spaces under consideration refer all to the tangent bundle $T\mathscr{B}$ and/or to the co-tangent bundle $(T\mathscr{B})^*$ associated with the system's reference placement, we denote by $[T\mathscr{B}]^n$ the space of tensor fields that, decomposed in a given tensor basis, have $n \in \mathbb{N}$ contravariant components, with $n \geq 1$. Analogously, we write $[T\mathscr{B}]_n$ to indicate the space of tensor fields with n covariant components. For instance, the metric tensor field $\boldsymbol{G}$ can be understood as the map $\boldsymbol{G} : X \in \mathscr{B} \mapsto \boldsymbol{G}(X) \in [T_X\mathscr{B}]_2$ that associates each point X of $\mathscr{B}$ with the second-order tensor $\boldsymbol{G}(X)$ having covariant components and representing the metric at X. Analogously, it holds that $\boldsymbol{G}^{-1}(X) \in [T_X\mathscr{B}]^2$. In addition, the space of tensor fields having the first $n \geq 1$ indices of contravariant type and the second $m \geq 1$ indices of covariant type is given by $[T\mathscr{B}]^n{}_m$, whereas $[T\mathscr{B}]_n{}^m$ represents the opposite situation in which the first $n \geq 1$ indices are covariant and the second $m \geq 1$ indices are contravariant. Examples are $[T\mathscr{B}]^1{}_2 = T\mathscr{B} \otimes (T\mathscr{B})^* \otimes (T\mathscr{B})^*$ and $[T\mathscr{B}]_1{}^2 = (T\mathscr{B})^* \otimes T\mathscr{B} \otimes T\mathscr{B}$.

A similar notation can be used for the spaces of tensor fields involving the tangent bundle $T\mathscr{S}$ and/or the co-tangent bundle $(T\mathscr{S})^*$. The spatial metric tensor field, in fact, is represented by the map $\boldsymbol{g} : x \in \mathscr{S} \mapsto \boldsymbol{g}(x) \in [T_x\mathscr{S}]_2$, so that, for each $x \in \mathscr{S}$, $\boldsymbol{g}(x)$ is the second-order tensor with covariant components denoting the metric at x. Moreover, as for the inverse of the material metric tensor, it holds that $\boldsymbol{g}^{-1}(x) \in [T_x\mathscr{S}]^2$. For two-point tensor fields, like the deformation gradient $\boldsymbol{F}$ or the first Piola–Kirchhoff stress tensor fields of the solid and of the fluid phase, i.e., $\boldsymbol{P}_\mathrm{s}$ and $\boldsymbol{P}_\mathrm{f}$, we write $\boldsymbol{F} \in T\mathscr{S} \otimes (T\mathscr{B})^*$ and $\boldsymbol{P}_\mathrm{s}, \boldsymbol{P}_\mathrm{f} \in (T\mathscr{S})^* \otimes T\mathscr{B}$.

We emphasize that in our model the remodeling tensor $\boldsymbol{F}_\gamma$ is regarded as a *configurational* [10] kinematic descriptor taking into account the evolution of the medium's microstructure. Specifically, we re-formulate the "first-neighbor" approach by Gurtin and Anand [142], used in finite plasticity, within the context of the remodeling of biological mixtures.

A comment on $\mathrm{Curl}\boldsymbol{F}_\gamma$

Equation (6.3) provides the covariant definition of $\mathrm{Curl}\boldsymbol{F}_\gamma$, since it employs the covariant material gradient of $\boldsymbol{F}_\gamma$, and is thus valid in any coordinate system. In Cartesian coordinates, the Christoffel symbols are null, $\det[\boldsymbol{G}] = 1$, and, consequently, the definition of $\mathrm{Curl}\boldsymbol{F}_\gamma$ becomes identical to the one given by Gurtin and Anand [18]. In this case, if $\boldsymbol{F}_\gamma$ happens to be the Jacobian tensor of some sufficiently regular deformation-like map φ, so that $[\boldsymbol{F}_\gamma]^A{}_B = \partial\varphi^A/\partial X^B$, then $\mathrm{Curl}\boldsymbol{F}_\gamma$ vanishes by virtue of Schwartz's Theorem, i.e., $[\mathrm{Curl}\boldsymbol{F}_\gamma]^{DA} = \epsilon^{DCB}\partial^2\varphi^A/\partial X^B\partial X^C = 0$, for all $D, A = 1, 2, 3$.

This conclusion, however, is less immediate when the covariant gradient of $\boldsymbol{F}_\gamma$ is used. Indeed, even by setting $[\boldsymbol{F}_\gamma]^A{}_B = \partial\varphi^A/\partial X^B$ and enforcing the symmetry property of the Christoffel symbols, say $\Gamma^P{}_{BC}$, in the lower indices B and C, Equation (6.3) returns

$$\big[\mathrm{Curl}\boldsymbol{F}_\gamma\big]^{DA} = \frac{1}{\sqrt{\det[\boldsymbol{G}]}}\epsilon^{DCB}[\boldsymbol{F}_\gamma]^L{}_B\Gamma^A{}_{LC} = \frac{1}{\sqrt{\det[\boldsymbol{G}]}}\epsilon^{DCB}\frac{\partial\varphi^L}{\partial X^B}\Gamma^A{}_{LC}, \quad (6.5)$$

which, to be zero, requires the symmetry of $(\partial\varphi^L/\partial X^B)\Gamma^A{}_{LC}$ in the indices B and C. Yet, this is in general not the case unless it holds that $\partial\varphi^L/\partial X^B = c\,\delta^L{}_B$, for some

$c \in]0, +\infty[$, which yields (for $c = 1$)

$$\left[\mathrm{Curl}\boldsymbol{F}_\gamma\right]^{DA} = \frac{1}{\sqrt{\det[\boldsymbol{G}]}}\epsilon^{DCB}\delta^{L}{}_{B}\Gamma^{A}{}_{LC} = \frac{1}{\sqrt{\det[\boldsymbol{G}]}}\epsilon^{DCB}\Gamma^{A}{}_{BC} = 0, \tag{6.6}$$

since $\Gamma^{A}{}_{BC} = \Gamma^{A}{}_{CB}$.

The non-vanishing of $[\mathrm{Curl}\boldsymbol{F}_\gamma]^{DA}$ in Equation (6.5) follows from regarding the generic basis vector field $\boldsymbol{E}_L$ of the decomposition $\boldsymbol{F}_\gamma = [\boldsymbol{F}_\gamma]^{L}{}_{M}\boldsymbol{E}_L \otimes \boldsymbol{E}^M$ as a function of X, so that its partial derivatives are given by

$$\frac{\partial \boldsymbol{E}_L}{\partial X^C} = \Gamma^{A}{}_{LC}\boldsymbol{E}_A, \qquad \text{with } L, C = 1, 2, 3. \tag{6.7}$$

On the other hand, if $\boldsymbol{F}_\gamma$ is to be identified with the Jacobian tensor field $D\psi$ of a C^2 map ψ, which defines a transformation of $\mathscr{B}$ into a new placement $\tilde{\mathscr{B}} := \psi(\mathscr{B})$, as is the case for configurational changes (see, e.g., the work by Grillo et al. [77] and Federico et al. [110]), then $\boldsymbol{F}_\gamma$ is naturally represented by a two-point tensor field and its decomposition reads

$$\boldsymbol{F}_\gamma = D\psi = \frac{\partial \psi^\alpha}{\partial X^B}[\mathfrak{e}_\alpha \circ \psi] \otimes \boldsymbol{E}^B, \qquad D\psi(X) : T_X\mathscr{B} \to T_{\psi(X)}\tilde{\mathscr{B}}, \tag{6.8}$$

where $\{\mathfrak{e}_\alpha(\psi(X))\}_{\alpha=1}^{3} \subset T_{\psi(X)}\tilde{\mathscr{B}}$ is a basis of the tangent space $T_{\psi(X)}\tilde{\mathscr{B}}$. Accordingly, the components of the covariant material gradient of $\boldsymbol{F}_\gamma$ become

$$[\mathrm{Grad}\boldsymbol{F}_\gamma]^{\alpha}{}_{BC} = [\mathrm{Grad}\, D\psi]^{\alpha}{}_{BC} = \frac{\partial^2 \psi^\alpha}{\partial X^B \partial X^C} + \frac{\partial \psi^\lambda}{\partial X^B}\gamma^{\alpha}{}_{\lambda\mu}\frac{\partial \psi^\mu}{\partial X^C} - \frac{\partial \psi^\alpha}{\partial X^D}\Gamma^{D}{}_{BC}, \tag{6.9}$$

with $\gamma^{\alpha}{}_{\lambda\mu}$ being the Christoffel symbols, composed with ψ, generated by the differentiation of the generic basis vector field $\mathfrak{e}_\alpha$ with respect to the coordinates (locally) covering $\tilde{\mathscr{B}}$. Hence, unlike Equation (6.5), the components of $\mathrm{Curl}\boldsymbol{F}_\gamma$ are given by

$$\begin{aligned}[\mathrm{Curl}\boldsymbol{F}_\gamma]^{D\alpha} &= \frac{1}{\sqrt{\det[\boldsymbol{G}]}}\epsilon^{DCB}[\mathrm{Grad}\, D\psi]^{\alpha}{}_{BC} \\ &= \frac{1}{\sqrt{\det[\boldsymbol{G}]}}\epsilon^{DCB}\frac{\partial \psi^\lambda}{\partial X^B}\gamma^{\alpha}{}_{\lambda\mu}\frac{\partial \psi^\mu}{\partial X^C} = 0\end{aligned} \tag{6.10}$$

(see also the work by Bonet et al. [189], in which the definition of the curl of a second-order tensor field is the transpose of the one adopted by Gurtin and Anand [142]). Indeed, while the first term and the third term on the right-hand side of Equation (6.9) do not contribute to $[\mathrm{Curl}\boldsymbol{F}_\gamma]^{D\alpha}$ because of Schwartz's Theorem and because of the symmetry of the Christoffel symbols $\Gamma^D{}_{BC}$ in the indices B and C, the second term yields the vanishing of $[\mathrm{Curl}\boldsymbol{F}_\gamma]^{D\alpha}$ since the symmetry of $\gamma^\alpha{}_{\lambda\mu}$ in the indices λ and μ makes it symmetric in B and C, too, for each $\alpha = 1, 2, 3$.

Finally, we consider the case in which $\boldsymbol{F}_\gamma$ is given by $\boldsymbol{F}_\gamma = \boldsymbol{M}_\gamma D\psi$, where ψ and $D\psi$ are defined as before and $\boldsymbol{M}_\gamma(\tilde{X}, t) : T_{\tilde{X}}\mathscr{B} \to \mathscr{N}_{\tilde{X}}(t)$ is intrinsically incompatible, unless it trivially reduces to the identity tensor $\boldsymbol{I}$ from $T_{\tilde{X}}\tilde{\mathscr{B}}$ into itself (see, e.g., the work by Ciancio et al. [190]). According to this decomposition of $\boldsymbol{F}_\gamma$, $\boldsymbol{F}_\gamma$ is a two-point tensor with components $[\boldsymbol{F}_\gamma]^\alpha{}_B = [\boldsymbol{M}_\gamma]^\alpha{}_\beta\,(\partial\psi^\beta/\partial X^B)$ and $\mathrm{Curl}\boldsymbol{F}_\gamma$ vanishes when $\boldsymbol{M}_\gamma = \boldsymbol{I}$.

Note that, however, when we say that $\boldsymbol{F}_\gamma$ is a "mixed, but (formally) not two-point, tensor field", we are considering the opposite situation, in which $\boldsymbol{F}_\gamma$ is intrinsically incompatible and, thus, coinciding with $\boldsymbol{M}_\gamma$ up to an unessential shift from $T_X\mathscr{B}$ to $T_{\tilde{X}}\tilde{\mathscr{B}}$. This condition, in fact, is met by considering the trivial maps $\psi^\beta(X) := \delta^\beta{}_B X^B + c_0^\beta$, where $\delta^\beta{}_B$ are the components of the shifter operator [24] and c_0^β are real constants (which may be taken to be null). Hence, by disregarding the unessential shifter and using uppercase indices only, our approach amounts to taking $\boldsymbol{F}_\gamma$ as the fully incompatible element of the class of tensors of the type $\boldsymbol{M}_\gamma D\psi$. Hence, granted the identification $\boldsymbol{F}_\gamma \equiv \boldsymbol{M}_\gamma$, $\mathrm{Curl}\boldsymbol{F}_\gamma$ is non-null and the case in which it reduces to the Jacobian tensor field of a deformation-like map is excluded.

6.2.2 Mass balances and the mixture incompressibility constraint

We model the multicellular aggregate under study as a biphasic mixture, comprising a soft solid phase and an interstitial fluid. To account for the mass balance of each phase, we introduce the *intrinsic* mass densities ϱ_s and ϱ_f, the volumetric fractions ϕ_s and ϕ_f, the *apparent* mass densities $\rho_\mathrm{s} := \phi_\mathrm{s}\varrho_\mathrm{s}$ and $\rho_\mathrm{f} := \phi_\mathrm{f}\varrho_\mathrm{f}$, as well as the apparent density of the mixture $\rho = \rho_\mathrm{s} + \rho_\mathrm{f}$. The volumetric fractions are regarded as real-valued, non-negative functions of the current placement fulfilling the *saturation* condition $\phi_\mathrm{s}(x, t) + \phi_\mathrm{f}(x, t) = 1$ for all pairs $(x, t) \in \mathscr{B}(t) \times \mathscr{I}$. Hence, we can write $\phi_\mathrm{s}(\,\cdot\,, t) : \mathscr{B}(t) \to [0, 1]$ and $\phi_\mathrm{f}(\,\cdot\,, t) : \mathscr{B}(t) \to [0, 1]$. We require ϱ_s and ϱ_f to be

constant, so that the evolution of the apparent mass densities ρ_s and ρ_f is entirely due to the variations of the volumetric fractions ϕ_s and $\phi_\mathrm{f} = 1 - \phi_\mathrm{s}$.

In our model we neglect growth, be it volumetric or appositional, and, in general, any phenomena representing mass exchanges between the phases. Under this assumption, and dropping the constant intrinsic mass densities, the mass balance equations for the biphasic mixture read

$$\partial_t \phi_\mathrm{s} + \mathrm{div}(\phi_\mathrm{s} \boldsymbol{v}_\mathrm{s}) = 0, \qquad \text{in } \mathscr{B}(t), \tag{6.11a}$$

$$\partial_t \phi_\mathrm{f} + \mathrm{div}(\phi_\mathrm{f} \boldsymbol{v}_\mathrm{f}) = 0, \qquad \text{in } \mathscr{B}(t), \tag{6.11b}$$

where $\boldsymbol{v}_\mathrm{s}$ and $\boldsymbol{v}_\mathrm{f}$ denote the velocity fields of the solid and fluid phases, respectively. Summing Equations (6.11a) and (6.11b) yields the so-called *"mixture incompressibility condition"* [180], which is given by

$$\mathrm{div}(\phi_\mathrm{s} \boldsymbol{v}_\mathrm{s} + \phi_\mathrm{f} \boldsymbol{v}_\mathrm{f}) = 0, \qquad \text{in } \mathscr{B}(t). \tag{6.12}$$

By introducing the substantial derivative operator with respect to the velocity of the solid phase, i.e., $\mathrm{D}_\mathrm{s} f := \partial_t f + (\mathrm{grad} f)\boldsymbol{v}_\mathrm{s}$, with f being a differentiable scalar function, Equation (6.11a) can be recast in the form $\mathrm{D}_\mathrm{s}\phi_\mathrm{s} + \phi_\mathrm{s}\mathrm{div}\boldsymbol{v}_\mathrm{s} = 0$. Moreover, upon denoting by $\mathcal{T} : \mathscr{B} \times \mathscr{I} \to \mathscr{I}$ the time-projection map [24, 191], defined such that $(X, t) \mapsto \mathcal{T}(X, t) = t$, and recalling the identity $\dot{J} = J[\mathrm{div}\boldsymbol{v}_\mathrm{s} \circ (\chi, \mathcal{T})]$, we can compute the solid phase volumetric fractions associated with the natural state and with the reference placement as $\Phi_{\mathrm{s}\nu} := J_\mathrm{e}[\phi_\mathrm{s} \circ (\chi, \mathcal{T})]$ and $\Phi_{\mathrm{sR}} := J[\phi_\mathrm{s} \circ (\chi, \mathcal{T})] = J_\gamma \Phi_{\mathrm{s}\nu}$, respectively. The composition of functions, expressed by the symbol "$\circ$", gives $f(X, t) = [\hat{f} \circ h](X, t) = \hat{f}(h(X, t))$, for any triple of functions f, $\hat{f}$, and h. Note that h can also be a collection of functions defined in $\mathscr{B} \times \mathscr{I}$, as is the case for $(\chi, \mathcal{T})$. Then, we obtain

$$\dot{\Phi}_{\mathrm{sR}} = \dot{\overline{J_\gamma \Phi_{\mathrm{s}\nu}}} = 0 \quad \Longrightarrow \quad J_\gamma\{\dot{\Phi}_{\mathrm{s}\nu} + \Phi_{\mathrm{s}\nu}\mathrm{tr}(\boldsymbol{F}_\gamma^{-1}\dot{\boldsymbol{F}}_\gamma)\} = 0, \tag{6.13}$$

where $\Phi_{\mathrm{s}\nu}$ and Φ_{sR} are the backward Piola transformations of ϕ_s to the natural state and to the reference placement of the medium, respectively. In particular, Equation (6.13) prescribes that Φ_{sR} is constant in time, and that $\Phi_{\mathrm{s}\nu}$ can be obtained as $\Phi_{\mathrm{s}\nu} = J_\gamma^{-1}\Phi_{\mathrm{sR}}$. In fact, this expression of $\Phi_{\mathrm{s}\nu}$ is the solution to Equation (6.13). Moreover, if Φ_{sR} is regarded as given, e.g., in terms of the (initial) distribution of

the solid phase in the medium's reference placement, then $\Phi_{s\nu}$ describes how the volumetric fraction of the solid phase evolves in response to the volumetric anelastic distortions, modeled by J_γ.

The condition of incompressibility (6.12) can be pulled back to $\mathscr{B}$ and recast in the two equivalent forms

$$\dot{J} + \mathrm{Div}[\Phi_{fR}(\boldsymbol{V}_f - \boldsymbol{V}_s)\boldsymbol{F}^{-T}] = 0, \qquad \text{in } \mathscr{B}, \tag{6.14a}$$

$$\mathrm{Div}[(\Phi_{sR}\boldsymbol{V}_s + \Phi_{fR}\boldsymbol{V}_f)\boldsymbol{F}^{-T}] = 0, \qquad \text{in } \mathscr{B}, \tag{6.14b}$$

where $\Phi_{fR} \coloneqq J - \Phi_{sR}$ is the volumetric fraction of the fluid phase per unit volume of $\mathscr{B}$, while $\boldsymbol{V}_s \coloneqq \boldsymbol{v}_s \circ (\chi, \mathcal{T})$ and $\boldsymbol{V}_f \coloneqq \boldsymbol{v}_f \circ (\chi, \mathcal{T})$ are the velocity fields of the solid and of the fluid phase defined over $\mathscr{B} \times \mathscr{I}$. In spite of their being one equivalent to the other, Equations (6.14a) and (6.14b) will be handled in a different way. Indeed, Equation (6.14a) represents the *condition of incompressibility* as typically handled in the mechanics of porous media, whereas Equation (6.14b) expresses how such condition *constrains* the velocities of the solid and of the fluid phase and, in the forthcoming sections, it will be used to perform the variations on these velocities. In this respect, Equation (6.14b) is, in the biphasic setting, the counterpart of the condition that the velocity of an incompressible monophasic medium be divergence free. Indeed, in a monophasic continuum in which mass is locally conserved (e.g., in the absence of growth or similar phenomena), the condition of incompressibility is reflected by the kinematic constraint that the velocity of the medium have zero divergence. On the other hand, in a saturated biphasic medium, it is the so-called *"composite velocity"* [192], i.e., $\phi_s\boldsymbol{v}_s + \phi_f\boldsymbol{v}_f$, that has to be divergence free when both phases are intrinsically incompressible. The composite velocity, pulled back to the medium's reference placement, returns the argument of the divergence in Equation (6.14b). This point of view has been exploited in [4].

6.2.3 Constraints on the rate of remodeling distortions

Following Gurtin and Anand [142], we hypothesize that the remodeling distortions represented by $\boldsymbol{F}_\gamma$ are isochoric and yield vanishing spin. In our notation, these two conditions, holding at all points of $\mathscr{B}$ and at all instants of $\mathscr{I}$, read

$$J_\gamma \equiv \det \boldsymbol{F}_\gamma = 1, \qquad \boldsymbol{W}_\gamma \equiv \tfrac{1}{2}\big[\boldsymbol{G}\dot{\boldsymbol{F}}_\gamma\boldsymbol{F}_\gamma^{-1} - (\dot{\boldsymbol{F}}_\gamma\boldsymbol{F}_\gamma^{-1})^T\boldsymbol{G}\big] = \boldsymbol{O}, \tag{6.15}$$

where $\boldsymbol{O}$ is the null tensor field of the second order. Gurtin and Anand [142] handled these assumptions *in strong form*, thereby developing their theory on the kinematic descriptor $\boldsymbol{D}_\gamma$, naturally compliant with the condition $(6.15)_2$, and which they took deviatoric as a direct consequence of $(6.15)_1$. However, by adhering to the framework of the Analytical Mechanics of constrained systems [11, 12, 14, 13], we view the conditions (6.15) as two independent *constraints* on $\boldsymbol{F}_\gamma$ and $\dot{\boldsymbol{F}}_\gamma$. This is a methodological alternative to that used by Gurtin and Anand [142], and is based on some recent works of our group [23, 32, 1, 2, 6] and on the references therein.

While the constraint of isochoric remodeling distortions is *holonomic* [11], meaning that, as stated in $(6.15)_1$, it is expressed as a function of $\boldsymbol{F}_\gamma$, the constraint of vanishing spin is in general *nonholonomic* [11], since it conveys a restriction on the admissible values of $\dot{\boldsymbol{F}}_\gamma$. However, for the forthcoming formulation it is convenient to express also Equation $(6.15)_1$ in differential form, so that, in terms of $\boldsymbol{L}_\gamma \coloneqq \dot{\boldsymbol{F}}_\gamma \boldsymbol{F}_\gamma^{-1}$, we obtain:

$$\mathcal{C}_{\mathrm{dev}} = \hat{\mathcal{C}}_{\mathrm{dev}} \circ \boldsymbol{L}_\gamma \coloneqq \langle J_\gamma \boldsymbol{I}^{\mathrm{T}} | \boldsymbol{L}_\gamma \rangle = \langle J_\gamma \boldsymbol{G}^{-1} | \boldsymbol{G}\boldsymbol{L}_\gamma \rangle = 0, \tag{6.16a}$$

$$\mathcal{C}_{\mathrm{sym}} = \hat{\mathcal{C}}_{\mathrm{sym}} \circ \boldsymbol{L}_\gamma \coloneqq \tfrac{1}{2}\big[\boldsymbol{G}\boldsymbol{L}_\gamma - (\boldsymbol{G}\boldsymbol{L}_\gamma)^{\mathrm{T}}\big] = \boldsymbol{O}, \tag{6.16b}$$

where $\boldsymbol{I} : T\mathscr{B} \to T\mathscr{B}$ is the material identity tensor field. Here, the subscripts "dev" and "sym" indicate that $\boldsymbol{L}_\gamma$ and $\boldsymbol{G}\boldsymbol{L}_\gamma$ have to be "deviatoric" (isochoric remodeling) and "symmetric", respectively. Moreover, for a generic kinematic quantity $\boldsymbol{f}$ —be it a vector or a tensor field— and its dual $\boldsymbol{\beta}$, the angular brackets $\langle \boldsymbol{\beta} | \boldsymbol{f} \rangle$ denote the duality products between $\boldsymbol{\beta}$ and $\boldsymbol{f}$.

Equations (6.13), $(6.15)_1$ and (6.16a) imply that $\Phi_{\mathrm{s}\nu}$ is constant in time and that its numerical value coincides with that of the volumetric fraction of the solid phase in the reference placement, i.e., with Φ_{sR}.

To handle $\mathrm{Grad}\boldsymbol{L}_\gamma$ with the restrictions placed on $\boldsymbol{L}_\gamma$, one could also take the gradient of Equations (6.16a) and (6.16b), and regard the resulting expressions as additional constraints. This approach is followed, e.g., by Anderson et al. [193], Chen and Fried [194], and Pastore et al. [6] for uniaxial nematic elastomers, and by Bertram and Glüge [195] for incompressible second-gradient monophasic media. In the present work, however, we do not follow this path.

6.2.4 Chetaev's conditions

The constraints (6.16a) and (6.16b) restrict the set of the admissible virtual velocities associated with $\dot{\boldsymbol{F}}_\gamma$ or $\boldsymbol{L}_\gamma$. Indeed, upon denoting by $\boldsymbol{L}_{\gamma\mathrm{v}}$ the virtual velocity associated with $\boldsymbol{L}_\gamma$, and introducing the hypothesis of *"ideal constraints"* [11, 16, 23, 32, 1, 2], $\boldsymbol{L}_{\gamma\mathrm{v}}$ must comply with so-called *Chetaev's conditions* [16, 1]:

$$\begin{aligned}\mathcal{A}_{\mathrm{dev}} &:= \hat{\mathcal{A}}_{\mathrm{dev}} \circ (\boldsymbol{L}_\gamma, \boldsymbol{L}_{\gamma\mathrm{v}}) \\ &= \left(\frac{\partial \hat{\mathcal{C}}_{\mathrm{dev}}}{\partial \boldsymbol{L}_\gamma} \circ \boldsymbol{L}_\gamma\right)[\boldsymbol{L}_{\gamma\mathrm{v}}] = \langle J_\gamma \boldsymbol{I}^{\mathrm{T}} | \boldsymbol{L}_{\gamma\mathrm{v}} \rangle = \langle J_\gamma \boldsymbol{G}^{-1} | \boldsymbol{G}\boldsymbol{L}_{\gamma\mathrm{v}} \rangle = 0, \qquad (6.17a) \\ \boldsymbol{\mathcal{A}}_{\mathrm{sym}} &:= \hat{\boldsymbol{\mathcal{A}}}_{\mathrm{sym}} \circ (\boldsymbol{L}_\gamma, \boldsymbol{L}_{\gamma\mathrm{v}}) \\ &= \left(\frac{\partial \hat{\boldsymbol{\mathcal{C}}}_{\mathrm{sym}}}{\partial \boldsymbol{L}_\gamma} \circ \boldsymbol{L}_\gamma\right)[\boldsymbol{L}_{\gamma\mathrm{v}}] = \tfrac{1}{2}\left[\boldsymbol{G}\boldsymbol{L}_{\gamma\mathrm{v}} - (\boldsymbol{G}\boldsymbol{L}_{\gamma\mathrm{v}})^{\mathrm{T}}\right] = \boldsymbol{O}, \qquad (6.17b)\end{aligned}$$

where $(\partial_{\boldsymbol{L}_\gamma} \hat{\mathcal{C}}_{\mathrm{dev}} \circ \boldsymbol{L}_\gamma)[\boldsymbol{L}_{\gamma\mathrm{v}}]$ and $(\partial_{\boldsymbol{L}_\gamma} \hat{\boldsymbol{\mathcal{C}}}_{\mathrm{sym}} \circ \boldsymbol{L}_\gamma)[\boldsymbol{L}_{\gamma\mathrm{v}}]$ are the Gâteaux derivatives of $\hat{\mathcal{C}}_{\mathrm{dev}}$ and $\hat{\boldsymbol{\mathcal{C}}}_{\mathrm{sym}}$ evaluated in $\boldsymbol{L}_\gamma$ and along $\boldsymbol{L}_{\gamma\mathrm{v}}$. Accordingly, the virtual velocities $\boldsymbol{L}_{\gamma\mathrm{v}}$ must be deviatoric and symmetric with respect to the metric tensor field $\boldsymbol{G}$. Also, $\boldsymbol{L}_{\gamma\mathrm{v}}$ can be expressed as $\boldsymbol{L}_{\gamma\mathrm{v}} := \boldsymbol{\mathcal{V}}_{\gamma\mathrm{v}} \boldsymbol{F}_\gamma^{-1}$, with $\boldsymbol{\mathcal{V}}_{\gamma\mathrm{v}}$ being the virtual velocity field associated with the time derivative of the remodeling tensor.

Note that, since the constraint functions $\hat{\mathcal{C}}_{\mathrm{dev}}$ and $\hat{\boldsymbol{\mathcal{C}}}_{\mathrm{sym}}$ are both linear in $\boldsymbol{L}_\gamma$, the corresponding functions $\hat{\mathcal{A}}_{\mathrm{dev}}$ and $\hat{\boldsymbol{\mathcal{A}}}_{\mathrm{sym}}$ are independent of $\boldsymbol{L}_\gamma$ and depend linearly on $\boldsymbol{L}_{\gamma\mathrm{v}}$. For this reason, to simplify the notation, we shall write $\hat{\mathcal{A}}_{\mathrm{dev}} \circ \boldsymbol{L}_{\gamma\mathrm{v}}$ and $\hat{\boldsymbol{\mathcal{A}}}_{\mathrm{sym}} \circ \boldsymbol{L}_{\gamma\mathrm{v}}$ from here on.

Quite differently from Equations (6.17a) and (6.17b), in which the Gâteaux derivatives are performed by direct differentiation of the constraints (6.16a) and (6.16b) with respect to $\boldsymbol{L}_\gamma$, Chetaev's condition associated with the constraint (6.14b) is obtained as follows. First, we redefine Equation (6.14b) through the functional

$$\mathcal{C}_{\mathrm{inc}} := \hat{\mathcal{C}}_{\mathrm{inc}} \circ (\boldsymbol{V}_{\mathrm{s}}, \boldsymbol{V}_{\mathrm{f}}) = \mathrm{Div}[(\Phi_{\mathrm{sR}} \boldsymbol{V}_{\mathrm{s}} + \Phi_{\mathrm{fR}} \boldsymbol{V}_{\mathrm{f}}) \boldsymbol{F}^{-\mathrm{T}}] = 0, \qquad (6.18)$$

which is linear in the velocities $\boldsymbol{V}_{\mathrm{s}}$ and $\boldsymbol{V}_{\mathrm{f}}$ (we adopt this notation for convenience, but $\hat{\mathcal{C}}_{\mathrm{inc}}$ could also be defined as a function of $\boldsymbol{V}_{\mathrm{s}}$, $\boldsymbol{V}_{\mathrm{f}}$, $\mathrm{Grad}\boldsymbol{V}_{\mathrm{s}}$ and $\mathrm{Grad}\boldsymbol{V}_{\mathrm{f}}$). Then, we introduce the homotopies $\boldsymbol{V}_{\mathrm{s}} \mapsto \boldsymbol{V}_{\mathrm{s}} + \varepsilon \boldsymbol{V}_{\mathrm{sv}}$ and $\boldsymbol{V}_{\mathrm{f}} \mapsto \boldsymbol{V}_{\mathrm{f}} + \varepsilon \boldsymbol{V}_{\mathrm{fv}}$, where ε is a

non-dimensional smallness parameter, and we define the function

$$\begin{aligned}\tilde{\mathcal{C}}_{\mathrm{inc}}(\varepsilon) &:= \hat{\mathcal{C}}_{\mathrm{inc}} \circ (\boldsymbol{V}_{\mathrm{s}} + \varepsilon \boldsymbol{V}_{\mathrm{sv}}, \boldsymbol{V}_{\mathrm{f}} + \varepsilon \boldsymbol{V}_{\mathrm{fv}}) \\ &= \mathrm{Div}[(\Phi_{\mathrm{sR}}(\boldsymbol{V}_{\mathrm{s}} + \varepsilon \boldsymbol{V}_{\mathrm{sv}}) + \Phi_{\mathrm{fR}}(\boldsymbol{V}_{\mathrm{f}} + \varepsilon \boldsymbol{V}_{\mathrm{fv}}))\boldsymbol{F}^{-\mathrm{T}}] \\ &= \mathrm{Div}[(\Phi_{\mathrm{sR}}\boldsymbol{V}_{\mathrm{s}} + \Phi_{\mathrm{fR}}\boldsymbol{V}_{\mathrm{f}})\boldsymbol{F}^{-\mathrm{T}}] + \varepsilon \mathrm{Div}[(\Phi_{\mathrm{sR}}\boldsymbol{V}_{\mathrm{sv}} + \Phi_{\mathrm{fR}}\boldsymbol{V}_{\mathrm{fv}})\boldsymbol{F}^{-\mathrm{T}}]. \quad (6.19)\end{aligned}$$

Thus, Chetaev's condition is given by (see the work by Giammarini et al. [4] for an analogous expression)

$$\begin{aligned}\mathcal{A}_{\mathrm{inc}} := \frac{\mathrm{d}\tilde{\mathcal{C}}_{\mathrm{inc}}}{\mathrm{d}\varepsilon}(0) &= (D\hat{\mathcal{C}}_{\mathrm{inc}} \circ (\boldsymbol{V}_{\mathrm{s}}, \boldsymbol{V}_{\mathrm{f}}))[\boldsymbol{V}_{\mathrm{sv}}, \boldsymbol{V}_{\mathrm{fv}}] \\ &= \mathrm{Div}[(\Phi_{\mathrm{sR}}\boldsymbol{V}_{\mathrm{sv}} + \Phi_{\mathrm{fR}}\boldsymbol{V}_{\mathrm{fv}})\boldsymbol{F}^{-\mathrm{T}}] = 0, \quad (6.20)\end{aligned}$$

where $(D\hat{\mathcal{C}}_{\mathrm{inc}} \circ (\boldsymbol{V}_{\mathrm{s}}, \boldsymbol{V}_{\mathrm{f}}))[\boldsymbol{V}_{\mathrm{sv}}, \boldsymbol{V}_{\mathrm{fv}}]$ is the Gâteaux derivative of $\hat{\mathcal{C}}_{\mathrm{inc}}$, evaluated at $(\boldsymbol{V}_{\mathrm{s}}, \boldsymbol{V}_{\mathrm{f}})$ and along the virtual velocities $\boldsymbol{V}_{\mathrm{sv}}$ and $\boldsymbol{V}_{\mathrm{fv}}$. For future use, we write $\mathcal{A}_{\mathrm{inc}} := \hat{\mathcal{A}}_{\mathrm{inc}} \circ (\boldsymbol{V}_{\mathrm{sv}}, \boldsymbol{V}_{\mathrm{fv}})$. Also for $\hat{\mathcal{A}}_{\mathrm{inc}}$ the same notational considerations hold that have been reported in the parentheses after Equation (6.18), but in terms of the virtual fields.

6.3 Force balances in biphasic mixtures undergoing remodeling

We complete the kinematic picture of the system under study by defining, for each of the considered degrees of freedom, the generalized virtual velocity field chosen as descriptor. From here on, unless there is room for confusion, we use "virtual velocity field" and "virtual velocity" interchangeably.

Next, we introduce the generalized force fields acting on the system. We do this by identifying each of such fields with the entity that represents the *virtual power* expended on the corresponding virtual velocity. Each virtual power constructed this way is, by definition, a linear functional in the associated virtual velocity. This functional has the property of being bounded in this virtual velocity, and continuous. Also for the force fields, we shall simply speak of "forces" when there is no lack of clarity.

To define the generalized forces, we distinguish them between internal and external. Furthermore, we classify the external forces as bulk forces and surface forces, depending on how they act on the system.

For the framework of the Principle of Virtual Power, we refer to the foundational works by Germain [137] and Epstein and Segev [138].

6.3.1 Principle of Virtual Power (PVP) with constraints

Granted the kinematical setting outlined in Section 2, we consider the collections

$$\mathscr{M} := \{\boldsymbol{V}_{\mathrm{s}} \equiv \dot{\chi}, \boldsymbol{V}_{\mathrm{f}}, \mathrm{Grad}\boldsymbol{V}_{\mathrm{s}}, \mathrm{Grad}\boldsymbol{V}_{\mathrm{f}}, \boldsymbol{L}_{\gamma}, \mathrm{Grad}\boldsymbol{L}_{\gamma}\}, \tag{6.21a}$$

$$\mathscr{M}_{\mathrm{v}} := \{\boldsymbol{V}_{\mathrm{sv}}, \boldsymbol{V}_{\mathrm{fv}}, \mathrm{Grad}\boldsymbol{V}_{\mathrm{sv}}, \mathrm{Grad}\boldsymbol{V}_{\mathrm{fv}}, \boldsymbol{L}_{\gamma\mathrm{v}}, \mathrm{Grad}\boldsymbol{L}_{\gamma\mathrm{v}}\}, \tag{6.21b}$$

comprising the generalized velocity fields of the system under study and the corresponding virtual fields, respectively, and in which $\boldsymbol{V}_{\mathrm{s}}$ and $\boldsymbol{V}_{\mathrm{f}}$, as well as $\boldsymbol{V}_{\mathrm{sv}}$ and $\boldsymbol{V}_{\mathrm{fv}}$, comply with the constraint (6.14b), while $\boldsymbol{L}_{\gamma}$ and $\boldsymbol{L}_{\gamma\mathrm{v}}$ comply with (6.16a) and (6.16b) (in fact, the virtual fields comply with Chetaev's conditions (6.20), (6.17a) and (6.17b)). The subscript "v" stands for "virtual" in all the symbols in which it appears. The fields $\boldsymbol{V}_{\mathrm{s}}$, $\boldsymbol{V}_{\mathrm{f}}$ and $\boldsymbol{L}_{\gamma}$, and their virtual counterparts $\boldsymbol{V}_{\mathrm{sv}}$, $\boldsymbol{V}_{\mathrm{fv}}$ and $\boldsymbol{L}_{\gamma\mathrm{v}}$ are defined on the topological closure of $\mathscr{B}$, i.e., on $\overline{\mathscr{B}} = \mathscr{B} \cup \partial\mathscr{B}$.

To define the virtual power, we introduce the functional spaces which $\boldsymbol{V}_{\mathrm{sv}}$, $\boldsymbol{V}_{\mathrm{fv}}$ and $\boldsymbol{L}_{\gamma\mathrm{v}}$ belong to, and we denote them by $\mathscr{V}_{\mathrm{sv}}$, $\mathscr{V}_{\mathrm{fv}}$ and $\mathscr{V}_{\gamma\mathrm{v}}$, respectively. For $\alpha = \mathrm{s,f}$, $\mathscr{V}_{\alpha\mathrm{v}}$ is a subset of the Sobolev space $H^1(\mathscr{B}; T\mathscr{S})$ of functions valued in $T\mathscr{S}$, characterized by the Dirichlet boundary conditions assigned to the motion of the solid and of the fluid phase. Analogously, $\mathscr{V}_{\gamma\mathrm{v}}$ is, in general, a subspace of $H^1(\mathscr{B}; [T\mathscr{B}]^1{}_1)$ of tensor functions valued in $[T\mathscr{B}]^1{}_1$. We recall that, for a given scalar, vector, or tensor space $\mathbb{S}$, $H^1(\mathscr{B}; \mathbb{S})$ is the Sobolev space of fields defined over $\overline{\mathscr{B}}$, valued in $\mathbb{S}$, square-integrable in $\mathscr{B}$, and with distributional gradient square-integrable in $\mathscr{B}$. Integrability is understood in the sense of Lebesgue, and the space of $\mathbb{S}$-valued fields that are square-integrable in $\mathscr{B}$ according to Lebesgue's measure is denoted by $L^2(\mathscr{B}; \mathbb{S})$ [196].

To handle the values attained by $\boldsymbol{V}_{\alpha}$ and $\boldsymbol{V}_{\alpha\mathrm{v}}$ on the boundary of $\mathscr{B}$, we have recourse to the *trace operators* [196], which, in the present setting, map a given field of $H^1(\mathscr{B}; T\mathscr{S})$ into a field of $L^2(\partial\mathscr{B}; T\mathscr{S})$. However, since it is known from

Functional Analysis that the trace operators defined in this way are not surjective [196], they are re-defined as $\wp : H^1(\mathscr{B};T\mathscr{S}) \to H^{1/2}(\partial\mathscr{B};T\mathscr{S})$, where $H^{1/2}(\partial\mathscr{B};T\mathscr{S})$ is given by $H^{1/2}(\partial\mathscr{B};T\mathscr{S}) \coloneqq \{\wp(\boldsymbol{W}) : \ \boldsymbol{W} \in H^1(\mathscr{B};T\mathscr{S})\} \subset L^2(\partial\mathscr{B};T\mathscr{S})$, and $\wp(\boldsymbol{W})$ is said to be the trace of $\boldsymbol{W}$ on $\partial\mathscr{B}$. To simplify the notation, we shall omit the symbol $\wp(\boldsymbol{W})$ to indicate that $\boldsymbol{W}$ is evaluated on $\partial\mathscr{B}$, or on a portion of it. However, such evaluation will be understood in the sense of the trace of $\boldsymbol{W}$. The same shall apply to the evaluation of a component of $\boldsymbol{W}$ in a given vector basis.

Since in this work we deal with second-order tensors for which their algebraic trace "tr" has to be evaluated, the operator "tr" should not be confused with the trace operator of Functional Analysis. However, it will be clear from the context which operator is meant.

For d = 1,2,3, let Γ^d_{sD} and Γ^d_{fD} be the portions of $\partial\mathscr{B}$ on which, in a given local coordinate system and in the associated vector basis, the dth component of the solid phase motion χ and of the fluid velocity $\boldsymbol{V}_{\mathrm{f}}$ are prescribed by means of Dirichlet boundary conditions. On Γ^d_{sD} and Γ^d_{fD}, the dth component of $\boldsymbol{V}_{\mathrm{sv}}$ and $\boldsymbol{V}_{\mathrm{fv}}$, i.e., V^d_{sv} and V^d_{fv}, are identically null by construction. On the other hand, since we prescribe no Dirichlet conditions on $\boldsymbol{F}_\gamma$ or on $\boldsymbol{L}_\gamma$, no restriction of this type is required for $\boldsymbol{L}_{\gamma\mathrm{v}}$. Hence, we set[1]

$$\mathscr{V}_{\mathrm{sv}} = \{\boldsymbol{V}_{\mathrm{sv}} \in H^1(\mathscr{B};T\mathscr{S}) : \ V^d_{\mathrm{sv}} = 0 \text{ on } \Gamma^d_{\mathrm{sD}}, \quad d \in \{1,2,3\}\}, \tag{6.22a}$$

$$\mathscr{V}_{\mathrm{fv}} = \{\boldsymbol{V}_{\mathrm{fv}} \in H^1(\mathscr{B};T\mathscr{S}) : \ V^d_{\mathrm{fv}} = 0 \text{ on } \Gamma^d_{\mathrm{fD}}, \quad d \in \{1,2,3\}\}, \tag{6.22b}$$

$$\mathscr{V}_{\gamma\mathrm{v}} \equiv H^1(\mathscr{B};[T\mathscr{B}]^1{}_1). \tag{6.22c}$$

Internal virtual power. Given $\mathscr{V}_{\mathrm{sv}}$, $\mathscr{V}_{\mathrm{fv}}$ and $\mathscr{V}_{\gamma\mathrm{v}}$, we define the *internal virtual power* as

$$\mathscr{P}^{(\mathrm{i})}_{\mathrm{v}} : \mathscr{V}_{\mathrm{sv}} \times \mathscr{V}_{\mathrm{fv}} \times \mathscr{V}_{\gamma\mathrm{v}} \to \mathbb{R}, \tag{6.23a}$$

$$\begin{aligned}\mathscr{P}^{(\mathrm{i})}_{\mathrm{v}}(\boldsymbol{V}_{\mathrm{sv}},\boldsymbol{V}_{\mathrm{fv}},\boldsymbol{L}_{\gamma\mathrm{v}}) \coloneqq &\int_{\mathscr{B}}\sum_{\alpha}\left\{\langle J\boldsymbol{m}_\alpha|\boldsymbol{V}_{\alpha\mathrm{v}}\rangle + \langle \boldsymbol{P}_\alpha|\mathrm{Grad}\boldsymbol{V}_{\alpha\mathrm{v}}\rangle\right\}\\ &+\int_{\mathscr{B}}\left\{\langle \boldsymbol{Y}_{\mathrm{u}}|\boldsymbol{L}_{\gamma\mathrm{v}}\rangle + \langle \mathbb{Y}_{\mathrm{u}}\,|\,\mathrm{Grad}\boldsymbol{L}_{\gamma\mathrm{v}}\rangle\right\},\end{aligned} \tag{6.23b}$$

[1] In order to emphasize the Functional Analysis aspects of the topic addressed in this chapter, the dependence of the virtual powers on the virtual (test) velocity fields has been given explicitly. Virtual powers, indeed, are linear functionals over the virtual velocity fields, as already indicated in Equation (5.18) of Section 5.2.3.

where $\boldsymbol{Jm}_\alpha$ is the active part of the force, expressed per unit volume of the reference placement, that the αth phase, $\alpha \in \{\mathrm{s}, \mathrm{f}\}$, exchanges with the other one [182] (it is here referred to as "active" because it is not directly related to the constraints and, in the following, it will be expressed constitutively); $\boldsymbol{P}_\alpha$ is the active part of the first Piola–Kirchhoff stress tensor associated with the αth phase; $\boldsymbol{Y}_\mathrm{u}$ is the active stress-like generalized force dual to $\boldsymbol{L}_{\gamma\mathrm{v}}$; finally, $\mathbb{Y}_\mathrm{u}$ is the tensor field of the third order that expresses the active generalized stress dual to $\mathrm{Grad}\boldsymbol{L}_{\gamma\mathrm{v}}$.

The generalized forces $\boldsymbol{Jm}_\alpha$, $\boldsymbol{P}_\alpha$, $\boldsymbol{Y}_\mathrm{u}$ and $\mathbb{Y}_\mathrm{u}$ must belong to functional spaces that guarantee the existence and finiteness of the integrals of Equation (6.23b). Moreover, $\mathcal{P}_\mathrm{v}^{(\mathrm{i})}$ should be linear and bounded in each of its arguments.

Null reactive virtual power. Since the constraints (6.16a) and (6.16b) are *"ideal"* [11, 16], the reaction forces generated by them expend *zero* virtual power against any admissible virtual velocity field. We enforce this property *weakly* by employing the Lagrange multiplier technique. Hence, we introduce a scalar Lagrange multiplier η and a tensorial Lagrange multiplier $\boldsymbol{\Upsilon}$, their associated virtual fields η_v and $\boldsymbol{\Upsilon}_\mathrm{v}$, and we conjugate η_v and $\boldsymbol{\Upsilon}_\mathrm{v}$ with (6.16a) and (6.16b), respectively, and η and $\boldsymbol{\Upsilon}$ with Chetaev's conditions (6.17a) and (6.17b). Note that η, η_v, $\boldsymbol{\Upsilon}$ and $\boldsymbol{\Upsilon}_\mathrm{v}$ have physical units of mechanical stress.

Analogous considerations are made for the incompressibility constraint, expressed in the form (6.14b) and in Chetaev's condition (6.20). The condition (6.20) is conjugated with a Lagrange multiplier p, acquiring the meaning of a *pressure*, while the constraint (6.14b) is conjugated with the virtual pressure p_v.

We denote by $\mathscr{V}_{\eta\mathrm{v}}$, $\mathscr{V}_{\boldsymbol{\Upsilon}\mathrm{v}}$, and $\mathscr{V}_{\mathrm{pv}}$ the functional spaces in which the virtual multipliers η_v, $\boldsymbol{\Upsilon}_\mathrm{v}$, and p_v live, and we define them as

$$\mathscr{V}_{\eta\mathrm{v}} = L^2(\mathscr{B};\mathbb{R}), \qquad \mathscr{V}_{\boldsymbol{\Upsilon}\mathrm{v}} = L^2(\mathscr{B};[T\mathscr{B}]^2), \qquad \mathscr{V}_{\mathrm{pv}} = H^1(\mathscr{B};\mathbb{R}). \tag{6.24}$$

Then, we write the *null* virtual powers expended by the reaction forces on the constraints as

$$\mathcal{P}_\mathrm{v}^{(\mathrm{dev})} : \mathscr{V}_{\gamma\mathrm{v}} \times \mathscr{V}_{\eta\mathrm{v}} \to \mathbb{R}, \tag{6.25a}$$

$$\mathcal{P}_\mathrm{v}^{(\mathrm{dev})}(\boldsymbol{L}_{\gamma\mathrm{v}};\eta_\mathrm{v}) \coloneqq \int_{\mathscr{B}} \eta[\hat{\mathcal{A}}_{\mathrm{dev}} \circ \boldsymbol{L}_{\gamma\mathrm{v}}] + \int_{\mathscr{B}} \eta_\mathrm{v}[\hat{\mathcal{C}}_{\mathrm{dev}} \circ \boldsymbol{L}_\gamma] = 0, \tag{6.25b}$$

$$\mathcal{P}_{\mathrm{v}}^{(\mathrm{sym})} : \mathscr{V}_{\gamma\mathrm{v}} \times \mathscr{V}_{\boldsymbol{\Upsilon}\mathrm{v}} \to \mathbb{R}, \tag{6.25c}$$

$$\mathcal{P}_{\mathrm{v}}^{(\mathrm{sym})}(\boldsymbol{L}_{\gamma\mathrm{v}}; \boldsymbol{\Upsilon}_{\mathrm{v}}) := \int_{\mathscr{B}} \langle \boldsymbol{\Upsilon} | \hat{\boldsymbol{\mathcal{A}}}_{\mathrm{sym}} \circ \boldsymbol{L}_{\gamma\mathrm{v}} \rangle + \int_{\mathscr{B}} \langle \boldsymbol{\Upsilon}_{\mathrm{v}} | \hat{\mathfrak{C}}_{\mathrm{sym}} \circ \boldsymbol{L}_{\gamma} \rangle = 0, \tag{6.25d}$$

$$\mathcal{P}_{\mathrm{v}}^{(\mathrm{inc})} : \mathscr{V}_{\mathrm{sv}} \times \mathscr{V}_{\mathrm{fv}} \times \mathscr{V}_{\mathrm{pv}} \to \mathbb{R}, \tag{6.25e}$$

$$\begin{aligned} \mathcal{P}_{\mathrm{v}}^{(\mathrm{inc})}(\boldsymbol{V}_{\mathrm{sv}}, \boldsymbol{V}_{\mathrm{fv}}; p_{\mathrm{v}}) := &- \int_{\mathscr{B}} p\,[\hat{\mathcal{A}}_{\mathrm{inc}} \circ (\boldsymbol{V}_{\mathrm{sv}}, \boldsymbol{V}_{\mathrm{fv}})] \\ &- \int_{\mathscr{B}} p_{\mathrm{v}}\,[\hat{\mathfrak{C}}_{\mathrm{inc}} \circ (\boldsymbol{V}_{\mathrm{s}}, \boldsymbol{V}_{\mathrm{f}})] = 0. \end{aligned} \tag{6.25f}$$

As for $\mathcal{P}_{\mathrm{v}}^{(\mathrm{i})}$, the functional spaces of the "true" Lagrange multipliers η, $\boldsymbol{\Upsilon}$ and p, of the "true" velocity fields $\boldsymbol{V}_{\mathrm{s}}$ and $\boldsymbol{V}_{\mathrm{f}}$, and of the motion χ must be such that the integrals in Equations (6.25b), (6.25d) and (6.25f) exist and be finite. Moreover, the total (null) virtual power done by the reaction forces on the constraints is linear and bounded in its arguments and is given by

$$\begin{aligned} &\mathcal{P}_{\mathrm{v}}^{(\mathrm{c})}(\boldsymbol{V}_{\mathrm{sv}}, \boldsymbol{V}_{\mathrm{fv}}, \boldsymbol{L}_{\gamma\mathrm{v}}; p_{\mathrm{v}}, \eta_{\mathrm{v}}, \boldsymbol{\Upsilon}_{\mathrm{v}}) \\ &:= \mathcal{P}_{\mathrm{v}}^{(\mathrm{dev})}(\boldsymbol{L}_{\gamma\mathrm{v}}; \eta_{\mathrm{v}}) + \mathcal{P}_{\mathrm{v}}^{(\mathrm{sym})}(\boldsymbol{L}_{\gamma\mathrm{v}}; \boldsymbol{\Upsilon}_{\mathrm{v}}) + \mathcal{P}_{\mathrm{v}}^{(\mathrm{inc})}(\boldsymbol{V}_{\mathrm{sv}}, \boldsymbol{V}_{\mathrm{fv}}; p_{\mathrm{v}}) = 0. \end{aligned} \tag{6.26}$$

Although Equations (6.25b) and (6.25d) state that the virtual power done by the reaction forces is zero, η and $\boldsymbol{\Upsilon}$ *are not* the reaction forces, in general. They are, however, related to these forces, as will become clear in Equations (6.27a) and (6.27b) below. Note also that, since η_{v} and $\boldsymbol{\Upsilon}_{\mathrm{v}}$ can be taken arbitrarily (see the forthcoming calculations), the last summands of Equations (6.25b) and (6.25d) return the constraints (6.16a) and (6.16b) in strong form. Moreover, if the last integrals of Equations (6.25b) and (6.25d) are evaluated for the "true" values of $\boldsymbol{L}_{\gamma}$, i.e., for the velocities solving the dynamic problem under study, which have to fulfill the constraints, then $\hat{\mathfrak{C}}_{\mathrm{dev}} \circ \boldsymbol{L}_{\gamma}$ and $\hat{\mathfrak{C}}_{\mathrm{sym}} \circ \boldsymbol{L}_{\gamma}$ vanish identically. The same holds true for the velocities $\boldsymbol{V}_{\mathrm{s}}$ and $\boldsymbol{V}_{\mathrm{f}}$ in the last integral of Equation (6.25f).

To identify explicitly the reaction forces associated with the constraints on $\boldsymbol{L}_{\gamma}$, let us rewrite the integrands $\eta[\hat{\mathcal{A}}_{\mathrm{dev}} \circ \boldsymbol{L}_{\gamma\mathrm{v}}]$ and $\langle \boldsymbol{\Upsilon} | \hat{\boldsymbol{\mathcal{A}}}_{\mathrm{sym}} \circ \boldsymbol{L}_{\gamma\mathrm{v}} \rangle$ in Equations (6.25b) and (6.25d) as

$$\eta[\hat{\mathcal{A}}_{\mathrm{dev}} \circ \boldsymbol{L}_{\gamma\mathrm{v}}] = \langle J_{\gamma} \eta \boldsymbol{I}^{\mathrm{T}} | \boldsymbol{L}_{\gamma\mathrm{v}} \rangle = 0, \tag{6.27a}$$

$$\langle \boldsymbol{\Upsilon} | \hat{\boldsymbol{\mathcal{A}}}_{\mathrm{sym}} \circ \boldsymbol{L}_{\gamma\mathrm{v}} \rangle = \langle \boldsymbol{G}(\mathrm{Skew}\boldsymbol{\Upsilon}) | \boldsymbol{L}_{\gamma\mathrm{v}} \rangle = 0. \tag{6.27b}$$

These expressions make it clear that the reaction forces are dual to $\boldsymbol{L}_{\gamma\mathrm{v}}$ and are represented by the tensor fields $J_\gamma \eta \boldsymbol{I}^{\mathrm{T}}$ and $\boldsymbol{G}(\mathrm{Skew}\boldsymbol{\Upsilon})$. These quantities, in turn, viewed as real-valued linear maps acting on $\mathscr{V}_{\gamma\mathrm{v}}$, read $\langle J_\gamma \eta \boldsymbol{I}^{\mathrm{T}} | \cdot \rangle$ and $\langle \boldsymbol{G}(\mathrm{Skew}\boldsymbol{\Upsilon}) | \cdot \rangle$. Consistently with this picture, the generalized virtual velocities $\boldsymbol{L}_{\gamma\mathrm{v}}$ must belong to the intersection of the kernels of $\langle J_\gamma \eta \boldsymbol{I}^{\mathrm{T}} | \cdot \rangle$ and $\langle \boldsymbol{G}(\mathrm{Skew}\boldsymbol{\Upsilon}) | \cdot \rangle$. Hence, we write

$$\boldsymbol{L}_{\gamma\mathrm{v}} \in \mathrm{Ker}\langle J_\gamma \eta \boldsymbol{I}^{\mathrm{T}} | \cdot \rangle \cap \mathrm{Ker}\langle \boldsymbol{G}(\mathrm{Skew}\boldsymbol{\Upsilon}) | \cdot \rangle, \tag{6.28}$$

which implies that a generic $\boldsymbol{L}_{\gamma\mathrm{v}}$ is admissible if it is deviatoric and symmetric with respect to the metric tensor field $\boldsymbol{G}$. These conditions are prescribed on $\boldsymbol{L}_\gamma$ by the constraints (6.16a) and (6.16b), and allow us to rewrite the first two summands on the right-hand side of Equation (6.26) as

$$\begin{aligned}
&\mathcal{P}_{\mathrm{v}}^{(\mathrm{dev})}(\boldsymbol{L}_{\gamma\mathrm{v}}; \eta_{\mathrm{v}}) + \mathcal{P}_{\mathrm{v}}^{(\mathrm{sym})}(\boldsymbol{L}_{\gamma\mathrm{v}}; \boldsymbol{\Upsilon}_{\mathrm{v}}) \\
&= \int_{\mathscr{B}} \langle J_\gamma \eta \boldsymbol{I}^{\mathrm{T}} + \boldsymbol{G}(\mathrm{Skew}\boldsymbol{\Upsilon}) | \boldsymbol{L}_{\gamma\mathrm{v}} \rangle \\
&+ \int_{\mathscr{B}} \eta_{\mathrm{v}} [\hat{\mathfrak{C}}_{\mathrm{dev}} \circ \boldsymbol{L}_\gamma] + \int_{\mathscr{B}} \langle \boldsymbol{\Upsilon}_{\mathrm{v}} | \hat{\mathfrak{C}}_{\mathrm{sym}} \circ \boldsymbol{L}_\gamma \rangle = 0.
\end{aligned} \tag{6.29}$$

On the same footing, we can determine the reaction forces associated with the Lagrange multiplier p by working out the first integrand on the right-hand side of Equation (6.25f). Indeed, by expanding the divergence in $\hat{\mathcal{A}}_{\mathrm{inc}} \circ (\boldsymbol{V}_{\mathrm{sv}}, \boldsymbol{V}_{\mathrm{fv}})$, and using the Piola identity, we obtain

$$\begin{aligned}
\mathcal{P}_{\mathrm{v}}^{(\mathrm{inc})}(\boldsymbol{V}_{\mathrm{sv}}, \boldsymbol{V}_{\mathrm{fv}}; p_{\mathrm{v}}) = \int_{\mathscr{B}} \sum_\alpha \left\{ \langle -Jp\, \boldsymbol{F}^{-\mathrm{T}} \mathrm{Grad}\phi_{\alpha\mathrm{R}} | \boldsymbol{V}_{\alpha\mathrm{v}} \rangle + \langle -\Phi_{\alpha\mathrm{R}} p \boldsymbol{F}^{-\mathrm{T}} | \mathrm{Grad}\boldsymbol{V}_{\alpha\mathrm{v}} \rangle \right\} \\
- \int_{\mathscr{B}} p_{\mathrm{v}} [\hat{\mathfrak{C}}_{\mathrm{inc}} \circ (\boldsymbol{V}_{\mathrm{s}}, \boldsymbol{V}_{\mathrm{f}})],
\end{aligned} \tag{6.30}$$

where $\phi_{\alpha\mathrm{R}} \equiv \phi_\alpha \circ (\chi, \mathcal{T}) = \Phi_{\alpha\mathrm{R}}/J$. Hence, for $\alpha = \mathrm{s,f}$, we identify the reactive contributions

$$-Jp\, \boldsymbol{F}^{-\mathrm{T}} \mathrm{Grad}\phi_{\alpha\mathrm{R}} \equiv -Jp\, [\mathrm{grad}\phi_\alpha \circ (\chi, \mathcal{T})], \qquad -\Phi_{\alpha\mathrm{R}} p \boldsymbol{F}^{-\mathrm{T}}. \tag{6.31}$$

The force in Equation $(6.31)_1$ is the reaction part of the internal force due to the momentum exchange between the solid and the fluid phase of the considered medium. For $\alpha = \mathrm{s,f}$, $-Jp\, \boldsymbol{F}^{-\mathrm{T}} \mathrm{Grad}\phi_{\alpha\mathrm{R}}$ adds to $J\boldsymbol{m}_\alpha$ to determine the overall internal force

dual to $\boldsymbol{V}_{\alpha\mathrm{v}}$. Moreover, it satisfies the requirement that the sum over α = s,f of the internal forces should be null. This follows from the saturation condition $\sum_\alpha \phi_{\alpha\mathrm{R}} = 1$, which yields $-\sum_\alpha Jp\,\boldsymbol{F}^{-\mathrm{T}}\mathrm{Grad}\phi_{\alpha\mathrm{R}} = -Jp\boldsymbol{F}^{-\mathrm{T}}\mathrm{Grad}\big(\sum_\alpha \phi_{\alpha\mathrm{R}}\big) = \boldsymbol{0}$. Similarly, the stress contribution $-\Phi_{\alpha\mathrm{R}}p\boldsymbol{F}^{-\mathrm{T}}$ in Equation $(6.31)_2$ identifies the reaction part of the first Piola–Kirchhoff stress tensor of the αth phase dual to the gradient $\mathrm{Grad}\boldsymbol{V}_{\alpha\mathrm{v}}$ of the corresponding virtual velocity.

External virtual power. Next, we define the *external virtual power* as

$$\mathcal{P}_{\mathrm{v}}^{(\mathrm{e})} : \mathscr{V}_{\mathrm{sv}} \times \mathscr{V}_{\mathrm{fv}} \times \mathscr{V}_{\gamma\mathrm{v}} \to \mathbb{R}, \tag{6.32a}$$

$$\begin{aligned}\mathcal{P}_{\mathrm{v}}^{(\mathrm{e})}(\boldsymbol{V}_{\mathrm{sv}}, \boldsymbol{V}_{\mathrm{fv}}, \boldsymbol{L}_{\gamma\mathrm{v}}) \coloneqq &\int_{\mathscr{B}} \sum_\alpha \langle \boldsymbol{f}_\alpha | \boldsymbol{V}_{\alpha\mathrm{v}} \rangle + \sum_\alpha \sum_{d=1}^{3} \int_{\partial\mathscr{B}\setminus\Gamma_{\alpha\mathrm{D}}^d} \tau_{\alpha d} V_{\alpha\mathrm{v}}^d \\ &+ \int_{\mathscr{B}} \langle \boldsymbol{Z} | \boldsymbol{L}_{\gamma\mathrm{v}} \rangle,\end{aligned} \tag{6.32b}$$

where $\boldsymbol{f}_\alpha \coloneqq \Phi_{\alpha\mathrm{R}}\varrho_\alpha \boldsymbol{f}$ is the amount of the external force per unit mass $\boldsymbol{f}$ felt by the αth phase [182]; $\tau_{\alpha d}$ is the dth component, in the given basis of co-vector fields $\{\boldsymbol{e}^c\}_{c=1}^3 \subset (T\mathscr{S})^*$, of the contact force $\boldsymbol{\tau}_\alpha$, relative to the αth phase, that is assumed to act on the portion of $\partial\mathscr{B}$ complementary to $\Gamma_{\alpha\mathrm{D}}^d$ (see Hughes [197]); $\boldsymbol{Z}$ is the external force density associated with the remodeling process acting on the remodeling rate $\boldsymbol{L}_\gamma$. The forces $\boldsymbol{f}_\alpha$, $\boldsymbol{\tau}_\alpha$, and $\boldsymbol{Z}$ must guarantee the existence and finiteness of the integrals in Equation (6.32b), and $\mathcal{P}_{\mathrm{v}}^{(\mathrm{e})}$ must be linear and bounded in each of its arguments. Moreover, we assume negligible inertial forces and no external forces dual to the functional trace of the virtual remodeling rate on $\partial\mathscr{B}$. It is worth emphasizing that, as evidenced by Gurtin and Anand [18], one could also account for an additional supply of external work manifested in the form of "remodeling" contact forces operating on the boundary $\partial\mathscr{B}$. However, we do not introduce these external agencies here and, consequently, we restrict our investigation to what Gurtin and Anand [18] call *"microscopically free"* boundaries[2].

Principle of Virtual Power. The definition (6.26) of $\mathcal{P}_{\mathrm{v}}^{(\mathrm{c})}$ as a useful tool for studying constrained systems by means of the Principle of Virtual Power (PVP) is

[2]The generalized forces $\boldsymbol{Y}_{\mathrm{u}}$ and $\boldsymbol{Z}$ introduced in this chapter, although sharing the same notation with the generalized forces employed in Chapter 5, are the push-forwards of their counterparts in Chapter 5 since they are dual to the virtual variations associated with the *natural* rate of remodeling $\boldsymbol{L}_\gamma \equiv \dot{\boldsymbol{F}}_\gamma \boldsymbol{F}_\gamma^{-1}$ rather than to the virtual variations related to the *material* rate of remodeling $\boldsymbol{\Lambda}_\gamma \equiv \boldsymbol{F}_\gamma^{-1}\dot{\boldsymbol{F}}_\gamma$.

taken from the book by Bonet and Wood [106], in which the PVP is formulated for computational problems. Following this methodology, we employ a *constrained* form of the PVP, which requires the fulfillment of the condition

$$\mathcal{P}_{\mathrm{v}}^{(\mathrm{i})}(\boldsymbol{V}_{\mathrm{sv}}, \boldsymbol{V}_{\mathrm{fv}}, \boldsymbol{L}_{\gamma\mathrm{v}}) + \mathcal{P}_{\mathrm{v}}^{(\mathrm{c})}(\boldsymbol{V}_{\mathrm{sv}}, \boldsymbol{V}_{\mathrm{fv}}, \boldsymbol{L}_{\gamma\mathrm{v}}; p_{\mathrm{v}}, \eta_{\mathrm{v}}, \boldsymbol{\Upsilon}_{\mathrm{v}}) = \mathcal{P}_{\mathrm{v}}^{(\mathrm{e})}(\boldsymbol{V}_{\mathrm{sv}}, \boldsymbol{V}_{\mathrm{fv}}, \boldsymbol{L}_{\gamma\mathrm{v}}) \quad (6.33)$$

for all the triples $(\boldsymbol{V}_{\mathrm{sv}}, \boldsymbol{V}_{\mathrm{fv}}, \boldsymbol{L}_{\gamma\mathrm{v}}) \in \mathscr{V}_{\mathrm{sv}} \times \mathscr{V}_{\mathrm{fv}} \times \mathscr{V}_{\gamma\mathrm{v}}$ and $(p_{\mathrm{v}}, \eta_{\mathrm{v}}, \boldsymbol{\Upsilon}_{\mathrm{v}}) \in \mathscr{V}_{\mathrm{pv}} \times \mathscr{V}_{\eta\mathrm{v}} \times \mathscr{V}_{\boldsymbol{\Upsilon}\mathrm{v}}$. A similar treatment of the constraints of the mixture incompressibility and of the isochoricity of the remodeling tensor is given in the work of Giammarini et al. [4].

From here on, we introduce the notation

$$\boldsymbol{\Pi}_{\alpha} \coloneqq -\Phi_{\alpha\mathrm{R}}\, p\boldsymbol{F}^{-\mathrm{T}} + \boldsymbol{P}_{\alpha}, \qquad \alpha = \mathrm{s,f}, \quad (6.34)$$

and, by invoking Gauss' Theorem and Leibniz rule of differentiation, and recalling that the dth component of the virtual velocity $\boldsymbol{V}_{\alpha\mathrm{v}}$ vanishes identically on $\Gamma^{d}_{\alpha\mathrm{D}}$, we recast Equation (6.33) in the form

$$\begin{aligned}
&\int_{\mathscr{B}} \sum_{\alpha} \langle J\boldsymbol{m}_{\alpha} - Jp\boldsymbol{F}^{-\mathrm{T}}\mathrm{Grad}\phi_{\alpha\mathrm{R}} - \mathrm{Div}\boldsymbol{\Pi}_{\alpha} - \Phi_{\alpha\mathrm{R}}\varrho_{\alpha}\boldsymbol{f} | \boldsymbol{V}_{\alpha\mathrm{v}} \rangle \\
&+ \int_{\mathscr{B}} \langle \boldsymbol{Y}_{\mathrm{u}} + \eta J_{\gamma}\boldsymbol{I}^{\mathrm{T}} + \boldsymbol{G}(\mathrm{Skew}\boldsymbol{\Upsilon}) - \mathrm{Div}\mathbb{Y}_{\mathrm{u}} - \boldsymbol{Z} | \boldsymbol{L}_{\gamma\mathrm{v}} \rangle \\
&+ \sum_{\alpha} \sum_{d=1}^{3} \int_{\partial\mathscr{B}\setminus\Gamma^{d}_{\alpha\mathrm{D}}} \{[\boldsymbol{\Pi}_{\alpha}\boldsymbol{N}]_{d} - \tau_{\alpha d}\} V^{d}_{\alpha\mathrm{v}} + \int_{\partial\mathscr{B}} \langle \mathbb{Y}_{\mathrm{u}}\boldsymbol{N} | \boldsymbol{L}_{\gamma\mathrm{v}} \rangle \\
&- \int_{\mathscr{B}} p_{\mathrm{v}}[\hat{\mathbb{C}}_{\mathrm{inc}} \circ (\boldsymbol{V}_{\mathrm{s}}, \boldsymbol{V}_{\mathrm{f}})] + \int_{\mathscr{B}} \eta_{\mathrm{v}}[\hat{\mathbb{C}}_{\mathrm{dev}} \circ \boldsymbol{L}_{\gamma}] + \int_{\mathscr{B}} \langle \boldsymbol{\Upsilon}_{\mathrm{v}} | \hat{\mathfrak{C}}_{\mathrm{sym}} \circ \boldsymbol{L}_{\gamma} \rangle = 0, \quad (6.35)
\end{aligned}$$

with $[\boldsymbol{\Pi}_{\alpha}\boldsymbol{N}]_{d} = [\boldsymbol{\Pi}_{\alpha}]_{d}{}^{B}N_{B}$, and $\boldsymbol{N}$ being the field of co-normals associated with $\partial\mathscr{B}$. Finally, as shown in Equation (6.27b), only the skew-symmetric part of $\boldsymbol{\Upsilon}$ is accounted for in Equation (6.35) because the symmetric part, $\mathrm{Sym}\boldsymbol{\Upsilon}$, is filtered out by the duality product with $\hat{\boldsymbol{\mathcal{A}}}_{\mathrm{sym}} \circ \boldsymbol{L}_{\gamma\mathrm{v}}$, which is a skew-symmetric tensor field.

To deduce Equation (6.35), we first apply Leibniz rule to $\langle \boldsymbol{P}_{\alpha} | \mathrm{Grad}\boldsymbol{V}_{\alpha\mathrm{v}} \rangle$ and $\langle \mathbb{Y}_{\mathrm{u}} | \mathrm{Grad}\boldsymbol{L}_{\gamma\mathrm{v}} \rangle$ in Equation (6.23b) and to $\langle -\Phi_{\alpha\mathrm{R}}\, p\boldsymbol{F}^{-\mathrm{T}} | \mathrm{Grad}\boldsymbol{V}_{\alpha\mathrm{v}} \rangle$ in Equation (6.30), i.e.,

$$\langle \boldsymbol{P}_{\alpha} | \mathrm{Grad}\boldsymbol{V}_{\alpha\mathrm{v}} \rangle = \mathrm{Div}(\boldsymbol{P}_{\alpha}^{\mathrm{T}}\boldsymbol{V}_{\alpha\mathrm{v}}) - \langle \mathrm{Div}\boldsymbol{P}_{\alpha} | \boldsymbol{V}_{\alpha\mathrm{v}} \rangle, \quad (6.36a)$$

$$\langle \mathbb{Y}_{\mathrm{u}} | \mathrm{Grad}\boldsymbol{L}_{\gamma\mathrm{v}} \rangle = \mathrm{Div}(\, \mathbb{Y}_{\mathrm{u}}^{\mathrm{T}} : \boldsymbol{L}_{\gamma\mathrm{v}}) - \langle \mathrm{Div}\mathbb{Y}_{\mathrm{u}} | \boldsymbol{L}_{\gamma\mathrm{v}} \rangle, \quad (6.36b)$$

$$\langle -\Phi_{\alpha\mathrm{R}}\, p\boldsymbol{F}^{-\mathrm{T}} | \mathrm{Grad}\boldsymbol{V}_{\alpha\mathrm{v}} \rangle = \mathrm{Div}(-\Phi_{\alpha\mathrm{R}}\, p\boldsymbol{F}^{-1}\boldsymbol{V}_{\alpha\mathrm{v}}) - \langle \mathrm{Div}(-\Phi_{\alpha\mathrm{R}}\, p\boldsymbol{F}^{-\mathrm{T}}) | \boldsymbol{V}_{\alpha\mathrm{v}} \rangle. \quad (6.36c)$$

The transposed tensor $\mathbb{Y}_{\mathrm{u}}^{\mathrm{T}}$ in (6.36b) has components $[\mathbb{Y}_{\mathrm{u}}^{\mathrm{T}}]^{L}{}_{M}{}^{N}$ (instead, $\mathbb{Y}_{\mathrm{u}}$ has indices placed as in $[\mathbb{Y}_{\mathrm{u}}]_{M}{}^{NL}$) and $\mathbb{Y}_{\mathrm{u}}^{\mathrm{T}} : \boldsymbol{L}_{\gamma\mathrm{v}}$ represents a pseudo-vector field with components $[\ \mathbb{Y}_{\mathrm{u}}^{\mathrm{T}} : \boldsymbol{L}_{\gamma\mathrm{v}}]^{A} = [\ \mathbb{Y}_{\mathrm{u}}^{\mathrm{T}}]^{A}{}_{B}{}^{C}[\boldsymbol{L}_{\gamma\mathrm{v}}]^{B}{}_{C}$.

The products $[\boldsymbol{\Pi}_{\alpha}\boldsymbol{N}]_{d}V_{\alpha\mathrm{v}}^{d}$ (no summation over $d = 1,2,3$) and $\langle \mathbb{Y}_{\mathrm{u}}\boldsymbol{N} | \boldsymbol{L}_{\gamma\mathrm{v}} \rangle$ in the surface integrals over $\partial\mathscr{B}\backslash\Gamma_{\alpha\mathrm{D}}^{d}$ and $\partial\mathscr{B}$ of Equation (6.35) descend from the application of Gauss' Theorem to $\mathrm{Div}(\boldsymbol{\Pi}_{\alpha}^{\mathrm{T}}\boldsymbol{V}_{\alpha\mathrm{v}})$ and $\mathrm{Div}(\ \mathbb{Y}_{\mathrm{u}}^{\mathrm{T}} : \boldsymbol{L}_{\gamma\mathrm{v}})$, which arise by working out Equation (6.33) and adding Equations (6.36a) and (6.36c) term by term. On $\partial\mathscr{B}\backslash\Gamma_{\alpha\mathrm{D}}^{d}$, the components $V_{\alpha\mathrm{v}}^{d}$ of the generalized virtual velocities need not vanish identically. Hence, we find:

$$\int_{\mathscr{B}} \sum_{\alpha} \mathrm{Div}(\boldsymbol{\Pi}_{\alpha}^{\mathrm{T}}\boldsymbol{V}_{\alpha\mathrm{v}}) = \int_{\partial\mathscr{B}} \sum_{\alpha} \langle \boldsymbol{\Pi}_{\alpha}^{\mathrm{T}}\boldsymbol{V}_{\alpha\mathrm{v}} | \boldsymbol{N} \rangle = \sum_{\alpha} \sum_{d=1}^{3} \int_{\partial\mathscr{B}\backslash\Gamma_{\alpha\mathrm{D}}^{d}} [\boldsymbol{\Pi}_{\alpha}\boldsymbol{N}]_{d}V_{\alpha\mathrm{v}}^{d}, \quad (6.37a)$$

$$\int_{\mathscr{B}} \mathrm{Div}(\ \mathbb{Y}_{\mathrm{u}}^{\mathrm{T}} : \boldsymbol{L}_{\gamma\mathrm{v}}) = \int_{\partial\mathscr{B}} \langle\ \mathbb{Y}_{\mathrm{u}}^{\mathrm{T}} : \boldsymbol{L}_{\gamma\mathrm{v}} | \boldsymbol{N} \rangle = \int_{\partial\mathscr{B}} \langle \mathbb{Y}_{\mathrm{u}}\boldsymbol{N} | \boldsymbol{L}_{\gamma\mathrm{v}} \rangle, \quad (6.37b)$$

where the identities $\langle \boldsymbol{\Pi}_{\alpha}^{\mathrm{T}}\boldsymbol{V}_{\alpha\mathrm{v}} | \boldsymbol{N} \rangle \equiv \langle \boldsymbol{\Pi}_{\alpha}\boldsymbol{N} | \boldsymbol{V}_{\alpha\mathrm{v}} \rangle$ and $\langle\ \mathbb{Y}_{\mathrm{u}}^{\mathrm{T}} : \boldsymbol{L}_{\gamma\mathrm{v}} | \boldsymbol{N} \rangle \equiv \langle \mathbb{Y}_{\mathrm{u}}\boldsymbol{N} | \boldsymbol{L}_{\gamma\mathrm{v}} \rangle$ are used.

To obtain Equations (6.35), (6.37a), and (6.37b), we have adapted a result of Functional Analysis (see Corollary 7.1, page 413 of the book by Salsa [196]), which requires $\boldsymbol{\Pi}_{\alpha} \in H^{1}(\mathscr{B}; (T\mathscr{S})^{*} \otimes T\mathscr{B})$ and $\mathbb{Y}_{\mathrm{u}} \in H^{1}(\mathscr{B}; [T\mathscr{B}]_{1}{}^{2})$. This implies $-\mathrm{Div}\boldsymbol{\Pi}_{\alpha} \in L^{2}(\mathscr{B}; (T\mathscr{S})^{*})$ and $-\mathrm{Div}\mathbb{Y}_{\mathrm{u}} \in L^{2}(\mathscr{B}; [T\mathscr{B}]_{1}{}^{1})$.

6.3.2 Strong form of the problem

Starting from Equation (6.35), classical localization procedures yield the force balances and the constraints of the system under consideration in *local form*, i.e.,

$$J\boldsymbol{m}_{\mathrm{s}} - Jp\boldsymbol{F}^{-\mathrm{T}}\mathrm{Grad}\phi_{\mathrm{sR}} - \mathrm{Div}(-\Phi_{\mathrm{sR}}\, p\boldsymbol{F}^{-\mathrm{T}} + \boldsymbol{P}_{\mathrm{s}}) - \boldsymbol{f}_{\mathrm{s}} = \boldsymbol{0}, \quad \text{in } \mathscr{B}, \quad (6.38a)$$

$$J\boldsymbol{m}_{\mathrm{f}} - Jp\boldsymbol{F}^{-\mathrm{T}}\mathrm{Grad}\phi_{\mathrm{fR}} - \mathrm{Div}(-\Phi_{\mathrm{fR}}\, p\boldsymbol{F}^{-\mathrm{T}} + \boldsymbol{P}_{\mathrm{f}}) - \boldsymbol{f}_{\mathrm{f}} = \boldsymbol{0}, \quad \text{in } \mathscr{B}, \quad (6.38b)$$

$$[(-\Phi_{\mathrm{sR}}\, p\boldsymbol{F}^{-\mathrm{T}} + \boldsymbol{P}_{\mathrm{s}})\boldsymbol{N}]_{d} = \tau_{\mathrm{s}d}, \quad d = 1,2,3, \quad \text{on } \partial\mathscr{B}\backslash\Gamma_{\mathrm{sD}}^{d}, \quad (6.38c)$$

$$[(-\Phi_{\mathrm{fR}}\, p\boldsymbol{F}^{-\mathrm{T}} + \boldsymbol{P}_{\mathrm{f}})\boldsymbol{N}]_{d} = \tau_{\mathrm{f}d}, \quad d = 1,2,3, \quad \text{on } \partial\mathscr{B}\backslash\Gamma_{\mathrm{fD}}^{d}, \quad (6.38d)$$

$$\boldsymbol{Y}_{\mathrm{u}} + \eta J_{\gamma}\boldsymbol{I}^{\mathrm{T}} + \boldsymbol{G}(\mathrm{Skew}\boldsymbol{\Upsilon}) - \mathrm{Div}\mathbb{Y}_{\mathrm{u}} - \boldsymbol{Z} = \boldsymbol{O}, \quad \text{in } \mathscr{B}, \quad (6.38e)$$

$$\mathbb{Y}_{\mathrm{u}}\boldsymbol{N} = \boldsymbol{O}, \qquad \text{on } \partial\mathscr{B}, \tag{6.38f}$$

$$\hat{\mathcal{C}}_{\mathrm{inc}} \circ (\boldsymbol{V}_{\mathrm{s}}, \boldsymbol{V}_{\mathrm{f}}) = \mathrm{Div}[(\Phi_{\mathrm{sR}}\boldsymbol{V}_{\mathrm{s}} + \Phi_{\mathrm{fR}}\boldsymbol{V}_{\mathrm{f}})\boldsymbol{F}^{-\mathrm{T}}] = 0, \qquad \text{in } \mathscr{B}, \tag{6.38g}$$

$$\hat{\mathcal{C}}_{\mathrm{dev}} \circ \boldsymbol{L}_\gamma = \langle J_\gamma \boldsymbol{I}^{\mathrm{T}} | \boldsymbol{L}_\gamma \rangle = J_\gamma \mathrm{tr}\boldsymbol{L}_\gamma = 0, \qquad \text{in } \mathscr{B}, \tag{6.38h}$$

$$\hat{\mathfrak{C}}_{\mathrm{sym}} \circ \boldsymbol{L}_\gamma = \tfrac{1}{2}[\boldsymbol{G}\boldsymbol{L}_\gamma - (\boldsymbol{G}\boldsymbol{L}_\gamma)^{\mathrm{T}}] = \boldsymbol{O}, \qquad \text{in } \mathscr{B}. \tag{6.38i}$$

Aside from the natural boundary conditions (6.38c), (6.38d) and (6.38f), the system (6.38a)–(6.38i) yields 20 independent scalar equations and features 80 unknown scalars fields: 20 of these are given by the basic kinematic variables χ, $\boldsymbol{V}_{\mathrm{f}}$, and $\boldsymbol{F}_\gamma$ (15 scalar unknowns) and by the Lagrange multipliers p, η, and $\mathrm{Skew}\boldsymbol{\Upsilon}$ (5 scalar unknowns), while the remaining 60 unknowns are the components of the fields $\boldsymbol{m}_{\mathrm{s}}$, $\boldsymbol{m}_{\mathrm{f}}$, $\boldsymbol{P}_{\mathrm{s}}$, $\boldsymbol{P}_{\mathrm{f}}$, $\boldsymbol{Y}_{\mathrm{u}}$, and $\mathbb{Y}_{\mathrm{u}}$. We recall that Φ_{sR} is regarded as known, while $\Phi_{\mathrm{fR}} = J - \Phi_{\mathrm{sR}}$, $\phi_{\mathrm{sR}} = \Phi_{\mathrm{sR}}/J$, and $\phi_{\mathrm{fR}} = \Phi_{\mathrm{fR}}/J$ are expressed as functions of J, as per Equation $(6.13)_1$. Similar considerations have recently been done in the work by Giammarini et al. [4]. Moreover, Equation (6.38e) splits as

$$\eta = -\tfrac{1}{3}\mathrm{tr}\big[J_\gamma^{-1}(\boldsymbol{Y}_{\mathrm{u}} - \mathrm{Div}\mathbb{Y}_{\mathrm{u}} - \boldsymbol{Z})\big], \tag{6.39a}$$

$$\mathrm{Skew}\boldsymbol{\Upsilon} = -\mathrm{Skew}[\boldsymbol{G}^{-1}(\boldsymbol{Y}_{\mathrm{u}} - \mathrm{Div}\mathbb{Y}_{\mathrm{u}} - \boldsymbol{Z})], \tag{6.39b}$$

$$\mathrm{Dev}_{\boldsymbol{G}}\mathrm{Sym}[\boldsymbol{G}^{-1}(\boldsymbol{Y}_{\mathrm{u}} - \mathrm{Div}\mathbb{Y}_{\mathrm{u}} - \boldsymbol{Z})] = \boldsymbol{O}, \tag{6.39c}$$

with $\mathrm{Dev}_{\boldsymbol{G}}\boldsymbol{A} \coloneqq \boldsymbol{A} - \frac{1}{3}\langle \boldsymbol{G}|\boldsymbol{A}\rangle\boldsymbol{G}^{-1}$, for any $\boldsymbol{A} = A^{MN}\boldsymbol{E}_M \otimes \boldsymbol{E}_N$, $\boldsymbol{A} = \boldsymbol{A}^{\mathrm{T}}$ (see [23, 87, 4]). Hence, η and $\mathrm{Skew}\boldsymbol{\Upsilon}$ can be computed separately, and the balance law (6.39c), which is equivalent to 5 scalar equations, replaces (6.38e) in the system (6.38a)–(6.38i). This reduces the number of coupled scalar equations to 16 and the number of effective unknowns to 76. However, granted the restrictions $\boldsymbol{m}_{\mathrm{s}} + \boldsymbol{m}_{\mathrm{f}} = \boldsymbol{0}$ and $\boldsymbol{g}^{-1}\boldsymbol{P}_\alpha\boldsymbol{F}^{\mathrm{T}} = (\boldsymbol{g}^{-1}\boldsymbol{P}_\alpha\boldsymbol{F}^{\mathrm{T}})^{\mathrm{T}}$, for $\alpha = \mathrm{s,f}$, which originate from the invariance of the internal virtual power under the superposition of arbitrary translational and rotational rigid motions [137, 182], the fields $\boldsymbol{m}_{\mathrm{f}}$, $\boldsymbol{P}_{\mathrm{s}}$, $\boldsymbol{P}_{\mathrm{f}}$, $\boldsymbol{Y}_{\mathrm{u}}$, and $\mathbb{Y}_{\mathrm{u}}$ will be assigned constitutively, thereby providing 60 scalar constitutive functions.

6.4 Constitutive assignments

For brevity, we concentrate on the consistency of the constitutive relations with objectivity and with the dissipation inequality of the system under study, while we give for granted all the other axioms of the general theory of constitutive laws

[198]. Following Cermelli and Gurtin [188] and Gurtin and Anand [142], some constitutive functions depend solely on the remodeling descriptors $\boldsymbol{F}_\gamma$ and $\mathrm{Curl}\boldsymbol{F}_\gamma$, and are defined so as to be invariant under smooth transformations of the reference placement of the system.

6.4.1 Dissipation inequality

By adapting the approaches of Cermelli and Gurtin [188], Cermelli et al. [70] and Gurtin and Anand [142] to biphasic mixtures, we consider a fixed region $\mathscr{R} \subset \mathscr{B}$ and the Helmholtz free energy density ψ_α of the αth phase, with $\alpha = \mathrm{s,f}$, per unit mass of the same phase. Then, we write the dissipation inequality:

$$\begin{aligned}\int_{\mathscr{R}} \mathcal{D} \coloneqq &- \overline{\int_{\mathscr{R}} \sum_\alpha \Phi_{\alpha\mathrm{R}}\varrho_\alpha\psi_\alpha}^{\cdot} - \int_{\partial\mathscr{R}} \langle \Phi_{\mathrm{fR}}\varrho_\mathrm{f}\psi_\mathrm{f}[\boldsymbol{V}_\mathrm{f} - \boldsymbol{V}_\mathrm{s}]\boldsymbol{F}^{-\mathrm{T}}|\boldsymbol{N}\rangle \\ &+ \int_{\mathscr{R}} \sum_\alpha \langle \boldsymbol{f}_\alpha|\boldsymbol{V}_\alpha\rangle + \int_{\partial\mathscr{R}} \sum_\alpha \langle(-\Phi_{\alpha\mathrm{R}}\, p\boldsymbol{F}^{-\mathrm{T}} + \boldsymbol{P}_\alpha)\boldsymbol{N}|\boldsymbol{V}_\alpha\rangle \\ &+ \int_{\mathscr{R}} \langle \boldsymbol{Z}|\boldsymbol{L}_\gamma\rangle + \int_{\partial\mathscr{R}} \langle \mathbb{Y}_\mathrm{u}\boldsymbol{N}|\boldsymbol{L}_\gamma\rangle \geq 0. \end{aligned} \tag{6.40}$$

Given a region $\mathscr{R}(t) \subset \mathscr{B}(t)$ contained in the current placement of the system, and the spatial (or Eulerian) representation of an $\mathbb{S}$-valued field ${}^{\mathrm{e}}f : \mathscr{R}(t) \times \mathscr{I} \to \mathbb{S}$, where $\mathbb{S}$ is $\mathbb{R}$ or any vector or tensor space, we define $f \coloneqq {}^{\mathrm{e}}f \circ (\chi, \mathcal{T}) : \mathscr{R}\times\mathscr{I} \to \mathbb{S}$, with $\mathscr{R} = [\hat{\chi}(\,\cdot\,, t)]^{-1}(\mathscr{R}(t)) \subset \mathscr{B}$ and $[\hat{\chi}(\,\cdot\,, t)]^{-1} \equiv \hat{\chi}_t^{-1}$. Hence, the time derivative of the integral of f over $\mathscr{R}$ reads

$$\overline{\int_{\mathscr{R}} f}^{\cdot} = \int_{\mathscr{R}} \dot{f}, \text{ with } \dot{f} = (D_\mathrm{s}\,{}^{\mathrm{e}}f) \circ (\chi, \mathcal{T}) \equiv [\partial_t\,{}^{\mathrm{e}}f + (\mathrm{grad}\,{}^{\mathrm{e}}f)\boldsymbol{v}_\mathrm{s}] \circ (\chi, \mathcal{T}). \tag{6.41}$$

The quantity $\dot{f} = (D_\mathrm{s}\,{}^{\mathrm{e}}f) \circ (\chi, \mathcal{T})$ is the time derivative of ${}^{\mathrm{e}}f$ with respect to the solid phase motion.

The second term on the right-hand side of Equation (6.40) compensates for the fact that, in the first term, the derivative of $\Phi_{\alpha\mathrm{R}}\varrho_\alpha\psi_\alpha$ is taken with respect to the velocity of the solid phase even for $\alpha = \mathrm{f}$. Then, by working out the time derivatives,

and invoking Gauss' Theorem, the mass balances[3], the incompressibility constraint (6.14b), the force balances (6.38a) and (6.38b), and the condition $\boldsymbol{m}_\mathrm{s} + \boldsymbol{m}_\mathrm{f} = \boldsymbol{0}$, we obtain

$$\begin{aligned}\int_{\mathscr{R}} \mathcal{D} = &- \int_{\mathscr{R}} \sum_{\alpha} \left[\Phi_{\alpha \mathrm{R}} \varrho_\alpha \dot{\psi}_\alpha - \langle \boldsymbol{P}_\alpha | \mathrm{Grad} \boldsymbol{V}_\alpha \rangle\right] \\ &+ \int_{\mathscr{R}} \langle J \boldsymbol{m}_\mathrm{f} - \Phi_{\mathrm{fR}} \varrho_\mathrm{f} \boldsymbol{F}^{-\mathrm{T}} \mathrm{Grad}\, \psi_\mathrm{f} | \boldsymbol{V}_\mathrm{f} - \boldsymbol{V}_\mathrm{s} \rangle \\ &+ \int_{\mathscr{R}} \left\{ \langle \boldsymbol{Y}_\mathrm{u} + \eta J_\gamma \boldsymbol{I}^{\mathrm{T}} + \boldsymbol{G}(\mathrm{Skew} \boldsymbol{\Upsilon}) | \boldsymbol{L}_\gamma \rangle + \langle \mathbb{Y}_\mathrm{u} | \mathrm{Grad} \boldsymbol{L}_\gamma \rangle \right\} \geq 0. \end{aligned} \tag{6.42}$$

Moreover, by neglecting the variability of ψ_f in space and time, localizing Equation (6.42), and recalling that the constraints (6.16a) and (6.16b) imply the identity

$$\langle \eta J_\gamma \boldsymbol{I}^{\mathrm{T}} + \boldsymbol{G}(\mathrm{Skew} \boldsymbol{\Upsilon}) | \boldsymbol{L}_\gamma \rangle = \eta J_\gamma \underbrace{\mathrm{tr} \boldsymbol{L}_\gamma}_{=0} + \langle \mathrm{Skew} \boldsymbol{\Upsilon} | \underbrace{\mathrm{Skew}(\boldsymbol{G} \boldsymbol{L}_\gamma)}_{=\boldsymbol{O}} \rangle = 0, \tag{6.43}$$

we obtain the following local form of the dissipation inequality [180, 153, 139]:

$$\begin{aligned}\mathcal{D} = &- \Phi_{\mathrm{sR}} \varrho_\mathrm{s} \dot{\psi}_\mathrm{s} + \langle J \boldsymbol{m}_\mathrm{f} | \boldsymbol{V}_\mathrm{f} - \boldsymbol{V}_\mathrm{s} \rangle + \langle \boldsymbol{P}_\mathrm{s} | \mathrm{Grad} \boldsymbol{V}_\mathrm{s} \rangle + \langle \boldsymbol{P}_\mathrm{f} | \mathrm{Grad} \boldsymbol{V}_\mathrm{f} \rangle \\ &+ \langle \boldsymbol{Y}_\mathrm{u} | \boldsymbol{L}_\gamma \rangle + \langle \mathbb{Y}_\mathrm{u} | \mathrm{Grad} \boldsymbol{L}_\gamma \rangle \geq 0. \end{aligned} \tag{6.44}$$

6.4.2 Constitutive descriptors and residual dissipation

From here on, we make three fundamental hypotheses:

Hp. 1 The stress response of the solid phase is hyperelastic.

Hp. 2 Aside from the exchange interactions with the fluid, the solid phase dissipates energy because of the remodeling of its internal structure.

Hp. 3 The fluid phase features two sources of dissipation: one is due to the exchange interactions with the solid phase, while the other one is due to the viscosity of the fluid, and results into a dissipative stress tensor, here identified with $\boldsymbol{P}_\mathrm{f}$.

[3] We refer to the identities $\overset{\cdot}{\overline{(\Phi_{\mathrm{sR}} \varrho_\mathrm{s})}} \equiv 0$ and $\overset{\cdot}{\overline{(\Phi_{\mathrm{fR}} \varrho_\mathrm{f})}} \equiv \dot{J}_{\varrho_\mathrm{f}} = -\mathrm{Div}(\Phi_{\mathrm{fR}} \varrho_\mathrm{f} [\boldsymbol{V}_\mathrm{f} - \boldsymbol{V}_\mathrm{s}] \boldsymbol{F}^{-\mathrm{T}})$ coming from the considerations reported in Section 6.2.2. Recall that the intrinsic mass densities ϱ_s and ϱ_f are assumed to be constant throughout this work.

To deal with these hypotheses, we choose the following collection of *independent constitutive variables*:

$$\mathcal{U} \coloneqq (\boldsymbol{F}, \boldsymbol{F}_\gamma, \mathfrak{B}, \boldsymbol{L}_\gamma, \mathrm{Grad}\boldsymbol{L}_\gamma, \mathrm{Grad}\boldsymbol{V}_\mathrm{f}, \boldsymbol{V}_\mathrm{fs}), \qquad \text{with } \boldsymbol{V}_\mathrm{fs} \coloneqq \boldsymbol{V}_\mathrm{f} - \boldsymbol{V}_\mathrm{s}. \tag{6.45}$$

The tensor fields $\boldsymbol{F}$ and $\boldsymbol{F}_\gamma$ account for the fact that the solid phase is hyperelastic (Hp. 1) and undergoes remodeling (Hp. 2). In fact, the elastic distortions and those due to the remodeling are described by $\boldsymbol{F}_\mathrm{e}$ and $\boldsymbol{F}_\gamma$, respectively, with $\boldsymbol{F}_\mathrm{e} = \boldsymbol{F}\boldsymbol{F}_\gamma^{-1}$. Thus, $\boldsymbol{F}_\mathrm{e}$ could be selected in lieu of $\boldsymbol{F}$ in the collection (6.45). However, since $\boldsymbol{F}$ is directly related to the motion of the solid phase, we find it more intuitive to use $\boldsymbol{F}$.

The Burgers tensor $\mathfrak{B}$ resolves the spatial variability of $\boldsymbol{F}_\gamma$ in a way that is unaffected by changes of the system's reference placement [199], while $\boldsymbol{L}_\gamma$ and $\mathrm{Grad}\boldsymbol{L}_\gamma$ account for the dissipation induced by the remodeling within a first-grade theory in $\boldsymbol{L}_\gamma$. Both $\mathfrak{B}$ and $\mathrm{Grad}\boldsymbol{L}_\gamma$ have their own length scale [142].

The relative velocity $\boldsymbol{V}_\mathrm{fs}$ is power-conjugate to the dissipative exchange interactions between the solid and the fluid phase, whereas $\mathrm{Grad}\boldsymbol{V}_\mathrm{f}$ is introduced because, at variance with the Darcian regime, the overall stress tensor of the fluid phase, $\boldsymbol{\Pi}_\mathrm{f}$, features the dissipative contribution $\boldsymbol{P}_\mathrm{f}$ in addition to the non-dissipative and hydrostatic term $-\Phi_\mathrm{fR} p \boldsymbol{F}^{-\mathrm{T}}$ (Hp. 3). This generalization captures also more complex behaviors of the fluid flow, such as boundary effects, and yields the Darcy–Brinkman model of the flow [174].

The fields ψ_s, $\boldsymbol{m}_\mathrm{f}$, $\boldsymbol{P}_\mathrm{s}$, $\boldsymbol{P}_\mathrm{f}$, $\boldsymbol{Y}_\mathrm{u}$, and $\mathbb{Y}_\mathrm{u}$ in the inequality (6.44) are the *dependent constitutive variables* of the present framework, and are assumed to be representable as functions of the collection $\mathcal{U}$, i.e.,

$$\psi_\mathrm{s} = \hat{\psi}_\mathrm{s} \circ \mathcal{U}, \qquad \boldsymbol{P}_\mathrm{s} = \hat{\boldsymbol{P}}_\mathrm{s} \circ \mathcal{U}, \qquad \boldsymbol{Y}_\mathrm{u} = \hat{\boldsymbol{Y}}_\mathrm{u} \circ \mathcal{U}, \qquad \mathbb{Y}_\mathrm{u} = \hat{\mathbb{Y}}_\mathrm{u} \circ \mathcal{U}, \tag{6.46a}$$

$$\boldsymbol{P}_\mathrm{f} = \hat{\boldsymbol{P}}_\mathrm{f} \circ \mathcal{U}, \qquad \boldsymbol{m}_\mathrm{f} = \hat{\boldsymbol{m}}_\mathrm{f} \circ \mathcal{U}. \tag{6.46b}$$

Since the dissipation of the system depends on $\mathcal{U}$ through the quantities (6.46a) and (6.46b), and since $\dot{\psi}_\mathrm{s}$ can be formally written as $\dot{\psi}_\mathrm{s} = \langle \partial_\mathcal{U} \hat{\psi}_\mathrm{s} \circ \mathcal{U} | \dot{\mathcal{U}} \rangle$, $\mathcal{D}$ admits the representation $\mathcal{D} = \hat{\mathcal{D}} \circ (\mathcal{U}, \dot{\mathcal{U}})$.

Computing $\dot{\psi}_\mathrm{s}$ permits to combine the partial derivatives $\partial_{\boldsymbol{F}} \hat{\psi}_\mathrm{s}$, $\partial_{\boldsymbol{F}_\gamma} \hat{\psi}_\mathrm{s}$, and $\partial_{\mathfrak{B}} \hat{\psi}_\mathrm{s}$ with $\hat{\boldsymbol{P}}_\mathrm{s}$, $\hat{\boldsymbol{Y}}_\mathrm{u}$, and $\hat{\mathbb{Y}}_\mathrm{u}$, respectively, as can be proven by recalling the identities $\dot{\boldsymbol{F}} \equiv \mathrm{Grad}\boldsymbol{V}_\mathrm{s}$ and $\dot{\boldsymbol{F}}_\gamma \equiv \boldsymbol{L}_\gamma \boldsymbol{F}_\gamma$, and noticing that $\dot{\mathfrak{B}}$ can be written as (cf. Equation

(6.8) of Gurtin and Anand [18])

$$\dot{\mathfrak{B}} = \boldsymbol{L}_\gamma \mathfrak{B} + \mathfrak{B}\boldsymbol{L}_\gamma^{\mathrm{T}} - J_\gamma^{-1}(\boldsymbol{F}_\gamma \times \boldsymbol{F}_\gamma)^{\mathrm{t}} : (\mathrm{Grad}\boldsymbol{L}_\gamma)^{\mathrm{t}}, \tag{6.47}$$

in which the condition $\mathrm{tr}\boldsymbol{L}_\gamma = 0$ has been enforced explicitly, and the cross product between two second-order tensors $\boldsymbol{A}$ and $\boldsymbol{B}$ of $[T\mathscr{B}]^1{}_1$ is defined as (cf. with Gurtin and Anand [18])

$$\begin{aligned} &[\boldsymbol{A} \times \boldsymbol{B}]^{ABC} = \frac{1}{\sqrt{\det[\boldsymbol{G}]}} \epsilon^{ADE} [\boldsymbol{A}]^B{}_D [\boldsymbol{B}]^C{}_E, \\ &\text{and } \ [(\boldsymbol{A} \times \boldsymbol{B})^{\mathrm{t}}]^{LMN} \coloneqq (\boldsymbol{A} \times \boldsymbol{B})^{NLM}. \end{aligned} \tag{6.48}$$

The relation (6.47) can be recast in the form $\mathcal{O}_\gamma \mathfrak{B} = -J_\gamma^{-1}(\boldsymbol{F}_\gamma \times \boldsymbol{F}_\gamma)^{\mathrm{t}} : (\mathrm{Grad}\boldsymbol{L}_\gamma)^{\mathrm{t}}$, where $\mathcal{O}_\gamma \mathfrak{B}$ is the Oldroyd derivative of $\mathfrak{B}$ with respect to $\boldsymbol{F}_\gamma$, defined as $\mathcal{O}_\gamma \mathfrak{B} \coloneqq \dot{\mathfrak{B}} - \boldsymbol{L}_\gamma \mathfrak{B} - \mathfrak{B}\boldsymbol{L}_\gamma^{\mathrm{T}}$.

On the other hand, the summands of $\dot{\psi}_{\mathrm{s}}$ given by

$$\langle \partial_{\boldsymbol{L}_\gamma} \hat{\psi}_{\mathrm{s}} \circ \mathcal{U} | \dot{\boldsymbol{L}}_\gamma \rangle, \qquad \langle \partial_{\mathrm{Grad}\boldsymbol{L}_\gamma} \hat{\psi}_{\mathrm{s}} \circ \mathcal{U} | \overline{\dot{\mathrm{Grad}\boldsymbol{L}_\gamma}} \rangle, \tag{6.49a}$$

$$\langle \partial_{\mathrm{Grad}\boldsymbol{V}_{\mathrm{f}}} \hat{\psi}_{\mathrm{s}} \circ \mathcal{U} | \overline{\dot{\mathrm{Grad}\boldsymbol{V}_{\mathrm{f}}}} \rangle, \qquad \langle \partial_{\boldsymbol{V}_{\mathrm{fs}}} \hat{\psi}_{\mathrm{s}} \circ \mathcal{U} | \overline{\dot{\boldsymbol{V}}_{\mathrm{fs}}} \rangle \tag{6.49b}$$

cannot be combined with any other term of the inequality (6.44), and, since $\hat{\mathcal{D}}$ is affine in the rates $\dot{\boldsymbol{L}}_\gamma$, $\overline{\dot{\mathrm{Grad}\boldsymbol{L}_\gamma}}$, $\overline{\dot{\mathrm{Grad}\boldsymbol{V}_{\mathrm{f}}}}$, and $\overline{\dot{\boldsymbol{V}}_{\mathrm{fs}}}$, which can be varied arbitrarily, the duality products in (6.49a) and (6.49b) could take on any real value and violate the non-negativity of $\hat{\mathcal{D}}$. Thus, to prevent this occurrence, we require the partial derivatives $\partial_{\boldsymbol{L}_\gamma}\hat{\psi}_{\mathrm{s}}$, $\partial_{\mathrm{Grad}\boldsymbol{L}_\gamma}\hat{\psi}_{\mathrm{s}}$, $\partial_{\mathrm{Grad}\boldsymbol{V}_{\mathrm{f}}}\hat{\psi}_{\mathrm{s}}$, and $\partial_{\boldsymbol{V}_{\mathrm{fs}}}\hat{\psi}_{\mathrm{s}}$ to vanish identically. This can be achieved by redefining the constitutive expression of ψ_{s} as a function of $\boldsymbol{F}$, $\boldsymbol{F}_\gamma$, and $\mathfrak{B}$, only. To this end, we find it convenient to introduce the solid phase Helmholtz free energy density per unit volume of $\mathscr{B}$, i.e., $W_{\mathrm{sR}} \coloneqq \Phi_{\mathrm{sR}} \varrho_{\mathrm{s}} \psi_{\mathrm{s}}$, for which it holds that $\dot{W}_{\mathrm{sR}} = \Phi_{\mathrm{sR}} \varrho_{\mathrm{s}} \dot{\psi}_{\mathrm{s}}$, since ϱ_{s} is assumed to be constant, while Φ_{sR} is constant by virtue of Equation (6.13). Then, following Gurtin and Anand [18], we write

$$W_{\mathrm{sR}} = \hat{W}_{\mathrm{sR}} \circ (\boldsymbol{F}, \boldsymbol{F}_\gamma, \mathfrak{B}) = \hat{W}_{\mathrm{se}} \circ (\boldsymbol{F}, \boldsymbol{F}_\gamma) + \hat{W}_{\mathrm{sD}} \circ \mathfrak{B}, \tag{6.50}$$

where $\hat{W}_{\mathrm{se}}$ is a hyperelastic free energy density of the solid phase, while $\hat{W}_{\mathrm{sD}}$ is referred to as a "defect" free energy [18] and resolves explicitly the spatial variability of $\boldsymbol{F}_\gamma$ within a first-order theory in the remodeling tensor (accounted for through

$\mathfrak{B}$). In our work, this is done to account also for the influence of *boundary effects* on remodeling. Yet, the formalism from which we are departing adopts $\mathrm{Grad}\boldsymbol{F}_\gamma$ to describe geometric incompatibilities that, for example, arise in metals at the scale of the lattice due to concentrated defects such as dislocations and disclinations [76, 199, 188, 79, 151, 200, 3].

To ensure objectivity, $\hat{W}_{\mathrm{se}}$ depends on $\boldsymbol{F}$ and $\boldsymbol{F}_\gamma$ through the elastic Cauchy–Green deformation tensor $\boldsymbol{C}_{\mathrm{e}} = \boldsymbol{F}_{\mathrm{e}}^{\mathrm{T}}\boldsymbol{g}\boldsymbol{F}_{\mathrm{e}}$. Hence, we set $\hat{W}_{\mathrm{se}} \circ (\boldsymbol{F}, \boldsymbol{F}_\gamma) \equiv \hat{W}_{\mathrm{sE}} \circ \boldsymbol{C}_{\mathrm{e}}$, and we reformulate $\hat{W}_{\mathrm{sR}}$ as

$$W_{\mathrm{sR}} = \hat{W}_{\mathrm{sR}} \circ (\boldsymbol{F}, \boldsymbol{F}_\gamma, \mathfrak{B}) = \hat{W}_{\mathrm{sE}} \circ \boldsymbol{C}_{\mathrm{e}} + \hat{W}_{\mathrm{sD}} \circ \mathfrak{B}, \tag{6.51}$$

where $\hat{W}_{\mathrm{sE}}$ and $\hat{W}_{\mathrm{sD}}$ are to be assigned. Hence, upon introducing the short-hand notation

$$\partial_{\boldsymbol{C}_{\mathrm{e}}} W_{\mathrm{sE}} \equiv \partial_{\boldsymbol{C}_{\mathrm{e}}} \hat{W}_{\mathrm{sE}} \circ \boldsymbol{C}_{\mathrm{e}}, \qquad \partial_{\mathfrak{B}} W_{\mathrm{sD}} \equiv \partial_{\mathfrak{B}} \hat{W}_{\mathrm{sD}} \circ \mathfrak{B}, \tag{6.52}$$

the term $\Phi_{\mathrm{sR}}\varrho_{\mathrm{s}}\dot{\psi}_{\mathrm{s}} \equiv \dot{W}_{\mathrm{sR}}$ in the inequality (6.44) admits the following representation [142]:

$$\begin{aligned}\Phi_{\mathrm{sR}}\varrho_{\mathrm{s}}\dot{\psi}_{\mathrm{s}} = {} & \langle \boldsymbol{g}\boldsymbol{F}_{\mathrm{e}}(2\partial_{\boldsymbol{C}_{\mathrm{e}}} W_{\mathrm{sE}})\boldsymbol{F}_\gamma^{-\mathrm{T}} | \dot{\boldsymbol{F}} \rangle \\ & + \big\langle -\boldsymbol{C}_{\mathrm{e}}(2\partial_{\boldsymbol{C}_{\mathrm{e}}} W_{\mathrm{sE}}) + [(\partial_{\mathfrak{B}} W_{\mathrm{sD}})\mathfrak{B}^{\mathrm{T}} + (\partial_{\mathfrak{B}} W_{\mathrm{sD}})^{\mathrm{T}}\mathfrak{B}] \big| \boldsymbol{L}_\gamma \big\rangle \\ & + \big\langle -J_\gamma^{-1}(\partial_{\mathfrak{B}} W_{\mathrm{sD}})^{\mathrm{T}}(\boldsymbol{F}_\gamma \times \boldsymbol{F}_\gamma)^{\mathrm{t}} \big| \mathrm{Grad}\boldsymbol{L}_\gamma \big\rangle. \end{aligned} \tag{6.53}$$

By plugging the derivative (6.53) into (6.44), the dissipation inequality becomes

$$\begin{aligned}\hat{\mathcal{D}} \circ (\mathcal{U}, \dot{\boldsymbol{F}}) = {} & \langle \hat{\boldsymbol{P}}_{\mathrm{s}} \circ \mathcal{U} - \boldsymbol{g}\boldsymbol{F}_{\mathrm{e}}(2\partial_{\boldsymbol{C}_{\mathrm{e}}} W_{\mathrm{sE}})\boldsymbol{F}_\gamma^{-\mathrm{T}} | \dot{\boldsymbol{F}} \rangle + \langle \hat{\boldsymbol{P}}_{\mathrm{f}} \circ \mathcal{U} | \mathrm{Grad}\boldsymbol{V}_{\mathrm{f}} \rangle + \langle J\hat{\boldsymbol{m}}_{\mathrm{f}} \circ \mathcal{U} | \boldsymbol{V}_{\mathrm{fs}} \rangle \\ & + \big\langle \hat{\mathbb{Y}}_{\mathrm{u}} \circ \mathcal{U} + \boldsymbol{C}_{\mathrm{e}}(2\partial_{\boldsymbol{C}_{\mathrm{e}}} W_{\mathrm{sE}}) - [(\partial_{\mathfrak{B}} W_{\mathrm{sD}})\mathfrak{B}^{\mathrm{T}} + (\partial_{\mathfrak{B}} W_{\mathrm{sD}})^{\mathrm{T}}\mathfrak{B}] \big| \boldsymbol{L}_\gamma \big\rangle \\ & + \big\langle \hat{\mathbb{Y}}_{\mathrm{u}} \circ \mathcal{U} + J_\gamma^{-1}(\partial_{\mathfrak{B}} W_{\mathrm{sD}})^{\mathrm{T}}(\boldsymbol{F}_\gamma \times \boldsymbol{F}_\gamma)^{\mathrm{t}} \big| \mathrm{Grad}\boldsymbol{L}_\gamma \big\rangle \geq 0, \end{aligned} \tag{6.54}$$

where, with a slight abuse of notation, we have reformulated $\hat{\mathcal{D}}$ as a function of $\mathcal{U}$ and $\dot{\boldsymbol{F}}$, only. However, $\hat{\mathcal{D}}$ is affine in $\dot{\boldsymbol{F}}$. Hence, following the same reasoning that has conducted to Equation (6.50), the entity dual to $\dot{\boldsymbol{F}}$ in the inequality (6.54) must vanish, and the active stress tensor $\boldsymbol{P}_{\mathrm{s}}$ is represented by

$$\boldsymbol{P}_{\mathrm{s}} = \hat{\boldsymbol{P}}_{\mathrm{s}} \circ (\boldsymbol{F}, \boldsymbol{F}_\gamma) = \boldsymbol{g}\boldsymbol{F}\boldsymbol{F}_\gamma^{-1}(2\partial_{\boldsymbol{C}_{\mathrm{e}}} W_{\mathrm{sE}})\boldsymbol{F}_\gamma^{-\mathrm{T}}. \tag{6.55}$$

Now, we particularize the hypotheses Hp. 2 and Hp. 3 by requiring each summand on the right-hand side of the inequality (6.54) to be non-negative independently of the other ones (the first summand satisfies trivially this requirement, since it is zero by virtue of Equation (6.55)). Moreover, as for the fluid, for which $\boldsymbol{P}_\mathrm{f}$ and $\boldsymbol{m}_\mathrm{f}$ are a dissipative stress and a dissipative force density, we define the dissipative stress-like quantities

$$\boldsymbol{Y}_\mathrm{ud} = \hat{\boldsymbol{Y}}_\mathrm{ud} \circ \mathcal{U} \coloneqq \hat{\boldsymbol{Y}}_\mathrm{u} \circ \mathcal{U} + \boldsymbol{C}_\mathrm{e}(2\partial_{\boldsymbol{C}_\mathrm{e}} W_\mathrm{sE}) - \left[(\partial_{\mathfrak{B}} W_\mathrm{sD})\mathfrak{B}^\mathrm{T} + (\partial_{\mathfrak{B}} W_\mathrm{sD})^\mathrm{T}\mathfrak{B}\right], \tag{6.56a}$$

$$\mathbb{Y}_\mathrm{ud} = \hat{\mathbb{Y}}_\mathrm{ud} \circ \mathcal{U} \coloneqq \hat{\mathbb{Y}}_\mathrm{u} \circ \mathcal{U} + J_\gamma^{-1}(\partial_{\mathfrak{B}} W_\mathrm{sD})^\mathrm{T}(\boldsymbol{F}_\gamma \times \boldsymbol{F}_\gamma)^\mathrm{t}, \tag{6.56b}$$

and, by recalling the result (6.55), we write the *residual dissipation inequality* as

$$\begin{aligned}\hat{\mathcal{D}} \circ \mathcal{U} = {} & \langle \hat{\boldsymbol{P}}_\mathrm{f} \circ \mathcal{U} | \mathrm{Grad}\boldsymbol{V}_\mathrm{f}\rangle + \langle J\hat{\boldsymbol{m}}_\mathrm{f} \circ \mathcal{U} | \boldsymbol{V}_\mathrm{fs}\rangle \\ & + \left\langle \hat{\boldsymbol{Y}}_\mathrm{ud} \circ \mathcal{U} \middle| \boldsymbol{L}_\gamma \right\rangle + \left\langle \hat{\mathbb{Y}}_\mathrm{ud} \circ \mathcal{U} \middle| \mathrm{Grad}\boldsymbol{L}_\gamma \right\rangle \geq 0.\end{aligned} \tag{6.57}$$

In the inequality (6.57), we split $\mathcal{U}$ into the two sub-collections of variables $\mathcal{E} \coloneqq (\boldsymbol{F}, \boldsymbol{F}_\gamma, \mathfrak{B})$ and $\mathcal{R} \coloneqq (\boldsymbol{L}_\gamma, \mathrm{Grad}\boldsymbol{L}_\gamma, \mathrm{Grad}\boldsymbol{V}_\mathrm{f}, \boldsymbol{V}_\mathrm{fs})$, with the latter comprising all the rates considered in the model, and we require $\hat{\mathcal{D}} \circ \mathcal{U} \equiv \hat{\mathcal{D}} \circ (\mathcal{E}; \mathcal{R})$ to be non-negative for all $\mathcal{E}$ and $\mathcal{R}$, null for $\mathcal{R} = 0$ independently of $\mathcal{E}$ (i.e., $\hat{\mathcal{D}} \circ (\mathcal{E}; 0) = 0$ uniformly with respect to $\mathcal{E}$), continuous and differentiable in $\mathcal{E}$, and at least continuous in $\mathcal{R}$. The continuity of $\hat{\mathcal{D}}$ in $\mathcal{R}$ is needed to ensure that $\hat{\mathcal{D}} \circ (\mathcal{E}; \mathcal{R})$ tends to zero for indefinitely small rates $\mathcal{R}$. We refer to the work by Cermelli et al. [70] for the reasoning reported so far.

In the following, we further assume $\hat{\mathcal{D}}$ to be *quadratic* in the rates $\mathcal{R}$, as specified by the law

$$\begin{aligned}\hat{\mathcal{D}} \circ (\mathcal{E}; \mathcal{R}) = {} & \Phi_\mathrm{fR}\langle \mathbb{V} : \mathrm{Grad}\boldsymbol{V}_\mathrm{f} | \mathrm{Grad}\boldsymbol{V}_\mathrm{f}\rangle + \Phi_\mathrm{fR}\langle \boldsymbol{r}\boldsymbol{V}_\mathrm{fs} | \boldsymbol{V}_\mathrm{fs}\rangle \\ & + \Phi_\mathrm{sR} S_\mathrm{y} \|\boldsymbol{L}_\gamma\|^2 + \Phi_\mathrm{sR} S_\mathrm{y} \ell^2 \|\mathrm{Grad}\boldsymbol{L}_\gamma\|^2 \geq 0,\end{aligned} \tag{6.58}$$

where $\Phi_\mathrm{fR} = J - \Phi_\mathrm{sR} \geq 0$ depends on $\boldsymbol{F}$ through J; $\mathbb{V} \coloneqq \hat{\mathbb{V}} \circ \mathcal{E}$ and $\boldsymbol{r} = \hat{\boldsymbol{r}} \circ \mathcal{E}$ are a fourth-order and a second-order tensor field, both positive semi-definite; $S_\mathrm{y} > 0$ and $\ell > 0$ are constants representing a characteristic mechanical stress of the solid phase, multiplied by a characteristic time scale,[4] and the characteristic length of $\boldsymbol{L}_\gamma$,

[4] The text "multiplied by a characteristic time scale" is going to appear in Prof. Alfio Grillo's IRIS institutional profile and is intended to be submitted to the journal *Mathematics and Mechanics of Solids* as part of a *Corrigendum*.

respectively [142]; the squared norms $\|\boldsymbol{L}_\gamma\|^2$ and $\|\mathrm{Grad}\boldsymbol{L}_\gamma\|^2$ are defined by

$$\|\boldsymbol{L}_\gamma\|^2 = \langle \boldsymbol{L}_\gamma^* | \boldsymbol{L}_\gamma \rangle = G_{AB}[\boldsymbol{L}_\gamma]^B{}_C G^{CD}[\boldsymbol{L}_\gamma]^A{}_D = \mathrm{tr}[\boldsymbol{L}_\gamma^{*\mathrm{T}}\boldsymbol{L}_\gamma], \tag{6.59a}$$

$$\begin{aligned}\|\mathrm{Grad}\boldsymbol{L}_\gamma\|^2 &= \langle (\mathrm{Grad}\boldsymbol{L}_\gamma)^* | \mathrm{Grad}\boldsymbol{L}_\gamma \rangle \\ &= G_{AH}[\mathrm{Grad}\boldsymbol{L}_\gamma]^H{}_{MN} G^{MB} G^{NC} [\mathrm{Grad}\boldsymbol{L}_\gamma]^A{}_{BC},\end{aligned} \tag{6.59b}$$

where $\boldsymbol{L}_\gamma^* \coloneqq \boldsymbol{G}\boldsymbol{L}_\gamma\boldsymbol{G}^{-1}$ and $(\mathrm{Grad}\boldsymbol{L}_\gamma)^*$ are the tensor fields *dual* to $\boldsymbol{L}_\gamma$ and $\mathrm{Grad}\boldsymbol{L}_\gamma$. The components of $(\mathrm{Grad}\boldsymbol{L}_\gamma)^*$ are given by the product of the first four factors on the right-hand side of Equation (6.59b).

Since in this work we need the stronger condition that $\hat{\mathcal{D}} \circ (\mathcal{E}; \mathcal{R})$ be zero if, and only if, all the rates are null, i.e., $\mathcal{R} = 0$, we consider only positive definite tensor-valued functions $\hat{\mathbb{V}} \circ \mathcal{E}$ and $\hat{\boldsymbol{r}} \circ \mathcal{E}$. Analogously, although Φ_{fR} is non-negative in general, we assume $\Phi_{\mathrm{fR}} > 0$, meaning no compaction. Moreover, since the duality products in Equation (6.58) symmetrize $\mathbb{V}$ and $\boldsymbol{r}$, we shall assume from here on that $\mathbb{V}$ possesses major symmetry and that $\boldsymbol{r}$ is symmetric. Hence, in components, we have $\mathbb{V}_a{}^A{}_b{}^B = \mathbb{V}_b{}^B{}_a{}^A$ and $r_{ab} = r_{ba}$.

Starting from the inequality (6.58), we retrieve the Darcy–Brinkman model of the flow and a strain-gradient theory of remodeling *à la* Gurtin and Anand [142] by invoking the Principle of Maximum Dissipation (see, e.g., Hackl and Fischer [201]).

6.4.3 Elastic energy and "defect" energy

To supply constitutive expressions for $\boldsymbol{P}_\mathrm{s}$, $\boldsymbol{Y}_\mathrm{u}$, and $\mathbb{Y}_\mathrm{u}$, we prescribe a Neo-Hookean strain energy density for the hyperelastic behavior of the solid phase and, following Gurtin and Anand [142], a "defect" energy density quadratic in the Burgers tensor, i.e.,

$$\hat{W}_{\mathrm{sE}} \circ \boldsymbol{C}_\mathrm{e} = \tfrac{1}{2}\Phi_{\mathrm{sR}}\mu_\mathrm{s}[\mathrm{tr}(\boldsymbol{G}^{-1}\boldsymbol{C}_\mathrm{e}) - 3] - \Phi_{\mathrm{sR}}\mu_\mathrm{s}\log J_\mathrm{e} + \tfrac{1}{2}\Phi_{\mathrm{sR}}\lambda_\mathrm{s}[\log J_\mathrm{e}]^2, \tag{6.60a}$$

$$\hat{W}_{\mathrm{sD}} \circ \mathfrak{B} = \tfrac{1}{2}\Phi_{\mathrm{sR}}\mu_\mathrm{s}L^2\|\mathfrak{B}\|^2, \qquad \text{with } \|\mathfrak{B}\|^2 = \langle \mathfrak{B}^* | \mathfrak{B} \rangle = \mathrm{tr}(\mathfrak{B}^{*\mathrm{T}}\mathfrak{B}), \tag{6.60b}$$

where $\mathfrak{B}^* \coloneqq \boldsymbol{G}\mathfrak{B}\boldsymbol{G}$ is the dual of the Burgers tensor, μ_s and λ_s are the first and the second Lamé parameters, and L is a phenomenological length scale that, as remarked by Gurtin and Anand [142], should be determined experimentally. Then, with $J_\gamma = 1$,

the relations (6.55), (6.56a), and (6.56b) take on the form

$$\boldsymbol{P}_{\mathrm{s}} = \hat{\boldsymbol{P}}_{\mathrm{s}} \circ (\boldsymbol{F}, \boldsymbol{F}_\gamma) = \Phi_{\mathrm{sR}}\mu_{\mathrm{s}}[\boldsymbol{g}\boldsymbol{F}\boldsymbol{B}_\gamma - \boldsymbol{F}^{-\mathrm{T}}] + (\Phi_{\mathrm{sR}}\lambda_{\mathrm{s}}\log J)\boldsymbol{F}^{-\mathrm{T}}, \tag{6.61a}$$

$$\boldsymbol{Y}_{\mathrm{u}} = \hat{\boldsymbol{Y}}_{\mathrm{u}} \circ \mathcal{U} = \hat{\boldsymbol{Y}}_{\mathrm{ud}} \circ \mathcal{U} - \boldsymbol{F}_\gamma^{-\mathrm{T}}[\boldsymbol{F}^{\mathrm{T}}\boldsymbol{P}_{\mathrm{s}}]\boldsymbol{F}_\gamma^{\mathrm{T}} + \Phi_{\mathrm{sR}}\mu_{\mathrm{s}}L^2\big[\mathfrak{B}^*\mathfrak{B}^{\mathrm{T}} + \mathfrak{B}^{*\mathrm{T}}\mathfrak{B}\big], \tag{6.61b}$$

$$\mathbb{Y}_{\mathrm{u}} = \hat{\mathbb{Y}}_{\mathrm{u}} \circ \mathcal{U} = \hat{\mathbb{Y}}_{\mathrm{ud}} \circ \mathcal{U} - \Phi_{\mathrm{sR}}\mu_{\mathrm{s}}L^2\mathfrak{B}^{*\mathrm{T}}(\boldsymbol{F}_\gamma \times \boldsymbol{F}_\gamma)^{\mathrm{t}}, \tag{6.61c}$$

with $\boldsymbol{F}^{\mathrm{T}}\boldsymbol{P}_{\mathrm{s}}$ being the Mandel stress tensor of the solid phase, associated with the reference placement.

6.4.4 Strain-gradient remodeling equation *a là* Gurtin and Anand

Applying the Principle of Maximum Dissipation [201] to the summands of the dissipation inequality (6.58) associated with the remodeling yields

$$\boldsymbol{Y}_{\mathrm{ud}} = \hat{\boldsymbol{Y}}_{\mathrm{ud}} \circ \boldsymbol{L}_\gamma \coloneqq \frac{1}{2}\left(\frac{\partial\hat{\mathcal{D}}}{\partial\boldsymbol{L}_\gamma} \circ (\mathcal{E};\mathcal{R})\right) = \Phi_{\mathrm{sR}}S_{\mathrm{y}}\,\boldsymbol{L}_\gamma^*, \tag{6.62a}$$

$$\mathbb{Y}_{\mathrm{ud}} = \hat{\mathbb{Y}}_{\mathrm{ud}} \circ \mathrm{Grad}\boldsymbol{L}_\gamma \coloneqq \frac{1}{2}\left(\frac{\partial\hat{\mathcal{D}}}{\partial\mathrm{Grad}\boldsymbol{L}_\gamma} \circ (\mathcal{E};\mathcal{R})\right) = \Phi_{\mathrm{sR}}S_{\mathrm{y}}\ell^2(\mathrm{Grad}\boldsymbol{L}_\gamma)^*. \tag{6.62b}$$

The relations (6.62a) and (6.62b) are a rewriting, in covariant formalism, and up to the rescaling of S_{y} through Φ_{sR} and the choice of some model parameters, of the constitutive laws proposed in Equation (6.17) of the work by Gurtin and Anand [142]. Indeed, in Cartesian coordinates, they read $\boldsymbol{Y}_{\mathrm{ud}} = \Phi_{\mathrm{sR}}S_{\mathrm{y}}\,\boldsymbol{L}_\gamma$ and $\mathbb{Y}_{\mathrm{ud}} = \Phi_{\mathrm{sR}}S_{\mathrm{y}}\ell^2\,\mathrm{Grad}\boldsymbol{L}_\gamma$, which are identical to the laws reported in the work by Gurtin and Anand [142] upon taking an identically null *"hardening (softening) function"* and unitary *"rate-sensitivity parameter"* [142], and by incorporating the model's *"reference flow-rate"* [142], taken unitary, into S_{y} (although S_{y} has physical dimensions of viscosity, with a slight abuse of terminology we call it "rescaled yield stress" or "rescaled strength" in the following).[5] Moreover, if the constraint (6.16b) is enforced explicitly, as done by Gurtin and Anand [142], then $\boldsymbol{L}_\gamma$ and $\mathrm{Grad}\boldsymbol{L}_\gamma$ can be substituted with $\boldsymbol{D}_\gamma$ and $\mathrm{Grad}\boldsymbol{D}_\gamma$ in the relations (6.62a) and (6.62b).

[5]The text "and by incorporating ... in the following)" is going to appear in Prof. Alfio Grillo's IRIS institutional profile and is intended to be submitted to the journal *Mathematics and Mechanics of Solids* as part of a *Corrigendum*.

Within their theory of strain-gradient plasticity, Gurtin and Anand [142] call $S_{\mathrm{y}} > 0$ *"coarse grain yield strength"* of the material, and introduce the length scale $\ell > 0$ to characterize the dissipation associated with the spatial inhomogeneity of $\boldsymbol{L}_\gamma$.

In our framework, we neglect any hardening or softening effects as well as any nonlinear relations similar to the *"nearly rate-independent behavior"* accounted for by Gurtin and Anand [142]. Indeed, the functional forms (6.62a) and (6.62b) are linear in $\boldsymbol{L}_\gamma$ and $\mathrm{Grad}\boldsymbol{L}_\gamma$, respectively, and have been obtained by requiring $\hat{\mathcal{D}}$ to be quadratic in each of these variables. Hence, they may fail to capture some particular physical aspects of remodeling. However, a more general picture can be obtained by hypothesizing $\boldsymbol{Y}_{\mathrm{ud}}$ and $\mathbb{Y}_{\mathrm{ud}}$ to be nonlinear in $\boldsymbol{L}_\gamma$ and $\mathrm{Grad}\boldsymbol{L}_\gamma$ [142], and showing that the resulting dissipation is non-negative.

Substituting the relations (6.62a) and (6.62b) into the expressions (6.61b) and (6.61c) for $\boldsymbol{Y}_{\mathrm{u}}$ and $\mathbb{Y}_{\mathrm{u}}$, and defining the apparent material parameters $\bar{S}_{\mathrm{y}} \coloneqq \Phi_{\mathrm{sR}} S_{\mathrm{y}}$, $\bar{\mu}_{\mathrm{s}} \coloneqq \Phi_{\mathrm{sR}}\mu_{\mathrm{s}}$ and $\bar{\lambda}_{\mathrm{s}} = \Phi_{\mathrm{sR}}\lambda_{\mathrm{s}}$ lead to

$$\boldsymbol{Y}_{\mathrm{u}} = \hat{\boldsymbol{Y}}_{\mathrm{u}} \circ (\mathcal{E}; \boldsymbol{L}_\gamma) = \bar{S}_{\mathrm{y}}\boldsymbol{L}_\gamma^* - \boldsymbol{F}_\gamma^{-\mathrm{T}}[\boldsymbol{F}^{\mathrm{T}}\boldsymbol{P}_{\mathrm{s}}]\boldsymbol{F}_\gamma^{\mathrm{T}} + \bar{\mu}_{\mathrm{s}}L^2\big[\mathfrak{B}^*\mathfrak{B}^{\mathrm{T}} + \mathfrak{B}^{*\mathrm{T}}\mathfrak{B}\big], \tag{6.63a}$$

$$\mathbb{Y}_{\mathrm{u}} = \hat{\mathbb{Y}}_{\mathrm{u}} \circ (\mathcal{E}; \mathrm{Grad}\boldsymbol{L}_\gamma) = \bar{S}_{\mathrm{y}}\ell^2(\mathrm{Grad}\boldsymbol{L}_\gamma)^* - \bar{\mu}_{\mathrm{s}}L^2\mathfrak{B}^{*\mathrm{T}}(\boldsymbol{F}_\gamma \times \boldsymbol{F}_\gamma)^{\mathrm{t}}, \tag{6.63b}$$

where we have set $J_\gamma = 1$ and, with a slight abuse of notation, we have retained the sole dependence on $\boldsymbol{L}_\gamma$ and $\mathrm{Grad}\boldsymbol{L}_\gamma$. Finally, by using the results (6.63a) and (6.63b), Equation (6.38e) becomes

$$\begin{aligned}&\bar{S}_{\mathrm{y}}\boldsymbol{L}_\gamma^* - \boldsymbol{F}_\gamma^{-\mathrm{T}}[\boldsymbol{F}^{\mathrm{T}}\boldsymbol{P}_{\mathrm{s}}]\boldsymbol{F}_\gamma^{\mathrm{T}} + \bar{\mu}_{\mathrm{s}}L^2\big[\mathfrak{B}^*\mathfrak{B}^{\mathrm{T}} + \mathfrak{B}^{*\mathrm{T}}\mathfrak{B}\big] + \eta\boldsymbol{I}^{\mathrm{T}} + \boldsymbol{G}(\mathrm{Skew}\boldsymbol{\Upsilon})\\ &- \mathrm{Div}\big\{\bar{S}_{\mathrm{y}}\ell^2(\mathrm{Grad}\boldsymbol{L}_\gamma)^* - \bar{\mu}_{\mathrm{s}}L^2\mathfrak{B}^{*\mathrm{T}}(\boldsymbol{F}_\gamma \times \boldsymbol{F}_\gamma)^{\mathrm{t}}\big\} - \boldsymbol{Z} = \boldsymbol{O}.\end{aligned} \tag{6.64}$$

The partial differential equation (6.64) and the constraints (6.38h) and (6.38i) rephrase, for remodeling, one of the main results of the theory of strain-gradient plasticity of Gurtin and Anand [142], formulated for $\boldsymbol{D}_\gamma$. In our derivation, we develop the model for $\boldsymbol{L}_\gamma$ and enforce the constraints on it via the Lagrange multiplier technique (see Section 2.3), which generates the reaction force $\eta\boldsymbol{I}^{\mathrm{T}} + \boldsymbol{G}(\mathrm{Skew}\boldsymbol{\Upsilon})$ in Equation (6.64). This can be eliminated by projecting Equation (6.64) onto the space of deviatoric and symmetric second-order tensor fields, as shown in Equation (6.39c), thereby retrieving Gurtin and Anand's strain-gradient *"micro-force balance"* [142]. Moreover, in our work, this result is framed within the context of solid-fluid mixtures. However, the coupling with the fluid is indirect and occurs through the influence that

the fields associated with the fluid (i.e., pressure p and velocity field $\boldsymbol{V}_\mathrm{f}$) exert on $\boldsymbol{F}$ (and, thus, on $\boldsymbol{P}_\mathrm{s}$). Another generalization is the presence of $\boldsymbol{Z}$, unaccounted for in the work by Gurtin and Anand [142], but relevant in the certain biological contexts, as is the case for growth [69, 87].

6.4.5 Darcy–Brinkman model for the flow of the interstitial fluid

The *Darcy–Brinkman model* [174] of the flow accounts for two independent types of dissipation, both related to the fluid (see Hp. 3). One is intrinsic to the fluid and hypothesizes a macroscopically viscous behavior, described by the dissipative stress tensor $\boldsymbol{P}_\mathrm{f}$. The other one, instead, stems from the dissipative character of the interactions between the solid and the fluid, described by $\boldsymbol{m}_\mathrm{f}$. By applying the formulation of the Principle of Maximum Dissipation presented by Hackl and Fischer [201] to the terms in the dissipation inequality (6.58) associated with the fluid flow, we find

$$\boldsymbol{P}_\mathrm{f} = \hat{\boldsymbol{P}}_\mathrm{f} \circ (\mathcal{E}; \mathcal{R}) \coloneqq \frac{1}{2}\left(\frac{\partial \hat{\mathcal{D}}}{\partial \mathrm{Grad}\boldsymbol{V}_\mathrm{f}} \circ (\mathcal{E}; \mathcal{R})\right) = \Phi_\mathrm{fR}[\hat{\mathbb{V}} \circ \mathcal{E}] : \mathrm{Grad}\boldsymbol{V}_\mathrm{f}, \tag{6.65a}$$

$$J\boldsymbol{m}_\mathrm{f} = J[\hat{\boldsymbol{m}}_\mathrm{f} \circ (\mathcal{E}; \mathcal{R})] \coloneqq \frac{1}{2}\left(\frac{\partial \hat{\mathcal{D}}}{\partial \boldsymbol{V}_\mathrm{fs}} \circ (\mathcal{E}; \mathcal{R})\right) = \Phi_\mathrm{fR}[\hat{\boldsymbol{r}} \circ \mathcal{E}]\boldsymbol{V}_\mathrm{fs}, \tag{6.65b}$$

where $\mathbb{V} = \hat{\mathbb{V}} \circ \mathcal{E}$ is a fourth-order tensor field of *generalized Brinkman viscosities* and $\boldsymbol{r} = \hat{\boldsymbol{r}} \circ \mathcal{E}$ is the (spatial) *resistivity* tensor field of the porous medium (as specified above, $\mathbb{V}$ enjoys major symmetry and $\boldsymbol{r}$ is symmetric). Since $\boldsymbol{r}$ is positive definite, it is invertible, and we identify its inverse with the expression

$$\boldsymbol{r}^{-1} = \phi_\mathrm{fR}^{-1}\boldsymbol{k}, \tag{6.66}$$

where $\boldsymbol{k}$ is the tensor field of the hydraulic conductivity of the medium (i.e., the permeability tensor field divided by the fluid dynamic viscosity). The tensor field $\boldsymbol{k}$ is symmetric and positive definite, too. We prescribe it to be a function of $\boldsymbol{F}$ only, and, since we are modeling biological tissues, we express it as suggested by Holmes and Mow [152], i.e.,

$$\boldsymbol{k} = \hat{\boldsymbol{k}} \circ \boldsymbol{F} = k_0\left[\frac{J - \Phi_\mathrm{sR}}{1 - \Phi_\mathrm{sR}}\right]^\kappa \exp\left(\tfrac{1}{2}m_0[J^2 - 1]\right)\boldsymbol{g}^{-1}, \tag{6.67}$$

where k_0, κ, and m_0 are positive material parameters (see Table 6.1).

To assign $\mathbb{V} = \hat{\mathbb{V}} \circ \mathcal{E}$, we start from the constitutive expression of the Cauchy stress tensor of the fluid phase, i.e., $\boldsymbol{\sigma}_\mathrm{f} = J^{-1}\boldsymbol{P}_\mathrm{f}\boldsymbol{F}^\mathrm{T}$, which, under the hypothesis of Newtonian-like behavior, can be written as

$$\boldsymbol{\sigma}_\mathrm{f} = \tfrac{1}{3}\phi_\mathrm{f}\mathfrak{a}\,(\mathrm{div}\boldsymbol{v}_\mathrm{f})\,\boldsymbol{\imath}^\mathrm{T} + 2\phi_\mathrm{f}\mathfrak{b}\,\mathrm{sym}(\boldsymbol{g}\,\mathrm{grad}\boldsymbol{v}_\mathrm{f})\boldsymbol{g}^{-1}, \tag{6.68}$$

where $\mathfrak{a}/3$ and $\mathfrak{b}$ are the Brinkman viscosity coefficients, fulfilling the inequalities $\mathfrak{a} + 2\mathfrak{b} > 0$ and $\mathfrak{b} > 0$, and $\boldsymbol{\imath} : T\mathscr{S} \to T\mathscr{S}$ is the spatial identity tensor field (note that, for simplicity, in these calculations we are omitting the composition of the involved fields with the maps χ and $\mathcal{T}$). Then, by computing $\boldsymbol{P}_\mathrm{f} = J\boldsymbol{\sigma}_\mathrm{f}\boldsymbol{F}^{-\mathrm{T}}$, we obtain the expression (6.65a) with

$$\mathbb{V} = \hat{\mathbb{V}} \circ \boldsymbol{F} \coloneqq \tfrac{1}{3}\mathfrak{a}\boldsymbol{F}^{-\mathrm{T}} \otimes \boldsymbol{F}^{-\mathrm{T}} + \mathfrak{b}\big(\boldsymbol{g} \underline{\otimes} \boldsymbol{C}^{-1} + \boldsymbol{F}^{-\mathrm{T}} \overline{\otimes} \boldsymbol{F}^{-1}\big), \tag{6.69a}$$

$$\mathbb{V}_a{}^A{}_b{}^B = \tfrac{1}{3}\mathfrak{a}[\boldsymbol{F}^{-\mathrm{T}}]_a{}^A[\boldsymbol{F}^{-\mathrm{T}}]_b{}^B + \mathfrak{b}\big(g_{ab}[\boldsymbol{C}^{-1}]^{AB} + [\boldsymbol{F}^{-\mathrm{T}}]_a{}^B[\boldsymbol{F}^{-1}]^A{}_b\big), \tag{6.69b}$$

where $\hat{\mathbb{V}}$ has been redefined as a function of $\boldsymbol{F}$ alone, and the notation introduced by Curnier et al. [202] has been adopted for the tensor products $\underline{\otimes}$ and $\overline{\otimes}$. Note that, by virtue of Equation (6.69a), and recalling that $\Phi_\mathrm{fR} = J - \Phi_\mathrm{sR}$, the constitutive representation of $\boldsymbol{P}_\mathrm{f}$ can be reformulated as

$$\boldsymbol{P}_\mathrm{f} = \hat{\boldsymbol{P}}_\mathrm{f} \circ (\boldsymbol{F}, \mathrm{Grad}\boldsymbol{V}_\mathrm{f}) = (J - \Phi_\mathrm{sR})(\hat{\mathbb{V}} \circ \boldsymbol{F}) : \mathrm{Grad}\boldsymbol{V}_\mathrm{f}. \tag{6.70}$$

The quantity $\frac{1}{3}\mathfrak{a}$ corresponds to the so-called "second viscosity", also known as "bulk viscosity" or "volume viscosity", that, within the monophasic framework, features in the compressible Navier–Stokes equation. However, in spite of this formal correspondence, $\frac{1}{3}\mathfrak{a}$ is physically distinct from the second viscosity of a compressible fluid (see Remark 6.1 below). From here on, we refer to $\frac{1}{3}\mathfrak{a}$ and $\mathfrak{b}$ as *Brinkman second viscosity* and *Brinkman dynamic viscosity*, respectively. Often, $\mathfrak{b}$ is also referred to as *effective viscosity* and is assumed to be different from the "true" viscosity of the fluid. Bear and Bachmat [203] express $\mathfrak{b}$ as proportional to the fluid true shear viscosity, with the proportionality factor being the ratio between the (scalar) tortuosity and the porosity of the porous medium in which the flow takes place.

Differently from the Darcian model, in which the Cauchy stress tensor of the fluid phase is the hydrostatic term $-\phi_\mathrm{f} p\,\boldsymbol{\imath}^\mathrm{T}$, the Darcy–Brinkman model distinguishes the

pressure contribution due to the Lagrange multiplier p from the viscous one. In other words, the fluid pressure is given by

$$p_{\mathrm{f}} \coloneqq -\tfrac{1}{3}\mathrm{tr}(-\phi_{\mathrm{f}} p\, \boldsymbol{\imath}^{\mathrm{T}} + \boldsymbol{\sigma}_{\mathrm{f}}) = \phi_{\mathrm{f}} p - \phi_{\mathrm{f}} \tfrac{\mathfrak{a}+2\mathfrak{b}}{3} \mathrm{div}\boldsymbol{v}_{\mathrm{f}}. \tag{6.71}$$

Although the fluid phase is assumed to be incompressible, the divergence of $\boldsymbol{v}_{\mathrm{f}}$ is not zero. Rather, the hypothesis of incompressibility, enforced also for the solid phase, is expressed by Equation (6.12), and the model of flow features the *Brinkman bulk viscosity* $(\mathfrak{a} + 2\mathfrak{b})/3$. However, if the velocity field of the solid phase is null and the volumetric fraction of the fluid phase is constant in space, Equation (6.12) reduces to $\mathrm{div}\boldsymbol{v}_{\mathrm{f}} = 0$ and, thus, $\boldsymbol{\sigma}_{\mathrm{f}}$ features only the contribution due to the Brinkman dynamic viscosity $\mathfrak{b}$. This approximation is often used in hydro-geological problems based on the Darcy–Brinkman flow model.

By substituting the relations (6.65a) and (6.65b) into (6.38b), and using (6.66), we obtain

$$\mathrm{Div}\big(\Phi_{\mathrm{fR}} \mathbb{V} : \mathrm{Grad}\boldsymbol{V}_{\mathrm{f}}\big) - \Phi_{\mathrm{fR}}\big[\big(\boldsymbol{F}^{-\mathrm{T}}\mathrm{Grad}p - \varrho_{\mathrm{f}}\boldsymbol{f}\big) + \phi_{\mathrm{fR}}\boldsymbol{k}^{-1}(\boldsymbol{V}_{\mathrm{f}} - \boldsymbol{V}_{\mathrm{s}})\big] = \boldsymbol{0}. \tag{6.72}$$

Equation (6.72) is a partial differential equation for the fluid velocity field $\boldsymbol{V}_{\mathrm{f}}$, coupled with the pressure field p and with the velocity field $\boldsymbol{V}_{\mathrm{s}}$ and deformation of the solid phase. Since $\mathbb{V}$ is positive definite and $\Phi_{\mathrm{fR}} > 0$, Equation (6.72) is elliptic in $\boldsymbol{V}_{\mathrm{f}}$.

Remark 6.1 (Comparison with the stress tensor of a compressible fluid in the monophasic framework).
Within the monophasic framework, the dissipative part of the stress tensor of a compressible fluid features the volumetric contribution $\zeta\,(\mathrm{div}\boldsymbol{v})\,\boldsymbol{\imath}^{\mathrm{T}}$, in which $\boldsymbol{v}$ is the velocity field of the fluid and ζ is a positive quantity termed *volume viscosity coefficient* (in the Newtonian case, ζ is independent of the velocity gradient). Yet, ζ is not necessarily equal to $(\mathfrak{a} + 2\mathfrak{b})/3$. There are two main reasons for this. First, ζ pertains to the description of a *compressible fluid* in the monophasic framework, whereas the bulk Brinkman viscosity $(\mathfrak{a} + 2\mathfrak{b})/3$ is defined also for an incompressible fluid phase in a fluid-solid biphasic mixture. Second, the Brinkman viscosities need not be equal to the viscosities that the same fluid would have if it were considered alone, i.e., decontextualized from the framework of mixture theory [174], although the two types of viscosities take values that become increasingly closer to each other for relatively small volumetric fractions of the solid phase.

6.5 Boundary-value problem, weak form, and numerical results

By substituting the constitutive relations (6.55), (6.63a), (6.63b), (6.65a), and (6.65b) into the system (6.38a)–(6.38i), and applying Dirichlet boundary conditions and initial conditions, we state an initial- and boundary-value problem (IBVP) for χ, $\boldsymbol{F}_\gamma$, $\boldsymbol{V}_\mathrm{f}$ and p. However, the boundary condition (6.38f), i.e.,

$$\mathbb{Y}_\mathrm{u}\boldsymbol{N} = \bar{S}_\mathrm{y}\ell^2(\mathrm{Grad}\boldsymbol{L}_\gamma)^*\boldsymbol{N} - \bar{\mu}_\mathrm{s}L^2\mathfrak{B}^{*\mathrm{T}}(\boldsymbol{F}_\gamma\times\boldsymbol{F}_\gamma)^\mathrm{t}\boldsymbol{N} = \boldsymbol{O}, \qquad \text{on } \partial\mathscr{B}, \tag{6.73}$$

does not have the expression of a classical Neumann boundary condition in $\boldsymbol{F}_\gamma$, since it involves also $\dot{\boldsymbol{F}}_\gamma$, $\mathrm{Grad}\dot{\boldsymbol{F}}_\gamma$, and $\mathrm{Curl}\boldsymbol{F}_\gamma$, as can be recognized by writing it explicitly.

To overcome this difficulty, we reformulate the IBVP by regarding $\boldsymbol{L}_\gamma$ as a primary unknown, rather than as a derived quantity, and we regard the relation $\dot{\boldsymbol{F}}_\gamma = \boldsymbol{L}_\gamma\boldsymbol{F}_\gamma$ as the additional equation for determining $\boldsymbol{F}_\gamma$. By doing so, Equation (6.64) can be recast in the form of a (linear) *modified Helmholtz equation* [204] in $\boldsymbol{L}_\gamma$, with a right-hand side that is highly nonlinear in $\boldsymbol{F}$ and $\boldsymbol{F}_\gamma$, and Equation (6.73) can be interpreted as a linear, nonhomogeneous, Neumann boundary condition for $\boldsymbol{L}_\gamma$, in which the non-homogeneity term depends on $\boldsymbol{F}_\gamma$ through $\boldsymbol{F}_\gamma\times\boldsymbol{F}_\gamma$ and the Burgers tensor $\mathfrak{B}$. Moreover, the constraints (6.38h) and (6.38i) become algebraic equations for $\boldsymbol{L}_\gamma$. This fact permits us to resolve them explicitly and, thus, to replace the nine unknown components of $\boldsymbol{L}_\gamma$ with the five unknown components of the symmetric and deviatoric tensor $\tilde{\boldsymbol{D}}_\gamma$, which satisfies identically the conditions $\tilde{\boldsymbol{D}}_\gamma = \tilde{\boldsymbol{D}}_\gamma^\mathrm{T}$ and $\langle\boldsymbol{G}^{-1}|\tilde{\boldsymbol{D}}_\gamma\rangle = 0$. Moreover, the reaction force $\eta\boldsymbol{I}^\mathrm{T} + \boldsymbol{G}(\mathrm{Skew}\Upsilon)$ can be eliminated from Equation (6.64) by projecting it onto the space of symmetric and deviatoric second-order tensors, as done in Equation (6.39c).

From here on, we neglect the external force densities $\Phi_{\mathrm{sR}}\varrho_\mathrm{s}\boldsymbol{f}$ and $\Phi_{\mathrm{fR}}\varrho_\mathrm{f}\boldsymbol{f}$, and, to visualize the reformulated IBVP, we rewrite Equations (6.38a), (6.38b), (6.38e) and (6.38g)–(6.38i) as

$$-\mathrm{Div}(\hat{\boldsymbol{P}}_\mathrm{s}\circ(\boldsymbol{F},\boldsymbol{F}_\gamma)) + J\phi_{\mathrm{fR}}^2\boldsymbol{k}^{-1}[\boldsymbol{V}_\mathrm{s}-\boldsymbol{V}_\mathrm{f}] + \Phi_{\mathrm{sR}}\boldsymbol{F}^{-\mathrm{T}}\mathrm{Grad}p = \boldsymbol{0}, \tag{6.74a}$$

$$-\mathrm{Div}\big(\Phi_{\mathrm{fR}}\mathbb{V} : \mathrm{Grad}\boldsymbol{V}_\mathrm{f}\big) + J\phi_{\mathrm{fR}}^2\boldsymbol{k}^{-1}[\boldsymbol{V}_\mathrm{f}-\boldsymbol{V}_\mathrm{s}] + \Phi_{\mathrm{fR}}\boldsymbol{F}^{-\mathrm{T}}\mathrm{Grad}p = \boldsymbol{0}, \tag{6.74b}$$

$$-\mathrm{Div}\big\{\bar{S}_\mathrm{y}\ell^2(\mathrm{Grad}\tilde{\boldsymbol{D}}_\gamma)^* - \tilde{\mathfrak{S}}^\sharp\big\} + \bar{S}_\mathrm{y}\tilde{\boldsymbol{D}}_\gamma^* = \tilde{\boldsymbol{A}}^\sharp + \tilde{\boldsymbol{Z}}^\sharp, \tag{6.74c}$$

$$-\mathrm{Div}[\Phi_{\mathrm{sR}}\boldsymbol{V}_\mathrm{s}\boldsymbol{F}^{-\mathrm{T}} + \Phi_{\mathrm{fR}}\boldsymbol{V}_\mathrm{f}\boldsymbol{F}^{-\mathrm{T}}] = 0, \tag{6.74d}$$

$$\dot{\chi} = \boldsymbol{V}_{\mathrm{s}}, \tag{6.74e}$$

$$\dot{\boldsymbol{F}}_{\gamma} = \boldsymbol{G}^{-1}\tilde{\boldsymbol{D}}_{\gamma}\boldsymbol{F}_{\gamma}, \tag{6.74f}$$

where we have introduced the auxiliary terms

$$\tilde{\boldsymbol{D}}^{*}_{\gamma} := \boldsymbol{G}^{-1}\tilde{\boldsymbol{D}}_{\gamma}\boldsymbol{G}^{-1}, \tag{6.75a}$$

$$\mathfrak{S} := \bar{\mu}_{\mathrm{s}}L^{2}\mathfrak{B}^{*\mathrm{T}}(\boldsymbol{F}_{\gamma}\times\boldsymbol{F}_{\gamma})^{\mathrm{t}}, \tag{6.75b}$$

$$\tilde{\mathfrak{S}}^{\sharp} := \tfrac{1}{2}\big[\boldsymbol{G}^{-1}\mathfrak{S} + (\boldsymbol{G}^{-1}\mathfrak{S})^{(\mathrm{t},\cdot)}\big] - \tfrac{1}{3}\boldsymbol{G}^{-1}\otimes\mathfrak{s}, \qquad \mathfrak{s}^{C} = \mathfrak{S}_{N}{}^{NC}, \tag{6.75c}$$

$$\boldsymbol{A} := \boldsymbol{F}_{\gamma}^{-\mathrm{T}}[\boldsymbol{F}^{\mathrm{T}}\boldsymbol{P}_{\mathrm{s}}]\boldsymbol{F}_{\gamma}^{\mathrm{T}} - \bar{\mu}_{\mathrm{s}}L^{2}\big[\mathfrak{B}^{*}\mathfrak{B}^{\mathrm{T}} + \mathfrak{B}^{*\mathrm{T}}\mathfrak{B}\big], \tag{6.75d}$$

$$\tilde{\boldsymbol{A}}^{\sharp} := \mathrm{Dev}_{\boldsymbol{G}}\mathrm{Sym}(\boldsymbol{G}^{-1}\boldsymbol{A}), \qquad \tilde{\boldsymbol{Z}}^{\sharp} := \mathrm{Dev}_{\boldsymbol{G}}\mathrm{Sym}(\boldsymbol{G}^{-1}\boldsymbol{Z}), \tag{6.75e}$$

and $\boldsymbol{V}_{\mathrm{s}}$ is viewed as an additional unknown, related to the solid phase motion χ through Equation (6.74e).

The components of $(\mathrm{Grad}\tilde{\boldsymbol{D}}_{\gamma})^{*}$, i.e., of the third-order tensor field dual to $\mathrm{Grad}\tilde{\boldsymbol{D}}_{\gamma}$, are given by $[(\mathrm{Grad}\tilde{\boldsymbol{D}}_{\gamma})^{*}]^{ABC} = G^{AM}[\mathrm{Grad}\boldsymbol{D}_{\gamma}]_{MNP}G^{NB}G^{PC}$. Moreover, for an arbitrary third-order tensor field $\mathfrak{T}$ of $[T\mathscr{B}]^{3}$, the transpose $\mathfrak{T}^{(\mathrm{t},\cdot)}$ means, in components, $[\mathfrak{T}^{(\mathrm{t},\cdot)}]^{ABC} = \mathfrak{T}^{BAC}$.

The system (6.74a)–(6.74f) consists of 24 scalar equations in the 24 scalar unknowns supplied by the components of χ, $\boldsymbol{F}_{\gamma}$, $\boldsymbol{V}_{\mathrm{s}}$, $\boldsymbol{V}_{\mathrm{f}}$, $\tilde{\boldsymbol{D}}_{\gamma}$ and by p, and is endowed with the boundary conditions

$$[(\hat{\boldsymbol{P}}_{\mathrm{s}}\circ(\boldsymbol{F},\boldsymbol{F}_{\gamma}) - \Phi_{\mathrm{sR}}p\boldsymbol{F}^{-\mathrm{T}})\boldsymbol{N}]_{d} = \tau_{\mathrm{s}d}, \quad \text{on } \partial\mathscr{B}\backslash\Gamma^{d}_{\mathrm{sD}}, \quad d\in\{1,2,3\}, \tag{6.76a}$$

$$[(\Phi_{\mathrm{fR}}\mathbb{V} : \mathrm{Grad}\boldsymbol{V}_{\mathrm{f}} - \Phi_{\mathrm{fR}}p\boldsymbol{F}^{-\mathrm{T}})\boldsymbol{N}]_{d} = \tau_{\mathrm{f}d}, \quad \text{on } \partial\mathscr{B}\backslash\Gamma^{d}_{\mathrm{fD}}, \quad d\in\{1,2,3\}, \tag{6.76b}$$

$$\chi^{d} = \chi^{d}_{\mathrm{b}}, \quad \text{on } \Gamma^{d}_{\mathrm{sD}}, \quad d\in\{1,2,3\}, \tag{6.76c}$$

$$V^{d}_{\mathrm{f}} = V^{d}_{\mathrm{fb}}, \quad \text{on } \Gamma^{d}_{\mathrm{fD}}, \quad d\in\{1,2,3\}, \tag{6.76d}$$

$$\{\bar{S}_{\mathrm{y}}\ell^{2}(\mathrm{Grad}\tilde{\boldsymbol{D}}_{\gamma})^{*} - \tilde{\mathfrak{S}}^{\sharp}\}\boldsymbol{N} = \boldsymbol{O}, \quad \text{on } \partial\mathscr{B}, \tag{6.76e}$$

where χ^{d}_{b} and V^{d}_{fb} are known boundary data on the solid phase motion and fluid velocity.

6.5.1 Initial- and boundary-value problem (IBVP)

The typical experimental apparatus for the compression test of multicellular aggregates consists of a chamber filled with water, kept at the temperature of 20°C, and two rigid and impermeable plates, usually made of resin or steel, placed within the chamber, parallel to each other, and oriented horizontally.

We consider a cylindrical specimen of a multicellular aggregate inserted between the plates and we study the case in which its bottom and upper surfaces are glued to the plates.

For the experiment under study, we assume the specimen's reference placement, i.e., $\mathscr{B}$, to coincide with its just described initial placement, and we partition the boundary of $\mathscr{B}$ as $\partial\mathscr{B} = \Gamma_B \cup \Gamma_L \cup \Gamma_U$, with Γ_B, Γ_L, and Γ_U denoting the bottom, lateral, and upper surface of the specimen, respectively.

The test is carried out in displacement control: a displacement ramp is applied uniformly to all the points of the upper plate (which, thus, remains parallel to its initial position) and, because of the hypothesis of rigidity, it is perfectly transmitted to Γ_U. The lower plate is kept fixed.

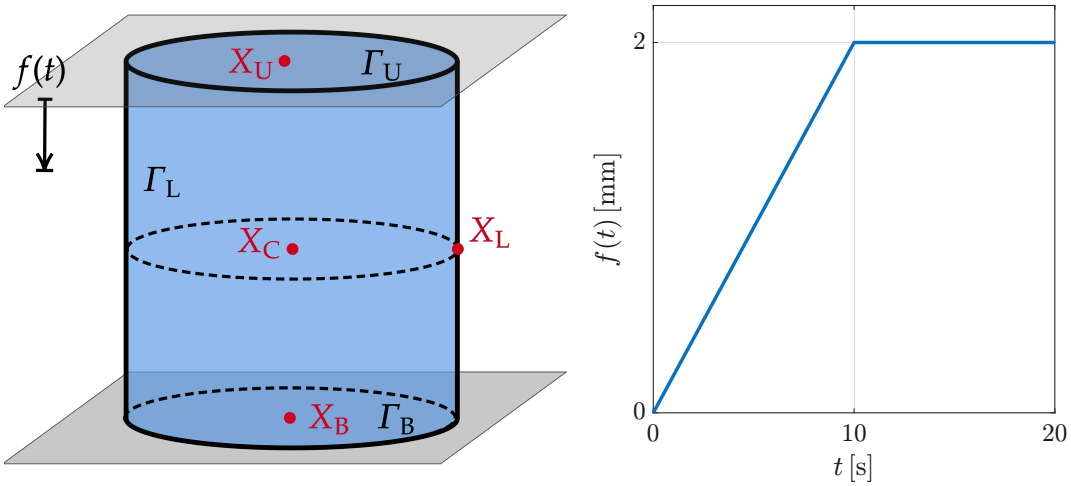

Fig. 6.2 Left panel: Graphical representation of the compression test simulated in this section. Right panel: Time trend of the magnitude of the (non-smoothed) compression ramp. This images were first showed during the conference "XI International Conference on Computational Bioengineering (ICCB 2025)" held in Rome, Italy, on September 8-10, 2025, within the presentation of the abstract "Coupling inelastic distortions and Darcy–Brinkman fluid flow in the modeling of multicellular aggregates under compression", authored by A. Pastore, A. Giammarini, A. Ramírez-Torres, A. Grillo.

Since the aggregate and the plates are glued together in the contact areas, and since the entity of the imposed displacement is relatively low (although large enough to generate finite deformations), the contact areas do not change in time.

The motion of the solid phase on the points of Γ_U and Γ_B is fully determined by the prescribed displacements: only the imposed vertical motion is allowed on Γ_U, while no motions are permitted on Γ_B. For the fluid phase, we prescribe no-slip conditions on Γ_U and Γ_B, so that the fluid velocity on the points of Γ_U equals the (vertical) velocity of the upper plate and is null on Γ_B. We assume Γ_L to be traction-free. For the remodeling, we assume that $\partial\mathscr{B} = \Gamma_U \cup \Gamma_B \cup \Gamma_L$ is *"microscopically free"*, to use the words of Gurtin and Anand [142].

By gathering the items of information collected so far, we obtain

BCs on Γ_U:	BCs on Γ_B:	BCs on Γ_L:	
$\chi(X,t) - \chi(X,0) = -f(t)\boldsymbol{e}_3,$	$\chi(X,t) - \chi(X,0) = \boldsymbol{0},$	$(\boldsymbol{P}_s - \Phi_{sR} p \boldsymbol{F}^{-T})\boldsymbol{N} = \boldsymbol{0},$	(6.77a)
$\boldsymbol{V}_f(X,t) = -\dot{f}(t)\boldsymbol{e}_3,$	$\boldsymbol{V}_f(X,t) = \boldsymbol{0},$	$(\boldsymbol{P}_f - \Phi_{fR} p \boldsymbol{F}^{-T})\boldsymbol{N} = \boldsymbol{0},$	(6.77b)
$\mathbb{Y}_u(X,t)\boldsymbol{N} = \boldsymbol{O},$	$\mathbb{Y}_u(X,t)\boldsymbol{N} = \boldsymbol{O},$	$\mathbb{Y}_u(X,t)\boldsymbol{N} = \boldsymbol{O},$	(6.77c)

with $f(t) = [H(t)H(t_r - t)t/t_r]f_{max} + [H(t_e - t)H(t - t_r)]f_{max}$, f_{max} specified in Table 6.1, and $H(s)$ being the Heaviside function, i.e., $H(s) = 1$ for $s > 0$, $H(s) = 0$ for $s < 0$, and $H(s) = 1/2$ for $s = 0$. Here, t_r is the instant of time at which the loading ramp ceases, while t_e is the final time of the simulation. Note that the solid phase velocity field on Γ_U is undefined for $t = t_r$, and we obtain $\boldsymbol{V}_s(X,t) = \boldsymbol{V}_{sb}(X,t) \equiv -(f_{max}/t_r)\,\boldsymbol{e}_3$ for $t \in]0, t_r[$, and $\boldsymbol{V}_s(X,t) = \boldsymbol{V}_{sb}(X,t) \equiv 0\,\boldsymbol{e}_3$ for $t \in]t_r, t_e[$. The same applies to the velocity of the fluid phase on Γ_U.

The prescribed initial conditions for the IBVP are

$$\chi(X,0) = \chi_{in}(X), \qquad \boldsymbol{V}_f(X,0) = \boldsymbol{0}, \qquad \boldsymbol{F}_\gamma(X,0) = \boldsymbol{I}, \tag{6.78}$$

with $\chi_{in}(X) = (X^1, X^2, X^3)$ for all $X \in \mathscr{B}$, and $\boldsymbol{I} : T_X\mathscr{B} \to T_X\mathscr{B}$ the "material" identity tensor.

Although our IBVP is inspired by an experiment, our simulations do not aim to recover experimental curves, at this stage. To do so, indeed, one necessitates a careful calibration of the model parameters.

Parameter	Symbol	Numerical value	Unit of measure	Reference
Initial radius	R	5.0	mm	-
Initial height	H	10.0	mm	-
Referential solidity	Φ_{sR}	0.6	-	-
Ref. hydraulic conductivity	k_0	$2.557 \cdot 10^{-2}$	$\mathrm{mm}^4/(\mathrm{N} \cdot \mathrm{s})$	-
Material parameter	m_0	0.0848	-	[205]
Material parameter	κ	4.6380	-	[205]
First Lamé's constant	λ_{s}	$1.3 \cdot 10^4$	Pa	-
Second Lamé's constant	μ_{s}	$2.0 \cdot 10^4$	Pa	-
Rescaled** coarse grain yield strength	S_{y}	$1.0 \cdot 10^3$	$\mathrm{Pa} \cdot \mathrm{s}$	-
Dissipative length [142]	ℓ	1.0	mm	-
Energetic length [142]	L	1.0	mm	-
Volumetric fluid viscosity coef.	$\mathfrak{a}$	0.0*	$\mathrm{Pa} \cdot \mathrm{s}$	-
Shear fluid viscosity coef.	$\mathfrak{b}$	$1.0 \cdot 10^{-3}$	$\mathrm{Pa} \cdot \mathrm{s}$	-
Prescribed displacement	$f_{\max}$	2.0	mm	-
Loading time	t_{r}	10.0	s	-
End time	t_{e}	20.0	s	-

Table 6.1 Values of the material parameters used for the numerical simulations. (*) Note that, in some simulations, the value $\mathfrak{a} = 100.0\,\mathrm{Pa} \cdot \mathrm{s}$ is assigned to obtain the Brinkman viscosity $\mathfrak{a}/3$. (**) The word "Rescaled" is going to appear in Prof. Alfio Grillo's IRIS institutional profile and is intended to be submitted to the journal *Mathematics and Mechanics of Solids* as part of a *Corrigendum*.

6.5.2 The weak form of the IBVP used in this work

The boundary conditions (6.77a)–(6.77c) suggest a weak formulation of the problem, based on Equations (6.74a)–(6.74f), that is customary when Darcy's regime is assumed, and consists of three main steps: (i) adding together the force balances (6.74a) and (6.74b); (ii) rewriting (6.74b) in a form in which the overall fluid stress tensor, i.e., $\boldsymbol{\Pi}_{\mathrm{f}} = -\Phi_{\mathrm{fR}} p \boldsymbol{F}^{-\mathrm{T}} + \Phi_{\mathrm{fR}} \mathbb{V} : \mathrm{Grad}\boldsymbol{V}_{\mathrm{f}}$, features under the divergence operator; (iii) recasting the condition (6.74d) as $\mathrm{Div}[\Phi_{\mathrm{fR}}(\boldsymbol{V}_{\mathrm{f}} - \boldsymbol{V}_{\mathrm{s}})\boldsymbol{F}^{-\mathrm{T}}] + \dot{J} = 0$. Accordingly, we obtain:

$$\int_{\mathscr{B}} \langle \hat{\boldsymbol{P}}_{\mathrm{s}} \circ (\boldsymbol{F}, \boldsymbol{F}_\gamma) + \hat{\boldsymbol{P}}_{\mathrm{f}} \circ (\boldsymbol{F}, \mathrm{Grad}\boldsymbol{V}_{\mathrm{f}}) | \mathrm{Grad}\boldsymbol{V}_{\mathrm{sv}} \rangle + \int_{\mathscr{B}} \langle -Jp\boldsymbol{F}^{-\mathrm{T}} | \mathrm{Grad}\boldsymbol{V}_{\mathrm{sv}} \rangle = 0, \tag{6.79a}$$

$$\int_{\mathscr{B}} \langle \hat{\boldsymbol{P}}_{\mathrm{f}} \circ (\boldsymbol{F}, \mathrm{Grad}\boldsymbol{V}_{\mathrm{f}}) - \Phi_{\mathrm{fR}} p \boldsymbol{F}^{-\mathrm{T}} | \mathrm{Grad}\boldsymbol{V}_{\mathrm{fv}} \rangle + \int_{\mathscr{B}} \langle J\phi_{\mathrm{fR}}^2 \boldsymbol{k}^{-1}[\boldsymbol{V}_{\mathrm{f}} - \boldsymbol{V}_{\mathrm{s}}] - p\,\mathrm{Div}(\Phi_{\mathrm{fR}}\boldsymbol{F}^{-\mathrm{T}}) | \boldsymbol{V}_{\mathrm{fv}} \rangle = 0, \tag{6.79b}$$

$$\int_{\mathscr{B}} \langle \Phi_{\mathrm{fR}}[\boldsymbol{V}_{\mathrm{f}} - \boldsymbol{V}_{\mathrm{s}}]\boldsymbol{F}^{-\mathrm{T}} | \mathrm{Grad}p_{\mathrm{v}} \rangle - \int_{\Gamma_{\mathrm{L}}} \langle \Phi_{\mathrm{fR}}[\boldsymbol{V}_{\mathrm{f}} - \boldsymbol{V}_{\mathrm{s}}]\boldsymbol{F}^{-\mathrm{T}}\boldsymbol{N} | p_{\mathrm{v}} \rangle - \int_{\mathscr{B}} \dot{J} p_{\mathrm{v}} = 0, \tag{6.79c}$$

$$\int_{\mathscr{B}} \left\{ \langle \bar{S}_{\mathrm{y}} \ell^2 (\mathrm{Grad}\tilde{\boldsymbol{D}}_\gamma)^* | \mathrm{Grad}\tilde{\boldsymbol{D}}_{\gamma\mathrm{v}} \rangle + \langle \bar{S}_{\mathrm{y}} \tilde{\boldsymbol{D}}_\gamma^* | \tilde{\boldsymbol{D}}_{\gamma\mathrm{v}} \rangle \right\} = \int_{\mathscr{B}} \left\{ \langle \tilde{\boldsymbol{A}}^\sharp + \tilde{\boldsymbol{Z}}^\sharp | \tilde{\boldsymbol{D}}_{\gamma\mathrm{v}} \rangle + \langle \tilde{\boldsymbol{\mathfrak{S}}}^\sharp | \mathrm{Grad}\tilde{\boldsymbol{D}}_{\gamma\mathrm{v}} \rangle \right\}. \tag{6.79d}$$

The absence of surface integrals in Equations (6.79a) and (6.79b) is due to the fact that Γ_{L} is a traction-free boundary both for the overall stress tensor and for the

fluid stress tensor, while Γ_{U} and Γ_{B} are Dirichlet boundaries for each of the three components of $\boldsymbol{V}_{\mathrm{s}}$ and $\boldsymbol{V}_{\mathrm{f}}$. In what follows, we assume $\boldsymbol{Z} = \boldsymbol{O}$.

A more detailed presentation of the weak form of the considered problem, written for more general boundary conditions, is provided in Appendix C.

6.5.3 Discussion of the numerical results

In this section we depart from the IBVP described in Section 5.1 and we simulate two benchmarks.

For the *first benchmark* we disregard remodeling and we compare the generalized Darcy–Brinkman model with the "classical" poroelastic model based on Darcy's law.

In the *second benchmark*, we consider also remodeling and we study two scenarios:

- the "Grade-0" case, or model, characterized by Darcy's law for the fluid and by $\boldsymbol{F}_\gamma$ for remodeling (we refer to this type of remodeling as "grade-0 remodeling"), with no spatial derivatives of $\boldsymbol{F}_\gamma$ explicitly featuring in the constitutive framework (at a glance, the Brinkman viscosities are set equal to zero, i.e., $\mathfrak{a} = 0\,\mathrm{Pa}\cdot\mathrm{s}$ and $\mathfrak{b} = 0\,\mathrm{Pa}\cdot\mathrm{s}$, and the remodeling lengths ℓ and L are null, i.e., $\ell = 0\,\mathrm{m}$ and $L = 0\,\mathrm{m}$);
- the "Grade-1" case, or model, characterized by the Darcy–Brinkman model for the fluid flow and by $\boldsymbol{F}_\gamma$ and $\mathrm{Grad}\boldsymbol{F}_\gamma$ for remodeling, as presented above (we refer to this type of remodeling as "grade-1 remodeling").

For the second benchmark, we compare the results predicted by the Grade-1 and the Grade-0 cases. The latter model can be retrieved by reverting to Darcy's regime, neglecting the terms associated with the Burgers tensor $\mathfrak{B}$ and $\mathrm{Grad}\boldsymbol{L}_\gamma$, or $\mathrm{Grad}\tilde{\boldsymbol{D}}_\gamma$ (by virtue of the constraints put on $\boldsymbol{L}_\gamma$), and disregarding the boundary conditions prescribed on $\boldsymbol{L}_\gamma$..

We use COMSOL Multiphysics® v5.3 to solve numerically the two benchmarks. In particular, for both problems, we generate a mesh consisting of 7656 volume elements, 1576 surface elements and 168 line elements. For the simulations of the Grade-1 model, we use quadratic Lagrange elements for the deformation χ, linear Lagrange elements for the fluid velocity $\boldsymbol{V}_{\mathrm{f}}$, linear Lagrange elements for the pressure field p, and, when remodeling is considered, linear discontinuous Lagrange elements

for the remodeling tensor $\boldsymbol{F}_\gamma$ and linear Lagrange elements for the remodeling rate $\tilde{\boldsymbol{D}}_\gamma$. For the simulations of the Grade-0 model, we employ linear Lagrange elements for χ, linear Lagrange elements for p and, when remodeling is considered, linear discontinuous Lagrange elements for $\boldsymbol{F}_\gamma$. We did not carry out convergence tests with mesh refinement.

To reach convergence in the simulations of Equations (6.79a)–(6.79d), we adopt one strategy, provided directly by COMSOL Multiphysics® v5.3. Namely, we regularize the imposed displacement on the upper surface of the specimen by slightly modifying the slope of the displacement ramp $f(t)$. In particular, we smooth the edges of the ramp at $t = 0\,\mathrm{s}$ and $t = t_\mathrm{r} = 10\,\mathrm{s}$, and we make it steeper over the time window $[0.5\,\mathrm{s}, t_\mathrm{r} - 1\,\mathrm{s}]$. Hence, in some simulations, the end of the increasing part of the non-regularized compressive ramp, i.e., $t_\mathrm{r} = 10\,\mathrm{s}$, does not coincide with the instant of time at which the registered value of quantities such as fluid pressure and mechanical stress acquire their highest values. Rather, these quantities reach their maxima before $t_\mathrm{r} = 10\,\mathrm{s}$.

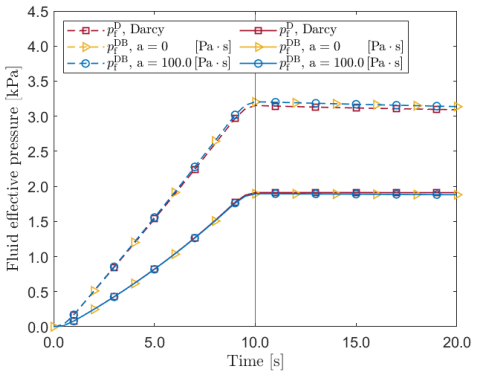

(a) Fluid effective pressure p_f at $X_\mathrm{U} \in \Gamma_\mathrm{U}$ and at X_C (no remodeling)

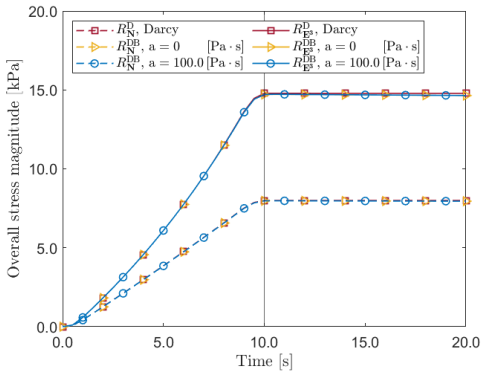

(b) Overall stress magnitudes $R_{\boldsymbol{N}}$ at $X_\mathrm{U} \in \Gamma_\mathrm{U}$ and $R_{\boldsymbol{E}^3}$ at X_C (no remodeling)

Fig. 6.3 Left panel: Fluid effective pressure p_f (see Equation (6.71)) evaluated at the middle point X_U of the upper surface Γ_U of the specimen (dashed lines), and at the center of the specimen X_C (solid lines). Right panel: Overall stress magnitudes $R_{\boldsymbol{N}}$ (see Equation (6.80a)), evaluated at the middle point X_U of the upper surface Γ_U of the specimen (dashed lines), and $R_{\boldsymbol{E}^3}$ (see Equation (6.80b)), evaluated at the center of the specimen X_C (solid lines). We consider three cases for the fluid flow: Darcian regime ("D"); Darcy–Brinkman model ("DB") with $\mathfrak{a} = 0\,\mathrm{Pa} \cdot \mathrm{s}$; and Darcy–Brinkman model ("DB") with $\mathfrak{a} = 100.0\,\mathrm{Pa} \cdot \mathrm{s}$.

First benchmark: Poroelastic Darcy–Brinkman model (no remodeling).

The purpose of this benchmark is to evaluate how switching from Darcy's model to the Darcy–Brinkman model presented in our work influences the fluid pressure and the overall stress in the considered specimen. To this end, we select some representative points of the specimen. In particular, we discuss the role of the *Brinkman second viscosity* $\mathfrak{a}$, since, in our model, the stress associated with it is nonzero in spite of the incompressibility of the fluid phase. This is a major difference with respect to the Darcy–Brinkman models of porous media that do not account for the deformation of the solid matrix and for the spatial variability of the porosity. Indeed, in these models, the fluid phase velocity field turns out to be divergence-free and the fluid Cauchy stress tensor becomes $\boldsymbol{\sigma}_{\mathrm{f}} = 2\phi_{\mathrm{f}}\mathfrak{b}\,\mathrm{sym}(\boldsymbol{g}\,\mathrm{grad}\boldsymbol{v}_{\mathrm{f}})\boldsymbol{g}^{-1}$, where $\mathrm{grad}\boldsymbol{v}_{\mathrm{f}}$ is deviatoric. In our framework, instead, $\boldsymbol{\sigma}_{\mathrm{f}}$ is given by Equation (6.68), since $\mathrm{div}\boldsymbol{v}_{\mathrm{f}}$ is nonzero as a consequence of the deformation of the solid phase and variability of the medium's porosity.

Figure 6.3. In Figure 6.3a, we plot the fluid effective pressure field p_{f} (in Darcy's case, $p_{\mathrm{f}} \equiv \phi_{\mathrm{f}} p$) versus time, evaluated both at the middle point X_{U} of the upper interface Γ_{U} between the specimen and the upper plate (dashed lines) and at the center of the specimen, X_{C} (solid lines).

In Figure 6.3b, we plot the time trend of the following overall stress magnitudes:

$$R_{\boldsymbol{N}} := \left\|\{-Jp\boldsymbol{F}^{-\mathrm{T}} + \hat{\boldsymbol{P}}_{\mathrm{s}} \circ (\boldsymbol{F}, \boldsymbol{F}_{\gamma}) + (J - \Phi_{\mathrm{sR}})(\hat{\mathbb{V}} \circ \boldsymbol{F}) : \mathrm{Grad}\boldsymbol{V}_{\mathrm{f}}\}\boldsymbol{N}\right\|, \quad \text{on } \Gamma_{\mathrm{U}}, \quad (6.80a)$$

$$R_{\boldsymbol{E}^3} := \left\|\{-Jp\boldsymbol{F}^{-\mathrm{T}} + \hat{\boldsymbol{P}}_{\mathrm{s}} \circ (\boldsymbol{F}, \boldsymbol{F}_{\gamma}) + (J - \Phi_{\mathrm{sR}})(\hat{\mathbb{V}} \circ \boldsymbol{F}) : \mathrm{Grad}\boldsymbol{V}_{\mathrm{f}}\}\boldsymbol{E}^3\right\|, \quad \text{on } \Gamma_{\mathrm{C}}, \quad (6.80b)$$

where $\boldsymbol{N}$ is the field of co-normals associated with Γ_{U} and $\boldsymbol{E}^3$ is the unit co-vector field of the basis $\{\boldsymbol{E}^A\}_{A=1}^3$, taken as the field of co-normals associated with the surface Γ_{C} passing through X_{C} and orthogonal to the specimen's symmetry axis. We evaluate $R_{\boldsymbol{N}}$ at X_{U} and $R_{\boldsymbol{E}^3}$ at X_{C}.

For the simulations that involve the Darcy–Brinkman model, we observe the response of the system for $\mathfrak{a} = 0\,\mathrm{Pa}\cdot\mathrm{s}$ and for $\mathfrak{a} = 100.0\,\mathrm{Pa}\cdot\mathrm{s}$. The reason for choosing these values, which, to our knowledge, are not supported by experimental data, is to estimate the impact of the parameter $\mathfrak{a}$ on p_{f}, $R_{\boldsymbol{N}}$, and $R_{\boldsymbol{E}^3}$. For this purpose, we consider both $\mathfrak{a} = 0\,\mathrm{Pa}\cdot\mathrm{s}$ and $\mathfrak{a} = 100.0\,\mathrm{Pa}\cdot\mathrm{s}$, which is five orders of magnitude greater than $\mathfrak{b}$ and much bigger than the volume viscosity coefficient

of fluids that are often regarded as incompressible in biological media (about four orders of magnitude greater than water volume viscosity at 25°C).

We denote by $p_{\mathrm{f}}^{\mathrm{D}}$, $R_{\boldsymbol{N}}^{\mathrm{D}}$ and $R_{\boldsymbol{E}^3}^{\mathrm{D}}$ the curves obtained by using Darcy's model, and by $p_{\mathrm{f}}^{\mathrm{DB}}$, $R_{\boldsymbol{N}}^{\mathrm{DB}}$ and $R_{\boldsymbol{E}^3}^{\mathrm{DB}}$ those obtained by switching to the Darcy–Brinkman model.

Figures 6.3a and 6.3b compare the time trends of $p_{\mathrm{f}}^{\mathrm{D}}$, $R_{\boldsymbol{N}}^{\mathrm{D}}$ and $R_{\boldsymbol{E}^3}^{\mathrm{D}}$ (squares) with those of $p_{\mathrm{f}}^{\mathrm{DB}}$, $R_{\boldsymbol{N}}^{\mathrm{DB}}$ and $R_{\boldsymbol{E}^3}^{\mathrm{DB}}$ for $\mathfrak{a} = 0$ Pa · s (triangles) and $\mathfrak{a} = 100.0$ Pa · s (circles). In Figure 6.3a, the transition from the Darcian model to the Darcy–Brinkman model produces, for both values of $\mathfrak{a}$, appreciable changes in the values of p_{f} only at X_{U} (dashed lines) and for $t \in]t_{\mathrm{r}}, t_{\mathrm{e}}[$, while it yields very modest differences at X_{C} and over the same time window (solid lines). In Figure 6.3b, instead, no remarkably appreciable differences are observed in the time trends of $R_{\boldsymbol{N}}$ and $R_{\boldsymbol{E}^3}$, regardless of the values attributed to $\mathfrak{a}$. These results could be related to the simple geometry of the contact zones between the specimen and the plates, which do not give rise to particularly noticeable boundary effects (at least, as long as remodeling is deactivated). Hence, for the next simulations we take $\mathfrak{a} = 0\,\mathrm{Pa} \cdot \mathrm{s}$.

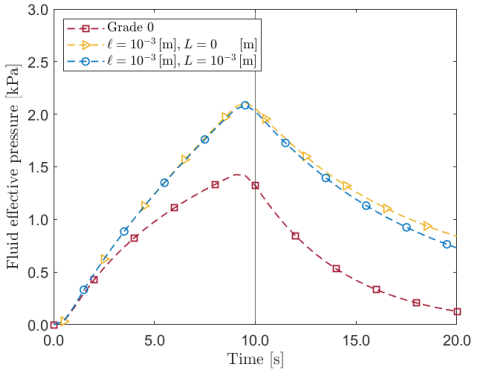

(a) Fluid effective pressure p_{f} at $X_{\mathrm{U}} \in \Gamma_{\mathrm{U}}$ (case with remodeling)

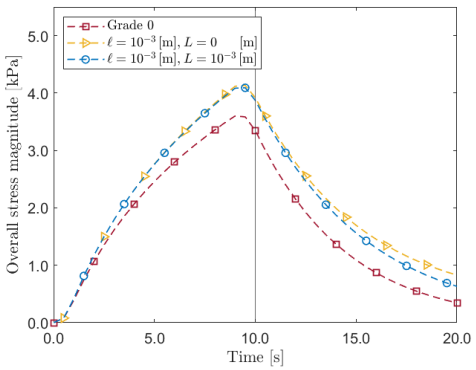

(b) Overall stress magnitudes $R_{\boldsymbol{N}}$ at $X_{\mathrm{U}} \in \Gamma_{\mathrm{U}}$ (case with remodeling)

Fig. 6.4 Left panel: Fluid effective pressure p_{f} (see Equation (6.71)) evaluated at the middle point X_{U} of the upper surface Γ_{U} of the specimen. Right panel: Overall stress magnitude $R_{\boldsymbol{N}}$ (see Equation (6.80a)) evaluated at the middle point X_{U} of the upper surface Γ_{U} of the specimen. The solid vertical line at $t = t_{\mathrm{r}} = 10\,\mathrm{s}$ indicates the instant of time in which the compressive ramp exerts the maximum displacement. Because of the regularization of the compressive ramp, the maxima of all the plotted curves are attained at time $t_{\max} = t_{\mathrm{r}} - 1 = 9\,\mathrm{s}$.

Second benchmark: Darcy–Brinkman model with strain-gradient remodeling.

We discuss the evolution of the system with remodeling. We compare three cases: (i) the flow is in Darcian regime and the remodeling distortions evolve according to a grade-0 theory in $\boldsymbol{F}_\gamma$, i.e., with Grad$\tilde{\boldsymbol{D}}_\gamma$ and $\mathfrak{B}$ absent from Equation (6.74c), which thus reduces to $\bar{S}_\mathrm{y}\tilde{\boldsymbol{D}}_\gamma^* = \tilde{\boldsymbol{A}}^\sharp$, with $\boldsymbol{A} = \boldsymbol{F}_\gamma^{-\mathrm{T}}[\boldsymbol{F}^\mathrm{T}\boldsymbol{P}_\mathrm{s}]\boldsymbol{F}_\gamma^\mathrm{T}$; (ii) the fluid obeys the Darcy–Brinkman model, but the non-dissipative effects of remodeling associated with W_sD are neglected, which amounts to prescribe $L = 0\,\mathrm{m}$; (iii) the full IBVP of Section 5 is solved.

Figure 6.4. In Figure 6.4a we report the evaluation of the fluid effective pressure p_f in the middle point X_U of the specimen's upper surface Γ_U, and over the time interval $[0\,\mathrm{s}, t_\mathrm{e} = 20\,\mathrm{s}]$. In Figure 6.4b we show the evaluation of R_N at the same point and over the same time interval. In both figures, we observe changes in the time trend when we pass from Darcy's model and grade-0 remodeling, i.e., the "Grade-0" case, to the Darcy–Brinkman model and grade-1 remodeling, i.e., the "Grade-1" case (identified by the values given to the length scales ℓ and L). For conciseness, we denote by $p_\mathrm{f}^{\mathrm{G0}}$ and R_N^{G0} the curves referring to the Grade-0 case (squares) and by $p_\mathrm{f}^{\mathrm{G1}}$ and R_N^{G1} those referring to the Grade-1 case (triangles and circles). Note that, for all these simulations, the Brinkman viscosity $\mathfrak{a}$ is set equal to zero, while $\mathfrak{b}$ is given the value reported in Table 6.1.

A noticeable result is that, when remodeling is activated, the values of both p_f and R_N are appreciably smaller than those appearing in the case in which remodeling is switched off. This behavior is expected as a consequence of the mitigating effect that remodeling has on the distribution of the stresses in a medium. Moreover, the presence of remodeling accelerates the relaxation of all the curves plotted in Figures 6.4a and 6.4b towards a state of lower pressure and stress.

Aside from the considerations made above, to us one result is noteworthy: the curves of $p_\mathrm{f}^{\mathrm{G1}}$ and R_N^{G1}, obtained for $L = 0\,\mathrm{m}$ and $L = 10^{-3}\,\mathrm{m}$, share a time trend qualitatively similar to those of $p_\mathrm{f}^{\mathrm{G0}}$ and R_N^{G0}, although there is an appreciable difference after a certain instant of time greater than the instant t_max at which all the curves attain their maxima. In fact, for $L = 0\,\mathrm{m}$, the values of $p_\mathrm{f}^{\mathrm{G1}}$ and of R_N^{G1} (triangles) are higher than the corresponding ones obtained for $L = 10^{-3}\,\mathrm{m}$ (circles). This means that, although the Grade-1 curves are all above the Grade-0

ones, the activation of the length scale L, related to the non-dissipative parts of $\boldsymbol{Y}_{\mathrm{u}}$ and $\mathbb{Y}_{\mathrm{u}}$, plays a mitigating role both on the pressure and on the overall stress, thereby accelerating their relaxation.

Figure 6.5. In Figures 6.5a–6.5d we plot the time trends of the radial, circumferential, and axial components of $\boldsymbol{F}_\gamma$ as well as of the radial-axial (13-)component of $\boldsymbol{F}_\gamma$. All these evaluations are taken at the point $X_{\mathrm{L}} \in \Gamma_{\mathrm{L}}$ of coordinates $(5.0, 0.0, 5.0)$ mm, lying at half of the height of the specimen's lateral boundary, Γ_{L}. We indicate with $\boldsymbol{F}_\gamma^{\mathrm{G0}}$ the remodeling tensor related to the Grade-0 case (squares), and with $\boldsymbol{F}_\gamma^{\mathrm{G1}}$ the same quantity obtained within the Grade-1 case (circles for non-vanishing "defect" free energy density W_{sD}, i.e., $L = 10^{-3}\,\mathrm{m}$, and triangles for vanishing W_{sD}, i.e., $L = 0\,\mathrm{m}$).

A relevant feature of Figure 6.5 is that, after a certain instant of time in the interval $[0\,\mathrm{s}, 5\,\mathrm{s}]$, $[\boldsymbol{F}_\gamma^{\mathrm{G1}}]^1{}_1$ becomes larger than $[\boldsymbol{F}_\gamma^{\mathrm{G0}}]^1{}_1$ both for $L = 0\,\mathrm{m}$ and for $L = 10^{-3}\,\mathrm{m}$ (see Figure 6.5a), while $[\boldsymbol{F}_\gamma^{\mathrm{G1}}]^2{}_2$ remains smaller than $[\boldsymbol{F}_\gamma^{\mathrm{G0}}]^2{}_2$ for almost the entire duration of the simulation (see Figure 6.5b), although, at $t = t_{\mathrm{e}}$, $[\boldsymbol{F}_\gamma^{\mathrm{G1}}]^2{}_2$ for $L = 0\,\mathrm{m}$ (triangles) comes closer to the value attained by $[\boldsymbol{F}_\gamma^{\mathrm{G0}}]^2{}_2$ at t_{e} (squares). Moreover, both for $L = 0\,\mathrm{m}$ and for $L = 10^{-3}\,\mathrm{m}$ (triangles and circles), the curves of $[\boldsymbol{F}_\gamma^{\mathrm{G1}}]^3{}_3$ intersect the curve of $[\boldsymbol{F}_\gamma^{\mathrm{G0}}]^3{}_3$ (squares) at an instant of time t_* in the interval $]5\,\mathrm{s}, t_{\mathrm{r}} - 1[$, and, in particular, they attain smaller values after t_* (see Figure 6.5c). Finally, both for the Grade-0 case and for the Grade-1 case, the values of $[\boldsymbol{F}_\gamma]^1{}_3$ are negligibly small with respect to the diagonal components of the remodeling tensor (see Figure 6.5d). Although we expect this result, due to the symmetries of the problem under investigation, we notice that, while $[\boldsymbol{F}_\gamma^{\mathrm{G0}}]^1{}_3$ is zero (in fact, its simulated values are of the order of 10^{-16}), $[\boldsymbol{F}_\gamma^{\mathrm{G1}}]^1{}_3$ is of the order of 10^{-7}.

We remark that, in Figures 6.5a, 6.5c, and 6.5d, switching from $L = 0\,\mathrm{m}$ to $L = 10^{-3}\,\mathrm{m}$ yields appreciable differences in the examined components of the remodeling tensor, while these differences are less marked in Figure 6.5b. In particular, in the Grade-1 model, and during the relaxation phase, the presence of the energetic contributions to $\boldsymbol{Y}_{\mathrm{u}}$ and $\mathbb{Y}_{\mathrm{u}}$ due to $L = 10^{-3}\,\mathrm{m}$ (circles) tend to decrease $[\boldsymbol{F}_\gamma^{\mathrm{G1}}]^1{}_1$ and $[\boldsymbol{F}_\gamma^{\mathrm{G1}}]^2{}_2$ and to increase $[\boldsymbol{F}_\gamma^{\mathrm{G1}}]^3{}_3$ with respect to the case $L = 0\,\mathrm{m}$. Hence, we conclude that these energetic contributions tend to hinder these components of the remodeling tensor near the lateral boundary.

Figure 6.6. In Figure 6.6a, we report the 33-component of $\boldsymbol{F}_\gamma^{\mathrm{G1}}$ and $\boldsymbol{F}_\gamma^{\mathrm{G0}}$ at $t = t_{\mathrm{r}} = 10\,\mathrm{s}$ and at $t = t_{\mathrm{e}} = 20\,\mathrm{s}$ (final time of observation). The curves of $[\boldsymbol{F}_\gamma^{\mathrm{G0}}]^3{}_3$ (squares) take on unitary values at the extrema of the spatial interval $[0\,\mathrm{mm}, 10\,\mathrm{mm}]$, corresponding to the middle points of the bottom and upper surfaces, denoted by $X_{\mathrm{B}} = (0, 0, 0)\,\mathrm{mm}$ and $X_{\mathrm{U}} = (0, 0, 10)\,\mathrm{mm}$, respectively. The evolution of the remodeling is testified by the fact that, at the end of the simulation, i.e., for $t = t_{\mathrm{e}}$, the curve of $[\boldsymbol{F}_\gamma^{\mathrm{G0}}]^3{}_3$ (solid line marked by squares) is below the one obtained for $t = t_{\mathrm{r}}$ (dashed line marked by squares). We notice that the derivative of $[\boldsymbol{F}_\gamma^{\mathrm{G0}}]^3{}_3$ along the axial direction, and evaluated at the points X_{B} and X_{U}, is nonzero.

A quite different behavior can be observed for $[\boldsymbol{F}_\gamma^{\mathrm{G1}}]^3{}_3$. In this case, indeed, although the curves plotted for $t = t_{\mathrm{r}} = 10\,\mathrm{s}$ (dashed lines marked with triangles and circles) and for $t = t_{\mathrm{e}} = 20\,\mathrm{s}$ (solid lines marked with triangles and circles) are symmetric with respect to the straight line of equation $X^3 = 5\,\mathrm{mm}$ (corresponding to transverse plane passing through X_{C}), the derivatives of $[\boldsymbol{F}_\gamma^{\mathrm{G1}}]^3{}_3$ along the axial direction, and evaluated at the points X_{B} and X_{U}, are (almost) zero, in accordance with the boundary conditions $\mathbb{Y}_{\mathrm{u}}\boldsymbol{N} = \boldsymbol{O}$ (see Equation (6.73)). This is, in fact, an effect of the boundary that is not visible for the Grade-0 model.

In Figure 6.6b we show the radial component $[\boldsymbol{F}_\gamma^{\mathrm{G1}}]^1{}_1$ and $[\boldsymbol{F}_\gamma^{\mathrm{G0}}]^1{}_1$. As one expects, for each curve, the maximum is attained at the symmetry axis.

It is worth mentioning that, as shown in Figures 6.6a and 6.6b, in the inner region of the specimen the components $[\boldsymbol{F}_\gamma^{\mathrm{G1}}]^3{}_3$ and $[\boldsymbol{F}_\gamma^{\mathrm{G1}}]^1{}_1$ for $t = t_{\mathrm{r}} = 10\,\mathrm{s}$ (dashed lines marked with triangles and circles) assume values closer to unity than their Grade-0 counterparts do. However, for $t = t_{\mathrm{e}} = 20\,\mathrm{s}$, the values of $[\boldsymbol{F}_\gamma^{\mathrm{G1}}]^3{}_3$ and $[\boldsymbol{F}_\gamma^{\mathrm{G1}}]^1{}_1$ (solid lines marked with triangles and circles) become very similar to the ones predicted by the Grade-0 theory. This suggests that $[\boldsymbol{F}_\gamma^{\mathrm{G1}}]^3{}_3$ and $[\boldsymbol{F}_\gamma^{\mathrm{G1}}]^1{}_1$ distance themselves from unity on the interval $[t_{\mathrm{r}}, t_{\mathrm{e}}]$ a little bit more than their Grade-0 counterparts.

6.6 Concluding remarks

We have studied the mechanics of a multicellular aggregate within a strain-gradient theory of remodeling (re-proposed from the work by Gurtin and Anand [142]) and a Darcy–Brinkman model for the interstitial fluid. This framework has been obtained

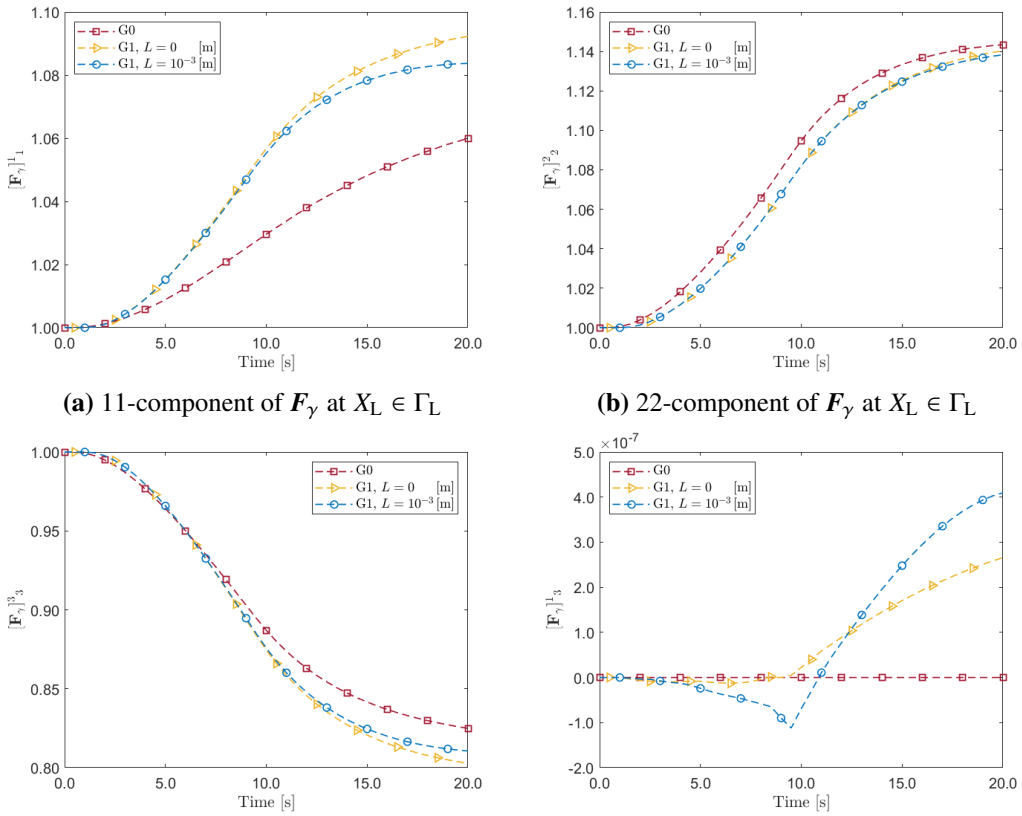

(a) 11-component of $\boldsymbol{F}_\gamma$ at $X_\mathrm{L} \in \Gamma_\mathrm{L}$

(b) 22-component of $\boldsymbol{F}_\gamma$ at $X_\mathrm{L} \in \Gamma_\mathrm{L}$

(c) 33-component of $\boldsymbol{F}_\gamma$ at $X_\mathrm{L} \in \Gamma_\mathrm{L}$

(d) 13-component of $\boldsymbol{F}_\gamma$ at $X_\mathrm{L} \in \Gamma_\mathrm{L}$

Fig. 6.5 Evolution of the radial (a), circumferential (b), axial (c), and radial-axial shear component of $\boldsymbol{F}_\gamma$ (d) at the point X_L of coordinates $(5.0, 0.0, 5.0)$ mm of the specimen's lateral surface Γ_L.

by selecting the motion of the solid phase, the velocity field of the fluid phase and the remodeling tensor as basic kinematic fields for the system under consideration.

Our results show that, *in the absence of remodeling*, the Darcy–Brinkman model for simulating the compression test of a homogeneous and isotropic cylindrical specimen leads to rather modest variations of the fluid effective pressure and to almost no appreciable changes in the stress distribution as compared with the same quantities predicted by standard Darcy's law. As discussed in the presentation of the figures, this could be partially imputable to the simple geometry of the specimen's boundary and to the loading conditions, which do not alter such geometry, thereby not giving room to strong boundary effects. In this respect, the benchmark test that we have simulated may seem to be inappropriate for justifying the Brinkman correction. However, the fact that there appear differences in the fluid effective pressure already

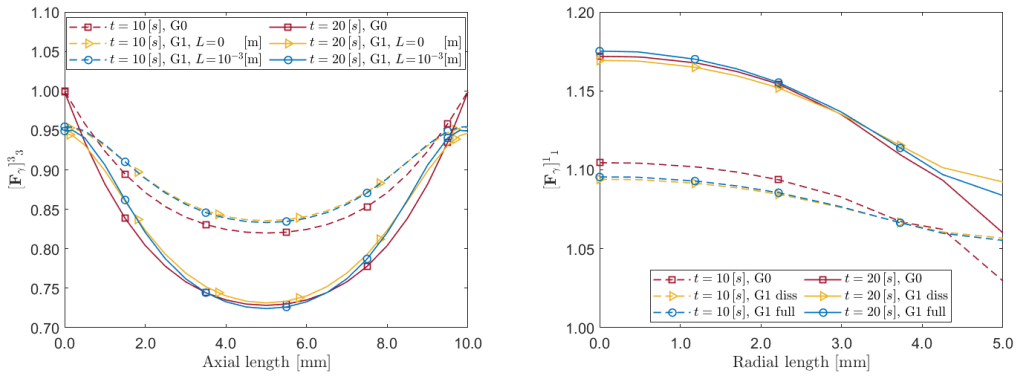

(a) Symmetry axis, 33-component of $\boldsymbol{F}_\gamma$ **(b)** Radial segment, 11-component of $\boldsymbol{F}_\gamma$

Fig. 6.6 Left panel: Comparison of the components $[\boldsymbol{F}_\gamma]^3{}_3$ computed within the Grade-0 model, i.e., $[\boldsymbol{F}_\gamma^{\mathrm{G0}}]^3{}_3$, with the same quantities computed within the Grade-1 model, i.e., $[\boldsymbol{F}_\gamma^{\mathrm{G1}}]^3{}_3$; the evaluation is done along the symmetry axis of the specimen. Right panel: Comparison of the components $[\boldsymbol{F}_\gamma]^1{}_1$ computed within the Grade-0 model, i.e., $[\boldsymbol{F}_\gamma^{\mathrm{G0}}]^1{}_1$, with the same quantities computed within the Grade-1 model, i.e., $[\boldsymbol{F}_\gamma^{\mathrm{G1}}]^1{}_1$; the evaluation is done along the radial segment comprised between the points $(0.0, 0.0, 5.0)$ mm and $(5.0, 0.0, 5.0)$ mm. In both panels, the cases $L = 0\,\mathrm{m}$ and $L = 10^{-3}\,\mathrm{m}$ characterize the Grade-1 model.

in the simple situation analyzed in our work suggests that the Darcy–Brinkman model could become important in situations generating strong gradients of the fluid velocity field. These could involve, for instance, twist tests or indentation tests, in which the original geometry of the specimen is remarkably modified, or transport problems in which the fluid is injected into the tested medium.

A different consideration concerns the role of the bulk viscosity parameter $\mathfrak{a}$. For the values considered in our work, $\mathfrak{a}$ does not alter significantly the evolution of the system, but we have not assessed yet whether, from the point of view of computing, $\mathfrak{a}$ could stabilize the numerical solution.

These considerations notwithstanding, appreciable differences in the fluid effective pressure, stress distribution within the specimen, and in the components of the remodeling tensor emerge when the Grade-0 model is compared with the Grade-1 model. In this respect, we remark that, while strain-gradient theories in the anelastic descriptor have been historically introduced to account for size effects in crystalline solids, and their importance cannot be understated (see e.g. the review by Voyiadjis and collaborators [171]), the determination of the phenomenological length scales ℓ and L in biological media is still an open problem. To the authors' knowledge, there is a lack of experimental protocols for the identification of size effects in biological

tissues, with a notable exception being the study of the mechanics of trabecular bone [206, 207]. In fact, following the opening of a crack, the neighboring region of the bone undergoes a remodeling process by developing plastic-like distortions and forming the so called *"plastic zone"* [206], which can be regarded as a size effect encompassing various elementary cells of a bone [206, 207] and determines a dissipative phenomenological length scale that can be estimated [206].

We conclude this discussion on the Darcy–Brinkman model with a remark. Auriault [208] obtains the Darcy–Brinkman model starting from Stokes' equation as a result of an up-scaling procedure that involves the asymptotic expansion of the fields of fluid pressure and velocity in a non-deforming porous medium made of *"swarms of fixed particles or fixed beds of fibers at very low concentration, only, and under precise conditions"*[208]. In this case, Auriault[208] finds that the so-called Brinkman viscosity equals the true viscosity of the fluid. However, he also warns that *"for isotropic and macroscopically homogeneous porous media [. . .] Brinkman's equation has no physical background"*[208]. While bearing this criticism in mind, we are aware of studies suggesting the usefulness of the Darcy–Brinkman model in addressing biomechanical problems[173]. Since biological porous media, especially when subjected to remodeling, have an internal structure that evolves and may deviate somewhat from the one of *"macroscopically homogeneous porous media"* [208], examining the influence of Brinkman's correction on the flow and its interaction with remodeling could deserve investigations. This has indeed motivated the present work and some results have been discussed in the previous section. Another case worthy of attention is provided by fiber-reinforced composites, which, besides the remodeling of the matrix, undergo also the reorientation of the fibers. Although the Darcy–Brinkman model in fiber-reinforced media is present in the literature (see, e.g., [209]), it could be useful to investigate how the non-spherical and dissipative stress tensor predicted by the Brinkman model couples with the fibers' distribution in the medium and whether it plays a role in the reorientation of the fibers themselves [4]. Clearly, all these considerations are at the moment conjectures and await experimental verification.

Appendix C

Weak form for general boundary conditions

The content of this appendix is taken from the appendix of [5].

In this appendix, we put Equations (6.74a)–(6.74d) and the boundary conditions (6.76a)–(6.76e) in *weak form*. Although this procedure has some similarities with the Principle of Virtual Power (PVP), it yields four important differences: first, the constitutive information is now fully exploited; second, the force balances (6.38a) and (6.38b), replaced by (6.74a) and (6.74b), are reformulated in a way in which, when put in weak form, the gradients of the volumetric fractions no longer appear; third, $\boldsymbol{L}_\gamma$ is replaced by the symmetric and deviatoric tensor field $\tilde{\boldsymbol{D}}_\gamma$; finally, $\tilde{\boldsymbol{D}}_\gamma$ and $\boldsymbol{F}_\gamma$ are regarded as kinematic variables that, although being formally independent of each other, are reciprocally related by Equation (6.74f). Note that, because of the identities $\phi_{\mathrm{sR}} = \Phi_{\mathrm{sR}}/J$ and $\phi_{\mathrm{fR}} = 1 - \Phi_{\mathrm{sR}}/J$, the elimination of the gradients of the volumetric fractions entails the elimination of the gradient of J and, thus, of $\boldsymbol{F}$, so that, when Equations (6.74a) and (6.74b) are put in weak form, the highest order of spatial differentiation of χ is the first.

To put Equation (6.74c) in weak form, we introduce as test field the generalized virtual rate $\tilde{\boldsymbol{D}}_{\gamma\mathrm{v}}$, which is symmetric and deviatoric by construction.

We compute the duality products of Equations (6.74a)–(6.74d) with $\boldsymbol{V}_{\mathrm{sv}}$, $\boldsymbol{V}_{\mathrm{fv}}$, $\tilde{\boldsymbol{D}}_{\gamma\mathrm{v}}$, and p_{v}, respectively, we integrate over $\mathscr{B}$, and we apply Leibnitz rule and

Gauss' Theorem. Hence, we obtain

$$\int_{\mathscr{B}}\langle\hat{\boldsymbol{P}}_{\mathrm{s}}\circ(\boldsymbol{F},\boldsymbol{F}_{\gamma})|\mathrm{Grad}\boldsymbol{V}_{\mathrm{sv}}\rangle+\int_{\mathscr{B}}\langle J\phi_{\mathrm{fR}}^{2}\boldsymbol{k}^{-1}\boldsymbol{V}_{\mathrm{s}}|\boldsymbol{V}_{\mathrm{sv}}\rangle+\int_{\mathscr{B}}\langle-J\phi_{\mathrm{fR}}^{2}\boldsymbol{k}^{-1}\boldsymbol{V}_{\mathrm{f}}|\boldsymbol{V}_{\mathrm{sv}}\rangle$$
$$+\int_{\mathscr{B}}\langle\Phi_{\mathrm{sR}}\boldsymbol{F}^{-\mathrm{T}}\mathrm{Grad}p|\boldsymbol{V}_{\mathrm{sv}}\rangle-\sum_{d=1}^{3}\int_{\partial\mathscr{B}\backslash\Gamma_{\mathrm{sD}}^{d}}[\Phi_{\mathrm{sR}}p\boldsymbol{F}^{-\mathrm{T}}\boldsymbol{N}]_{d}V_{\mathrm{sv}}^{d}=\sum_{d=1}^{3}\int_{\partial\mathscr{B}\backslash\Gamma_{\mathrm{sD}}^{d}}\tau_{\mathrm{s}d}V_{\mathrm{sv}}^{d},\tag{C.1a}$$

$$\int_{\mathscr{B}}\langle\Phi_{\mathrm{fR}}\mathbb{V}:\mathrm{Grad}\boldsymbol{V}_{\mathrm{f}}|\mathrm{Grad}\boldsymbol{V}_{\mathrm{fv}}\rangle+\int_{\mathscr{B}}\langle J\phi_{\mathrm{fR}}^{2}\boldsymbol{k}^{-1}\boldsymbol{V}_{\mathrm{f}}|\boldsymbol{V}_{\mathrm{fv}}\rangle+\int_{\mathscr{B}}\langle-J\phi_{\mathrm{fR}}^{2}\boldsymbol{k}^{-1}\boldsymbol{V}_{\mathrm{s}}|\boldsymbol{V}_{\mathrm{fv}}\rangle$$
$$+\int_{\mathscr{B}}\langle\Phi_{\mathrm{fR}}\boldsymbol{F}^{-\mathrm{T}}\mathrm{Grad}p|\boldsymbol{V}_{\mathrm{fv}}\rangle-\sum_{d=1}^{3}\int_{\partial\mathscr{B}\backslash\Gamma_{\mathrm{fD}}^{d}}[\Phi_{\mathrm{fR}}p\boldsymbol{F}^{-\mathrm{T}}\boldsymbol{N}]_{d}V_{\mathrm{fv}}^{d}=\sum_{d=1}^{3}\int_{\partial\mathscr{B}\backslash\Gamma_{\mathrm{fD}}^{d}}\tau_{\mathrm{f}d}V_{\mathrm{fv}}^{d},\tag{C.1b}$$

$$\int_{\mathscr{B}}\big\{\langle\bar{S}_{\mathrm{y}}\ell^{2}(\mathrm{Grad}\tilde{\boldsymbol{D}}_{\gamma})^{*}|\mathrm{Grad}\tilde{\boldsymbol{D}}_{\gamma\mathrm{v}}\rangle+\langle\bar{S}_{\mathrm{y}}\tilde{\boldsymbol{D}}_{\gamma}^{*}|\tilde{\boldsymbol{D}}_{\gamma\mathrm{v}}\rangle\big\}=\int_{\mathscr{B}}\big\{\langle\tilde{\boldsymbol{A}}^{\sharp}+\tilde{\boldsymbol{Z}}^{\sharp}|\tilde{\boldsymbol{D}}_{\gamma\mathrm{v}}\rangle+\langle\tilde{\boldsymbol{\mathfrak{S}}}^{\sharp}|\mathrm{Grad}\tilde{\boldsymbol{D}}_{\gamma\mathrm{v}}\rangle\big\},\tag{C.1c}$$

$$\int_{\mathscr{B}}\langle\Phi_{\mathrm{sR}}\boldsymbol{V}_{\mathrm{s}}\boldsymbol{F}^{-\mathrm{T}}|\mathrm{Grad}p_{\mathrm{v}}\rangle-\sum_{d=1}^{3}\int_{\partial\mathscr{B}\backslash\Gamma_{\mathrm{sD}}^{d}}[\Phi_{\mathrm{sR}}\boldsymbol{F}^{-\mathrm{T}}\boldsymbol{N}]_{d}V_{\mathrm{s}}^{d}\,p_{\mathrm{v}}+\int_{\mathscr{B}}\langle\Phi_{\mathrm{fR}}\boldsymbol{V}_{\mathrm{f}}\boldsymbol{F}^{-\mathrm{T}}|\mathrm{Grad}p_{\mathrm{v}}\rangle$$
$$-\sum_{d=1}^{3}\int_{\partial\mathscr{B}\backslash\Gamma_{\mathrm{fD}}^{d}}[\Phi_{\mathrm{fR}}\boldsymbol{F}^{-\mathrm{T}}\boldsymbol{N}]_{d}V_{\mathrm{f}}^{d}\,p_{\mathrm{v}}=\sum_{d=1}^{3}\int_{\Gamma_{\mathrm{sD}}^{d}}[\Phi_{\mathrm{sR}}\boldsymbol{F}^{-\mathrm{T}}\boldsymbol{N}]_{d}\dot{\chi}_{\mathrm{b}}^{d}\,p_{\mathrm{v}}+\sum_{d=1}^{3}\int_{\Gamma_{\mathrm{fD}}^{d}}[\Phi_{\mathrm{fR}}\boldsymbol{F}^{-\mathrm{T}}\boldsymbol{N}]_{d}V_{\mathrm{fb}}^{d}\,p_{\mathrm{v}}.\tag{C.1d}$$

The unknowns p, V_{s}^{d} and V_{f}^{d} feature also on the boundary portions complementary to the ones on which Dirichlet conditions are imposed on χ^{d} and V_{f}^{d}.

We do not put Equations (6.74e) and (6.74f) in weak form because they are solved pointwise. In view of the finite element implementation, they must be fulfilled by the nodal values of the discretized representations of $\boldsymbol{V}_{\mathrm{s}}$ and $\tilde{\boldsymbol{D}}_{\gamma}$, including the values at the nodes of $\partial\mathscr{B}\backslash\Gamma_{\mathrm{sD}}^{d}$ and $\partial\mathscr{B}$, respectively, which are unknown. In fact, if N_{s} and N_{γ} are the numbers of nodes of the discretizations of $\boldsymbol{V}_{\mathrm{s}}$ and $\tilde{\boldsymbol{D}}_{\gamma}$, respectively, then Equations (6.74e) and (6.74f), which amount to three and nine scalar equations, generate a number of conditions equal to $3N_{\mathrm{s}}+9N_{\gamma}$.

Let us now introduce the velocity field $\check{\boldsymbol{V}}_{\mathrm{sb}}$, associated with the solid phase, and defined as follows: let $d\in\{1,2,3\}$ be the index identifying, in a given basis $\{\boldsymbol{e}_{a}\}_{a=1}^{3}$, the component of the trace of the solid phase velocity field prescribed on Γ_{sD}^{d}, so that $V_{\mathrm{s}}^{d}=\dot{\chi}_{\mathrm{b}}^{d}$ on Γ_{sD}^{d} in the sense of the trace operators. Then, we introduce $\check{\boldsymbol{V}}_{\mathrm{sb}}=\sum_{a=1}^{3}\check{V}_{\mathrm{sb}}^{a}\boldsymbol{e}_{a}$ as a vector field defined on $\overline{\mathscr{B}}=\mathscr{B}\cup\partial\mathscr{B}$ and having components that, on the given Γ_{sD}^{d}, satisfy $\check{V}_{\mathrm{sb}}^{a}\equiv\dot{\chi}_{\mathrm{b}}^{d}$ for $a=d$, and $\check{V}_{\mathrm{sb}}^{a}\equiv 0$ for $a\neq d$. In fact, $\check{\boldsymbol{V}}_{\mathrm{sb}}$ prolongs the Dirichlet boundary data prescribed on Γ_{sD}^{d} for the solid phase velocity to the inner points of $\mathscr{B}$ and onto $\partial\mathscr{B}\backslash\Gamma_{\mathrm{sD}}^{d}$. Introducing $\check{\boldsymbol{V}}_{\mathrm{sb}}$ permits us to rewrite $\boldsymbol{V}_{\mathrm{s}}$ as $\boldsymbol{V}_{\mathrm{s}}=\boldsymbol{U}_{\mathrm{s}}+\check{\boldsymbol{V}}_{\mathrm{sb}}$, where the *rescaled* velocity field $\boldsymbol{U}_{\mathrm{s}}:=\boldsymbol{V}_{\mathrm{s}}-\check{\boldsymbol{V}}_{\mathrm{sb}}$ is such that, on

Γ^d_{sD}, its components satisfy $U^a_{\mathrm{s}} = 0$ for $a = d$, and $U^a_{\mathrm{s}} = V^a_{\mathrm{s}}$ for $a \neq d$. Hence, $\boldsymbol{U}_{\mathrm{s}}$ belongs to the same functional space as $\boldsymbol{V}_{\mathrm{sv}}$, i.e., $\boldsymbol{U}_{\mathrm{s}} \in \mathscr{V}_{\mathrm{sv}}$.

We apply now an identical reasoning to the fluid phase velocity field, thereby rewriting $\boldsymbol{V}_{\mathrm{f}}$ as $\boldsymbol{V}_{\mathrm{f}} = \boldsymbol{U}_{\mathrm{f}} + \check{\boldsymbol{V}}_{\mathrm{fb}}$, with $\boldsymbol{U}_{\mathrm{f}} \coloneqq \boldsymbol{V}_{\mathrm{f}} - \check{\boldsymbol{V}}_{\mathrm{fb}} \in \mathscr{V}_{\mathrm{fv}}$, and where $\check{\boldsymbol{V}}_{\mathrm{fb}} = \sum_{a=1}^{3} \check{V}^a_{\mathrm{fb}} \boldsymbol{e}_a$ is a vector field defined on $\overline{\mathscr{B}}$ such that, on Γ^d_{fD} (for some $d \in \{1,2,3\}$), its components satisfy $\check{V}^a_{\mathrm{fb}} \equiv V^d_{\mathrm{fb}}$ for $a = d$, and $\check{V}^a_{\mathrm{fd}} = 0$ for $a \neq d$.

The structure of the weak forms (C.1a)–(C.1d) and the rescaled velocity fields $\boldsymbol{U}_{\mathrm{s}}$ and $\boldsymbol{U}_{\mathrm{f}}$ yield

$$
\begin{aligned}
\mathcal{M}_{\mathrm{ss}}(\chi, \boldsymbol{F}_\gamma; \boldsymbol{U}_{\mathrm{s}}|\boldsymbol{V}_{\mathrm{sv}}) + \mathcal{M}_{\mathrm{sf}}(\chi; \boldsymbol{U}_{\mathrm{f}}|\boldsymbol{V}_{\mathrm{sv}}) + \mathcal{M}_{\mathrm{sp}}(\chi; p|\boldsymbol{V}_{\mathrm{sv}}) &= T_{\mathrm{s}}(\chi; \boldsymbol{V}_{\mathrm{sv}}), && \text{(C.2a)}\\
\mathcal{M}^{\dagger}_{\mathrm{sf}}(\chi; \boldsymbol{U}_{\mathrm{s}}|\boldsymbol{V}_{\mathrm{fv}}) + \mathcal{M}_{\mathrm{ff}}(\chi; \boldsymbol{U}_{\mathrm{f}}|\boldsymbol{V}_{\mathrm{fv}}) + \mathcal{M}_{\mathrm{fp}}(\chi; p|\boldsymbol{V}_{\mathrm{fv}}) &= T_{\mathrm{f}}(\chi; \boldsymbol{V}_{\mathrm{fv}}), && \text{(C.2b)}\\
\mathcal{M}^{\dagger}_{\mathrm{sp}}(\chi; \boldsymbol{U}_{\mathrm{s}}|p_{\mathrm{v}}) + \mathcal{M}^{\dagger}_{\mathrm{fp}}(\chi; \boldsymbol{U}_{\mathrm{f}}|p_{\mathrm{v}}) &= T_{\mathrm{p}}(\chi; p_{\mathrm{v}}), && \text{(C.2c)}\\
\mathcal{M}_{\gamma\gamma}(\tilde{\boldsymbol{D}}_\gamma|\tilde{\boldsymbol{D}}_{\gamma\mathrm{v}}) &= T_\gamma(\chi, \boldsymbol{F}_\gamma; \tilde{\boldsymbol{D}}_{\gamma\mathrm{v}}), && \text{(C.2d)}
\end{aligned}
$$

where we have used the dagger "†" to indicate the adjoint of an operator, we have switched Equations (C.1c) and (C.1d), now corresponding to (C.2d) and (C.2c), and we have introduced the functionals

$$
\begin{aligned}
\mathcal{M}_{\mathrm{ss}}(\chi, \boldsymbol{F}_\gamma; \boldsymbol{U}_{\mathrm{s}}|\boldsymbol{V}_{\mathrm{sv}}) &\coloneqq \int_{\mathscr{B}} \langle \hat{\boldsymbol{P}}_{\mathrm{s}} \circ (\boldsymbol{F}, \boldsymbol{F}_\gamma) | \mathrm{Grad}\boldsymbol{V}_{\mathrm{sv}} \rangle + \int_{\mathscr{B}} \langle J\phi^2_{\mathrm{fR}} \boldsymbol{k}^{-1} \boldsymbol{U}_{\mathrm{s}} | \boldsymbol{V}_{\mathrm{sv}} \rangle, && \text{(C.3a)}\\
\mathcal{M}_{\mathrm{sf}}(\chi; \boldsymbol{U}_{\mathrm{f}}|\boldsymbol{V}_{\mathrm{sv}}) &\coloneqq \int_{\mathscr{B}} \langle -J\phi^2_{\mathrm{fR}} \boldsymbol{k}^{-1} \boldsymbol{U}_{\mathrm{f}} | \boldsymbol{V}_{\mathrm{sv}} \rangle, && \text{(C.3b)}\\
\mathcal{M}_{\mathrm{sp}}(\chi; p|\boldsymbol{V}_{\mathrm{sv}}) &\coloneqq \int_{\mathscr{B}} \langle \Phi_{\mathrm{sR}} \boldsymbol{F}^{-\mathrm{T}} \mathrm{Grad} p | \boldsymbol{V}_{\mathrm{sv}} \rangle - \sum_{d=1}^{3} \int_{\partial\mathscr{B}\setminus\Gamma^d_{\mathrm{sD}}} [\Phi_{\mathrm{sR}} p \boldsymbol{F}^{-\mathrm{T}} \boldsymbol{N}]_d V^d_{\mathrm{sv}}, && \text{(C.3c)}\\
T_{\mathrm{s}}(\chi; \boldsymbol{V}_{\mathrm{sv}}) &\coloneqq \sum_{d=1}^{3} \int_{\partial\mathscr{B}\setminus\Gamma^d_{\mathrm{sD}}} \tau_{\mathrm{s}d} V^d_{\mathrm{sv}} - \int_{\mathscr{B}} \langle J\phi^2_{\mathrm{fR}} \boldsymbol{k}^{-1} (\check{\boldsymbol{V}}_{\mathrm{sb}} - \check{\boldsymbol{V}}_{\mathrm{fb}}) | \boldsymbol{V}_{\mathrm{sv}} \rangle, && \text{(C.3d)}\\
\mathcal{M}_{\mathrm{ff}}(\chi; \boldsymbol{U}_{\mathrm{f}}|\boldsymbol{V}_{\mathrm{fv}}) &\coloneqq \int_{\mathscr{B}} \langle \Phi_{\mathrm{fR}} \mathbb{V} : \mathrm{Grad}\boldsymbol{U}_{\mathrm{f}} | \mathrm{Grad}\boldsymbol{V}_{\mathrm{fv}} \rangle + \int_{\mathscr{B}} \langle J\phi^2_{\mathrm{fR}} \boldsymbol{k}^{-1} \boldsymbol{U}_{\mathrm{f}} | \boldsymbol{V}_{\mathrm{fv}} \rangle, && \text{(C.3e)}\\
\mathcal{M}_{\mathrm{fp}}(\chi; p|\boldsymbol{V}_{\mathrm{fv}}) &\coloneqq \int_{\mathscr{B}} \langle \Phi_{\mathrm{fR}} \boldsymbol{F}^{-\mathrm{T}} \mathrm{Grad} p | \boldsymbol{V}_{\mathrm{fv}} \rangle - \sum_{d=1}^{3} \int_{\partial\mathscr{B}\setminus\Gamma^d_{\mathrm{fD}}} [\Phi_{\mathrm{fR}} p \boldsymbol{F}^{-\mathrm{T}} \boldsymbol{N}]_d V^d_{\mathrm{fv}}, && \text{(C.3f)}\\
T_{\mathrm{f}}(\chi; \boldsymbol{V}_{\mathrm{fv}}) &\coloneqq \sum_{d=1}^{3} \int_{\partial\mathscr{B}\setminus\Gamma^d_{\mathrm{fD}}} \tau_{\mathrm{f}d} V^d_{\mathrm{fv}} - \int_{\mathscr{B}} \langle J\phi^2_{\mathrm{fR}} \boldsymbol{k}^{-1} (\check{\boldsymbol{V}}_{\mathrm{fb}} - \check{\boldsymbol{V}}_{\mathrm{sb}}) | \boldsymbol{V}_{\mathrm{fv}} \rangle\\
&\quad - \int_{\mathscr{B}} \langle \Phi_{\mathrm{fR}} \mathbb{V} : \mathrm{Grad}\check{\boldsymbol{V}}_{\mathrm{fb}} | \mathrm{Grad}\boldsymbol{V}_{\mathrm{fv}} \rangle, && \text{(C.3g)}\\
T_{\mathrm{p}}(\chi; p_{\mathrm{v}}) &\coloneqq - \int_{\mathscr{B}} \langle \Phi_{\mathrm{sR}} \check{\boldsymbol{V}}_{\mathrm{sb}} \boldsymbol{F}^{-\mathrm{T}} | \mathrm{Grad} p_{\mathrm{v}} \rangle + \sum_{d=1}^{3} \int_{\Gamma^d_{\mathrm{sD}}} [\Phi_{\mathrm{sR}} \boldsymbol{F}^{-\mathrm{T}} \boldsymbol{N}]_d \dot{\chi}^d_{\mathrm{b}}\, p_{\mathrm{v}}\\
&\quad - \int_{\mathscr{B}} \langle \Phi_{\mathrm{fR}} \check{\boldsymbol{V}}_{\mathrm{fb}} \boldsymbol{F}^{-\mathrm{T}} | \mathrm{Grad} p_{\mathrm{v}} \rangle + \sum_{d=1}^{3} \int_{\Gamma^d_{\mathrm{fD}}} [\Phi_{\mathrm{fR}} \boldsymbol{F}^{-\mathrm{T}} \boldsymbol{N}]_d V^d_{\mathrm{fb}}\, p_{\mathrm{v}}
\end{aligned}
$$

$$+\sum_{d=1}^{3}\int_{\partial\mathscr{B}\setminus\Gamma^d_{\mathrm{sD}}}[\Phi_{\mathrm{sR}}\boldsymbol{F}^{-\mathrm{T}}\boldsymbol{N}]_d\check{V}^d_{\mathrm{sb}}\,p_{\mathrm{v}}+\sum_{d=1}^{3}\int_{\partial\mathscr{B}\setminus\Gamma^d_{\mathrm{fD}}}[\Phi_{\mathrm{fR}}\boldsymbol{F}^{-\mathrm{T}}\boldsymbol{N}]_d\check{V}^d_{\mathrm{fb}}\,p_{\mathrm{v}},\quad\text{(C.3h)}$$

$$\mathcal{M}_{\gamma\gamma}(\tilde{\boldsymbol{D}}_\gamma|\tilde{\boldsymbol{D}}_{\gamma\mathrm{v}}):=\int_{\mathscr{B}}\langle\bar{S}_{\mathrm{y}}\ell^2(\mathrm{Grad}\tilde{\boldsymbol{D}}_\gamma)^*|\mathrm{Grad}\tilde{\boldsymbol{D}}_{\gamma\mathrm{v}}\rangle+\int_{\mathscr{B}}\langle\bar{S}_{\mathrm{y}}\tilde{\boldsymbol{D}}^*_\gamma|\tilde{\boldsymbol{D}}_{\gamma\mathrm{v}}\rangle,\quad\text{(C.3i)}$$

$$T_\gamma(\chi,\boldsymbol{F}_\gamma;\tilde{\boldsymbol{D}}_{\gamma\mathrm{v}}):=\int_{\mathscr{B}}\left\{\langle\tilde{\boldsymbol{A}}^\sharp+\tilde{\boldsymbol{Z}}^\sharp|\tilde{\boldsymbol{D}}_{\gamma\mathrm{v}}\rangle+\langle\tilde{\boldsymbol{\mathfrak{S}}}^\sharp|\mathrm{Grad}\tilde{\boldsymbol{D}}_{\gamma\mathrm{v}}\rangle\right\}.\quad\text{(C.3j)}$$

To determine the dependence of T_γ on χ and $\boldsymbol{F}_\gamma$, we have assumed that $\tilde{\boldsymbol{Z}}^\sharp$ can be represented as a function of $\boldsymbol{F}$ and $\boldsymbol{F}_\gamma$. This hypothesis allows for a feedback of $\boldsymbol{F}$ and $\boldsymbol{F}_\gamma$ on the external generalized force density described by $\boldsymbol{Z}$.

With the exception of $\mathcal{M}_{\gamma\gamma}$, the functionals appearing in Equations (C.2a)–(C.2d) are all nonlinear in χ, while $\mathcal{M}_{\mathrm{ss}}$ and T_γ are nonlinear also in $\boldsymbol{F}_\gamma$. Clearly, more general situations can be envisaged, for example when the constitutive representations of $\boldsymbol{k}$ and $\mathbb{V}$ are also functions of $\boldsymbol{F}_\gamma$. Moreover, each functional of (C.3a)–(C.3j) is linear in the corresponding virtual field. Similarly, $\mathcal{M}_{\mathrm{ss}}$, $\mathcal{M}_{\mathrm{sf}}$, $\mathcal{M}_{\mathrm{sp}}$, $\mathcal{M}_{\mathrm{ff}}$, $\mathcal{M}_{\mathrm{fp}}$ and $\mathcal{M}_{\gamma\gamma}$ are linear also in the field featuring in the slot on the left-hand side of "|", i.e., in $\boldsymbol{U}_{\mathrm{s}}$, $\boldsymbol{U}_{\mathrm{f}}$, p, and $\tilde{\boldsymbol{D}}_\gamma$.

Performing the numerical analysis of the system (C.2a)–(C.2d) requires the identification of the functional spaces hosting the entities dual to the virtual fields and to their gradients as well as the linearization of the functionals (C.3a)–(C.3j). While these aspects of the problem are out of the scopes of the present work (indeed, we use a commercial software to determine a numerical solution to our problem), we notice that Equations (C.2a)–(C.2d) constitute a symmetric system. Its well posedness relies on the functional properties of the solid phase Helmholtz free energy density function —and, thus, of the constitutive expressions of $\boldsymbol{P}_{\mathrm{s}}$, $\tilde{\boldsymbol{A}}^\sharp$ and $\tilde{\boldsymbol{\mathfrak{S}}}^\sharp$—, on the positive-definiteness of the permeability tensor $\hat{\boldsymbol{k}}\circ\boldsymbol{F}$ and of the Brinkman viscosity tensor $\hat{\mathbb{V}}\circ\boldsymbol{F}$, and on the positivity of the rescaled[1] yield stress $\bar{S}_{\mathrm{y}}$. In particular, we notice that $\mathcal{M}_{\gamma\gamma}$ defines a scalar product in the functional space $H^1(\mathscr{B};\mathrm{Dev}_{\boldsymbol{G}}\mathrm{Sym}[T\mathscr{B}]_2)$ (see, e.g., the book by Salsa [196] for details). Equation (C.1b) generalizes to the present framework some results obtained in the work by Vacca [210] in the case of the Darcy–Brinkman model studied for a non-deforming porous medium, and velocity of the fluid phase assumed to be divergence-free and satisfying homogeneous Dirichlet conditions on the entire boundary of the computational domain.

[1]The word "rescaled" is going to appear in Prof. Alfio Grillo's IRIS institutional profile and is intended to be submitted to the journal *Mathematics and Mechanics of Solids* as part of a *Corrigendum*.

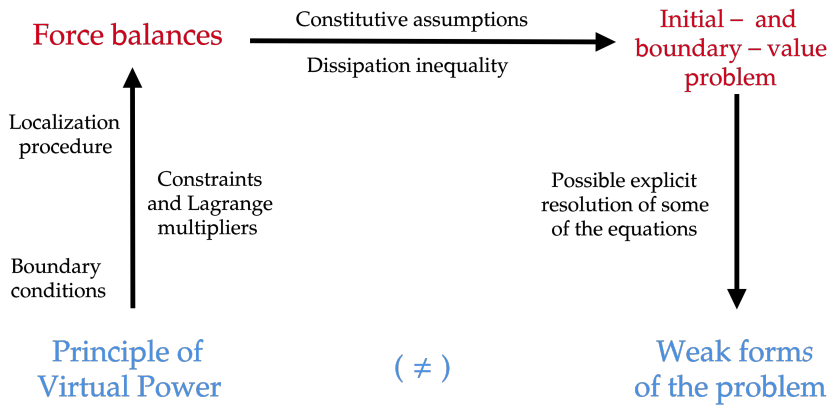

Fig. C.1 Graphical representation of the machinery employed in Chapter 6. It is important to remark that, in general, for a given mechanical problem, multiple weak form*s* are possible to construct, and do not necessarily share the same structure as that of the original form of the postulated PVP. In fact, manipulating, merging, or explicitly enforcing some of the model's equations can directly affect the resulting weak form of the model. This is indeed the *leitmotiv* of the last sections of Chapter 6 and, especially, of this appendix. This image was first showed during the conference "XI International Conference on Computational Bioengineering (ICCB 2025)" held in Rome, Italy, on September 8-10, 2025, within the presentation of the abstract "Coupling inelastic distortions and Darcy–Brinkman fluid flow in the modeling of multicellular aggregates under compression", authored by A. Pastore, A. Giammarini, A. Ramírez-Torres, A. Grillo.

Comparison with the "classical" Darcy model. Apart from the equations describing remodeling, i.e., (6.74c) in the strong formulation and (C.2d) in the weak, operatorial, setting, the way in which our problem is posed is rather different from the classical formulation of the finite-deformation poro-mechanics in Darcian regime[156, 155, 157, 129, 184, 183, 134]. The first, and most important, difference is that the force balance (6.74b) cannot be eliminated to obtain Darcy's law $\Phi_{\mathrm{fR}}\boldsymbol{F}^{-1}[\boldsymbol{V}_{\mathrm{f}}-\boldsymbol{V}_{\mathrm{s}}]=-\boldsymbol{K}\mathrm{Grad}\,p$, with $\boldsymbol{K}\coloneqq J\boldsymbol{F}^{-1}\boldsymbol{k}\boldsymbol{F}^{-\mathrm{T}}$ being the material permeability tensor field. This is obviously due to the presence of the dissipative stress $\Phi_{\mathrm{fR}}\mathbb{V}:\mathrm{Grad}\boldsymbol{V}_{\mathrm{f}}$, which is the core of Brinkman's model. The second difference is a direct consequence of the non applicability of Darcy's law. Indeed, in the Darcian case, it is computationally advantageous to substitute Darcy's law into the force balance (6.74a) and into the incompressibility condition (6.74d), thereby transforming (6.74d) into a Poisson equation for the pressure field and making (6.74a) equivalent to the sum of (6.74a) and (6.74b). In fact, even though similar steps can be done also for the Darcy–Brinkman model, they are not always so computationally advantageous as in the case of the Darcian regime. The third difference pertains to

the boundary conditions. Indeed, adding the stresses implies that also the boundary conditions (6.76a) and (6.76b) must be added together and, thus, that they have to hold on the same boundary portions. In particular, Equation (6.76b) imposes a relation, modulated by the deformation, between p and $\boldsymbol{V}_{\mathrm{f}}$. In addition, while Equation (6.76c) remains unchanged when passing from the Darcy–Brinkman model to Darcy's one, the Dirichlet condition (6.76d) on the fluid velocity is replaced by a condition on the relative velocity $\boldsymbol{V}_{\mathrm{f}} - \boldsymbol{V}_{\mathrm{s}}$, which, again, requires Equations (6.76c) and (6.76d) to be defined on the same boundary portion. In this case, however, given the relation $\Phi_{\mathrm{fR}}\boldsymbol{F}^{-1}[\boldsymbol{V}_{\mathrm{f}} - \boldsymbol{V}_{\mathrm{s}}] = -\boldsymbol{K}\mathrm{Grad}\, p$, the boundary condition on $\boldsymbol{V}_{\mathrm{f}} - \boldsymbol{V}_{\mathrm{s}}$ becomes a Neumann boundary condition on the pressure.

Part III

Materials science problems

Chapter 7

Dissipative dynamics of Volterra disclinations

The content of this chapter is taken from [3].

In what follows we abandon the covariant formalism of the previous chapters. Specifically, from here on: (i) we do not distinguish between "points" and "vectors" attached to such points; (ii) we identify "vectors" and "co-vectors" via the trivial metric induced by Cartesian coordinates over the three-dimensional Euclidean space; (iii) and in place of the duality brackets $\langle \cdot | \cdot \rangle$, representing the action of a co-vector against a vector, we use the inner (scalar) products between two vectors, with the usual dot notation "$\cdot$". We opted for this change in notation to adhere to the formalism employed in the original paper [3] and to focus on the mathematical analysis aspects of the problem hereafter investigated.

7.1 Introduction to disclinations and dislocations

Wedge disclinations, defined by the corresponding Frank angles, are asymmetries observed at the lattice level in various materials and systems relevant to technological applications, such as elastic crystals [211, 212], shape memory alloys [20, 213, 214], metal alloys [215, 216], graphene [217, 218], and more. Alongside dislocations (translational defects), disclinations represent the classical lattice rotational irregularities envisioned by Volterra [219]. See also later developments [220, 221].

The investigation and modeling of disclinations, particularly regarding their formation, motion, and interaction with other defects, are crucial for understanding the structure-property relationships in the corresponding materials. For instance, in graphene, wedge disclinations with opposite angles tend to attract and interact, forming disclination dipoles [222], Stone–Wales defects [223], and even more complex configurations commonly referred to as "flowers" [224], which dramatically influence electrical/magnetic/mechanical properties and chemical reactivity. In metal alloys and elastic crystals, moving disclination dipoles create shear similar to that of deformation twins in the context of accommodating plastic deformations [225, 226], thereby affecting mechanical behavior, such as stress concentration in the system.

While dislocation dynamics has been extensively studied by experimentalists (see [227–229] and the references therein), modellers [230–232] and theoreticians [233, 234, 199, 235–240, 118], the investigation of disclination dynamics has received less attention. An example can be found in [241], where partial dislocations in the context of high-temperature plasticity of graphene are observed. It is shown that these dislocations result from the arrangement of positive and negative wedge disclinations. The motion of these configurations is governed by the coordinated motion of the corresponding disclinations, which constitutes an important migration mechanism in annealing processes. For further insight into the challenges of experimentally observing disclinations and their modeling based on quantum chemistry, especially in relation to inverse design and optimization of graphene structures, see [242].

A general mathematical theory of moving disclinations in linear elasticity has been presented in [243, 244], where the equations of motion are expressed in terms of the total (i.e., elastic + plastic) deformation (see also the references to earlier works contained therein, as well as [245], and [246, 247]). The dynamics of disclinations, along with other types of defects and misfits, including dislocations, grain boundaries, and more, have been studied in the context of generalized disclination theory [248], which is a theory designed to treat Volterra defects within a continuously distributed defects framework (see [249]). For an approach to modeling thermodynamic driving forces on line and planar defects via iso-geometric analysis, see [250]; for a geometrically nonlinear approach, see, e.g., [251]. We refer to [252, 253] for a probabilistic model of the evolution of self-similar martensitic microstructures, which are systems known to be associated with lattice mismatches, particularly disclinations. In [254], forces acting on defects interacting with external fields of mechanical stresses are calculated. It is found that wedge disclinations are influenced

by the presence of the boundary of the elastic body and tend to get ejected from it. To the best of our knowledge a systematic analysis of these equations is not available as of yet.

The goal of this chapter is to get insight from a simple conceptual model of the evolution of a system of disclinations, and to study some of the consequences of their dynamics, e.g., dynamic equilibrium and stability, through the solution of a few selected benchmarks.

We follow the mathematical modeling presented in [200], which is based on the mechanical modeling work of [255, 256, 219], where wedge disclinations are described by concentrated singularities that are point sources of kinematic incompatibility. Precisely, each wedge disclination is represented by a Dirac delta distribution located at point y_i, with a multiplicative factor $s_i \in \mathbb{R} \setminus \{0\}$ denoting the Frank angle, which corresponds to the angular mismatch. With some abuse of notation, we will refer to the Frank angles as (signed) charges, in analogy with electrostatics.

Our modeling work is conceptual in nature, as we consider an ideal system with planar strain kinematics applied to a linear elastic isotropic and homogeneous medium. In this configuration, disclinations are subject to driving forces arising from their mutual interactions with the surrounding disclinations, as well as to additional forces pushing them towards the domain boundary. This approach allows us to address fundamental questions regarding the dynamics of finite systems of disclinations, particularly their spontaneous reorganization starting from prescribed initial configurations in the absence of external forcing. This is a basic modeling question that, to the best of our knowledge, has not been addressed in the literature.

We emphasize that the dynamics of the disclinations has been investigated also in relation to topological charges, phase transitions, and spontaneous symmetry breaking. In this respect, and within an approach based on statistical mechanics, mention must be made of the celebrated KTHNY theory [257, 258]. In what follows, however, rather than following methods based on statistical mechanics, we study the dynamics of a system of N disclinations viewed as *charged point particles*.

At mechanical equilibrium, we describe the mechanical stress using the Airy potential function of the system [200, 259, 219]. Under these circumstances, and in analogy with the second-order case of the electrostatic potential, we find that the dynamics of a system with finite number of wedge disclinations is modeled by the

evolution of a finite collection of charges under the effect of the fourth-order Airy potential field generated by the disclinations themselves.

Outline of the content of Chapter 7. Our main results are as follows. In analogy with the case of dislocations [199], we characterize the dynamics of a system of disclinations by applying the principle of dissipation to the mechanical energy of the system (7.2). This dynamics is driven by the negative gradient of the elastic energy of the disclination system [234, 260], leading to a set of coupled, highly nonlinear ordinary differential equations (ODEs) that describe the positions of the disclinations, which can be derived exactly in Section 7.3.1. However, in contrast to [199], where the study of dislocation dynamics required renormalization of the mechanical energy, we show that the disclination dynamics can be derived directly from the mechanical energy of the disclination system, which is not singular and does not require any renormalization. From the theoretical point of view, we provide analytical tools in the form of exact solutions for a single disclination in a disk (Section 7.3.2) and we characterize the asymptotic behavior of a system of two disclinations in various configurations in such a disk, hereafter also referred to as circular domain (Section 7.3.3). Our model indicates that disclinations collide in infinite time (Remark 7.1), and reach the boundary of the disk also in infinite time (Remark 7.6). This is a striking difference with dislocations, where a similar modeling approach based on dissipation for an analogous continuum model in planar, linear kinematics indicates that these types of collision occur at finite characteristic times [236]. Finally, since exact solutions are not available even in simple cases, we present numerical examples of these solutions, with a particular focus on the dynamics of disclination systems with non-zero total Frank angle (Section 7.4). Specifically, four benchmark problems are examined and are reported in the following sections: Benchmark #1 in Section 7.4.1, Benchmark #2 in Section 7.4.2, Benchmark #3 in Section 7.4.3 and Benchmark #4 in Section 7.4.4.

We conclude Chapter 7 with our initial attempt to incorporate anisotropy into the system by considering dynamics over a finite set of glide directions. Since the analysis proposed closely follows the dislocation analysis from [234], we have placed this discussion in Appendix D, which can be consulted separately from the main body of the paper. More systematic efforts to model realistic defect dynamics will require incorporating disclination-dislocation interactions, as well as accounting for general

asymmetries such as elastic/plastic microstructures, grain boundaries, interfaces, and more. These topics are left for future investigation.

7.2 Mechanical model formulation

In this section, we briefly recall the main ingredients of the mechanical setting developed by Cesana, De Luca, and Morandotti [200] to study the dynamics of disclinations in *plane strain* through a variational theory of concentrated defects in elastic media undergoing infinitesimal deformations.

Let us consider an open, bounded, and simply connected set $\Omega \subset \mathbb{R}^2$, and let $\phi \in H^2_0(\Omega)$ denote the Airy potential function describing the plane strain linear elastic problem under study, formulated under the assumption of traction-free boundary and no volume forces. Accordingly, the relations $\partial^2_{x_1x_1}\phi = \sigma_{22}$, $\partial^2_{x_1x_2}\phi = -\sigma_{12}$, and $\partial^2_{x_2x_2}\phi = \sigma_{11}$ hold true, where σ is the symmetric mechanical stress tensor. We recall that $\phi \in H^2_0(\Omega)$ is, for simply connected domains, equivalent to requiring the normal component of the mechanical stress σ to be zero on $\partial\Omega$, as proved in [200, Section 1.3]. This condition is compatible with the hypothesis that the body is traction-free on its boundary and in mechanical equilibrium. Then the elastic energy functional of the medium in terms of the Airy potential function reads as

$$\mathcal{W}(\phi;\Omega) := \frac{1}{2}\frac{1+\nu}{E}\int_\Omega (|\nabla^2\phi|^2 - \nu(\Delta\phi)^2) = \frac{1}{2}\frac{1-\nu^2}{E}\int_\Omega (\Delta\phi)^2, \qquad (7.1)$$

where E and ν are the material's Young modulus and Poisson ratio, respectively, $\nabla^2\phi$ is the Hessian of ϕ, and $\Delta\phi$ is the Laplacian of ϕ. Note that, granted the hypothesis of homogeneous material (i.e., with ν constant), the second equality holds true for functions ϕ in $H^2_0(\Omega)$, because, owing to the properties of such functions, it can be shown that $\int_\Omega |\nabla^2\phi|^2$ is equal to $\int_\Omega (\Delta\phi)^2$. In this work, we choose $-1 < \nu < 1/2$ so that the functional in Equation (7.1) is strictly positive definite. We recall that the Airy potential permits to express the components of Cauchy stress in a way that the indefinite equations of mechanical equilibrium are identically satisfied.

Following [200], to account for concentrated wedge disclinations in Ω, we introduce the *incompatibility measure* θ, which describes the kinematic incompatibility associated with the *rotational* symmetry breaking of the material at the point in

which a wedge disclination appears. To define such disclinations properly, we use the concept of *Frank angle* [261], i.e., the angle that defines the aperture of a wedge-type defect of the material lattice from its ideal, regular, arrangement. In this regard, we consider the set $\mathcal{S} \subset \mathbb{R} \setminus \{0\}$ of admissible, or possible, values taken by the Frank angle associated with each wedge disclination, and we give the following definition.

Definition 7.1 (Disclination)**.** A disclination in Ω is a pair $d \equiv (s, y) \in \mathcal{S} \times \Omega$, where $s \in \mathcal{S}$ is the Frank angle associated with the disclination, and $y \in \Omega$ is the point in which the disclination is placed.

If we assume the presence of $N \in \mathbb{N}$ disclinations in Ω, denoted by $d_1, \dots, d_N$, so that $d_k = (s_k, y_k)$, with $k = 1, \dots, N$, the incompatibility measure is [200, 261, 256]

$$\theta \equiv \sum_{k=1}^{N} \theta_k \coloneqq \sum_{k=1}^{N} s_k \delta_{y_k}, \qquad \theta_k \coloneqq s_k \delta_{y_k}, \tag{7.2}$$

where, for each $k = 1, \dots, N$, δ_{y_k} represents the Dirac delta distribution located in $y_k \in \Omega$ and has physical dimensions of the reciprocal of a length squared. Notice that in measuring the Frank angles we adopt the notation of [200].

Upon taking the duality product $\langle \theta, \phi \rangle$, which, by virtue of Equation (7.2), returns $\langle \theta, \phi \rangle = \sum_{k=1}^{N} s_k \phi(y_k)$, we can define the total energy functional [200, Equation (0.2)]

$$\mathcal{J}^{\theta}(\phi; \Omega) \coloneqq \mathcal{W}(\phi; \Omega) + \langle \theta, \phi \rangle = \mathcal{W}(\phi; \Omega) + \sum_{k=1}^{N} s_k \phi(y_k). \tag{7.3}$$

This represents the total energy of the system and is composed by the elastic energy functional $\mathcal{W}(\phi; \Omega)$ and the energy associated with the incompatibilities $\langle \theta, \phi \rangle$.

At static equilibrium, the partial differential equation governing the system is the Euler–Lagrange equation obtained by imposing the vanishing of the first variation of $\mathcal{J}^{\theta}(\cdot, \Omega)$ with respect to the Airy potential. Its solution $\bar{\phi}$ is sought for in $H_0^2(\Omega)$ by solving the biharmonic boundary value problem

$$\frac{1 - \nu^2}{E} \Delta^2 \phi = -\theta \quad \text{in } \Omega, \qquad \phi = 0 \quad \text{on } \partial\Omega, \qquad \partial_{\boldsymbol{n}} \phi = 0 \quad \text{on } \partial\Omega, \tag{7.4}$$

and, due to the strict convexity of $\mathcal{J}^\theta(\,\cdot\,;\Omega)$ with respect to $\phi \in H_0^2(\Omega)$, $\bar{\phi}$ is such that

$$\bar{\phi} = \operatorname{argmin}\{\mathcal{J}^\theta(\phi;\Omega) \mid \phi \in H_0^2(\Omega)\}. \tag{7.5}$$

Upon setting $W := \mathcal{W}(\bar{\phi};\Omega)$ to indicate the elastic energy of the system determined by substituting the Airy potential $\phi \equiv \bar{\phi}$, which solves Equation (7.4), into the elastic energy functional $\mathcal{W}(\,\cdot\,;\Omega)$, we have recourse to the following theorem.

Theorem 7.1 (Clapeyron's theorem in $H_0^2(\Omega)$)**.** *Given $\bar{\phi} \in H_0^2(\Omega)$, the solution to the biharmonic problem* (7.4)*, it follows that the elastic energy $W := \mathcal{W}(\bar{\phi};\Omega)$ reads as*

$$W = -\frac{1}{2}\langle\theta, \bar{\phi}\rangle. \tag{7.6}$$

Proof. Since $\Omega \subset \mathbb{R}^2$, by the Sobolev embedding theorem, $\bar{\phi}$ is continuous. Then, upon testing (7.4) against the solution $\bar{\phi}$, we obtain

$$-\langle\theta, \bar{\phi}\rangle = \frac{1-\nu^2}{E}\int_\Omega (\Delta^2\bar{\phi})\bar{\phi} = \frac{1-\nu^2}{E}\int_\Omega (\Delta\bar{\phi})^2 = 2W, \tag{7.7}$$

where the second equality follows from the boundary conditions in Equation (7.4). □

We recall that the result conveyed by Clapeyron's theorem, largely used in the field of strength of materials, states that, in a mechanical system governed by a linear relationship between stress and strain, the elastic energy of the system is one-half of the virtual work done by the external forces acting on the system itself. The elastic energy is the one that the system acquires in the elastic loading process that brings it from its unstressed and undeformed state to the loaded state. Clearly, this result has to be re-contextualized to our framework, in which the role of the "displacements" is played by the Airy functions. Note that the work has to be *virtual* because, otherwise, the "true" work would require an integration with respect to ϕ.

Under the assumption that the Frank angles of all the considered disclinations are constant, Clapeyron's theorem in the form of Equation (7.6) permits to express the elastic energy W in terms of the positions of the N disclinations as

$$W \equiv \hat{W}(y_1, \dots, y_N) = -\frac{1}{2}\sum_{k=1}^{N} s_k\bar{\phi}(y_k). \tag{7.8}$$

Note that, in principle, the Frank angle of each disclination may have dynamics of its own, thereby requiring $\hat{W}$ to be a function of $d_1, \ldots, d_N$ altogether. However, in the rest of this work we assume that the Frank angles do not vary.

In what follows we compute W according to Equation (7.8) for an open ball of radius $R > 0$ centered in the origin, i.e., $\Omega \equiv B_R(0)$, and for a general arrangement of disclinations. In fact, we consider N disclinations $d_1, \ldots, d_N$ assumed to occupy known positions inside Ω, as if we were looking at a *photograph* of the system, with Equation (7.8) representing the elastic energy in the *static* scenario. However, we use the energy $W = \mathcal{W}(\bar{\phi}; \Omega)$ computed this way to study the evolution in time of the considered disclinations.

7.2.1 The single disclination scenario

As a point of departure, we consider the problem of a single disclination ($N = 1$) placed at $y \in \Omega$. In this case, the incompatibility measure θ in Equation (7.4) reduces to the single Dirac delta centered in y, i.e., $\theta \equiv s\delta_y$. For $y = 0$, the corresponding Airy potential was computed in [200]. However, the generalization to a disclination located at $y \neq 0$ can be achieved by determining the Green function associated with the distribution $\theta \equiv s\delta_y$ (see e.g. the *"clamped disk"* problem [262, Section 4]). In this case, the Green function is the solution $\bar{\phi} \in H_0^2(\Omega)$ to Equation (7.4), which reads

$$\begin{aligned}\bar{\phi}(x) \coloneqq &- \frac{E}{1-\nu^2}\frac{sR^2}{16\pi}\frac{|x-y|^2}{R^2}\log\frac{|x-y|^2}{R^2} - \frac{E}{1-\nu^2}\frac{sR^2}{16\pi}\left(1-\frac{|x|^2}{R^2}\right)\left(1-\frac{|y|^2}{R^2}\right)\\ &+ \frac{E}{1-\nu^2}\frac{sR^2}{16\pi}\frac{|x-y|^2}{R^2}\log\frac{R^4 - 2R^2 x\cdot y + |x|^2|y|^2}{R^4}\end{aligned} \tag{7.9}$$

for $x \in \Omega \setminus \{y\}$ (the Green function is sometimes denoted by $\bar{\phi}_y(x)$ to emphasize its dependence on the point in which the Dirac delta is centered). In contrast to the case of unbounded domains, Equation (7.9) loses translational invariance, since it cannot be written as a function of $|x - y|$. The extension by continuity of $\bar{\phi}$ in $x = y$ yields

$$\bar{\phi}(y) \coloneqq -\frac{E}{1-\nu^2}\frac{sR^2}{16\pi}\left(1-\frac{|y|^2}{R^2}\right)^2. \tag{7.10}$$

The first term on the right-hand side of Equation (7.9) is the Green function of the biharmonic problem in $\mathbb{R}^2$ with the singularity being situated in $x = y$; the second

and the third terms are due to the boundedness of Ω. In particular, the third term stems from the disclination not being placed at the origin, and features the quantity

$$\frac{R^4 - 2R^2 x \cdot y + |x|^2|y|^2}{R^4} = \left(1 - \frac{|x|^2}{R^2}\right)\left(1 - \frac{|y|^2}{R^2}\right) + \frac{|x-y|^2}{R^2}, \tag{7.11}$$

which appears when applying the method of *sources*, or of *image charges*, to look for Green functions in bounded domains (see, e.g., [263, Chapter IV]).

By employing Theorem 7.1, the elastic energy reads

$$W = -\frac{1}{2} s\bar{\phi}(y) = \frac{E}{1-\nu^2}\frac{s^2R^2}{32\pi}\left(1 - \frac{|y|^2}{R^2}\right)^2, \tag{7.12}$$

and we can see that the resulting elastic energy W is the same as the one computed in [200] for $y = 0$; the energy $W \equiv \hat{W}(y)$ depends on y solely through the distance between the origin and y, i.e., $W \equiv \check{W}(|y|)$, thereby making W *invariant* with respect to *rotations* of the disclination's position vector about the origin; moreover, $\check{W}$ has a maximum for $|y| = 0$, i.e., in the origin, and $\check{W}$ goes to zero *quadratically* as y approaches the boundary, i.e., $\check{W}(|y|) = O((R - |y|)^2)$ for $|y| \to R$.

Although the mechanical stress of a single disclination is singular with logarithmic behavior towards its center, its stored elastic energy is finite. This is evident when taking $y = 0$ in (7.12), which also yields that the elastic energy W scales quadratically with the size of the domain (see, e.g., [255, 256, 219]). This contrasts the behavior of a dislocation placed at the center of $B_R(0)$, in which case the energy scales with $\log R$, sufficiently far away from the origin (see, e.g., [199]). This is the main reason why disclinations in hard solids are not found in isolation.

7.2.2 The N disclinations scenario

When N disclinations are present in Ω, then the Airy potential characterizing the system is given by the solution $\bar{\phi} \in H_0^2(\Omega)$ of the biharmonic problem (7.4) with the incompatibility measure specified in (7.2). By the linearity of Equation (7.4), and by the *homogeneity* of the associated Dirichlet and Neumann boundary conditions, it can be proved that $\bar{\phi}$ is given according to *superposition principle* as the summation $\bar{\phi} = \bar{\phi}_1 + \cdots + \bar{\phi}_N$, where the hth function $\bar{\phi}_h$, with $h = 1, \ldots, N$, is the solution of

the hth subproblem

$$\frac{1-\nu^2}{E}\Delta^2\phi = -\theta_h \quad \text{in } \Omega, \qquad \phi = 0 \quad \text{on } \partial\Omega, \qquad \partial_{\boldsymbol{n}}\phi = 0 \quad \text{on } \partial\Omega. \tag{7.13}$$

Since each $\bar{\phi}_h$ is of the type reported in Section 7.2.1, we conclude that, upon setting $C \coloneqq ER^2/(16\pi(1-\nu^2))$, the solution $\bar{\phi}$ is given by

$$\bar{\phi}(x) = \sum_{h=1}^{N} \bar{\phi}_h(x), \tag{7.14}$$

where, for each $h = 1, \ldots, N$, $\bar{\phi}_h(x)$ is defined for any $x \in \Omega \setminus \{y_h\}$ as

$$\begin{aligned}\bar{\phi}_h(x) = &- Cs_h \frac{|x-y_h|^2}{R^2}\log\frac{|x-y_h|^2}{R^2} - Cs_h\left(1-\frac{|x|^2}{R^2}\right)\left(1-\frac{|y_h|^2}{R^2}\right)\\ &+ Cs_h\frac{|x-y_h|^2}{R^2}\log\frac{R^4 - 2R^2 x\cdot y_h + |x|^2|y_h|^2}{R^4},\end{aligned} \tag{7.15}$$

and $\bar{\phi}_h(y_h)$ is defined by continuity as

$$\bar{\phi}_h(y_h) \coloneqq -Cs_h\left(1-\frac{|y_h|^2}{R^2}\right)^2. \tag{7.16}$$

The argument of the logarithm in the third term can be written as in Equation (7.11).

By virtue of Equation (7.15), we can state the following theorem, the proof of which follows from a direct computation.

Theorem 7.2 (Reciprocity — Betti's theorem in $H_0^2(\Omega)$)**.** *Given the incompatibility measure $\theta = \theta_1 + \cdots + \theta_N$ and the solution $\bar{\phi} = \bar{\phi}_1 + \cdots + \bar{\phi}_N$ to the biharmonic problem* (7.4) *reported in Equation* (7.14)*, it follows that*

$$\langle \theta_k, \bar{\phi}_h\rangle \equiv s_k\bar{\phi}_h(y_k) = s_h\bar{\phi}_k(y_h) \equiv \langle \theta_h, \bar{\phi}_k\rangle, \qquad h,k = 1,\ldots,N. \tag{7.17}$$

Betti's theorem constitutes another important result in the field of strength of materials and, more generally, in the linear response theory. In words, it can be stated as follows: let a linear elastic body be subjected to two different systems of external forces, each of which determines a particular elastic state for the body, defined by displacements, deformation, and stress. One can compute the virtual work that the first system of external forces expends on the displacements of the elastic state

produced by the second system of forces. Reciprocally, one can also compute the virtual work that the second system of external forces expends on the displacements of the elastic state of the first system. Then it is possible to prove that the two virtual works computed this way are equal. Also in this case, the work is *virtual* because, for a given system of external forces, we are using as test functions the displacements of the other system. Note that, again, in our context, Betti's theorem is formulated with the Airy functions playing the role of the displacements.

The result of Theorem 7.2 has the following important consequence.

Corollary 7.1 (Consequence of Betti's theorem)**.** *Given $\bar{\phi} = \bar{\phi}_1 + \cdots + \bar{\phi}_N$, the elastic energy W of the system can be expressed as the following sum:*

$$W = \sum_{k=1}^{N} W_k + \sum_{k=1}^{N} \sum_{h=k+1}^{N} W_{kh}, \tag{7.18}$$

where we have defined the energetic contributions

$$W_k \coloneqq \frac{1}{2} C s_k^2 \Big(1 - \frac{|y_k|^2}{R^2}\Big)^2, \tag{7.19a}$$

$$\begin{aligned} W_{kh} \coloneqq {} & C s_h s_k \frac{|y_h - y_k|^2}{R^2} \log \frac{|y_h - y_k|^2}{R^2} + C s_h s_k \Big(1 - \frac{|y_h|^2}{R^2}\Big)\Big(1 - \frac{|y_k|^2}{R^2}\Big) \\ & - C s_h s_k \frac{|y_h - y_k|^2}{R^2} \log \frac{R^4 - 2R^2 y_k \cdot y_h + |y_k|^2 |y_h|^2}{R^4}, \end{aligned} \tag{7.19b}$$

and the argument of the logarithm in the last summand of (7.19b) *admits the same decomposition as the one shown in Equation* (7.11)*, with $x \equiv y_k$ and $y \equiv y_h$.*

Proof. By substituting the decomposition $\bar{\phi} = \sum_{h=1}^{N} \bar{\phi}_h$ into Equation (7.8) and employing Theorem 7.2, the elastic energy in (7.8) becomes

$$\begin{aligned} W = -\frac{1}{2} \sum_{k=1}^{N} s_k \bar{\phi}(y_k) &= -\frac{1}{2} \sum_{k=1}^{N} \sum_{h=1}^{N} s_k \bar{\phi}_h(y_k) \\ &= -\frac{1}{2} \sum_{k=1}^{N} s_k \bar{\phi}_k(y_k) - \sum_{k=1}^{N} \sum_{h=k+1}^{N} s_k \bar{\phi}_h(y_k), \end{aligned} \tag{7.20}$$

which, by virtue of Equations (7.19a) and (7.19b), proves the thesis. □

According to Equation (7.1), which descends from the *superposition principle*, the elastic energy can be expressed as the sum of N self-energies W_k, with $k = 1, \dots, N$, and $N(N-1)/2$ interaction energies W_{kh}, with $h, k = 1, \dots, N$ and $k < h$. Moreover, Betti's theorem provides the following meaning for the energies in Equations (7.19a) and (7.19b): W_k is the elastic energy associated with the kth subproblem (7.13), i.e., the one in which only the kth disclination d_k is present in Ω; W_{kh} is twice the elastic energy associated with a "fictitious" system in which the Airy potential is $\bar{\phi}_h$ and the incompatibility measure is θ_k, or vice versa.

7.3 Disclination dynamics

As done in [234], to emphasize the dependence of the energies in Equation (7.18) on the positions of the disclinations $y_1, \dots, y_N$, we rewrite the elastic energy W in the following way:

$$W \equiv \hat{W}(\boldsymbol{y}) = \sum_{k=1}^{N} \hat{W}_k(\boldsymbol{y}) + \sum_{k=1}^{N} \sum_{h=k+1}^{N} \hat{W}_{kh}(\boldsymbol{y}), \qquad \boldsymbol{y} \in \mathcal{Y} \coloneqq \Omega^N \setminus \Pi, \tag{7.21}$$

$\boldsymbol{y} \coloneqq (y_1, \dots, y_N)$ being the array collecting the positions of the disclinations, and $\Pi \subset \Omega^N$ being the set, referred to as the *collision set*, defined by

$$\Pi \coloneqq \bigcup_{k=1}^{N} \bigcup_{h=k+1}^{N} \Pi_{kh}, \qquad \Pi_{kh} \coloneqq \left\{ \boldsymbol{y} \in \Omega^N \,\middle|\, y_k = y_h, k \neq h \right\} \tag{7.22}$$

(see [234, Equation (2.13)]). In the terminology of [234], it is said that two different disclinations, say d_k and d_h, with $k \neq h$, experience *"collisions"* if they share the same position $y_k = y_h$. In our work, however, we prove that this event may occur only in infinite time. Thus, two different disclinations, in fact, never meet each other dynamically, whereas they can share their position only in a thought experiment in which the two disclinations are prepared in this particular configuration. Yet, two different disclinations may *tend to collide*, which is when $|y_k - y_h| \to 0$. This situation requires special care (see Remark 7.3), and can be handled computationally by introducing a smallness real parameter $\varepsilon_c > 0$, and stipulating that a "collision" occurs if $|y_k - y_h| \leq \varepsilon_c$.

It is worth noticing that the energy is well-defined even in the case in which, for example, two disclinations $d_{\bar{k}}$ and $d_{\bar{h}}$, with $\bar{k}, \bar{h} \in \{1, \dots, N\}$, and $\bar{k} \neq \bar{h}$, share the same position, say, at the initial time of observation. The energy, in such a particular configuration, can be computed by evaluating the limit of $\hat{W}(\boldsymbol{y})$ in (7.21) for $|y_{\bar{k}} - y_{\bar{h}}| \to 0$ and would correspond to the energy of a system in which the two superposed disclinations are (virtually) replaced by one equivalent disclination having Frank angle $s_{\bar{k}} + s_{\bar{h}}$. In this respect, one may say that the limit is *configurational* and performed virtually, rather than representing a process of dynamic superposition. The latter, although leading to the superposition of two disclinations in infinite time, would still be associated with a finite energy. This is in striking contrast to the case of dislocations where the elastic energy becomes singular if collisions occur [234, 260].

As put forward in Section 7.1, we *assume* that the dynamics of the kth disclination in Ω, for $k = 1, \dots, N$, is dissipative and driven by the negative of the gradient of $\hat{W}$ in Equation (7.21) with respect to y_k, thereby yielding a force $\hat{F}_k \coloneqq -\nabla_{y_k} \hat{W}$, formally similar to the Peach–Koehler forces acting on dislocations [76]. Note that the functional form of Equation (7.21) is such that each force $\hat{F}_k$ is continuous in $\mathcal{Y}$, and can be extended by continuity in Ω^N.

Upon assigning initial conditions $y_k(0) = y_{k,\mathrm{i}}$, with $k = 1, \dots, N$, the dynamics of the N disclinations considered in Ω is governed by the Cauchy problem [234]

$$\begin{cases} \dot{y}_k(t) = -\lambda_k \nabla_{y_k} \hat{W}(y_1(t), \dots, y_N(t)), & k = 1, \dots, N, \\ y_k(0) = y_{k,\mathrm{i}}, & k = 1, \dots, N, \end{cases} \tag{7.23}$$

where $\dot{y}_k$ is the derivative of y_k with respect to time, and $\lambda_k > 0$ is a positive scalar quantity having the meaning of the inverse of a generalized viscous friction coefficient. For the sake of simplicity, we assume all the coefficients λ_k, with $k = 1, \dots, N$, to be equal to some $\lambda > 0$. Models of this type are already used in [199, 234] for dislocations.

While some analytical issues of Equation (7.23), such as existence and uniqueness of the solution, are addressed in Section 7.3.1, we mainly focus on the modeling aspects of Equation (7.23) through the description of two *archetypal* scenarios for a system of disclinations in Ω: these are the "one-disclination problem" and the "two-disclination problem," handled in Sections 7.3.2 and 7.3.3, respectively. We include, in Section 7.4, numerical experiments involving more than two disclinations.

7.3.1 Non-dimensionalization

We rewrite the system (7.23) in non-dimensional form so as to study the dynamics of the disclinations in terms of the rescaled variables $x \mapsto x/R$ and $t \mapsto (\lambda C/R^2)t$, where we recall that $C = ER^2/(16\pi(1-\nu^2))$. Hence, upon defining the non-dimensional position of the kth disclination as $y_k \mapsto y_k/R$, and scaling the energy W accordingly as $W \mapsto W/C$, we can recast Equation (7.23) as

$$\begin{cases} \dot{y}_k(t) = -\nabla_{y_k}\hat{W}(y_1(t),\dots,y_N(t)), & k = 1,\dots,N, \\ y_k(0) = y_{k,\mathrm{i}}, & k = 1,\dots,N, \end{cases} \tag{7.24}$$

where $\dot{y}_k \equiv \mathrm{d}y_k/\mathrm{d}t$ from here on denotes differentiation with respect to the non-dimensional time t, and $W = \hat{W}(y_1,\dots,y_N)$ is the elastic energy of the non-dimensional system, which reads

$$\begin{aligned} \hat{W}(y_1,\dots,y_N) = \frac{1}{2}\sum_{k=1}^{N} s_k^2(1-|y_k|^2)^2 + \sum_{k=1}^{N}\sum_{h=k+1}^{N} s_k s_h(1-|y_h|^2)(1-|y_k|^2) \\ + \sum_{k=1}^{N}\sum_{h=k+1}^{N} s_k s_h |y_h - y_k|^2 \log r_{kh}. \end{aligned} \tag{7.25}$$

In Equation (7.25), we have expressed the non-dimensional elastic energy in terms of the quantities r_{kh}, with $h,k = 1,\dots,N$, which are ratios depending on the positions y_k and y_h, and are defined as

$$r_{kh} := \frac{|y_k - y_h|^2}{|y_k - y_h|^2 + (1-|y_k|^2)(1-|y_h|^2)}, \qquad \text{with } r_{kh} = r_{hk}. \tag{7.26}$$

Moreover, r_{kh} vanishes identically for $k = h$, and tends to unity from below in the limits $|y_k| \to 1^-$ and/or $|y_h| \to 1^-$, for $k \neq h$. Yet, we have to exclude the value $r_{kh} = 0$ to appropriately define the logarithm in (7.25), so that we have $0 < r_{kh} < 1$. A last remark concerns the fact that the elastic energy in Equation (7.25) can be extended by continuity to the case in which one or more disclinations are on the boundary of $B_1(0)$. In particular, if the disclinations $d_1,\dots,d_N$ are all placed on the boundary, then it holds that $\hat{W}(y_1,\dots,y_N) = 0$. If, instead, the disclinations are all prepared in a superposed configuration placed at the origin of the domain Ω, then $\hat{W}(0,\dots,0) = (\frac{1}{\sqrt{2}}\sum_{k=1}^{N} s_k)^2$. This configuration is energetically very "expensive" in general, unless the "charges" are such that $\sum_{k=1}^{N} s_k = 0$.

To close this section, we remark that, upon employing the expression of $\hat{W}$ in Equation (7.25), it is possible to introduce in (7.24) the non-dimensional forces $\hat{F}_k \coloneqq -\nabla_{y_k}\hat{W}$, with $k = 1, \dots, N$, which read as

$$\hat{F}_k(y_1, \dots, y_N) = \hat{F}_k^{(1)}(y_k) + \sum_{h=1, h\neq k}^{N} \hat{F}_{kh}^{(2)}(y_k, y_h) + \sum_{h=1, h\neq k}^{N} \hat{F}_{kh}^{(3)}(y_k, y_h), \quad (7.27)$$

where, given $k, h = 1, \dots, N$, with $h \neq k$, we have introduced the notation

$$F_k^{(1)} \equiv \hat{F}_k^{(1)}(y_k) = 2s_k^2(1 - |y_k|^2)y_k, \quad (7.28a)$$

$$F_{kh}^{(2)} \equiv \hat{F}_{kh}^{(2)}(y_k, y_h) = 2s_k s_h(1 - r_{kh})(1 - |y_h|^2)y_k, \quad (7.28b)$$

$$F_{kh}^{(3)} \equiv \hat{F}_{kh}^{(3)}(y_k, y_h) = 2s_k s_h(1 - r_{kh} + \log r_{kh})(y_h - y_k). \quad (7.28c)$$

Each force $\hat{F}_k$ comprises one contribution due solely to $\partial B_1(0)$ (see Equation (7.28a)), $N - 1$ contributions that account for the effect of $\partial B_1(0)$ on y_k, modulated by the remaining $N - 1$ disclinations (see Equation (7.28b)), and $N - 1$ terms stemming from the mutual interactions with the other disclinations (see Equation (7.28c)).

Notice that the forces featuring in Equations (7.28a)–(7.28c) are obtained directly as the gradient of the elastic energy without any additional renormalization nor limit process, in striking difference with the case of dislocations [199]. Moreover, in the limit for $|y_h - y_k| \to 0$ for fixed $h, k = 1, \dots, N$, Equations (7.28b) and (7.28c) can be extended by continuity in any $\boldsymbol{y} \in \Pi_{kh}$, thereby allowing for the *superposition* of the kth and hth disclinations. While this condition is possible by assigning $y_{k,\mathrm{i}} = y_{h,\mathrm{i}}$, in the next section we show that collisions cannot be reached in finite time. This is addressed in more depth for $N = 2$ in Section 7.3.3.

For future use, we also define

$$F_k^{(2)} \equiv \hat{F}_k^{(2)}(y_1, \dots, y_N) \coloneqq \sum_{h=1, h\neq k}^{N} \hat{F}_{kh}^{(2)}(y_k, y_h), \quad (7.29a)$$

$$F_k^{(3)} \equiv \hat{F}_k^{(3)}(y_1, \dots, y_N) \coloneqq \sum_{h=1, h\neq k}^{N} \hat{F}_{kh}^{(3)}(y_k, y_h). \quad (7.29b)$$

Since each $\hat{F}_k$ does not depend explicitly on time, the system is autonomous and thus trivially continuous with respect to time. Moreover, since each $\hat{F}_k$ is

Lipschitz-continuous in each of its arguments, uniformly with respect to time, in every compact subset of $\mathcal{Y}$ of the type

$$\mathcal{R} := \bigtimes_{k=1}^{N} \left([y^1_{k,\mathrm{i}} - b^1_k, y^1_{k,\mathrm{i}} + b^1_k] \times [y^2_{k,\mathrm{i}} - b^2_k, y^2_{k,\mathrm{i}} + b^2_k]\right), \tag{7.30}$$

and having empty intersection with Π, then, by the *theorem of local existence and uniqueness*, there exists a unique solution to the Cauchy problem in (7.24).

7.3.2 One-disclination problem: the effect of the boundary

We now discuss the dynamics of a single disclination, initially located in $y_{\mathrm{i}} \in B_1(0)$. Hence, upon specializing Equation (7.24) to the case $N = 1$, we find

$$\begin{cases} \dot{y}(t) = 2s^2(1 - |y(t)|^2)y(t), \quad t > 0, \\ y(0) = y_{\mathrm{i}}, \end{cases} \tag{7.31}$$

which has the structure of a Cauchy problem with a *logistic* differential equation. To solve it, it is convenient to express y in polar coordinates $y(t) \equiv \rho(t)\exp(i\vartheta(t))$, where $\rho\colon [0, +\infty[\to [0, 1[$ and $\vartheta\colon [0, +\infty[\to \mathbb{R}$. Thus, upon setting $y_{\mathrm{i}} \equiv \rho_{\mathrm{i}} \exp(i\vartheta_{\mathrm{i}})$, Equation (7.31) can be rewritten as

$$\begin{cases} \dot{\rho}(t) = 2s^2(1 - \rho(t)^2)\rho(t), \quad t > 0, \\ \rho(0) = \rho_{\mathrm{i}}, \end{cases} \qquad \begin{cases} \dot{\vartheta}(t) = 0, \quad t > 0, \\ \vartheta(0) = \vartheta_{\mathrm{i}}. \end{cases} \tag{7.32}$$

The stationary solutions $\rho_{\mathrm{s}0}(t) = 0$ and $\rho_{\mathrm{s}1}(t) = 1$ of the differential equation of the Cauchy problem $(7.32)_1$ are admissible if and only if the initial condition is taken to be $\rho_{\mathrm{i}} = 0$ and $\rho_{\mathrm{i}} = 1$, respectively. However, assuming y_{i} to be a point of the open ball $B_1(0)$ implies the restriction $\rho_{\mathrm{i}} \in [0, 1[$, which makes $\rho_{\mathrm{s}1}(t)$ not admissible. Hence, $\rho_{\mathrm{s}0}(t) = 0$ is the only admissible stationary solution, provided $\rho_{\mathrm{i}} = 0$. Moreover, for $\rho_{\mathrm{i}} \in]0, 1[$, and upon setting $\mu_{\mathrm{i}} := (1 - \rho^2_{\mathrm{i}})/\rho^2_{\mathrm{i}}$, the Cauchy problem $(7.32)_1$ admits the one-parameter family of solutions

$$\rho(t) = \frac{1}{\sqrt{1 + \mu_{\mathrm{i}} \exp(-4s^2 t)}}, \qquad \vartheta(t) = \vartheta_{\mathrm{i}}, \qquad \forall\, t \in [0, +\infty[\,. \tag{7.33}$$

This result states that the dynamics of the disclination $d = (s, y)$, i.e., the evolution in time of $y(t)$ for a given value of s, is solely *radial*, as one expects from the fact that the right-hand side of Equation (7.31), i.e., the non-dimensional force, is *radial*.

Our physical interpretation of the results of this subsection is that a system with a single disclination (modeled, here, as a point defect) either tries to minimize its energy by moving the defect towards the boundary or places the defect in the position that maximizes energy, i.e., at the center of the circular domain, thereby preserving symmetry. If, however, the symmetry is broken by putting the disclination out of the center of the domain, which corresponds to an *unstable* configuration, the disclination goes towards the boundary of the domain, where the equilibrium is stable. Yet, this may occur only in infinite time, so that the disclination cannot leave the domain.

Remark 7.1. Notice that the boundary, which behaves as an attractor (indeed, $\rho(t) \to 1$ if $t \to +\infty$), has an effect that could be interpreted as stemming from an "interaction potential", *quadratic* as ρ approaches unity (see (7.32), as discussed at the end of Section 7.2.1). We emphasize that this behavior contrasts with that of one screw dislocation in $B_1(0)\backslash\{0\}$, which reaches the boundary in finite time [234, 236].

7.3.3 Two-disclination problem: interactions among disclinations

We consider now the dynamics of two disclinations in $B_1(0)$, namely $d_1 = (s_1, y_1)$ and $d_2 = (s_2, y_2)$, thereby specializing (7.24) to $N = 2$, i.e.,

$$\begin{cases} \dot{y}_1(t) = \hat{F}_1(y_1(t), y_2(t)), & \dot{y}_2(t) = \hat{F}_2(y_1(t), y_2(t)), \quad t > 0, \\ y_1(0) = y_{1,\mathrm{i}}, & y_2(0) = y_{2,\mathrm{i}}, \end{cases} \tag{7.34}$$

where the non-dimensional forces $\hat{F}_1 := -\nabla_{y_1}\hat{W}$ and $\hat{F}_2 := -\nabla_{y_2}\hat{W}$ read as

$$\hat{F}_1(y_1, y_2) = \hat{F}_1^{(1)}(y_1) + \hat{F}_1^{(2)}(y_1, y_2) + \hat{F}_1^{(3)}(y_1, y_2), \tag{7.35a}$$

$$\hat{F}_2(y_1, y_2) = \hat{F}_2^{(1)}(y_2) + \hat{F}_2^{(2)}(y_1, y_2) + \hat{F}_2^{(3)}(y_1, y_2). \tag{7.35b}$$

Similarly to the general case of N disclinations, the force $\hat{F}_1$ acting on d_1 features three contributions: $\hat{F}_1^{(1)}$ is formally the same *radial* force that would act on d_1 if d_2 were absent (see Section 7.3.2); $\hat{F}_1^{(2)}$ is the agency due to the boundary, modulated by d_2; and $\hat{F}_1^{(3)}$ is the *mutual* interaction between d_1 and d_2. In particular, $\hat{F}_1^{(2)}$ is *radial*, and $\hat{F}_1^{(3)}$ is directed along the segment connecting y_1 and y_2, while their signs

depend solely on the product of the Frank angles $s_1 s_2$. Indeed, within the range $0 < r_{12} < 1$, it holds true that $1 - r_{12} > 0$ and $1 - r_{12} + \log r_{12} < 0$. The same discussion can be done also for the force featuring in Equation (7.35b).

If s_1 and s_2 have the same sign, i.e., if $s_1 s_2 > 0$, then, for each disclination, the second force tends to move the disclination radially towards the boundary, in synergy with the first force, and the third force describes a *repulsion* between the two disclinations. On the other hand, if s_1 and s_2 have opposite sign, i.e., if $s_1 s_2 < 0$, the second force operates against the first one by pushing the disclinations towards the center, and the third force describes an *attraction* between the two disclinations.

A consequence of the discussion reported above is that disclinations in an elastic medium behave qualitatively as *charged particles* (see the notion of topological charges [258]), with the Frank angles playing the role of electric charges. Thus, two disclinations with Frank angles of opposite sign attract each other, whereas two disclinations with Frank angles of the same sign repel each other.

To better understand the scenarios of a disclination approaching the boundary and of two superposing disclinations, we give the following remarks.

Remark 7.2 (A disclination goes to the boundary). Let us suppose that d_2 approaches the boundary, which amounts to taking the limit $|y_2| \to 1^-$. Then, the force $\hat{F}_2$ tends to vanish and, accordingly, the evolution of y_2 tends to stop, while the force $\hat{F}_1$ acting on d_1 tends to equal the first (radial) contribution of Equation (7.35a), i.e., $\hat{F}_1(y_1, y_2) \sim 2s_1^2(1 - |y_1|^2)y_1$, since d_1 is the only disclination *effectively* remaining in the system. It is important to highlight that, in fact, $\hat{F}_1$ becomes independent of the position taken by d_2 on the boundary.

Remark 7.3 (Superposition of two disclinations). Let us study the case in which the system is prepared in such a way that two disclinations d_1 and d_2 are superposed at the same point $y_e \in B_1(0)$. The energy of this configuration can be obtained by taking the limit of Equation (7.25) for y_1 and y_2 tending to the same point y_e, i.e.,

$$\check{W}(y_e) \coloneqq \lim_{y_2 \to y_1} \hat{W}(y_1, y_2) = \frac{1}{2}(s_1 + s_2)^2(1 - |y_e|^2)^2. \tag{7.36}$$

We emphasize that this limit should not be understood in dynamic sense. Rather, it represents the energetic output of a virtual process of superposition of the two disclinations at *frozen time*, e.g., at the initial time of observation. On the other hand, to study the dynamics of a system of two disclinations that are initially superposed,

one should solve (7.34), with $y_1(0) = y_2(0) = y_{\mathrm{e,i}}$ and the forces specified in Equations (7.35a) and (7.35b). In this respect, it could be instructive to notice that, as long as $y_1(t)$ and $y_2(t)$ are such that, for $t > 0$, the distance $|y_2(t) - y_1(t)|$ is sufficiently small, then the forces F_1 and F_2 can be approximated as

$$F_1 = \hat{F}_1(y_1, y_2) \sim 2s_1^2(1 - |y_1|^2)y_1 + 2s_1s_2(1 - |y_2|^2)y_1, \tag{7.37a}$$

$$F_2 = \hat{F}_2(y_1, y_2) \sim 2s_2^2(1 - |y_2|^2)y_2 + 2s_1s_2(1 - |y_1|^2)y_2, \tag{7.37b}$$

and Equation (7.34) should be modified accordingly, i.e., with Equations (7.37a) and (7.37b) in lieu of (7.35a) and (7.35b). Hence, inspecting the approximated forces F_1 and F_2 permits to assess that d_1 and d_2 remain superposed for $t > 0$ in two cases: (i) if $|s_1| \neq |s_2|$, then the solutions $y_1(t) = y_2(t) = y_{\mathrm{e}}(t)$ for $t > 0$, with $y_{\mathrm{e}}(t)$ obtained by solving either $(7.34)_1$ or $(7.34)_2$, are admissible if and only if $y_{\mathrm{e}}(t) = 0$ or $y_{\mathrm{e}}(t) = 1$, which requires $y_{\mathrm{e,i}} = 0$ and $y_{\mathrm{e,i}} = 1$, respectively, and means that, in fact, the superposed disclinations do not move; (ii) if $|s_1| = |s_2|$, then d_1 and d_2 remain superposed for $t > 0$, regardless of their coincident initial position, and are allowed to move according to the applied forces. In particular, if $s_1 = s_2$ and $y_{\mathrm{e,i}} \neq 0$, then the disclinations, while being superposed, move towards the boundary; more importantly, if $s_1 = -s_2$, then, independently of $y_{\mathrm{e,i}}$, the first and second summands in each of the expressions of the forces in Equations (7.37a) and (7.37b) compensate each other out, and, thus, the disclinations do not move from their initial superposed configuration. In the terminology of [258], the two disclinations are said to *annihilate* each other, thereby restoring the compatibility of the deformation at the superposition point. Finally, we notice that Equations (7.37a) and (7.37b) characterize also the situation in which the two disclinations that are not superposed *tend to collide*. Indeed, if $|y_2(t) - y_1(t)| \leq \varepsilon_{\mathrm{c}}$, then the term r_{12} in Equation (7.26) scales with $\varepsilon_{\mathrm{c}}^2$, so that the force $F_{12}^{(2)}$ is approximated as in the second summand on the right-hand side of (7.37a), while $F_{12}^{(3)}$ becomes negligible, since it scales with ε_{c}.

Remark 7.4 (Splitting of two disclinations). As pointed out in Remark 7.3, two disclinations initially placed at the same position $y_{1,\mathrm{i}} = y_{2,\mathrm{i}} = y_{\mathrm{e,i}}$ do *not* remain superposed for $t > 0$ if $|s_1| \neq |s_2|$ and $y_{\mathrm{e,i}} \in B_1(0) \setminus \{0\}$. This is because the two disclinations move towards the boundary $\partial B_1(0)$ with forces that, differing in magnitude, *split* the two disclinations dynamically. This situation is simulated in Benchmark #2 in Section 7.4. Yet, although maintaining the conditions $|s_1| \neq |s_2|$ and $y_{\mathrm{e,i}} \in B_1(0) \setminus \{0\}$, we may enforce a *constraint* that restricts the two disclinations

to remain superposed at all times. This is useful, for instance, to quantify the reactive forces necessary to maintain the superposition also for $t > 0$. A possible way of doing this is to assume the disclinations form a dipole of infinitesimal length and then to perform the limit in which this length approaches zero. Hence, we introduce the *holonomic* constraint $\hat{C}(y_1, y_2; \varepsilon) \coloneqq y_1 - y_2 - \varepsilon = 0$, with ε being a vector with arbitrarily small, but strictly positive, magnitude, and the *augmented* Lagrangian function [11]

$$\mathcal{L} \equiv \hat{\mathcal{L}}(y_1, y_2; \lambda, \varepsilon) \coloneqq -\hat{W}(y_1, y_2) + \lambda \cdot \hat{C}(y_1, y_2; \varepsilon), \tag{7.38}$$

with λ being the vector-like Lagrange multiplier associated with the constraint (not to be confused with the inverse of the friction coefficient in the dynamic equations). Note that ε is introduced to prevent the logarithm in the forces presented above to be ill-defined, and that the "true" Lagrangian of the system is given by $L \equiv \hat{L}(y_1, y_2) \coloneqq -\hat{W}(y_1, y_2)$ in the present framework (no inertial forces are attributed to the disclinations). Because of the constraint in Equation (7.38), the dynamic problem (7.34) changes into

$$\dot{y}_1(t) = \nabla_{y_1}\hat{\mathcal{L}}(y_1(t), y_2(t); \lambda(t), \varepsilon(t)) = -\nabla_{y_1}\hat{W}(y_1(t), y_2(t)) + \lambda(t), \tag{7.39a}$$

$$\dot{y}_2(t) = \nabla_{y_2}\hat{\mathcal{L}}(y_1(t), y_2(t); \lambda(t), \varepsilon(t)) = -\nabla_{y_2}\hat{W}(y_1(t), y_2(t)) - \lambda(t), \tag{7.39b}$$

$$0 = \nabla_{\lambda}\hat{\mathcal{L}}(y_1(t), y_2(t); \lambda(t), \varepsilon(t)) = y_1(t) - y_2(t) - \varepsilon(t), \tag{7.39c}$$

which holds for $t > 0$. By differentiating Equation (7.39c) with respect to time, the system in (7.39a)–(7.39c) can be rewritten in the decoupled form

$$\dot{y}_1(t) = -\tfrac{1}{2}\left[\nabla_{y_1}\hat{W}\big(y_1(t), y_1(t) - \varepsilon(t)\big) + \nabla_{y_2}\hat{W}\big(y_1(t), y_1(t) - \varepsilon(t)\big)\right] + \tfrac{1}{2}\dot{\varepsilon}(t), \tag{7.40a}$$

$$\dot{y}_2(t) = -\tfrac{1}{2}\left[\nabla_{y_1}\hat{W}\big(y_2(t) + \varepsilon(t), y_2(t)\big) + \nabla_{y_2}\hat{W}\big(y_2(t) + \varepsilon(t), y_2(t)\big)\right] - \tfrac{1}{2}\dot{\varepsilon}(t), \tag{7.40b}$$

$$\lambda(t) = +\tfrac{1}{2}\left[\nabla_{y_1}\hat{W}\big(y_1(t), y_2(t)\big) - \nabla_{y_2}\hat{W}\big(y_1(t), y_2(t)\big)\right] + \tfrac{1}{2}\dot{\varepsilon}(t). \tag{7.40c}$$

The solution to Equations (7.40a)–(7.40c) that comply with the initial conditions $y_1(0) = y_{1,\mathrm{i}}$ and $y_2(0) = y_{1,\mathrm{i}} - \varepsilon(0)$ is the triple $(y_1(t), y_2(t); \lambda(t))$, which, in the

limit $\varepsilon(t) \to 0$ uniformly with respect to t, converges to the solution of the problem

$$\begin{cases} \dot{y}_{\mathrm{e}}(t) = \hat{F}_{\mathrm{e}}(y_{\mathrm{e}}(t)) = 2s_{\mathrm{e}}^2(1 - |y_{\mathrm{e}}(t)|^2)y_{\mathrm{e}}(t), & t > 0, \\ \lambda(t) = (s_2^2 - s_1^2)(1 - |y_{\mathrm{e}}(t)|^2)y_{\mathrm{e}}(t), & t > 0, \quad s_{\mathrm{e}} \coloneqq \dfrac{s_1 + s_2}{\sqrt{2}}. \\ y_{\mathrm{e}}(0) = y_{\mathrm{e,i}}, \end{cases} \tag{7.41}$$

Thus, if the constraint of "persisting superposition" is fulfilled, the two disclinations follow together the same kind of dynamics addressed in Section 7.2.1, as if they were a single disclination, initially positioned in $y_{\mathrm{e,i}}$, and with an "effective" Frank angle equal to $s_{\mathrm{e}} \coloneqq (s_1 + s_2)/\sqrt{2}$, which can be zero or different from zero. However, the force on the right-hand side of $(7.41)_1$ is different from the one that would stem from the differentiation of the energy $\check{W}$ in Equation (7.36) with respect to y_{e}. The "price to pay" for maintaining this dynamics is given by the reaction forces $\lambda(t)$ and $-\lambda(t)$, which are characterized by the following property: they have the same functional dependence on y_{e} as the force in $(7.41)_1$, but they depend on the difference between the squares of the Frank angles of the two disclinations. Hence, the reactive forces vanish identically both when the Frank angles are equal to each other and when they are opposite to each other, i.e., when $|s_1| = |s_2|$. This means that constraining the two disclinations to persist in their initial superposed configuration yields null reaction forces for the subsequent instants of time, since the two disclinations remain together naturally. This is because, in the just discussed situation, the superposition of the two disclinations annihilates the attractive or repulsive forces that they mutually exchange, and only modulates the influence of the boundary. On the contrary, the reaction forces are non-null for $|s_1| \neq |s_2|$, and their magnitudes increase with the absolute value $|s_2^2 - s_1^2|$, since the "price" for keeping them superposed increases with their tendency to separate. This is consistent with Remark 7.3. An example of the dynamics of the "effective" disclination associated with two initially superposed disclinations is discussed in Benchmark #2 of Section 7.4.

Remark 7.5 (Superposition breaking due to a third disclination). We conclude this series of remarks by noting that the initial superposition of two disclinations does not persist, in general, if interactions with other disclinations are perceived. Indeed, even though one prepares an "experiment" (*in silico*, for this work) in which two disclinations with opposite Frank angles are superposed at the initial time of their dynamics, this compatible configuration of the system breaks dynamically as soon as the interaction with another disclination is felt. On the one hand, this behavior is

intuitive, because one switches from a two-disclination to a three-disclination system. On the other hand, the *splitting* phenomenon is important because it shows that two initially superposed disclinations with opposite Frank angles and interacting with a third disclination *are not equivalent* to a system of one disclination only (the third one). This situation is simulated in Benchmark #3 of Section 7.4.

7.3.4 Two disclinations with zero total Frank angle

To better understand the behaviour of the "two-disclination problem", we now consider the case in which $s_1 = -s_2 = s$, and the disclinations are initially placed in $B_1(0)$ symmetrically with respect to the origin. In this case, Equation (7.34) reduces to a Cauchy problem with a single ordinary differential equation in the non-dimensional distance $\Delta := |y_1 - y_2|$ between d_1 and d_2, and with initial condition $\Delta(0) = \Delta_\mathrm{i} := |y_{1,\mathrm{i}} - y_{2,\mathrm{i}}|$, i.e.,

$$\begin{cases} \dot{\Delta}(t) = \hat{G}(\Delta(t)), \quad t > 0, \\ \Delta(0) = \Delta_\mathrm{i}, \end{cases} \tag{7.42}$$

where the forcing term $\hat{G}(\Delta) := \hat{F}_1(y_1, y_2) - \hat{F}_2(y_1, y_2)$ is given by

$$\hat{G}(\Delta) := 4s^2\Delta\left[\frac{4-\Delta^2}{4+\Delta^2} + 2\log\frac{4\Delta}{4+\Delta^2}\right], \qquad \Delta \in \,]0, 2[\,, \tag{7.43}$$

and is obtained because, in the symmetric condition under investigation, it holds that $y_1 = (\frac{1}{2}\Delta, 0)$ and $y_2 = (-\frac{1}{2}\Delta, 0)$.

The function $\hat{G}$ in Equation (7.43) admits only one zero in the open interval $\,]0, 2[\,$, computed numerically and approximately given by $\Delta_\mathrm{eq} \simeq 0.8$. Since $\hat{G}(\Delta_\mathrm{eq}) = 0$, Δ_eq is the sole equilibrium configuration for the system. This configuration is *unstable* and divides the range of admissible values of Δ into two basins of attraction, as shown in Figure 7.1. The instability of Δ_eq descends from the fact that, if we choose $\Delta_\mathrm{i} < \Delta_\mathrm{eq}$ in the Cauchy problem (7.42), then it holds that $\Delta(t) \to 0^+$ for $t \to +\infty$, which means that if the initial distance between the two disclinations is smaller than the equilibrium one, it tends to decrease indefinitely, so that the disclinations *tend to collide* in the origin. Moreover, if $\Delta_\mathrm{i} > \Delta_\mathrm{eq}$, then $\Delta(t) \to 2^-$ for $t \to +\infty$, i.e., the disclinations increase their reciprocal distance with respect to the initial one and

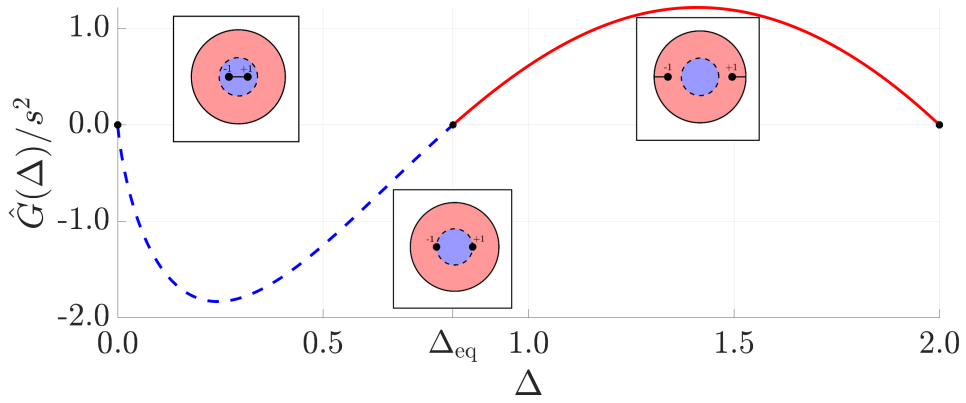

Fig. 7.1 Plot of $\hat{G}(\Delta)/s^2$ in Equation (7.43): the basins of attraction for $\Delta = 0$, i.e., $]0, \Delta_{eq}[$, and for $\Delta = 2$, i.e., $]\Delta_{eq}, 2[$, are highlighted with dashed and solid lines, respectively. Three simulations of two symmetrically placed disclinations having Frank angles $+1$ and -1 have been carried out over a normalized time window of width $T = 2$ (see Section 7.4 for the implementation details). The trajectories for three values of Δ_i are depicted in the three squares. The results are coherent with the expected behavior since the disclinations come closer for $\Delta_i < \Delta_{eq}$, move apart for $\Delta_i > \Delta_{eq}$, and do not move if $\Delta_i = \Delta_{eq}$.

move towards the boundary. Hence, if one now sees the domain of $\hat{G}$ as $]0, 2]$, and extends by continuity $\hat{G}$ in $\Delta = 0$, the values $\Delta = 0$ and $\Delta = 2$ can be "promoted" to two configurations of *stable equilibrium*.

What has been described so far can be formalized by taking the principal parts of $\hat{G}(\Delta)$ in the limits $\Delta \to 0^+$ and $\Delta \to 2^-$, which permit one to approximate $\hat{G}(\Delta)$ as

$$\hat{G}(\Delta)/s^2 \sim 8\Delta \log\Delta, \qquad \Delta \to 0^+, \tag{7.44a}$$

$$\hat{G}(\Delta)/s^2 \sim 4(2 - \Delta), \qquad \Delta \to 2^-. \tag{7.44b}$$

Then, by solving the corresponding approximated Cauchy problems in small neighborhoods $I^+(0)$ and $I^-(2)$ of the values $\Delta = 0$ and $\Delta = 2$, we have that

$$\begin{cases} \dot{\Delta}(t) = 8s^2\Delta(t)\log\Delta(t), \\ \Delta(0) = \Delta_i \in I^+(0), \end{cases} \Rightarrow \Delta(t) = \exp[(\log\Delta_i)\exp(+8s^2t)], \tag{7.45a}$$

$$\begin{cases} \dot{\Delta}(t) = 4s^2(2 - \Delta(t)), \\ \Delta(0) = \Delta_i \in I^-(2), \end{cases} \Rightarrow \Delta(t) = 2 - (2 - \Delta_i)\exp(-4s^2t). \tag{7.45b}$$

The results in Equations (7.45a) and (7.45b) imply that the values $\Delta = 0$ and $\Delta = 2$ are attractors for the system under study. In particular, although $\Delta = 0$ is not in the domain of $\hat{G}$, it describes the case of two disclinations with opposite Frank angles that tend to collide, and is consistent with the predictions of Remark 7.4 for $s_e = 0$ and $y_{e,i} = 0$ (the latter condition preserves the compliance with the geometric constraint that the two disclinations are placed symmetrically with respect to the origin).

Even more importantly, from the just discussed situation (two disclinations placed symmetrically and with opposite Frank angles) we deduce that the value Δ_{eq} is the system's *critical distance* such that two behaviors are observed: for $\Delta_i < \Delta_{eq}$, the attractive forces between the disclinations are predominant with respect to the effect of the boundary, and thus, as one would expect, the disclinations tend to come indefinitely closer to each other; for $\Delta_i > \Delta_{eq}$, the presence of the boundary overcomes the attractive forces, and, even though the disclinations have opposite Frank angles, they move apart.

Remark 7.6. Equations (7.45a) and (7.45b) show that, for the symmetric system of disclinations under study, the phenomena of "collision" between the disclinations and of the two disclinations reaching the boundary occur in infinite time, thereby manifesting another striking difference with the case of screw dislocations [236].

Before moving to Section 7.4, we emphasize that the results provided in Section 7.3.4 would be significantly different if the total Frank angle of the system were non-zero, i.e., $s_1 + s_2 \neq 0$, since an underlying symmetry would be lost. The behavior of a system of this type is numerically analyzed in Benchmark #1 of Section 7.4.

7.4 Non-trivial rearrangements of disclinations

In this section, we report on four *benchmark* problems that we deem remarkable. Our goal is to present and discuss non-trivial rearrangements of disclinations towards *stable* equilibria by numerically solving the Cauchy problem in (7.24) for different choices of the number of disclinations N and of the initial distribution $\boldsymbol{y}_i$. The simulations are carried out in MATLAB [264] by having recourse to the `ode45` function [265]. In the subsequent figures, the disclinations with positive Frank angle are associated with red color and solid lines, whereas the ones with negative Frank

angle are associated with blue color and dashed lines. Additional simulation details, as the time of observation, are provided in the benchmark descriptions.

7.4.1 Two disclinations with nonzero total Frank angle

We consider the case of two disclinations d_1 and d_2 with Frank angles $s_1 = +1$ and $s_2 = -2$, placed symmetrically with respect to the origin of $B_1(0)$, at the initial positions $y_{1,\mathrm{i}} = (+0.3, 0.0)$ and $y_{2\mathrm{i}} = (-0.3, 0.0)$. As can be seen in Figure 7.2, the predominant forces in the initial instants of time are the ones of mutual interaction. This makes the two disclinations move one towards the other, with d_1 being moved at higher velocity. Then, after d_1 passes through the center of the circular domain, and d_1 and d_2 are sufficiently close to each other, they start moving together towards the boundary (the attraction towards the boundary become the predominant effect). The forces of mutual interaction keep d_1 and d_2 near to each other but never in superposition.

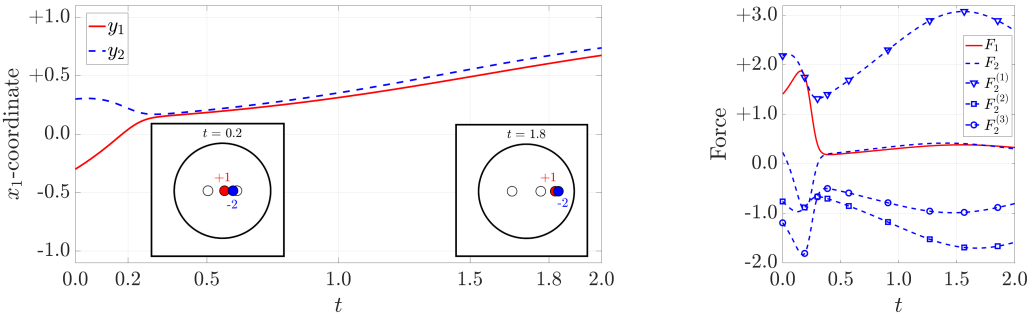

Fig. 7.2 (Left) Time trend along the x_1-axis of the positions of the disclinations of Benchmark #1, with snapshots at $t = 0.2$ and $t = 1.8$, over a time window of width $T = 2$. (Right) Time trend of F_1, F_2, and of the summands of F_2.

7.4.2 Superposition breaking: unbalance of the Frank angles

We consider two disclinations d_1 and d_2, so that $s_1 = +1$ and $s_2 = -2$, respectively, which are initially superposed in $y_{\mathrm{e,i}} = (+0.3, 0.0)$. This system is depicted in Figure 7.3 where its dynamics is studied with and without the constraint of "persisting superposition" of Remark 7.4. The simulations confirm the predictions of Remarks 7.3 and 7.4, since d_1 and d_2 naturally tend to split, so that the inequality $y_1(t) \neq y_2(t)$,

for $t > 0$, holds true if no constraint is enforced. This is because the difference in the Frank angles produces different interactions and weighs differently the effect of the boundary $\partial B_1(0)$, as visualized in Figure 7.3. Instead, when the constraint is enforced, d_1 and d_2 remain superposed and move together as one "effective" disclination d_e having Frank angle $s_e = -1/\sqrt{2}$.

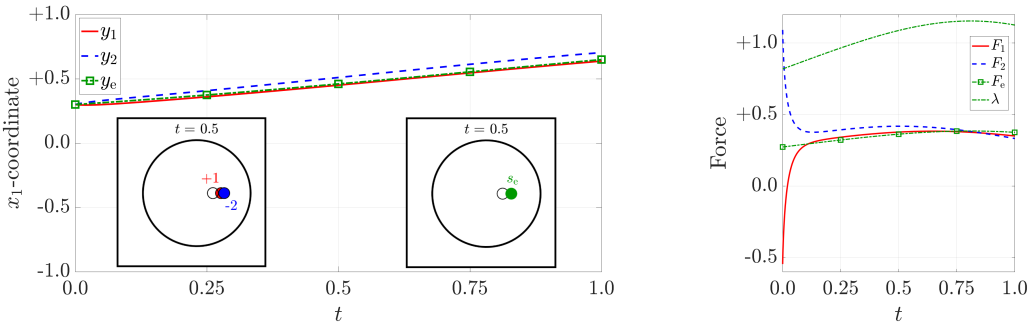

Fig. 7.3 (Left) Time trend along the x_1-axis of the positions of the disclinations of Benchmark #2 and of the "effective" disclination $d_e = (y_e, s_e)$, with snapshots at $t = 0.5$, over a time window of width $T = 1$. (Right) Time trend of F_1 , F_2 , F_e and λ.

7.4.3 Superposition breaking due to a third disclination

We consider three disclinations, denoted by d_1, d_2, and d_3, with $s_1 = +1$, $s_2 = -1$, and $s_3 = +1$, where d_1 and d_2 are initially superposed, so that their initial common position is $y_{1,i} = y_{2,i} = (+0.3, 0.0)$, and $y_{3,i} = (-0.3, 0.0)$. As expected from Remark 7.5, the presence of d_3 breaks the initial superposition of d_1 and d_2 by attracting d_2 and repelling d_1 due to the signs of the considered Frank angles. Hence, d_1 and d_2 *split*. However, as d_3 approaches the boundary, these interactions tend to vanish, so that d_1 and d_2 approach each other again.

7.4.4 Odd number of disclinations: vertices of a regular polygon

It is noteworthy to examine the behavior of a system of N disclinations initially placed at the vertices of a regular polygon. The initial positions can be expressed in polar coordinates as $y_{k,i} \equiv \rho \exp(i(k-1)\pi/N)$, for $k = 1, \dots, N$ and fixed ρ, while the Frank angles can be chosen as $s_k = (-1)^{k-1}$, for $k = 1, \dots, N$. On the one hand, the case of an even number of disclinations can be seen as a "generalization" of the

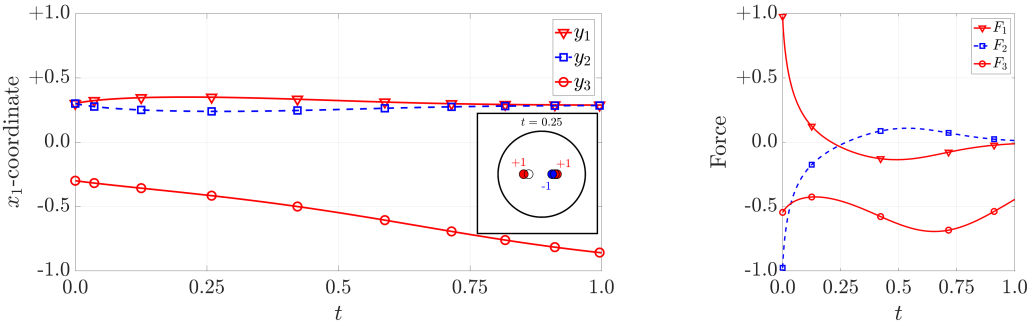

Fig. 7.4 (Left) Time trend of the positions of the disclinations of benchmark #3, with a snapshot at $t = 0.25$, over a time window of width $T = 2$. (Right) Time trend of F_1 , F_2 , and F_3. Note that, as also in Figures 7.2 and 7.3, the time derivative of the functions plotted on the left are the functions plotted on the right. For instance, at about $t = 0.25$, where y_1 and y_2 have critical points, F_1 and F_2 vanish.

scenario examined in Section 7.3.4, since $\sum_{k=1}^{N} s_k = 0$ (neutral total "charge"), and, for a sufficiently small ρ, the N disclinations move towards the center (this is shown, for $N = 4$, in Figure D.1 of Appendix D). On the other hand, the case of an odd number of disclinations N is more interesting, since $\sum_{k=1}^{N} s_k \neq 0$, and the trajectories of the disclinations exhibit highly-nonlinear behaviors, as can be seen in Figure 7.5.

For $N = 3$ (a *triplet*, left panel of Figure 7.5), the disclinations with positive Frank angles, d_1 and d_3, initially repel each other (they have Frank angles of the same sign). However, rather then moving in straight line, they start their motion with two specular circles (because, at the initial times, repulsive forces are stronger) before moving towards the boundary. The presence of the circles is strongly dependent on the choice of ρ (distance of each disclination from the center). Indeed, for smaller values of ρ, the circles are not observed, and one sees a more sudden change in direction from the phase of distancing to the phase in which the trajectories approach each other (data not shown). The negative disclination d_2 follows the other two disclinations, in a symmetric way, by virtue of the two attractive forces dominating over the effect of the boundary. Eventually, the three disclinations move together towards the boundary by placing themselves at the vertices of a triangle, which is maintained by the balance among the repulsive force characterizing the pair (d_1, d_3) and the attractive forces characterizing the pairs (d_1, d_2) and (d_2, d_3). We find this result interesting because the disclinations d_1 and d_3 tend to migrate towards the boundary very close to each other in spite of them having Frank angle of the same sign. This is made possible by d_2, which, having Frank angle of opposite sign, mitigates their mutual repulsion and

induces a *shielding effect* for d_1 and d_3. To us, this behavior is reminiscent of Cooper pairs in superconductors [66], although the physics of our problem is very different.

For $N=5$ (a *quintet*, central panel of Figure 7.5), the repulsive forces between the two positive disclinations closest to each other allow one to see the dynamics of the system as essentially dictated by two main behaviors: the first one is identified by two pairs of disclinations, each of which features two disclinations of opposite sign that tend to collide by moving along curved trajectories; the second one is identified by the unpaired disclination that moves towards the boundary in the direction opposite to the other disclinations. In our opinion, this benchmark is remarkable since, in spite of the high non-linearity of the problem, we are still able to track the behavior of the disclinations: indeed, they are characterized by two phenomena that we have individually addressed in this work, i.e., collisions (at infinite time) between disclinations of opposite sign, and the motion towards the boundary of the unpaired disclination.

For $N = 7$ (a *septet*, right panel of Figure 7.5), the phenomena characterizing this initial configuration are the collisions (occurring in infinite time) within the two pairs of disclinations of opposite sign moving, again, along curved trajectories, and the motion of the three unpaired disclinations forming a *triplet* that moves towards the boundary.

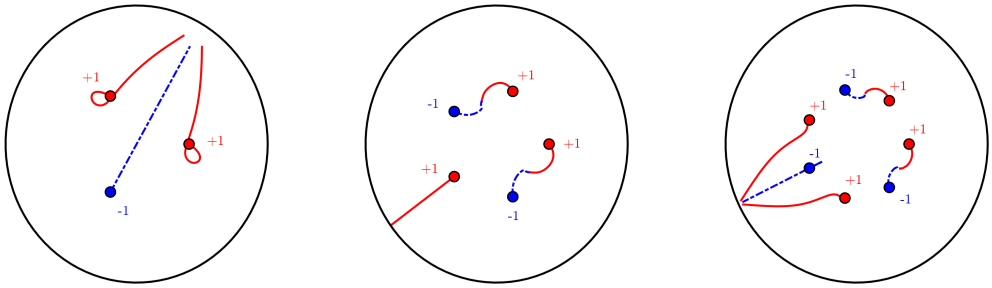

Fig. 7.5 Trajectories of a system of $N = 3$, $N = 5$, $N = 7$ disclinations initially placed at the vertices of a regular polygon ($\rho = 0.4$). The starting locations of the disclinations are marked with circles. The trajectories, departing from the markers, are shown over a normalized time window of width $T = 8$.

Appendix D

Modeling the crystalline structure in disclination dynamics

The content of this appendix is taken from the appendix of [3].

This appendix is devoted to showing what our model predicts in the presence of preferred directions of motion. Our primary objective here is theoretical: to demonstrate how the modeling concept of glide directions, as introduced in [199] and further explored in [234] for dislocations, applies to disclinations. We emphasize, however, that, to the best of our knowledge, there is currently no experimental evidence directly supporting the idea that the spontaneous dynamics of disclinations are restricted by slip systems as in the case of dislocations. At the same time, we acknowledge several observations and theoretical arguments suggesting that the dynamics of disclinations are likely influenced by the underlying lattice structure. In the context of graphene, for example, there is evidence indicating that disclination motion depends on preferred directions within the hexagonal lattice and specific angles. The nucleation mechanism of single disclinations and their associated kinetics, as described in [242], is thought to involve initial 90-degree bond rotations, followed by the migration of dislocation-disclination dipole systems (for further exploration of this topic, see [266–268]). We hope that the predictions outlined in this section will inspire future experimental studies aimed at elucidating the rules governing the kinematics of disclinations.

In this section, we denote by $\boldsymbol{y} = (y_1, \dots, y_N) \in [B_1(0)]^N$ the configuration of the N disclinations and we shall abandon the "hat" notation; recalling Equation

(7.27), the system in (7.24) reads then (with $\boldsymbol{F}(\boldsymbol{y}) \coloneqq (F_1(\boldsymbol{y}), \dots, F_N(\boldsymbol{y})) \in \mathbb{R}^{2N}$) as

$$\begin{cases} \dot{\boldsymbol{y}}(t) = \boldsymbol{F}(\boldsymbol{y}(t)), \quad t > 0, \\ \boldsymbol{y}(0) = \boldsymbol{y}_{\mathrm{i}}. \end{cases} \tag{D.1}$$

Let $\mathcal{G}$ be a set of $M \in \mathbb{N}$ unit vectors, with the requirements that $\operatorname{Span} \mathcal{G} = \mathbb{R}^2$ and that $g \in \mathcal{G} \iff -g \in \mathcal{G}$. The directions $g_k(\boldsymbol{y}) \in \mathcal{G}$ along which the disclination $d_k = (s_k, y_k)$ moves are determined as the ones along which the force F_k is the most aligned, namely

$$g_k(\boldsymbol{y}) \in \arg\max_{g \in \mathcal{G}} \{F_k(\boldsymbol{y}) \cdot g\}\,; \tag{D.2}$$

we let $\mathcal{G}_k(\boldsymbol{y}) \coloneqq \{g_k(\boldsymbol{y}) \in \mathcal{G} : \text{(D.2) holds}\}$. Finally, we define

$$\mathcal{F}_k(\boldsymbol{y}) = \big\{(F_k(\boldsymbol{y}) \cdot g_k(\boldsymbol{y}))g_k(\boldsymbol{y}) \,\big|\, g_k(\boldsymbol{y}) \in \mathcal{G}_k(\boldsymbol{y})\big\}. \tag{D.3}$$

For geometric reasons, there are only three possible scenarios:

(1) If $F_k(\boldsymbol{y}) = 0$ (the force on disclination d_k vanishes), then $\mathcal{G}_k(\boldsymbol{y}) = \mathcal{G}$, and trivially $\mathcal{F}_k(\boldsymbol{y}) = \{0\}$.

(2) If $F_k(\boldsymbol{y}) \neq 0$ and there is only one direction maximizing $F_k(\boldsymbol{y}) \cdot g$ in Equation (D.2), namely $\mathcal{G}_k(\boldsymbol{y}) = \{g_k(\boldsymbol{y})\}$, then $\mathcal{F}_k(\boldsymbol{y}) = \{(F_k(\boldsymbol{y}) \cdot g_k(\boldsymbol{y}))g_k(\boldsymbol{y})\}$.

(3) If $F_k(\boldsymbol{y}) \neq 0$ and there exist two different directions both maximizing $F_k(\boldsymbol{y}) \cdot g$ in Equation (D.2), namely $\mathcal{G}_k(\boldsymbol{y}) = \{g_k^-(\boldsymbol{y}), g_k^+(\boldsymbol{y})\}$, then $\mathcal{F}_k(\boldsymbol{y}) = \{(F_k(\boldsymbol{y}) \cdot g_k^\pm(\boldsymbol{y}))g_k^-(\boldsymbol{y}), (F_k(\boldsymbol{y}) \cdot g_k^\pm(\boldsymbol{y}))g_k^+(\boldsymbol{y})\}$. This case occurs when the force $F_k(\boldsymbol{y})$ bisects the angle formed by $g_k^-(\boldsymbol{y})$ and $g_k^+(\boldsymbol{y})$.

These three cases can be resumed in the following formula:

$$\mathcal{F}_k(\boldsymbol{y}) = \begin{cases} \{0\}, & \text{if } F_k(\boldsymbol{y}) = 0, \\ \{(F_k(\boldsymbol{y}) \cdot g_k(\boldsymbol{y}))g_k(\boldsymbol{y})\}, & \text{if } F_k(\boldsymbol{y}) \neq 0 \text{ and } \mathcal{G}_k(\boldsymbol{y}) = \{g_k(\boldsymbol{y})\}, \\ \{(F_k(\boldsymbol{y}) \cdot g_k^\pm(\boldsymbol{y}))g_k^\pm(\boldsymbol{y})\}, & \text{if } F_k(\boldsymbol{y}) \neq 0 \text{ and } \mathcal{G}_k(\boldsymbol{y}) = \{g_k^\pm(\boldsymbol{y})\}, \end{cases} \tag{D.4}$$

and Equation (D.1) takes the form of the following differential inclusion:

$$\begin{cases} \dot{\boldsymbol{y}}(t) \in \boldsymbol{\mathcal{F}}(\boldsymbol{y}(t)) \quad t > 0, \\ \boldsymbol{y}(0) = \boldsymbol{y}_{\mathrm{i}}\,, \end{cases} \tag{D.5}$$

where $\boldsymbol{\mathcal{F}}(\boldsymbol{y}) \coloneqq \mathcal{F}_1(\boldsymbol{y}) \times \cdots \times \mathcal{F}_N(\boldsymbol{y}) \subset \mathbb{R}^{2N}$; notice that (D.5) is a dynamics in $\mathbb{R}^{2N}$, and it is indeed a differential inclusion when scenario (3) occurs for at least one $k \in \{1, \dots, N\}$.

The set-valued function $\boldsymbol{\mathcal{F}}$ is defined on the set $[B_1(0)]^N \setminus \Pi$, which makes each F_k well defined; nonetheless, recalling the arguments in Section 7.3.1 and Remark 7.2, it is possible to extend each F_k by continuity to the whole closed unit disk, so that we will consider $\operatorname{dom} \boldsymbol{\mathcal{F}} = \left[\overline{B}_1(0)\right]^N$; the set-valued function $\boldsymbol{\mathcal{F}}$ turns out to be upper semicontinuous (in the sense of [269, p. 65]; see [234, Lemma 2.11] for a proof). The theory of differential inclusions [269] provides a suitable notion of solution to Equation (D.5).

Definition D.1. A solution to Equation (D.5) is an absolutely continuous curve $t \mapsto \boldsymbol{y}(t) \in [B_1(0)]^N$ such that

$$\begin{cases} \dot{\boldsymbol{y}}(t) \in \operatorname{co} \boldsymbol{\mathcal{F}}(\boldsymbol{y}(t)), & t > 0, \\ \boldsymbol{y}(0) = \boldsymbol{y}_{\mathrm{i}} \in [B_1(0)]^N \setminus \Pi, \end{cases} \tag{D.6}$$

where $\operatorname{co} \boldsymbol{\mathcal{F}}$ is the convex hull of the set $\boldsymbol{\mathcal{F}}$.

Our case is analogous to that of [234, Lemma 2.10], therefore $\operatorname{co} \boldsymbol{\mathcal{F}}(\boldsymbol{y}) = (\operatorname{co} \mathcal{F}_1(\boldsymbol{y})) \times \cdots \times (\operatorname{co} \mathcal{F}_N(\boldsymbol{y})) \subset \mathbb{R}^{2N}$ for all $\boldsymbol{y} \in [\overline{B}_1(0)]^N$, and, from Equation D.4, we have that for each $k = 1, \dots, N$ the term $\operatorname{co} \mathcal{F}_k(\boldsymbol{y})$ is

$$\operatorname{co} \mathcal{F}_k(\boldsymbol{y}) = \begin{cases} \{0\}, & \text{if } F_k(\boldsymbol{y}) = 0, \\ \{(F_k(\boldsymbol{y}) \cdot g_k(\boldsymbol{y}))g_k(\boldsymbol{y})\}, & \text{if } F_k(\boldsymbol{y}) \neq 0 \text{ and } \mathcal{G}_k(\boldsymbol{y}) = \{g_k(\boldsymbol{y})\}, \\ \Sigma_k(\boldsymbol{y}), & \text{if } F_k(\boldsymbol{y}) \neq 0 \text{ and } \mathcal{G}_k(\boldsymbol{y}) = \{g_k^{\pm}(\boldsymbol{y})\}, \end{cases} \tag{D.7}$$

where $\Sigma_k(\boldsymbol{y})$ is the segment joining $(F_k(\boldsymbol{y}) \cdot g_k^{\pm}(\boldsymbol{y}))g_k^{-}(\boldsymbol{y})$ and $(F_k(\boldsymbol{y}) \cdot g_k^{\pm}(\boldsymbol{y}))g_k^{+}(\boldsymbol{y})$. We stress that scenario (3) must occur for having $\operatorname{co} \mathcal{F}_k(\boldsymbol{y}) = \Sigma_k(\boldsymbol{y})$.

We can now state the local existence theorem.

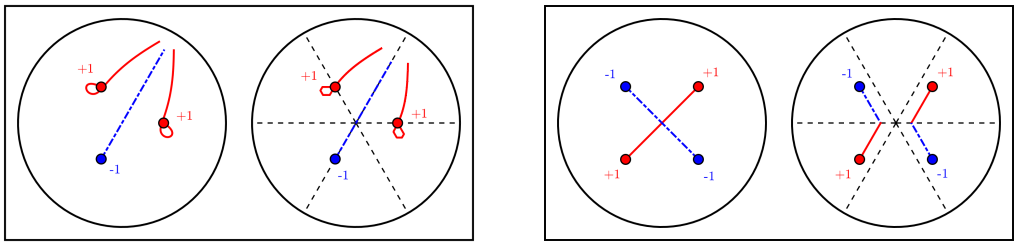

Fig. D.1 (Left) Numerical simulation of a *triplet*, without and with a hexagonal glide system over a time window of $T = 8$. It can be observed that the "circular" motion of the two positive disclinations is approximated by a *cross-slip* motion for their constrained counterparts, moving only in the allowed hexagonal directions. Moreover, the constrained disclinations experience a transition towards a *fine cross-slip* motion after passing again through their initial positions. It is important to observe that, since the forces are projected, the constrained disclinations move slower compared to their unconstrained counterparts. (Right) Numerical simulation of a system of a *quartet* without and with an hexagonal glide system over a time window of $T = 8$. The introduction of preferred directions of motion in the constrained case changes the equilibrium points towards which the system is attracted. Indeed, instead of *annihilating* in the center of the domain, as in the isotropic case, the disclinations prefer to annihilate in pairs, in points differing from the center, by moving along the glide directions.

Theorem D.1 (see [234, Theorem 2.13]). *Let* $\mathcal{F}\colon [\overline{B}_1(0)]^N \to \mathcal{P}(\mathbb{R}^{2N})$ *be defined as above, and let* $\boldsymbol{y}_{\mathrm{i}} \in [B_1(0)]^N \setminus \Pi$. *Then there exists* $t^* > 0$ *such that Equation D.5 admits a solution* $[-t^*, t^*] \ni t \mapsto \boldsymbol{y}(t) \in [B_1(0)]^N \setminus \Pi$ *in the sense of D.1.*

To discuss the local uniqueness of the solution, we distinguish two possibilities: if either case (1) or case (2) occurs, namely if either $\operatorname{co} \mathcal{F}_k(\boldsymbol{y}) = \{0\}$ or $\operatorname{co} \mathcal{F}_k(\boldsymbol{y}) = \{(F_k(\boldsymbol{y}) \cdot g_k(\boldsymbol{y}))g_k(\boldsymbol{y})\}$, for all $k = 1, \dots, N$, then uniqueness is immediate, owing to the Lipschitz continuity of the $\mathbb{R}^{2N}$-valued function $\mathcal{F}$, whereas two distinct phenomena can occur in case (3), namely when there exists (at least one index) $k \in \{1, \dots, N\}$ such that $\operatorname{co} \mathcal{F}_k(\boldsymbol{y}) = \Sigma_k(\boldsymbol{y})$. This last situation includes the phenomena that in the context of dislocation dynamics are called *cross-slip* and *fine cross-slip*: they were pictured in [199] and have been addressed mathematically in [234].

To tackle uniqueness in the latter case, we need to look carefully at the condition leading to $\operatorname{co} \mathcal{F}_k(\boldsymbol{y}) = \Sigma_k(\boldsymbol{y})$; from Equation (D.7), this occurs when $\operatorname{card} \mathcal{G}_k(\boldsymbol{y}) = 2$, so that we define $\mathcal{A}_k := \left\{\boldsymbol{y} \in [\overline{B}_1(0)]^N : \operatorname{card} \mathcal{G}_k(\boldsymbol{y}) = 2\right\}$ and $\mathcal{A} := \cup_{k=1}^N \mathcal{A}_k$ (cf. [234, formula (2.19)]). Given that in case (3) $F_k(\boldsymbol{y}) \neq 0$, the sets $\mathcal{A}_k$ are identified by the condition $F_k(\boldsymbol{y}) \cdot g_0(\boldsymbol{y}) = 0$, for the vector $g_0(\boldsymbol{y}) := g_k^+(\boldsymbol{y}) - g_k^-(\boldsymbol{y})$. Invoking the analitycity results for biharmonic functions contained in [270], we obtain that

$\mathcal{F}_k(\boldsymbol{y})$ are analytic, so that all of the $\mathcal{A}_k$'s are locally smooth manifolds; this yields that the normal unit vector $\mathbb{N}(\boldsymbol{y})$ is well defined for almost all $\boldsymbol{y} \in \mathcal{A}$ (and we assume, without loss of generality, that it points from the side of $\mathcal{A}_k$ where $g_k^-(\boldsymbol{y})$ is the only direction satisfying Equation (D.2) to the side of $\mathcal{A}_k$ where $g_k^+(\boldsymbol{y})$ is the only direction satisfying Equation (D.2)). This fails when $\mathcal{A}_k$ and $\mathcal{A}_h$ intersect transversally for $h \neq k$. These points, however, belong to a set of co-dimension greater than or equal to 2 in $\mathbb{R}^{2N}$. Accordingly, given $\widehat{\boldsymbol{y}} \in \mathcal{A}_k$ and B a neighborhood of $\widehat{\boldsymbol{y}}$, we denote by B^+ the "half" of B on the side of $\mathcal{A}_k$ containing $\boldsymbol{N}(\widehat{\boldsymbol{y}})$ and by B^- the other half and we let

$$F_k^{\pm}(\boldsymbol{y}) \coloneqq (F_k(\boldsymbol{y}) \cdot g_k^{\pm}(\widehat{\boldsymbol{y}}))g_k^{\pm}(\widehat{\boldsymbol{y}}) \qquad \text{for } \boldsymbol{y} \in B^{\pm}, \tag{D.8}$$

and we extend it smoothly to points $\boldsymbol{y} \in B \cap \mathcal{A}_k$ (cf. [234, formula (2.29)]). We let $\boldsymbol{F}^{\pm}(\boldsymbol{y})$ be the corresponding forces. Then, if at time $\widehat{t}$ it occurs that $\boldsymbol{y}(\widehat{t}) =: \widehat{\boldsymbol{y}} \in \mathcal{A}_k$, and $\boldsymbol{y}(t) \in B^-$ for $0 < \widehat{t} - t$ sufficiently small, and $\boldsymbol{y}(t) \in B^+$ for $0 < t - \widehat{t}$ sufficiently small, we have the following two scenarios.

(a) *Cross-slip* (see [234, Theorem 2.19]): the disclination d_k switches from moving along direction $g_k^-(\boldsymbol{y})$ to moving along direction $g_k^+(\boldsymbol{y})$ if

$$\boldsymbol{F}^-(\widehat{\boldsymbol{y}}) \cdot \boldsymbol{N}(\widehat{\boldsymbol{y}}) > 0 \qquad \text{and} \qquad \boldsymbol{F}^+(\widehat{\boldsymbol{y}}) \cdot \boldsymbol{N}(\widehat{\boldsymbol{y}}) > 0. \tag{D.9}$$

(b) *Fine cross-slip* (see [234, Theorem 2.20]): the disclination d_k switches from moving along direction $g_k^-(\boldsymbol{y})$ to moving along a convex combination $g_k^0(\boldsymbol{y}) \notin \mathcal{G}$ of directions $g_k^-(\boldsymbol{y})$ and $g_k^+(\boldsymbol{y})$ if

$$\boldsymbol{F}^-(\widehat{\boldsymbol{y}}) \cdot \boldsymbol{N}(\widehat{\boldsymbol{y}}) > 0 \qquad \text{and} \qquad \boldsymbol{F}^+(\widehat{\boldsymbol{y}}) \cdot \boldsymbol{N}(\widehat{\boldsymbol{y}}) < 0. \tag{D.10}$$

The force $\boldsymbol{F}^0(\boldsymbol{y}) \in \operatorname{co}\mathcal{F}(\boldsymbol{y})$ is determined by $\boldsymbol{F}^0(\boldsymbol{y}) = (1 - \alpha(\boldsymbol{y}))\boldsymbol{F}^-(\boldsymbol{y}) + \alpha(\boldsymbol{y})\boldsymbol{F}^+(\boldsymbol{y})$, where

$$\alpha(\boldsymbol{y}) = \frac{\boldsymbol{F}^-(\boldsymbol{y}) \cdot \boldsymbol{N}(\boldsymbol{y})}{\boldsymbol{F}^-(\boldsymbol{y}) \cdot \boldsymbol{N}(\boldsymbol{y}) - \boldsymbol{F}^+(\boldsymbol{y}) \cdot \boldsymbol{N}(\boldsymbol{y})}. \tag{D.11}$$

This motion occurs for $t > \widehat{t}$ and is confined to the set $\mathcal{A}_k$ (which makes the formula for $\alpha(\boldsymbol{y})$ well defined) and abandons it (tangentially to $\mathcal{A}_k(\boldsymbol{y})$) to continue in the direction $g_k^+(\boldsymbol{y})$.

Both scenarios (a) and (b) described above, as well as the result for right uniqueness in the case of single-valued forces $\mathcal{F}_k(\boldsymbol{y})$ satisfy the conditions for right uniqueness of [234, Theorem 2.17]. We refer the interested reader to [234, Section 2] for the precise statements of these theorems and for some technical mathematical details that we omitted in our discussion, without consequences for the understanding of the dynamics.

Figure D.1 offers a comparison of the motion for two systems of disclinations without and with glide directions. The chosen glide directions are those of the hexagonal lattice, which is the relevant one for graphene structures, i.e., $g_n \equiv \pm \exp(in\pi/3)$, with $n = 0, 1, 2$. Operatively, we numerically solve the two benchmark tests presented in Figure D.1 by modifying the implementation addressed in Section 7.4 and computing, at each time step, the projection of the N forces $F_1, \ldots, F_N$ along the glide directions, following the evolution rule reported in Equation (D.4).

Appendix E

The stationary behavior of systems of many disclinations

In this appendix, adding to the numerical experiments carried out in [3] and reported in Chapter 7 for small number of disclinations, we focus on a particular class of disclination systems. Specifically, we discuss the stationary behavior of systems of an even number, N, of disclinations $d_k = (y_k, s_k)$, with $k = 1, \ldots, N$, such that the condition of "zero total charge" holds true, i.e., $\sum_{k=1}^{N} s_k = 0$, and the Frank angles s_k are pairwise taken as "+1" and "−1".

Disclination systems with an initial "random" distribution. We first simulate a family of systems of N disclinations in which the defects are placed, at time $t = 0$, in random points of the unitary disk, representing the elastic domain in the non-dimensional setting. The disclinations organize themselves according to Equation (7.24). The simulated trajectories are reported in Figure E.1 and tracked from $t = 0$ to a time $t = T$, large enough to simulate the stationary state.

As can be seen from Figure E.1, the highly nonlinear right-hand side of Equation (7.24), due to the structure of Equation (7.25), makes the disclinations follow trajectories that strongly deviate from straight lines. In fact, such trajectories feature nontrivial curvature, "almost-sharp" turns, and turnarounds. These phenomena make the motion of a single disclination difficult to track, while they suggest quite naturally to look at the collective motion of the disclinations as a whole.

By recalling that the disclinations reorganize themselves due to their mutual interactions, through the elastic energy, and also due to the influence of the boundary, Figure E.1 makes it easy to see that the disclinations of a given pair, which are sufficiently near one with the other, tend to merge. This leads to their mutual annihilation in the limit in which time tends to infinity. In turn, disclinations which are sufficiently far away from other disclinations perceive, as leading force, the attraction towards the boundary, thereby following trajectories that asymptotically terminate there. These are all indications of *emerging behaviors* that could be further investigated.

Disclination systems with an initial "structured" distribution. The second family of scenarios that we simulate consists of two systems of disclinations in which, at time $t = 0$, the defects are placed so as to form structured patterns and the charge distributions respect some prescribed symmetries. Specifically, we consider the scenario in which disclinations of positive and negative Frank angles are *well separated* into two regions of the disk (see Figure E.2a) and the scenario in which the disclinations form successive *layers* of positive and negative Frank angles (see Figure E.2b). Although the disclinations are arranged according to predetermined patterns, in this experiment some randomness is introduced in their initial positions in order to break the geometric symmetry.

It is interesting to notice that, as shown in Figure E.2a, the positive and negative disclinations that are initially found at the "interface" between the two regions are attracted towards each others, identifying, in the stationary limit, a central region in which the "collisions" generated by these disclinations appear. On the same footing, the disclinations which are the farthest at the initial time from the "interface" will all behave the same, independently from their Frank angle. In fact, they approach the boundary almost radially (we say "almost" because of the influence of the other disclinations).

Concerning the case pictured in Figure E.2b, also in this scenario the initial structure is lost due to the mutual interactions among the disclinations. Still, it is remarkable that the disclinations of different layers move towards each others and the "collision points" approximately lie over the middle line identified by the two layers. As in the previous case, the disclinations nearer the boundary are attracted towards it.

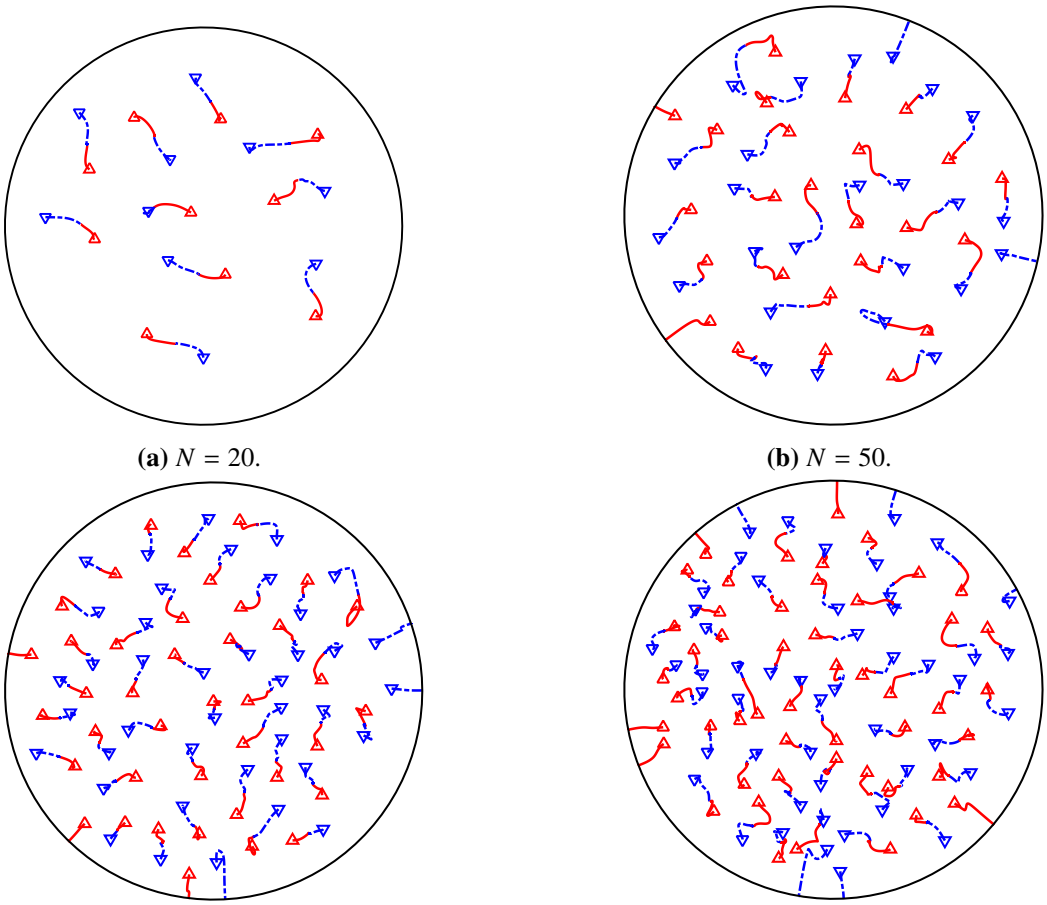

(a) $N = 20$. **(b)** $N = 50$.

(c) $N = 80$. **(d)** $N = 100$.

Fig. E.1 Trajectories of four systems of N disclinations initially placed at random points.

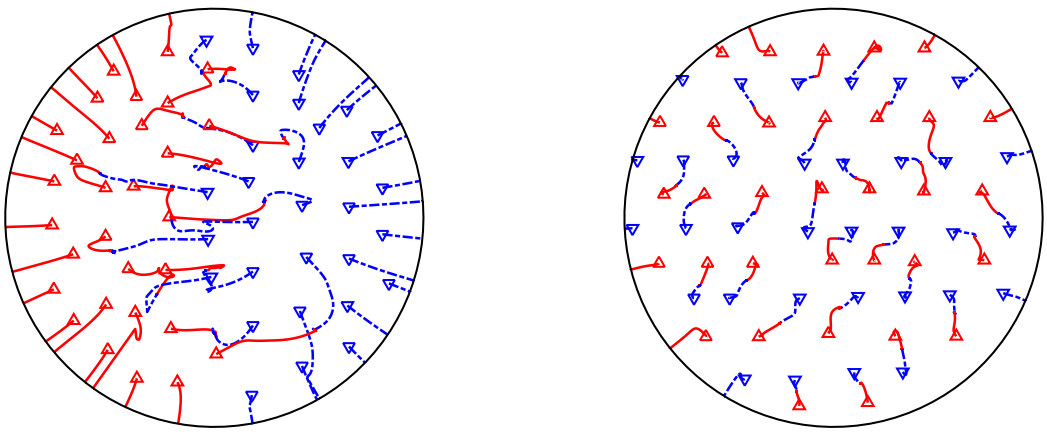

(a) "Initial charge separation" ($N = 60$). **(b)** "Initial layerings of charges" ($N = 66$).

Fig. E.2 Two examples of systems of N disclinations having an initial structure.

References

[1] A. Pastore, A. Giammarini, and A. Grillo. Reconciling Kozlov's vakonomic method with the traditional non-holonomic method: solution of two benchmark problems. *Acta Mech.*, 235:2341–2379, 2024.

[2] A. Grillo, A. Pastore, and S. Di Stefano. An Approach to Growth Mechanics based on the Analytical Mechanics of Nonholonomic Systems. *J Elast*, 153(3), 2025.

[3] P. Cesana, A. Grillo, M. Morandotti, and A. Pastore. Dissipative dynamics of Volterra Disclinations. *SIAM J. Appl. Math.*, 85(4):1361–1386, 2025.

[4] A. Giammarini, A. Pastore, and A. Grillo. A model of fiber reorientation in fiber-reinforced biological materials combining statistical and configurational mechanics. *Math. Mech. Solids*, 30(11):2619–2656, 2025.

[5] A. Giammarini, A. Pastore, A. Ramírez-Torres, and A. Grillo. A first-gradient approach to the remodeling and fluid flow in saturated porous media. *Math. Mech. Solids*, 30(9):2185–2223, 2025.

[6] A. Pastore, A. Grillo, and E. Fried. Internal constraints and gauge relations in the theory of uniaxial nematic elastomers. *J Elast*, 158(10), 2026.

[7] E. Bibbona, L. Fatibene, and M. Francaviglia. Chetaev vs. vakonomic prescriptions in constrained field theories with parametrized variational calculus. *J. Math. Phys.*, **48**:032903, 2007.

[8] J. Vankerschaver, F. Cantrijn, J.M. de León, and D. Martín de Diego. Geometric aspects of nonholonomic field theories. *Reports on Mathematical Physics*, 56(3):387–411, 2005.

[9] Romano G., Barretta R., and Diaco M. On continuum dynamics. *J. Math. Phys.*, 50:102903, 2009.

[10] M. E. Gurtin. The nature of configurational forces. *Arch. Rational Mech. Anal.*, 131:67–100., 1995.

[11] C. Lanczos. *The Variational Principles of Mechanics*. Dover Publications, Inc. New York, 1970.

[12] L. A. Pars. *A Treatise on Analytical Dynamics*. Heinemann, London, 1965.

[13] Ju.I. Neimark and N.A. Fufaev. *"Dynamics of Nonholonomic Systems"*, volume 33. Translation of Mathematical Monographs, 1972.

[14] F. Gantmacher. *Lectures in Analytical Mechanics*. MIR Publishers, Moscow, 1975.

[15] A. M. Bloch. *Nonholonomic Mechanics and Control*. Springer, New York, 2003.

[16] J. Llibre, R. Ramírez, and N. Sadovskaia. A new approach to the vakonomic mechanics. *Nonlinear Dyn.*, 78:2219–2247, 2014.

[17] N.A. Lemos. Complete inequivalence of nonholonomic and vakonomic mechanics. *Acta Mech.*, 233:47–56, 2022.

[18] M. E. Gurtin and L. Anand. A theory of strain-gradient plasticity for isotropic, plastically irrotational materials. Part II: Finite deformations. *Int. J. Plasticity*, 21:2297–2318, 2005.

[19] K. Hagihara, N. Yokotani, and Y. Umakoshi. Plastic deformation behavior of mg12yzn with 18r long-period stacking ordered structure. *Intermetallics*, 18(2):267–276, 2010.

[20] T. Inamura. Geometry of kink microstructure analysed by rank-1 connection. *Acta Mater.*, 173:270–280, 2019.

[21] M.R. Flannery. d'Alembert–Lagrange analytical dynamics for nonholonomic systems. *Journal of Mathematical Physics*, **52**:032705, 2011.

[22] A. Borisov and A. Tsiganov. On rheonomic nonholonomic deformations of the Euler equations proposed by Bilimovich. *Theoret Appl Mech*, 47(2):155–168, 2020.

[23] A. Grillo and S. Di Stefano. A formulation of volumetric growth as a mechanical problem subjected to non-holonomic and rheonomic constraint. *Math. Mech. Solids*, 28(10):2215–2241, 2023.

[24] J.E. Marsden and T.J.R. Hughes. *Mathematical Foundations of Elasticity*. Dover Publications, New York, 1983.

[25] J.M. Maruskin, A.M. Bloch, J.E. Marsden, and D.V. Zenkov. A fiber bundle approach to the transpositional relations in nonholonomic mechanics. *J. Nonlinear Sci.*, 22:431–461, 2012.

[26] P. V. Kharlamov. A critique of some mathematical models of mechanical systems with differential constraints. *J. Appl. Math. Mech.*, **56**:584–594, 1992.

[27] G. Zampieri. Nonholonomic versus vakonomic dynamics. *Journal of Differential Equations*, 163:335–347, 2000.

[28] J. G. Papastavridis. *Analytical Mechanics: A Comprehensive Treatise on the Dynamics of Constrained Systems*. Oxford University Press, Oxford, 2002.

[29] D.T. Greenwood. *Advanced Dynamics*. Cambridge University Press, Cambridge, 2003.

[30] E. Jarzębowska. Quasi-coordinates based dynamics modeling and control design for nonholonomic systems. *Nonlinear Anal. Theory Methods Appl.*, 71(12):118–131, 2009.

[31] E. Bibbona, L. Fatibene, and M. Francaviglia. Gauge-natural parameterized variational problems, vakonomic field theories and relativistic hydrodynamics of a charged fluid. *International Journal of Geometric Methods in Modern Physics*, 03:1573–1608, 2006.

[32] A. Grillo and S. Di Stefano. Addendum to *"A formulation of volumetric growth as a mechanical problem subjected to non-holonomic and rheonomic constraint"*. *Math. Mech. Solids*, 29(1):62–70, 2024.

[33] I. Giorgio, F. dell'Isola, U. Andreus, and A. Misra. An orthotropic continuum model with substructure evolution for describing bone remodeling: an interpretation of the primary mechanism behind Wolff's law. *Biomech Model Mechanobiol*, 22:2135–2152, 2023.

[34] N. Sansonetto and M. Zoppello. On the Trajectory Generation of the Hydrodynamic Chaplygin Sleigh. *IEEE Control Systems Letters*, **4**(4):922–927, 2020.

[35] R. M. Murray, S. Shankar Sastry, and L. Zexiang. *A Mathematical Introduction to Robotic Manipulation*. CRC Press, Boca Raton, United States, 1994.

[36] A. De Luca and G. Oriolo. Modelling and control of nonholonomic mechanical systems. In J. Angeles and A. Kecskeméthy, editors, *Kinematics and Dynamics of Multi-Body Systems*, pages 277–342. Springer Vienna, Vienna, 1995.

[37] P. Souéres and J.-D. Boissonnat. Optimal trajectories of nonholonomic mobile robots. In J.-P. Laumond, editor, *Robot Motion Planning and Control*. Springer New York, New York, 1998.

[38] E. Todorov. Convex and analytically-invertible dynamics with contacts and constraints: Theory and implementation in MuJuCo. In *2014 IEEE International Conference on Robotics and Automation (ICRA), Hong Kong, China*, pages 6054–6061, 2014.

[39] M.R. Flannery. The elusive d'Alembert-Lagrange dynamics of nonholonomic systems. *American Journal of Physics*, **79(9)**:932–944, 2011.

[40] N.A. Lemos. *Analytical Mechanics*. Cambridge University Press, Cambridge, 2018.

[41] V. V. Kozlov. Dynamics of systems with non-integrable restrictions i. *Vestn. Mosk. Univ., Ser. I Mat. Mekh.*, 3:92–100, 1982.

[42] V. V. Kozlov. Dynamics of systems with non-integrable restrictions ii. *Vestn. Mosk. Univ., Ser. I Mat. Mekh.*, 3:70–76, 1982.

[43] V. V. Kozlov. Dynamics of systems with non-integrable restrictions iii. *Vestn. Mosk. Univ., Ser. I Mat. Mekh.*, 3:102–111, 1983.

[44] V. V. Kozlov. Realization of nonintegrable constraints in classical mechanics. *Sov. Phys. Dokl.*, **28**:735–737, 1983.

[45] A. Nadile. Sull'esistenza per i sistemi anolonomi soggetti a vincoli reonomi di un integrale analogo a quello dell'energia. *Bollettino Unione Matematica Italiana*, 5:297–301, 1950.

[46] A. M. Bloch, P. S. Krishnaprasad, J. E. Marsden, and R. M. Murray. "Non-holonomic mechanical systems with symmetry". *Arch. Rational Mech. Anal.*, **136**:21–99, 1996.

[47] C. Cronstrom and T. Raita. On non-holonomic systems and variational principles. *J. Math. Phys.*, 50:042901, 2009.

[48] A. M. Bloch, J. E. Marsden, and D. V. Zenkov. "Quasivelocities and symmetries in non-holonomic systems". *Dynamical Systems*, **24(2)**:187–222, 2009.

[49] O. Krupkova. The nonholonomic variational principle. *J. Phys. A: Math. Theor.*, 42:185201, 2009.

[50] A. D. Lewis and R. M. Murray. Variational principles for constrained systems: Theory and experiment. *International Journal of Non-Linear Mechanics*, 30(6):793–815, 1995.

[51] M. Favretti. Equivalence of Dynamics for Nonholonomic Systems with Transverse Constraints. *Journal of Dynamics and Differential Equations*, **10(4)**:511–536, 1998.

[52] M. Jóźwikowski and W. Respondek. "A comparison of vakonomic and nonholonomic dynamics with applications to non-invariant chaplygin systems". *Journal of Geometric Mechanics*, **11**:77–122, 2019.

[53] X. Gràcia, J. Marín-Solano, and M-C. Muñoz-Lecanda. Some geometric aspects of variational calculus in constrained systems. *Reports on Mathematical Physics*, 51(1):127–148, 2003.

[54] O.E. Fernandez and A.M. Bloch. Equivalence of the dynamics of nonholonomic and variational nonholonomic systems for certain initial data. *J. Phys. A: Math. Theor.*, 41:344005, 2008.

[55] F. Cardin and M. Favretti. On nonholonomic and vakonomic dynamics of mechanical systems with nonintegrable constraints. *J. Geom. Phys.*, 18:295–325, 1995.

[56] J. Cortés, M. De León, D. Martín De Diego, and S. Martínez. Geometric description of vakonomic and nonholonomic dynamics. Comparison of solutions. *J. Control Optim.*, 41:1389–1412, 2002.

[57] K. Grabowska and J. Grabowski. Variational calculus with constraints on general algebroids. *Journal of Physics A: Mathematical and Theoretical*, 41(17):175204, 2008.

[58] A.D. Lewis. Nonholonomic and constrained variational mechanics. *Journal of Geometric Mechanics*, 12:165–308, 2020.

[59] R. Ramírez and N. Sadovskaia. On the dynamics of nonholonomic systems. *Reports on Mathematical Physics*, 60(3):427–451, 2007.

[60] G. K. Suslov. On a particular variant of d'Alembert principle. *Math. Sb.*, **22**:687–691, 1901.

[61] P. Voronets. On the equations of motion for nonholonomic systems. *Math. Sb.*, **22**:659–686, 1901.

[62] V. I. Kirgetov. On the transpositional relations in mechanics. *J. Appl. Math. Mech.*, **22**:682–693, 1958.

[63] F. Fassò and N. Sansonetto. An elemental overview of the nonholonomic noether theorem. *Int. J. Geom. Methods Mod. Phys.*, 6(8):1343–1355, 2009.

[64] M.K. Salehani. A geometric approach to the transpositional relations in dynamics of nonholonomic systems. *Int. Jour. of Geom. Met. in Mod. Phys.*, 15:1850112, 2018.

[65] P. Urbánski. Double vector bundles and duality. *Archivum Mathematicum*, 35:59–95, 1999.

[66] B. Felsager. *Geometry, particles, and fields*. Springer, Heidelberg, 1998.

[67] M. Safeea, P. Neto, and R. Bearee. Robot dynamics: A recursive algorithm for efficient calculation of Christoffel symbols. *Mechanism and Machine Theory*, 142:103589, 2019.

[68] M. Crampin and T. Mestdag. "Anholonomic frames in constrained dynamics". *Dynamical Systems*, **25**(**2**):159–187, 2010.

[69] A. DiCarlo and S. Quiligotti. Growth and balance. *Mech. Res. Commun.*, 29(6):449–456, 2002.

[70] P. Cermelli, E. Fried, and S. Sellers. Configurational stress, yield and flow in rate-independent plasticity. *Proc. R. Soc. Lond. A*, 457:1447–1467, 2001.

[71] M. E. Gurtin. Generalized Ginzburg-Landau and Cahn-Hilliard equations based on a microforce balance. *Physica D*, 92:178–192, 1996.

[72] F. dell'Isola and L. Placidi. *Variational principles are a powerful tool also for formulating field theories*, pages 1–15. COURSES AND LECTURES, Springer, 2011.

[73] M. Epstein and G.A. Maugin. Thermomechanics of volumetric growth in uniform bodies. *Int. J. Plasticity*, 16(7-8):951–978, 2000.

[74] P. Podio-Guidugli. Configurational balances via variational arguments. *Interface Free Bound.*, 3:323–332, 2011.

[75] E. Hill. Hamilton's principle and the conservation theorems of mathematical physics. *Review of Modern Physics*, 23(3):253–260, 1951.

[76] G. A. Maugin. *Material Inhomogeneities in Elasticity*. Chapman and Hall, London, 1993.

[77] A. Grillo, S. Di Stefano, and S. Federico. Growth and remodelling from the perspective of Noether's theorem. *Mech. Res. Commun.*, 97:89–95, 2019.

[78] A. Yavari. A geometric theory of growth mechanics. *J. Nonlinear Sci.*, 20:781–830, 2010.

[79] A. Yavari and A. Goriely. Weyl geometry and the nonlinear mechanics of distributed point defects. *Proc. R. Soc. A*, 468:3902–3922, 2012.

[80] A. Goriely. *The Mathematics and Mechanics of Biological Growth*. Springer, New York, 2017.

[81] E.K. Rodriguez, A. Hoger, and A.D. McCulloch. Stress-dependent finite growth in soft elastic tissues. *J. Biomech.*, 27:455–467, 1994.

[82] M. Javadi, M. Epstein, and M. Asghari. Thermomechanics of material growth and remodeling in uniform bodies based on the micromorphic theory. *Journal of the Mechanics and Physics of Solids*, 138:103904–16, 2020.

[83] L.A. Taber. Biomechanics of growth, remodeling, and morphogenesis. *Appl. Mech. Rev.*, 48(8):487, 1995.

[84] D. Ambrosi and L. Preziosi. Cell adhesion mechanisms and stress relaxation in the mechanics of tumours. *Biomech. Model. Mechanobiol.*, 8:397–413, 2009.

[85] P. Mascheroni, C. Stigliano, M. Carfagna, D.P. Boso, L. Preziosi, P. Decuzzi, and B.A. Schrefler. Predicting the growth of glioblastoma multiforme spheroids using a multiphase porous media model. *Biomech. Model. Mechanobiol.*, 15(5):1215–1228, 2016.

[86] A. DiCarlo. Surface and bulk growth unified. In Maugin G.A. Steinmann P., editor, *Mechanics of Material Forces. Advances in Mechanics and Mathematics*, volume 11, pages 53–64. Springer, Boston, MA, 2005.

[87] A. Grillo and S. Di Stefano. An *a posteriori* approach to the mechanics of volumetric growth. *Math. Mech. Complex Syst.*, 11(1):57–86, 2023.

[88] V.A. Lubarda and A. Hoger. On the mechanics of solids with a growing mass. *J. Mech. Phys. Solids*, 39:4627–4664, 2002.

[89] D. Ambrosi and L. Preziosi. On the closure of mass balance models for tumor growth. *Math. Models Methods Appl. Sci.*, 12(05):737–754, 2002.

[90] D. Ambrosi and F. Guana. Stress-modulated growth. *Math. Mech. Solids*, 12:319–342, 2007.

[91] A. Grillo and S. Di Stefano. Comparison between different viewpoints on bulk growth mechanics. *Math. Mech. Complex Syst.*, 11(2):287–311, 2023.

[92] D. Ambrosi, G.A. Ateshian, E.M. Arruda, S.C. Cowin, J. Dumais, A. Goriely, G.A. Holzapfel, J.D. Humphrey, R. Kemkemer, E. Kuhl, J.E. Olberding, L.A. Taber, and K. Garikipati. Perspectives on biological growth and remodeling. *J. Mech. Phys. Solids*, 59(4):863–883, 2011.

[93] D. Ambrosi, M. B. Amar, C. J. Cyron, A. DeSimone, A. Goriely, J. D. Humphrey, and E. Kuhl. Growth and remodelling of living tissues: perspectives, challenges and opportunities. *J. R. Soc. Interface*, 16:20190233, 2019.

[94] C. Giverso and L. Preziosi. Influence of the mechanical properties of the necrotic core on the growth and remodelling of tumour spheroids. *Int. J. of Nonlinear Mech.*, 108:20–32, 2019.

[95] D. Ambrosi and F. Mollica. On the mechanics of a growing tumor. *Int. J. Eng. Sci.*, 40(12):1297–1316, 2002.

[96] A. Agosti, C. Cattaneo, C. Giverso, D. Ambrosi, and P. Ciarletta. A computational framework for the personalized clinical treatment of glioblastoma multiforme. *Zeitschrift für Angewandte Mathematik und Mechanik - ZAMM*, 98:2307–2327, 2018.

[97] A. Agosti, C. Giverso, E. Faggiano, A. Stamm, and P. Ciarletta. A personalized mathematical tool for neuro-oncology: A clinical case study. *International Journal of Non-Linear Mechanics*, 107:170–181, 2018.

[98] P. Ciarletta, D. Ambrosi, G.A. Maugin, and L. Preziosi. Mechano-transduction in tumour growth modelling. *Eur. Phys. J. E*, 36:23, 2013.

[99] V. V. Kozlov. The problem of realizing constraints in dynamics. *J. Appl. Math. Mech.*, 56:594–600, 1992.

[100] A. M. Bloch, J. E. Marsden, and Zenkov D.V. Quasivelocities and symmetries in non-holonomic systems. *Dynamical Systems*, 24(2):187–222, 2009.

[101] T. Olsson and A. Klarbring. Residual stresses in soft tissue as a consequence of growth and remodeling: application to an arterial geometry. *Eur. J. Mech. A*, 27(6):959–974, 2008.

[102] P. Mascheroni, M. Carfagna, A. Grillo, D.P. Boso, and B.A. Schrefler. An avascular tumor growth model based on porous media mechanics and evolving natural states. *Math. Mech. Solids*, 23(4):686–712, 2018.

[103] J. Ciambella and P. Nardinocchi. Torque-induced reorientation in active fibre-reinforced materials. *Soft Matter*, 15(9):2081–2091, 2019.

[104] J. Ciambella, G. Lucci, P. Nardinocchi, and L. Preziosi. Passive and active fiber reorientation in anisotropic materials. *Int. J. Eng. Sci.*, 176(103688):1–10, 2022.

[105] G. Batra. On hamilton's principle for thermo-elastic fluids and solids, and internal constraints in thermo-elasticity. *Archive for Rational Mechanics and Analysis*, 99:37–59, 1987.

[106] J. Bonet and R. D. Wood. *Nonlinear Continuum Mechanics for Finite Element Analysis*. Cambridge University Press, New York, 2008.

[107] S. Di Stefano, A. Ramírez-Torres, R. Penta, and A. Grillo. Self-influenced growth through evolving material inhomogeneities. *Int. J. Nonlinear Mech.*, 106:174–187, 2018.

[108] A. Grillo, S. Di Stefano, A. Ramírez-Torres, and M. Loverre. A study of growth and remodeling in isotropic tissues, based on the Anand-Aslan-Chester theory of strain-gradient plasticity. *GAMM-Mitteilungen*, 42(4), may 2019.

[109] S. Sadik and A. Yavari. On the origins of the idea of the multiplicative decomposition of the deformation gradient. *Math. Mech. Solids*, 22(4):771–772, 2017.

[110] S. Federico, M. F. Alhasadi, and A. Grillo. Eshelby's inclusion theory in light of Noether's theorem. *Mathematics and Mechanics of Complex Systems*, 7(3):247–285, 2019.

[111] W. Noll. Materially uniform simple bodies with inhomogeneities. *Arch. Rational Mech. Anal.*, 27:1–32, 1967.

[112] M. Epstein and M. Elżanowski. *Material Inhomogeneities and their Evolution — A Geometric Approach*. Springer-Verlag Berlin Heidelberg, 1 edition, 2007.

[113] B.A. Bilby, L.R.T. Gardner, and A.N. Stroh. Continuous distributions of dislocations and the theory of plasticity. *Extrait des Actes du IX^e Congres Int. de Mecanique Appliquee, Brussels*, pages 35–44, 1957.

[114] E. Kröner. Allgemeine Kontinuumstheorie der Versetzungen und Eigenspannungen. *Arch. Ration. Mech. Analysis*, 4:273–334, 1960.

[115] C.-C Wang. On the geometric structures of simple bodies, a mathematical foundation for the theory of continuous distributions of dislocations. *Arch. Rational Mech. Anal.*, 27:33–94, 1967.

[116] M.V. Mićunović. *Thermomechanics of Viscoplasticity*. Springer New York, 2009.

[117] E.I. Rashba. Stress determination in bulks due to own weight taking into account the construction sequence. *Proc. Inst. Struct. Mech. Acad. Sci. Ukrainian SSR*, 18:23–27, 1953.

[118] A. Yavari and A. Goriely. Riemann–Cartan Geometry of Nonlinear Dislocation Mechanics. *Arch. Rational Mech. Anal.*, 205:59–118, 2012.

[119] S.A. Lychev and A.V. Manzhirov. Reference Configurations of Growing Bodies. *Mech. Solids*, 48(5):553–560, 2013.

[120] S.A. Lychev and A.V. Manzhirov. The mathematical theory of growing bodies. Finite deformations. *J. Appl. Math. Mech.*, 77(4):421–432, 2013.

[121] S. Lychev and K. Koifman. *Geometry of Incompatible Deformations: Differential Geometry in Continuum Mechanics*. De Gruyter, 2019.

[122] S. Lychev and K. Koifman. Nonlinear evolutionary problem for a laminated inhomogeneous spherical shell. *Acta Mech*, 230:3989–4020, 2019.

[123] S.A. Lychev, G.V. Kostin, K.G. Koifman, and T.N. Lycheva. Non-euclidean Geometry and Defected Structure for Bodies with Variable Material Composition. *J. Phys.: Conf. Ser.*, 1250.012035, 2019.

[124] S.A. Lychev and K.G. Koifman. Material Affine Connections for Growing Solids. *Lobachevskii J. Math*, 41(10):2034–2052, 2020.

[125] S.A. Lychev and K.G. Koifman. Contorsion of Material Connection in Growing Solids. *Lobachevskii J Math*, 42:1852–1875, 2021.

[126] K. Garikipati, E.M. Arruda, K. Grosh, H. Narayanan, and S. Calve. A continuum treatment of growth in biological tissue: the coupling of mass transport and mechanics. *J. Mech. Phys. Solids*, 52:1595–1625, 2004.

[127] B. Loret and F.M.F. Simões. A framework for deformation, generalized diffusion, mass transfer and growth in multi-species multi-phase biological tissues. *Eur. J. Mech. A*, 24:757–781, 2005.

[128] D. Ambrosi, S. Pezzuto, D. Riccobelli, T. Stylianopoulos, and P. Ciarletta. Solid tumors are poroelastic solids with a chemo-mechanical feedback on growth. *J. Elast.*, 129:107–124, 2017.

[129] L. Preziosi, D. Ambrosi, and C. Verdier. An elasto-visco-plastic model of cell aggregates. *J. Theor. Biol.*, 262(1):35–47, 2010.

[130] L. Preziosi and G. Vitale. A multiphase model of tumor and tissue growth including cell adhesion and plastic reorganization. *Math. Models Methods Appl. Sci.*, 21(09):1901–1932, 2011.

[131] M.A.J. Chaplain, L. Graziano, and L. Preziosi. Mathematical modelling of the loss of tissue compression responsiveness and its role in solid tumour development. *Mathematical Medicine and Biology: A Journal of the IMA*, 23(3):197–229, 2006.

[132] N.Kh. Arutyunyan and A.D. Drozdov. Mechanics of growing viscoelastic bodies subject to aging at finite strains. *Doklady AN SSSR*, 276(4):821–825, 1984.

[133] G. Forgacs, R.A. Foty, Y. Shafrir, and M.S. Steinberg. Viscoelastic properties of living embryonic tissues: a quantitative study. *Biophysical Journal*, 74:2227–2234, 1998.

[134] S. Di Stefano, A. Giammarini, C. Giverso, and A. Grillo. An elasto-plastic biphasic model of the compression of multicellular aggregates: the influence of fluid on stress and deformation. *Z. Angew. Math. Phys.*, 73:79–118, 2022.

[135] A. Tatone and F. Recrosi. Volumetric growth, microstructure, and kinetic energy. *European Journal of Mechanics - A/Solids*, 103:105154, 2024.

[136] F. dell'Isola and L. Placidi. Variational principles are a powerful tool also for formulating field theories. In F. dell'Isola and S. Gavrilyuk, editors, *Variational Models and Methods in Solid and Fluid Mechanics. CISM Courses and Lectures*, pages 1–15. Springer, Vienna, 2011.

[137] P. Germain. The method of virtual power in continuum mechanics. part 2: Microstructure. *SIAM J. Appl. Math.*, 25(3):556–575, 1973.

[138] M. Epstein and R. Segev. Differentiable manifolds and the principle of virtual work in continuum mechanics. *J. Math. Phys.*, 21(5):1243–1245, 1980.

[139] A. Grillo, S. Federico, and G. Wittum. Growth, mass transfer, and remodeling in fiber-reinforced, multi-constituent materials. *Int. J. Nonlinear Mech.*, 47:388–401, 2012.

[140] M. Epstein and Maugin G. A. The energy-momentum tensor and material uniformity in finite elasticity. *Acta Mechanica*, **83**(3-4):127–133, 1990.

[141] S. Cleja-Tigoiu and G. A. Maugin. Eshelby's stress tensors in finite elastoplasticity. *Acta Mechanica*, 139(1-4):231–249, 2000.

[142] M. E. Gurtin and L. Anand. A theory of strain-gradient plasticity for isotropic, plastically irrotational materials. Part I: Small deformations. *J. Mech. Phys. Solids*, 53:1624–1649, 2005.

[143] E. Crevacore, S. Di Stefano, and A. Grillo. Coupling among deformation, fluid flow, structural reorganisation and fibre reorientation in fibre-reinforced, transversely isotropic biological tissues. *Int. J. Nonlinear Mech.*, 111:1–13, 2019.

[144] I. Giorgio, F. dell'Isola, U. Andreaus, F. Alzahrani, T. Hayat, and T. Lekszycki. On mechanically driven biological stimulus for bone remodeling as a diffusive phenomenon. *Biomech Model Mechanobiol*, 18(6):1639–1663, 2019.

[145] A. Di Carlo, M. E. Gurtin, and P. Podio-Guidugli. A Regularized Equation for Anisotropic Motion-by-Curvature. *SIAM Journal on Applied Mathematics*, 52(4):1111–1119, 1992.

[146] S. Quiligotti. On bulk growth mechanics of solid-fluid mixtures: kinematics and invariance requirements. *Theoret. Appl. Mech.*, 28-29:277–288, 2002.

[147] M. Epstein and A. Goriely. Self-diffusion in remodeling and growth. *Z. Angew. Math. Phys.*, 63:339–355, 2012.

[148] P. Moreo, J. M. García-Aznar, and M. Boblaré. Modeling mechanosensing and its effect on the migration and proliferation of adherent cells. *Acta Biomaterialia*, 4(3):613–621, 2008.

[149] Y. Chen, L. Ju, M. Rushdi, C. Ge, and C. Zhu. Receptor-mediated cell mechanosensing. *Molecular Biology of the Cell*, 28(23):3134–3155, 2017.

[150] M. Minozzi, P. Nardinocchi, L. Teresi, and V. Varano. Growth-induced compatible strains. *Math. Mech. Solids*, 22(1):62–71, 2016.

[151] S. Cleja-Tigoiu. Dislocations and disclinations: continuously distributed defects in elasto-plastic crystalline materials. *Archive of Applied Mechanics*, 84(9-1):1293–1306, 2014.

[152] M.H. Holmes and V.C. Mow. The nonlinear characteristics of soft gels and hydrated connective tissues in ultrafiltration. *Journal of biomechanics*, 23:1145–1156, 1990.

[153] L.S. Bennethum, M.A. Murad, and J.H. Cushman. Macroscale thermodynamics and the chemical potential for swelling porous media. *Transport in Porous Media*, 39(2):187–225, 2000.

[154] R.V. Huyghe, J.M. Loon and F. Baaijens. Fluid-solid mixtures and electrochemomechanics: the simplicity of lagrangian mixture theory. *Clinics*, 23, 2004.

[155] G.A. Ateshian. On the theory of reactive mixtures for modeling biological growth. *Biomech. Model. Mechanobiol.*, 6(6):423–445, jan 2007.

[156] H. Byrne and L. Preziosi. Modelling solid tumour growth using the theory of mixtures. *Mathematical Medicine and Biology*, 20(4):341–366, dec 2003.

[157] D. Ambrosi, L. Preziosi, and G. Vitale. The insight of mixtures theory for growth and remodeling. *Z. Angew. Math. Phys.*, 61:177–191, 2010.

[158] P. Marmottant, A. Mgharbel, J. Käfer, B. Audren, J-P Rieu, J-C Vial, B. van der Sanden, A.F.M. Marée, F. Graner, and H. Delanoë-Ayari. The role of fluctuations and stress on the effective viscosity of cell aggregates. *Proc. Natl. Acad. Sci. U. S. A.*, 106(41):17271–17275, October 2009.

[159] C. Giverso and L. Preziosi. Modelling the compression and reorganization of cell aggregates. *Mathematical Medicine and Biology*, 29:181–204, 2012.

[160] Y.C. Fung. *Biomechanics. Motion, flow, stress, and growth*. Springer, New York, 1990.

[161] S.C. Cowin. How is a tissue built? *J Biomech Eng*, 122:553–569, 2000.

[162] M. Epstein. The split between remodelling and aging. *International Journal of Non-Linear Mechanics*, 44(6):604–609, jul 2009.

[163] Lisa D. Muiznieks and Fred W. Keeley. Molecular assembly and mechanical properties of the extracellular matrix: A fibrous protein perspective. *Biochim Biophys Acta*, 1832(7):866–875, 2013.

[164] Jaime A. Espina, Marilia H. Cordeiro, and Elias H. Barriga. Tissue interplay during morphogenesis. *Seminars in Cell and Developmental Biology*, 147, March 2023.

[165] R. Vandiver and A. Goriely. Morpho-elastodynamics: The long-time dynamics of elastic growth. *Journal of Biological Dynamics.*, 3:180–195, 2009.

[166] Alain Goriely. *The Mathematics and Mechanics of Biological Growth*. Springer New York, 2017.

[167] M. Minozzi, Paola Nardinocchi, Luciano Teresi, and Valerio Varano. Growth-induced compatible strains. *Math. Mech. Solids*, 22(1):62–71, aug 2017.

[168] W.J. Lin, M.D. Iafrati, R.A. Peattie, and L. Dorfmann. Growth and remodeling with application to abdominal aortic aneurysms. *J. Eng. Math.*, In press:1–25, 2017.

[169] M. Epstein. Self-driven continuous dislocations and growth. In Maugin G.A. Steinmann P., editor, *Mechanics of Material Forces. Advances in Mechanics and Mathematics*, volume 11, pages 129–139. Springer, Boston, MA, 2005.

[170] M. Epstein. *The geometric language of continuum mechanics*. Cambridge University Press, 2010.

[171] George Z. Voyiadjis and Yooseob Song. Strain gradient continuum plasticity theories: Theoretical, numerical and experimental investigations. *International Journal of Plasticity*, 121:21–75, October 2019.

[172] K. Vafai and C.L. Tien. Boundary and inertia effects on convective mass transfer in porous media. *Int. J. Heat Mass Transf.*, 25(8):1183–1190, August 1982.

[173] A. R. A. Khaled and K. Vafai. The role of porous media in modeling flow and heat transfer in biological tissues. *Int. J. Heat Mass Transf.*, 46(26):4989–5003, dec 2003.

[174] H. C. Brinkman. A calculation of the viscous force exerted by a flowing fluid on a dense swarm of particles. *Flow, Turbulence and Combustion*, 1(1), dec 1949.

[175] R.K. Dash, K.N. Mehta, and G. Jayaraman. Casson fluid flow in a pipe filled with a homogeneous porous medium. *International Journal of Engineering Science*, 34(10):1145–1156, August 1996.

[176] Shigeru Tada and John M. Tarbell. Interstitial flow through the internal elastic lamina affects shear stress on arterial smooth muscle cells. *American Journal of Physiology-Heart and Circulatory Physiology*, 278(5):H1589–H1597, May 2000.

[177] C. Giverso, M. Scianna, and A. Grillo. Growing avascular tumours as elasto-plastic bodies by the theory of evolving natural configurations. *Mech. Res. Commun.*, 68:31–39, 2015.

[178] Morton E. Gurtin and Paolo Podio Guidugli. The thermodynamics of constrained materials. *Archive for Rational Mechanics and Analysis*, 51(3):192–208, 1973.

[179] S.M. Hassanizadeh. Derivation of basic equations of mass transp. porous med., part 2. generalized darcy's and fick's laws. *Adv. Water Resour.*, 9:207–222, 1986.

[180] S. M. Hassanizadeh. Derivation of basic equations of mass transp. porous med., part 2. generalized Darcy's and Fick's laws. *Adv. Water Resour.*, 9:207–222, 1986.

[181] Sachin Gunda, Alessandro Giammarini, Ariel Ramírez-Torres, Sundararajan Natarajan, Olga Barrera, and Alfio Grillo. Fractionalization of Forchheimer's correction to Darcy's law in porous media in large deformations. *Mathematics and Mechanics of Solids*, 30(4):809–849, August 2024.

[182] S. Quiligotti, G.A. Maugin, and F. dell'Isola. An eshelbian approach to the nonlinear mechanics of constrained solid-fluid mixtures. *Acta Mech.*, 160:45–60, 2003.

[183] C. Giverso, S. Di Stefano, A. Grillo, and L. Preziosi. A three dimensional model of multicellular aggregate compression. *Soft Matter*, 15(48):10005–10019, 2019.

[184] A. Grillo, R. Prohl, and G. Wittum. A poroplastic model of structural reorganisation in porous media of biomechanical interest. *Continuum Mech. Therm.*, 28:579–601, 2016.

[185] Ariel Ramírez-Torres, Salvatore Di Stefano, and Alfio Grillo. Influence of non-local diffusion in avascular tumour growth. *Math. Mech. Solids*, 26(9):1264–1293, 2021.

[186] D. J. Steigmann. Gradient plasticity in isotropic solids. *Mathematics and Mechanics of Solids*, 27(10):1896–1912, nov 2021.

[187] Mircea Bîrsan and Patrizio Neff. *On the Dislocation Density Tensor in the Cosserat Theory of Elastic Shells*. Springer Singapore, 2016.

[188] Paolo Cermelli and Morton E. Gurtin. On the characterization of geometrically necessary dislocations in finite plasticity. *Journal of the Mechanics and Physics of Solids*, 49(7):1539–1568, July 2001.

[189] J. Bonet, A. J. Gil, and R. Ortigosa. On a tensor cross product based formulation of large strain solid mechanics. *International Journal of Solids and Structures*, 84:49–63, 2016.

[190] V. Ciancio, M. Dolfin, M. Francaviglia, and S. Preston. Uniform materials and the multiplicative decomposition of the deformation gradient in finite elasto-plasticity. *J. Non-Equilib. Thermodyn.*, 33(3):199–234, 2008.

[191] Salvatore Federico. The truesdell rate in continuum mechanics. *Zeitschrift für angewandte Mathematik und Physik*, 73(3), apr 2022.

[192] D. Ambrosi and L. Preziosi. Modeling injection molding processes with deformable porous preforms. *SIAM Journal on Applied Mathematics*, 61(1):22–42, 2000.

[193] D.R. Anderson, D.E. Carlson, and E. Fried. A Continuum-Mechanical Theory for Nematic Elastomers. *Journal of Elasticity*, 56:33–58, 1999.

[194] Y. Chen and E. Fried. Uniaxial nematic elastomers: constitutive framework and a simple application. *Proc. R. Soc. A*, 462:1295–1314, 2006.

[195] A. Bertram and R. Glüge. Gradient materials with internal constraints. *Math. Mech. Complex Syst.*, 4(1):1–15, 2016.

[196] Sandro Salsa. *Partial Differential Equations in Action*. Springer International Publishing, 2015.

[197] T. J. R. Hughes. *The Finite Element Method – Linear Static and Dynamic Finite Element Analysis*. Prentice-Hall, Inc., Englewood Cliffs, New Jersey, 1987.

[198] A. C. Eringen. *Mechanics of Continua*. R. E. Krieger Publishing Company, Huntington, New York, 1980.

[199] Paolo Cermelli and Morton E. Gurtin. The motion of screw dislocations in crystalline materials undergoing antiplane shear: Glide, cross-slip, fine cross-slip. *Archive for Rational Mechanics and Analysis*, 148(1):3–52, 1999.

[200] Pierluigi Cesana, Lucia De Luca, and Marco Morandotti. Semidiscrete modeling of systems of wedge disclinations and edge dislocations via the airy stress function method. *SIAM Journal on Mathematical Analysis*, 56:79–136, 01 2024.

[201] Klaus Hackl and Franz Dieter Fischer. On the relation between the principle of maximum dissipation and inelastic evolution given by dissipation potentials. *Proceedings of the Royal Society A: Mathematical, Physical and Engineering Sciences*, 464(2089):117–132, oct 2007.

[202] Alain Curnier, Qi-Chang He, and Philippe Zysset. Conewise linear elastic materials. *Journal of Elasticity*, 37(1):1–38, 1995.

[203] J. Bear and Y. Bachmat. *Introduction to Modeling of Transport Phenomena in Porous Media*. Kluwer, Dordrecht, 1990.

[204] A. S. Fokas. On the integrability of linear and nonlinear partial differential equations. *J. Math. Phys.*, 41(6):4188–4237, 2000.

[205] M. H. Holmes. Finite deformation of soft tissue: Analysis of a mixture model in uni-axial compression. *Journal of Biomechanical Engineering*, 108(4):372–381, November 1986.

[206] D.M. Robertson, D. Robertson, and C.R. Barrett. Fracture toughness, critical crack length and plastic zone size in bone. *Journal of Biomechanics*, 11(8–9):359–364, 1978.

[207] R. Ritchie, M. Buehler, and P. Hansma. Plasticity and toughness in bone. *Physics Today - PHYS TODAY*, 62(6):41–47, 2009.

[208] Jean-Louis Auriault. On the domain of validity of Brinkman's equation. *Transport in Porous Media*, 79(2):215–223, December 2008.

[209] Wook Ryol Hwang and Suresh G. Advani. Numerical simulations of Stokes–Brinkman equations for permeability prediction of dual scale fibrous porous media. *Physics of Fluids*, 22(11), November 2010.

[210] Giuseppe Vacca. An H1-conforming virtual element for Darcy and Brinkman equations. *Mathematical Models and Methods in Applied Sciences*, 28(01):159–194, December 2017.

[211] E. Orowan. Zur Kristallplastizität. III. *Z. Physik*, 89:634–659, 1934.

[212] M. Polanyi. Über eine Art Gitterstörung, die einen Kristall plastisch machen könnte. *Z. Physik*, 89:660–664, 1934.

[213] T. Inamura, H. Hosoda, and S. Miyazaki. Incompatibility and preferred morphology in the self-accommodation microstructure of β-titanium shape memory alloy. *Philosophical Magazine*, 93(6):618–634, 2013.

[214] T. Inamura, M. Li, M. Tahara, and H. Hosoda. Formation process of the incompatible martensite microstructure in a beta-titanium shape memory alloy. *Acta Mater.*, 124:351–359, 2017.

[215] D. Essmann and H. Träuble. The Direct Observation of Individual Flux Lines in Type II Superconductors. *Phys. Letters*, 24A(526), 1967.

[216] H. Träuble and D. Essmann. Fehler im Flussliniengitter von Supraleitern zweiter Art. *Phys. Stat. Sol.*, 25(373), 1968.

[217] F. Banhart, J. Kotakoski, and A. V. Krasheninnikov. Structural defects in graphene. *ACS Nano*, 5(1):26–41, 2011. PMID: 21090760.

[218] G. Yang, L. Li, W. B. Lee, and M. C. Ng. Structure of graphene and its disorders: a review. *Science and Technology of Advanced Materials*, 19(1):613–648, 2018.

[219] V. Volterra. Sur l'équilibre des corps élastiques multiplement connexes. *Annales scientifiques de l'École Normale Supérieure*, 24:401–517, 1907.

[220] J. P. Hirth and R. W. Armstrong. Straight and curved disclinations and dislocation equivalents. *Philosophical Magazine*, 101(1):25–37, 2021.

[221] John P. Hirth, Greg Hirth, and Jian Wang. Disclinations and disconnections in minerals and metals. *Proceedings of the National Academy of Sciences*, 117(1):196–204, 2020.

[222] A. E. Romanov, M. A. Rozhkov, and A. L. Kolesnikova. Disclinations in polycrystalline graphene and pseudo-graphenes. review. *Letters on Materials*, 8(4):384–400, 2018.

[223] M. Kabir and K. J. Van Vliet. Kinetics of Topological Stone–Wales Defect Formation in Single-Walled Carbon Nanotubes. *J. Phys. Chem. C*, 120(3):1989–1993, 2016.

[224] J. Lu, Y. Bao, C. L. Su, and K. P. Loh. Properties of Strained Structures and Topological Defects in Graphene. *ACS Nano*, 7(10):8350–8357, 2013.

[225] B. I. Smirnov. Disclination Mode of Intergrain Fracture in LiF Bicrystals under Single Slip Deformation. *Solid State Phenomena*, 87:301–0, 2002.

[226] Tsubasa Tokuzumi, Masatoshi Mitsuhara, Shigeto Yamasaki, Tomonari Inamura, Toshiyuki Fujii, and Hideharu Nakashima. Role of disclinations around kink bands on deformation behavior in Mg–Zn–Y alloys with a long-period stacking ordered phase. *Acta Mater.*, 248:118785, 2023.

[227] Sh. Akhondzadeh, Minju Kang, Ryan B. Sills, K.T. Ramesh, and Wei Cai. Direct comparison between experiments and dislocation dynamics simulations of high rate deformation of single crystal copper. *Acta Mater.*, 250:118851, 2023.

[228] J. E. Dorn, J. Mitchell, and F. Hauser. Dislocation dynamics. *Experimental Mechanics*, 5:353–362, 1965.

[229] J.S. Robach, I.M. Robertson, H.-J. Lee, and B.D. Wirth. Dynamic observations and atomistic simulations of dislocation–defect interactions in rapidly quenched copper and gold. *Acta Mater.*, 54(6):1679–1690, 2006.

[230] Amit Acharya. A model of crystal plasticity based on the theory of continuously distributed dislocations. *Journal of the Mechanics and Physics of Solids*, 49(4):761–784, 2001.

[231] Amit Acharya. New inroads in an old subject: Plasticity, from around the atomic to the macroscopic scale. *Journal of the Mechanics and Physics of Solids*, 58(5):766–778, 2010.

[232] Xiaohan Zhang, Amit Acharya, Noel J. Walkington, and Jacobo Bielak. A single theory for some quasi-static, supersonic, atomic, and tectonic scale applications of dislocations. *Journal of the Mechanics and Physics of Solids*, 84:145–195, 2015.

[233] Roberto Alicandro, Lucia De Luca, Adriana Garroni, and Marcello Ponsiglione. Minimising movements for the motion of discrete screw dislocations along glide directions. *Calc. Var. Partial Differential Equations*, 56(5):Paper No. 148, 19, 2017.

[234] T. Blass, I. Fonseca, G. Leoni, and M. Morandotti. Dynamics for systems of screw dislocations. *SIAM Journal on Applied Mathematics*, 75(2):393–419, 2015.

[235] A. Garroni, P. van Meurs, M. A. Peletier, and L. Scardia. Convergence and non-convergence of many-particle evolutions with multiple signs. *Arch. Ration. Mech. Anal.*, 235(1):3–49, 2020.

[236] Thomas Hudson and Marco Morandotti. Properties of screw dislocation dynamics: time estimates on boundary and interior collisions. *SIAM J. Appl. Math.*, 77(5):1678–1705, 2017.

[237] Maria Giovanna Mora, Mark A. Peletier, and Lucia Scardia. Convergence of interaction-driven evolutions of dislocations with Wasserstein dissipation and slip-plane confinement. *SIAM J. Math. Anal.*, 49(5):4149–4205, 2017.

[238] Stefania Patrizi and Tharathep Sangsawang. From the Peierls-Nabarro model to the equation of motion of the dislocation continuum. *Nonlinear Anal.*, 202:Paper No. 112096, 50, 2021.

[239] Patrick van Meurs and Marco Morandotti. Discrete-to-continuum limits of particles with an annihilation rule. *SIAM J. Appl. Math.*, 79(5):1940–1966, 2019.

[240] Patrick van Meurs and Stefania Patrizi. Discrete dislocation dynamics with annihilation as the limit of the Peierls-Nabarro model in one dimension. *SIAM J. Math. Anal.*, 56(1):197–233, 2024.

[241] Alex W. Robertson, Gun-Do Lee, Kuang He, Ye Fan, Christopher S. Allen, Sungwoo Lee, Heeyeon Kim, Euijoon Yoon, Haimei Zheng, Angus I. Kirkland, and Jamie H. Warner. Partial dislocations in graphene and their atomic level migration dynamics. *Nano Letters*, 15(9):5950–5955, 2015.

[242] E. Annevelink, H. T. Johnson, and E. Ertekin. Pathways to controlled 3D deformation of graphene: Manipulating the motion of topological defects. *Current Opinion in Solid State & Materials Science*, page 100893, 2021.

[243] E. Kossecka and R. de Wit. Disclination dynamics. *Arch. Mech.*, 29:749–767, 1977.

[244] E. Kossecka and R. de Wit. Disclination kinematics. *Arch. Mech.*, 29:633–651, 1977.

[245] A. E. Romanov and V. I. Vladimirov. Disclinations in solids. *physica status solidi (a)*, 78:11–34, 1983.

[246] C. Fressengeas, V. Taupin, and L. Capolungo. An elasto-plastic theory of dislocation and disclination fields. *International Journal of Solids and Structures*, 48(25):3499–3509, 2011.

[247] V. Taupin, L. Capolungo, C. Fressengeas, A. Das, and M. Upadhyay. A theory of disclination and dislocation fields for grain boundary plasticity. In Holm Altenbach, Samuel Forest, and Anton Krivtsov, editors, *Generalized Continua as Models for Materials: With Multi-scale Effects or Under Multi-field Actions*, pages 303–320. Springer Berlin Heidelberg, Berlin, Heidelberg, 2013.

[248] Chiqun Zhang, Amit Acharya, and Saurabh Puri. Finite element approximation of the fields of bulk and interfacial line defects. *Journal of the Mechanics and Physics of Solids*, 114:258–302, 2018.

[249] Amit Acharya and Claude Fressengeas. Continuum mechanics of the interaction of phase boundaries and dislocations in solids. In Gui-Qiang G. Chen, Michael Grinfeld, and R. J. Knops, editors, *Differential Geometry and Continuum Mechanics*, pages 123–165, Cham, 2015. Springer International Publishing.

[250] E. Zegpi, H. Casquero, Y. J. Zhang, and A. Acharya. IGA Approximations of Elastic Interfaces and their Defects in an Elastic Medium with Couple Stress. *Engineering with Computers*, 40:4109–4140, 2024.

[251] A. Yavari and A. Goriely. Riemann-Cartan geometry of nonlinear disclination mechanics. *Mathematics and Mechanics of Solids*, 18(1):91–102, 2013.

[252] J. Ball, P. Cesana, and B. Hambly. A probabilistic model for martensitic avalanches. *MATEC Web of Conferences*, 33, 2015.

[253] P. Cesana and B. M. Hambly. A probabilistic model for interfaces in a martensitic phase transition. *Journal of Applied Probability*, 59(4):1081–1105, 2022.

[254] E. Kossecka. Interaction of defects with the elastic field. *Arch. Mech.*, 31:851–859, 1979.

[255] R. de Wit. Linear theory of static disclinations. In *J. A. Simmons, R. de Wit, and R. Bullough (eds.) Fundamental Aspects of Dislocation Theory*, volume I, pages 651–673. Nat. Bur. Stand. (US), Spec. Publ. 317, 1970.

[256] H. S. Seung and D. R. Nelson. Defects in flexible membranes with crystalline order. *Physical Review A*, 38:1005–1018, 1988.

[257] J.M. Kosterlitz and D.J. Thouless. Ordering, metastability and phase transitions in two-dimensional systems. *Journal of Physics C: Solid State Physics*, 6(7):1181, 1973.

[258] Qi Wei-Kai, Zhu Tao, Chen Yong, and Ren Ji-Rong. Topological aspect of disclinations in two-dimensional crystals. *Chinese Physics B*, 18(3):1002, mar 2009.

[259] J. H. Michell. On the Direct Determination of Stress in an Elastic Solid, with application to the Theory of Plates. *Proceedings of the London Mathematical Society*, s1-31(1):100–124, 04 1899.

[260] T. Blass and M. Morandotti. Renormalized energy and Peach-Köhler forces for screw dislocations with antiplane shear. *Journal of Convex Analysis*, 24(2):547–570, 2017.

[261] A. E. Romanov and V. I. Vladimirov. Disclinations in crystalline solids. In F.R.N. Nabarro, editor, *Dislocations in solids*, volume 9, pages 191–402. North-Holland Publ. Co., Amsterdam, 1992.

[262] Mitsuru Nakai and Leo Sario. Green's function of the clamped punctured disk. *J. Austral. Math. Soc.*, **20** (Series B):175–181, 1978.

[263] A.N. Tikhonov and A.A. Samarskii. *Equations of Mathematical Physics*. Dover Books on Physics. Dover Publications, 2013.

[264] The MathWorks, Inc. *MATLAB*. MathWorks, Natick, Massachusetts, 2024. Version R2024b.

[265] L. F. Shampine and M. W. Reichelt. The MATLAB ODE Suite. *SIAM Journal on Scientific Computing*, 18, 1997.

[266] J. D. Eshelby. A simple derivation of the elastic field of an edge dislocation. *British Journal of Applied Physics*, 17(9):1131–1135, sep 1966.

[267] A. Yavari. On the wedge dispiration in an inhomogeneous isotropic nonlinear elastic solid. *Mech. Res. Commun.*, 78:55–59, 2016.

[268] A. Yavari and A. Goriely. The geometry of discombinations and its applications to semi-inverse problems in anelasticity. *Proc. R. Soc. A*, 470:20140403, 2014.

[269] A. F. Filippov. *Differential equations with discontinuous righthand sides*, volume 18 of *Mathematics and its Applications (Soviet Series)*. Kluwer Academic Publishers Group, Dordrecht, 1988. Translated from the Russian.

[270] N. I. Muskhelishvili. Sur l'intégration de l'équation biharmonique. *Bull. de l'Académie des Sciences de Russie*, 17:663–686, 1919.